DARCOM PAMPHLET DARCOM-P 706-358

ENGINEERING DESIGN HANDBOOK

ANALYSIS AND DESIGN OF AUTOMOTIVE BRAKE SYSTEMS

HQ, US ARMY MATERIEL DEVELOPMENT & READINESS COMMAND DECEMBER 1976

LIST OF ILLUSTRATIONS

LIST OF ILLUSTRATIONS (Continued)

LIST OF ILLUSTRATIONS (Continued)

LIST OF ILLUSTRATIONS (Continued)

LIST OF ILLUSTRATIONS (Continued)

LIST OF ILLUSTRATIONS (Continued)

LIST OF TABLES

PREFACE

The Engineering Design Handbook Series of the US Army Materiel Development and Readiness Command is a coordinated series of handbooks containing basic information and fundamental data useful in the analysis, design, and development of Army materiel and systems.

This handbook treats the braking of motor vehicles such as passenger cars, trucks, and trailers. No attempt has been made to address fully the braking of specialty vehicles. However, the engineering relationships presented can be applied to the analysis of any automotive braking system, including those of tanks and special carriers.

The text is structured so that it can be used by junior engineers with a minimum of supervision provided by a senior engineer. Chapters 2, 3, 4, 5, and 6 present the analysis of brake system components and should provide sufficient detail for the computations required for the analysis of entire brake systems. Chapter 7 and those that follow address the analysis and design of the brake system of motor vehicles including the computation of partial braking performance with the brake system in a failed condition. The examples in Chapter 14 are presented in considerable detail to provide the engineer with insight into the methodology used in solving brake problems. A brief description of brake system hardware is provided in Chapter 15 for the engineer not fully familiar with the functioning of various brake system components.

This Handbook was written by Dr. Rudolf Limpert, Salt Lake City, Utah, for the Engineering Handbook Office, Research Triangle Institute, prime contractor to the US Army Materiel Development and Readiness Command. The handbook is based on lecture material and practical experience gained in industry and university research.

The Engineering Design Handbooks fall into two basic categories, those approved for release and sale, and those classified for security reasons. The US Army Materiel Development and Readiness Command policy is to release these Engineering Design Handbooks in accordance with current DOD Directive 7230.7, dated 18 September 1973. All unclassified Handbooks can be obtained from the National Technical Information Service (NTIS). Procedures for acquiring these Handbooks follow:

a. All Department of Army activities having need for the Handbooks must submit their request on an official requisition form (DA Form 17, date Jan 70) directly to:

Commander
Letterkenny Army Depot
ATTN: DRXLE-ATD
Chambersburg, PA 17201

(Requests for classified documents must be submitted, with appropriate "Need to Know" justification, to Letterkenny Army Depot.) DA activities will not requisition Handbooks for further free distribution.

b. All other requestors, DOD, Navy, Air Force, Marine Corps, nonmilitary Government agencies, contractors, private industry, individuals, universities, and others must purchase these Handbooks from:

National Technical Information Service
Department of Commerce
Springfield, VA 22151

Classified documents may be released on a "Need to Know" basis verified by an official Department of Army representative and processed from Defense Documentation Center (DDC), ATTN: DDC-TSR, Cameron Station, Alexandria, VA 22314.

Comments and suggestions on this Handbook are welcome and should be addressed to:

Commander
US Army Materiel Development and Readiness Command
Alexandria, VA 22333

(DA Forms 2028, Recommended Changes to Publications, which are available through normal publications supply channels, may be used for comments/suggestions.)

DEPARTMENT OF THE ARMY
HEADQUARTERS US ARMY MATERIEL DEVELOPMENT AND READINESS COMMAND
5001 Eisenhower Ave, Alexandria, VA 22333

DARCOM PAMPHLET
No. 706-358

1 December 1976

ENGINEERING DESIGN HANDBOOK
ANALYSIS AND DESIGN OF AUTOMOTIVE BRAKE SYSTEMS

TABLE OF CONTENTS

TABLE OF CONTENTS (Continued)

TABLE OF CONTENTS (Continued)

TABLE OF CONTENTS (Continued)

TABLE OF CONTENTS (Continued)

TABLE OF CONTENTS (Continued)

TABLE OF CONTENTS (Continued)

CHAPTER 1
INTRODUCTION

In this chapter some basic relationships are presented that show how stopping distance is dependent upon speed, deceleration, and time. The concept of tire-road friction utilization is introduced briefly. Significant problems of braking are introduced. Methods for improving braking performance are reviewed briefly.

1-0 LIST OF SYMBOLS

a = deceleration, g-units
a_m = mean deceleration, g-units
a_{max} = maximum deceleration, g-units
g = gravitational constant, ft/s²
S_a = stopping distance associated with maximum deceleration, ft
S_{actual} = actual stopping distance, ft
S_μ = minimum stopping distance, ft
t_a = application time, s
t_b = buildup time, s
V = vehicle speed, ft/s
μ = tire-road friction coefficient, d'less*

1-1 FACTORS INFLUENCING STOPPING DISTANCE

The vehicle is connected to the roadway by the traction forces produced by the tires. Consequently, only circumferential tire forces equal to or less than the product of normal force and tire-roadway friction coefficient can be transmitted by the wheels. Exceptions are provided by special designs using aerodynamic effects or rocket down thrusters resulting in greater normal forces on the tires than the vehicle weight.

This fundamental consideration yields a possible all wheels locked minimum stopping distance S_μ as given by the relationship

$$S_\mu = \frac{V^2}{2g\mu} \text{ , ft} \qquad (1\text{-}1)$$

where

g = gravitation constant, ft/s²
V = vehicle speed, ft/s
μ = tire-road friction coefficient (assumed constant in the derivation of Eq. 1-1), d'less

The stopping distance obtained from Eq. 1-1 represents the minimum possible for the tire-roadway condition specified by μ. However, this stopping distance will be achieved only when all wheels approach wheel slide conditions at the same instant. Since this is not the case for a variety of loading and road conditions, the stopping distance S_a associated with the maximum deceleration a_{max} attainable prior to wheel lockup will be given by the expression

$$S_a = \frac{V^2}{2ga_{max}} \text{ , ft} \qquad (1\text{-}2)$$

where

a_{max} = maximum deceleration, g-units

In Eq. 1-2 the deceleration is assumed to reach its maximum value at the instant of pedal application. The actual stopping distance is also affected by time delays required to apply the brakes and to build up brake force. If the application time t_a and buildup time t_b are idealized as shown in Fig. 1-1, the stopping distance associated with those time delays is given by the relationship

$$S_{actual} = \frac{V^2}{2ga_{max}} + \left(t_a + \frac{t_b}{2}\right)V - \frac{ga_{max}\,t_b^2}{24} \text{ , ft} \qquad (1\text{-}3)$$

where

t_a = application time, s
t_b = buildup time, s

The mean deceleration a_m, as indicated in Fig. 1-1, is assumed to be constant over the entire braking

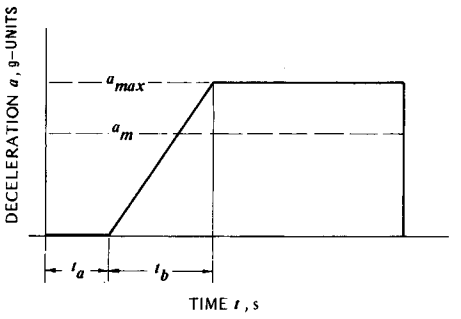

Figure 1-1. Idealized Deceleration Diagram

*d'less = dimensionless

process and may be determined from the initial velocity (ft/s), the maximum deceleration (g-units) and the application and buildup time (s) by the relationship

$$a_m = \frac{a_{max}}{1 + \frac{2ga_{max}}{V}(t_a + t_b/2)}, \text{ g-units} \quad (1\text{-}4)$$

Eq. 1-4 indicates that for equal values of a_{max}, t_a, and t_b, a_m will depend on V, i.e., for otherwise identical braking processes the mean deceleration will be different for different initial braking velocities. In Fig. 1-2 the different characteristics of a_m as a function of different velocities at the instant of brake pedal application and time delays of 0.2 s, 0.4 s, and 0.54 s are illustrated for a maximum deceleration of a_{max} = 0.81 g. A closer inspection of these curves indicates that, for example, for a velocity of 25 mph and a time delay $(t_a + t_b/2)$ of 0.4 s, the mean deceleration is only 0.50 g for a maximum deceleration of 0.81 g. For a velocity of 60 mph, the corresponding mean deceleration would be 0.65 g, indicating a significant difference in mean deceleration for otherwise identical braking conditions.

Eq. 1-3 may be rewritten in the form

$$S_{actual} = \frac{V^2}{2g\mu\left(\frac{a_{max}}{\mu}\right)} + \left[(t_a + t_b/2)\right]V - \frac{g\left(\frac{a_{max}}{\mu}\right)\mu(t_b)^2}{24}, \text{ ft} \quad (1\text{-}5)$$

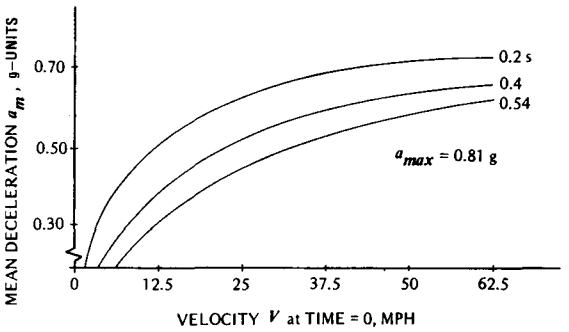

Figure 1-2. Mean Deceleration as a Function of Initial Velocity for a Maximum Deceleration of 0.81g and Different Time Delays

where the ratio a_{max}/μ expresses the extent to which the vehicle brake system uses the available tire-road friction, often termed braking efficiency. For example, when a_{max}/μ is less than unity, the available friction is not utilized fully. When a_{max}/μ is greater than unity, the wheel approaches wheel slide condition, i.e., the wheel is overbraked. Overbraking means that the ratio of actual brake force to dynamic axle load is greater than the deceleration expressed in g-units. If the required friction utilization for a particular axle is greater than the tire-road friction available, then the wheels tend to lock up and the lateral tire forces are decreased considerably. If wheel lockup is to be prevented, then the deceleration can be increased only to a level for which the friction utilization corresponds to the tire-roadway friction coefficient available. Given this condition, the vehicle deceleration in g-units is smaller than the tire-roadway friction coefficient, excluding the case in which all axles lock up simultaneously.

1-2 BRAKING DYNAMICS

A significant problem of braking arises as a result of dynamic load transfer induced by vehicle deceleration. This is especially important in the design of vehicles wherein a significant difference in center-of-gravity location exists between loaded and unloaded cases, e.g., station wagons and trucks. For example, a typical 3/4-ton pickup truck will experience a dynamic load transfer onto the front axle of approximately 500 lb for the empty case and 1000 lb for the loaded case for a deceleration of 16 ft/s^2. The static axle load distribution, the height of the center of gravity above the road surface, the wheel base, as well as the level of vehicle deceleration are factors influencing dynamic load transfer. The relationships for determining the dynamic axle loads for a variety of vehicles are presented in detail in Chapters 8 and 9. For a typical two-axle tractor coupled to a single-axle trailer, commonly termed as a 2-*S*1 combination, the dynamic axle loads as a function of vehicle deceleration are illustrated in Fig. 1-3. These curves indicate that the rear axle load of the tractor is little affected by deceleration, whereas the front axle and the trailer axle show significant changes in their respective dynamic axle loads.

For vehicles having a significant change of axle load during braking, the distribution of braking forces among the axles needs to be analyzed carefully in order to achieve acceptable braking performance on slippery and dry road surfaces for both the empty and loaded driving conditions.

Another significant problem of braking stems from the frictional character of the tire-roadway interface.

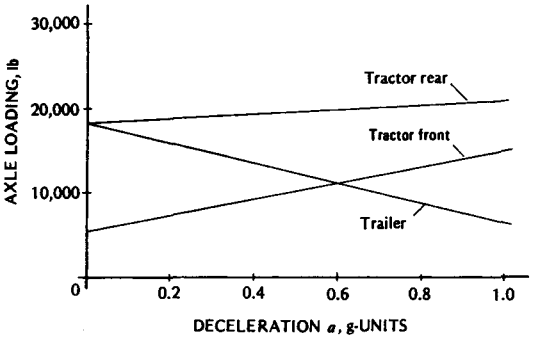

Figure 1-3. Dynamic Axle Load of a 3-Axle Tractor-Semitrailer

Fig. 6-1 shows a typical friction-slip curve for a standard automobile tire. The friction force increases with increasing values of slip up to the peak friction point. Beyond this point the friction force generally decreases with increasing slip values as indicated in Fig. 6-2 for speeds from 20 to 40 mph and in Fig. 6-3 for all speeds. This instability inherent in the friction curve calls for special provisions to use available friction near or at the peak friction value.

1-3 METHODS TO IMPROVE BRAKING CAPABILITY

Inspection of Eq. 1-5 indicates that the actual stopping distance is limited by four factors:

1. Tire-roadway friction coefficient μ
2. Efficient use of available road friction a_{max}/μ
3. Application time t_a strongly dependent upon the driver
4. Buildup time t_b strongly dependent upon the brake and suspension system.

Tire-road interface tests indicate that the tire-road friction coefficient of truck tires, both peak and sliding, is significantly less than that of passenger car tires. Carefully controlled road tests point up considerable variation in tire-road friction coefficient among the various types of truck tires. However, an overall increase in available tire-roadway friction levels will tend to decrease the stopping distance. Efficient use of the available friction requires: (a) that the distribution of braking forces among the axles is adjusted according to the normal forces on those axles during braking, and (b) that the brake torque levels are great enough for wheel slide conditions to be approached for all possible driving conditions, particularly for the loaded vehicle on dry road surfaces. Static and dynamic axle load sensitive devices have been used to distribute the braking forces according to the dynamic axle loads. Several mechanisms have been suggested for this purpose. A detailed discussion and analysis of proportional braking are presented in Chapter 9.

The time delays, especially in the case of air brakes, can be decreased significantly through the use of larger brake lines, smoother fittings, and special designs.

The instabilty inherent in the friction-slip curve of automobile tires has led to several designs using available friction. Wheel antilock systems have been developed that modulate the rotational velocity of the wheel, preventing wheel lockup. Experimental results indicate that improvements in braking performance along with a significant increase in vehicle stability are possible. In light of Eq. 1-5, this means that the vehicle brake system automatically operates near the maximum value of μ, tending to maximize the ratio a_{max}/μ and to minimize the time delay. A detailed discussion of wheel antilock braking is presented in Chapter 10.

1-4 OVERVIEW OF BRAKE SYSTEM DESIGN

The analysis and design of automotive brake systems draw mainly upon the physical laws of statics, dynamics, and heat transfer. In most cases practical engineering equations are used to determine braking performance and thermal response in a variety of braking situations.

The analysis and design of a brake system begin with an analysis of the brake torque produced by the wheel brakes. The mechanical analysis of friction brakes is presented in Chapter 2. Drum and disc brakes are considered. The drum brakes are divided into internal shoe brakes — the common drum wheel brake — and band brakes. Shoe brakes include leading, trailing, two-leading, and duo-servo brakes; these are the most common types of shoe brakes. The engineering equations presented in Chapter 2 can be modified easily to determine the torque production of other brake shoe configurations. Several band brake configurations are analyzed. Band brakes are used as emergency or parking brakes. The torque production of disc brakes is analyzed for the non-self-energizing disc brake — which is the most common one in use today — and the self-energizing disc brake. The equations presented in Chapter 2 may be used to determine the brake torque of brakes as part of a service brake system, or parking brake system.

The thermal analysis of drum and disc brakes is presented in Chapter 3. The determination of brake temperature is important for the analysis and design of a brake system. Excessive temperatures will cause

a decrease in brake torque production — commonly called brake fade — and may cause increased brake lining wear, brake system failure, and damage to adjacent components such as bearings and tires. The engineering equations used for determining brake temperatures for different braking modes are presented. Equations used for determining heat transfer coefficients for both drum and disc brakes are included. The development and computation of thermal stresses in disc brakes are discussed.

The analysis of auxiliary brakes is discussed in Chapter 4. Auxiliary brakes are provided in addition to the wheel brakes and are designed mainly to retard the vehicle in continued downhill braking operation. Engineering equations for engine braking, and hydrodynamic and electric retarders are presented.

The actual brake force production is discussed in Chapter 5. Engineering equations for pedal force, brake line pressure, brake torque, and tire braking force are presented for non-powered hydraulic brake systems, vacuum assisted brake systems, full power hydraulic brake systems, air brake systems, air-over-hydraulic brake systems, and mechanical systems. The mechanical systems are used commonly in emergency or parking brakes. Brake system design charts are provided for the size selection of vacuum assisted and full power hydraulic brakes. Engineering equations required for a brake fluid volume analysis are presented.

The effects of tire characteristics on braking are discussed in Chapter 6. The contribution of tire rolling resistance to braking are reviewed. Tire friction measurement schemes are evaluated and actual test data which are useful for the determination of tire braking forces are presented.

The effects of wheel brakes, tire characteristics, vehicle geometry, and loading conditions on braking performance are considered in Chapter 7. Presented are the five important measures or evaluation parameters of braking performance. A braking performance calculation program which permits the calculation of vehicle deceleration including tandem axle load transfer and brake fade is outlined. A step-by-step description of the operation of the computer program for a tractor-semitrailer is presented. Dynamic braking programs and tractor-trailer handling programs are reviewed. Engineering equations for the determination of aerodynamic drag and drag due to shock absorbers and a vehicle turning are presented. The braking performance calculation program of Chapter 7 is used as a basis for all braking performance calculations that follow.

The braking analysis of vehicles equipped with fixed-ratio braking systems is presented in Chapter 8. Fixed ratio brake systems are designed so that the brake force distribution — front-to-rear — does not change. Engineering equations for the optimum brake force distribution for straight line stops are presented. The important design difference for optimizing brake systems for straight and curved braking are discussed. The engineering equations required in the Braking Performance Calculation Program of Chapter 7 for a large number of solid frame and tractor-trailer combinations with and without tandem axles are presented. By the use of the Braking Performance Calculation Program the braking performance of a tandem axle truck, tractor-semitrailer (with and without tandem axles) and a tractor-semitrailer-double trailer combination are analyzed. The equations presented in Chapter 8 may be used to evaluate the braking performance of vehicles towing unbraked trailers.

The braking analysis of vehicles equipped with variable-ratio braking systems is presented in Chapter 9. A variable-ratio braking system exists when an intended variation of brake force distribution — front-to-rear — is designed into the brake system. Engineering equations for the determination of the optimum variable ratio brake force distribution for straight-line braking are presented. Design considerations for straight versus curved line braking are reviewed. Engineering equations for the design of variable-ratio brake systems for tractor-semitrailers are presented. By use of the Braking Performance Calculation Program of Chapter 7, the variable ratio braking performance of a tandem axle equipped tractor-semitrailer is analyzed.

The fundamentals involved in an analysis of wheel-antilock brake systems are presented in Chapter 10. Engineering equations associated with the locking process of a wheel are presented and general design considerations are reviewed. The functional relationships associated with air-brake-antiskid systems are presented. Vacuum-powered antiskid systems are analyzed and reasons for their below-optimum performance are noted. Experimental results and comparison of different antiskid systems are presented.

A brief introduction to the dynamic analysis of brake systems is presented in Chapter 11. A theoretical analysis of brake system dynamics requires extensive use of advanced dynamic and mathematical principles and is beyond the scope of this handbook. The discussion of hydraulic brake system dynamics is limited to an identification of critical components. For air brake systems functional relationships, developed from experiment, that determine the approximate time delay are presented. Brake response

times measured on a tractor-semitrailer combination are presented.

Analyses of brake system failures are presented in Chapter 12. The development of brake failures and their causes are noted. The engineering equations to determine the reduced braking performance associated with brake failure are presented for loss of line pressure in dual brake systems, loss of vacuum in an assisted brake system, and loss of braking effectiveness due to brake fade. Theoretical results in the form of increased pedal travels associated with loss of line pressure in dual brake systems are presented. A comparison of system complexity of various dual brake system designs is provided. The consequences of brake failure on increased stopping distance and vehicle instability are discussed.

Fundamentals involved in brake system testing are presented in Chapter 13. Major elements of a braking standard are introduced and measurement of braking performance is discussed. The effects of brake usage and brake maintenance and inspection on braking performance are discussed. Various schemes used for brake testing are evaluated. The brake test procedures developed by the US Department of Transportation relative to hydraulic and air brake systems are reviewed. The brake test procedures for military vehicles, including track vehicles, are presented in greater detail. Some details associated with brake lining laboratory testing are provided.

The concepts of brake system analysis are applied in Chapter 14 to various design examples. Specific design measures are presented and upper limits are provided. A brake system design check list is included. Design examples are a brake factor analysis, light and heavy truck brake analysis, vacuum assisted and full power hydraulic system analysis, tank disc brake analysis, and drum brake temperature analysis.

A description of automotive brake systems and their components is presented in Chapter 15. The objective is to provide a basis for the reader not familiar with brake system details to obtain sufficient information on component functions to be able to perform braking performance calculations. Chapter 15 is not intended to replace brake service manuals provided by manufacturers.

CHAPTER 2

MECHANICAL ANALYSIS OF FRICTION BRAKES

In this chapter the relationships important in the design and analysis of wheel brakes are presented. Brake shoe displacement, self-energizing and self-locking, and brake torque production of drum and disc brakes are analyzed. The problems involved in computing the brake torque developed by a nonrigid brake shoe are introduced briefly. Practical engineering equations for computing brake torque of a variety of disc and drum brakes are presented.

2-0 LIST OF SYMBOLS

a = brake dimension, in.
a_1 = brake dimension, in.
a_2 = brake dimension, in.
a' = brake dimension, in.
BF = brake factor, d'less*
BF_1 = brake factor of first shoe, d'less
BF_2 = brake factor of second shoe, d'less
b = brake dimension, in.
C_1 = factor collecting brake dimensions, d'less
C_2 = factor collecting brake dimensions, d'less
C' = constant for determining pressure distribution between lining and drum, psi
c = brake dimension, in.
D = drum diameter, in.
D_B = factor collecting brake dimensions, d'less
d = shoe tip displacement, in.
d_L = lining compression, in.
d_{Lo} = original lining thickness, in.
d_t = shoe tip displacement due to temperature, in.
dr = differential radius element, in.
E = elastic modulus of the lining material, psi
E_B = factor collecting brake dimensions, d'less
e = base of natural logarithms, d'less
F_a = application force, lb
F_{ax} = internal application force, lb
F_B = factor collecting brake dimensions, d'less
F_d = drag force, lb
F_{di} = drag force on ith segment, lb
F_{d1} = drag force on first shoe or segment, lb
F_{d2} = drag force on second shoe or segment, lb
F_{d3} = drag force on third segment, lb
F_{d4} = drag force on fourth segment, lb
F_n = normal force, lb
F_r = resultant drag force, lb
G_B = factor collecting brake dimensions, d'less
H_B = factor collecting brake dimensions, d'less
h = brake dimension, in.
i = ratio of application arms, d'less
K = application force for band brake, lb
k = constant for determining pressure distribution between lining and drum, d'less
K_1 = wear constant, s·in.^{4}/lb
K_2 = wear constant, s·in^4/lb
l = brake dimension, in.
M = moment about brake shoe pivot point, lb·in.
n = numerals 1,2,3,4, . . ., d'less
o = brake dimension, in.
p = pressure, psi
p_{mean} = mean pressure between pad and rotor, psi
$p(r)$ = pressure as function of radius, psi
R_i = inner radius of swept rotor area, in.
R_o = outer radius of swept rotor area, in.
r = brake drum radius, in.
r_d = radius, in.
r_k = disc brake dimension, in.
r_m = disc brake dimension, in.
S_B = brake sensitivity, d'less
S_1 = band force, lb
S_2 = band force, lb
v_1 = sliding speed, in./s
w_1 = wear measure, in.^{3}
α = lining angle, deg or rad
α_B = band angle, rad
α_n = brake dimension, deg
α_t = thermal expansion coefficient, in./in.·°F
α_0 = lining angle, deg
α_1 = brake dimension, deg
α_2 = brake dimension, deg
α_3 = brake dimension, deg
$\hat{\alpha}_0$ = arc of angle α_0, rad
β = brake dimension, deg
ΔBF = brake factor changes, d'less
ΔT = brake temperature increase, deg F
γ = brake dimension, deg
δ = disc brake ramp angle, deg
ϵ = strain of lining material, d'less
μ_L = lining friction coefficient, d'less

*d'less = dimensionless

$\mu_{L\infty}$ = value of lining friction coefficient causing self-locking of brake, d'less
μ_s = coefficient of friction for steel on steel, d'less
ρ = friction radius, in.
φ = shoe rotation, deg or rad
ψ = inclination angle, deg

2-1 DIFFERENT BRAKE DESIGNS

The friction brakes generally used in automotive applications can be divided into drum and disc brakes. The drum brakes subdivide into external band and internal shoe brakes. Typical shoe brakes subdivide further according to the shoe arrangement into leading-trailing, two-leading shoe, or duo-servo brakes. Drum brakes may be further divided according to the shoe abutment or anchorage into shoes supported by parallel or inclined sliding abutment, or pivoted shoes. A sliding abutment supports the tip of the shoe but permits a sliding of the shoe relative to the fixed abutment. If the abutment surface is oriented vertically, it is called parallel, otherwise inclined. The brake shoe actuation may be grouped into hydraulic wheel cylinder, wedge, cam, and mechanical linkage actuation. The disc brakes may be divided according to the caliper design into single cylinder floating caliper or opposing cylinder fixed caliper, and into fully covered disc brakes. The latter involve a circular pad covering the entire swept area of the disc brake rotor.

The basic shoe arrangements for drum brakes are illustrated in Fig. 2-1. In the case of the duo-servo brake both shoes serve the function of a leading shoe, however the individual shoes are called primary and secondary shoe. The basic caliper disc brake is shown in Fig. 2-2. The fixed and floating caliper disc brake designs are illustrated in Fig. 2-3.

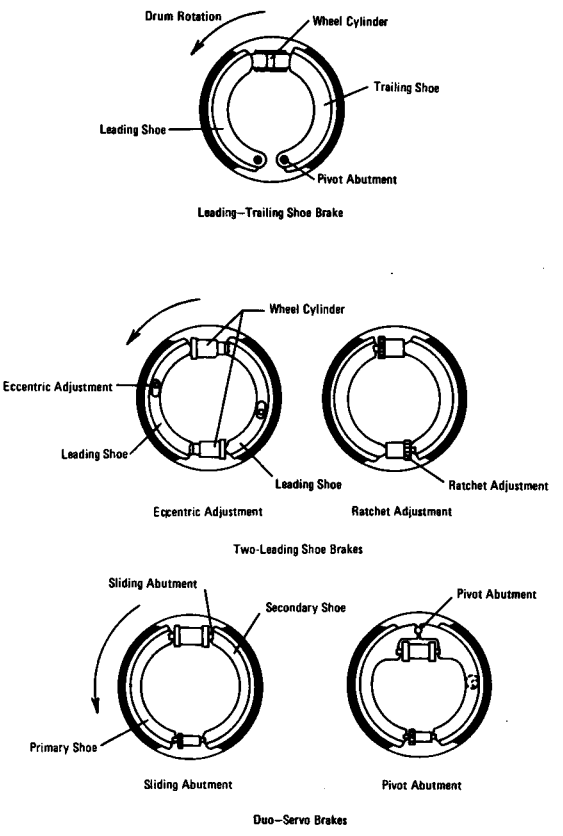

Figure 2-1. Basic Drum Brakes

2-2 BRAKE SHOE DISPLACEMENT AND APPLICATION

The shoe tip travel required to displace the brake shoe a certain distance is dependent upon a variety of factors among which are clearance, wear, lining compression, and drum distortion due to temperature and mechanical pressure. With the notation shown in Fig. 2-4, the shoe tip displacement d for "cold" brakes may be computed with sufficient accuracy by (Ref. 1)

$$d = 0.1\ h/a\ , \text{ in.} \qquad (2\text{-}1)$$

where
a = brake dimension, in.
h = brake dimension, in.

Drum as well as brake shoe distortion have not been incorporated in this analysis and should be considered by allowing an increased shoe displacement. Shoe tip displacement d_t resulting from a temperature increase ΔT may be approximated by

$$d_t = 0.5\,(h/a)\,\alpha_t\,D\,\Delta T\ , \text{ in.} \qquad (2\text{-}2)$$

where
D = drum diameter, in.
α_t = thermal expansion coefficient, in./in.·°F
ΔT = brake temperature increase, deg F

Application of Eqs. 2-1 and 2-2 to a brake with D = 10 in., h/a = 2.0, $\alpha_t = 6.6 \times 10^{-6}$ in./in.·°F, and ΔT = 700 deg F yields a total shoe tip displacement $(d + d_t)$ of 0.25 in.

For disc brakes the wheel cylinder piston travel required to cover clearance, caliper distortion, pad compression, and wear is approximately equal to 0.024 to 0.028 in.

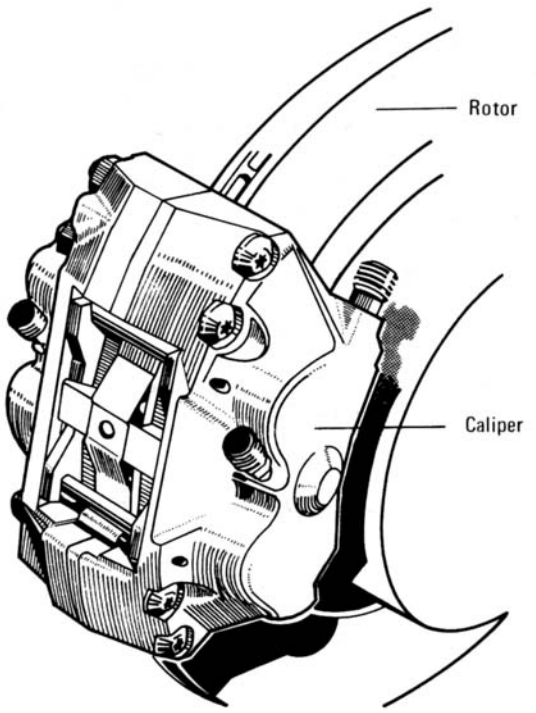

Figure 2-2. Disc Brake

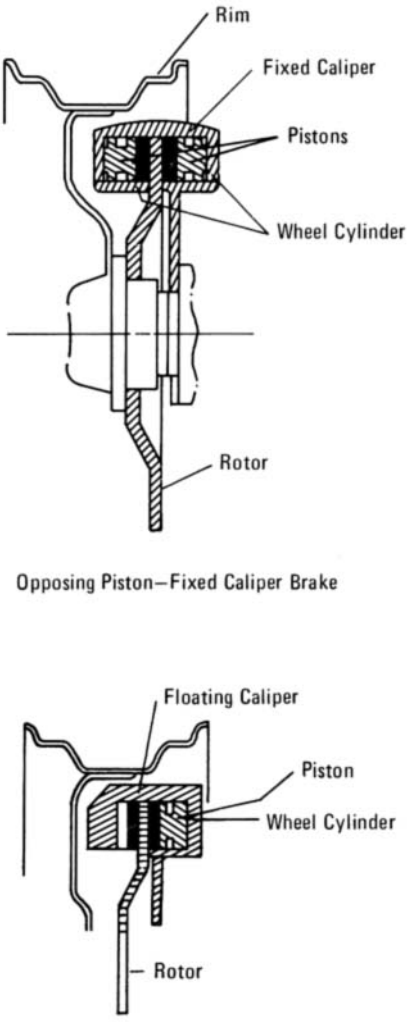

Figure 2-3. Basic Disc Brakes

2-3 BRAKE SHOE ADJUSTMENT

In order to keep the clearance between brake lining and drum at a minimum, adjustment becomes necessary as the linings wear. To accomplish this, either manual or automatic adjustment mechanisms are provided.

Manual adjusters should be adjusted only when the brakes are cold and the parking brake is released. The adjustment mechanism may be located on the shoe. At the wheel cylinder (see Fig. 15-6), or at the fixed or floating shoe abutment (see Fig. 15-9). In the case of the fixed abutment brake, two adjuster slots are provided in the backing plate; in the case of a floating abutment brake, only one slot is provided.

Automatic adjusters use the reverse braking action as input for brake adjustment. In one application, friction washers are used to produce the adjustment. The friction force must be greater than the shoe return spring force. Another ratchet type mechanism consists of a threaded eye-bolt and a split sleeve with corresponding thread fixed to the brake shoe. The adjustment is produced when the split sleeve springs into the next thread. The ratchet adjuster has also been designed to fit into the wheel cylinder. The design is such that each wheel cylinder piston adjusts independently of the other.

Brake adjustment in the case of disc brakes is accomplished automatically by the wheel cylinder piston seal. The seal is designed so that in the event of a piston displacement, it distorts elastically for about 0.006 in. Provided no pad wear has occurred, the piston seal pulls the piston back on releasing the brake line pressure, as shown in Fig. 2-5. If the clearance between pad and rotor becomes greater due to wear, the piston travels in excess of 0.006 in., and the

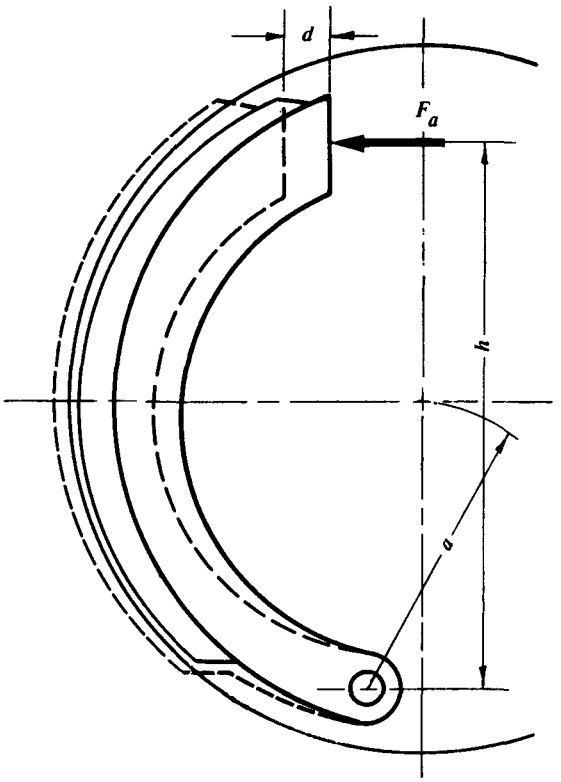

Figure 2-4. Brake Shoe Geometry

piston seal preload is overcome, forcing the piston closer to the rotor.

2-4 TORQUE ANALYSIS OF FRICTION BRAKES

Some fundamentals associated with the torque analysis of drum and disc brakes will be discussed next. In later paragraphs, only the equations usable for predicting the brake torque of various drum and disc brakes will be presented.

2-4.1 SELF-ENERGIZING AND SELF-LOCKING

In order to demonstrate the self-energizing effect of a brake shoe a more detailed analysis is carried out. The normal force between drum and brake lining segment as a result of the application force F_a for the brake shown in Fig. 2-6 is given by $F_a\ h/b$. This normal force causes a frictional force on the drum sliding surface of the magnitude $(F_a\ h/b)\ \mu_L$, where the friction coefficient between drum and brake lining segment is designated by μ_L, and b and h are brake dimensions.

The friction force causes a moment M about the pivot point A of magnitude $M = (F_a\ h/b)\mu_L c$; c is another brake dimension. This moment can only be counteracted at the contact area between brake lining segment and drum by a force of magnitude $[(F_a\ h/b) \times \mu_L]\ (c/b)$. This additional force again results in a friction force, producing an additional moment, and the cycle repeats itself. This phenomenon of increased brake effectiveness observed in the case of rotating the brake shoe in the direction of drum rotation is called the self-energizing effect of drum brakes, and the shoe is termed "leading shoe".

The summation of all friction forces as a result of the self-energizing may be expressed in terms of a series of the form (Ref. 1):

$$F_d = F_a\left(\frac{h}{b}\right)\mu_L\left[1 + \left(\mu_L\frac{c}{b}\right) + \left(\mu_L\frac{c}{b}\right)^2 + \left(\mu_L\frac{c}{b}\right)^3 + \cdots\right], \text{lb} \qquad (2\text{-}3)$$

The summation of which is given by

$$F_d = F_a\left(\frac{h}{b}\right)\mu_L\left[\frac{1 - \left(\mu_L\frac{c}{b}\right)^n}{1 - \mu_L\frac{c}{b}}\right], \text{ lb}$$

where

F_d = drag force, lb

n = numerals 1,2,3,4, . . ., d'less

A further simplification may be introduced by considering that $\mu_L c/b$ is less than unity for all practical purposes, causing the numerator to approach unity as n approaches infinity.

Hence,

$$F_d = F_a\left(\frac{h}{b}\right)\left(\frac{\mu_L}{1 - \mu_L\frac{c}{b}}\right), \text{ lb} \qquad (2\text{-}4)$$

The brake torque produced by the shoe is determined from the product of $F_d\ r$, where r = drum radius.

Eq. 2-4 may also be derived from a moment equilibrium consideration about point A, i.e.,

$$F_a h + F_d c - \frac{F_d}{\mu_L} b = 0 \ , \text{ lb·in.} \qquad (2\text{-}5)$$

from which Eq. 2-4 follows directly.

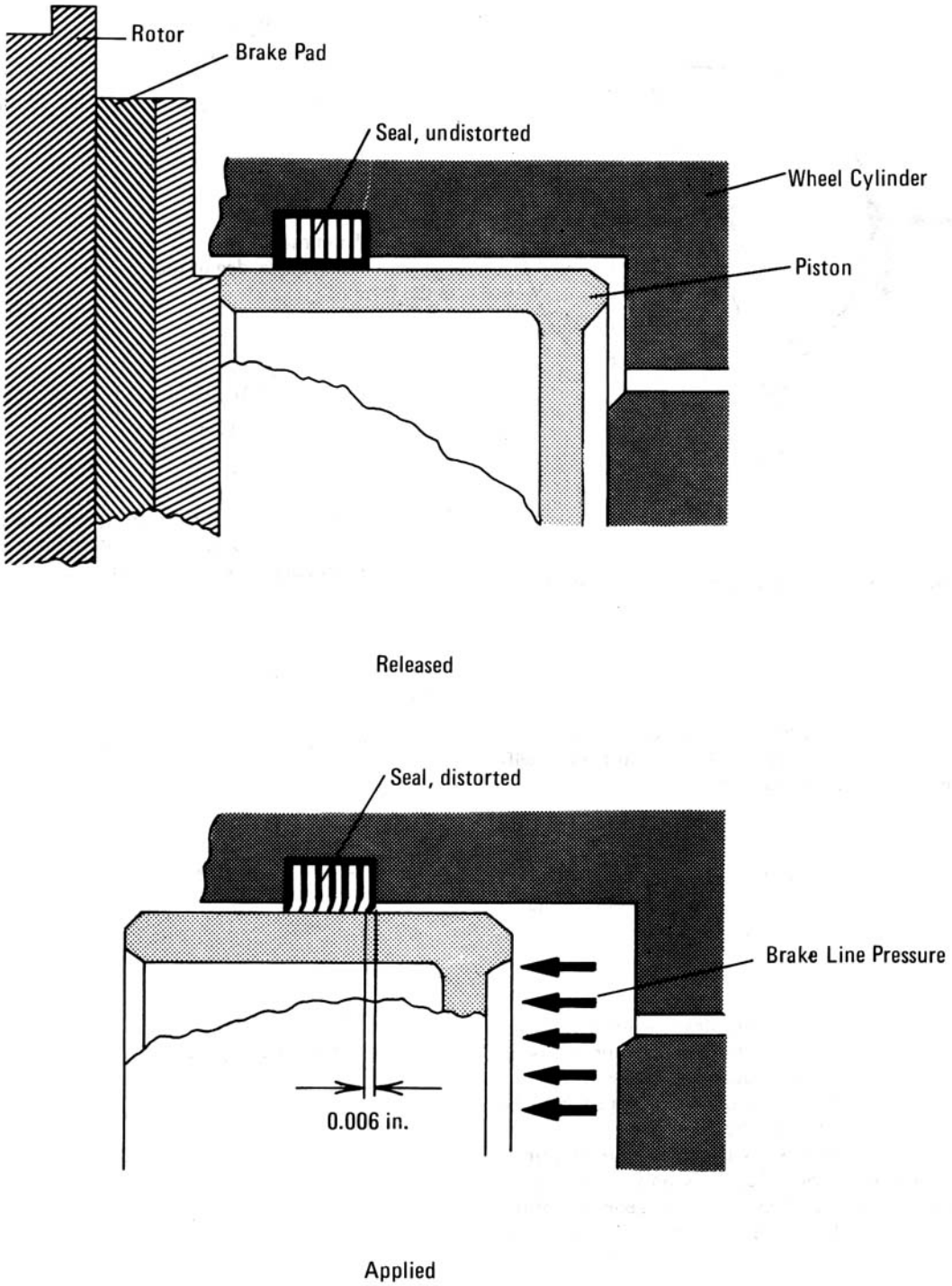

Figure 2-5. Disc Brake Clearance Adjustment

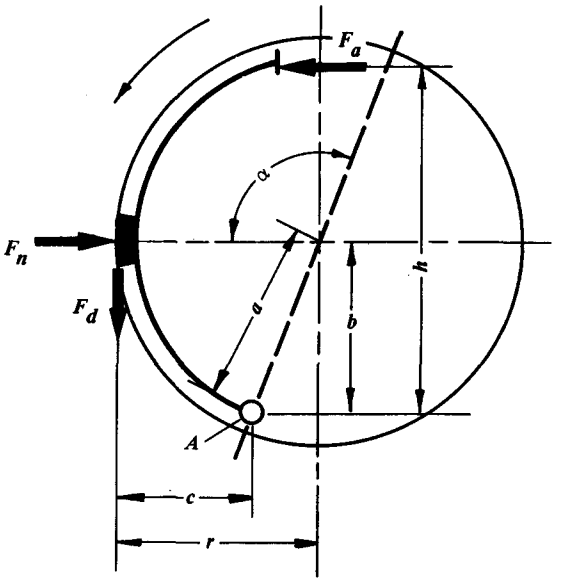

Figure 2-6. Self-Energizing in a Drum Brake

In the case of a reversal of rotation, the brake becomes a "trailing shoe" brake resulting in a self-deenergizing effect described by

$$F_d = F_a\left(\frac{h}{b}\right)\left(\frac{\mu_L}{1 + \mu_L\frac{c}{b}}\right), \text{ lb} \qquad (2\text{-}6)$$

Inspection of Eq. 2-4 indicates that for a finite application force F_a, the drum drag F_d approaches infinity when the denominator approaches zero, i.e., when the lining friction coefficient μ_L approaches the magnitude expressed by the ratio b/c. Under these conditions the brake will self-lock in spite of a finite application force. Self-locking is only a function of the lining friction coefficient and the geometry of the brake, and should not be confused with wheel lock-up found to occur when increased brake line pressure causes the brake force to exceed the tire-roadway traction limit.

If $\mu_{L\infty}$ designates the lining friction resulting in self-locking, then with the terminology of Fig. 2-6, Eq. 2-4 may be rewritten with

$$\mu_{L\infty} = \frac{b}{c} = \frac{a\sin\alpha}{r + a\cos\alpha} = \frac{\sin\alpha}{\frac{r}{a} + \cos\alpha}, \text{ d'less} \qquad (2\text{-}7)$$

where

r = drum radius, in.

α = lining angle, deg or rad

in the form of

$$F_d = F_a\left(\frac{h}{b}\right)\left(\frac{\mu_L}{1 - \frac{\mu_L}{\mu_{L\infty}}}\right), \text{ lb} \qquad (2\text{-}8)$$

If furthermore, $2h/b = 2h/(a\sin\alpha)$ is introduced, then the ratio of drum drag to application force in the case of the leading shoe may be expressed by

$$\frac{F_d}{F_a} = \frac{\mu_L\left(\frac{h}{a}\right)\frac{1}{\sin\alpha}}{1 - \mu_L\left(\frac{1}{\sin\alpha}\right)\left(\frac{r}{a} + \cos\alpha\right)} = \frac{\mu_L\left(\frac{C_1}{2}\right)}{1 - \frac{\mu_L}{\mu_{L\infty}}} \text{ d'less} \qquad (2\text{-}9)$$

where

$C_1 = 2h/(a\sin\alpha)$

Similarly, for the trailing shoe

$$\frac{F_d}{F_a} = \frac{\mu_L\left(\frac{C_1}{2}\right)}{1 + \frac{\mu_L}{\mu_{L\infty}}}, \text{ d'less} \qquad (2\text{-}10)$$

2-4.2 LEADING AND TRAILING SHOE

For a brake of typical design with longer linings, the entire lining may be considered to consist of

several small brake lining segments as shown in Fig. 2-7. Each individual lining segment produces a friction force F_{di}. The algebraic summation of all individual contributions F_{di} results in the total drum drag force F_d.

For purposes of computation, all individual friction forces F_{di} are geometrically collected into one resultant F_r acting a distance ρ (the friction radius) from the center point of the brake shoe. Since the condition $F_d r = F_r \rho$ has to be satisfied, it follows that ρ exceeds r, since the geometrical summation of F_{di} is less than the algebraic summation of F_{di}. If the normal force between lining and drum is located perpendicular to F_r and under the angle α_n to a straight line connecting shoe pivot point and brake center, then an analysis identical to that of a single brake lining segment will yield a similar brake force relationship. In this case, F_r replaces F_d, ρ replaces r, and α_n replaces α.

Hence, from Eq. 2-9 for the leading shoe

$$\frac{F_r}{F_a} = \frac{\mu_L\left(\frac{h}{a}\right)\left(\frac{1}{\sin\alpha_n}\right)}{1 - \mu_L\left(\frac{1}{\sin\alpha_n}\right)\left(\frac{\rho}{a} + \cos\alpha_n\right)}, \text{ d'less} \quad (2\text{-}11)$$

Using the equation $F_r = F_d\,(r/\rho)$, the following expression results

$$\frac{F_d}{F_a} = \frac{\mu_L\left(\frac{h}{a}\right)\left(\frac{\rho/r}{\sin\alpha_n}\right)}{1 - \mu_L\left(\frac{\rho/r}{\sin\alpha_n}\right)\left(\frac{r}{a} + \frac{\cos\alpha_n}{\rho/r}\right)}, \text{ d'less} \quad (2\text{-}12)$$

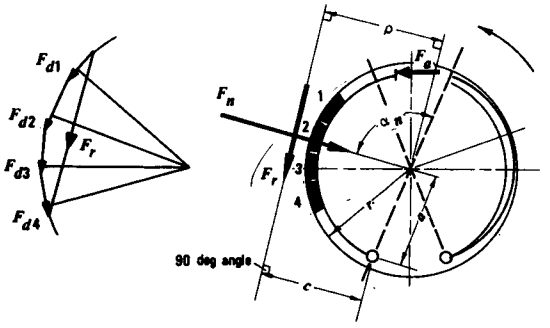

Figure 2-7. Leading Shoe Analysis

Eq. 2-12 may be rewritten in the form

$$\frac{F_d}{F_a} = \frac{\mu_L\left(\frac{C_2}{2}\right)}{1 - \frac{\mu_L}{\mu_{L\infty}}}, \text{ d'less} \quad (2\text{-}13)$$

where

$$C_2 = 2\left(\frac{h}{a}\right)\frac{\rho/r}{\sin\alpha_n}, \text{ d'less} \quad (2\text{-}14)$$

$$\mu_{L\infty} = \frac{1}{\frac{\rho/r}{\sin\alpha_n}\left(\frac{r}{a} + \frac{\cos\alpha_n}{\rho/r}\right)}, \text{ d'less} \quad (2\text{-}15)$$

The relationship for the trailing shoe is

$$\frac{F_d}{F_a} = \frac{\mu_L\left(\frac{C_2}{2}\right)}{1 + \frac{\mu_L}{\mu_{L\infty}}}, \text{ d'less} \quad (2\text{-}16)$$

Detailed mathematical analyses show that the ratio of F_d to F_r and ρ to r may be found from geometrical considerations and the pressure distribution along the brake lining. Since the mathematics involved in deriving the ratio ρ/r is rather complicated, only the final expressions for computing the shoe drag are presented in this chapter. In the next paragraphs some fundamentals relating to pressure distribution and lining wear are discussed.

2-4.3 PRESSURE DISTRIBUTION ALONG BRAKE LINING

If it is assumed that the brake drum and brake shoe are rigid and that all deformation occurs within the lining material, then the compression d_L of the lining as a result of the shoe displacement against the drum measured by the angle rotation φ is related to the strain ϵ and the original lining thickness d_{Lo} by

$$\epsilon = d_L/d_{Lo}, \text{ d'less} \quad (2\text{-}17)$$

where

d_L = lining compression, in.
d_{Lo} = original lining thickness, in.

Tests have shown that the pressure p is approximately proportional to strain, i.e., Hooke's Law is valid provided excessive mean pressures are avoided.

The actual pressure distribution between lining and drum is bound by functional relationships of the form

$$p = E\epsilon = E\frac{a\varphi}{d_{Lo}}\sin\alpha \text{ , psi} \quad (2\text{-}18)$$

and

$$p = c'\{\exp[(k\,a\,\varphi\,\sin\alpha)/d_{Lo}] - 1\} \text{ , psi} \quad (2\text{-}19)$$

where

a = brake dimension, in.
c' = constant for determining pressure distribution between lining and drum, psi
E = elastic modulus of the lining, psi
k = constant for determining pressure distribution between lining and drum, d'less
α = lining angle, deg
φ = shoe rotation, rad
ϵ = strain of lining material, d'less

The experimental results obtained for several lining materials with different elastic behaviors are presented in Fig. 2-8 where the pressure distribution over the lining angle is shown (Ref. 1). Inspection of Fig. 2-8 indicates that constant c' varies between 2.94 and 73.5 psi for the linings tested. The information contained in Fig. 2-8 may be used to compute the approximate strain values. At a lining angle of 50 deg the strain ϵ of the soft lining is approximately 0.05, that of the hard lining 0.005. The corresponding values of the elastic modulus are 2,400 and 17,500 psi for the soft and hard lining, respectively.

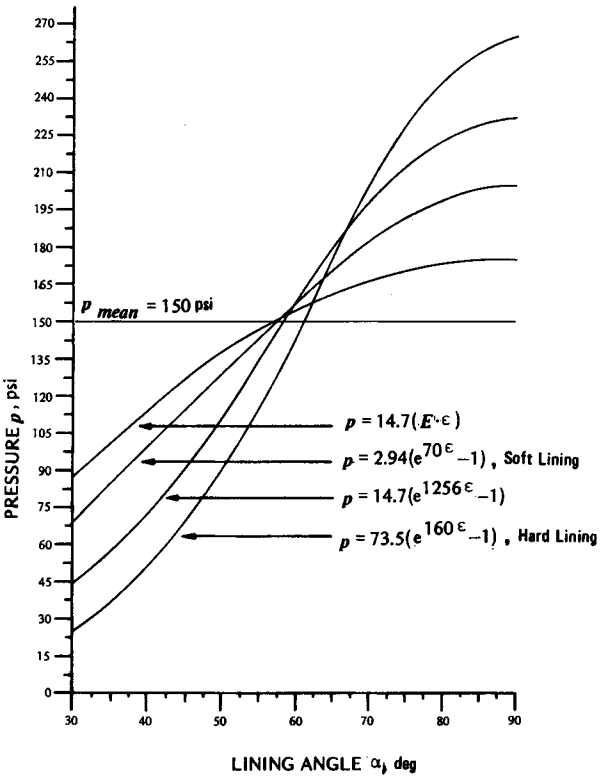

Figure 2-8. Measured Pressure Distribution Over Lining Angle α for Different Linings

2-4.4 LINING WEAR AND PRESSURE DISTRIBUTION

The lining material is in all practical applications the wear component of the brake, i.e., the wear of the drum or disc is negligible compared with the lining wear. If the wear behavior of the lining material is known, then it becomes possible to determine the pressure distribution along the lining. A detailed analysis is beyond the scope of this handbook, and only some of the important results obtained for a pivoted leading shoe are presented. A wear relationship w_1 of the form

$$w_1 = k_1\,\mu_L\,p\,v_1 \text{ , in.}^3 \quad (2\text{-}20)$$

is assumed,
where

k_1 = wear constant, s·in.^{4}/lb
p = pressure, psi
v_1 = sliding speed, in./s
μ_L = lining drum friction coefficient, d'less

With Eq. 2-20 a sinusoidal pressure distribution may be found to exist along the brake lining.

The pressure distributions obtained analytically after successive brake applications, and thus wear, are presented in Fig. 2-9. Inspection of Fig. 2-9 indicates that a sinusoidal distribution $p = 132.2 \sin\alpha$ is developed after 11 brake applications.

For a wear relationship of the form

$$W = k_2\,\mu_L\,p^2\,v_1^2 \text{ , in.}^3 \quad (2\text{-}21)$$

where

k_2 = wear constant, s^2·in.^{5}/lb

a pressure distribution of the form p = constant $\times \sqrt{\sin\alpha}$ is obtained. This pressure distribution is illustrated also in Fig. 2-9.

Inspection of the curves in Fig. 2-9 indicates that new brakes will have a different pressure distribution than brakes in service. For an exact prediction of pressure distribution, hence brake torque, a knowledge of both the wear relationship and the elastic behavior of the lining material is essential. It is a known

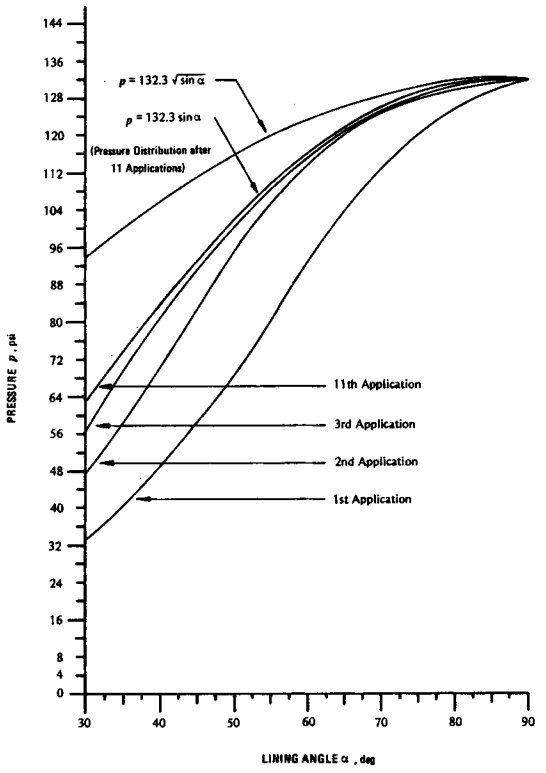

Figure 2-9. Computed Pressure Distribution as a Function of Wear After Successive Brake Applications

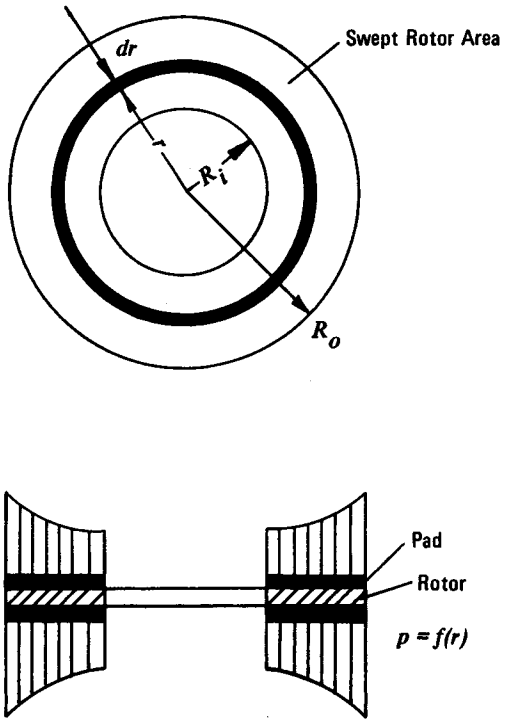

Figure 2-10. Pressure Distribution on a Disc Brake

fact that the pressure distribution changes during the run-in period (Refs. 2 and 3). Burnishing procedures subject the vehicle brake system to a series of brake applications during which the pressure distribution along the lining tends to approach run-in condition.

For disc brakes, the brake torque production depends upon the pressure distribution between pad and rotor as indicated in Fig. 2-10. The mean pressure p_{mean} may be computed from

$$p_{mean} = \frac{\int_{R_i}^{R_o} p(r)\, r\, dr}{\int_{R_i}^{R_o} r\, dr}, \text{ psi} \qquad (2\text{-}22)$$

where

dr = differential radius element, in.
$p(r)$ = pressure distribution as a function of radius, psi
R_i = inner radius of swept rotor area, in.
R_o = outer radius of swept rotor area, in.
r_d = radius, in.

The pressure distribution is determined by the elastic and wear characteristics of pad and rotor. In most cases it is assumed, however, that either the pressure (p = constant) or the product of pressure and sliding speed relative velocity is constant over the contact area ($p\, v_1$ = constant). Numerical evaluation of typical disc brakes has shown that the condition p = constant, which is applicable for new brakes, results in a mean effective radius and hence brake torque which is approximately 2 to 3% greater than is obtained with a $p\, v_1$ = constant condition, which is applicable for brakes in the burnished or run-in condition. For most practical cases the pressure therefore may be assumed to be inversely proportional to the radius. The mean effective radius may be assumed to be equal to the average value between outer and inner radius.

2-4.5 BRAKE FACTOR AND BRAKE SENSITIVITY

The brake factor *BF* is defined as the ratio of drum or rotor drag force to the actuating force of one shoe or pad. The brake factor of the entire brake consists of the summation of all brake factors associated with the individual brake shoes of the brake. The brake

factor may be considered as the gain of the brake. For example, for a leading-trailing shoe brake as illustrated in Fig. 2-6 the brake factor of the leading shoe is given by (see Eq. 2-13).

$$BF_1 = \frac{F_{d1}}{F_a} = \frac{\mu_L \left(\frac{C_2}{2}\right)}{1 - \frac{\mu_L}{\mu_{L\infty}}} \text{ , d'less}$$

and that of the trailing shoe by (see Eq. 2-16)

$$BF_2 = \frac{F_{d2}}{F_a} = \frac{\mu_L \left(\frac{C_2}{2}\right)}{1 + \frac{\mu_L}{\mu_{L\infty}}} \text{ , d'less}$$

and consequently, the brake factor of the entire brake is given by

$$BF = \frac{F_{d1} + F_{d2}}{F_a} = \frac{\mu_L C_2}{1 - \left(\frac{\mu_L}{\mu_{L\infty}}\right)^2} \text{ , d'less} \quad (2\text{-}23)$$

Since the brake factor is only a function of the lining friction coefficient for a given brake geometry, it seems advisable to determine the changes in brake factor associated with changes in lining friction coefficient. Changes in lining friction coefficient will occur as a result of changes in, e.g., temperature, speed, pressure, and moisture encountered during braking. The slope of the brake factor-friction coefficient curve may be used as a sensitivity indicator for the brake. The slope can be expressed in the form of brake sensitivity $S_B = d(BF)/d(\mu_L)$. For the leading-trailing shoe brake this results in

$$S_B = \frac{C_2 \left[1 + \left(\frac{\mu_L}{\mu_{L\infty}}\right)^2\right]}{\left[1 - \left(\frac{\mu_L}{\mu_{L\infty}}\right)^2\right]^2} \text{ , d'less} \quad (2\text{-}24)$$

For most practical purposes the brake sensitivity may be determined from the brake factor curve by piece-wise differentiation.

The brake factor of a brake is defined as the ratio of the sum of all tangential forces acting on the friction surface; i.e., the drag on the drum or disc, divided by the actuating force of one shoe or pad. In the analysis for computing the brake factor it is assumed that brake drum, shoe, and shoe pivot are rigid, and that the motion of the lining is constrained to the cylindrical shape of the drum. All equations given in the remainder of this chapter determine the brake factor as a function of brake geometry and lining friction only. Although drum distortions have been computed analytically and measured, the influence of distortion has not yet been incorporated into the brake factor analysis.

Current design practice yields brake factor and sensitivity values (approximate values for lining coefficient of friction of 0.35 and changes in μ_L of ± 0.05) as tabulated in Table 2-1.

For purposes of brake factor calculations, drum brakes can be grouped according to design (a) by brake shoe configuration, i.e., duo-servo, two-leading shoe, and one leading-one trailing shoe brakes; (b) by the way the brake torque is transmitted to the backing plate into pivot or sliding (parallel or inclined) abutments; and (c) by internal shoe or external band arrangement.

2-4.6 BRAKE FACTOR OF A CALIPER DISC BRAKE

For a nonself-energizing caliper disc brake, the brake factor BF is equal to

$$BF = \frac{F_d}{F_a} = 2\mu_L \text{ , d'less} \quad (2\text{-}25)$$

where

μ_L = lining coefficient of friction, d'less

The sensitivity S_B is constant with $S_B = 2$.

TABLE 2-1
DISC AND DRUM BRAKE COMPARISON

	BF	$\Delta BF(\%)$	S_B
disc brake	0.7	+14 to −14	2
leading/trailing shoe brake	2.0 to 2.8	+26 to −21	8
two-leading shoe brake	2.5 to 3.5	+36 to −28	12
duo-servo brake	3.0 to 7.0	+51 to −33	4

2-4.7 BRAKE FACTOR OF A LEADING-TRAILING SHOE BRAKE WITH PIVOT ON EACH SHOE

The schematic of one shoe is illustrated in Fig. 2-11. The total brake factor is the summation of the individual brake factors of the leading shoe BF_1 and of the trailing shoe BF_2.

$$BF = BF_1 + BF_2 = \frac{F_{d1}}{F_a} + \frac{F_{d2}}{F_a}, \text{ d'less (2-26)}$$

The brake factor of the leading shoe is given by the following expression using the minus sign in the denominator:

$$BF_1 = \frac{F_{d1}}{F_a}$$

$$= \mu_L\left(\frac{h}{r}\right)$$

$$\div\left[\left(\frac{a'}{r}\right)\left(\frac{\hat{\alpha}_0 - \sin\alpha_0 \cos\alpha_3}{4 \sin\frac{\alpha_0}{2}\sin\frac{\alpha_3}{2}}\right) \pm \mu_L\left(1 + \frac{a'}{r}\cos\frac{\alpha_0}{2}\cos\frac{\alpha_3}{2}\right)\right], \text{ d'less (2-27)}$$

where

a' = brake dimension, in.

$\hat{\alpha}_0$ = arc of the angle α_0, rad

$\alpha_3 = \alpha_1 + \alpha_2$, deg (as defined in Fig. 2-11)

The brake factor of the trailing shoe is determined by using the plus sign in Eq. 2-27. The dimension a' has a major effect on the brake factor of the leading-trailing shoe brake for a given lining coefficient of friction as illustrated in Fig. 2-12.

2-4.8 BRAKE FACTOR OF A TWO-LEADING SHOE BRAKE WITH PIVOT ON EACH SHOE

For this case, the brake factor can simply be determined from

$$BF = 2\,BF_1 = 2\left(\frac{F_{d1}}{F_a}\right), \text{ d'less} \quad (2\text{-}28)$$

with F_{d1}/F_a determined from Eq. 2-27 using the minus sign in the denominator.

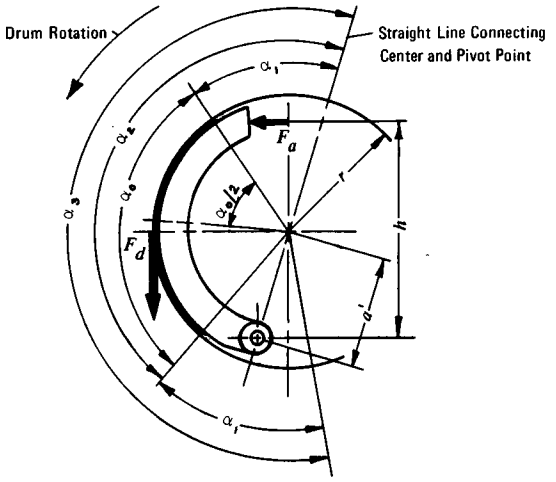

Figure 2-11. Leading Shoe With Pivot

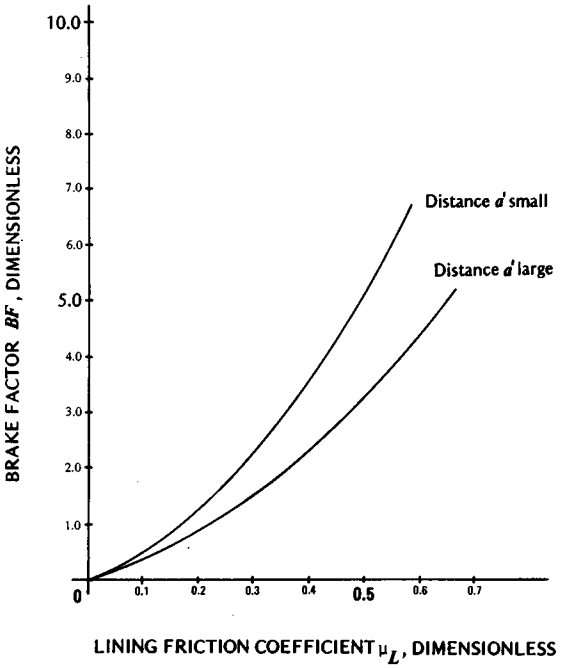

Figure 2-12. Brake Factor Curves for Different Lengths of Distance a'

2-4.9 BRAKE FACTOR OF A LEADING-TRAILING SHOE BRAKE WITH PARALLEL SLIDING ABUTMENT

The schematic of one shoe is illustrated in Fig. 2-13. The brake factor *BF* is determined by Eq. 2-26. The individual brake factors are:

for the leading shoe

$$BF_1 = \frac{F_{d1}}{F_a} = \left(\frac{\mu_L D_B + \mu_L^2 E_B}{F_B - \mu_L G_B + \mu_L^2 H_B}\right)_1 \text{, d'less(2-29a)}$$

for the trailing shoe

$$BF_2 = \frac{F_{d2}}{F_a} = \left(\frac{\mu_L D_B - \mu_L^2 E_B}{F_B + \mu_L G_B + \mu_L^2 H_B}\right)_2 \text{, d'less(2-29b)}$$

where

$$D_B = \left[\frac{c}{r} + \frac{a}{r} + \mu_s\left(\frac{o}{r}\right)\right]\cos\beta + \mu_s\left(\frac{c}{r}\right)\sin\beta \text{ , d'less}$$

$$E_B = \mu_s\left(\frac{c}{r}\right)\cos\beta - \left[\frac{c}{r} + \frac{a}{r} + \mu_s\left(\frac{o}{r}\right)\right]\sin\beta \text{ , d'less}$$

$$F_B = \frac{\hat{\alpha}_0 + \sin\alpha_0}{4\sin(\alpha_0/2)}\left[\frac{a}{r} + \mu_s\left(\frac{o}{r}\right)\right] \text{ , d'less}$$

$$G_B = \cos\beta + \mu_s \sin\beta \text{ , d'less}$$

$$H_B = F_B - (\mu_s\cos\beta - \sin\beta) \text{ , d'less}$$

The value of μ_s is associated with the sliding friction between the tip of the shoe and the abutment. For steel on steel $\mu_s \approx 0.2$ to 0.3. The value of the angle β is positive when $\gamma > \alpha_0/2$, and negative when $\gamma < \alpha_0/2$.

2-4.10 BRAKE FACTOR OF A TWO-LEADING SHOE BRAKE WITH PARALLEL SLIDING ABUTMENT

The brake factor can be determined from the general expression for two-leading shoe brakes, Eq. 2-28, with the brake factor of one shoe determined by Eq. 2-29a.

2-4.11 BRAKE FACTOR OF A LEADING-TRAILING SHOE BRAKE WITH INCLINED ABUTMENT

A schematic of a typical shoe is illustrated in Fig. 2-14. The total brake factor may be determined from Eq. 2-26, Eqs. 2-29a and 2-29b with the abutment friction coefficient μ_s replaced by $(\mu_s + \tan\psi)$ where ψ is the inclination angle of the abutment in deg.

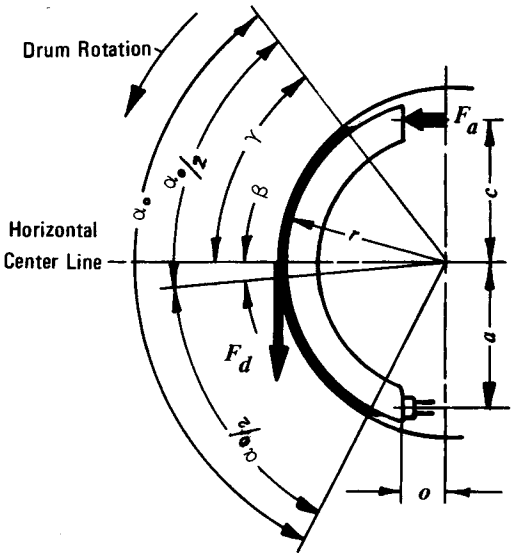

Figure 2-13. Leading Shoe With Parallel Sliding Abutment

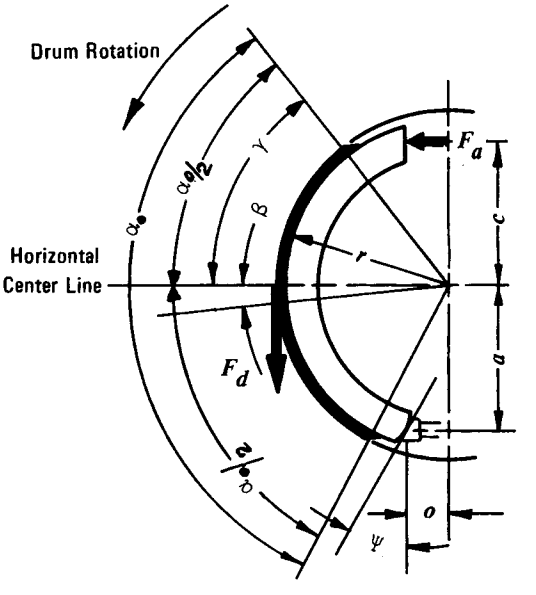

Figure 2-14. Leading Shoe With Inclined Abutment

2-4.12 BRAKE FACTOR OF A TWO-LEADING SHOE BRAKE WITH INCLINED ABUTMENT

The total brake factor may be determined from Eq. 2-28 and Eq. 2-29a with μ_s replaced by $(\mu_s + \tan \psi)$ where ψ is the inclination angle in deg.

2-4.13 BRAKE FACTOR OF A DUO-SERVO BRAKE WITH SLIDING ABUTMENT

The schematic of the brake is illustrated in Fig. 2-15. The relationships shown earlier can be used to determine the brake factor. In this case, however, the internal application force F_{ax} of the primary shoe designated by 1, becomes the actuation force of the secondary shoe designated by 2.

The total brake factor BF is determined by

$$BF = BF_1 + BF_2 = \frac{F_{d1}}{F_a} + \frac{F_{d2}}{F_a}$$

$$= \frac{F_{d1}}{F_a} + \left(\frac{F_{d2}}{F_{ax}}\right)\left(\frac{F_{ax}}{F_a}\right), \text{ d'less} \qquad (2\text{-}30)$$

where

$$\frac{F_{d1}}{F_a} = \frac{\mu_L D_B + \mu_L^2 E_B}{F_B - \mu_L G_B + \mu_L^2 H_B}, \text{ d'less}$$

$$\frac{F_{d2}}{F_{ax}} = \frac{\mu_L D_B + \mu_L^2 E_B}{F_B - \mu_L G_B + \mu_L^2 E_B}, \text{ d'less}$$

The relative support force F_{ax}/F_a is given by

$$\frac{F_{ax}}{F_a} = \frac{c}{a} + \left(\frac{F_{d1}}{F_a}\right)\left(\frac{r}{a}\right), \text{ d'less} \qquad (2\text{-}31)$$

2-4.14 BRAKE FACTOR OF A DUO-SERVO BRAKE WITH PIVOT SUPPORT

A schematic of the brake is shown in Fig. 2-16. The total brake factor can be determined from Eqs. 2-30 and 2-31, with the brake factor of the primary shoe given by Eq. 2-29a and the brake factor F_{d2}/F_{ax} of the secondary shoe given by Eq. 2-27; the minus sign is used in the denominator.

2-5 EFFECT OF SHOE AND DRUM STIFFNESS ON BRAKE TORQUE

The derivation of the brake factor in the previous paragraphs was based on a rigid shoe and drum. All elastic deformation was assumed to occur in the lining material. Test results show a significant effect of brake shoe elasticity on brake torque. Experimental data obtained for the "rigid" and "elastic" brake shoe geometries shown in Fig. 2-17 are presented in Fig. 2-18 (Ref. 4). Although both shoes exhibit identical dimensions, their actual brake force production is different. Reasons for this difference are found in the change in pressure distribution between lining and drum in the case of the elastic brake

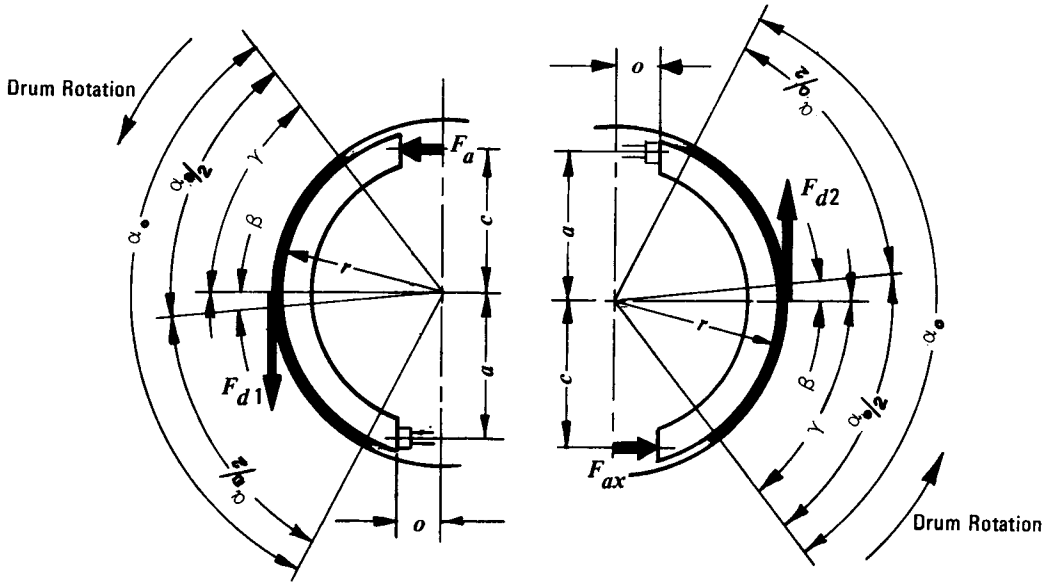

Figure 2-15. Duo-Servo Brake With Sliding Abutment

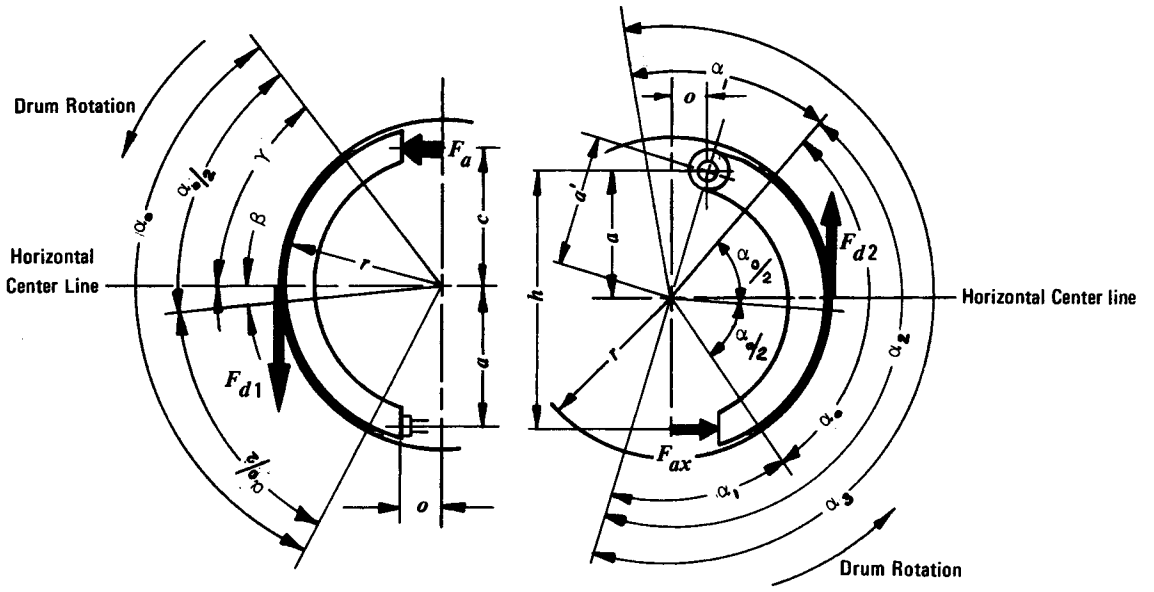

Figure 2-16. Duo-Servo Brake With Pivot

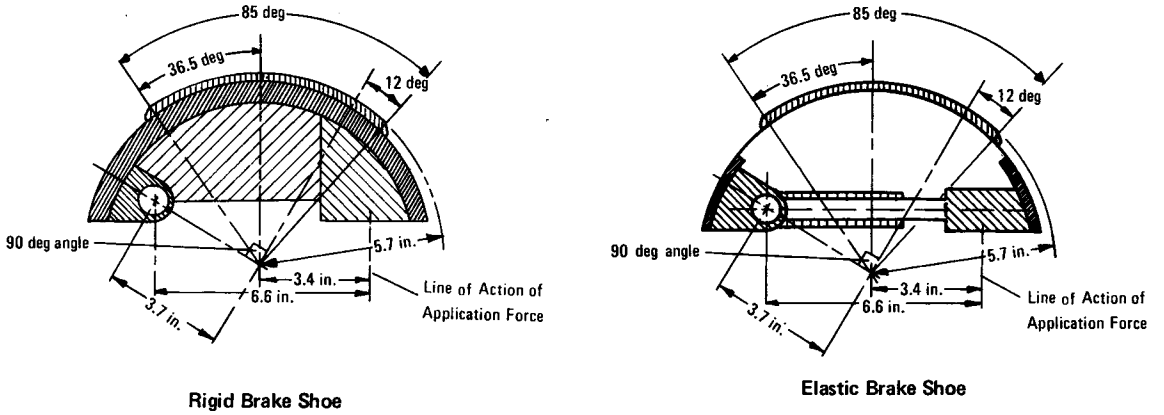

Figure 2-17. Brake Shoes of Different Stiffness

shoe. As indicated by Eq. 2-18, in the case of a rigid shoe the pressure distribution is approximated by $p = (E\ a\ \varphi\ \sin\alpha)/d_{Lo}$. An elastic shoe produces a pressure distribution that exhibits higher pressure concentrations at or near the ends of the lining. The pressure distribution may be approximated by

$$p = (a\,\varphi\,E/d_{Lo})(2\sin\alpha + \cos 2\alpha)\ ,\text{psi} \qquad (2\text{-}32)$$

Application of this pressure distribution to the brake factor analysis under consideration of an elastic shoe yields fairly complicated equations for predicting brake torque. The analysis is made difficult by the complicated designs found in many brake shoes which prevent the establishment of a simple equation for the elastic deformation.

The effect of the difference in pressure distribution may be analyzed by increasing the angle β (Fig. 2-13) from a typical value of 3 deg to 30 or 40 deg (Refs. 4 and 5). This change would effectively alter the pressure distribution so as to concentrate pressure near the end of the lining. Application of this change to

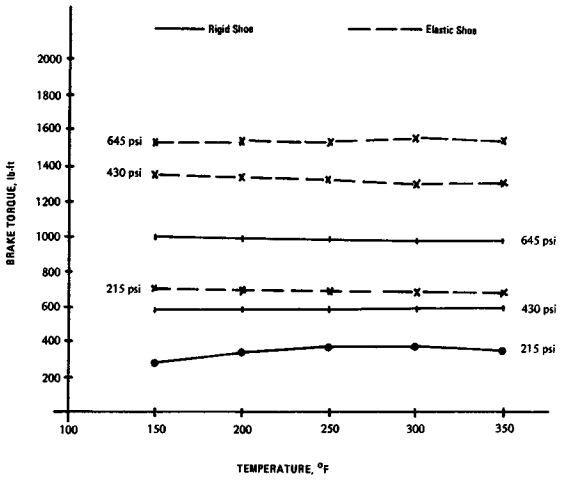

Figure 2-18. Brake Torque vs Temperature for Different Brake Line Pressures (215, 430, 645 psi)

the brake factor equations yields significantly higher brake factors at moderate values of lining friction coefficients. The undesirable side effect is increased lining wear.

Truck brakes generally are designed so that they do not exhibit any appreciable elastic effects on the brake torque production. Some earlier passenger car brakes of US manufacture were designed to produce a limited amount of elastic deformation, and hence an increase in brake torque production.

2-6 ANALYSIS OF EXTERNAL BAND BRAKES

Motor vehicles are sometimes equipped with emergency or parking brakes mounted directly on the drive shaft. In most cases, the brakes are so-called band or external friction brakes. Some of the disadvantages are high bearing forces, possibility for extensive contamination, and often degraded thermal capacity.

For the band brake shown in Fig. 2-19 the following equilibrium conditions apply:

$$\left.\begin{aligned} Kl - S_1 a_1 - S_2 a_2 &= 0 \\ S_1 - S_2 &= F_d \text{ , lb} \\ \frac{S_1}{S_2} &= e^{\mu_L \alpha_B} \text{ , d'less} \end{aligned}\right] \qquad (2\text{-}33)$$

where

a_1 = brake dimension, in.
a_2 = brake dimension, in.
K = application force, lb
l = brake dimension, in.
S_1 = band force, lb
S_2 = band force, lb
α_B = band angle, rad

In terms of the brake factor as defined earlier, the ratio of F_d to F_a represents the gain of the brake. The application force F_a for a simple band brake ($a_1 = 0$, $a_2 = a$) is given by

$$F_a = Kl/a \text{ , lb} \qquad (2\text{-}34)$$

The brake factor and brake sensitivity are given in the following paragraphs for most common band brakes illustrated in Figs. 2-20 through 2-22.

The band brake shown in Fig. 2-20 yields a brake factor for a clockwise rotation of

$$BF = \frac{F_d}{F_a} = e^{\mu_L \alpha_B} - 1 \text{ , d'less} \qquad (2\text{-}35a)$$

and a brake sensitivity of

$$S_B = \alpha_B e^{\mu_L \alpha_B} \text{ , d'less} \qquad (2\text{-}35b)$$

For counterclockwise rotation of the same band brake, the results are:

$$BF = \frac{F_d}{F_a} = \frac{e^{\mu_L \alpha_B} - 1}{e^{\mu_L \alpha_B}} \text{ , d'less} \qquad (2\text{-}36a)$$

$$S_B = \frac{\alpha_B}{e^{\mu_L \alpha_B}} \text{ , d'less} \qquad (2\text{-}36b)$$

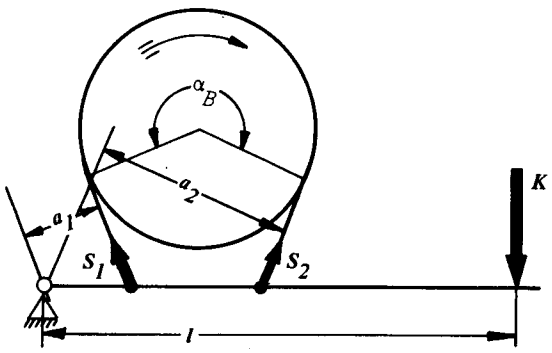

Figure 2-19. General Design of External Band Brake

For the hand brake shown in Fig. 2-21, the results are

$$BF = \frac{F_d}{F_a} = \frac{e^{\mu_L \alpha_B} - 1}{i - e^{\mu_L \alpha_B}} \text{ , d'less} \quad 2\text{-}37a)$$

$$S_B = \frac{\alpha\, e^{\mu_L \alpha_B}\,(i-1)}{(i - e^{\mu_L \alpha_B})^2} \text{ , d'less} \quad (2\text{-}37b)$$

where

i = ratio of application arms as defined in Fig. 2-21, d'less

For the brake shown in Fig. 2-22 the results for brake factor and sensitivity are

$$BF = \frac{F_d}{F_a} = \frac{e^{\mu_L \alpha_B} - 1}{e^{\mu_L \alpha_B} + 1} \text{ , d'less} \quad (2\text{-}38a)$$

$$S_b = \frac{2\alpha\, e^{\mu_L \alpha_B}}{(e^{\mu_L \alpha_B} + 1)^2} \text{ , d'less} \quad (2\text{-}38b)$$

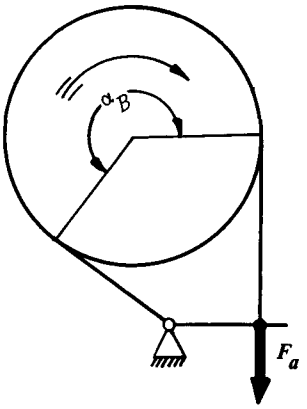

Figure 2-20. Single Application External Band Brake

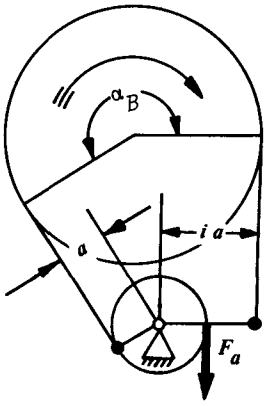

Figure 2-21. Opposing Application External Band Brake

2-7 ANALYSIS OF SELF-ENERGIZING DISC BRAKES

The basic wedge design of a self-energizing disc brake is illustrated in Fig. 2-23. The self-energizing effect is accomplished by means of a wedge shaped disc brake pad. The friction force between pad and rotor tends to force the pad into the wedge shaped piston. This small displacement of the pad causes an increased force between pad and piston and consequently between pad and rotor friction surface. This increased normal force between pad and rotor results in a larger rotor drag force and hence increased brake force. Caliper disc brakes commonly in use on automobiles and trucks do not use self-energizing mechanisms. Fully covered disc brakes have been designed to use the wedging effect to increase brake factor. The self-energizing mechanism consists in most cases of a ball-and-ramp type design as illustrated in Fig. 2-24. The actuating force is the force directly pressing against the disc. This force is increased by the friction force which causes an additional relative rotation and hence pushing apart of the circular brake pads and increased normal force by means of the ball-and-ramp mechanism, thus introducing self-energizing.

By use of the notation of Fig. 2-24, the friction force of one circular brake pad is given by the relationship

$$F_d = \mu_L \left[F_a + F_d \left(\frac{r_m}{r_k} \right) \right] \cot \delta \text{ , lb}$$

$$\frac{F_d}{F_a} = \frac{\mu_L \left(\frac{r_k}{r_m} \right)}{(\tan \delta)\left(\frac{r_k}{r_m} \right) - \mu_L} \text{ , d'less} \quad (2\text{-}39)$$

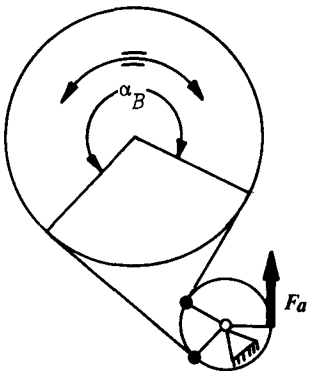

Figure 2-22. Inline Application External Band Brake

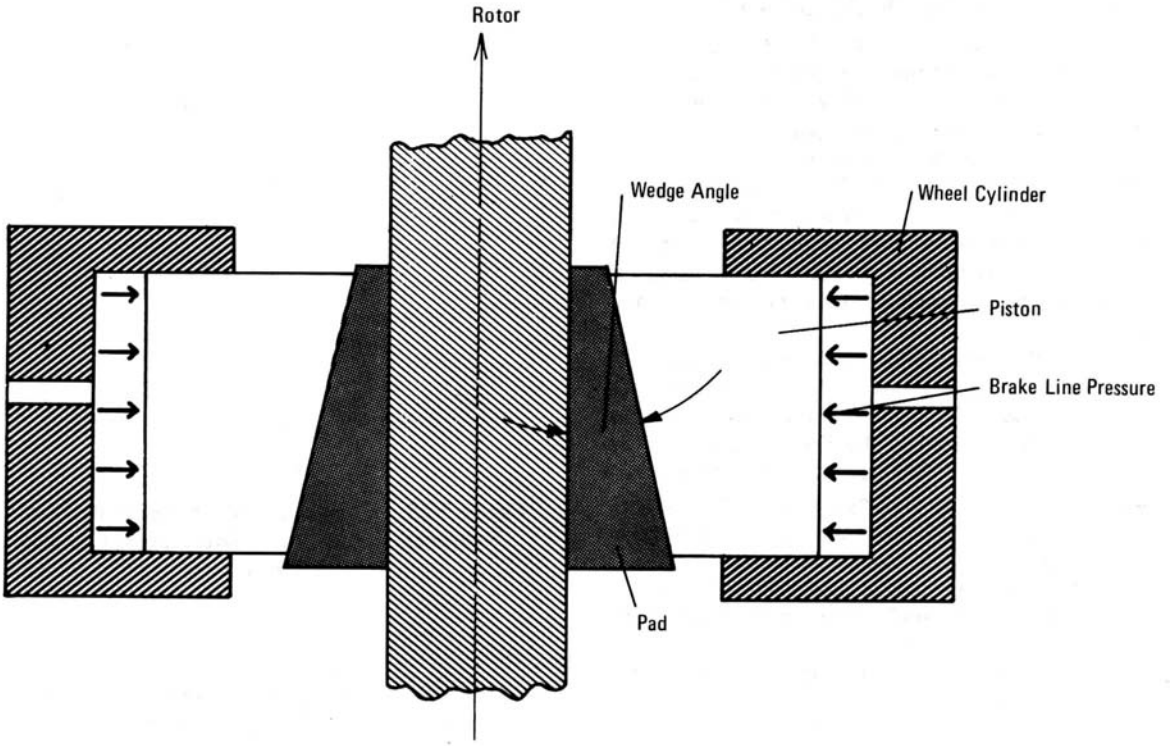

Figure 2-23. Self-Energizing of Caliper Disc Brake

where

r_k = disc brake dimension, in.
r_m = disc brake dimension, in.
δ = disc brake ramp angle, deg
μ_L = pad friction coefficient, d'less

Since two friction surfaces are present, the total brake factor becomes

$$BF = 2\left(\frac{r_k}{r_m}\right)\frac{\frac{\mu_L}{\mu_{L\infty}}}{1-\frac{\mu_L}{\mu_{L\infty}}}, \text{ d'less} \qquad (2\text{-}40)$$

where the self-locking limit is given by

$$\mu_{L\infty} = (\tan\delta)\frac{r_k}{r_m}, \text{ d'less}$$

The sensitivity of the brake is expressed by the relationship of the form:

$$S_B = \frac{2\cot\delta}{\left(1-\frac{\mu_L}{\mu_{L\infty}}\right)^2}, \text{ d'less} \qquad (2\text{-}41)$$

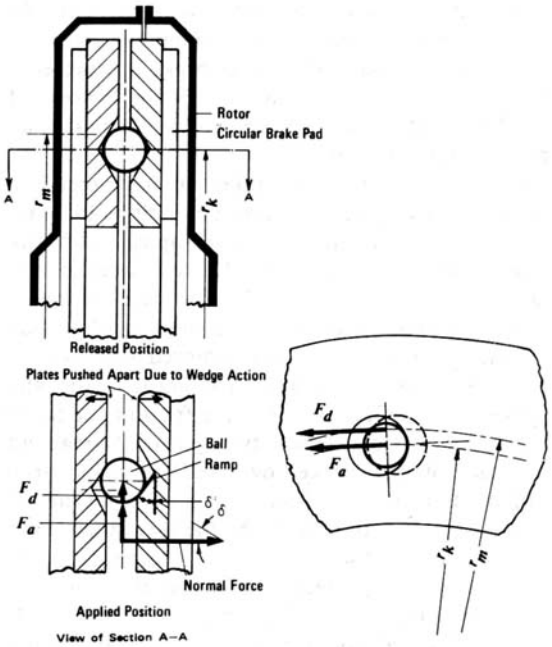

Figure 2-24. Schematic of Self-Energizing Full Covered Disc Brake

2-8 COMPARISON OF BRAKES

Duo-servo brakes show the highest brake factor and hence brake torque/line pressure gain. However, its high sensitivity is a disadvantage (Ref. 6). A vehicle equipped with the high gain duo-servo brakes easily may experience a yawing moment or change in front to rear brake force distribution during the braking process (Ref. 2). Also, the lining on the secondary shoe wears more rapidly than on the primary shoe. This often is provided for by using different friction materials on primary and secondary shoe.

Two-leading shoe brakes show a moderate brake factor as well as brake sensitivity. Their main disadvantage lies in the fact that in the case of a reversal of direction of rotation the brake factor may decrease by as much as 70% due to a change from a two-leading shoe to a two-trailing shoe operation. Expensive designs may be used to avoid this change in brake factor due to a reversal of rotation.

Leading-trailing shoe brakes exhibit the lowest brake factor and sensitivity. Since approximately 70% of the brake torque is generated on the leading shoe, the leading shoe lining will wear more rapidly than the trailing shoe.

The wear along a lining ideally should be uniform. A shoe held by an abutment will wear more uniformly than a pivoted shoe. An inclined abutment may result in a more uniform wear than a parallel abutment. The wear life predicted theoretically for "S" cam and wedge actuated drum brake agrees with experimental results. The wedge brake is expected to have a better wear life than the "S" cam brake (Ref. 3). (More details on "S" cam and wedge brakes are presented in Chapter 15.)

Experiments with disc brakes on commercial vehicles were carried out in Europe as early as 1957. Experimental results on trucks equipped with disc brakes were published in the United States in 1969 and are presented in Fig. 2-25. The decelerations of 0.8g to 1g were exceptionally high compared with decelerations of 0.6g to 0.65g achieved with vehicles equipped with drum brakes. The linear relationship between brake factors and lining friction coefficient and hence constant sensitivity, is one of the main advantages of disc brakes over self-energizing drum brakes. For constant lining friction coefficient the brake factor is little affected by thermal expansion of the caliper or disc. For drums, however, during severe braking the effective drum radius will increase more than the radius of the brake shoe due to the smaller thermal conductivity of the brake linings (Ref. 2). This may result in a change of pressure distribution over the brake lining and in a reduction of the brake factor of up to 20%, and hence lower brake performance. During the cooling period the drum will attain lower temperatures than the brake shoe, and will therefore have a smaller effective drum radius. This may result in a high pressure between lining and drum at both ends of the lining and in an increase of up to 40% in brake factor over normal operating conditions.

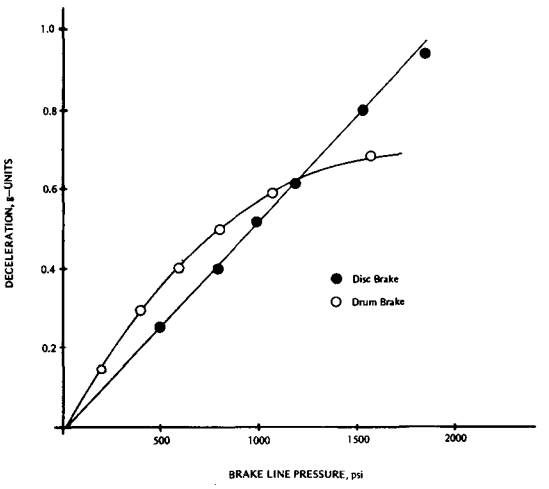

Figure 2-25. Comparison of Measured Braking Performance of Disc and Drum Brakes for a Truck

The greatest disadvantage of disc brakes is their low brake factor. On the average, the brake factor is only about 25% of that for a two-leading shoe brake. However, this can easily be resolved by using power assisted braking systems. Also, disc brakes tend to produce somewhat smaller brake torques during run-in conditions than in the new condition, while drum brakes exhibit the opposite behavior.

REFERENCES

1. H. Strien, *Computation and Testing of Automotive Brakes,* Dissertation, Technical University, Braunschweig, Germany, 1949.
2. J. L. Winge, *Instrumentation and Methods for the Evaluation of Variables in Passenger Car Brakes,* SAE Paper No. 361B, SAE Summer Meeting 1961.
3. G. B. Stroh, M. H. Lawrence, and W. T. Deibel, *Effects of Shoe Force Geometry on Heavy Duty*

Internal Shoe Brake Performance, SAE Paper No. 680432, May 1968.

4. W. Muller, "Contribution to the Analysis and Testing of Motor-Vehicle Drum Brake", *Deutsche Kraftfahrtforschung und Strassenverkehrstechnik* No. 207, 1971.
5. G. A. G. Fazekas, "Brake Torque", *Automobile Engineer,* Vol. 41, No. 540, May 1959, pp. 185-89.
6. J. G. Oetzel, *Relating Lining Characteristics to Brake Design,* SAE Preprint, Summer Meeting, June 5-9, 1961.

CHAPTER 3
THERMAL ANALYSIS OF FRICTION BRAKES

In this chapter the basic relationships for predicting brake temperature as a result of a single, repeated, or continued brake application are presented. Equations for the computation of the convective heat transfer coefficients of drum and disc brakes are given. Finite-difference techniques are discussed for the case of a one-dimensional analysis.

In the thermal stress analysis, relationships for predicting surface stresses of solid rotors are developed. Solution outlines for the ventilated rotor are discussed.

3-0 LIST OF SYMBOLS

A_f = friction area of one rotor side, ft²
A_{in} = inlet area, ft²
A_{out} = outlet area, ft²
A_P = pad surface area, ft²
A_R = rotor surface area, ft²
A_{rad} = cooling area of radiator, ft²
A_{WC} = wheel cylinder area, in.²
a = vehicle deceleration, g-units
a_t = thermal diffusivity, ft²/h
a_x = vehicle deceleration, ft/s²
BF = brake factor, d'less*
b = plate width, ft
C = heat transfer constant, d'less
c_a = specific heat of air, BTU/lbm·°F
c_P = specific heat of the pad, BTU/lbm·°F
c_R = specific heat of the rotor, BTU/lbm·°F
D = drum diameter, ft
D = outer diameter, ft
d = inner diameter, ft
d = differential operator, d'less
d_h = hydraulic diameter, ft
E = elastic modulus, psi
f = thermal fade factor, (°F)$^{-1}$
G = road gradient, d'less
h_p = convective heat transfer coefficient of pad, BTU/h·°F·ft²
h_R = convective heat transfer coefficient of rotor or drum, BTU/h·°F·ft²
$h_{R,rad}$ = radiative heat transfer coefficient, BTU/h·°F·ft²
h_{rad} = convective heat transfer coefficient of radiator, BTU/h·°F·ft²
k = thermal conductivity of drum, BTU/h·°F·ft
k_a = thermal conductivity of air, BTU/h·°F·ft
k_P = thermal conductivity of the pad material, BTU/h·°F·ft
k_R = thermal conductivity of the rotor, BTU/h·°F·ft
k_S = thermal conductivity of the pad support, BTU/h·°F·ft
L = one-half rotor thickness, ft
L = drum thickness, ft
L_c = characteristic length, ft
l = length of cooling vane, ft
M = parameter, d'less
m = heat transfer parameter, d'less
m_a = air flow rate, ft³/s
N = parameter, d'less
Nu = Nusselt number, d'less
n_a = number of brake application, d'less
n_h = heat transfer parameter, d'less
n_r = revolutions per minute of the rotor, rpm
n = numerals 1, 2, 3, . . ., d'less
n_c = number of calipers per axle, d'less
Pr = Prandtl number, d'less
p_l = brake line pressure, psi
q_{ij} = heat flow between nodal points i and j, BTU/h
q_o = average braking energy of the vehicle, BTU/h
q_o = braking energy absorbed by the rotor, BTU/h
$q_{o,B}$ = braking energy absorbed by a single brake, BTU/h
$q_{o,RB}$ = braking energy absorbed per rear brake, BTU/h
$q''_{(o)}$ = time-varying heat flux into rotor at time $t = 0$, BTU/h·ft²
q''_o = average heat flux into rotor, BTU/h·ft²
q''_P = heat flux into pad, BTU/h·ft²
q''_R = heat flux into rotor, BTU/h·ft²
q''_{rad} = radiation heat flux, BTU/h·ft²
$q''(t)$ = time varying heat flux, BTU/h·ft²
$q''(\tau)$ = time varying heat flux, BTU/h·ft²
R = effective tire radius, ft
Re = Reynolds number, d'less

*d'less = dimensionless

R_P = thermal resistance to conductive heat flow in pad, h·°F/BTU
R_R = thermal resistance to conductive heat flow in rotor, h·°F/BTU
R_r = tire rolling resistance coefficient, d'less
r_i = distance of nodal point i from center of rotor, ft
r_m = effective rotor radius, ft
s = tire slip, d'less
T = temperature at time t, °F
T_i = temperature of node i, °F
T_i = initial temperature, °F
T_j = temperature of node j, °F
T_R = rotor surface temperature, °R
$T(t)$ = maximum temperature, °F
$T(z)$ = temperature distribution over z, °F
$T(z, t)$ = transient temperature distribution in rotor, °F
T_0 = temperature of surface node, °F
$T_0(z, t)$ = transient temperature distribution in rotor due to a constant heat flux, °F
T_1 = temperature of node 1, °F
T_2 = temperature of node 2, °F
T_3 = temperature of node 3, °F
T'_o = temperature of node 0 after time interval Δt, °F
T'_2 = temperature of node 2 after time interval Δt, °F
T_∞ = ambient temperature, °F or °R
T_n = temperature of node n, °F
T'_n = temperature of node n after time interval Δt, °F
t = time, h or s
t_a = time during which brakes are applied, h
t_c = cooling time, h
t_s = braking time to a stop, h
V = vehicle speed, ft/s
$V_{average}$ = average velocity in vane, ft/s
V_{in} = inlet velocity, ft/s
V_{out} = outlet velocity, ft/s
v_R = rotor volume, ft³
V_1 = initial vehicle speed, ft/s
V_2 = final vehicle speed, ft/s
W = vehicle weight, lb
z = horizontal distance measured from center of rotor, ft
z = distance measured from friction surface, ft

α_t = thermal expansion coefficient, in./°F·in.
β = parameter, BTU·s/h·°F·ft³
γ = relative braking energy absorbed by rotor, d'less
Δh = enthalpy change, BTU/lbm
ΔT = temperature change, deg F
ΔT_{rad} = mean temperature difference of cooling liquid and air in radiator, deg F
Δt = time interval, s or h
Δx = horizontal distance between two adjacent nodal points, ft
Δy = vertical distance between two adjacent nodal points, ft
δ_m = differential mass, lbm
δ_P = pad thickness, ft
δ_S = pad support thickness, ft
ϵ_R = rotor surface emissivity, d'less
η = mechanical efficiency, d'less
$\theta(z, t)$ = $T(z, t) - T_\infty$, relative temperature of brake resulting from time-varying heat flux, deg F
θ_i = initial temperature difference between brake and ambient $T_i - T_\infty$, deg F
$\theta_o(z, t)$ = $T_0(z, t) - T_\infty$, relative temperature of brake resulting from constant heat flux, deg F
λ_n = $n\pi/L$, ft⁻¹
μ_a = viscosity of air, lbm/ft·s
μ_L = lining/rotor friction coefficient, d'less
μ_{Lc} = lining/rotor friction coefficient for cold brake, d'less
μ_{Lh} = lining/rotor friction coefficient for hot brake, d'less
ν = Poisson's ratio, d'less
ρ = density, lbm/ft³
ρ_a = density of air, lbm/ft³
ρ_P = density of the pad, lbm/ft³
ρ_R = density of the rotor, lbm/ft³
σ = stress, psi
σ = Stefan-Boltzmann constant = 0.1714 × 10⁻⁸ BTU/h·ft²·°R⁴
σ_x = stress in x-direction, psi
σ_y = stress in y-direction, psi
$\sigma(z, t)$ = stress resulting from time-varying heat flux, psi
$\sigma_o(z, t)$ = stress resulting from constant heat flux, psi
τ = time, h
ϕ = rear axle brake force divided by total brake force, d'less
$\partial T/\partial x$ = temperature gradient, deg F/ft

3-1 TEMPERATURE ANALYSIS

3-1.1 THE FRICTION BRAKE AS A HEAT EXCHANGER

During braking, the potential energy and kinetic energy of a vehicle are converted into thermal energy via the mechanism of deforming the friction partners. In the automobile retarding mechanism, there are

two different locations where frictional forces are produced and where heat generation may occur. Heat generation occurs when a relative motion exists between the friction partners. A vehicle that is being decelerated with its tires operating near their maximum braking capability, without complete wheel lockup occurring, will have the tires operating at approximately 8 to 12% slip. A tire slip of 12%, for example, means that the circumferential velocity of the tire is only 88% of the longitudinal velocity of the vehicle. This indicates that only 88% of the kinetic energy of the vehicle is absorbed by the brakes. The remaining 12% is absorbed by the tires and the road surface. For conditions in which the brake torque is significantly less than that associated with maximum tire braking forces, most braking energy will be absorbed by the brakes.

The average braking energy q_o of the vehicle, thought to be constant over the entire braking process, may be obtained from the summation of the forces in a horizontal plane and is given by

$$q_o = \frac{(1-s)W(V_1 + V_2)\,a \times 3600}{2 \times 778}, \text{BTU/h} \qquad (3\text{-}1)$$

where

a = vehicle deceleration, g-units
s = tire slip, defined by the ratio of difference between vehicle forward speed and circumferential tire speed to vehicle forward speed, d'less
V_1 = initial vehicle speed, ft/s
V_2 = final vehicle speed, ft/s
w = vehicle weight, lb

If an unbraked trailer is towed by the vehicle, the combination weight must be used in Eq. 3-1.

The maximum braking energy produced at the onset of braking is equal to $2q_o$.

Not included in the braking energy given by Eq. 3-1 are the rotational energies of wheels, axles, and shafts. In many applications these additional energies are assumed equal to retarding effects produced by rolling resistance and aerodynamic drag. To account for rotational energies of a particular vehicle, the vehicle weight must be multiplied by a factor whose value is determined from the rotational masses and transmission ratios.

Use the example of w = 20,000 lb, V_1 = 88 ft/s, V_2 = 0, a = 0.6g, and s = 0.1, and apply Eq. 3-1; a maximum rate of braking energy at the instant of brake initiation of 4,397,738 BTU/h or 1727 hp is yielded. The average brake horsepower of 863 hp must be absorbed by the vehicle brake system. The duration of the effectiveness stop is 4.55 s — computed by dividing speed by deceleration expressed as ft/s^2.

During a continued downhill brake application, the energy per hour q_o absorbed by the vehicle brakes is

$$q_o = \frac{W\,V\,(G - R_r)\,3600}{778}, \text{BTU/h} \qquad (3\text{-}2)$$

where

G = road gradient, d'less
R_r = tire rolling resistance coefficient, d'less
V = vehicle speed, ft/s

Use the vehicle data of the earlier example and V = 58.67 ft/s on a gradient G = 7%, R_r = 0.015 (value obtained from Table 6-1) and apply Eq. 3-2; a brake power of 298,629 BTU/h or 117 hp is yielded. Comparison of the brake power values obtained for a single stop and continued braking appears to identify the effectiveness stop as the more critical application. However, as shown earlier, this high level of braking power is limited to 4.55 s, whereas a continued brake application may eventually lead to high temperatures and a significant decrease in braking performance.

The thermal capacity of a brake may be compared to that of a combustion engine. A vehicle having a gross vehicle weight of 20,000 lb may have an engine of 130-180 hp. An approximate estimate of the total energy balance indicates that about 1/3 of the fuel energy is dissipated through the cooling system, 1/3 through the exhaust gases, and 1/3 in the form of mechanical engine work. Consequently, an engine rated at 130 hp has a cooling system designed for dissipating approximately 130 hp. Upon comparing the elaborate design of a motor-cooling system to that available to the foundation brakes, it is apparent that most brakes found on our trucks today are ill-suited for prolonged brake application unless special provision for cooling is provided.

3-1.2 FUNDAMENTALS ASSOCIATED WITH BRAKE TEMPERATURE ANALYSIS

One of the functions of a brake is to store and/or dissipate thermal energy generated at the interface. Since the structural integrity of a brake can be related to the temperature at the friction surface, most theoretical investigations are addressed to the determination of the temperature rise expected during braking in a single stop and during repeated or continuous braking. Results indicate that in the case of braking

to a single stop the friction surface should be as large as possible to reduce the temperature. However, for continued braking, the heat capacity and convective heat-transfer are essential, i.e., the important design parameters for stop-braking differ from those for continued braking. The theoretical investigations also indicate for organic linings that, of the heat generated during stop-braking, approximately 95% is absorbed by the drum or disc, and 5% by the brake lining or pad. Sintered-iron linings use metal plugs in the lining to transfer a greater portion of the generated heat to the brake shoes or pad support because of the increased thermal conductivity of this friction material.

The distribution of braking energy between pad and rotor cannot be predicted readily. The distribution of thermal energy between the pad and the rotor is related directly to the thermal resistance associated with both sides of the interface. It is assumed that the heat transfer into the rotor and pad may be determined from the equivalent resistance network. For the steady-state conditions this may be expressed as (Ref. 1)

$$\frac{q_R''}{q_P''} = \frac{\sum R_P}{\sum R_R}, \text{ d'less} \qquad (3\text{-}3)$$

where

q_R'' = heat flux into rotor, BTU/h·ft²
q_P'' = heat flux into pad, BTU/h·ft²
R_P = thermal resistance to conductive heat flow in pad, h·°F/BTU
R_R = thermal resistance to conductive heat flow in rotor, h·°F/BTU

For short brake application times, the pad and rotor may be considered as semi-infinite solids. Under these conditions, the requirement for identical temperatures at the interface and that the total heat generation equals the heat generation absorbed by the rotor and the pad yields with Eq. 3-3

$$\frac{q_R''}{q_P''} = \left(\frac{\rho_R c_R k_R}{\rho_P c_P k_P}\right)^{1/2}, \text{ d'less} \qquad (3\text{-}4)$$

where

c_P = pad specific heat, BTU/lbm·°F
c_R = rotor specific heat, BTU/lbm·°F
k_P = pad thermal conductivity, BTU/h·°F·ft
k_R = rotor thermal conductivity, BTU/h·°F·ft
ρ_P = pad density, lbm/ft³
ρ_R = rotor density, lbm/ft³

It becomes convenient to express the portion of the total heat generation absorbed by the rotor in terms of the material properties. The requirement that the total heat generated equals $q_R'' + q_P''$ and Eq. 3-4 yield for the relative braking energy γ absorbed by the rotor

$$\gamma = \frac{q_R''}{q_R'' + q_P''} = \frac{1}{1 + \left(\frac{\rho_P c_P k_P}{\rho_R c_R k_R}\right)^{1/2}}, \text{ d'less} \qquad (3\text{-}5)$$

For continued braking or repeated brake applications, Eq. 3-5 assumes a more complicated form due to the convective heat transfer occurring as a result of higher brake temperatures. The schematic is illustrated in Fig. 3-1. For steady-state conditions no energy will be stored in the rotor. Consequently, the thermal resistance R_R associated with the rotor is given by

$$\sum R_R = \frac{1}{h_R A_R}, \text{ h·°F/BTU} \qquad (3\text{-}6)$$

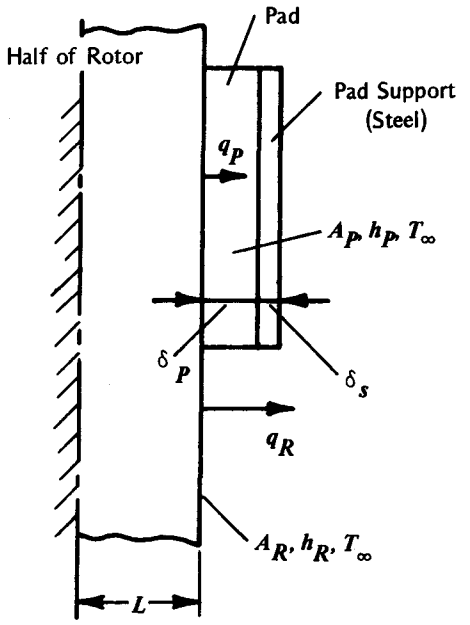

Figure 3-1. Heat Distribution for Continued Braking

where

A_R = rotor surface area, ft²

h_R = convective heat transfer coefficient of the rotor, BTU/h·°F·ft²

The thermal resistance R_P associated with the pad is (Ref. 2)

$$\sum R_P = \frac{1}{h_P A_P} + \frac{\delta_P}{k_P A_P} + \frac{\delta_S}{k_S A_P}, \text{ h·°F/BTU} \quad (3\text{-}7)$$

where

A_P = pad surface area, ft²

h_P = convective heat transfer coefficient of the pad, BTU/h·°F·ft²

k_P = thermal conductivity of pad material, BTU/h·°F·ft

k_S = thermal conductivity of pad support, BTU/h·°F·ft

δ_P = pad thickness, ft

δ_S = pad support thickness, ft

With the heat distribution factor defined in Eqs. 3-5 and 3-3 as

$$\gamma = \frac{q''_R}{q''_R + q''_P} = \frac{1}{1 + \frac{\sum R_R}{\sum R_P}}, \text{ d'less}$$

the heat distribution to the rotor is given by

$$\gamma = 1 + \left[\frac{h_P k_P k_S A_P}{h_R A_R (k_P k_S + \delta_P h_P k_s + \delta_S h_P k_P)}\right]^{-1}, \text{ d'less} \quad (3\text{-}8)$$

Some difficulty may arise from the determination of the convective heat transfer coefficient of the disc. Investigations of heat transfer from a rotating disc have been carried out. However, the influence of a caliper located on the disc has not yet been incorporated in any theoretical analysis.

If the ventilated and solid disc are of equal weight, only a small average temperature difference can be expected during the first few stops, but ultimately, or during continued braking, the ventilated disc will tend to reach approximately 60% of the temperature of the solid disc.

The effects of radiation are neglected in most applications since they contribute only about 5 to 10% to the heat transfer from the drum or disc. However, for brakes attaining high temperatures, as can be expected in the case of sintered iron plug linings, thermal radiation may contribute substantially to the heat transfer. In a complete thermal analysis of brakes, the entire brake assembly should be considered — i.e., wheel cylinder, axle bearings, and tire should be included.

Certain other design variations, such as bimetallic brake drums, liquid-cooled brakes, as well as the mentioned modified brake linings, have been used to reduce temperature.

3-1.3 PREDICTION OF BRAKE TEMPERATURE DURING CONTINUED BRAKING

The derivation of the temperature distribution through the thickness of the rotor in case of a ventilated rotor is extremely complicated (Ref. 3).

For a solid rotor, the conditions permit an analytical solution (Fig. 3-2).

$$\theta_o(z,t) = \frac{q''_o}{h_R}\left[2\left(\frac{\theta_i h_R}{q''_o} - 1\right) \times \sum_{n=1}^{\infty} \frac{\sin(\lambda_n L)}{\lambda_n L + \sin(\lambda_n L)\cos(\lambda_n L)} e^{-a_t \lambda_n^2 t} \times \cos(\lambda_n z) + 1\right], \text{ deg F} \quad (3\text{-}9)$$

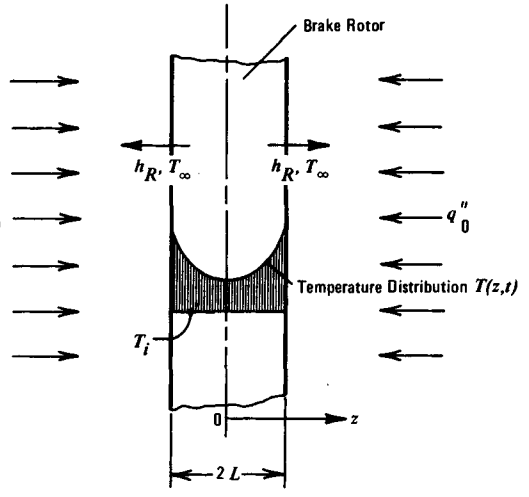

Figure 3-2. Physical System Representing Brake Rotor

where

a_t = $k_R/(\rho_R c_R)$ = thermal diffusivity, ft²/h
h_R = convective heat transfer coefficient of rotor, BTU/h·°F·ft²
L = one-half rotor thickness, ft
n = numerals 1, 2, 3, . . ., d'less
q''_o = average heat flux into rotor, BTU/h·ft²
T_i = initial temperature, °F
$T_o(z, t)$ = transient temperature distribution in rotor due to a constant heat flux, °F
T_∞ = ambient temperature, °F
t = time, h
z = horizontal distance measured from center of rotor, ft
θ_i = initial temperature difference between brake and ambient $T_i - T_\infty$, deg F
$\theta_o(z, t) = T_o(z, t) - T_\infty$ relative temperature of brake resulting from constant heat flux, deg F
$\lambda_n = n\pi/L$, (ft)$^{-1}$

The value of $\lambda_n L$ is determined from the transcendental equation

$$(\lambda_n L)\tan(\lambda_n L) - h_R L/k = 0$$

Inherent in the derivation of Eq. 3-9 are the following assumptions:

1. The temperature is only a function of the coordinate normal to the friction surface and time.
2. The heat transfer coefficient h_R is constant and evaluated at some mean velocity.
3. The heat flux is in the direction of the normal to the friction surface. Heat conduction parallel to the friction surface is negligible. First, the heat flux into the rotor is assumed to be constant. The analysis will yield the equations describing the temperature response for continued braking. Later the application of Duhamel's theorem will produce the equations describing the temperature response resulting from a time-varying heat flux.
4. The thermal properties of both friction partners are constant when evaluated at some mean temperature.
5. The ambient temperature T_∞ = constant.
6. Radiative heat transfer is included in terms of an equivalent radiative heat transfer coefficient (see Fig. 3-4).

The temperature attained by a drum brake is (Ref. 3)

$$\theta_o(z, t) = \frac{q''_o L}{k}\left\{1 - \frac{z}{L} + \frac{k}{h_R L} - 2\sum_{n=1}^{\infty}\frac{e^{-a_t\lambda_n^2 t}\cos(\lambda_n z)}{(\lambda_n L)[(\lambda_n L + \sin(\lambda_n L)\cos(\lambda_n L)]}\right\}, \text{deg F} \quad (3\text{-}10)$$

where

k = thermal conductivity of drum, BTU/h·°F·ft
L = drum thickness, ft
z = distance measured from friction surface, ft

Eq. 3-10 also may be used for computing the brake temperatures of ventilated rotors when the convective heat transfer at the friction surfaces is negligible as in the case of a shielded rotor. A few roots of the transcendental equation of practical importance for typical brakes are presented in Table 3-1.

3-1.4 PREDICTION OF BRAKE TEMPERATURE DURING A SINGLE STOP

Eq. 3-9 computes the temperature response resulting from a constant heat flux at the rotor surface. When the vehicle is decelerated in a single stop, the heat flux varies with time. In most cases a linearly decreasing heat flux can be assumed. The temperature response of the brake rotor may be obtained directly from the temperature solution associated with the time independent heat flux q''_o by application of Duhamel's theorem. The application of Duhamel's superposition integral results in the following expression for the temperature change resulting from a time-varying heat flux (Ref. 3)

$$\theta(z, t) = \frac{q''_{(o)}}{q''_o}\theta_0(z, t) + \frac{1}{q''_o}\int_0^t \frac{dq''(\tau)}{d(\tau)}\theta_0(z, t-\tau)d\tau, \text{deg F} \quad (3\text{-}11)$$

where

d = differential operator, d'less
$q''_{(o)}$ = time-varying heat flux into rotor at time $t = 0$, BTU/h·ft²
$q''(\tau)$ = time-varying heat flux, BTU/h·ft²
t = time, h
$\theta_o(z, t) = T_o(z, t) - T_\infty$ = relative temperature of brake resulting from constant heat flux, deg F
τ = time, h

TABLE 3-1
ROOTS OF TRANSCENDENTAL EQUATION

$h_R L/k$	$\lambda_1 L$	$\lambda_2 L$	$\lambda_3 L$	$\lambda_4 L$	$\lambda_5 L$	$\lambda_6 L$
0.01	0.0998	3.1448	6.2848	9.4258	12.5672	15.7086
0.02	0.1410	3.1479	6.3864	9.4269	12.5680	15.7092
0.04	0.1987	3.1543	6.2895	9.4290	12.5696	15.7105
0.06	0.0774	3.1435	6.2841	9.4254	12.5668	15.7085

If a time-varying heat flux $q''(t)$

$$q''(t) = q''_{(o)}\left(1 - \frac{t}{t_s}\right), \text{BTU/h·ft}^2 \quad (3\text{-}12)$$

is assumed, where t = time, h and t_s = braking time to a stop, h; then integration of Eq. 3-11 with Eq. 3-9 and $\theta_i = 0$ yields the temperature response resulting from a time-varying heat flux (Refs. 2 and 4)

$$\theta(z,t) = \frac{q''_{(o)}}{q''_o}\theta_o(z,t) - \frac{q''_{(o)}}{t_s h_R} \times \left[t - 2\sum_{n=1}^{\infty} \frac{\sin(\lambda_n L)}{\lambda_n L + \sin(\lambda_n L)\cos(\lambda_n L)} \times \left(\frac{1 - e^{-a_t\lambda_n^2 t}}{a_t\lambda_n^2}\right)\cos(\lambda_n z)\right], \text{deg F} \quad (3\text{-}13)$$

where

$q''_{(o)}$ = time varying heat flux into the rotor at time $t = 0$, BTU/h·ft²

q''_o = average heat flux into rotor, BTU/h·ft² = $q''_{(o)}/2$

t_s = braking time to a stop, h

$\theta_o(z,t)$ = relative temperature of brake resulting from constant heat flux, deg F (obtained from Eq. 3-9)

The temperature response of a drum brake resulting from a time-varying heat flux is

$$\theta(z,t) = \frac{q''_{(o)}}{q''_o}\theta_o(z,t) - \frac{q''_{(o)}L}{k\,t_s} \times \left[t\left(1 + \frac{k}{h_R L} - \frac{z}{L}\right) - 2\sum_{n=1}^{\infty} \frac{\sin(\lambda_n L)}{(\lambda_n L) + \sin(\lambda_n L)\cos(\lambda_n L)}\right] \times \left(\frac{1 - e^{-a_t\lambda_n^2 t}}{a_t\lambda_n^2}\right)\cos(\lambda_n z), \text{deg F} \quad (3\text{-}14)$$

where

$\theta_o(z,t)$ is obtained from Eq. 3-10.

An evaluation of the prior equations for the temperature response of a brake requires the use of some kind of computing machine. The equations are necessary for a critical evaluation of more complicated finite-difference methods used for predicting temperature response. They also are used in computing the thermal stresses developed during rapid and severe braking to a stop.

In many cases a simpler equation is helpful in predicting the temperature response during a single stop. For the time domain in which the heat flux has not yet penetrated through the drum or flange thickness of the ventilated rotor, practical solutions to the differential equation yield as the maximum temperature $T(t)$ at the friction surface (Ref. 5)

$$T(t) = \frac{0.52\,q''_{(o)}\,(t_s)^{1/2}}{(\rho_R\,c_R\,k_R)^{1/2}} + T_i, \text{°F} \quad (3\text{-}15)$$

Eq. 3-15 assumes that all braking energy is absorbed and stored by the rotor during the single stop.

The evaluation of the temperature equations requires information of the thermal properties of lining and pad materials of drum and disc brakes, respectively, as well as for the brake rotors.

No specific thermal properties can be assigned since they are a function of lining composition, burnishing procedures, and temperature. The values shown in Table 3-2 may be used for design evaluation only when typical drum and lining materials are used (Refs. 2 and 6).

3-1.5 PREDICTION OF BRAKE TEMPERATURE DURING REPEATED BRAKING

During repeated braking, the vehicle is decelerated at a given deceleration from, e.g., 60 mph to zero speed, after which the vehicle is accelerated again to test speed and the next braking cycle is carried out. Repeated brake applications if not decelerated to zero speed usually are termed snubs. The rotor temperatures attained during repeated braking may be computed from simple analytical solutions, provided the braking energy, cooling intervals, or braking times remain unchanged during the test.

TABLE 3-2
BRAKE DESIGN VALUES

	LINING	PAD	DRUM OR DISC	UNITS
ρ	127	162	455	lbm/ft³
c	0.30	0.35	0.10	BTU/lbm·°F
k	0.67	0.7	28	BTU/h·°F·ft
a_t	0.0176	0.0124	0.615	ft²/h

Under these conditions the equation for computing the temperature increase during repeated brake applications may be expressed in a simple form. Assumptions are that the rotor can be treated as a lumped system — i.e., the rotor temperature is uniform throughout, that the heat transfer coefficient is constant, and that the thermal properties are constant. If the braking time is considerably less than the cooling time, then the cooling during braking may be neglected. In this case the rotor temperature will increase uniformly by (Ref. 2)

$$\Delta T = \frac{q_o t_s}{\rho_R c_R v_R} = \text{constant, deg F} \quad (3\text{-}16)$$

where

q_o = braking energy absorbed by the rotor, BTU/h
t_s = braking time to a stop, h
c_R = specific heat of rotor, BTU/lbm·°F
v_R = rotor volume, ft³
ρ_R = rotor density, lbm/ft³

The lumped formulation results in a differential equation describing the cooling of the brake after a brake application

$$\rho_R c_R v_R \frac{dT}{dt} = -h_R A_R (T - T_\infty) \text{ , BTU/h} \quad (3\text{-}17)$$

where

A_R = rotor surface area, ft²
h_R = heat transfer coefficient, BTU/h·°F·ft²
T = temperature at time t, °F
T_∞ = ambient temperature, °F

With an initial temperature of T_i, integration of Eq. 3-17 yields a cooling temperature response

$$\frac{T(t) - T_\infty}{T_i - T_\infty} = \exp\{[-h_R A_R/(\rho_R c_R v_R)]t\} \text{ , d'less} \quad (3\text{-}18)$$

An analysis combining heating by means of Eq. 3-16 and cooling by means of Eq. 3-18 may be developed to derive the temperatures of a brake before or after the first, second, third or nth brake application. The relative brake temperature before the nth brake application is

$$[T(t) - T_\infty]_b = \Delta T \left\langle 1 - \exp\{[-(n_a - 1)h_R A_R/(\rho_R c_R v_R)]t_c\} \times \exp\{[-h_R A_R/(\rho_R c_R v_R)]t_c\} \right\rangle \div \left\langle 1 - \exp\{[-h_R A_R/(\rho_R c_R v_R)]t_c\} \right\rangle, \text{deg F} \quad (3\text{-}19)$$

where

n_a = number of brake application, d'less
t_c = cooling time ≈ cycle time, h

The relative brake temperature after the nth application is

$$[T(t) - T_\infty]_a = \Delta T \left\langle 1 - \exp\{[-n_a h_R A_R/(\rho_R c_R v_R)]\, t_c\} \right\rangle \div \left\langle 1 - \exp\{[-h_R A_R/(\rho_R c_R v_R)]\, t_c\} \right\rangle, \text{deg F} \quad (3\text{-}20)$$

The limit values of the temperature before and after braking for a large number of cycles ($n \to \infty$) may be obtained from Eqs. 3-19 and 3-20 by dropping the term involving the factor n_a.

Road tests have shown that the minimum cooling times of most cars and light trucks are approximately 60 s between stops due to engine power limitations. The minimum braking time from 60 mph is approximately 5 s. Consequently, Eqs. 3-19 and 3-20 may be used in many applications for evaluating the brake temperatures attained during repeated braking.

However, if the braking time is not negligible as compared with the cooling time, then the cooling during braking has to be included in the analysis. The formulation results in the temperature response

$$T(t) = \{T_i - [T_\infty + q_o/(A_R h_R)]\} \times \exp\{[-h_R A_R/(\rho_R c_R v_R)]\, t_a\} + T_\infty + q_o/(A_R h_R) \text{ , °F} \quad (3\text{-}21)$$

where

q_o = braking energy absorbed by rotor, BTU/h
t_a = time during which brakes are applied, h

Eq. 3-21 gives the temperature rise during the brake period.

An analysis including heat transfer during braking may be developed in a similar fashion. In this case, Eq. 3-21 replaces Eq. 3-16. The cooling characteristics of the brake again are determined from Eq. 3-17. The resulting equations are lengthy and are not presented here.

3-1.6 PREDICTION OF CONVECTIVE HEAT TRANSFER COEFFICIENT

The computation of brake temperatures requires information on the convective heat transfer coefficient which varies with vehicle speed. In many cases it is sufficient to evaluate the heat transfer coefficient at some mean speed.

Computer solutions make it convenient to predict brake temperatures when the heat generation or convective heat transfer coefficient is variable during the braking process. Repeated brake applications, for example, which are encountered during snub testing, also may be evaluated by means of computer methods.

At the outset it should be stated that any relationships expressing the convective heat transfer coefficient will yield only approximate results. A difference between predicted and measured temperature levels of 10 to 30% may be considered normal. Often excellent "correlation" is obtained by adjusting the convective heat transfer coefficient until agreement between prediction and measurement is achieved.

It has been shown that experimental results of a cooling analysis can be represented by the product of dimensionless numbers raised to some power (Ref 6).

$$Nu = C\,Re^{m}\,Pr^{n_h} \quad \text{, d'less} \qquad (3\text{-}22)$$

where

$Nu = h_R L_c / k_a$ = Nusselt number, d'less
C = heat transfer constant, d'less
$Re = v\rho_a L_c / \mu_a$ = Reynolds number, d'less
$Pr = 3600 c_a \mu_a / k_a$ = Prandtl number, d'less
c_a = specific heat of air, BTU/lbm·°F
h_R = convective heat transfer coefficient, BTU/h·°F·ft²
L_c = characteristic length, ft
k_a = thermal conductivity of air, BTU/h·°F·ft
m = heat transfer parameter, d'less
n_h = heat transfer parameter, d'less
V = vehicle speed, ft/s
ρ_a = density of air, lbm/ft³
μ_a = viscosity of air, lbm/ft·s

The constant C in Eq. 3-22 is a function of the geometry of the brake and assumes different values for brake drums, solid rotors, and ventilated rotors. For ventilated rotors the value of C depends upon the shape of the vanes used for ventilation.

The heat transfer parameter m is a function of the type of flow, i.e., turbulent, laminar, or transition flow. For most practical cases m is a function of vehicle velocity and the associated brake rotor angular velocity. The heat transfer parameter n_h depends upon the thermal properties of the air. Since these properties are a function of temperature, the Prandtl number effect is nearly constant for most cases and is often included in the constant C of Eq. 3-22. The characteristic length L_c is either a length or diameter depending on the definition of the Nusselt or Reynolds number.

Textbooks on heat transfer provide a large number of empirical equations for predicting the convective heat transfer coefficient for a variety of test conditions and geometries. These equations generally apply to rotors not obstructed by tire and rim or disc brake caliper and are those associated with a cylinder (brake drum) or rotating circular disc (disc brake rotor).

For brake drums fully exposed to the air flow, the heat transfer coefficient h_R is (Ref. 7)

$$h_R = 0.1 \left(\frac{k_a}{D}\right) Re^{2/3} \quad \text{, BTU/h·°F·ft²} \qquad (3\text{-}23)$$

where

D = drum diameter, ft
k_a = thermal conductivity of air, BTU/h·°F·ft

For example, a 15-in. diameter drum moving through air at a speed of 60 mph at an ambient temperature of 100°F will exhibit a convective heat transfer coefficient of approximately 9 BTU/h·°F·ft². At 20 mph the convective heat transfer coefficient will only be about 3.5 BTU/ h·°F·ft². Eq. 3-23 is valid only for Reynolds numbers greater than 1000, i.e., driving conditions in which the forced convection outweighs the contribution due to natural convection.

For solid-rotor disc brakes the convection heat transfer coefficient associated with laminar flow may be approximated by

$$h_R = 0.70 \left(\frac{k_a}{D}\right) Re^{0.55} \quad \text{, BTU/h·°F·ft²} \qquad (3\text{-}24)$$

where

D = outer diameter, ft

For $Re > 2.4 \times 10^5$ the flow characteristics will become turbulent and the heat transfer coefficient may be expressed as

$$h_R = 0.04 \left(\frac{k_a}{D}\right) Re^{0.8} \quad \text{, BTU/h·°F·ft²} \qquad (3\text{-}25)$$

Eqs. 3-24 and 3-25 were obtained from experimental data collected with a disc brake system of a light truck (Ref. 2). Use the data of the previous example; a 15-in. outer diameter rotor at 60 mph will exhibit a convective heat transfer coefficient of approximately 20 BTU/h·°F·ft². For the example chosen, the transition from laminar to turbulent flow lies at about 24

mph. Consequently, the convective heat transfer coefficient at 20 mph is computed by Eq. 3-24 to be approximately 7 BTU/h·°F·ft².

A comparison of the computed heat transfer coefficient indicates clearly that a disc brake exhibits a higher convective heat transfer coefficient than a drum brake.

It should be noted that Eqs. 3-24 and 3-25 were obtained from experiments with two calipers located horizontally 180 deg apart (Ref. 2). The particular location of the caliper relative to the air flow may have a significant effect upon the cooling capacity of the disc brake.

Ventilated disc brakes generally exhibit convective heat transfer coefficients approximately twice as large as those associated with solid discs. The cooling effectiveness associated with the internal vanes tends to decrease somewhat for higher speeds due to the increased stagnation pressure of the air. The pumping action of the rotor is reduced as ambient air tends to enter the rotor at the front portion of brake due to vehicle speed.

For estimating purposes the following relationship may be used to obtain the heat coefficient inside the vanes of the brake rotor (Refs. 6 and 7).

$$h_R = 0.023 \left[1 + \left(\frac{d_h}{l}\right)^{0.67}\right] \times Re^{0.8} Pr^{0.33} \left(\frac{k_a}{d_h}\right), \text{BTU/h·°F·ft}^2 \quad (3\text{-}26)$$

where

$Re = (\rho_a d_h/\mu_a)\, V_{average}$, d'less
d_h = hydraulic diameter, ft
l = length of cooling vane, ft
$V_{average}$ = average velocity in vane, ft/s

Eq. 3-26 is valid for $Re > 10^4$, i.e., for turbulent flow. The hydraulic diameter is defined as the ratio of four times the cross-sectional flow area (wetted area) divided by the wetted perimeter as illustrated in Fig. 3-3. For vanes with varying cross-sectional size, an average hydraulic diameter is determined from the dimensions of the inlet and outlet locations on the vane.

The velocity associated with the Reynolds number is that existing in the vanes which is not identical to the foward speed of the vehicle.

For low values of velocity, laminar flow will exist in the vanes. For $Re < 10^4$ the convective heat transfer coefficient may be approximated by (Ref. 6)

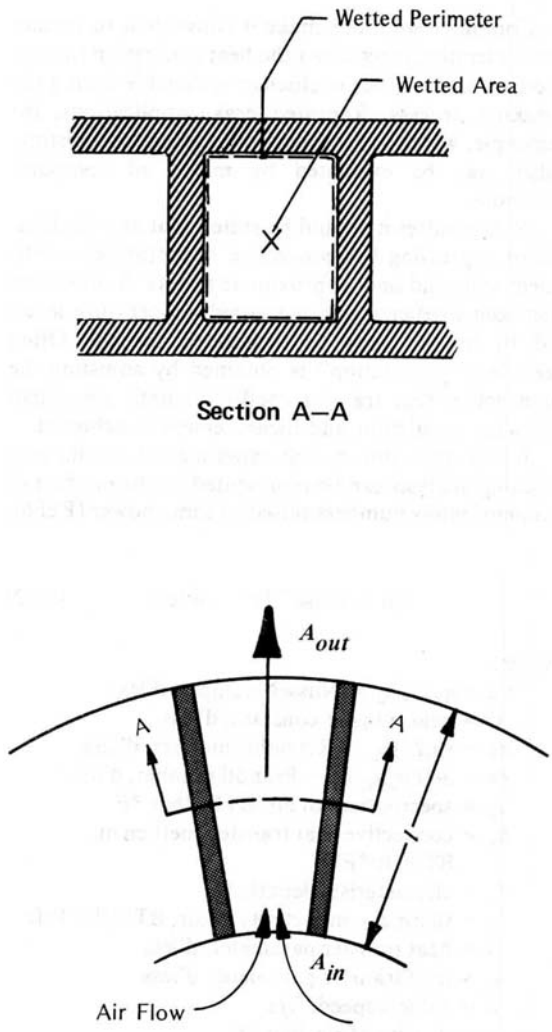

Figure 3-3. Ventilated Disc

$$h_R = 1.86(Re\ Pr)^{1/3} \left(\frac{d_h}{l}\right)^{0.33} \times \left(\frac{k_a}{d_h}\right), \text{BTU/h·°F·ft}^2 \quad (3\text{-}27)$$

The average velocity through the cooling vanes can be computed by

$$V_{average} = \frac{V_{in} + V_{out}}{2} \text{ , ft/s} \qquad (3\text{-}28)$$

where

$V_{in} = 0.052\, n_r\, (D^2 - d^2)^{1/2}$, ft/s
$V_{out} = V_{in}\, (A_{in}/A_{out})$, ft/s
A_{in} = inlet area, ft²
A_{out} = outlet area, ft²
D = outer diameter, ft
d = inner diameter, ft
n_r = revolutions per minute of rotor, rpm

The air flow rate m_a is determined by

$$m_a = 0.052\, n_r\, [(D^2 - d^2)\, A_{in}^2]^{1/2} \text{ , ft}^3\text{/s} \qquad (3\text{-}29)$$

The following example illustrates the use of Eqs. 3-26 through 3-28. A ventilated rotor with an outer diameter D = 1.25 ft, an inner diameter d = 0.75 ft, rotating at 800 rpm exhibits an inlet velocity of 41.6 ft/s as computed by the prior equation for inlet velocity. If the rotor has 30 vanes with a fin thickness of 0.25 in., then the ratio of inlet area to outlet area is 0.521. The outlet velocity is 21.68 ft/s. Consequently, the average velocity will be 31.64 ft/s. The Reynolds number is 10,719 based on an average hydraulic diameter of 0.974 in. The hydraulic diameter was computed for an inner vane width of 1 in. The convective heat transfer coefficient computed with Eq. 3-26 is 10.8 BTU/h·°F·ft². The detailed analysis of Eq. 3-26 indicates that the entrance effects cause an increase of the convective heat transfer coefficient by approximately 47%. If the rotor rotates at 300 rpm, the convective heat transfer coefficient is 3.8 BTU/h·°F·ft² as computed by Eq. 3-27.

If the ventilated rotor is exposed to the air, i.e., the friction surfaces are not shielded, then the convective heat transfer coefficient is obtained by the summation of the heat transfer coefficients of Eq. 3-25 and 3-26, or 3-24 and 3-27, depending on whether turbulent or laminar flow exists.

At higher temperatures the radiative cooling capacity of the brake has to be considered. A radiative heat transfer coefficient $h_{R,\,rad}$ may be defined by (Refs. 2 and 6)

$$h_{R,\,rad} = \frac{\sigma\, \epsilon_R\, (T_R^4 - T_\infty^4)}{T_R - T_\infty} \text{ , BTU/h·°F·ft}^2 \qquad (3\text{-}30)$$

where

T_R = rotor surface temperature, °R
T_∞ = ambient temperature, °R
ϵ_R = rotor surface emissivity, d'less
σ = Stefan-Boltzmann constant
= 0.1714×10^{-8} BTU/h·ft²·°R⁴

Evaluation of Eq. 3-30 using ϵ_R = 0.55, a value typical of machined cast iron surfaces of brake rotors, yields the radiative heat transfer characteristics illustrated in Fig. 3-4. It is apparent that significant radiation cooling does not occur until high brake temperatures are attained.

Road test data obtained from testing of heavy vehicles indicate that the convective heat transfer coefficient associated with drum brakes may be approximated by a functional relationship of the form (Ref. 8)

$$h_R = 0.92 + \beta\, V \times \exp(-V/328) \text{ , BTU/h·°F·ft}^2 \qquad (3\text{-}31)$$

where

V = vehicle speed, ft/s
β = 0.70 for front brake drum, BTU·s/h·°F·ft³
β = 0.30 for rear brake drum, BTU·s/h·°F·ft³

The corresponding values of β associated with the heat transfer from the brake shoes inside the brake

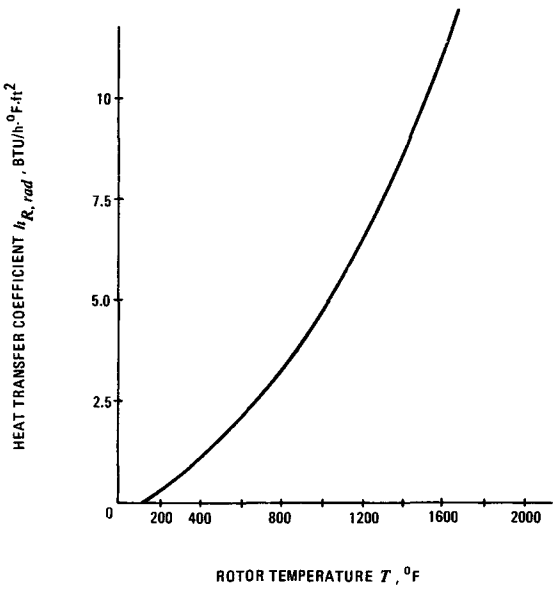

Figure 3-4. Radiative Heat Transfer Coefficient as Function of Temperature

assembly were found to be 0.15 and 0.06, respectively. When the vehicle is braked to rest, the convective cooling capacity is reduced to that of natural convection indicated by 0.92 BTU/h·°F·ft² in Eq. 3-31.

3-1.7 COMPUTER METHODS FOR PREDICTING BRAKE TEMPERATURE

The numerical methods for solving steady-state problems are not discussed here, since the steady-state temperatures are of less importance in braking analysis than time-dependent temperature distributions. The reader is referred to standard text books on heat transfer (Refs. 3 and 6). In the unsteady-state system the initial temperature distribution is known; however, its variation with time must be determined.

The system, i.e., the drum or disc thickness is divided into a number of discrete nodal points as illustrated in Fig. 3-5. Application of the first law of thermodynamics to each individual node results in a set of algebraic equations whose solution will yield individual nodal temperatures for each finite time interval. It is therefore necessary to deduce the temperature distribution at some future time from a given distribution at an earlier time, the earliest time being that associated with the known initial distribution.

The relationship expressing heat conduction between two nodes is known as Fourier's Conduction Law and may be stated in the form of an exact integral

$$q_{ij} = \int_{\Delta y} -k\left(\frac{\partial T}{\partial x}\right) b\, dy \text{ , BTU/h}$$

$$\approx -k\left(\frac{dT}{dx}\right)_{average} b\,\Delta y \approx -k\left(\frac{\Delta T}{\Delta x}\right)_{av} b\,\Delta y \qquad (3\text{-}32)$$

where

q_{ij} = heat flow between nodal points i and j, BTU/h
b = width of plate, ft
Δx = horizontal distance between two adjacent nodal points, ft
Δy = vertical distance between two adjacent nodal points, ft
$\partial T/\partial x$ = temperature gradient, deg F/ft

The distances Δx, Δy, and b designate control volume size, and k the thermal conductivity of the material. Eq. 3-32 may be rewritten in the form of the temperature of the two nodal points

$$q_{ij} = -\frac{k(T_j - T_i)\, b\, \Delta y}{\Delta x} \text{ , BTU/h} \qquad (3\text{-}33)$$

where

T_i = temperature of node i, °F
T_j = temperature of node j, °F

For two-dimensional problems and a square grid with $\Delta x = \Delta y$, the basic heat conduction between two nodal points becomes

$$q_{ij} = k(T_i - T_j)\, b \text{ , BTU/h} \qquad (3\text{-}34)$$

For one-dimensional systems such as brake rotors under consideration, the basic heat conduction equation with Δy equal to unity becomes

$$q_{ij} = \frac{k_R(T_i - T_j)\, b}{\Delta x} \text{ , BTU/h} \qquad (3\text{-}35)$$

With the mass contained in the control volume of thickness Δx, $\delta m = \rho_R \Delta x b(1)$, and the change in enthalpy, $\Delta h = c_R\, \Delta T$, the first law of thermodynamics

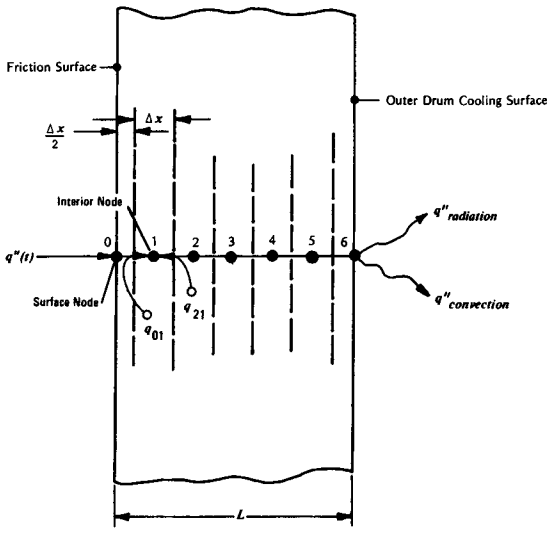

Figure 3-5. Thermal Model for Finite Difference Computation (Drum Brake Shown)

applied, e.g., to the interior node 2 results in the expression (Fig. 3-5)

$$\rho_R \Delta x\, b\, c_R \left(\frac{T_2' - T_2}{\Delta t}\right)$$

$$= k_R \left(\frac{T_1 - T_2}{\Delta x}\right) b + k_R \left(\frac{T_3 - T_2}{\Delta x}\right) b \text{ , BTU/h}$$

Here T_2' represents the temperature attained by node 2 after the time interval Δt has elapsed. Solving for T_2' yields

$$T_2' = \frac{1}{M}(T_3 + T_1) + \left(1 - \frac{2}{M}\right) T_2 \text{ , °F} \quad (3\text{-}36)$$

where

$M = (\Delta x)^2/(a_t \Delta t)$, d'less
a_t = thermal diffusivity, ft²/h
Δt = time interval, h

Eq. 3-36 may be expressed for any arbitrary interior point n in the form

$$T_n' = \frac{1}{M}(T_{n+1} + T_{n-1}) + \left(1 - \frac{2}{M}\right) T_n \text{ , °F} \quad (3\text{-}37)$$

Application of the first law to a surface point yields (Fig. 3-5)

$$T_o' = \left(1 - \frac{2N + 2}{M}\right) T_o + \frac{2N}{M} T_\infty + \frac{2}{M} T_1$$

$$+ \left(\frac{2\Delta x}{k_R M}\right) q_R'' - \left(\frac{2\Delta x}{k_R M}\right) q''_{rad} \text{, °F} \quad (3\text{-}38)$$

where

$M = (\Delta x)^2/(a_t \Delta t)$, d'less
$N = h_R \Delta x/k$, d'less
q''_{rad} = radiation heat flux away from surface
$= \epsilon\, \sigma[(T_o + 460)^4 - (T_\infty + 460)^4]$, BTU/h·ft²
q_R'' = heat flux absorbed by the rotor computed from Eq. 3-43, BTU/h·ft²
T_∞ = ambient temperature, °F
ϵ_R = emissivity, ≈ 0.8 for black drum surfaces, 0.55 for metallic disc surfaces, d'less
σ = Stefan-Boltzmann constant, 0.1714 × 10^{-8}, BTU/h·ft²·°R⁴

Stability conditions require that M be chosen equal to or greater than $2N + 2$, i.e.,

$$M \geq 2N + 2 \text{ , d'less} \quad (3\text{-}39)$$

Otherwise the coefficient of T_o assumes negative values resulting in an unstable temperature solution. The time step Δt and grid size may be chosen arbitrarily, provided the condition in Eq. 3-39 is satisfied.

This type of finite difference method is sometimes called "marching type solution" since the new temperatures of each node after the first time step are computed from Eqs. 3-37 and 3-38 with the initial temperatures introduced on the right-hand side of the equations. The computed temperatures are then used to determine the new temperature of each nodal point after the second time interval.

Other important equations used in the finite-difference analysis are presented next.

The deceleration a_x of the vehicle can be determined from design information (Ref. 4) as

$$a_x = \frac{32.2}{W} \sum_{i\,=\,\text{no. of axles}} \left[n_C\, p_l\, A_{WC}\, \eta\, BF \left(\frac{r_m}{R}\right)\right], \text{ ft/s}^2 \quad (3\text{-}40)$$

where

A_{WC} = wheel cylinder area, in.²
BF = brake factor, defined as ratio of rotor drag force to applying normal force of one caliper or brake shoe, d'less
n_C = number of calipers per axle, d'less
p_l = brake line pressure, psi
R = effective tire radius, ft
r_m = effective rotor radius, ft
W = test weight of the vehicle, lb
η = mechanical efficiency, 0.96 accounting for frictional losses in the wheel cylinder, d'less

The coefficient of friction required for computing the brake factor was assumed to be a function of brake temperature. The frictional characteristics of the brake pads used in this investigation can be described by a functional relationship of the form

$$\mu_L = \mu_{Lc} - f \Delta T \text{ , d'less} \quad (3\text{-}41)$$

where

$f = (\mu_{Lc} - \mu_{Lh})/\Delta T$, a thermal fade factor expressing the change in pad friction coefficient per °F, (°F)⁻¹
ΔT = brake temperature change, deg F

μ_L = lining/rotor friction coefficient, d'less
μ_{Lc} = coefficient of friction for the cold brake (below 200°F), d'less
μ_{Lh} = coefficient of friction at high temperatures, d'less

The instantaneous velocity V of the test vehicle is given by the relationship

$$V = V_1 - a_x \Delta t, \text{ ft/s} \qquad (3\text{-}42)$$

where
a_x = vehicle deceleration, ft/s²
V_1 = speed at commencement of Δt, ft/s
Δt = time step used in the finite-difference program, s

The instantaneous heat flux q''_R per rotor friction surface is determined from

$$q''_R = \mu_L p_l A_{WC} \eta (1 - s) V (r_i/R)(n_c/2) \times \frac{3600}{(778)(2)} \left(\frac{\gamma}{A_f}\right), \text{BTU/h·ft}^2 \qquad (3\text{-}43)$$

where
A_f = friction area of one rotor side, ft²
r_i = distance of nodal point i from the center of rotor, ft
s = tire slip, d'less
γ = heat distribution to the rotor computed from Eq. 3-5 or 3-8, d'less

For drum brakes r_i = constant = radius to drum friction surface and A_f = total swept area.

Some results obtained with computer programs for predicting brake temperature during repeated (fade test) and continuous application (brake rating test) are presented next.

In the fade test the vehicle was decelerated from 60 mph to 10 mph and subsequently accelerated again to 60 mph as fast as possible. Typical temperatures obtained for a 25,000-lb GVW truck after each snub during a three snub test are presented in Fig. 3-6 in which the lining temperature, measured approximately 0.1 in. below the friction surface, is compared to theoretical predictions. The test data shown are the average values between the left and right rear wheels. Although the correlation as shown in Fig. 3-6 is good, in general, differences between experimental and theoretical results as high as 20-30% may be encountered in experimental and analytical results.

In the brake rating test the vehicle is pulled with its brakes applied to a specific brake line pressure. The test is continued until the draw bar pull has decreased to a certain value. Typical results obtained for a 25,000-lb GVW are illustrated in Fig. 3-7, in which the measured brake lining temperatures, averaged between the left and right rear brakes, are compared to theoretical predictions.

3-1.8 ANALYSIS OF SEALED BRAKES

The sealed brake is designed to accomplish two basic functions:

1. Absorb and dissipate the kinetic energy of the vehicle at its maximum speed.
2. Protect the brake against damage from adverse environment such as ice, snow, water, mud, dirt, and dust.

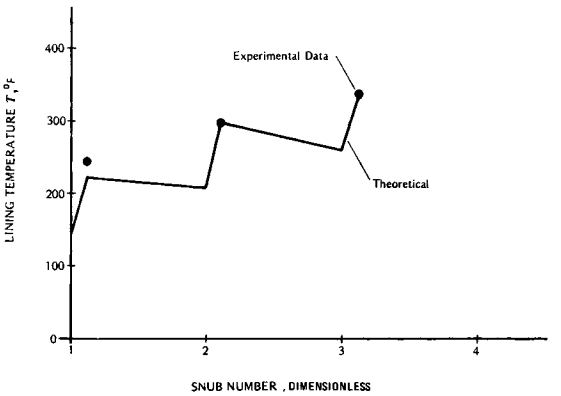

Figure 3-6. Brake Lining Temperature Attained in Fade Test

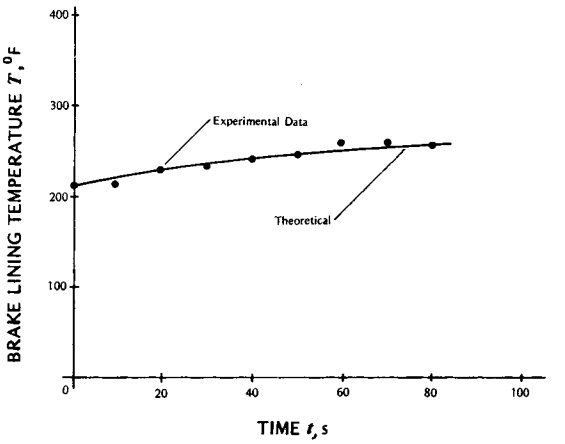

Figure 3-7. Brake Lining Temperature Attained in Brake Rating Test

Sealing the brakes allows the vehicle to be operated in an off-road environment by keeping the internal brake parts free from outside contamination. The exclusion of abrasive elements results in greater safety, high reliability, and increased life for lining and metal surfaces. This reduces vehicle down time required for replacement and servicing of brake parts due to normal wear. An important consideration is the rubbing speed of the seals. Sealed brakes are often designed so that the seal is resting on the sliding surface only at low speeds, while at higher speeds centrifugal force or air pressure forces the seal off the sliding surface. Since high vehicle speeds in off-road terrain are unlikely, the life of the seals is increased significantly with speed sensitive sealing designs.

Dissipation of heat generated during braking is accomplished by circulating cooling fluid around the metal surfaces of the brake. A study of the energy absorption capacity of the various fluids shows that oil has an outstanding capacity, and that air is reasonably close to oil. Water is also good, but its freezing characteristics make it a poor candidate. An eutectic mixture of water and ethlene glycol eliminates the freezing problem but has only about one-third of the energy absorption capacity of oil and one-half that of air, as shown in Table 3-3.

An example of an oil-cooled disc brake system is represented by a sealed-oil-cooled, multi-disc, self-adjusting service brake. The brake assembly is made up of a set of multiple disc plates, an annular piston, a coolant pump, a face type seal assembly, a labyrinth seal assembly, an automatic adjuster sleeve, and a piston return spring assembled within the brake housing and cover. The brake is actuated by hydraulic pressure from a hydraulic supply system acting on the annular piston.

TABLE 3-3
ENERGY ABSORPTION CAPACITY OF VARIOUS FLUIDS

Fluid	State	Energy Absorption Capacity, ft·lb/lbm
Air	Gas	74,000
Water	Liquid	62,200
Oil	Liquid	99,500
Mixture water and ethylene glycol	Liquid	≈33,000

As braking action takes place between stationary and rotating discs, cooling oil is pumped through the assembly to absorb the heat generated. The coolant is pumped either by an integral turbine type pump which is driven by a floating gear between two driven discs, or by an external pump. The cooling oil flows from the brake assembly through piping to an oil-to-water heat exchanger mounted within the truck radiator. Piping returns the cooled oil to the brake disc pack cavity, completing the cooling oil hydraulic loop. A "zero" line also is routed from the oil reservoir to the pump inlet to eliminate the possibility of cavitation.

During braking, the cooling oil pump delivers maximum oil flow under low pressure to the heat exchanger. However, when the brake actuating force is removed, releasing the brake disc, the pump drive gear settles into a neutral position between its two adjacent driven discs. The increased operating clearances between the pump and the discs reduces the output effectiveness of the coolant pump. The resulting reduced cooling flow provides sufficient after cooling with negligible spin losses when the brakes are not applied.

Assembly sealing is divided into two elements: (1) sealing the hydraulic supply system from the cooling oil system and (2) sealing internal components from the external environment.

To provide adequate cooling at the surface of the disc plates, the cooling oil must be distributed uniformly to all the discs and directed through the discs to obtain maximum heat transfer from the discs to the oil. Uniform distribution of oil to all discs in the stack is obtained by design of plate hubs and housing for optimum coolant flow and by proper location of oil inlet and outlet connections to the brake housing. The direction of oil flow must be from the outside periphery to the inside diameter of the discs in order to counter the natural pumping action of the plates and insure even distribution of cooling oil across the face of the discs. Experience has shown that oil flowing from inside to outside diameter tends to channel in a few grooves in the lined discs, resulting in local hot spots. Oil flow through the discs is provided by grooves cut in the friction material. The engine radiator is used frequently as heat exchanger for cooling the liquid (Ref. 9).

In specialty vehicles such as earth moving equipment sealed oil-cooled brakes use a large reservoir in the wheel rather than a pump circulating the coolant.

The temperature analysis of liquid cooled brakes is similar to that of an engine heat exchange process. The heat generated at the wheel brakes is dissipated to the ambient air by means of a heat exchanger or

radiator. The heat generation at the friction brake is determined from Eq. 3-1 or 3-2.

For example, for the downhill braking mode the energy $q_{o,RB}$ absorbed by one brake of the rear axle of a two-axle vehicle is (Ref. 10)

$$q_{o,RB} = \frac{W V (G - R_r) \phi \times 3600}{(778)(2)}, \text{BTU/h} \quad (3\text{-}44)$$

where

ϕ = rear axle brake force divided by total brake force, d'less

For continued braking, the capacity of the liquid cooled brakes is not limited, provided the radiator heat transfer is

$$h_{rad} A_{rad} \Delta T_{rad} = \sum_{\text{no. of brakes}} q_{o,B}, \text{BTU/h} \quad (3\text{-}45)$$

where

h_{rad} = convective heat transfer coefficient of the radiator, BTU/h·°F·ft²

A_{rad} = cooling area of radiator, ft²

ΔT_{rad} = mean temperature difference of cooling liquid and air in radiator, deg F

$q_{o,B}$ = energy absorbed per single brake, BTU/h

A rough estimate indicates that the cooling capacity of the engine radiator is approximately 90 to 100% of the engine horsepower. Additional cooling of about 10 to 20% is provided by external heat transfer from the wheel brake surfaces and connecting lines being exposed to convective air flow. The heat transfer coefficient of the engine radiator is dependent on speed and assumes values between 20 to 30 BTU/h·°F·ft² for vehicle speeds of 60 mph.

For a sealed brake of another design, air was selected as the coolant for the brakes since its heat absorption capacity based on mass compares favorably with other suitable fluids. A ventilated or fan type disc was selected to aid in circulating the cooling air and to increase the heat exchange surface by the area of the radial fan blades. This cooling action is needed to disperse the heat which has been stored during the stop from the disc. When the vehicle is regaining speed, the ventilated disc has about twice the dissipation rate of a solid disc. The greater kinetic energy conversion capacity of the ventilated disc makes it most appropriate for the system.

After air was selected as a coolant the following design problems were considered:

1. Since air is a gas, the volume of fluid to be circulated in the brake system is much greater than for a liquid. Therefore, the air ducting is larger than hydraulic tubing.

2. The sealing problem was not considered to be serious because it is necessary to circulate air through the brake enclosure. The air being expelled past a simple labyrinth at a slight pressure prevents contaminates from entering the brake assembly.

3. Cooling is accomplished by circulating the air from the blower around the disc to dissipate the heat generated by each stop within the time the vehicle can be accelerated again to full speed.

4. Dust generated by the friction material is blown from the enclosed brake.

5. The ducts bringing the cooling air into the sealed brake assembly are flexible, to allow front wheel steering movement and the relative motion between the axles and the vehicle frame.

The design of the brake rotor is based on Eq. 3-21 for a continued downhill brake operation. The convective heat transfer coefficient required for sufficient cooling may be determined from par. 3-1.6. The heat transfer coefficient necessitates a minimum level of air convected over the rotor surfaces. Consequently, the blower must satisfy the requirements for sufficient air flow as well as for sufficient air pressure to keep the brakes free from contamination. The minimum air pressure required to push water out of the brake depends upon the water depth through which the vehicle may travel and the specific weight of the water or mud.

3-2 THERMAL STRESS ANALYSIS

3-2.1 FUNDAMENTALS ASSOCIATED WITH THERMAL CRACKS

Surface cracking due to thermal loading may occur as the result of two phenomena: thermal shock and/or thermal fatigue. Thermal shock exists when a single application of the heat flux and subsequent cooling produce surface failure. Thermal fatigue exists when a series of heating and cooling cycles results in surface failure. If temperature changes of sufficient magnitude exist at the rotor surface, then heat cracks generally oriented in a radial direction will develop. One of the requirements for heat cracking to occur is that the thermal stresses exceed the elastic limit of the material, causing plastic deformations to develop at the surface. In the subsequent cooling cycle the original dimensions can no longer be attained, thus producing tensile stresses which exceed the ultimate strength of the material (Ref. 4).

This process may be illustrated by the simple analysis that follows. An element taken out of the x-y plane of the surface of an infinite plate is illustrated in Fig. 3-8. Upon severe thermal loading the high temperature difference between the suffface and the interior will cause compressive stresses. At the instant the material near the surface exceeds the yield strength, the stress state can only cause a material flow in the direction of the surface as schematically indicated in Fig. 3-8. During the cooling period the compressive stresses change into tensile stresses. The plastic flow in the opposite direction cannot be completed to its original geometrical form, giving rise to tensile stresses that exceed the ultimate strength of the material. This may be considered as the onset of surface cracking.

The approximate compressive stresses σ developed in the surface layer of a flat plate as a result of a sudden temperature increase are (Refs. 4 and 11)

$$\sigma = -\left(\frac{E}{1-\nu}\right)\alpha_t \Delta T, \text{ psi} \qquad (3\text{-}46)$$

where

E = elastic modulus, psi
α_t = thermal expansion coefficient, in./°F·in.
ΔT = temperature increase, deg F
ν = Poisson's ratio, d'less

If one uses typical cast iron material properties, the theoretical temperature increase required for the compressive stresses to exceed the yield strength of the material is approximately equal to 1500 deg F. However, data on material properties of cast iron are not too reliable. For example, the tensile strength of ferritic malleable iron decreases with temperature to as much as 20% of the strength exhibited at room temperature. Also, the elastic modulus may vary. If one considers these factors, a sudden temperature increase at the surface of only 300 to 500 deg F may be sufficient for failure to occur.

Temperature analyses have shown that the brake rotor is almost at a uniformly decreasing temperature during cooling. However, thermal fatigue will exist when the cooling characteristics of the brake are such that the highly elongated surface layer can no longer attain the original length, resulting in residual tensile stresses in the generally highly loaded friction surface.

The occurrence of surface cracking depends, among other things, upon the sensitivity of the material to temperature changes at the surface as expressed by Eq. 3-46. In a more complete analysis at least the following parameters or variables are considered to have an effect upon the sensitivity of the material to thermal shock fatigue produced by temperature changes:

1. Thermal diffusivity
2. Thermal expansion coefficient
3. Elastic modulus
4. Poisson's ratio
5. Rate of change of temperature
6. Temperature gradient at the surface
7. Maximum and minimum temperature difference during repeated braking
8. The change of stress produced by a change of strain
9. Geometry of the rotor.

Furthermore, some of the parameters are dependent upon the stress state and temperature, indicating that an exact theoretical prediction, e.g., the number of cycles required for surface failure to occur is a difficult task. However, the number of cycles of repeated braking has been found to be convenient for

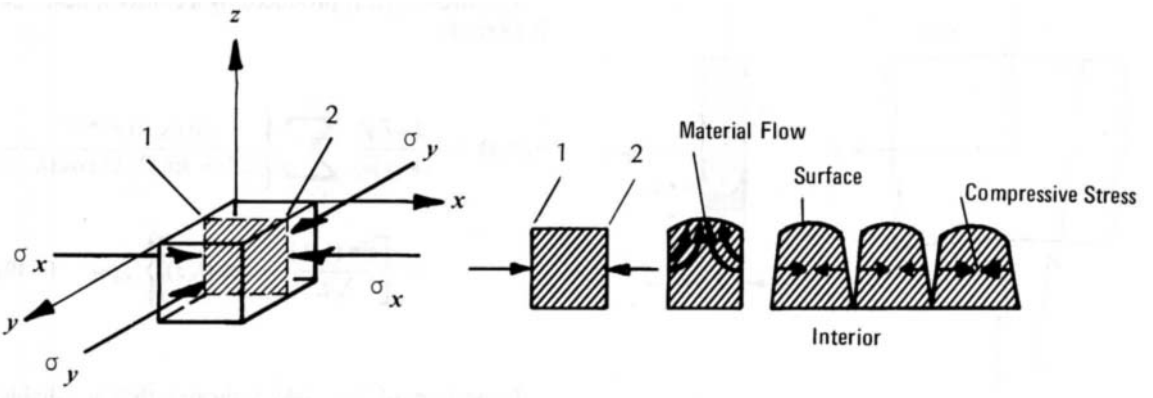

Figure 3-8. Thermally Loaded Surface Element Resulting in Surface Rupture

expressing the capability of the brake rotor to withstand surface failure under certain thermal braking conditions. The sensitivity of the rotor to changes in surface temperature may then be expressed by the reciprocal of the number of cycles required for surface failure to occur.

3-2.2 THERMAL STRESSES IN SOLID-ROTOR DISC BRAKES

The thermal stresses result from nonuniform temperature distributions. In addition, mechanical stresses may arise from body deformation or body forces. In most practical thermal stress problems it is permissible to separate the temperature problem from the stress problem and solve both consecutively. This approach contains the assumption that the temperature response is only a function of thermal conditions and is not affected by body deformation. It also is assumed that inertia effects resulting from body deformation are negligible.

In Eq. 3-46 the approximate surface stresses attained in an infinite plane were determined. An improvement can be obtained by treating the rotor as a thin plate as illustrated in Fig. 3-9, yielding a plane stress problem. Although this approximation does not describe the stresses accurately over the entire friction surface, adequate accuracy is obtained at distances from the edges larger than about one-half plate thickness. The assumptions which follow were made using the schematic shown in Fig. 3-9:

1. Surface traction is negligible.
2. Body forces are negligible.
3. The temperature is a function of thickness z and time t only.
4. The temperature distribution is symmetrical.

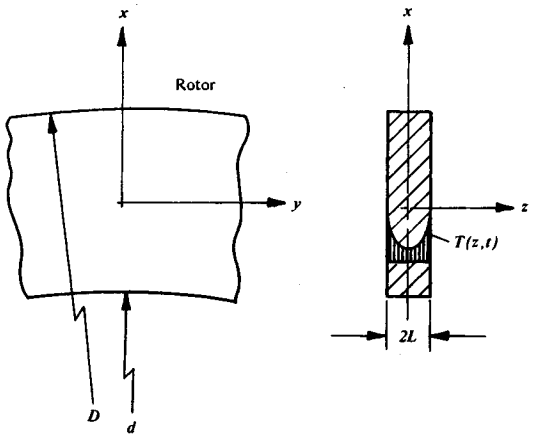

Figure 3-9. Flat Plate Representation of Brake Rotor

The stress analysis of a free plate yields the expression for computing the thermal stresses in the rotor

$$\sigma_x = \sigma_y = \frac{\alpha_t E}{1-\nu}\left[-T(z) + \frac{1}{L}\int_0^L T(z)\,dz\right], \text{ psi} \quad (3\text{-}47)$$

where

L = one half rotor thickness, ft
$T(z)$ = temperature distribution over z, °F
σ_x = stress in x-direction, psi
σ_y = stress in y-direction, psi

The thermal stresses $\sigma(z, t)$ produced by a linearly decreasing heat flux are determined from the temperature response given by Eq. 3-13 for a solid rotor and Eq. 3-47 as (Ref. 4)

$$\sigma(z,t) = \frac{q''_{(o)}}{q''_o}\sigma_o(z,t) + \frac{2q''_{(o)}\alpha_t E}{t_s(1-\nu)h_R} \times \sum_{n=1}^{\infty}\left\{\frac{\sin(\lambda_n L)}{\lambda_n L + \sin(\lambda_n L)\cos(\lambda_n L)} \times \frac{1-e^{-\alpha_t\lambda_n^2 t}}{\alpha_t\lambda_n^2} \times \left[\frac{\sin(\lambda_n L)}{\lambda_n L} - \cos(\lambda_n z)\right]\right\}, \text{ psi} \quad (3\text{-}48)$$

where

L = one-half rotor thickness, ft
t_s = stopping time, h
$\sigma_o(z, t)$ = stress produced by a constant heat flux, psi

The stress $\sigma_o(z, t)$ produced by a constant heat flux is (Ref. 4)

$$\sigma_o(z,t) = \frac{2\alpha_t E q''_o}{(1-\nu)h_R}\sum_{n=1}^{\infty}\left\{\frac{\sin(\lambda_n L)\,e^{-\alpha_t\lambda_n^2 t}}{\lambda_n L + \sin(\lambda_n L)\cos(\lambda_n L)} \times \left[\frac{\sin(\lambda_n L)}{\lambda_n L} - \cos(\lambda_n z)\right]\right\}, \text{ psi} \quad (3\text{-}49)$$

Inspection of Eq. 3-48 indicates that a reliable evaluation requires the use of a computer.

The theoretical thermal stresses at the surface computed from Eq. 3-48 for stops from 60 and 80 mph are illustrated in Fig. 3-10. The stresses at the surface are also the maximum stresses exhibited by the rotor. This is evident from the term cos $(\lambda_n z)$ in Eq. 3-48. For example, the stresses at the mid plane with $z = 0$ will be at a minimum since cos 0 = 1. Inspection of the curves in Fig. 3-10 indicates a maximum near a braking time of 1 s. The maximum compressive stress attained in a stop from 60 mph is approximately equal to 25,000 psi. The total compressive stress easily may attain values between 27,000 and 28,000 psi when the mechanical stresses resulting from centrifugal forces and torque transmission are considered also.

Since thermal shock and subsequent surface cracking is a direct function of the initial temperature gradient at the swept rotor surface, Eq. 3-48 also may be used to approximate the thermal stresses produced in the ventilated rotor. In this case L equals the flange thickness.

3-2.3 THERMAL STRESSES IN BRAKE DRUMS

The detailed equations for predicting the thermal stresses in brake drums are very complicated. Approximate equations may be given for drums with the ratio of drum width to drum radius much less than unity (Refs. 12 and 13). However, this approach would exclude a large number of brakes, especially those for heavy vehicles.

A rough estimate of the thermal stresses produced in a single stop may be obtained from Eq. 4-46.

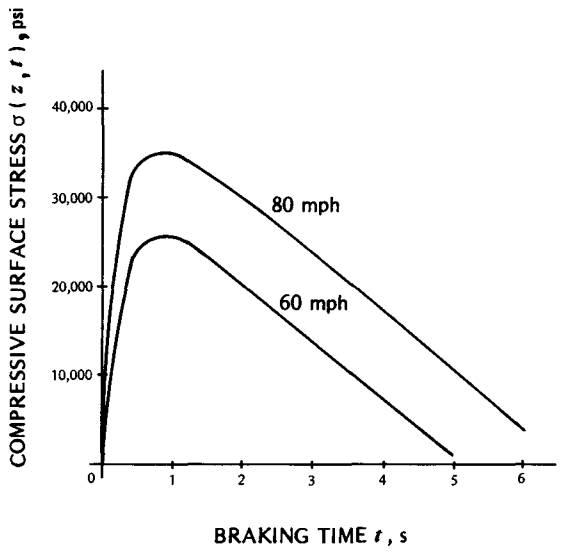

Figure 3-10. Thermal Stresses at the Surface Attained in Stops from 60 and 80 mph

REFERENCES

1. H. Dorner, "Fundamental Principles for the Calculation of the Braking Potential of Motor Vehicle Brakes During Continuous and Intermittent Application", *Deutsche Kraftfahrtforschung und Strassenverkehrstecknik*, No. 165, 1963.
2. R. Limpert, *Temperature and Stress Analysis of Solid-Rotor Disc Brakes*, Ph.D. dissertation, University of Michigan, 1972.
3. V. Arpaci, *Conduction Heat Transfer*, Addison-Wesley Publishing Company, Reading, Massachusetts, 1966.
4. R. Limpert, *An Investigation of Thermal Conditions Leading to Surface Rupture of Cast Iron Rotors*, SAE Paper No. 720447, Detroit, May 1972.
5. R. Limpert, *The Thermal Performance of Automotive Disc Brakes*, SAE Paper No. 750873, Detroit, October 1975.
6. F. Kreith, *Principles of Heat Transfer*, International Textbook Company, Scranton, Pennsylvania, 1965.
7. R. Limpert, *Cooling Analysis of Disc Brake Rotors*, SAE Paper No. 751014, Truck Meeting, Philadelphia, November 1975.
8. R. Murphy, et al., *Bus, Truck, Tractor-Trailer Braking System Performance*, Final Report, Contract FH-11-7290, U.S. Department of Transportation, March 1971.
9. AMCP 706-361, Engineering Design Handbook, *Military Vehicle Power Plant Cooling*.
10. R. Limpert, *An Investigation of Integrated Retarder/Foundation Brake Systems for Commercial Vehicles*, SAE Paper No. 750126, Detroit, February 1975.
11. Boley and Weiner, *Theory of Thermal Stresses*, John Wiley & Sons, Inc., New York, 1967.
12. Youngdahl and Sternberg, "Transient Thermal Stresses in a Circular Cylinder", *ASME Journal of Applied Mechanics*, 1961.
13. H. Hasselgruber, "On the Calculation of Thermal Stresses in Brake Drums of Motor Vehicles During Braking to a Stop", *Automobiltechnische Zeitschrift*, Vol. 56, No. 2, Februrary 1954, pp. 47-50.

CHAPTER 4
ANALYSIS OF AUXILIARY BRAKES

In this chapter several different auxiliary retarding devices are discussed. Exhaust brakes, and hydrodynamic and electric retarders are compared in their effectiveness.

Simplified engineering equations are presented for a general evaluation of auxiliary brakes.

The advantages of integrated retarder/foundation brake controls are discussed.

4-0 LIST OF SYMBOLS

A_{rad} = cooling area of radiator, ft²
c_p = specific heat of air at constant pressure, BTU/°F·lbm
F_{ret} = retarding force at vehicle drive wheels, lb
G = road gradient, d'less*
h_{rad} = heat transfer coefficient of engine radiator, BTU/h·°F·ft²
M_e = engine retarding torque, lb·ft
m_a = mass flow rate of cooling air, lbm/h
p_m = average retarding pressure in combustion chamber, psi
R = effective tire radius, ft
R_r = rolling resistance coefficient, d'less
V = vehicle speed, ft/s
v_e = engine displacement, in.³
W = vehicle weight, lb
W_1 = weight of truck, lb
W_2 = weight of trailer, lb
α = slope angle, deg
ΔT_R = difference of temperature of air entering and leaving rotor, deg F
ΔT_{rad} = mean temperature difference of water and air in radiator, deg F
n_T = efficiency of transmission, d'less
μ_R = tire-road friction coefficient of braked rear axle, d'less
ρ = transmission ratio between engine and wheels, d'less
χ = height of center of gravity of truck divided by wheel base of truck, d'less
ψ = static rear axle load of truck divided by truck weight, d'less

4-1 EXHAUST BRAKES

Auxiliary brakes may be divided into two classes: engine brakes and transmission or propeller shaft brakes. In the case of the engine brake, the retarding torque transmission can be interrupted by disengaging the clutch or selecting a neutral gear position. The propeller shaft brake, once applied, can be disconnected from the retarded wheels only through release of the control lever.

The engine of a vehicle in motion will, if the throttle is closed, exert a retarding force on the vehicle as a portion of the kinetic energy is absorbed by the frictional, compressive, and other mechanical losses in the engine (Refs. 1, 2, and 3). This retarding force is, however, very limited, and various methods have been devised for increasing the effectiveness of the engine as a brake. One such improvement consists of increasing the compressor action of the engine by closing off the exhaust. Retarders of this type are generally termed exhaust brakes. This type of retarder consists of a throttle in the exhaust system which can be closed either by mechanical, electrical, or pneumatic means. The brake torque generated depends on the gearing and engine speed. In general, at moderate and high velocities the primary braking system also must be applied since the generated brake torque is limited to about 70% of the motor drive torque. The major limiting design factor of an exhaust brake is associated with the exit valve spring. Increased pressure in the exhaust system tends to overcome the valve spring, forcing the valve to stay open and consequently limiting the compressor action.

Further improvement in engine brake torque can be achieved by altering the camshaft timing such that the compressor action of the engine is increased. The engine brake torque may be over 100% of the maximum drive torque of the engine. Large retarding torques, however, can only be achieved by using a low gear, which in turn results in undesirably low cruising speeds and thus increased per mile operating costs. No adverse effects on engine wear have been observed with this type of brake (Ref. 4). It is claimed that shoe and drum wear can be reduced from 25-50% with the use of exhaust brakes, depending on conditions. Reference throughout has been to diesel-engine equipped vehicles for which the brake specifically is intended, but an exhaust brake also can be fitted to a gasoline engine. Its performance may be

*d'less = dimensionless

slightly lower since the gasoline engine, operating on a lower compression ratio, necessarily has a larger clearance volume and is thus less effective when used as a compressor. Of significance is the effect of engine braking on the thermal state of the combustion engine. Changing thermal conditions (undercooling) may cause premature wear and related problems. Research findings indicate that, when braking on a downhill grade while using the wheel brakes, the combustion cylinder surface temperature decreased from 401° to 167°F. The same test with exhaust brakes showed a temperature decrease from 401° to 302°F, indicating more favorable thermal engine operating conditions.

The main findings regarding exhaust brakes may be summarized as:

1. There was only a small increase in the maximum braking performance of the vehicle when using the exhaust brake in addition to the normal wheel brakes for an emergency stop.
2. The mean overall vehicle deceleration when using the engine alone was approximately 0.015g; with the exhaust brake in operation, the mean overall deceleration increased to nearly 0.03g.
3. To maintain a steady speed of about 20 mph on down gradients with the vehicle in top gear, it was not necessary to use the foundation brake on slopes of 1 in 22 or less. On gradients of 1 in 10, a savings of about 33% in usage of the main brakes was observed.
4. In normal traffic applications, savings of about 20% in usage of the main wheel brakes may be expected.

The retarding moment M_e of a combustion engine may be computed from the approximate relationship (Ref. 5).

$$M_e = 0.0065 p_m v_e \text{ , lb·ft} \qquad (4\text{-}1)$$

where

p_m = average retarding pressure in combustion chamber, psi
v_e = engine displacement, in.^{3}

The average retarding pressure associated with engine braking ranges from approximately 45 to 75 psi for gasoline engines and 60 to 95 psi for diesel engines. The upper values are associated with high levels of revolutions per minute of the engine crank shaft, the lower values with low levels.

The retarding force F_{ret} at the drive wheels of the vehicle is

$$F_{ret} = \frac{M_e \rho}{\eta_T R} \text{ , lb} \qquad (4\text{-}2)$$

where

R = effective tire radius, ft
η_T = efficiency of transmission, d'less
ρ = transmission ratio between engine and wheels, d'less

4-2 HYDRODYNAMIC RETARDERS

The hydrodynamic retarder is a device that uses viscous damping as the mechanism for producing a retarding torque (Refs. 6, 7, and 8). The viscous damping or internal fluid friction is transformed into thermal energy and dissipated by a heat exchanger. In its design, the hydrodynamic retarder is similar to that of a hydrodynamic clutch; however, its turbine or drive rotor is stationary. The retarding torque is produced by the rotor which pumps a fluid against the stator. The stator reflects the fluid back against the rotor, and a continuous internal pumping cycle is developed. The reaction forces, and hence the retarding torque, are absorbed by the rotor which is connected to the drive wheels of the vehicle. The magnitude of the retarding torque depends upon the amount of fluid in the retarder and the pressure level at which it is introduced into the retarder.

The application of the retarder may result from a hand lever movement or a combined service brake/ retarder control such as the foot pedal as shown in Fig. 4-1. Depending upon the level of applied control force, compressed air travels over the relay valve to the charge tank and control valve. The compressed air in the charge tank forces the retarder fluid into the hydrodynamic brake, simultaneously disconnecting the line between the control valve and the retarder. For a given control input force the control valve allows a constant retarding torque to develop. The degree of fluid application to the retarder determines the amount of fluid and fluid pressure and, consequently, retarding torque. Due to the pumping action of the rotor of the hydrodynamic brake, a pressure difference is produced at the inlet and exit ports, allowing a portion of the service fluid to be circulated through the retarder fluid/water heat exchanger.

One important advantage of this type of retarder is that the retarding force is greater at higher vehicle speeds (Ref. 9). Hydrodynamic retarders operate independently of the engine, clutch, transmission, or electrical power supply. They are connected to the drive axle and represent an almost indestructible no-wear braking element when designed properly. When used on a trailer, a separate cooler becomes necessary. Skidding at the wheels is impossible since the retarding torque approaches zero with decreasing

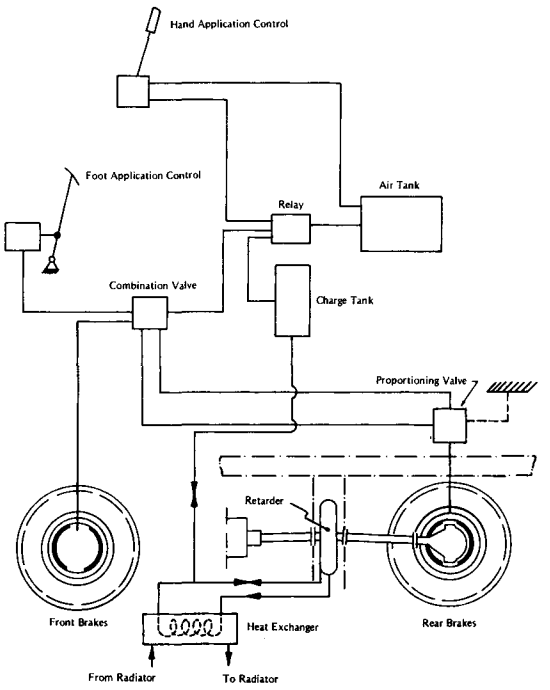

Figure 4-1. Integrated Foundation Brake/Retarder Control System

retarder drive shaft speed. When the retarder is installed in a powered unit, it prevents undercooling of the engine below normal operating temperature on long mountain grades by transferring the thermal energy generated through viscous damping in the retarder to the engine cooling system.

Depending on the downhill operating conditions, the retarder may absorb all or a portion of the vehicle braking energy. For economic reasons, the retarding capacity has to be a function of intended vehicle use, traffic conditions, and other related factors. For a continued application in downhill operation, the retarding capacity of the hydrodynamic retarder is not limited, provided the following relationship is satisfied

$$\frac{W\,V(G - R_r) \times 3600}{778} = h_{rad}\,A_{rad}\,\Delta T_{rad}\ ,\ \text{BTU/h} \qquad (4\text{-}3)$$

where

A_{rad} = cooling area of radiator, ft²
G = road gradient, d'less
h_{rad} = heat transfer coefficient of engine radiator, BTU/h·°F·ft²
R_r = rolling resistance coefficient, d'less
V = vehicle speed, ft/s
W = vehicle weight, lb
ΔT_{rad} = mean temperature difference of water and air in radiator, deg F

The right-hand term of Eq. 4-3 identifies the cooling capacity available in the engine radiator in connection with an additional water/retarder fluid heat exchanger. A rough estimate indicates that the cooling capacity of the engine radiator is approximately 90-100% of the engine horsepower. Additional cooling of about 10% is provided by the retarder and connecting lines being exposed to convective air flow. The heat transfer coefficient of the engine radiators may be estimated from heat transfer relationships. Typical values range from 20-30 BTU/h·°F·ft².

Eq. 4-3 can be used to determine the maximum safe traffic speed a truck may travel for a given road gradient without having to use the foundation brakes.

4-3 ELECTRIC RETARDERS

The principle of the electric retarder is based on the production of eddy currents within a metal disc rotating between two electromagnets which develop a retarding torque on the rotating disc. When the electromagnets are partially energized, the retarding torque is reduced. When the electromagnets are not energized, the retarding torque is zero. The eddy currents result in the heating of the disc. The cooling of the disc is accomplished by means of convection heat transfer with ventilated rotors. Initially, all retarding energy is absorbed by and stored in the rotor material. Only at elevated temperatures does cooling occur. The major problem of the eddy current retarder is associated with the necessity of high brake temperatures for efficient convective cooling capacity — similar to that experienced with friction-type wheel brakes. The high temperatures cause a decrease in retarding effectiveness due to the demagnetizing of the rotor. Depending on the particular material composition involved, this limiting temperature lies near 1350°F.

The maximum retarding performance of an eddy current retarder is limited by the cooling capacity of the ventilated rotor. Eq. 4-3 may be restated for this case as

$$\frac{W\,V(G - R_r) \times 3600}{778} = m_a\,c_p\,\Delta T_R\ ,\ \text{BTU/h} \qquad (4\text{-}4)$$

where

c_p = specific heat of air at constant pressure, BTU/°F·lbm

m_a = mass flow rate of cooling air pumped through the rotor, lbm/h

ΔT_R = difference of temperature of air entering and leaving rotor, deg F

In order to limit the demagnetizing effects, the operating temperatures should not exceed values of 700° to 900°F. At these levels a reduction in retarding effectiveness of approximately 20 to 30% exists.

4-4 ANALYSIS OF INTEGRATED RETARDER/FOUNDATION BRAKE SYSTEMS

If the retarder-foundation brake system is designed so that, for any braking requirement first the retarder, and then the foundation brakes are applied, a truck brake system may be developed that provides essentially fade-free brakes and significantly extended brake-lining life. Since nearly all continued braking energy will be absorbed by the retarder, no temperature increases exist during downhill braking. Under these conditions approximately 40% lower weight foundation brakes may be installed. This weight saving more than compensates for the weight of the retarder. Consequently, no payload penalties are suffered by the truck (Ref. 10).

In order to utilize better the retarder for both single and repeated brake applications, as may be experienced in city-type operation (as well as during downhill braking), the foundation brake and retarder must be integrated with the help of a control system so that, for each brake application, first the retarder and then the foundation brakes are applied. The major portion of the kinetic energy of the vehicle is absorbed by the retarder. When the vehicle speed is decreased, the foundation brakes are required to absorb the remaining kinetic energy of the vehicle due to the reduced brake torque of the retarder, resulting from a drop in drive shaft speed. Furthermore, the control system should be adjustable to both static and dynamic parameters during the braking process to redistribute better the kinetic energy of the vehicle between the retarder and foundation brakes.

If the hydrodynamic retarder produced braking performance is not sufficient, increased levels of foot-pedal force will result in application of the foundation brakes and hence further increased deceleration levels.

A simplified integrated hydrodynamic retarder/brake schematic is shown in Fig. 4-1, identifying the essential components for retarder application and heat exchange.

The design of the control system may be optimized relative to maximum lining life or maximum deceleration. The retarding characteristics of a typical hydrodynamic retarder are shown in Fig. 4-2 (Ref. 7). The maximum retarding torque of 2100 lb·ft is attained for a charge pressure of approximately 75 psi. Inspection of the curves indicates that the retarding torque is nearly constant for shaft speeds ranging from 800-2800 rpm.

In an integrated system designed for a frame vehicle such that the full retarder performance produces a loaded vehicle deceleration of 0.3g, the portions of braking energy absorbed by the hydrodynamic retarder and foundation brakes are distributed as shown in Fig. 4-3. In this case the integrated control system is designed so that only after complete utilization of the retarder capacity do the foundation brakes produce brake force and absorb any kinetic energy of the vehicle. For the empty loading condition the retarder/brake energy ratio is increased, indicating more braking energy absorbed by the retarder at deceleration levels above 0.3g. Inspection of the curves in Fig. 4-3 indicates that for stops below 0.3g (about 10 ft/s²) the foundation brakes are used only to absorb the small remaining kinetic energy of the vehicle associated with speeds below 15-20 mph. At this low level of speed the hydrodynamic retarder braking capacity is reduced significantly and approaches zero for a stationary propeller shaft as shown in Fig. 4-2.

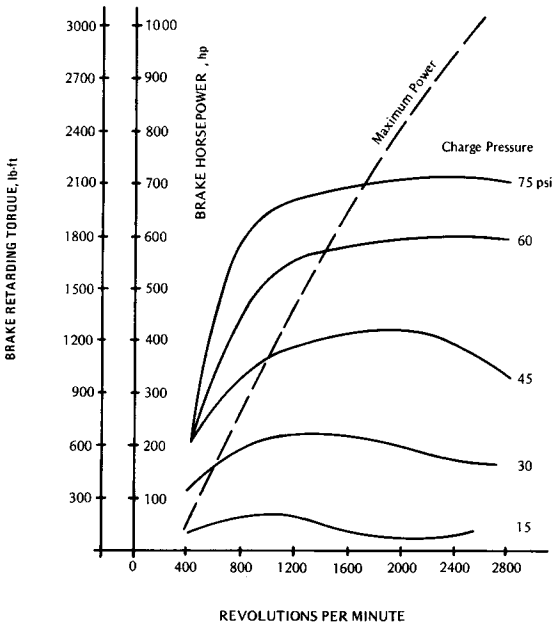

Figure 4-2. Hydrodynamic Retarder Performance Characteristics

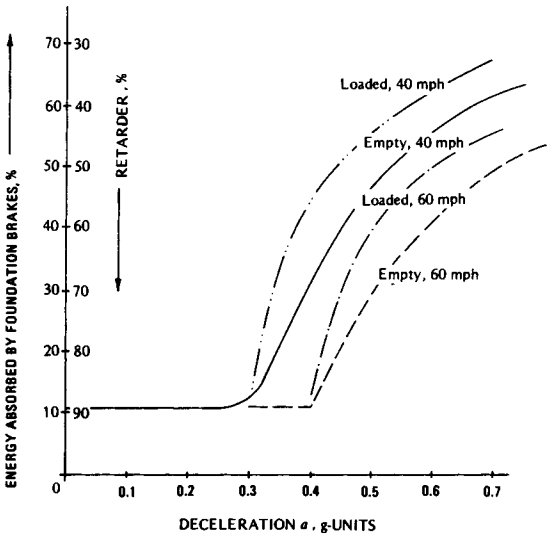

Figure 4-3. Distribution of Braking Energy Between Retarder and Foundation Brakes for 60 and 40 mph Stops for Optimum Lining Life Design

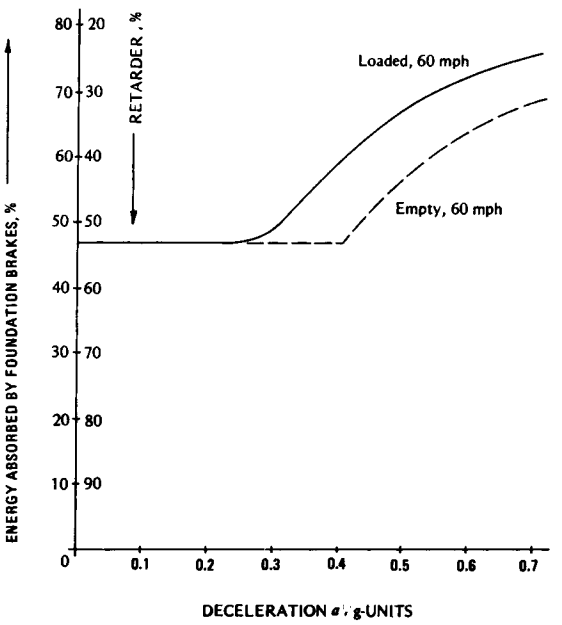

Figure 4-4. Distribution of Braking Energy Between Retarder and Foundation Brakes for a 60 mph Stop for Minimum Stopping Distance Design

Lining wear has been found to be nearly proportional to brake energy but to increase rapidly with brake temperature. Since retarder-equipped vehicles operate at much lower brake temperatures and truck highway decelerations in excess of 0.3g rarely are required, significant increases in brake-lining life result. The brake-lining life may increase by a factor as high as ten, provided vehicle decelerations do not exceed the retarder design limit of 0.3g. Practical increases of brake lining life are expected to be three to six times those associated with standard brake systems. Additional cost savings result from less out-of-service times and increased operating speeds.

If maximum levels of braking are required, then the integrated system must be designed such that all axles are braked near their tire-road friction limit with a minimum level of delay. When a 0.3g-limit retarder and with the control system design directed towards maximum deceleration is installed into a frame vehicle, the braking energy absorbed by retarder and foundation brakes is distributed as shown in Fig. 4-4. The accomplishment of these design objectives requires the use of load or deceleration sensitive proportioning valves for the retarder braked axle in order to increase the utility of the control system. Comparison of Figs. 4-3 and 4-4 shows that integrated brake systems in typical stops at decelerations less than 0.3g have 55-90% of the total energy absorbed by the retarder for speeds in excess of 15-20 mph.

Since safety considerations may require that integrated brake systems be designed relative to maximum deceleration, it appears desirable to make the operational mode of the brake system an automatic function of the braking severity. Brake applications that do not require minimum stopping distance may allow the system to operate in the lining-saving mode, whereas emergency stops automatically force the system to operate in the maximum deceleration mode. The automatic adjustment could be achieved by means of sensing the rate of change of vehicle deceleration or related parameters. It is expected that stopping-distance differences for trucks designed for either maximum lining life or minimum stopping distance do not assume significant values. A preliminary estimate indicates increases in stopping distance of less than 20-30 ft for stops from 60 mph for a truck having an integrated brake system designed for maximum lining life.

Since existing and proposed braking standards necessitate the use of wheel-antilock brake systems, the function of both control systems must be matched properly to achieve optimal braking performance under all operating conditions. For example, when braking on a slippery road surface at less than 0.3g deceleration, the antiskid unit associated with the retarder-equipped axle needs to operate only for

speeds below 15-20 mph, a level at which the retarder force drops to zero.

Retarders installed in tractor-semitrailer combinations similarly will yield significant savings in brake-lining life. Since economic considerations require the installation of the retarder in the tractor rather than in the trailer, integrated brake system designs will result in approximately 25-30% of the total effectiveness stop braking energy absorbed by the retarder. This is because only the tractor drive wheels are retarded by means of the hydrodynamic retarder. For continued downhill braking, the retarder can be designed to absorb all braking energy developed on existing highway gradients.

The economical design of a retarder/brake system in many cases requires that only the motor vehicle drive axle be braked. In this case it may be necessary to determine the downhill road gradient upon which the vehicle or vehicle combination can safely operate with its retarder in the applied position without exceeding the traction limit on the retarder axle.

The slope α that can safely be driven on by a solid-frame vehicle with the retarder applied is (Ref. 6)

$$\tan \alpha \leq \frac{\mu_R \psi + R_r}{1 + \mu_R \chi} \text{, d'less} \qquad (4\text{-}5)$$

where

R_r = rolling resistance coefficient, d'less
α = slope angle, deg
μ_R = tire-road friction coefficient of braked rear axle, d'less
χ = height of center of gravity of truck divided by wheel base of truck, d'less
ψ = static rear axle load of truck divided by truck weight, d'less

If a truck-trailer combination is retarded over the truck rear axle, the approximate slope that can be operated on is

$$\tan \alpha \leq \frac{\mu_R \psi + R_r(1 + W_2/W_1)}{\mu_R \chi + 1 + W_2/W_1} \text{, d'less} \qquad (4\text{-}6)$$

where

W_1 = truck weight, lb
W_2 = trailer weight, lb

REFERENCES

1. "Auxiliary Braking Systems", *Automobile Engineer*, Vol. 47, No. 7, July 1957, pp. 282-86.
2. E. Rohne, "Ueberlegungen Zur Ausfuehrung Von Dauerbremsen fuer Kraftfahrzeuge", *ATZ*, Vol. 69, No. 5, 1967, pp. 145-49.
3. D. D. Cummins, *The Jacobs Engine Drake Application and Performance*, Paper 660740 presented at SAE combined powerplant and transportation meetings, Chicago, October 1966.
4. E. Johannis, "The Effect of Engine Braking on the Thermal State of the Diesel Engine", *ATZ*, Vol. 57, No. 7, 1957.
5. M. Mitschke, *The Dynamics of Motor Vehicles*, Springer Publisher, Berlin, Heidelberg, New York 1972.
6. H. Strien and O. Mehmet, "Continuous Braking System for Truck-Trailer Combination", *Automobil-Industrie*, Vol. 12, No. 3, September 1967, pp. 83-87, 89-92.
7. O. Depenheuer and H. Strien, *The Retarder for Commercial Vehicles and Its Effects on Traffic Flow and Safety*, Teves GmbH Special Publication, October 1972.
8. H. Mueller, "The Voith Hydraulic Retarder for Vehicles", *ATZ*, Vol. 69, No. 5, 1967, pp. 142-44.
9. W. S. Nagel, *Full Retarder-Design and Development*, Society of Automotive Engineers, Inc., Paper 650626, August 1965.
10. R. Limpert, *An Investigation of Integrated Retarder/Foundation Brake Systems for Commercial Vehicles*, SAE Paper No. 750126, Detroit, 1975.

CHAPTER 5
BRAKE FORCE PRODUCTION

In this chapter the brake forces produced by hydraulic, pneumatic, and mechanical brake systems are analyzed. Equations that determine the maximum vehicle weight that can be decelerated safely with manual or vacuum-assisted brakes are derived. The different components used in powered brake systems are described briefly. Electrical brakes are reviewed.

5-0 LIST OF SYMBOLS

A_A = assist unit area, in.^{2}
A_C = brake chamber area, in.^{2}
A_{MC} = master cylinder area, in.^{2}
A_{WC} = wheel cylinder area, in.^{2}
A_1 = control piston area, in.^{2}
A_2 = control disc area, in.^{2}
a = deceleration, g-units
a_1 = deceleration of truck, g-units
a_2 = deceleration of trailer, g-units
B = assist characteristic, d'less*
BF = brake factor, d'less
BF_F = brake factor of front brakes, d'less
BF_R = brake factor of rear brakes, d'less
D_B = booster piston diameter, in.
D_C = output or master cylinder diameter, in.
D_P = pushrod diameter, in.
d = wheel cylinder piston displacement, in.
d = displacement of tip of brake shoe, in.
d_C = brake chamber piston displacement, in.
d_F = wheel cylinder piston displacement of front wheels, in.
d_R = wheel cylinder piston displacement of rear wheels, in.
F_A = effective assist unit force, lb
F_A' = assist unit force plus return spring force, lb
F_T = tongue force, lb
F_C = control piston force, lb
F_H = hand force, lb
F_P = pedal force, lb
F_x = brake force, lb
$F_{x,\,total}$ = total brake force, lb
F_{x1} = brake force of truck, lb
F_{x2} = brake force of trailer, lb
G = system gain, d'less
IC = booster input characteristic, d'less
$l_h = x/d$, hydraulic gain, d'less
l_c = effective cam radius, in.
l_p = pedal lever ratio, d'less
l_s = effective slack adjuster length, in.
l_1 = brake dimension, in.
l_2 = brake dimension, in.
l_3 = brake dimension, in.
l_4 = brake dimension, in.
l_5 = brake dimension, in.
n_B = number of wheel brakes, d'less
n_S = number of brake shoes, d'less
P = booster pressure ratio, d'less
p_A = accumulator pressure, psi
p_B = booster pressure, psi
p_C = control pressure, psi
p_G = charging pressure of accumulator gas, psi
p_l = brake line pressure, psi
p_o = pushout pressure, psi
R = effective tire radius, in.
r = drum or rotor radius, in.
T_B = brake torque, lb·in.
V_A = accumulator volume, in.^{3}
V_{MC} = master cylinder volume, in.^{3}
V_{ratio} = volume ratio, d'less
v = relative portion of master cylinder volume required for hose expansion, d'less
W = vehicle weight, lb
W_{max} = maximum vehicle weight which can be decelerated safely, lb
W_1 = weight of truck, lb
W_2 = weight of trailer, lb
X = master cylinder piston travel, in.
Y = pedal travel, in.
Y_H = available hand (or foot) travel for emergency brake, in.
α = wedge angle, deg
$\eta = \eta_p \eta_c$ efficiency, d'less
η_c = efficiency of wheel cylinder, d'less
η_H = mechanical efficiency of hand brake, d'less
η_m = mechanical efficiency between brake chamber and brake shoe or transmission and wheels, d'less
η_p = pedal lever efficiency, d'less

*d'less = dimensionless

ρ = lever ratio between brake chamber and brake shoe, d'less
ρ_B = emergency brake gain, d'less
ρ_D = differential gear ratio, d'less
ρ_H = displacement gain between hand brake application force and cable force, d'less
$\rho_l = l_p l_h$, product of pedal lever ratio and hydraulic gain, d'less
ϕ = rear axle brake force divided by total brake force, d'less

5-1 INTRODUCTION

During braking, the kinetic energy and potential energy of the vehicle are converted into thermal energy at the friction surface of the brake and at the tire-roadway interface. In the braking process the brake generates a retarding torque as a function of the applied pedal force. The pedal force-braking torque characteristics are determined by the mechanical/pneumatic or mechanical/hydraulic parameters of the braking system, whereas the actual deceleration of the vehicle is determined by the brake torque and the tire radius, the tire-roadway friction coefficient, and the normal force between tire and roadway. The normal forces change with the dynamic load transfer from the rear axle(s) to the front axle. For articulated vehicles, load transfer occurs on each unit of the vehicle combination as well as on individual axles of a tandem suspension.

5-2. NONPOWERED HYDRAULIC BRAKE SYSTEM

Fig. 5-1 illustrates a typical hydraulic brake system. Application of the pedal force F_p causes the brake pedal to be displaced through a distance Y. The pedal linkage is designed to produce a mechanical force advantage l_p between the pedal and the master cylinder piston, resulting in a displacement X of the piston which is less than the pedal displacement Y. The master cylinder, having an area A_{MC}, traps the brake fluid in the brake line, thereby developing a hydraulic brake line pressure p_l. Since there are frictional losses, a pedal lever efficiency η_p is assumed.

The hydraulic brake line pressure p_l in the brake line is

$$p_l = \frac{F_p l_p \eta_p}{A_{MC}}, \text{ psi} \qquad (5\text{-}1)$$

where

A_{MC} = master cylinder area, in.^{2}
F_p = pedal force, lb
l_p = pedal lever ratio, d'less
η_p = pedal lever efficiency, d'less

The pedal lever efficiency η_p represents the losses associated with the master cylinder and pedal linkage. The mechanical losses of the master cylinder are caused by friction between master cylinder wall and seal and the effect of the master cylinder piston return spring. The frictional losses of the master cylinder are

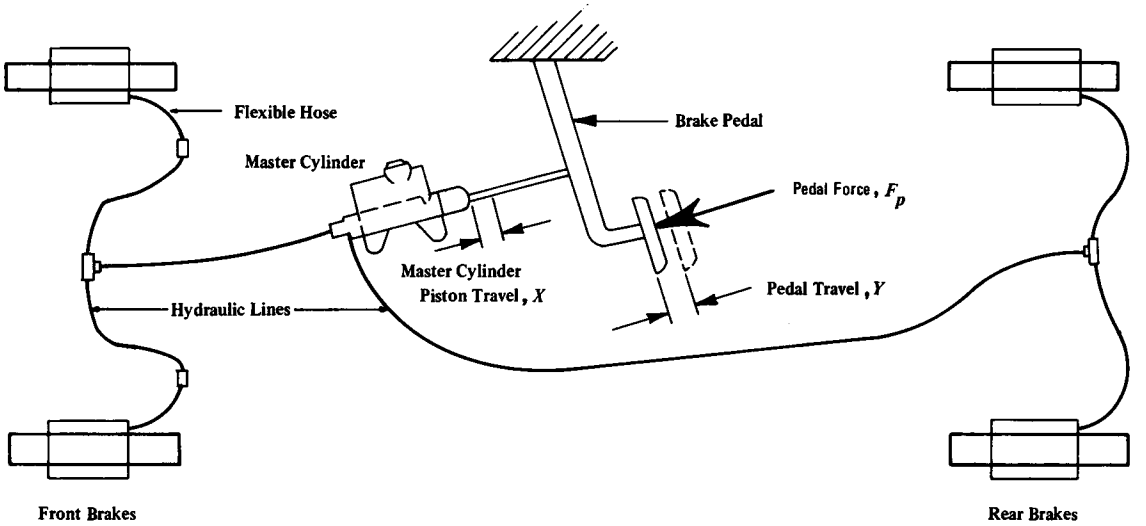

Figure 5-1. Hydraulic Brake System

expressed in terms of an efficiency determined by the ratio of equivalent output force at the master cylinder piston to input force at the pushrod. Typical efficiency values are 0.96 for a single circuit or standard master cylinder and 0.92 for dual circuit or tandem master cylinder. The mechanical efficiency associated with the pedal linkage is determined by the number of pivots required. Typical linkages using only one lever between pedal force application and master cylinder input exhibit efficiencies of approximately 0.85-0.90. Consequently, the pedal lever efficiency η_p may range from 0.78 to 0.86. A value of $\eta_p = 0.80$ is used in connection with a tandem master cylinder.

In the wheel brake, a friction material is pressed against the brake drum or disc, resulting in a brake torque. The brake torque is dependent upon brake geometry, brake line pressure, and lining friction coefficient. The brake torque T_B of one brake may be computed from the expression

$$T_B = (p_l - p_o)\, A_{WC}\, \eta_c\, BF\, r, \text{ lb·in.} \qquad (5\text{-}2)$$

where

A_{WC} = wheel cylinder area, in.^{2}
BF = brake factor, defined as the ratio of drag force on the drum friction surface to the actuating force of one shoe, d'less
p_o = pushout pressure, required to bring the brake shoe in contact with the drum, psi
r = drum radius, in.
η_c = efficiency corresponding to frictional losses in the wheel cylinder, d'less

The wheel cylinder efficiency η_c is approximately 0.96.

The development of vehicle deceleration by means of the brake torque may be analyzed by a simplified method. When wheel inertias are neglected and no wheel lockup occurs, then the brake force F_x (produced by one wheel) is (Ref. 1)

$$F_x = (p_l - p_o)\, A_{WC}\, \eta_c\, BF \left(\frac{r}{R}\right), \text{ lb} \qquad (5\text{-}3)$$

where

R = effective tire radius, in.

The effective tire radius is the vertical distance between wheel center and road surface. The effective tire radius is affected by inflation pressure, loading, and vehicle speed. Lower inflation pressure and increased loading decrease tire radius, whereas, increased speed tends to increase tire radius due to centrifugal forces associated with the tread material. The distance between wheel center and road surface measured on the stationary vehicle may be used as effective tire radius in most braking analyses. For a standing or slowly rotating tire, the tire radius of heavy trucks decreases by approximately 0.17 in. for 1000 lb increase in tire normal force (Ref. 2).

For a brake system having identical brakes on each wheel, the total brake force $F_{x,\,total}$ is

$$F_{x,\,total} = n_B\, (p_l - p_o)\, A_{WC}\, \eta_c\, BF \left(\frac{r}{R}\right), \text{ lb}$$

where

n_B = number of wheel brakes, d'less

Since the total brake force produced by the vehicle must be equal to the inertia force of the vehicle, the deceleration is related to total brake force by the following expression

$$aW = F_{x,\,total}, \text{ lb} \qquad (5\text{-}4)$$

or

$$aW = n_B\, (p_l - p)\, A_{WC}\, \eta_c\, BF \left(\frac{r}{R}\right), \text{ lb} \qquad (5\text{-}4a)$$

where

a = deceleration, g-units
W = vehicle weight, lb

This equation may be rewritten in a simpler and more useful form for illustrative purposes. Pushout pressures are generally between 50 and 100 psi for drum brakes and between 5 and 10 psi for disc brakes, and they may be neglected to simplify the analysis. The brake line pressure can be replaced by Eq. 5-1, yielding

$$aW = n_B \left(\frac{F_p\, l_p\, \eta_p}{A_{MC}}\right) A_{WC}\, \eta_c\, BF \left(\frac{r}{R}\right), \text{ lb} \qquad (5\text{-}5)$$

From a brake fluid volume analysis, it follows that the fluid displaced by the master cylinder equals the fluid displacements of the individual wheel cylinders, neglecting any hose expansion at this time. Hence, the volume V_{MC} produced by the master cylinder is

$$V_{MC} = A_{MC}\, X = n_S\, A_{WC}\, d, \text{ in.}^3$$

or

$$\frac{A_{WC}}{A_{MC}} = \frac{X}{n_S d}, \text{ d'less} \qquad (5\text{-}6)$$

where

d = wheel cylinder piston displacement, in.
n_S = number of brake shoes, d'less
X = master cylinder piston travel, in.

If the ratio of wheel cylinder area to master cylinder area (Eq. 5-6) is introduced in Eq. 5-5, the following expression results

$$aW = F_p l_p \eta_p \eta_c \left(\frac{X}{d}\right)(BF)\left(\frac{r}{R}\right)\left(\frac{n_B}{n_S}\right), \text{lb} \qquad (5\text{-}7)$$

Eq. 5-7 may be rewritten as

$$aW = F_p \rho_l \left(\frac{n_B}{n_S}\right) \eta\, BF \left(\frac{r}{R}\right), \text{lb} \qquad (5\text{-}8)$$

where

$\eta = \eta_p \eta_c$, d'less
$\rho_l = l_p l_h$, d'less
$l_h = X/d$ hydraulic gain, d'less

Eq. 5-8 may be expressed in terms of the system gain G as

$$aW = F_p G, \text{lb} \qquad (5\text{-}9)$$

where

$G = \rho_l (n_B/n_S)\, \eta\, BF\, (r/R)$, d'less

As can be seen immediately, not only the pedal force but also the total gain and hence the pedal travel and the shoe displacement are important in determining deceleration levels. For a given vehicle weight all parameters except the brake factor BF and the hydraulic gain ρ_l are more or less determined by intended vehicle use. Consequently, an increase in deceleration capability can be obtained only by increasing the brake factor and/or the gain. An increased brake factor — for example, a change from a leading-trailing shoe brake to a duo-servo brake — will be associated with a higher brake sensitivity, i.e., the vehicle may more easily experience a yawing moment during braking and may become directionally unstable. The use of too great gain values may result in an unsafe operation of the braking system. The pedal travel/master cylinder gain l_p is generally limited by the basic geometry and force capabilities of the human leg and is determined by the ratio of foot pedal travel to master cylinder piston travel. The hydraulic gain l_h between the master cylinder and the wheel cylinder is limited by the minimum shoe travel required to cover shoe play, lining compression, drum distortion, and wear. The gain l_h is determined by the ratio of master cylinder piston travel to the travel of a single wheel cylinder piston. The shoe tip travel required for a drum brake or the caliper piston of a disc brake may be obtained from Chapter 2.

With the equations presented so far it becomes possible to predict the vehicle weight that can be decelerated safely with a manual brake system.

The analysis is carried out in terms of the necessary work output from the master cylinder. From this information, the required pedal force and travel are easily determined, provided the pedal geometry and master cylinder piston stroke are known.

First, it is assumed that the front and rear axle are both equipped with brakes of the same type, i.e., either drum or disc brakes; later the weight limitation on a two-axle vehicle equipped with disc and drum brakes is derived.

The brake force F_x produced by one axle may be computed from Eq. 5-3 as

$$F_x = 2(p_l - p_o)\, \eta_c\, A_{WC}\, BF \left(\frac{r}{R}\right), \text{lb} \qquad (5\text{-}10)$$

The pedal force F_p required to produce the hydraulic brake line pressure p_l is given by Eq. 5-1 as

$$F_p = \frac{p_l A_{MC}}{l_p \eta_p}, \text{lb}$$

During braking, the inertia force acting at the center of gravity of the vehicle equals the retarding forces developed by the brake/tire system. Consequently, when ignoring the pushout pressure, one obtains by Eq. 5-10

$$aW = p_l \left[(A_{WC}\, BF)_F + (A_{WC}\, BF)_R\right] \times 2\left(\frac{r}{R}\right)\eta_c, \text{lb} \qquad (5\text{-}11)$$

where the subscripts F and R refer to the front and rear axle, respectively. The required fluid displacement produced by the master cylinder can be expressed as a function of the individual wheel cylinder volumes and the brake hose loss. For a vehicle equipped with four brakes this relationship is

$$V_{MC} = 4\left[(A_{WC}\, d)_F + (A_{WC}\, d)_R\right](1 + \nu), \text{in.}^3 \qquad (5\text{-}12)$$

where

ν = relative portion of V_{MC} require for hose expansion, d'less

A comparison of the brake factors and the minimum wheel cylinder piston displacement d allows approximate relationships to be written as

$$d = BF/(22 \text{ to } 30), \text{ in. for drum brakes}$$
$$d = BF/(25 \text{ to } 28), \text{ in for disc brakes}$$

Eq. 5-12 can be rewritten with $d = BF/30$ expressed in inches as

$$V_{MC} = \frac{4}{30}[(A_{WC}\,BF)_F + (A_{WC}BF)_R] \times (1 + v), \text{in.}^3$$

or (5-13)

$$\frac{30V_{MC}}{4(1 + v)} = [(A_{WC}\,BF)_F + (A_{WC}\,BF)_R], \text{in.}^2$$

Combining Eqs. 5-11 and 5-13 yields

$$\frac{Wa}{2(r/R)\,\eta\,p_l} = \frac{30V_{MC}}{4(1 + v)}, \text{in.}^2 \quad (5\text{-}14)$$

With work defined as the product of pressure and volume, the work output required from the master cylinder can now be computed as

$$p_l\,V_{MC} = \frac{Wa(1 + v)}{15(r/R)\,\eta}, \text{in.·lb} \quad (5\text{-}15)$$

The mechanical efficiency η is

$$\eta = \eta_p\,\eta_c, \text{ d'less} \quad (5\text{-}16)$$

where

η_c = efficiency of wheel cylinder, d'less
η_p = efficiency of pedal lever, d'less

Typical values for η_p are 0.92 to 0.94, and for η_c 0.96 and 0.88 for single piston and tandem master cylinders, respectively. A conservative value for $\eta = 0.80$ may be assumed for this analysis. The drum to tire radius ratio r/R varies somewhere between 0.32 and 0.40 for most road vehicles. A conservative estimate of the hose expansion of 30% of the total master cylinder volume may be assumed for trucks. For passenger cars a value of 10% may be used. For an arbitrarily specified deceleration capability of 20 ft/s² or 0.62g, the work output required from the master cylinder becomes by Eq. 5-15

$$p_l\,V_{MC} = W\frac{0.62\,(1 + 0.30)}{15\,(0.32 \text{ to } 0.40)\,0.8}, \text{in.·lb}$$

or (5-17)

$$p_l\,V_{MC} = (0.17 \text{ to } 0.21)\,W, \text{in.·lb}$$

Eq. 5-17 indicates that the master cylinder must provide a work output measured in in.·lb equal to the numerical value of 17 to 21% of the weight of the vehicle.

The work output from the master cylinder must be equal to the work input into the cylinder, thus equal to the work at the foot pedal:

$$F_p\,Y = (0.17 \text{ to } 0.21)\,W, \text{in.·lb} \quad (5\text{-}18)$$

With an assumed maximum pedal force $F_p = 150$ lb and a maximum pedal travel $Y = 6$ in. the maximum weight W_{max} that can be safely decelerated by hydraulic unpowered brakes is

$$W_{max} = \frac{F_p\,Y}{(0.17 \text{ to } 0.21)} = \frac{150 \times 6}{(0.17 \text{ to } 0.21)}$$
$$\approx 4300 \text{ to } 5300 \text{ lb}$$

Here it is assumed that the pedal force of 150 lb remains constant during the brake application, neglecting any dynamic effects of pedal force on pressure buildup.

This analysis indicates that motor vehicles having unpowered hydraulic brake systems and a total vehicle weight of approximately 5000 lb represent a "limit-vehicle" which can be decelerated safely by manual brake application. However, in order to ensure the high gains required, a careful and possibly automatic adjustment of the brakes becomes necessary. Heavier vehicles require powered brake systems such as vacuum assist, full hydraulic, or pneumatic systems.

In paragraph that follows, the weight limitation on a vehicle equipped with disc brakes on the front (or rear) and drum brakes on the rear (or front) is derived. The development is similar to the previous derivation and is as follows.

Divide Eq. 5-12 by Eq. 5-11 and rearrange:

$$p_l V_{MC} = \left[\frac{(A_{WC}\,d)_F + (A_{WC}\,d)_R}{(A_{WC}\,BF)_F + (A_{WC}\,BF)_R}\right] \times \left[\frac{4(1+\nu)}{2(r/R)\eta_c}\right] aW \text{ , in.·lb} \quad (5\text{-}19)$$

For identical drum and tire radii on front and rear axle the first bracket of the right-hand side of Eq. 5-19 may be rewritten as:

$$\frac{(A_{WC}\,d)_F + (A_{WC}\,d)_R}{(A_{WC}\,BF)_F + (A_{WC}\,BF)_R} = \frac{(A_{WC}\,d)_F + (A_{WC}\,d)_R}{\frac{1}{\phi}(A_{WC}\,BF)_R} \text{ , in.} \quad (5\text{-}20a)$$

where

ϕ = rear axle brake force divided by total brake force, d'less

Eq. 5-20a can be developed further by expressing the right-hand side in two terms

$$\phi\left[\frac{(A_{WC})_F}{(A_{WC})_R}\right]\left(\frac{d_F}{BF_R}\right) + \phi\left(\frac{d_R}{BF_R}\right), \text{ in.} \quad (5\text{-}20b)$$

or

$$\left[\frac{(A_{WC}\,BF)_R}{(A_{WC}\,BF)_F + (A_{WC}\,BF)_R}\right]\left[\frac{(A_{WC})_F}{(A_{WC})_R}\right]\left(\frac{d_F}{BF_R}\right) + \phi\left(\frac{d_R}{BF_R}\right), \text{ in.} \quad (5\text{-}20c)$$

However, the term $(A_{WC}\,BF)_R$ can be cancelled, and when denominator and numerator are multiplied by BF_F, the final expression is

$$\left[\frac{(A_{WC}\,BF)_F}{(A_{WC}\,BF)_F + (A_{WC}\,BF)_R}\right]\left(\frac{d_F}{BF_F}\right) + \phi\left(\frac{d_R}{BF_R}\right), \text{ in.} \quad (5\text{-}20d)$$

or

$$(1-\phi)\left(\frac{d_F}{BF_F}\right) + \phi\left(\frac{d_R}{BF_R}\right), \text{ in.} \quad (5\text{-}20e)$$

which is equal to the first bracket of the right-hand side of Eq. 5-19. Substitution of Eq. 5-20e into Eq. 5-19 yields the work output from the master cylinder as

$$p_l V_{MC} = \left[(1-\phi)\left(\frac{d_F}{BF_F}\right) + \phi\left(\frac{d_R}{BF_R}\right)\right] \times \left[\frac{4(1+\nu)}{2(r/R)\eta_c}\right] aW \text{ , in.·lb} \quad (5\text{-}21)$$

For a truck with $\nu = 0.30$, $0.32 \le r/R \le 0.40$, a = 0.62g, and $\eta_c = 0.80$:

$$\frac{4(1+\nu)\,a}{2(r/R)\,\eta} = \frac{4(1+0.3)\,0.62}{2\,(0.32 \text{ to } 0.40)\,0.8} = 5.04 \text{ to } 6.3 \text{ , d'less}$$

The final expression for the safe deceleration of a vehicle with a given weight is

$$p_l V_{MC} = (5.04 \text{ to } 6.3) \times \left[(1-\phi)\left(\frac{d_F}{BF_F}\right) + \phi\left(\frac{d_R}{BF_R}\right)\right] W \text{ , in.·lb} \quad (5\text{-}22)$$

Eq. 5-22 reduces to Eq. 5-17 for $d = BF/30$ for front and rear brakes. Eqs. 5-17 and 5-22 allow a quick, approximate evaluation of the stopping capability of a vehicle equipped with nonpowered hydraulic brakes in terms of the line pressure levels required for a 20 ft/s² stop. Stops of differing deceleration levels require proportionately changed pedal efforts. The analysis presented here can be extended easily to include three-axle vehicles, off-road vehicles with one or more axles braked, fork lifts, and other specialty vehicles.

5-3 VACUUM-ASSISTED HYDRAULIC BRAKE SYSTEM

For hydraulic brake systems equipped with vacuum assist, the work output from the master cylinder is equal to the pedal work plus the work provided by the vacuum assist. The power assist units for passenger cars, and light and medium size trucks utilize engine vacuum. There are basically two types of vacuum assist: mechanical and hydraulic control

of the vacuum application. The hydraulic control, often called hydrovac, requires two master cylinders and often a more involved valve arrangement. Its advantage is that the hydrovac unit can be located anywhere in the vehicle, whereas the mechanically controlled assist unit must be located opposite the foot pedal on the fire wall (Ref. 3).

The design of a typical hydrovac is seen in Fig. 5-2, showing the applied position of the brakes (Ref. 4). The hydrovac consists of the vacuum cylinder (1) with piston (2), return spring (3), and pushrod (4). The control pipe (5) connects the left chamber of the vacuum cylinder with the lower chamber of the membrane (6) of the vacuum valve, while the right chamber of the vacuum cylinder is connected to the vacuum inlet (7) leading to the engine manifold. The right side of the vacuum cylinder also is connected to the upper side of the membrane (8).

The secondary master cylinder consists of the cylinder (9), the secondary piston (10) equipped with a check valve (11), and the pushrod (4).

In the off position, the piston (2) is held at the left side of the vacuum cylinder by the return spring (3). In this position, the arm (12) of the secondary piston (10) rests against the back plate, and the ball of the check valve (11) is lifted from the seat. The control piston (13) is located at its uppermost position, thus separating the control valve (14) from the seat of the membrane.

During application of the primary master cylinder, the line pressure is transmitted through the check valve into the brake system and to the wheel brakes.

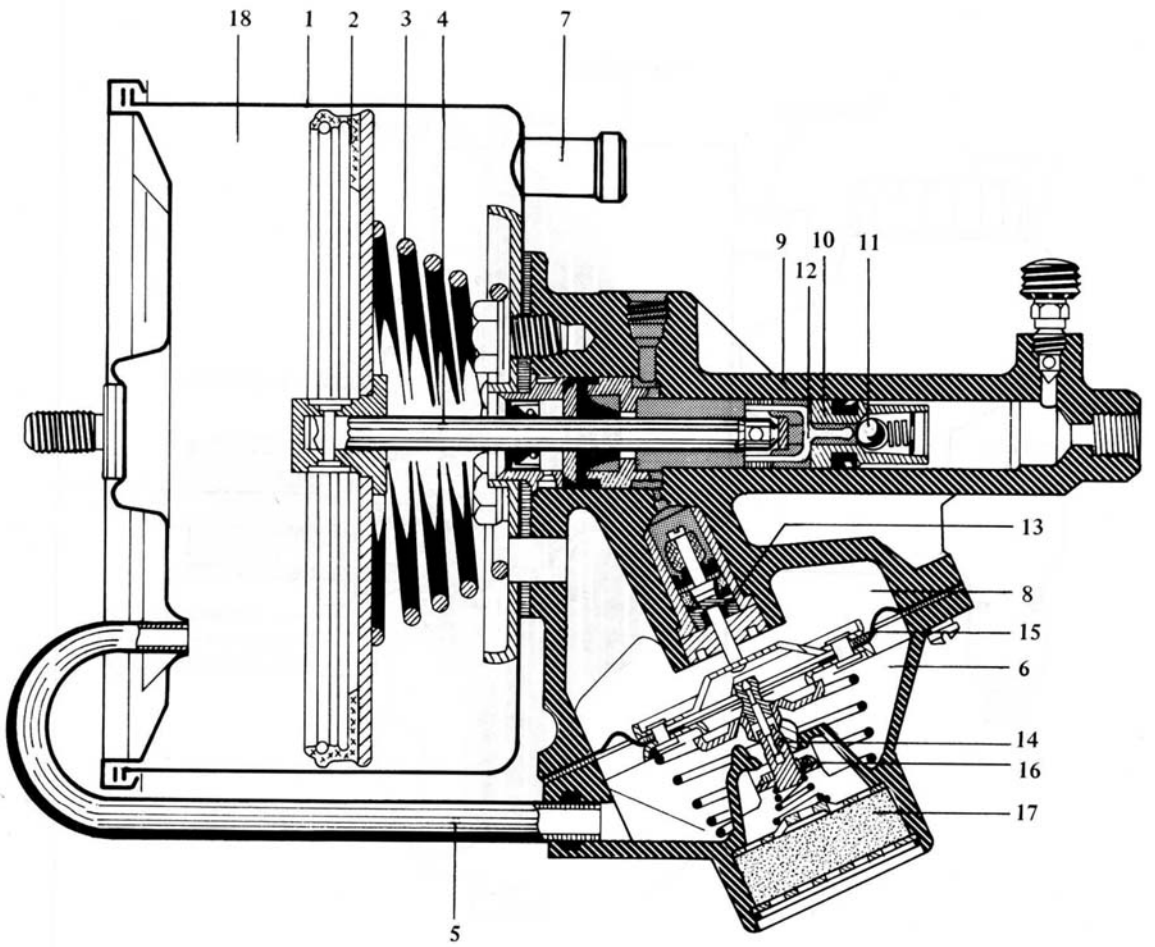

Figure 5-2. Hydrovac in On Position

At the same time the hydraulic pressure in front of the control piston (13) begins to rise, moving the piston and membrane downward until the membrane contacts the control valve (14). At this moment the two chambers to the left and right of the piston (2) are separated. Any further motion of the membrane (15) downward will open the ambient valve (16).

The atmospheric air flows past the air filter (17) through the ambient valve (16) into the valve chamber (6) and through the control pipe (5) into the cylinder chamber (18), resulting in a rightward motion of piston (2), pushrod (4), and secondary piston (10). The check valve (11) will be closed as a result of the secondary piston's movement to the right allowing the line pressure to increase and to be transmitted to the wheel brakes. The vacuum difference across piston (2) is identical to the pressure difference across the membrane (15). The position of membrane (15) is determined by the pressure in the pedal-master cylinder and the pressure differential across the membrane. Any change in pedal force will cause a corresponding change in vacuum application and hence pressure differential across piston (2), allowing a sensitive control of the brake application.

The operation of the mechanically controlled vacuum — often called mastervac — is explained in the next paragraphs. The schematic of the assist unit is illustrated in Fig. 5-3.

The assist characteristic B is defined as the ratio of pushrod force upon the master cylinder piston to the pedal force input into the mastervac.

The computations that follow are carried out for a single piston mastervac with an 8-in. diameter assist piston. The diameters of the control disc and control piston are 1.21 and 0.729 in., respectively.

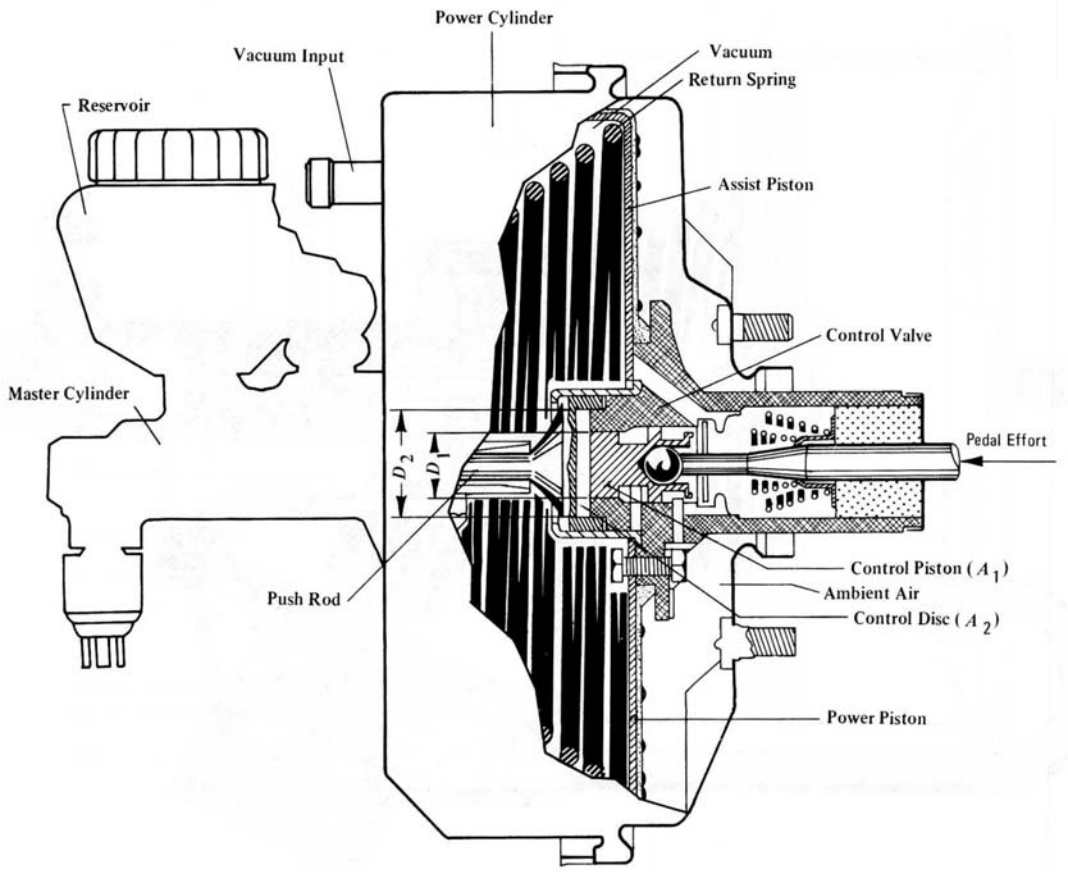

Figure 5-3. Mastervac in Applied Position

The effective assist unit area A_A is equal to the booster area minus the pushrod area,

$$A_A = \frac{8^2\pi}{4} - \frac{0.33^2\pi}{4} = 50.18 \text{ in.}^2$$

where a pushrod diameter = 0.33 in. was assumed.

The booster force F_A' for an effective vacuum of 11.5 psi and a mechanical efficiency of 0.95 is

$$F_A' = (50.18)(11.5)(0.95) = 548.2 \text{ lb}$$

The effective assist unit force F_A is smaller due to the booster piston return spring opposing the assist action. Hence,

$$F_A = 548.2 - 38 = 510.2 \text{ lb}$$

where a return spring force of 38 lb was assumed.

The rubber control disc acts similar to a pressurized hydraulic fluid. The pressure in the control disc p_C is equal to the effective booster force divided by the difference in cross-sectional area of the control disc A_2 and the control piston A_1

$$p_C = \frac{510.2}{[(1.21)^2 - (0.729)^2]\,\pi/4} = 696.5 \text{ psi}$$

The control pressure p_C is acting against any surface in contact with the control disc. Since the control piston is pushing against a portion of the control disc, the control piston force F_C is equal to the control pressure multiplied by the control piston area A_1

$$F_C = p_C A_1 = (696.5)\frac{(0.729)^2\pi}{4} = 290.71 \text{ lb}$$

The control piston force is opposed by the control piston return spring force. For an 8-in. diameter vacuum assist the return spring force is approximately 15 lb. Consequently, the effort into the master cylinder produced by the foot pedal is 290.7 + 15 = 305.7 lb.

The total force upon the master cylinder piston and hence the brake line pressure producing force is equal to the sum of the effective booster force and control piston force or 510.2 + 290.7 lb = 800.9 lb.

Finally, the vacuum assist characteristic B is given by the ratio of pushrod force upon the master cylinder piston to control piston force

$$B = \frac{800.9}{290.7} = 2.75$$

It is interesting to note that the assist characteristic B is also equal to the ratio of control disc area to control piston area

$$\frac{A_2}{A_1} = \frac{1.149}{0.4172} = 2.75$$

The theoretical results may be used to construct a diagram illustrating the booster performance. In Fig. 5-4, the pushrod force upon the master cylinder piston versus the pedal force multiplied by the pedal lever ratio is shown. As can be seen, the booster has a maximum boost assist of approximately 801 lb. For decelerations requiring higher pushrod forces, the additional work input into the brake system must come from the pedal effort, i.e., the driver. Also, the different booster output forces as a function of different levels of vacuum are illustrated in Fig. 5-4.

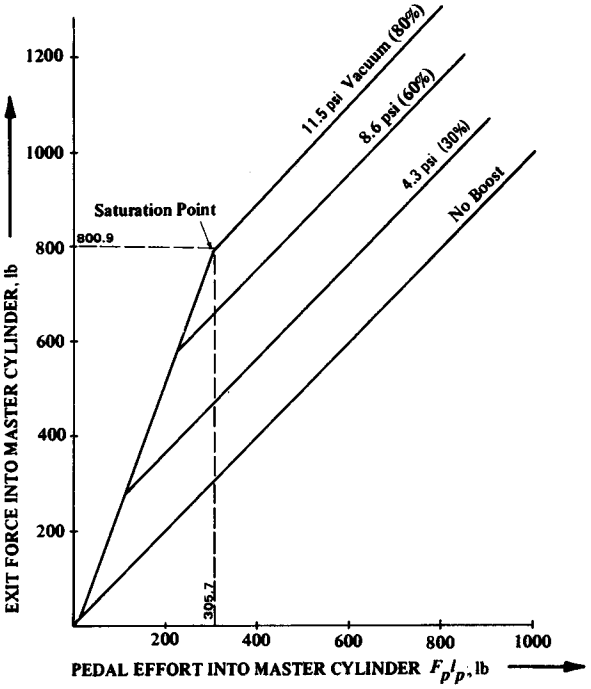

Figure 5-4. Mastervac Characteristics

With Eq. 5-17 and the vacuum assist characteristic B it becomes possible to determine the vehicle weight that can be decelerated safely with a vacuum-assisted brake system.

The hydraulic work $p_l V_{MC}$ of Eq. 5-17 is equal to the booster and pedal work

$$p_l V_{MC} = F_A X + F_p Y \text{, in.·lb} \qquad (5\text{-}23)$$

where

F_A = effective assist unit force, lb
F_p = pedal force, lb
X = effective master cylinder piston travel, in.
Y = pedal travel, in.

The hydraulic brake line pressure p_l developed by the pedal and booster force is

$$p_l = \frac{B F_p l_p}{A_{MC}} = \frac{B F_p Y}{V_{MC}} \text{, psi} \qquad (5\text{-}24)$$

Consequently, the work output from the master cylinder in terms of the booster characteristics and the pedal effort is

$$p_l V_{MC} = B F_p Y \text{, in.·lb} \qquad (5\text{-}25)$$

Since

$$B = \frac{F_p l_p + F_A}{F_p l_p} \text{, d'less}$$

and

$$l_p = \frac{Y}{X}$$

it follows that

$$\frac{F_A X}{F_p Y} = (B - 1) \text{, d'less} \qquad (5\text{-}26)$$

The vehicle weight that can be decelerated safely may be determined from Eqs. 5-17 and 5-25 in the form of

$$B F_p Y = (0.17 \text{ to } 0.21) W \text{, in.·lb} \qquad (5\text{-}27)$$

For example, with a pedal force F_p = 150 lb and an effective pedal travel of Y = 4 in., the vehicle weight would be equal to

$$W = \frac{B \times 150 \times 4}{(0.17 \text{ to } 0.21)} = B(2850 \text{ to } 3530) \text{, lb}$$

For a vacuum assist characteristic of B = 3, the maximum vehicle weight that could safely be decelerated is approximately 8,500 to 10,000 lb. Vacuum-assist-equipped vehicles generally use smaller pedal travels than manual brake systems.

The vacuum booster analysis may be presented graphically in the form of a design chart as shown in Fig. 5-5. The use of the chart is as follows. For a vehicle with the values that follow as

1. Given
   a. Pedal force F_P = 65 lb
   b. Pedal travel Y = 5.0 in.
   c. Brake line pressure p_l = 1300 psi
   d. Master cylinder volume V_{MC} = 0.7 in.^{3}
2. Find
   a. Booster work $F_A X$
   b. Assist characteristic B
   c. Booster diameter
   d. Relative vacuum
   e. Assist piston travel
   f. Pedal ratio l_P

from Fig. 5-5. The solution is illustrated by the broken lines on the chart.

3. Solution
   a. Booster work $F_A X$:

(1) Draw a horizontal line from the brake line pressure p_l = 1300 psi to the line representing V_{MC} = 0.7 in.^{3}

(2) From the point of intersection of the horizontal line with the line representing V_{MC} = 0.7 in.^{3} drop a vertical line to the second horizontal line on the chart.

(3) The intersection of the vertical line with the second horizontal line gives the booster work $F_A X$ which in this case is 800 in.·lb.

b. Assist characteristic B:

(1) Draw a vertical line from the pedal travel Y = 5.0 in. to the line representing pedal force F_P = 65 lb.

(2) From the intersection of the vertical line with F_P = 65 lb, draw a horizontal line to the left.

(3) From the point representing booster work $F_A X$ = 800 in.·lb draw a line extending upward at an angle of 45 deg.

(4) The intersection of the horizontal line with the one drawn at 45 deg gives an assist characteristic B = 2.5.

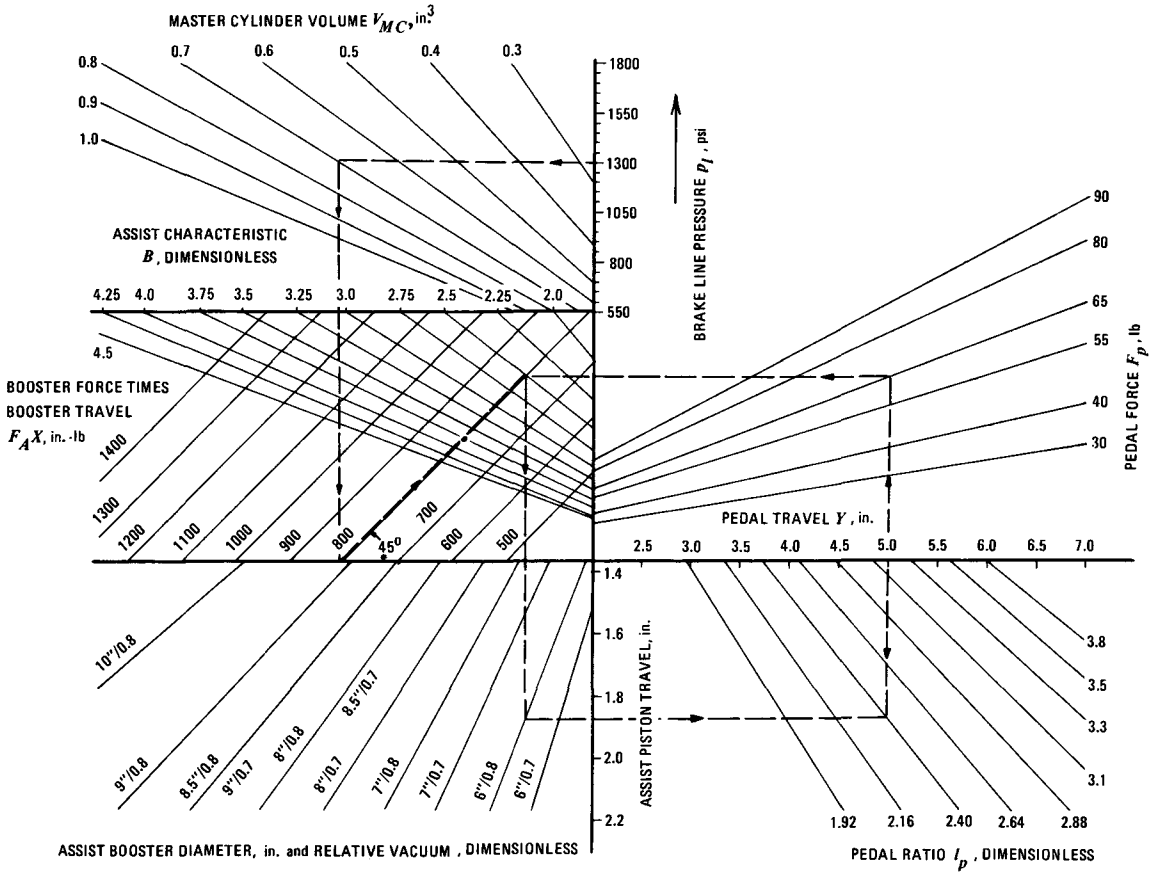

Figure 5-5. Vacuum Booster Design Chart

c. Booster diameter and relative vacuum:

(1) Drop a vertical line from the point established in b(4).

(2) The intersection of this vertical line with one of the booster lines gives acceptable values of booster diameter and relative vacuum. In this case let the vertical line intersect the line representing booster diameter and relative vacuum of 6"/0.8.

d. Pedal ratio l_p:

(1) Drop a vertical line from pedal travel Y = 5.0 in.

(2) Draw a horizontal line through the point established in c(2).

(3) The intersection of the vertical and horizontal lines gives the pedal ratio — in this case l_p = 2.4.

e. Assist piston travel. The intersection of the horizontal line established in d(2) with the vertical axis determines the assist piston travel — in this case approximately 1.87 in.

If a different booster diameter and/or relative vacuum is chosen, then the pedal ratio and assist piston travel change accordingly. For example with a booster diameter of 7 in. and a relative vacuum of 0.7, the pedal ratio becomes approximately 2.88 and the assist piston travel approximately 1.54 in. If desired, a pedal ratio may be selected rather than the booster diameter and/or relative vacuum. This selection will determine the booster diameter and relative vacuum. The choice of booster diameter or pedal ratio is a function of the space available for the installation of the booster or foot pedal.

5-4 FULL-POWER HYDRAULIC BRAKE SYSTEM

Two different designs of full-power hydraulic brake systems can be identified: (a) the pump brake system with master cylinder and (b) the pump brake

system with accumulator without master cylinder (Refs. 5, 6, and 7). Discussion follows:

1. Pump Brake System With Master Cylinder:

The pump system with master cylinder consists of the standard hydraulic brake system equipped with a special master cylinder. Connected to the master cylinder is the pump circuit. Both circuits are completely separate but use the same type of brake fluid so that in the event of leakage no fluid contamination occurs. The schematic of the system is shown in Fig. 5-6. The brake system consists of the pump (1), reservoir (2), the master cylinder (3), the assist unit (4), the standard hydraulic brakes with lines (5), wheel cylinders (6), and wheel brakes (7). The assist characteristics, defined as the ratio of force upon the master cylinder piston to pedal force into the master cylinder, is a function of the effective area and the pushrod area of the assist unit. In case of pump failure, the pedal effort is transmitted directly upon the master cylinder piston and a reduced manual brake application is available. A typical line pressure/pedal force diagram is illustrated in Fig. 5-7 for different modes of brake system operation. An important design consideration is the use of moderate assist characteristics so that no excessive pedal forces are required in the event of a power failure.

The pump is a separate pump or the pump of the steering system. It delivers a constant flow of fluid through the assist unit. In the event of brake application, the fluid flow is obstructed which results in an increase of fluid pressure. This pressure acts upon the master cylinder piston and the pedal force input rod. This condition allows a very sensitive pedal force modulation by the driver. The maximum pressure level is limited by a check valve. When the brake pedal is not applied, the assist fluid pressure is low and determined by the flow resistance of the circuit. When the brake pedal is actuated, the assist pressure must be built up to the desired level, resulting in a time delay between pedal displacement and maximum brake line pressure production. Modern full hydraulic brake systems use an energy storing element such as gas-pressurized accumulators. Here the pump pressure is used to produce a high fluid pressure stored by the accumulator. During brake application, the pressure is at the desired level resulting in a rapidly responding system. However, in the installation of the accumulator system care must be taken to avoid exposure of fluid lines between pump accumulator, and assist or booster unit, to low temperatures. Low fluid temperatures cause low fluid viscosity, and hence, increased response times.

The size of the accumulator is a function of the vehicle weight and the number of stops required by one accumulator charge. In the paragraphs that follow the procedure used for determining accumulator size is discussed (Ref. 7).

The schematic of a hydraulic booster unit is illustrated in Fig. 5-8. The pressure p_B supplied by the accumulator to the booster in addition to the pedal effort by the driver acts upon the master cylinder piston which produces the brake line pressure to the wheels.

The effective input force to the booster is determined by the booster area and the push rod cross-sectional area. The booster input characteristic IC may be defined by the ratio

$$IC = (D_B/D_P)^2 \text{ , d'less} \qquad (5\text{-}28)$$

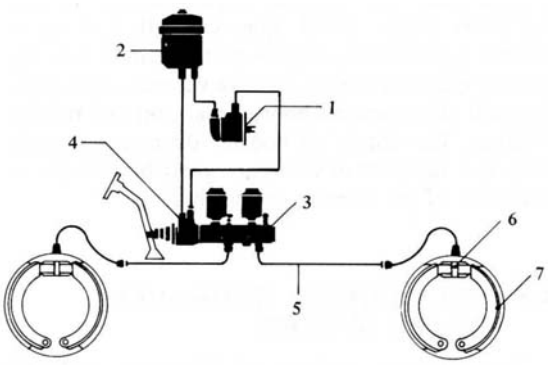

Figure 5-6. Schematic of Pump Power Hydraulic Brake System

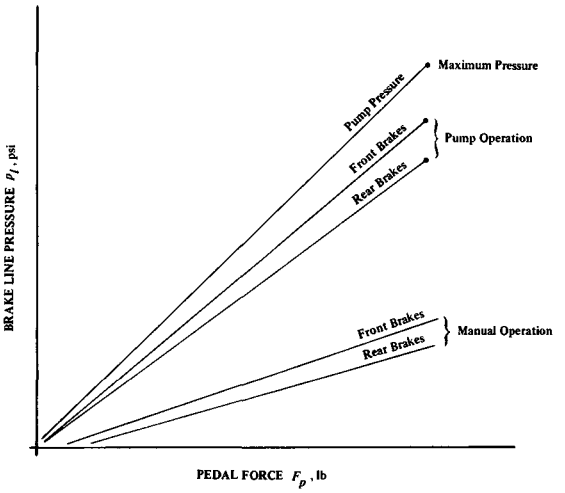

Figure 5-7. Line Pressure/Pedal Force Diagram for Full Power Hydraulic Brake System

where

D_B = booster piston diameter, in.

D_P = pushrod diameter, in.

The booster pressure ratio P is defined by the ratio of output pressure to input pressure and may be expressed in terms of diameters as

$$P = (D_B/D_C)^2 \text{, d'less} \qquad (5\text{-}29)$$

where

D_C = output or master cylinder diameter, in.

The brake line pressure may be determined for a given booster pressure (or accumulator pressure) once the booster pressure ratio has been computed.

The boost circuit fluid volume, i.e., size, and operating pressure range of the accumulator are a function of the maximum accumulator pressure P_A and the initial gas charge pressure P_G of the gas used for energy storage by the accumulator. The volume ratio V_{ratio} of the booster is defined by the ratio of volume displaced at the booster side to volume displaced at the output side and is determined by

$$V_{ratio} = P(1 - 1/IC) \text{, d'less} \qquad (5\text{-}30)$$

The minimum size of the accumulator required for the safe deceleration of a vehicle in successive stops may be obtained from the accumulator design chart shown in Fig. 5-9 (Ref. 7).

It is assumed for the preparation of the accumulator design chart that approximately 67% of the master cylinder displacement is required for an emergency stop. The example illustrated in Fig. 5-9 indicates that a vehicle having a master cylinder volume V_{MC} = 3.0 in.^{3}, five emergency stops, a volume ratio V_{ratio} = 2.4 computed by Eq. 5-30, and a pressure ratio P_G/P_A = 0.35 requires an approximate accumulator size of 38 in.^{3}

If the same energy had to be stored by a vacuum assist unit, a volume approximately 40-50 times larger than that associated with a medium pressure accumulator, or 100-130 times larger than that associated with a high pressure accumulator would be required.

The energy stored in the accumulator is affected by ambient temperature. The fluid volume available for braking at high pressures decreases with decreasing temperature. For example, an accumulator having a volume of 40 in.^{3} available between the pressure range of 2,100 and 2,600 psi when operating at 176°F, provides only 15 in.^{3} when the temperature is minus 40°F (Ref. 7).

2. Pump Brake System With Accumulator Without Master Cylinder:

The brake system consists of the pump, the accumulator, the foot valve, and the standard hydraulic brake system. The accumulator pressure is modulated by the foot valve and is applied directly upon the wheel cylinder of the wheel brakes. Since no master cylinder is used, no manual brake application is available in the event of a power source failure. For this reason a separate emergency brake system is provided in case the major system fails. In many cases the accumulator capacity is designed so that several brake applications are possible if the pump fails.

The pumps used in accumulator brake systems are either vane or radial piston designs. Vane pumps are

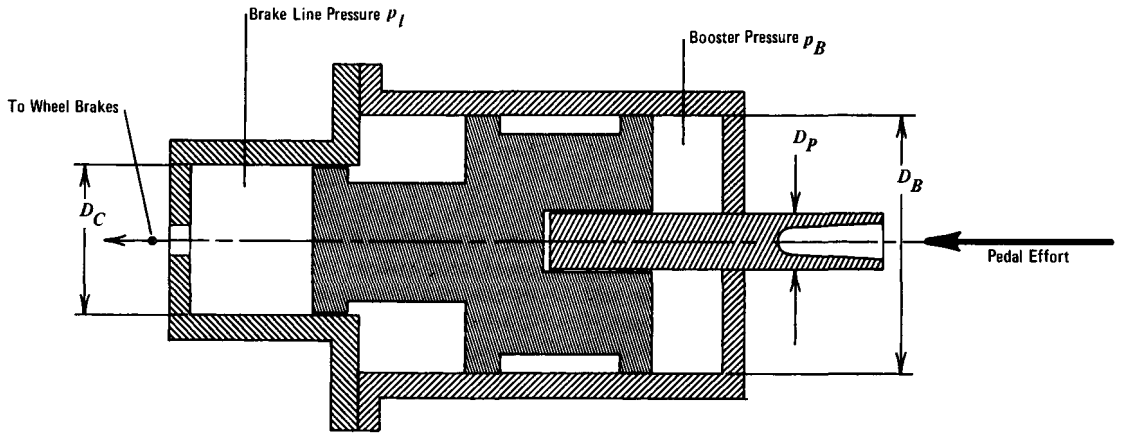

Figure 5-8. Schematic of Hydraulic Booster

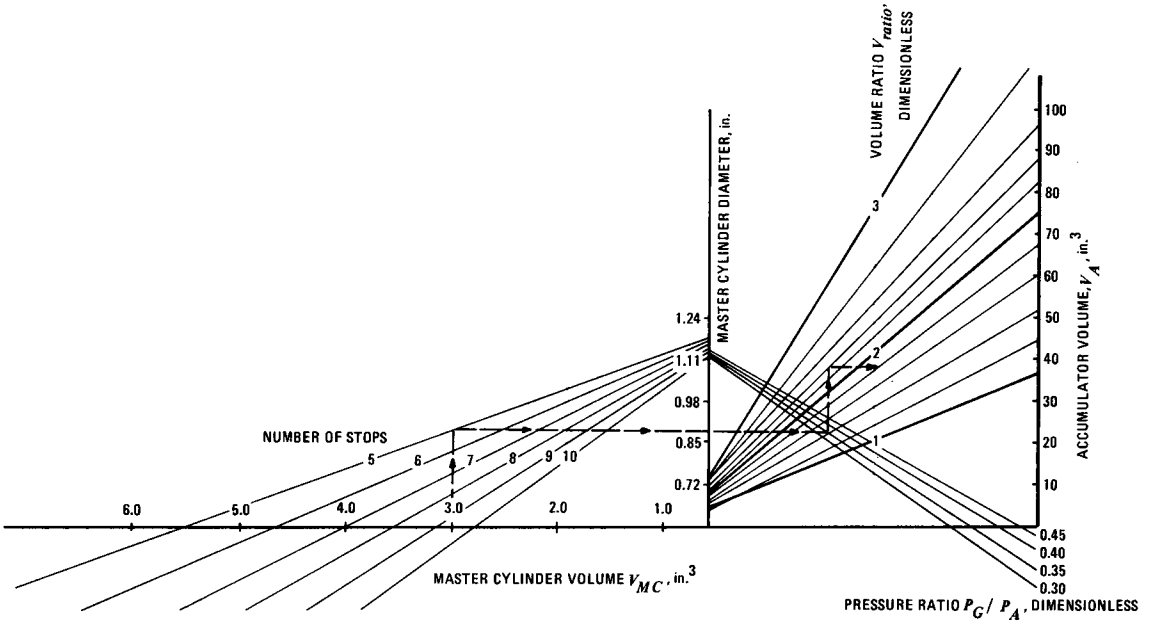

Figure 5-9. Accumulator Design Chart

generally limited to a pressure of approximately 1400 psi; extreme pressure levels may go as high as 2000 psi. Radial piston type pumps may produce pressures up to 3000 psi and volume flow rates of approximately 0.06 in.^{3} per revolution. Pumps are commonly driven directly by the vehicle engine by pulleys and belts or gears. In some applications electrically driven pumps are used. Some vehicles use the steering pump for charging the accumulator. Since steering pumps use mineral oil and not hydraulic brake fluid, separate circuits must be provided for the brake system and the steering system.

A comparison of full power systems with vacuum-assisted brakes indicates the latter to be the most economical power source, assuming a sufficient quantity of vacuum is available. However, exhaust emission regulations and fuel injection systems have reduced greatly the degree of vacuum available as a power source. Consequently, more and more future designs will require a hydraulic energy source consisting of a pump and, if necessary, a gas-loaded accumulator. The latter becomes necessary for the efficient and high-performance-oriented operation of advanced antilock brake systems. In the case of an accumulator installation, a relatively small pump, which only charges the accumulator when the charge pressure falls below a certain level, is sufficient. Operating pressures are as high as 2500 psi.

The computation of brake force and vehicle deceleration is accomplished in the same manner as for the manual brake system. The axle brake force produced by a full power hydraulic brake system is determined by Eq. 5-10. The vehicle deceleration is computed by Eq. 5-11. The pedal force/brake pressure is obtained from an analysis of the effective area of the assist unit, or from the brake assist characteristics specified by manufacturers.

5-5 AIR BRAKE SYSTEM

The principles involved in air brake systems are similar to those of full-power accumulator brake systems. The pedal force of the driver is used only to modulate the flow, and thus pressure, of the working fluid between the accumulator and the wheel brakes. As the name implies, the working fluid is air. Since air brake systems operate at maximum pressures of approximately 120 psi, the size of the components is significantly larger than those found in full power hydraulic brake systems (Refs. 8, 9, and 10).

Air brake systems consist of a variety of components which are used to maintain a supply of compressed air, to direct and control the flow of air, and to transform the stored energy of the air into mechanical force at the wheel brakes. A detailed discussion is presented in Chapter 15.

The brake force produced by an air brake is computed by an equation similar to Eq. 5-3. Since the application of the mechanical force to the brake shoes is accomplished by slack adjusters and cams or wedges, the general equation for the brake force F_x per axle of an air brake is (Ref. 2)

$$F_x = 2(p_l - p_o) A_C \eta_m BF\left(\frac{r}{R}\right)\rho \text{ , lb} \qquad (5\text{-}31)$$

where

A_C = brake chamber area, in.^{2}
p_l = brake line pressure, psi
η_m = mechanical efficiency between brake chamber and shoe actuation, d'less
ρ = lever ratio between brake chamber and brake shoe, d'less

For "S" cam brakes, the lever ratio is

$$\rho = \frac{l_s}{2l_c} \text{ , d'less} \qquad (5\text{-}32)$$

where

l_s = effective slack adjuster length, in.
l_c = effective cam radius, in.; for most brakes l_c = 0.5 in.

For wedge brakes the lever ratio is

$$\rho = \frac{1}{2\tan(\alpha/2)} \text{ , d'less} \qquad (5\text{-}33)$$

where

α = wedge angle, deg

The wedge angle ranges from 10 to 18 deg in 2-deg intervals. If the brakes are in good mechanical condition, the mechanical efficiencies exhibited by "S" cam and wedge brakes range from 0.70 to 0.75, and 0.80 to 0.88, respectively (Refs. 2, 11, and 12). The deceleration of the vehicle can be determined by Eq. 5-4.

The brake actuation force produced by the brake chamber decreases significantly as the chamber piston stroke increases beyond a certain travel. The drop in force is caused by the change in diaphragm geometry resulting in a smaller effective area. Tests have shown that a brake chamber with a 2.5 in. maximum stroke may exhibit a decrease in pushrod force of as high as 40% during the last 0.75 in. of stroke when actuated at 80 psi or more (Ref. 13). In order to limit the chamber piston stroke, it becomes necessary to control elastic air chamber bracket deflection, lining to drum clearance, and pushrod clevis setting in case of "S" cam brakes. Test results indicate that a clearance of 0.002 in. between lining and drum may result in a pushrod force of approximately 1,600 lb when actuated at 80 psi and may decrease to about 1,200 psi for a clearance of 0.02 in.

It is apparent that an accurate prediction of vehicle deceleration can be accomplished only when no significant nonlinearities are introduced in the brake force transmission line. For brakes in good mechanical condition — which requires control on clearance adjustment, slack adjuster clevis setting — the vehicle deceleration may be obtained by Eqs. 5-4 and 5-31. Prediction accuracy generally is within ± 5-10% and is limited only by the accuracy of the lining/drum friction coefficient data. If a prediction of the vehicle deceleration is attempted for vehicles with brakes that show brake chamber piston stroke in excess of 1.75 in., then Eq. 5-31 must be modified to account for the reduced effectiveness of the brake chamber. In this case the brake actuating force, given by the term $(p_l - p_o)A_C$, is replaced by an empirical relationship to yield an axle brake force

$$F_x = (5)(p_l - p_o)(A_C - 6.3d_C)\eta_m BF\left(\frac{r}{R}\right)\rho \text{ , lb} \qquad (5\text{-}34)$$

where

$d_C \geq 1.75$ in., brake chamber piston displacement

Inspection of Eq. 5-34 indicates the number 6.3 must have the units of length. Eq. 5-34 may be used only when the brake chamber piston displacement is equal or greater than 1.75 in. For cases in which the displacement is less than 1.75 in., Eq. 5-31 must be used.

5-6 COMPRESSED AIR-OVER-HYDRAULIC BRAKE SYSTEM

The air-over-hydraulic brake uses compressed air as an assist medium to actuate a standard master cylinder in the hydraulic brake circuit. The major advantage of the air-over-hydraulic brake is the availability of compressed air for braking trailers equipped with air brakes when connected to a hydraulically braked tractor.

The assist unit is axially mounted to the hydraulic master cylinder as illustrated in Fig. 5-10. The design avoids the transmission of reaction forces to the mounting bracket. The assist force is transmitted directly against the master cylinder piston which supplies the brake fluid to the wheel cylinders. Since no levers are required for the transmission of the force, a high mechanical efficiency is obtained.

Air-over-hydraulic brakes can be designed as dual circuits by either using two assist units or a tandem master cylinder connected to a single assist unit.

A single circuit air-over-hydraulic brake system is illustrated in Fig. 5-11 with all essential components identified. The air compressor (1) charges the air tank (2). The air pressure is adjusted by the pressure regulator (3). The application valve (4) controls the air flow to the assist unit (5) and force application to the master cylinder (6). Hydraulic brake line pressure is transmitted to the wheel brakes at the front (7) and rear axle (8). Air pressure is measured by the gauge (9). Trailer brake supply line connections are indicated (10).

A more efficient design is provided by combining the air application valve with the master cylinder into one unit. This system allows hydraulically braked trucks to tow pneumatically braked trailers, allows the combination of hydraulic and air brakes on the same vehicle, and provides for the efficient design of dual circuit brakes for heavy vehicles. An example of the application of the combination brake valve to the brakes of a tandem axle truck is illustrated in Fig. 5-12. The components are: compressor (1), air tank (2), pressure regulator (3), combination brake valve (4), assist unit (5), front brakes (6), rear brakes (7), pressure gauge (8), and trailer brake line (9).

The actual design of a brake system in terms of the size of the combination valve and assist unit depends upon the force required to press the brake shoes against the drum and hence the hydraulic brake line pressure to the wheel cylinders. Although the gain of the combination valve or assist unit can be calculated from design information in a manner similar to that of vacuum assisted brake systems, manufacturers provide pressure curves of the assist unit as illustrated in Fig. 5-13. The curves shown are those with and without air assist. Although the braking effectiveness is reduced significantly in the event of a failure in the compressed air circuit, manual application of the brakes is possible since the force transmission line remains in tact between the foot pedal and the wheel brakes. Pure air brakes do not exhibit this emergency braking feature.

The deceleration produced by an air-over-hydraulic brake system may be computed by Eq. 5-11 for a two-axle vehicle with the brake line pressure obtained from a graph similar to Fig. 5-13.

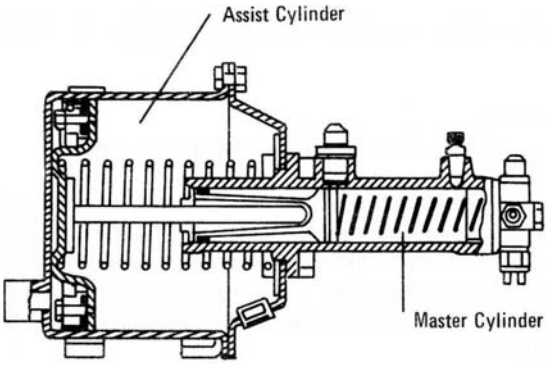

Figure 5-10. Air-Over-Hydraulic Brake Unit

5-7 MECHANICAL BRAKE SYSTEM

In current design practice, mechanical brake systems — often called hand brakes — are used for emergency or parking brakes. Their mechanical efficiency (65%) is lower than that of hydraulic (95%) or air brake systems (75%). Mechanical brake systems equipped with cables easily may exhibit efficiencies less than 60%.

For a typical parking brake design in the wheel brakes as illustrated in Fig. 5-14, the gain ρ_B between

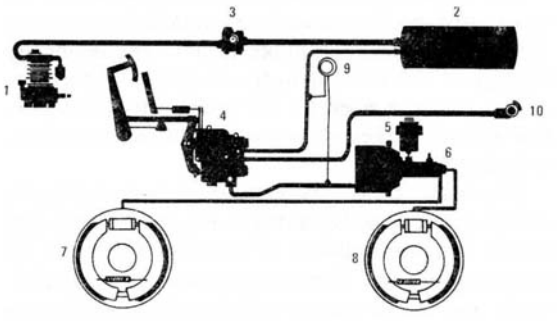

Figure 5-11. Air-Over-Hydraulic Brake System (Single Circuit)

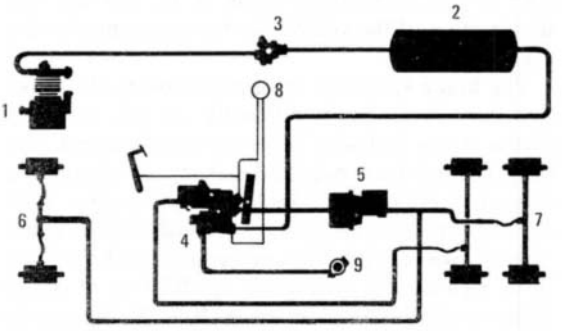

Figure 5-12. Air-Over-Hydraulic Brakes for Tandem Axle Truck

the cable force into the brake and average shoe actuation force is

$$\rho_B = \frac{1}{2}\left[\frac{l_2}{l_1 l_5}(l_3 - l_1) + \frac{l_3}{l_1 l_5}(l_2 - l_1)\right], \text{ d'less} \quad (5\text{-}35)$$

where l_1 through l_5 are brake dimensions, in., identified in Fig. 5-14.

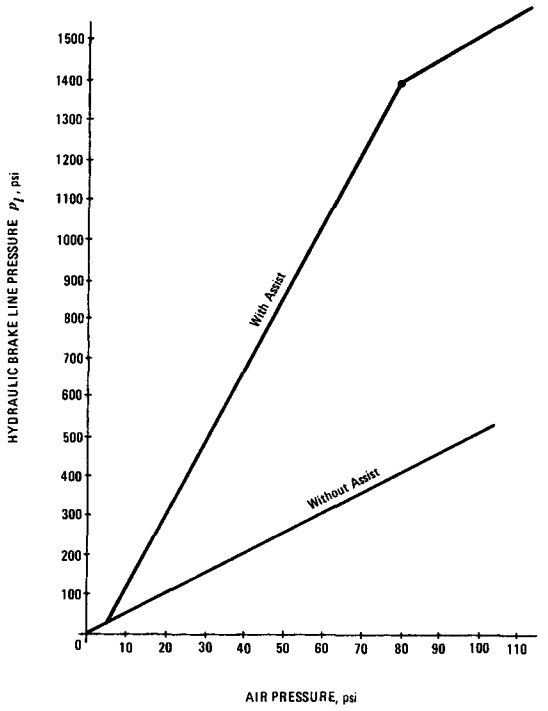

Figure 5-13. Air-Over-Hydraulic Brake Characteristic

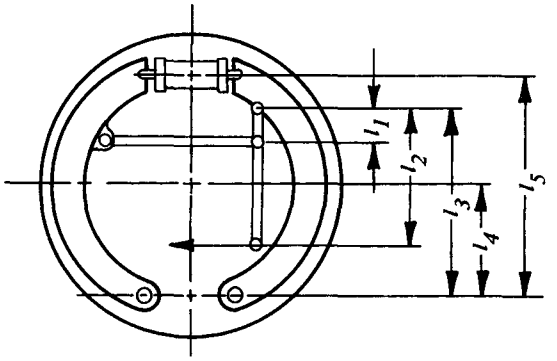

Figure 5-14. Schematic of Parking Brake

The total brake force F_x at the wheels braked by the mechanical system may be computed by

$$F_x = F_H \rho_H \rho_B \eta_H BF \left(\frac{r}{R}\right), \text{ lb} \quad (5\text{-}36)$$

where

F_H = hand force, lb
η_H = mechanical efficiency of hand brake, d'less
ρ_B = emergency brake gain, d'less
ρ_H = displacement gain between hand brake application force and cable force, d'less

The displacement gain ρ_H is equivalent to the pedal lever ratio of the foot-operated service brake. It is determined by the ratio of hand travel to cable travel. The average displacement d of the tip of the brake shoe, equivalent to wheel cylinder piston travel, is

$$d = \frac{Y_H}{\rho_B \rho_H}, \text{ in.} \quad (5\text{-}37)$$

where

Y_H = available hand or foot travel for emergency brake, in.

The corresponding brake shoe displacement d resulting from the nonpowered hydraulic service brake is given by the relationship

$$d = \frac{(Y/l_p - 0.1) A_{MC}}{4[(A_{WC})_F + (A_{WC})_R]}, \text{ in.} \quad (5\text{-}38)$$

A travel loss of 0.1 in. due to reservoir compensating hole clearance is assumed in Eq. 5-8.

Safety considerations require that the displacement associated with the emergency brake μ_s obtained by Eq. 5-37 be greater than that associated with the service brakes as obtained by Eq. 5-38.

Drive shaft mounted parking brakes retard the shaft between transmission and differential and thus operate at a higher number of revolutions per minute than the wheel brakes.

The total braking force F_x at the wheels retarded by the drive shaft mounted brake is

$$F_x = \frac{F_H \rho_H BF \eta_m \rho_D r}{\eta R}, \text{ lb} \quad (5\text{-}39)$$

where

η_m = mechanical efficiency between transmission and wheels, d'less
ρ_D = differential gear ratio, d'less

Brake factors *BF* of typical drive shaft mounted brakes such as band brakes are discussed in Chapter 2.

5-8 SURGE BRAKES

The trailer is connected to the truck by the tongue. If the trailer is not equipped with a braking system, the inertia force of the trailer during braking must be absorbed by the brakes of the truck. Light to medium weight trailers often are equipped with a surge brake. During braking, the inertia force of the trailer is transmitted through the tongue to the truck. The surge brake uses this tongue force to actuate either a mechanical system of linkages or a hydraulic master cylinder. The deceleration of the trailer is a function of the trailer weight. For trailers with varying loading conditions the surge brake offers significant advantages.

The analysis of surge brakes is accomplished by determining the deceleration of the truck a_1 in the absence of the trailer by

$$a_1 = \frac{F_{x1}}{W_1}, \text{ g-units} \qquad (5\text{-}40)$$

where

F_{x1} = braking force of truck, lb

W_1 = truck weight, lb

The trailer deceleration a_2 in the absence of the truck is

$$a_2 = \frac{F_{x2}}{W_2}, \text{ g-units} \qquad (5\text{-}41)$$

where

F_{x2} = braking force of trailer, lb

W_2 = trailer weight, lb

The deceleration a of the truck-trailer combination is

$$a = \frac{F_{x1} + F_{x2}}{W_1 + W_2} = a_1 \frac{W_1}{W_1 + W_2} + a_2 \frac{W_2}{W_1 + W_2}, \text{ g-units} \qquad (5\text{-}42)$$

The tongue force or surge brake actuating force F_T is determined by

$$F_T = F_{x2} - W_2 a, \text{ lb} \qquad (5\text{-}43)$$

The tongue force determined by Eq. 5-43 is used as actuating force of the trailer brake system.

Surge brakes generally are not used on heavy trailers. Since the surge brake requires that a tongue force exist between truck and trailer, the vehicle combination may become unstable when braking in a turn. The tongue force may be sufficiently large to cause the truck rear axle to slide sideways. Heavy trailers therefore are equipped with brakes that are actuated by a signal from the driver and not by the tongue force. Stability requirement on braking of heavy truck-trailer combinations to reduce the tongue force to zero for all braking and loading conditions. This requirement is achieved when $a_1 = a_2$.

5-9 ELECTRIC BRAKES

Electric brakes are used in trailers and are actuated by the driver by a special lever. A rotating and stationary ring face each other in the wheel brake. The stationary ring replaces the common hydraulic wheel cylinder and is used to actuate the brake shoe. As the driver displaces the trailer brake lever, electric current is provided to the stationary ring resulting in magnetizing it which results in the development of a torque between the stationary and rotating ring. The slight rotation of the stationary ring results in an application of the brake shoes against the drum. The use of electric brakes generally is limited to duo-servo and two-leading shoe brakes. Reasons for this limitation are that the rotation of the stationary ring can actuate brake shoes in one direction only. A leading-trailing shoe brake, for example, requires actuation of the leading shoe in the counter-clockwise direction and of the trailing shoe in the clockwise direction.

REFERENCES

1. R. Murphy, et al., *Development of Braking Performance Requirement for Buses, Trucks, and Tractor/Trailers,* SAE Paper No. 710046, January 1971.
2. J. T. Tielking, et al., *Mechanical Properties of Truck Tires,* SAE Paper No. 730183, January 1973.
3. "Vacuum-Hydraulic Brake Servo", *Automobile Engineer,* Vol. 52, No. 1, January 1962, pp. 26-29.
4. *ATE Brake Service Manual,* Frankfurt, Germany, 1972.
5. O. Depenheur and H. Strien, *Hydraulic Brake*

Activating Systems Under Consideration of Anti-lock Systems and Disc Brakes, SAE Paper No. 730535, May 1973.

6. R. T. Burnett, et al., "An Advanced Brake System for Heavy Trucks", *Bendix Technical Journal,* Autumn 1969, pp. 15-25.
7. H. C. Klein and H. Strien, *Hydraulically Boosted Brakes – An Important Part of Central Hydraulic Systems,* SAE Paper No. 750867, October 1975.
8. S. Johnson, *Pneumatic Power Control Systems for Trucks, Trailers, and Buses,* SAE Paper No. 52C, June 1958.
9. R. Hildebrandt, *Air Brake Control System on the New "L" Series Trucks,* SAE Paper No. 700504.
10. C. F. Smith, *Dual Air Brake Control Systems,* SAE Paper No. 700505.
11. J. W. Kourik, *Wedge Brake Versus Cam Brake – Theoretical Comparison,* SAE Paper No. 941A, October 1964.
12. E. J. Beatty, *Wedge Brake Versus Cam Brake – Road Test Comparison,* SAE Paper No. 941C, October 1964.
13. D. E. Steis, *Inertia Brake Dynamometer Testing Techniques for FMVSS121,* SAE Paper No. 751010, Philadelphia, November 1975.

CHAPTER 6
TIRE-ROAD FRICTION

In this chapter the effects of tire characteristics on braking are discussed. The contribution of tire rolling resistance to vehicle deceleration is introduced briefly. The different tire designs and their importance relative to braking are presented.

6-0 LIST OF SYMBOLS

F_R = rolling resistance, lb
$F_{z,res}$ = resultant force, lb
F_x = force in longitudinal direction, lb
F_z = normal force supported by tire, lb
h = distance from wheel center to road, ft
p = tire inflation pressure, psi
R_r = tire rolling resistance coefficient, d'less
S = locked-wheel stopping distance, ft
V = vehicle speed, mph
x = horizontal distance from wheel center to resultant force, ft
μ_x = longitudinal friction coefficient, d'less*
μ_y = lateral friction coefficient, d'less

6-1 TIRE-ROAD INTERFACE

The friction between tire and roadway limits the maximum braking capability of a vehicle. The friction can be defined in terms of the coefficient of friction which is equal to the ratio of the tangential force transmitted by the tire to the normal load carried by the tire. The coefficient of friction depends upon the material and surface geometries of the tire and the roadway; the nature and thickness of any film such as water, sand, or oil present in the contact area; sliding velocity, and operating temperature.

Tire-road friction is not a fully understood phenomenon (Ref. 1). Any measurement of the frictional properties of a surface is a measure of the performance of a particular tire on that surface and does not define the performance of another tire on the same surface.

Research has shown that the primary element in the production of rubber friction is the interaction of the tire tread rubber compound with the microtexture of the road surface (Ref. 2). This texture generally is concluded to be of extreme small scale in the order of 3 to 10 microns. On dry surfaces, the friction level is relatively independent of speed in the normal passenger car operating range. It can be concluded then that the friction level can be controlled by varying the microtexture in the road surface. This appears to be true for both wet and dry roads. However, on wet roads, the ability of the rubber to interact with the microtexture is hindered by the water. This lack of intimate rubber-microtexture contact is what creates lower friction levels on wet roads and is caused by two basic phenomena. These are viscous hydroplaning and dynamic hydroplaning. In the case of viscous hydroplaning, friction is lost by the inability of the individual microtexture elements to break through a viscous water film and contact the tread rubber.

Dynamic hydroplaning creates a loss of tire-road contact by exerting a lift on the tread contact patch due to water inertial effects. As the tire attempts to displace water in its path, the inertia of the water creates a hydrodynamic pressure which can lift the tire patch and reduce intimate tire road contact. The element of road structure that reduces this phenomenon is known as macro or large relief paths in the contact area. The relief paths reduce hydrodynamic pressure and tire contact patch lifting. Increasing macrotextures will increase high speed friction by reducing the build up of hydrodynamic pressure. In order to produce a specific set of frictional characteristics — namely, actual level and change of friction with speed — both the micro and macro texture of the road surface must be controlled. If both textures are controlled, a particular set of frictional characteristics will have been established for a defined water depth and a particular test tire.

6-2 ROAD FRICTION MEASUREMENT

The measured coefficient of friction of a public road is not constant and varies seasonally and from lane to lane on the highway. Measuring road friction may be done by several methods (Refs. 2 and 3). Three methods have been widely used: skid trailer, stopping distance measurements, and portable testers. Skid trailers can be used to measure peak and sliding friction. Comparisons between the British Portable Tester and automobile stopping distance measurements show good correlation of the results

*d'less = dimensionless

when patterned tires are used. In all skid resistance measurements the conditions must be controlled carefully in order to obtain consistent results. Each is discussed:

1. Skid Trailer. One useful test device is the braking skid trailer. A slave wheel is attached to a large vehicle. All tire forces can be measured while the wheel is made to spin up, brake to any speed, and operate over a range of slip values. This device produces considerable data, usually for equilibrium conditions of tire operation. In principle it is possible to impose quickly varying conditions on the tire to measure its transient behavior. However, to date it has not been possible to eliminate all of the unwanted transients from the test system.

In a different skid trailer design, side slip properties of a pneumatic tire are used. Side slip is defined as the angle between the wheel axis and the direction of motion. Since side slip angle, longitudinal slip, and tire-road friction coefficients are related, this procedure yields data on road traction capability. Tests have shown, however, that in this case tire wear has a pronounced effect upon tire traction, which, consequently, results in poorer correlation among test data (Ref. 2).

2. Automobile Stopping Distance Measurements. The major use of the automobile as a test device is in the braking test, and there are two major types of such tests. The oldest is the locked wheel stopping distance test. For such a test an average tire/road longitudinal friction coefficient μ_x is

$$\mu_x = \frac{V^2}{30S}, \text{ d'less} \qquad (6\text{-}1)$$

where

S = locked wheel stopping distance, ft

V = vehicle speed, mph

Stopping distance tests are simple, relatively low in cost, and reliable. They only can be conducted safely at low speed. An alternative test was developed where the brakes are applied for a short time without stopping the vehicle. For such tests the vehicle speed change may be measured during braking usually with a "fifth wheel" or indirectly by an accelerometer. In either case the test must last somewhat longer than the duration of the transients that accompany braking.

3. Portable Testers. A good number of small and portable test devices have been developed (Ref. 2). Of these, the most universally accepted is the British Portable Skid Resistance Tester. It is a pendulum device which measures the sliding friction based on the amount of energy lost as a test specimen of rubber on the pendulum slides over a sample of road material.

It is important that the test results obtained by one and the same method be repeatable. This means procedures are transferable to other geographic locations giving accurate assessments of road conditions and hence a reliable skid resistance inventory. In testing wet conditions, it appears that the amount of water specified for wetting a unit area of road surface is not always sufficient for defining a wet surface. Since the water film thickness is the controlling variable, side wind and road undulation do have a significant effect upon the measured skid resistance of a particular roadway.

6-3 TIRE FRICTION CHARACTERISTICS

A typical curve showing how the friction coefficient varies with longitudinal slip is given in Fig. 6-1 (Ref. 4). Longitudinal slip is defined as the ratio of the difference between the actual vehicle speed and the circumferential speed of the tire to actual vehicle speed times 100. A locked wheel corresponds to 100% longitudinal slip. The friction of a given tire-roadway combination can be specified by the peak and sliding coefficients. For a given tire, the shape and magnitude of the friction curve vary with both vehicle speed and road surface condition. It has been found that both the peak and sliding coefficient generally decrease with increasing speed, with the peak value decreasing at a lower rate (Ref. 5).

Typical data illustrating the influence of velocity on dry and wet road surfaces are presented in Figs. 6-2 and 6-3 (Ref. 6). Whereas the friction forces on dry

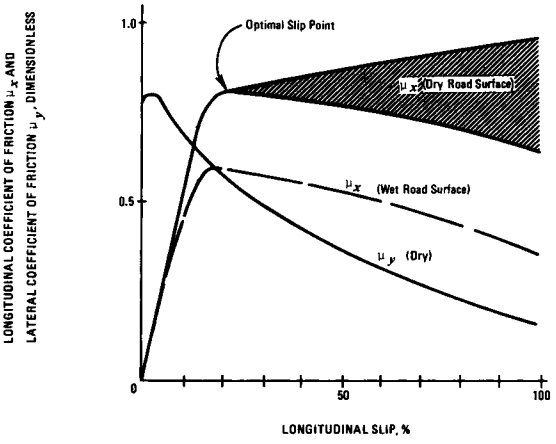

Figure 6-1. Tire Friction Versus Wheel Slip

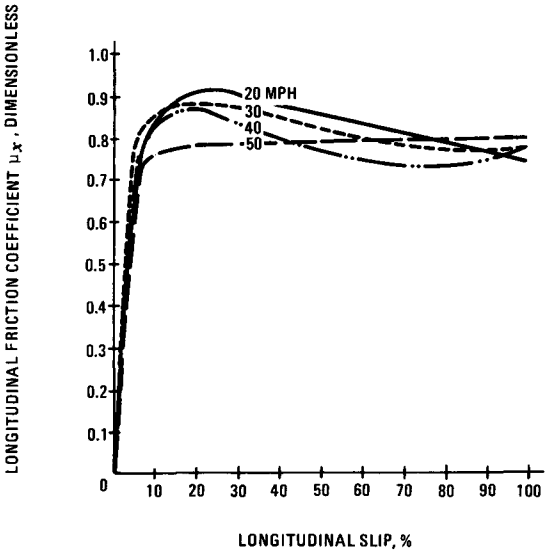

Figure 6-2. Friction-Slip Curve for Dry Concrete as Function of Speed

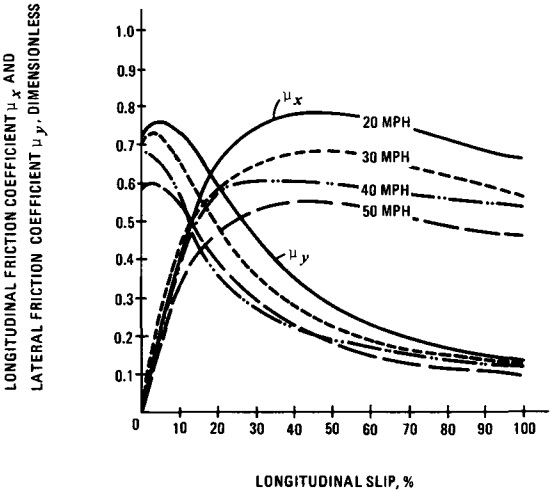

Figure 6-3. Friction-Slip Curve for Wet Concrete Road as a Function of Speed Obtained for an Automobile Tire

concrete are little affected by wheel slip values beyond 10% and vehicle speed, the results obtained on wet concrete indicate a pronounced effect of velocity and slip on the friction force produced by the tire. Typical friction data that may be used for design purposes of truck brake systems are presented in Fig. 6-4 (Refs. 7 and 8). For passenger car tires operating under similar conditions, the tire-road friction coefficients for dry surfaces are generally 10 to 20% higher. In the design evaluation of wheel antilock systems on dry roadways approximate values for maximum longitudinal friction coefficients of 0.85 to 0.90 and sliding friction coefficients of 0.70 to 0.75 may be used. For an exact investigation the particular tire properties must be individually measured. As can be seen from Fig. 6-2, on dry surfaces a wheel antilock brake system will not produce a substantial improvement in stopping distance reduction because the ratio of the peak friction coefficient to the sliding value is nearly unity. However, on wet surfaces a considerable decrease in stopping distance may be expected.

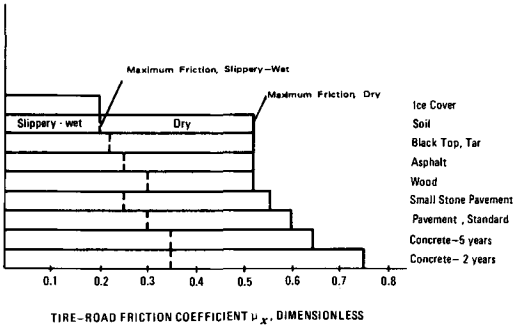

Figure 6-4. Typical Coefficient of Friction μ_x Between Tire and Road for Truck Tire

The curves in Fig. 6-1 also illustrate the basic characteristics of the lateral friction coefficient designated by μ_y. It is evident that a free rolling wheel will have a maximum lateral friction coefficient; whereas, a sliding wheel will have a minimum coefficient of friction μ_y. For braking on wet pavement, the optimum of providing maximum longitudinal and lateral friction lies probably somewhere near or before the peak value of the coefficient of friction μ_x for wet surfaces. Under these conditions a tire tends to produce sufficient lateral as well as longitudinal contact forces.

6-4 TIRE ROLLING RESISTANCE

Tire rolling resistance is that force developed by the rolling tire that resists forward motion. As a tire rotates, the tire deformation produced at the tire-road interface moves continuously around the periphery of the tire. As a result of this internal damping of the tire casing entering and leaving the contact patch, the pressure distribution in the contact area is shifted forward yielding the resultant force

$F_{z,res}$ which produces the rolling resistance as illustrated in Fig. 6-5. For a free rolling wheel with no moment acting on the shaft, the moment $F_{z,res}x$ must be balanced by the moment $F_R h$.

The rolling resistance force F_R may be computed by

$$F_R = R_r F_z \text{ , lb} \tag{6-2}$$

where

R_r = tire rolling resistance coefficient, d'less

F_z = normal force supported by tire, lb

The rolling resistance coefficient R_r is expressed by the functional relationship (Ref. 9).

$$R_r = 0.005 + \frac{0.15}{p} + \frac{0.0035}{p}\left(\frac{V^2}{100}\right) \text{ , d'less} \tag{6-3}$$

where

p = tire inflation pressure, psi

V = vehicle speed, mph

The rolling resistance increases when the tire is delivering tractive effort. The rolling resistance also increases with increasing slip angle.

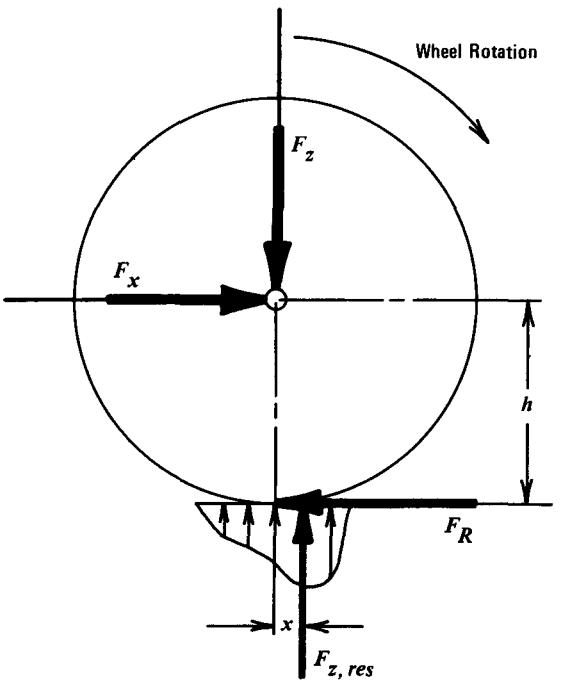

Figure 6-5. Forces Acting on a Free-Rolling Wheel

Tire materials and type of tire construction have an effect on rolling resistance. At low speed, nylon cord has the highest rolling resistance followed by rayon. Steel cord has the lowest rolling resistance. However, at high speed, rayon has a higher rolling resistance than nylon. Table 6-1 lists some typical values of rolling resistance measured on a passenger car tire.

Truck tires generally have a lower rolling resistance coefficient than passenger tires.

6-5 TIRE DESIGN AND COMPOSITION

Different tire construction, in general, influences the tire mechanical characteristics, and it is not possible to rate one type of tire superior to another in all respects. The carcass, an inflated enclosure of rubber fiber composite, is the basic tire structure. It is reinforced with the fibrous cord following a set path pattern, bias ply (the conventional tire) and radial ply, and consists of a different number of layers embedded in rubber or other commonly used polymer matrix. The cord structure provides the necessary structural rigidity to the otherwise soft and highly elastic rubber or polymer mix to withstand the static and dynamic stresses of inflation and other forces without excessive creep. Some tires are built with a belt under the tread to provide structural integrity. The belt is influential in controlling the wear characteristics of the tire.

There are two ways to apply the plies: bias and radial. For many years most tires were of the bias type. These had the plies crisscrossed with one layer running one way and the other running so that they were more or less perpendicular. This gave a carcass that was strong in all directions because of the overlapping plies. The difficulty was that the plies tended to move against each other, generating heat, particularly at high speed. Also, the tread tended to squirm as it met the road and this caused tread wear.

To remedy this problem, tires with radial plies were introduced. On these the plies all run parallel to each other and perpendicular to the tire rim. To provide

TABLE 6-1. TIRE ROLLING RESISTANCE COEFFICIENTS

ROADWAY	R_r
Smooth Asphalt Surface	0.015
Smooth Concrete Surface	0.017
Smooth Dirt Road	0.045
Loose Sand	0.05 to 0.30

strength in the direction parallel to the tire rim, belts are applied all the way around the tire. The tread is then vulcanized on top of the belts. The belts are made of rayon, glass fiber, or steel. All perform in a similar manner and provide additional strength to the circumference of the tire. In addition, the belted tire has a larger contact area. It is less stiff because of the radial plies and thinner sidewalls, and thus flexes more to apply a greater part of the tread to the road. Because the sidewalls can be thinner and more flexible, the tread has less tendency to heel up when cornering and provides increased traction in turns.

Bias-ply tires may also be belted. The belted-bias tire generally will have performance properties midway between the other tire types.

Tread design has little effect on a dry road traction. However, on wet road surfaces the tread must maintain effective tire-road contact by removing water coming under the tire. This removal becomes more difficult at high speeds because of the hydrodynamic forces generated due to the water between the tire and the road. The importance of tread design on wet road performance is well-recognized with individual design features such as sipes in the form of narrow slots, grooves, tread width, and crown radius influencing performance. An obvious improvement in the wet road performance is obtained with grooved tires compared to smooth tire surfaces with fine texture since the grooves provide escape channels for the interface water. The effectiveness of grooves increases with the number and width of grooves up to some limit with the sideway skidding resistance also increasing. Although straight circumferential grooves are very effective, some advantages may be gained using zig-zag circumferential grooves of some optimum dimension. The use of narrow slots or sipes also provides an improvement in the wet skidding performance, and this effect is more pronounced on polished smooth wet surfaces. The blades or sipes not only provide a wiping action through the exposed sharp cut edge at right angles to the tread sliding, but also act as reservoirs for water.

Another factor that normally influences the skid resistance directly is the amount and condition of the uneven wear pattern, and regular wearing of the tread. The latter reduces the flow capacity of drainage channels and reservoirs, and considerably impairs the advantages gained with tread pattern. Uneven wear of the tread occurs with tires in the form of significant wear at the leading end of the tread elements compared with the trailing edge. This loss of effective wet traction coefficient could be regained by reversing the direction of wheel rotation. The factors controlling tread wear are the composition, design, load, inflation pressure, and the mode of operation. The actual tread loss per mile travelled is influenced directly by the slip caused by the variety of maneuvers involving some proportion of cornering, traction, or braking and also the road surface characteristics.

Retreading and regrooving are the common techniques for improving the traction of a worn tire without having to replace it. The advantages gained by these methods are substantial and economical, but only when the tire carcass still has enough structural integrity. Regrooving will add the extra skid resistance only where the undertread has sufficient regrooving allowance which is commonly built in most of the truck and bus tires.

Tread pattern is not as influential on rough and harsh textured surfaces. It normally is said that it is the smooth road surfaces which discriminate between tread designs while rough surfaces discriminate between tread materials.

It has long been known that rubber sliding friction is dependent on velocity and load, and that this behavior is a function of the visco-elastic property of the rubber or rubber-like materials. Since the different rubbers are composed of different molecular structures with different mechanical properties, it is not strange to find that rubber possesses a wide range of frictional characteristics (Ref. 2).

Besides natural rubber a large number of rubber materials are used in tires. Laboratory and road skid tests indicate that polybutadiene is a longer wearing tread material than others with improved wet skid resistance. It also reduces tread groove cracking, and cutting and chipping of tire treads during service. The use of high hysteresis trend compounds gives improved wet skid resistance.

Truck tires generally have a larger amount of natural rubber content than passenger car tires, resulting in lower rolling resistance at the cost of a decreased longitudinal tire friction coefficient.

REFERENCES

1. A. Tross, "The Mechanism of Friction", *Glaser Annalen,* Vol. 86, No. 5, 1962, No. 11.
2. K. C. Ludema and B. Gujrati, *An Analysis of the Literature on Tire-Road Skid Resistance,* Mechanical Engineering Dept., University of Michigan, 1971.
3. J. A. Davisson, *Basic Test Methods for Evaluating Tire Traction,* SAE Paper No. 680136, 1968.
4. R. Limpert and C. Y. Warner, *Proportional Braking of Solid-Frame Vehicles,* SAE Paper No. 710047, January 1971.

5. E. Hoerz, "Requirements on the Brake Force Modulation of Passenger Cars", *ATZ*, Vol. 71, No. 6, 1969, pp. 189-193.
6. P. S. Fancher, Jr., et al., *Experimental Studies of Tire Shear Force Mechanics*, Highway Safety Research Institute, The University of Michigan, July 30, 1970.
7. *Truck Tire Trends*, SAE Paper No. SP-244, May 1963.
8. W. Hauer, "The Problems of Deceleration Heavy Commercial Vehicles", *Automobil Industrie*, April 1963, pp. 47-54.
9. S. F. Hoerner, *Fluid-Dynamic Drag*, published by the author, 1957.

CHAPTER 7
VEHICLE BRAKING PERFORMANCE

In this chapter performance measures important in the analysis of vehicle braking performance are introduced. The basic approach for computer prediction of vehicle braking performance is discussed. Nonbraking deceleration effects such as aerodynamic drag are briefly reviewed.

7-0 LIST OF SYMBOLS

A = frontal area, ft²
a = deceleration, g-units
a_y = lateral acceleration, g-units
BF = brake factor, d'less*
c_{AD} = aerodynamic drag coefficient, d'less
c_{DD} = damping coefficient, lb·s/ft
E_i = braking efficiency of the ith axle, d'less
E_R = braking efficiency of rear axle, d'less
e = base of natural logarithm
F_{AD} = aerodynamic drag force, lb
F_{DD} = viscous damping drag force, lb
F_p = pedal force, lb
F_{TD} = turning resistance force, lb
$F_{x,total}$ = total brake force, lb
F_{xi} = brake force of ith axle or wheel, lb
$F_{xi,slide}$ = sliding brake force of ith axle, lb
$F_{zF,dyn}$ = dynamic front axle normal force, lb
$F_{zi,dyn}$ = dynamic normal force on ith axle, lb
$F_{zR,dyn}$ = dynamic rear axle normal force, lb
$F_{zR,static}$ = static rear axle normal force, lb
F_{yi} = lateral tire force of ith wheel, lb
f = fade force associated with heavy truck drum brakes, in.²/lb
h = center of gravity height, in.
i = designates ith axle or wheel, d'less
k = factor characterizing road roughness, ft²/s²
L = wheel base, in.
n = number of damped wheels, d'less
p_l = brake line pressure, psi
R_T = turning resistance coefficient, d'less
V = vehicle speed, ft/s
V_{rel} = relative speed between vehicle and wind, ft/s
W = vehicle weight, lb
X_o = coordinate fixed in space, ft
x = longitudinal vehicle coordinate, ft
Y_o = coordinate fixed in space, ft
y = lateral vehicle coordinate, ft
α_F = slip angle on front wheels, deg
α_R = slip angle on rear wheels, deg
β = vehicle side slip angle, deg
γ = trailer articulation angle, deg
δ = front wheel steering angle, deg
μ = tire-road friction coefficient, d'less
μ_L = lining friction coefficient, d'less
μ_{Lh} = nonfaded lining friction coefficient, d'less
μ_{Ll} = faded lining friction coefficient, d'less
μ_{road} = actual tire-road friction coefficient, d'less
$\mu_{road,i}$ = tire-road friction required to prevent lock up of ith axle, d'less
ρ = air density, lbm/ft³
χ = center of gravity height divided by wheelbase, d'less
ψ = static rear axle load divided by vehicle weight, d'less

Subscript 1 = left front tractor wheel
2 = right front tractor wheel
3 = left rear tractor wheel
4 = right rear tractor wheel
5 = left trailer wheel
6 = right trailer wheel

*d'less = dimensionless

7-1 BRAKING PERFORMANCE MEASURES

The mechanics of the braking process suggest that there are at least five distinct facets of braking performance deserving of consideration for passenger cars and commercial vehicles. These facets or measures of braking performance may be referred to as effectiveness, efficiency, response time, controllability, and thermal effectiveness (Ref. 1).

7-1.1 EFFECTIVENESS

Braking effectiveness is the capability of a brake system to translate a given pedal force or brake line pressure into a retarding force acting between tire and ground. Braking effectiveness can be determined analytically by the equations presented in Chapters 2 and 5, or it can be measured either by means of a brake dynamometer or road tests with the vehicle. Dynamometer testing is straight forward and done

routinely for vehicles-in-use evaluation. In road tests when the braking level is lowered such that the tires are not being forced to operate near their adhesion or friction limit, the total braking force acting on a vehicle is linearly related to the total torque being generated by all of the brakes. Under these conditions, deceleration per unit value of brake line pressure or pedal force serves as an overall measure of the braking effectiveness of the vehicle. For pneumatic systems characterized by a limit value of line pressure, a finite value of effectiveness for a given brake means that there is an upper limit to the brake torque that can be generated. If this maximum torque is insufficient to produce wheel lock during the braking process, the maximum value of wheels-unlocked deceleration that can be achieved by the vehicle is degraded.

7-1.2 EFFICIENCY

Braking efficiency is a measure of the ability of a vehicle to use the friction forces available at the tire-road interface. Braking efficiency is defined as the ratio of the maximum wheels-unlocked deceleration capability of the vehicle on a given surface to the peak tire-road friction coefficient of that surface. When braking efficiency is determined experimentally, the surface on which the vehicle is tested must be measured to determine the peak tire-road friction coefficient. These measurements can be made as described in Chapter 6.

7-1.3 RESPONSE TIME

Brake response time is defined as the time required for a brake to reach a given level of effectiveness from the time that the brake control (pedal) is activated. Measurements of response time in an actual stop therefore would require torque sensors on each braked wheel. Consequently, a more common means for determining the response time is to measure the time from the instant of pedal application (resulting in a full, fast opening of the treadle valve) to the instant a given pressure level is reached in the brake chamber. The brake response time of any hydraulic systems is generally short enough (0.1 s or less) to be neglected. However, measurements show that the response times typically exhibited by air brake systems are sufficient to influence the braking performance of commercial vehicles, as measured either by average deceleration or stopping distance. Synchronization of brake timing is important for preventing instabilities in articulated vehicles. Brake release time is significant when the driver is attempting to modulate the brake force to prevent wheel lockup.

7-1.4 CONTROLLABILITY

Brake controllability is used here in the sense of the driver being able to modulate brake force under a wide variety of loading and road surface conditions to minimize stopping distance while preventing wheel lockup. In the absence of antiskid control systems controllability is increased for that driving condition where the driver, if he exceeds the pedal force limit and causes wheel lockup to occur, still finds his vehicle stable and regains complete control over the vehicle's steerability upon lowering the pedal force level. This requirement implies that the front wheels must lock before the rear wheels for all decelerations and hence friction levels ranging from zero to high. A vehicle having this characteristic may be thought of as having its own tire-road friction sensing system. The driver applies increasing levels of pedal force until the front wheels lock. This condition, especially on slippery surfaces, can be detected. At the instant of lockup the pedal force is reduced slightly to result in an almost ideal stop. Certain limits on pedal force/deceleration gain assist the driver in modulating the braking forces. High levels of pedal force/deceleration gain appear to be more desirable when braking on slippery roadways, low levels when braking on dry road surfaces.

7-1.5 THERMAL EFFECTIVENESS

Thermal effectiveness of a brake is defined as the ability to absorb heat during a single stop or to dissipate heat during continued braking. For a single stop nearly all the braking energy is absorbed by the brake rotor; consequently, a rotor weight effectiveness can be formulated which indicates how much of the weight of the rotor is used for temperature reduction. For continued braking the surface area of the rotor is an important measure, and thus an area effectiveness can be established that indicates how much of the surface area is used effectively in temperature reduction. Thermal effectiveness often is compared to thermal capacity or resistance to temperature fade of a brake. It is measured in terms of the level of braking effectiveness which can be maintained during a series of rapidly repeated snubs, or the number of snubs which can be accomplished in a given time interval, or the decrease in towbar force in a towing test.

7-2 BRAKE FORCE MODULATION

Automotive wheel brakes of the friction type exhibit the characteristic of changing effectiveness with changing relative velocity between the friction partners. In addition, the tire-road friction coefficient is

strongly dependent on speed as discussed in Chapter 6. The coefficient of friction between a tire and a wet road surface may be 0.7 at 5 mph and only 0.4 at 75 mph. The corresponding values for dry surfaces may be 0.9 and 0.7. An ideal stop would require that the driver modulates the pedal force such that each axle is braked near the existing friction level (Refs. 2 and 3). Since both braking efficiency and friction level change during the stop, the pedal force modulations required for an ideal stop place challenging demands on the typical driver. The pedal force in a passenger car may increase from 25 lb to 50 lb when braking from 75 mph to zero on a wet road surface. For dry road conditions the corresponding pedal forces generally increase only from 50 lb to 60 lb.

7-3 BRAKING PERFORMANCE PREDICTION AND ANALYSIS

With the equations of Chapters 2 and 5 the braking performance of a motor vehicle can be predicted. It was shown that pedal force versus line pressure characteristic, brake effectiveness, and pedal force versus deceleration gain could be calculated for a variety of brake system types based upon design data and specifications. At present only very complicated dynamic computer simulations of the brake system allow the computation of brake system response times. As shown in Chapter 11, simplified equations will be used to predict brake response times of pneumatic brake systems. Thus all braking performance measures defined in par. 7-1 may be predicted from vehicle and brake system design data. Further, by means of computer simulation of vehicle dynamics, the effects of tandem axles, trailers, and loading conditions upon braking performance can be predicted. The computer programs may be extended to include combined braking and turning as well as the dynamic response of the vehicle to various control inputs (Refs. 4, 5, and 6).

Three digital computer programs used in vehicle braking studies will be discussed: the Braking Performance Calculation Program, the Dynamic Braking Program, and the Tractor-Trailer Braking and Handling Program. Of these, the Braking Performance Calculation Program will be discussed in the most detail.

7-3.1 BRAKING PERFORMANCE CALCULATION PROGRAM

This program facilitates the calculations necessary to predict the braking performance of passenger cars, trucks, and tractor-trailers by using a simplified model. The measures of braking performance predicted by this model are brake effectiveness and braking efficiency. The approach consists of the basic steps that follow. A certain brakeline pressure results in a brake force, which produces vehicle deceleration, which causes dynamic axle loads, which may be used to compute the tire-road friction coefficient μ required to prevent wheel lockup.

The program consists of five steps:

1. Input. Vehicle data and specifications, brake data, loading condition, and tire-road friction values are entered into the program.
2. Initialization. Calculation of static axle loads and setting of brake line pressure at initial value.
3. Calculations. Necessary calculations including brake factor, brake force, deceleration, and dynamic axle loads are made. Wheel lockup is indicated if it occurs.
4. Output. Results from calculations are printed.
5. Increment/Stop. If line pressure is less than maximum value, it is incremented, and another set of calculations is made. If calculations have been made for the maximum brake line pressure, or if all wheels lock for a given pressure, the program is terminated.

Brakes may be specified on an axle by axle basis, and options include: no brakes, S-cam, dual or single wedge, duo-servo, two-leading shoe, leading-trailing shoe, and disc brakes. Single axle, walking beam, and elliptic leaf spring tandem suspensions can be specified. In later chapters equations for six vehicle configurations are presented.

1. 2-axle passenger car or straight truck
2. 3-axle straight truck
3. 2-axle tractor, single-axle trailer
4. 2-axle tractor, 2-axle trailer
5. 3-axle tractor, single-axle trailer
6. 3-axle tractor, 2-axle trailer.

The brake force produced on each axle for a given brake line pressure is determined from Eq. 5-10 for hydraulic brake systems, and Eq. 5-31 for air brake systems. The values for the brake factor of the various types of drum and disc brakes required in Eqs. 5-10 and 5-31 are calculated by means of analytical expressions given in Chapter 2. These expressions show that the brake factor is a function of brake type, brake geometry, and the coefficient of friction between the lining and the drum or disc. Brake factor/lining friction coefficient relationships for three commonly used brake types are given in Fig. 7-1.

If the value of the lining friction coefficient is held constant in the calculation of brake torque as a function of brake line pressure, the brake factor remains constant, and the line pressure-torque characteristic is a straight line. However, results from vehicle tests

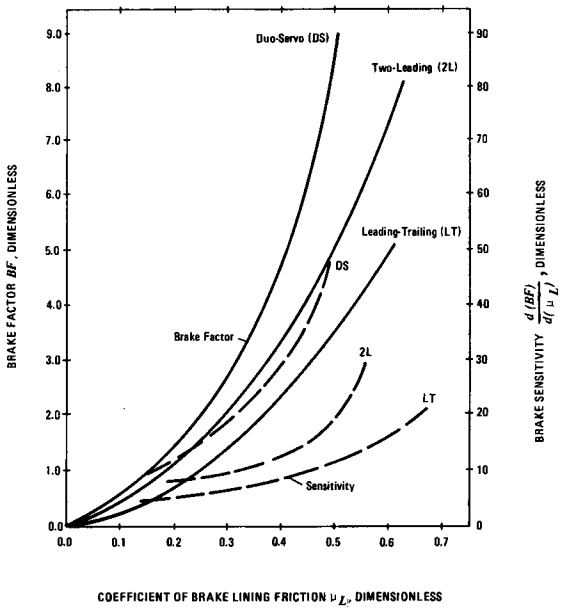

Figure 7-1. Brake Factor — Lining Friction Curves for Typical Drum Brakes

indicate that considerable brake fade is experienced, especially by loaded vehicles, when being decelerated from higher speeds. Thus a technique was devised to take fade effects into account by proper adjustment of the lining friction coefficient. Results from an extensive vehicle test program were used to verify the technique (Ref. 1).

An exponentially decaying dependence of the effective lining friction coefficient μ_L upon pressure was assumed

$$\mu_L = \mu_{Ll} + (\mu_{Lh} - \mu_{Ll})\, e^{-fp_l} \quad , \text{d'less} \qquad (7\text{-}1)$$

where

f = fade factor associated with heavy truck drum brakes, in.^{2}/lb
p_l = brake line pressure, psi
μ_L = lining friction coefficient, d'less
μ_{Lh} = nonfaded lining friction coefficient, d'less
μ_{Ll} = faded lining friction coefficient, d'less

Typical values of μ_{Lh} for S-cam and wedge brakes are 0.35 to 0.38 and 0.45 to 0.48, respectively. The fade factor f and the lower limit of the lining friction coefficient μ_{Ll} were determined from test data and curve fitting procedures. Vehicles with air brakes have fade factors of 0.018 in.^{2}/lb when loaded and 0.003 in.^{2}/lb when empty. For vehicles equipped with hydraulic brake systems the corresponding values for f are 0.00088 and 0.00028 in.^{2}/lb. Analysis of the experimental data indicates that the maximum reduction in lining friction coefficient can be approximated by $\mu_{Ll} = 0.70\,\mu_{Lh}$.

The decreasing lining friction coefficient as computed by Eq. 7-1 for increasing line pressures was then introduced in the brake factor BF of Eq. 5-10 or 5-31 to compute the brake force of a particular axle under faded conditions.

If vehicles are equipped with proportioning or limiting valves, line pressure may be introduced into Eqs. 5-10 or 5-31 as a variable determined by the proportioning or limiting used on a particular axle.

On evaluating Eq. 5-10 or 5-31 for each axle as a function of brake line pressure, the total brake force $F_{x,total}$ on the vehicle is obtained from

$$F_{x,total} = \sum_{i} F_{xi}, \text{ lb} \qquad (7\text{-}2)$$

where i designates the number of braked axles. The solution procedure is described in the analysis that follows, using the example of a two-axle truck.

For two-axle trucks, the equations describing dynamic axle loads induced by the brake force are (Fig. 7-2)

$$F_{zF,dyn} = [(1 - \psi) + \chi a]W \ , \text{lb} \qquad (7\text{-}3a)$$

$$F_{zR,dyn} = [\psi - \chi a]W \ , \text{lb} \qquad (7\text{-}3b)$$

where

$$\psi = \frac{F_{zR,static}}{W} \ , \text{ d'less} \qquad (7\text{-}4a)$$

$$\chi = \frac{\text{center of gravity height}}{\text{wheelbase}} \ , \text{ d'less} \qquad (7\text{-}4b)$$

W = vehicle weight, lb

$$a = \frac{F_{x,total}}{W} = \text{decleration, g-units} \qquad (7\text{-}4c)$$

$F_{zF,dyn}$ = dynamic front axle normal force, lb
$F_{zR,dyn}$ = dynamic rear axle normal force, lb
$F_{zR,static}$ = static rear axle normal force, lb

For tandem-axle trucks and tractor-semitrailer combinations Eqs. 7-2, 7-3, and 7-4 are considerably more complicated, but are nevertheless amenable to computer solution. For a given brake line pressure, Eqs. 7-2 to 7-4c serve to define the deceleration of the

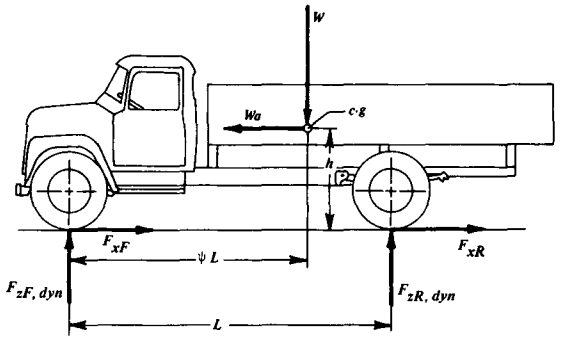

Figure 7-2. Forces Acting on a Decelerating Vehicle

vehicle and the dynamic axle loads existing at this deceleration. The tire-roadway friction coefficient $\mu_{road,i}$ required to prevent wheel lockup of the ith axle is

$$\mu_{road,i} = \frac{F_{xi}}{F_{zi,dyn}} \text{, d'less} \qquad (7\text{-}5)$$

where

F_{xi} = brake force of ith axle, lb

$F_{zi,dyn}$ = dynamic normal force of ith axle, lb

The resulting braking efficiency E_i achieved by individual axles is defined as

$$E_i = \frac{a}{\mu_{road,i}} \text{, d'less} \qquad (7\text{-}6)$$

where

a = deceleration, g-units

If wheel lockup is found to occur on some but not all axles at a given brake line pressure, the retarding force $F_{xi,\,slide}$ produced by the axle with locked wheels is assumed to be given by the following relationship:

$$F_{xi,slide} = \mu_{road} F_{zi,dyn} \text{, lb} \qquad (7\text{-}7)$$

where

μ_{road} = actual coefficient of friction existing at the tire road interface, d'less

As an example, the following step-by-step description of the operation of the computer program for a 3S-2 tractor-trailer combination, having all five axles braked, is given:

1. INPUT
   a. Vehicle geometric and loading parameters
   b. Initial velocity
   c. Tire/road interface coefficients
   d. Brake lining data
   e. Brake response time and push out pressures
   f. Brake data
      (1) Front brakes: chamber size, wedge, and dimensions, mechanical efficiency
      (2) Tractor rear brakes: chamber size, cam radius, slack adjuster length, dimensions, mechanical efficiency
2. INITIALIZE BRAKE LINE PRESSURE
3. CALCULATE
   a. Pressure at each brake
   b. Effective lining
   c. Brake factors at each brake
   d. Brake force
   e. If brake force is greater than the sliding force, set brake force equal to sliding force otherwise continue
   f. Sum brake forces
   g. Deceleration
   h. Stopping distance
   i. Normal wheel loads due to load transfer, including tandem suspension effects
   j. Fifth wheel kingpin forces
4. OUTPUT
   a. Deceleration
   b. Nominal line pressure and individual brake pressures
   c. Brake factors
   d. Brake effort: % front, % rear, % trailer
   e. Required friction coefficient for each axle
   f. Brake efficiency, each axle
   g. Kingpin and suspension forces
   h. Total brake force
   i. Brake force each axle
   j. Dynamic axle loads
   k. Average deceleration
   l. Stopping distance
5. INCREMENT LINE PRESSURE

If the line pressure at a wheel is less than maximum pressure, go back to Step 3, otherwise stop.

For passenger cars and two-axle trucks, it is often sufficient to compute the expected braking efficiencies by means of a slide rule or desk calculator. In this case, an average brake factor will be determined using the appropriate equations from Chapter 2, and upper and lower limits on the lining friction coefficient of μ_{Lh} and 0.70 μ_{Lh}, respectively.

The performance measures may be presented in the form of a performance diagram illustrated in Fig. 7-3 for a two-axle vehicle. It should be noted that the tire-roadway friction coefficients in Fig. 7-3 are those computed to prevent wheel lockup. For the same

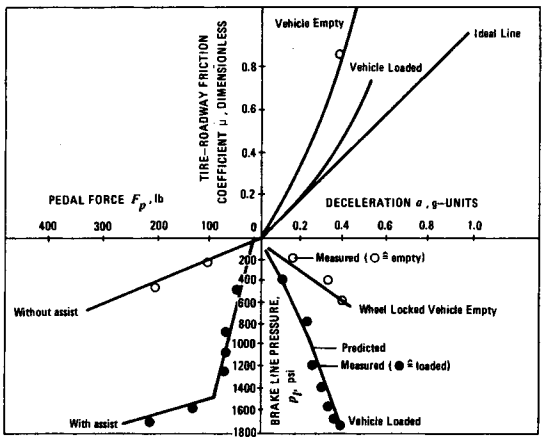

Figure 7-3. Braking Performance Diagram of a Two-Axle Truck

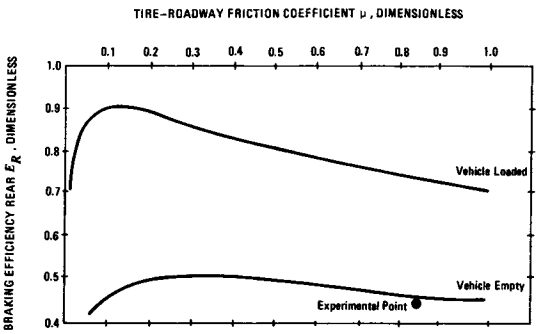

Figure 7-4. Braking Efficiency of a Two-Axle Truck

vehicle, the braking efficiency as a function of tire-roadway function coefficient is presented in Fig. 7-4 for the loaded and empty vehicle conditions. Good agreement is noted between experimental and theoretical results. This is due mainly to the fact that brake fade is included in the braking analysis.

The effects of brake response times upon the braking efficiency of vehicles equipped with pneumatic brake systems are of considerable significance, especially in longer combination vehicles. The equations used in the Braking Performance Calculation Program do not take into consideration the individual time delays of the different axles. However, this can be done easily in the dynamic simulation programs described in the next paragraph.

7-3.2 DYNAMIC BRAKING PROGRAM

The dynamic simulation program is based on a model that represents the physical system to be studied. The size of the program is a direct function of the complexity and detail of the system to be analyzed. The following is a description of a program used for the straight-line braking simulation of a three-axle tractor semitrailer or a two-axle truck (Ref. 5). Motions are constrained to the plane of vertical symmetry. Specifically, the wheels can bounce and spin, the chassis can bounce and pitch, and the vehicle can accelerate or decelerate. The braking system is modeled in a manner such that the brake torque-line pressure characteristic can be specified for each brake and variable time delays in torque response can be introduced. Thus, any desired brake force distribution can be specified.

The model has the following eleven degrees of freedom:

1. Vehicle forward displacement
2. Vertical displacement of center of gravity of tractor
3. Pitch angle of tractor
4. Vertical displacement of center of gravity of trailer
5. Pitch angle of trailer
6. Vertical displacement of tractor front wheels
7. Vertical displacement of tractor rear wheels
8. Vertical displacement of trailer wheels
9. Angular velocity of tractor front wheels
10. Angular velocity of tractor rear wheels
11. Angular velocity of trailer rear wheels.

To determine the value of these variables as functions of time, eleven differential equations of motion need to be solved simultaneously, along with ancillary equations defining intermediate variables such as suspension deflections, tire-road interface forces, normal forces on the tires, forces at the coupling point between the tractor and trailer, and horizontal forces acting on the sprung masses.

This simulation model may be used to determine the effect of variation of vehicle and loading parameters, brake time response, brake torque distribution, and various brake proportioning schemes on truck and tractor-trailer braking performance.

7-3.3 TRACTOR-TRAILER BRAKING AND HANDLING PROGRAM

Many research efforts have been conducted to simulate the response of a vehicle during combined braking and steering (Refs. 6 and 7). The number of variables involved is large, and difficulties may exist in accurately measuring all parameters required for the computer simulation. A physical model of a

three-axle tractor-semitrailer combination is illustrated in Fig. 7-5. It consists of two rigid bodies which translate parallel to a smooth, level surface and rotate about an axis perpendicular to this surface. The fifth-wheel coupling, which allows relative rotation of the two bodies, transmits lateral and longitudinal forces as well as a moment due to friction. Aerodynamic forces and moments, the rotational inertia of the wheels, and the rolling and pitching of the bodies on their suspensions are neglected.

The external forces acting on the vehicle model are the normal and frictional forces applied through the tire-road interface. The three moments which are created by moving the force system from its actual point of application to the center of tire contact with the road are assumed to have a negligible effect on the lateral and longitudinal motions of the vehicle and are disregarded. The frictional tire force in the plane of the road can be resolved into two components, as shown in Fig. 7-5: the lateral tire force F_{yi} perpendicular to the plane of the wheel, and the longitudinal tire force F_{xi} in the direction of the wheel heading. In addition, dual tires are assumed to have frictional tire forces which are twice the forces generated by a single tire operating at one-half the vertical load on the dual tires.

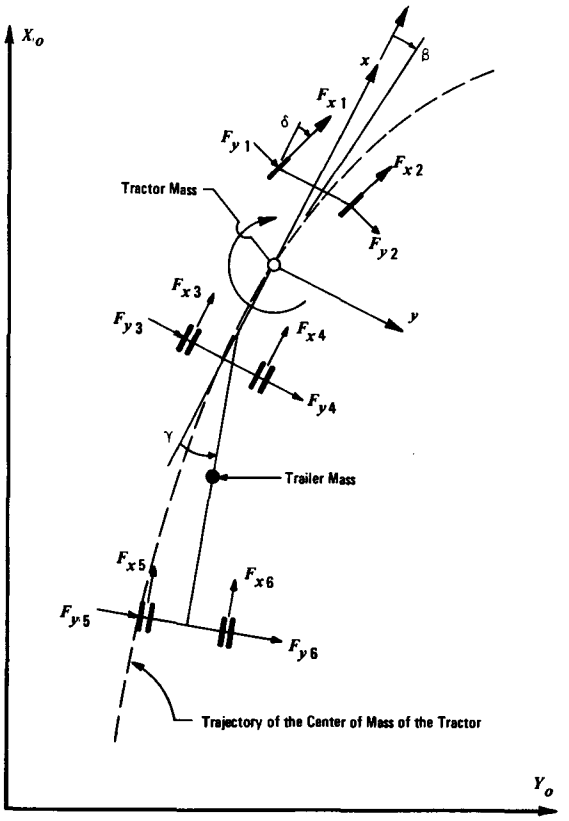

Figure 7-5. Tractor-Semitrailer Vehicle Model

In addition to providing support for the entire weight of the vehicle, the vertical force has a large influence on the magnitude of lateral and longitudinal tire forces that can be developed. The vertical load on each tire is determined by the static load plus any instantaneous change resulting from maneuvers of a vehicle having a center of mass above the ground plane. In this study, these load transfers were not determined as a function of the displacement and velocity of the suspension components, but rather as a quasi-static function of the acceleration of the center of gravity of each mass element. In this way, it is possible to simulate the major contribution of pitch and roll to the vehicle directional response without having to treat these motions as degrees of freedom.

This model may be used to determine the effect of vehicle and loading parameters, brake force distribution, brake proportioning, and environmental factors on stability of tractor-semitrailer vehicles.

7-4 VEHICLE DRAGS

The deceleration of a vehicle is caused by the resultant external force acting on the vehicle. The individual external forces may act on the tires or the vehicle body. Acting opposite to the drag is the effect of rotational energies of the wheels and shafts, which increases the braking energy to be absorbed by the brakes.

7-4.1 ROLLING RESISTANCE

The development of tire rolling resistance and its computation are discussed in detail in Chapter 6. For most automotive applications the effect of rolling resistance on vehicle retardation is set equal to the driving effects of rotational masses and, consequently, neither rolling resistance nor rotational energies are included in the braking analysis. Special vehicles such as tanks having large rotational masses require a detailed analysis of both rolling resistance and rotational energies.

7-4.2 AERODYNAMIC DRAG

A vehicle traveling on the ground has airflow forced under, around, and over the vehicle. The streamlines separate behind the vehicle. The airflow is turbulent in the speed ranges of interest to automotive use. The aerodynamic force is the result of a pressure difference between the front and the rear of

the vehicle and of the frictional forces between the surface area of the vehicle and the air.

The existing aerodynamic drag force F_{AD} is

$$F_{AD} = c_{AD} A [\rho/(32.2 \times 2)] V_{rel}^2, \text{ lb} \quad (7\text{-}8)$$

where

A = frontal area of vehicle, ft²
c_{AD} = aerodynamic drag coefficient, d'less
V_{rel} = relative speed between vehicle and wind, ft/s
ρ = air density, lbm/ft³

The aerodynamic drag coefficient c_{AD} ranges from 0.3 for race cars to 1.1 for tractor/trailer combinations.

7-4.3 VISCOUS DAMPING DRAG

On rough roads, an additional resistance to forward motion of the vehicle is produced by the energy absorbed by the shock absorbers (Ref. 3). Similar to the internal damping of a tire resulting in rolling resistance, the damping associated with vertical motion of a wheel produces the damping drag force F_{DD}.

$$F_{DD} = n c_{DD} k/V, \text{ lb} \quad (7\text{-}9)$$

where

n = number of damped wheels, d'less
c_{DD} = damping coefficient, lb·s/ft
k = factor characterizing road roughness, ft²/s²
V = vehicle speed, ft/s

Maximum values of the factor k at 75 mph range from 0.5 ft²/s² for smooth concrete roadways to 5 ft²/s² for gravel roads. At speeds below 15 mph the factor k approaches negligible values regardless of road surface roughness.

By Eq. 7-9 a four-wheel vehicle with a damping coefficient of 600 lb·s/ft yields a viscous damping drag of only approximately 11 lb on a smooth concrete road at 75 mph. The corresponding drag on a gravel road is approximately 109 lb.

7-4.4 DRAG DUE TO TURNING

The resistance produced by the tires to forward motion of a vehicle in a turn is a function of the severity of the turn.

The turning resistance coefficient R_T is (Ref. 3)

$$R_T = a_y[(1-\psi) \sin \alpha_F + \psi \sin \alpha_R], \text{ d'less} \quad (7\text{-}10)$$

where

a_y = lateral acceleration, g-units
ψ = static rear axle load divided by total vehicle weight, d'less
α_F = slip angle on front wheels, deg
α_R = slip angle on rear wheels, deg

Slip angle α is defined as the angle between a line perpendicular to the axis of wheel rotation and direction of wheel motion. The slip angle required for the side force production necessary to hold a vehicle in a desired turn is a function of a large number of vehicle parameters and changes in a nonlinear fashion with lateral acceleration. For purposes of estimating the turning resistance coefficient R_T equal slip angles front and rear may be assumed of the magnitude of 2 deg for a_y = 0.2g, 6 deg for a_y = 0.6g and 10 deg for a_y = 0.8g. The turning resistance force F_{TD} is

$$F_{TD} = R_T W, \text{ lb} \quad (7\text{-}11)$$

where

W = vehicle weight, lb

By Eq. 7-11 a 6,000-lb vehicle with ψ = 0.50 turning at 0.6g lateral acceleration yields a turning resistance force of approximately 376 lb. At 0.2g lateral acceleration, the corresponding value is only 42 lb.

7-4.5 ENGINE DRAG

The retarding effect of the engine is discussed in Chapter 4. The retarding force acting on the drive wheels is a function of the transmission ratio, the engine retarding moment, and the tire radius. In the case of continued downhill vehicle travel, the engine drag will always relieve the brakes. In an effectiveness stop the effect of the engine drag may not always result in an increased deceleration. Since the engine crank shaft is rotating at high revolutions per minute, the rotational energies may exceed the effect of the engine drag, and consequently increased stopping distances may result. Road test data indicate this condition exists, especially when braking from speeds below 30 mph.

REFERENCES

1. R. W. Murphy, R. Limpert, and L. Segel, *Bus, Truck and Tractor-Trailer Braking System Performance,* Final Report, Highway Safety Research Institute, the University of Michigan, to the National Highway Traffic Safety Administration, Contract FH-11-7290, March 1971.
2. R. G. Mortimer, et al., *Brake Force Requirement Study: Driver Vehicle Braking Performance as a Function of Brake System Design Variables.* Contract No. FH-11-6972, prepared for the National

Highway Safety Bureau, U.S. Department of Transportation, by the Highway Safety Research Institute, The University of Michigan, April 10, 1970.

3. M. Mitschke, *Dynamics of Motor Vehicles,* Springer Publisher, Berlin, Heidelberg, New York, 1972.
4. R. W. Murphy, *Analysis and Simulation of Tractor-Trailer Braking System Performance,* Proceedings of the 1971 Summer Computer Simulation Conference, BSC, Denver, Colo.
5. *A Computer Based Mathematical Method for Predicting the Braking Performance of Trucks and Tractor-Trailers,* Highway Safety Research Institute, University of Michigan, September 5, 1972.
6. *A Computer Based Mathematical Method for Predicting the Directional Response of Trucks and Tractor-Trailers,* Highway Safety Research Institute, University of Michigan, June 1, 1973.
7. P. M. Leucht, *Directional Dynamics of the Tractor-Semitrailer Vehicle,* Ph.D., Dissertation, University of Michigan, 1970.

CHAPTER 8
BRAKING OF VEHICLES EQUIPPED WITH FIXED RATIO BRAKING SYSTEM

In this chapter the braking analysis of solid-frame and articulated vehicles equipped with fixed brake torque distribution among the axles is presented. Important factors are dynamic and actual brake force distribution, friction utilization, and braking efficiency. Design techniques for optimizing brake force distribution are presented. A computer method presented in Chapter 7 is used in the analysis of multi-axle vehicles and vehicle combinations.

8-0 LIST OF SYMBOLS

A = parameter, d'less*
A_C = brake chamber area, in.^{2}
A_{WC} = wheel cylinder area, in.^{2}
a = deceleration, g-units
a_{max} = maximum deceleration, g-units
a_x = longitudinal deceleration, g-units
a_y = lateral acceleration, g-units
a_{x0} = deceleration in the absence of lateral acceleration, g-units
a_{y0} = lateral acceleration in the absence of braking, g-units
a_{1F} = tractor front wheels unlocked deceleration, g-units
a_{1R} = tractor rear wheels unlocked deceleration, g-units
a_{2R} = trailer wheels unlocked deceleration, g-units
B = parameter, d'less
BF = brake factor, d'less
b = dimension, tandem axle, in.
C_1 = parameter, d'less
C_2 = parameter, d'less
C_3 = parameter, d'less
c = dimension, tandem axle, in.
D = parameter, in.^{2}
d = dimension, tandem axle, in.
E = braking efficiency, d'less
E_F = braking efficiency of front axle, d'less
$E_{F,i}$ = braking efficiency of inner front wheel, d'less
E_{min} = minimum braking efficiency, d'less
E_R = braking efficiency of rear axle, d'less
E_T = total braking energy, ft·lb
e = dimension, tandem axle, in.
F_c = centrifugal force, lb
F_{cx} = centrifugal force component in x-direction, lb
F_{cy} = centrifugal force component in y-direction, lb
F_p = pedal force, lb
F_R = resultant force, lb
$F_{res,F,i}$ = resultant traction force on inner front wheel, lb
F_x = brake force, lb
F_{xF} = actual front axle brake force, lb
$F_{xF,i}$ = brake force of inner front wheel, lb
$F_{xF,o}$ = brake factor of outer front wheel, lb
F_{xR} = actual rear axle brake force, lb
F_{xRF} = actual brake force of tandem forward axle, lb
F_{xRR} = actual brake force of tandem rearward axle, lb
$F_{xR,i}$ = brake force of inner back wheel, lb
$F_{xR,o}$ = brake force of outer back wheel, lb
$F_{xF,dyn}$ = dynamic front axle brake force, lb
$F_{xR,dyn}$ = dynamic rear axle brake force, lb
$F_{x,total}$ = total brake force, lb
$F_{x1F,dyn}$ = dynamic brake force of tractor front axle, lb
$F_{x1R,dyn}$ = dynamic brake force of tractor rear axle, lb
F_{x1F} = actual brake force of tractor front axle, lb
F_{x1R} = actual brake force of tractor rear axle, lb
F_{x1RF} = actual brake force of tractor tandem forward axle, lb
F_{x1RR} = actual brake force of tractor tandem rearward axle, lb
F_{x2R} = actual brake force of semitrailer axle, lb
$F_{x2R,dyn}$ = dynamic brake force of trailer axle, lb
F_{x2RF} = actual brake force of semitrailer tandem forward axle, lb
F_{x2RR} = actual brake force of semitrailer tandem rearward axle, lb
F_{x3F} = actual brake force of double trailer front axle, lb
F_{x3R} = actual brake force of double trailer rear axle, lb

*d'less = dimensionless

$F^*_{xF,dyn}$ = dynamic front axle brake force divided by vehicle weight, d'less
$F^*_{xR,dyn}$ = dynamic rear axle brake force divided by vehicle weight, d'less
F_y = side force, lb
F_{yF} = front tire side force, lb
$F_{yF,i}$ = side force of inner front wheel, lb
$F_{yF,o}$ = side force of outer front wheel, lb
F_{yR} = rear tire side force, lb
$F_{yR,i}$ = side force of inner rear wheel, lb
$F_{yR,o}$ = side force of outer rear wheel, lb
F_z = normal force, lb
F_{zF} = dynamic normal force of front axle, lb
F_{zR} = dynamic normal force of rear axle, lb
$F_{zF,i}$ = normal force of inner front wheel, lb
$F_{zF,static}$ = static normal force of front axle, lb
$F_{zF,o}$ = normal force of outer front wheel, lb
F_{zRF} = normal force of truck tandem forward axle, lb
$F_{zR,i}$ = normal force of inner rear wheel, lb
$F_{zR,o}$ = normal force of outer rear wheel, lb
F_{zRR} = normal force of truck tandem rearward axle, lb
$F_{zR,static}$ = static normal force of rear axle, lb
F_{z1F} = normal force of tractor front axle, lb
F_{z1R} = normal force of tractor rear axle, lb
$F_{z1F,ap}$ = approximate normal force of tractor front axle, lb
$F_{z1R,ap}$ = approximate normal force of tractor rear axle, lb
F_{z2R} = normal force of trailer axle, lb
$F_{z2R,ap}$ = approximate normal force of trailer axle, lb
F_{z1RF} = normal force of tractor tandem forward axle, lb
F_{z1RR} = normal force of tractor tandem rearward axle, lb
F_{z2RF} = normal force of trailer tandem forward axle, lb
F_{z2RR} = normal force of trailer tandem rearward = axle, lb
F_{z3F} = normal force of double trailer front axle, lb
F_{z3R} = normal force of double trailer rear axle, lb
G = parameter, in.·lb
G_1 = parameter, in.·lb
g = gravitational constant, 32.2 ft/s²
g' = gravitational constant, 386 in./s²
H = parameter, in.
H_1 = parameter, in.
h = center of gravity height above roll axis, in.
h_F = center of gravity height of front unsprung mass, ft
h_r = distance between center of gravity and roll axis, ft
I = mass moment of inertia of rotating components decelerated by brakes, in.·lb·s²
I_d = mass moment of inertia of drive shaft, in.·lb·s²
I_e = mass moment of inertia associated with engine, in.·lb·s²
I_R = mass moment of inertia of rear wheels and connected shafts, in.·lb·s²
I_{TF} = mass moment of inertia of front wheels and brakes, in.·lb·s²
I_{TR} = mass moment of inertia referred to rear brakes, in.·lb·s²
K_F = front roll stiffness, ft·lb/rad
K_R = rear roll stiffness, ft·lb/rad
K_1 = parameter, d'less
K_2 = parameter, d'less
K_3 = parameter, d'less
L = wheel base, in. or ft
L_R = horizontal distance between center of gravity and rear axle, ft
L_1 = tractor wheel base, in.
L_2 = distance from fifth wheel to semitrailer axle, also called semitrailer base, in.
L_3 = wheel base of double trailer, in.
l_c = cam radius, in.
l_s = slack adjuster length, in.
l_r = lever ratio, d'less
m = tire factor, d'less
p = roll center height, in.
p_F = front roll center-to-ground distance, ft
p_l = brake line pressure, psi
q = dimension, tandem axle, in.
q_1 = dimension, tandem axle, in.
q_2 = dimension, tandem axle, in.
R = radius or distance between wheel center and ground, in.
r = effective drum or rotor radius, in.
r_s = scrub radius, in.
S_{act} = actual stopping distance, ft
S_F = front normalized roll stiffness, d'less
S_{min} = minimum stopping distance, ft
S_R = rear normalized roll stiffness, d'less
s = dimension, tandem axle, in.
s_1 = dimension, tandem axle, in.
s_2 = dimension, tandem axle, in.
T = parameter, lb·in.²
t = track width, in.
t_F = front track width, ft
t_a = application time, s
t_b = buildup time, s
u = dimension, tandem axle, in.

u_1 = dimension, tandem axle, in.
u_2 = dimension, tandem axle, in.
V = vehicle speed, ft/s
V_1 = initial vehicle speed, ft/s
V_2 = final vehicle speed, ft/s
v = dimension, tandem axle, in.
v_1 = dimension, tandem axle, in.
v_2 = dimension, tandem axle, in.
W = vehicle or combination weight, lb
W_{Tr} = trailer weight, lb
W_{Truck} = truck weight, lb
W_s = unsprung weight or weight of truck minus weight of tandem axle, lb
W_{s1} = tractor weight minus weight of tandem axle, lb
W_{s2} = semitrailer weight minus weight of tandem axle, lb
$(Wa)_{total}$ = translational inertia of vehicle increased by rotational effects, lb
W_1 = tractor weight, lb
W_2 = semitrailer weight, lb
W_3 = double trailer weight, lb
w_F = front suspension unsprung weight or unsprung weight of truck tandem forward axle, lb
w_R = unsprung weight of truck tandem rearward axle, lb
w_{1F} = unsprung weight of tractor tandem forward axle, lb
w_{1R} = unsprung weight of tractor tandem rearward axle, lb
X = horizontal fifth wheel force, lb
X_h = horizontal force of hitch point, lb
X_1 = horizontal suspension force, lb
X_2 = horizontal suspension force, lb
X_3 = horizontal suspension force, lb
X_4 = horizontal suspension force, lb
x = displacement of center of rotation of vehicle due to tire creep, ft
Y = vertical fifth wheel force, lb
Y_1 = vertical suspension force, lb
Y_2 = vertical suspension force, lb
Y_3 = vertical suspension force, lb
Y_4 = vertical suspension force, lb
y = horizontal distance between front wheels and fifth wheel divided by tractor wheel base L_1, d'less
Z_1 = fifth wheel height divided by tractor wheel base L_1, d'less
Z_2 = fifth wheel height divided by semitrailer base L_2, d'less
Z_3 = double trailer hitch height divided by double trailer wheel base L_3, d'less
Z_4 = double trailer hitch height divided by semitrailer base L_2, d'less
α = wedge angle, deg
α_v = vehicle side slip angle, deg
ΔF_{zF} = load transfer of one front wheel due to turning, lb
ΔF_{zR} = load transfer of one rear wheel due to turning, lb
ΔS = stopping distance increase, ft
$\Delta\chi$ = difference in relative center of gravity height, d'less
$\Delta\psi$ = difference in relative static rear axle load, loaded and empty, d'less
δ = rotational inertia factor, d'less
λ = tractor weight divided by total combination weight, d'less
μ = tire-road friction coefficient, d'less
μ_F = tire-road friction coefficient of front axle, d'less
$\mu_{F,i,req}$ = tire-road friction coefficient required to prevent wheel lock of inner front wheel, d'less
μ_R = tire-road friction coefficient of rear axle, d'less
μ_{1F} = tire-road friction coefficient of tractor front wheels, d'less
μ_{1R} = tire-road friction coefficient of tractor rear wheels, d'less
μ_{2R} = tire-road friction coefficient of trailer wheels, d'less
ρ = trailer brake force divided by total combination weight, d'less
ρ_c = radius of curvature, ft
ρ_d = differential ratio, d'less
ρ_t = transmission ratio, d'less
ϕ = rear axle brake force divided by total brake force, d'less
ϕ_{1F} = tractor front axle brake force divided by total brake force, d'less
ϕ_{1R} = tractor rear axle brake force divided by total brake force, d'less
ϕ_{2R} = trailer brake force divided by total brake force, d'less
χ = relative center of gravity height, i.e., center of gravity height divided by wheel base L, d'less
χ_o = center of gravity height divided by wheel base L, empty vehicle, d'less
χ_1 = tractor center of gravity height divided by tractor wheel base L_1, d'less
χ_2 = semitrailer center of gravity height divided by semitrailer base L_2, d'less
χ_3 = double trailer center of gravity height divided by double trailer wheel base L_3, d'less
ψ = static rear axle or tandem axle load divided by vehicle weight, d'less

ψ_o = static rear axle load divided by vehicle weight, empty vehicle, d'less
ψ_1 = empty tractor rear axle load (without semitrailer), divided by tractor weight, d'less
ψ_2 = static semitrailer axle load divided by semitrailer weight, d'less
ψ_3 = static double trailer rear axle load divided by double trailer weight, d'less
ω_d = angular velocity of drive shaft, rad/s
ω_e = angular velocity of engine shaft, rad/s
ω_R = angular velocity of rear wheel, rad/s
ω_1 = initial angular velocity of brake rotor, rad/s
ω_2 = final angular velocity of brake rotor, rad/s

Recurring subscripts:

F = front axle
R = rear axle
x = longitudinal direction (braking)
y = lateral direction (side)
z = normal direction (vertical)
1 = tractor
2 = semitrailer
3 = double trailer

8-1 BRAKING OF TWO-AXLE VEHICLE

The important relationships bearing upon the optimum brake system are derived in this paragraph.

8-1.1 DYNAMIC BRAKE FORCE

The forces acting on a decelerating two-axle vehicle are illustrated in Fig. 8-1. Aerodynamic drag, rolling resistance of the tires, and moments due to rotational energies are neglected. The dynamic axle loads during braking are given by Eqs. 7-3a and 7-3b as a function of deceleration, and vehicle geometrical and loading data. The graphical representation of the dynamic axle loads is that of a straight line similar to those shown in Fig. 1-3 for a tractor-semitrailer. The dynamic load transfer, e.g., from the rear axle is $\chi\, a\, W$. Typical values of the ratio χ of center of gravity height divided by the wheel base range from 0.20 for passenger cars to 0.45 for trucks. Consequently, a truck weighing 20,000 lb will experience as much as 5,400 lb load transfer in a 0.6g deceleration braking process. By assuming an even axle load distribution during nonbraking, i.e., the static axle loads are identical front and rear, and applying Eqs. 7-3a and 7-3b, the dynamic axle load on the front will attain 15,400 lb, the rear will decrease to 4,600 lb. For deceleration levels sufficiently low for wheel lock not to occur, the vehicle deceleration is computed by the equations presented in Chapter 5. Main factors are brake system design parameters affecting system gain and pedal force as indicated by Eq. 5-8. Maximum deceleration, however, is attained when both axles achieve wheel lock up simultaneously. Only for this condition will both axles produce maximum braking forces. By taking as an optimum the condition that the deceleration in g-units equals the coefficient of friction between tire and roadway, the dynamic and optimum braking forces for straight-line braking are obtained by multiplying the dynamic normal forces by the deceleration.

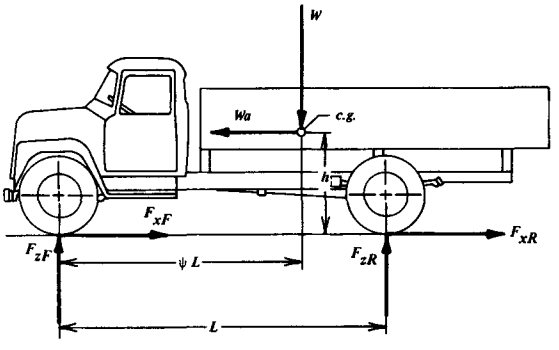

Figure 8-1. Forces Acting on a Decelerating Vehicle

$$\text{Front: } F_{xF,dyn} = [1 - \psi + \chi a]aW \text{ , lb} \qquad (8\text{-}1)$$

$$\text{Rear: } F_{xR,dyn} = [\psi - \chi a]aW \text{ , lb} \qquad (8\text{-}2)$$

where

a = deceleration, g-units
$F_{xF,dyn}$ = dynamic front axle brake force, lb
$F_{xR,dyn}$ = dynamic rear axle brake force, lb
W = vehicle or combination weight, lb
χ = center of gravity height divided by wheel base, d'less
ψ = static rear axle load divided by vehicle weight, d'less

A graphical representation of Eqs. 8-1 and 8-2 for ψ and χ values typical for a light truck is shown in Fig. 8-2. The nonlinear nature of the dynamic braking forces indicates the varying ratio of dynamic braking forces between front and rear axles which is required for optimum braking. As illustrated in Fig. 8-2, different deceleration scales are required for the empty and loaded vehicle condition. Inspection of Fig. 8-2 indicates that the distances between points defined, e.g., by a deceleration of 0.4g and 0.6g for

the empty and loaded cases are not identical. Consequently, different scales must be used for the empty and loaded vehicle condition in analyzing the dynamic brake forces.

A simplification of Eqs. 8-1 and 8-2 can be obtained by dividing the dynamic braking forces by the vehicle weight

$$\text{Front: } F^*_{xF,dyn} = \frac{F_{xF,dyn}}{W} = (1 - \psi + \chi a)\, a \text{ , d'less} \quad (8\text{-}3)$$

$$\text{Rear: } F^*_{xR,dyn} = \frac{F_{xR,dyn}}{W} = (\psi - \chi a)\, a \text{ , d'less} \quad (8\text{-}4)$$

where

$F^*_{xF,dyn}$ = dynamic front axle brake divided by vehicle weight, d'less

$F^*_{xR,dyn}$ = dynamic rear axle brake force divided by vehicle weight, d'less

The graphical representation of Eqs. 8-3 and 8-4 is illustrated in Fig. 8-3. Only one deceleration scale is required for all loading conditions. When the deceleration a in g-units is equal to the tire-road friction coefficient μ, the dynamic brake forces — front and rear — represent maximum use of a given road friction. For $a > \mu$, the demanded deceleration is greater than the available due to friction, and in the case of slippery roads and thus low decelerations the front axle tends to overbrake. In the case of dry roadways and high decelerations the rear axle tends to overbrake. Overbraking of an axle will occur when the ratio of actual brake force existing between tire and road to dynamic axle load exceeds the ratio of total brake force produced by the vehicle to vehicle weight. For braking conditions expressed by $a < \mu$, the given road friction is not used completely. The actual stopping distance is greater for both cases than the minimum achievable, i.e., $a \neq \mu$ represents nonoptimum straight-line braking.

The term "ideal" often is used to describe the dynamic braking forces. In the literature an ideal braking process has been described as that process in which the actual braking forces were always equal to the dynamic or "ideal" braking forces. The braking process considered was restricted to straight-line

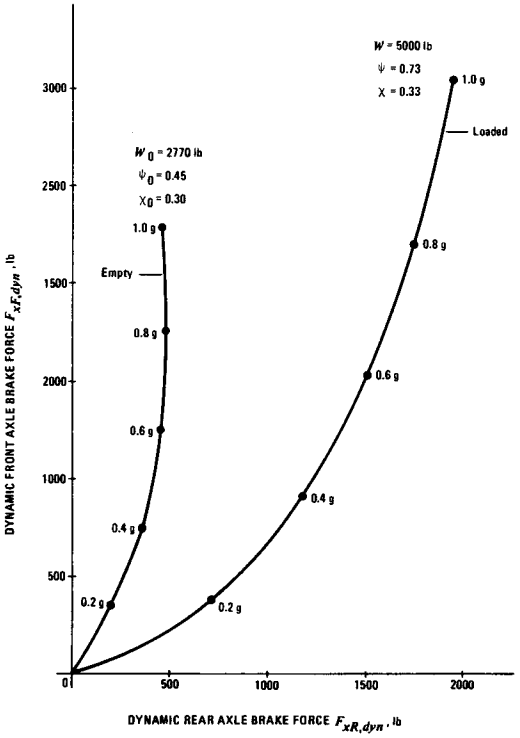

Figure 8-2. Dynamic Braking Forces

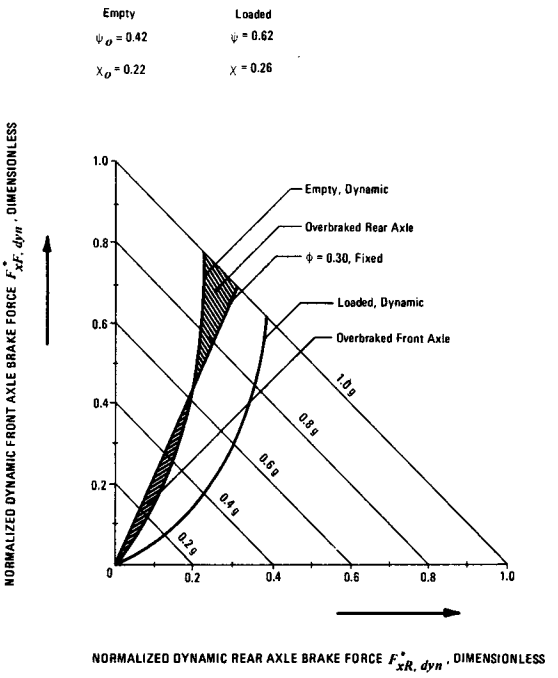

Figure 8-3. Normalized Dynamic Brake Forces

braking. Since the dynamic braking forces are different for straight-line braking and braking in turn, two different "ideal' conditions exist. The brake engineer must determine by the intended vehicle function whether a brake system should be optimized with respect to straight-line braking or braking in a turn. The word ideal should be used only for the description of a brake force distribution when no improvements in braking performance can be achieved by altering the distribution of brake forces among axles or wheels.

8-1.2 ACTUAL BRAKE FORCE DISTRIBUTION

The quality of a brake system is determined by comparing actual brake forces to dynamic brake forces. If the actual brake forces always were equal to the dynamic brake forces, the braking process would be optimum resulting in minimum straight-line stopping distances. For vehicles equipped with fixed ratio braking the actual brake forces produced by the front and rear axles may be represented by a straight line as illustrated in Figs. 8-3, 8-4, and 8-5. The distribution of the actual brake forces ϕ is defined as the ratio of the rear axle brake force to total brake force

$$\phi = \frac{F_{xR}}{F_{xF} + F_{xR}}, \text{ d'less} \qquad (8\text{-}5)$$

where

F_{xF} = actual front axle brake force, lb
F_{xR} = actual rear axle brake force, lb

Similarly, the relative front axle brake force is

$$1 - \phi = \frac{F_{xF}}{F_{xF} + F_{xR}}, \text{ lb} \qquad (8\text{-}6)$$

The individual axle brake forces may be computed by Eqs. 5-10 and 5-31 of Chapter 5. For small push-out pressures and equal tire radius front and rear, the brake force distribution ϕ is computed by the parameters of the components usually altered between front and rear axle

$$\phi = \frac{(A_{WC}BFr)_R}{(A_{WC}BFr)_F + (A_{WC}BFr)_R}, \text{ d'less} \qquad (8\text{-}7)$$

where

A_{WC} = wheel cylinder area, in.^{2}
BF = brake factor, d'less
r = effective drum or rotor radius, in.
F = subscript for front axle, d'less
R = subscript for rear axle, d'less

In Fig. 8-3 the dynamic braking forces are compared to an actual brake force distribution $\phi = 0.30$. Typical values for ϕ, ψ, and χ were used in this example. The point of change from front axle overbraking to rear axle overbraking is determined by the intersection of ϕ with the dynamic braking forces. It can be seen that for the unloaded driving condition overbraking of the front axle may occur for $a <$ 0.64g, whereas the rear axle tends to overbrake for a > 0.64g. For the loaded driving condition the front axle always tends to overbrake.

Improved straight-line braking performance will be obtained by a fixed brake force distribution minimizing the difference between actual and dynamic brake forces over a wide range of decelerations. Although diagrams such as illustrated in Fig. 8-3 are essential for an initial brake system analysis, more useful information about the braking process can be obtained from a tire-road friction utilization analysis.

The dynamic braking forces illustrated in Fig. 8-3 may be expanded to include both deceleration and acceleration of the vehicle as illustrated in Fig. 8-4. The zero points of the parabola of dynamic braking force and driving force are determined from Eqs. 8-3 and 8-4, respectively, with the dynamic brake forces set equal to zero. Dynamic driving forces are obtained by acceleration of the vehicle as opposed to deceleration.

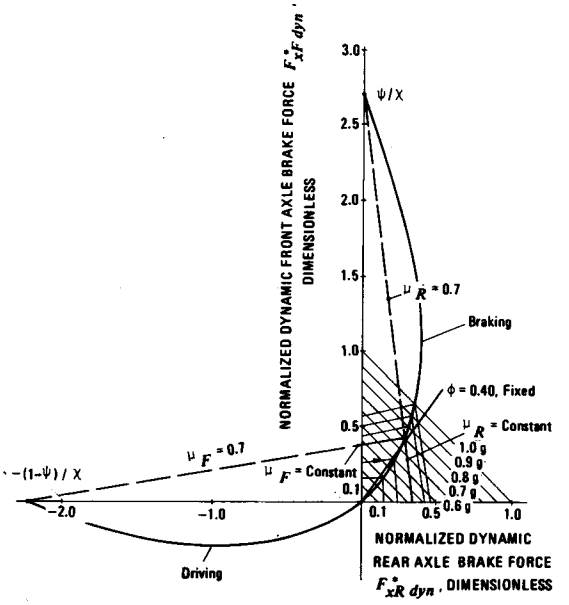

Figure 8-4. Parabola of Normalized Dynamic Braking and Driving Forces

A line of constant tire-road friction coefficient for either the front or rear axle is obtained by drawing a line through the intersection of the parabola with a line of constant deceleration and the appropriate zero points of the parabola. Lines of constant tire-road friction coefficient for the front axle are found by using the zero point $-(1-\psi)/\chi$ and for the rear axle by using the zero point ψ/χ. The use of the expanded dynamic braking force diagram (Fig. 8-4) is explained in the next paragraph for a vehicle having typical geometrical and loading data.

Of particular interest is the deceleration and hence stopping distance of a vehicle with no wheels locked, and with either the front or rear wheels locked. For a given vehicle, this deceleration can be determined most easily from the diagram illustrated in Fig. 8-5. The dynamic brake force — front and rear — normalized by the vehicle weight is shown to be a function of vehicle deceleration. If it is assumed that the peak tire-road friction is equal to the sliding friction value, which is nearly true for most tires operating on dry pavement, lines of constant tire-road friction coefficient on the front and rear wheels can be drawn as shown in Fig. 8-5. Also shown are straight lines

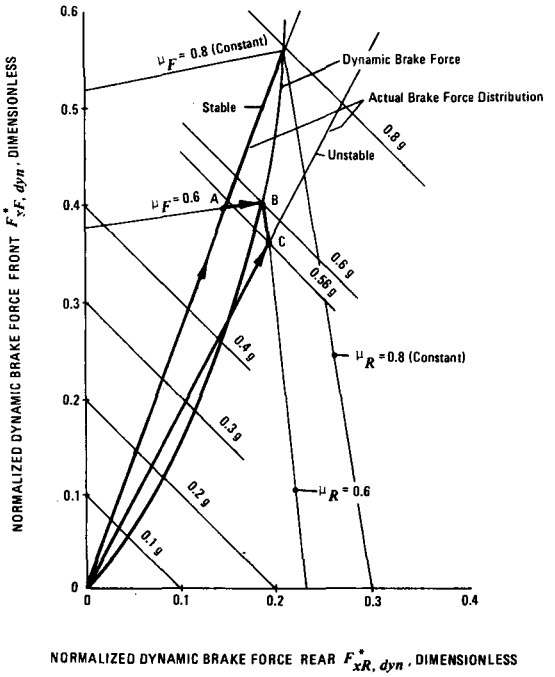

Figure 8-5. Normalized Dynamic and Actual Brake Forces

representing the normalized brake forces actually developed by the installed brakes. These lines are marked stable and unstable. When a pedal force is applied, e.g., for a vehicle having the stable brake force distribution, the brake forces — front and rear — increase along the stable line up to point A. If it is assumed that the tire-road friction coefficient is 0.6, the front wheels lock at point A. Further increase in pedal force results in increased rear wheel brake force and thus increased deceleration from 0.56g to 0.60g, designated by point B. The increased deceleration from 0.56g to 0.60g stems from increased rear brake force and the larger front wheel braking force due to increased normal force on the front tires. Since the front wheels lock before the rear wheels, a stable stop results. For a vehicle equipped with the unstable brake force distribution, the brake forces — front and rear — increase to a level indicated by point C, corresponding to a deceleration of 0.56g. For a maximum tire-road friction coefficient of 0.6 the rear wheels lock at the conditions marked by point C. Further increase in pedal force results in increased deceleration along line CB until all wheels are locked at a deceleration of 0.6g, indicated by point B. This stop is unstable because the rear wheels lock prior to the front wheels.

8-1.3 TIRE-ROAD FRICTION UTILIZATION

The concept of tire-road friction utilization was introduced in Chapter 7. The tire-road friction coefficient required on a particular axle to prevent wheel lockup may be computed by Eq. 7-5. For a two-axle vehicle the tire-road friction coefficient μ_R on the rear axle is

$$\mu_R = \frac{F_{xR}}{F_{zR}} = \frac{\phi\, a\, W}{(\psi - \chi a)W} = \frac{\phi\, a}{\psi - \chi a} \quad \text{,d'less(8-8)}$$

where

F_{xR} = actual rear axle brake force, lb

F_{zR} = dynamic normal force of rear axle, lb

Similarly, on the front axle the tire-road friction coefficient μ_F is

$$\mu_F = \frac{(1-\phi)a}{1 - \psi + \chi a}\text{, d'less} \qquad (8\text{-}9)$$

A graphical representation of Eqs. 8-8 and 8-9 is illustrated in Fig. 8-6 for the vehicle geometrical and loading data shown. The friction utilization computed by Eq. 8-8 is illustrated by the part of the curve labeled by "Rear Axle Overbrakes", the part corresponding to Eq. 8-9, by "Front Axle Overbrakes".

The optimum point corresponds to a = 0.62g. For deceleration below 0.62g, e.g., 0.4g, a friction coefficient between front tires and road of approximately 0.44 is required for wheels unlocked braking in the empty condition. For decelerations exceeding 0.62g, e.g., a = 0.9g, a friction coefficient of about 1.08 is required on the rear wheels.

8-1.4 BRAKING EFFICIENCY

The concept of tire-road friction utilization may be expanded to be more generally applicable to a braking analysis. Upon dividing the deceleration by the associated tire-road friction coefficient required for wheels unlocked braking the concept of braking efficiency is established. The braking efficiency expresses the extent a given tire-road friction coefficient available to the vehicle is transformed into vehicle deceleration (Refs. 1 and 2).

By starting with Eqs. 8-8 and 8-9, analytical expressions for the braking efficiency of rear and front axle may be derived. Eq. 8-8 can be rewritten as

$$\mu_R \psi - \mu_R \chi a = \phi a$$

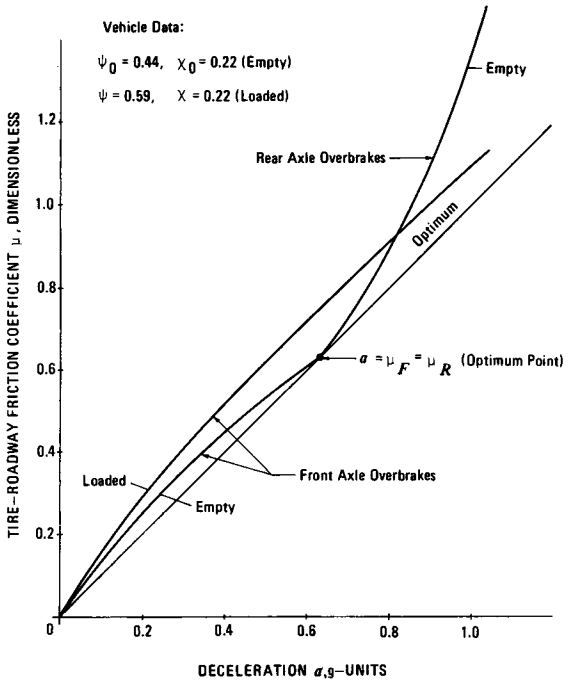

Figure 8-6. Tire-Road Friction Utilization

and collecting terms involving deceleration yields

$$a(\phi + \mu_R \chi) = \mu_R \psi$$

The braking efficiency E_R of the rear axle now becomes

$$E_R = (a/\mu)_R = \frac{\psi}{\phi + \mu_R \chi}, \text{ d'less} \quad (8\text{-}10)$$

Similarly, the braking efficiency E_F of the front axle becomes

$$E_F = (a/\mu)_F = \frac{1 - \psi}{1 - \phi - \mu_F \chi}, \text{ d'less} \quad (8\text{-}11)$$

Since the values of tire-road friction — front and rear — are nearly identical and may assume only slightly different values due to changes in normal forces during braking, the subscripts front and rear associated with the friction coefficients in Eqs. 8-10 and 8-11 may be ignored.

A graphical representation of Eqs. 8-10 and 8-11 is illustrated in Fig. 8-7 in which the braking efficiency is plotted as a function of tire-road friction coefficient. Inspection of Fig. 8-7 indicates that for μ = 0.40 the efficiency on the front axle is equal to approximately 0.88 for the empty driving condition. A braking efficiency of 88% indicates that 88% of the friction available for braking is used for vehicle deceleration by the front wheels.

Fig. 8-7 also shows the additional stopping distance over the minimum achievable with optimum

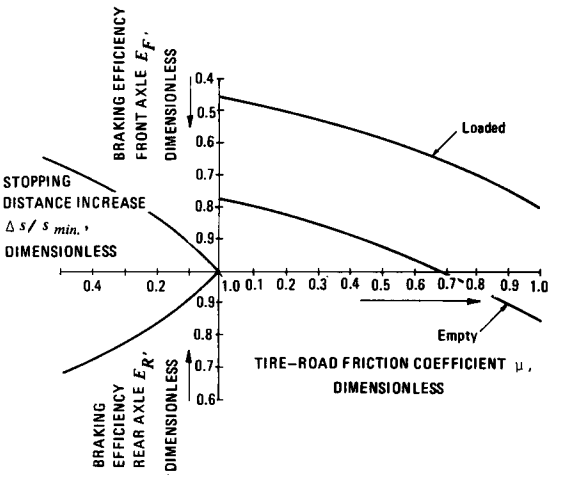

Figure 8-7. Braking Efficiency Diagram

braking. Starting with Eqs. 1-1 and 1-2, the ratio between stopping distance increase ΔS and minimum stopping distance S_{min} may be derived as

$$\Delta S/S_{min} = \frac{1-(a/\mu)}{(a/\mu)} \text{ , d'less} \quad (8\text{-}12)$$

It has been assumed, so far, that the deceleration a attains its maximum value instantaneously. However, when time delays are included as indicated by Eq. 1-3, a requirement on the minimum value of braking efficiency necessary for achieving a certain stopping distance can be formulated as

$$(a/\mu) = \frac{V^2}{2g\mu\left[S_{act} - \left(t_a + \frac{t_b}{2}\right)V\right]} \text{ , d'less} \quad (8\text{-}13)$$

where

g = gravitational constant, 32.2 ft/s^2
S_{act} = actual stopping distance, ft
t_a = application time, s
t_b = buildup time, s
V = vehicle speed, ft/s

The last term, i.e., $ga_{max}\, t_b^2/24$ of Eq. 1-3 generally assumes small values for typical buildup times t_b = 0.5 to 1.0 s and therefore is neglected in the derivation of Eq. 8-13. The maximum deceleration is identified by a_{max}.

By substitution of μ = 0.7, S_{act} = 216 ft, t_a = 0.1 s, t_b = 0.4 s and V = 88 ft/s into Eq. 8-13, the required braking efficiency becomes 91%. For μ = 0.8 the required braking efficiency would be 79%. Eq. 8-13 demonstrates the physical phenomenon that a given stopping distance can be achieved by a braking system having a large response time and high braking efficiency or short response times and low braking efficiency.

8-1.5 OPTIMUM BRAKING FORCE DISTRIBUTION FOR STRAIGHT-LINE BRAKING

Before designing the braking system of any motor vehicle, the questions to be answered are: (a) can specific wheels-unlocked decelerations be achieved over a wide range of loading and roadway conditions with a fixed brake force distribution, and (b) if so, what is the required brake force distribution?

For a two-axle vehicle Eqs. 8-10 and 8-11 may be used to develop a limiting relationship on the brake force distribution ϕ (Ref. 3)

$$\left(1 - \mu\chi - \frac{1-\psi}{E_{min}}\right) \le \phi \le \left(\frac{\psi}{E_{min}} - \mu\chi\right) \text{ , d'less} \quad (8\text{-}14)$$

where

E_{min} = minimum braking efficiency to be achieved by vehicle, d'less

Application of this inequality to the limiting conditions corresponding to $0.2 \le \mu \le 0.8$ and the loaded and empty cases defines an envelope for acceptable values of ϕ. A ϕ-value within this envelope may be used for design evaluation. Application of Eq. 8-14 normally will yield different values of ψ for the empty and loaded vehicle. The ϕ-value finally used for design purposes depends on the intended vehicle function. The decelerations achievable prior to wheel-lock have to be computed with the design distribution for slippery (μ = 0.2) as well as dry (μ = 0.8) road surfaces for both the empty and loaded vehicle. The expressions for computing the deceleration achievable can easily be obtained from Eqs. 8-10 and 8-11.

Rear Axle:

$$a = \frac{\mu\psi}{\phi + \mu\chi} \text{ , g-units} \quad (8\text{-}15)$$

Front Axle:

$$a = \frac{\mu(1-\psi)}{1 - \phi - \mu\chi} \text{ , g-units} \quad (8\text{-}16)$$

For a modified test vehicle, application of Eq. 8-14 resulted in a brake force distribution of ϕ = 0.38 for the empty driving condition and for μ = 0.2 and 0.8 (Ref. 2). The test vehicle was originally equipped with a distribution ϕ = 0.50. The computed decelerations achievable on slippery and dry pavements are equal to 0.19g and 0.60g, respectively, for ϕ = 0.38; and 0.15g and 0.50g, respectively, for ϕ = 0.50 for the empty driving condition. When the vehicle is loaded, the wheels unlocked decelerations are 0.12g and 0.71g, respectively, for ϕ = 0.38; and 0.17g and 0.69g, respectively, for ϕ = 0.50. The results indicate that the loaded vehicle with ϕ = 0.38 will tend to lose steering ability sooner, but improved braking performance for the empty case will probably be of more importance with respect to vehicle safety.

Often, it is of interest to know prior to finalizing the brake system design if a two-axle truck can produce certain braking efficiencies. An analysis is presented which allows a decision to be made on the necessity of a variable brake force distribution based upon geometric and loading information of the vehicle, i.e., will a particular vehicle achieve certain braking efficiencies with fixed ratio braking?

Eqs. 8-15 and 8-16 may be used to formulate a requirement on the brake force distribution ϕ for a vehicle braking on low friction (μ = 0.2) and high friction road surfaces (μ = 0.8) with a specified braking efficiency. The greatest difficulties exist in preventing premature rear wheel lockup when the empty vehicle is braking on dry road surfaces at high deceleration or preventing front wheel lockup when the loaded vehicle is braking at low decelerations on a slippery road surface. In the first case the static rear axle load is small since the vehicle is empty and large dynamic load transfer off the rear axle occurs due to a larger deceleration. In the second case the static front axle load is small and no significant dynamic load transfer to the front axle occurs. For these two conditions the braking efficiency generally presents the minimum limit value. For the cases of braking the loaded vehicle on a dry road surface or the empty vehicle on a slippery road surface the braking efficiencies are generally larger than those associated with the minimum limit value.

Based on these physical constraints, a requirement on the brake force distribution ϕ can be developed.

For the empty vehicle when braking on a high friction road surface (μ = 0.8) with a braking efficiency E_R = 0.65 Eq. 8-15 yields

$$0.65 \times 0.8 = 0.52 = \frac{0.8\,\psi_o}{\phi + 0.8\,\chi_o} \qquad (8\text{-}17)$$

The front axle of the empty vehicle generally operates at a braking efficiency higher than the minimum value when braking on a low friction road surface. For E_F = 0.80 and μ = 0.2 Eq. 8-16 yields

$$0.16 = \frac{(1 - \psi_o)\,0.2}{1 - \phi - 0.2\,\chi_o} \qquad (8\text{-}18)$$

For the loaded vehicle the rear axle generally operates at a braking efficiency higher than the minimum value when braking on a high friction surface. For E_R = 0.75 and μ = 0.8 Eq. 8-15 yields

$$0.60 = \frac{0.8\,\psi}{\phi + 0.8\chi} \qquad (8\text{-}19)$$

The front axle of the loaded vehicle operates at the minimum value of braking efficiency when braking on a low friction road surface. For E_F = 0.65 and μ = 0.2 Eq. 8-16 yields

$$0.13 = \frac{(1 - \psi)\,0.2}{1 - \phi - 0.2\chi} \qquad (8\text{-}20)$$

The subscript "o" designates the empty driving condition. From Eqs. 8-17 through 8-20 a requirement on the brake force distribution $\phi = f(\psi, \chi, \psi_o, \chi_o)$ as function of geometric and loading parameters may be formulated. Omit the algebra; the result from Eqs. 8-17 and 8-18 is

$$\phi = \frac{\psi_o\,(1 + 0.45\,\chi_o) - 0.65\,\chi_o}{1 - 0.1875\,(1 - \psi_o)}\ , \text{ d'less} \qquad (8\text{-}21)$$

and from Eqs. 8-19 and 8-20

$$\phi = \frac{\psi\,(1 + 0.72\chi) - 0.92\chi}{1 + 0.15\,(1 - \psi)}\ , \text{ d'less} \qquad (8\text{-}22)$$

Application of Eqs. 8-21 and 8-22 generally will result in different values of ϕ for the empty and loaded vehicle. But, if the values for ψ, χ, ψ_o, and χ_o are such that the brake force distributions ϕ computed from Eqs. 8-21 and 8-22 are identical, a fixed brake force distribution will be adequate, i.e., the differences in center-of-gravity location between the empty and loaded cases are so small that a proportional braking system is not necessary.

Eqs. 8-21 and 8-22 may be used to eliminate ϕ, and it becomes possible to derive a limiting condition on the relative static rear load $\psi_o = f(\psi, \chi, \chi_o)$ as a function of the remaining vehicle parameters. This condition must be satisfied before fixed ratio braking may be considered adequate for the braking process with a specified minimum braking efficiency. Omit the algebra; the results when plotted for different values of ψ and $\Delta\chi = \chi - \chi_o$ were found to be described by a functional relationship

$$\psi - \psi_o \leq \Delta\chi + 0.09\ , \text{d'less} \qquad (8\text{-}23)$$

The value of $\Delta\chi$ for trucks is generally small and less than 0.03 and, consequently, an approximate limiting condition on the change in relative static rear axle load is

$$\psi - \psi_o \leq 0.12\ , \text{d'less} \qquad (8\text{-}24)$$

The results indicate that vehicles equipped with fixed ratio braking systems are capable of achieving decelerations well within the requirements for safe braking performance, provided the vehicle experiences an increase in relative static rear axle load of not more than 12%, i.e., $\Delta\psi = \psi - \psi_o \leq 0.12$. This means, also, that load dependent proportioning will

yield only little or no improvement in braking performance for trucks whose difference in relative static rear axle load between the empty and loaded case is less than 12%.

The limiting condition on the brake force distribution, i.e., Eq. 8-14, was applied to a variety of commercial vehicles such as light and medium trucks and school buses (Refs. 4 and 5). Actual road tests were conducted to determine the maximum braking capabilities of the vehicles. The center-of-gravity location of the light truck remained almost unaffected by the loading as indicated by $\Delta\psi = \psi - \psi_0 = 0.674 - 0.595 = 0.079$ and $\Delta\chi = \chi - \chi_0 = 0.320 - 0.293 = 0.027$. The corresponding values for the medium truck were $\Delta\psi = 0.29$ and $\Delta\chi = 0.06$ indicating a significant horizontal change in the location of the center of gravity from the loaded to the unloaded case. The location of the center of gravity of the school bus changed little as indicated by $\Delta\psi = 0.105$ and $\Delta\chi = 0.001$. This result was to be expected due to the long wheel base of the vehicle.

Inspection of the $\Delta\psi$ values for the light truck and the school bus indicates that no difficulties exist in designing a braking system with fixed ratio braking for both vehicles which will yield an acceptable braking performance. The $\Delta\psi$ value of the medium truck is greater than the limit value $\Delta\psi = 0.12$, and therefore it becomes impossible to achieve acceptable braking performances with fixed ratio braking for the medium truck.

Assume a maximum and minimum value of μ equal to 0.8 and 0.2, respectively, and a minimum braking efficiency of 0.70; application of Eq. 8-14 to the light truck results in a theoretical value for $\phi = 0.51$, as contrasted with the actual brake force distribution of $\phi = 0.53$. The computed distribution $\phi = 0.51$ along with the appropriate vehicle data yields a minimum braking efficiency of 77% by use of Eq. 8-11 for the loaded vehicle operating on slippery road surfaces with $\mu = 0.2$. For all other loading and road surface conditions, the theoretical braking efficiencies are higher. For the dry road surface, the braking efficiencies computed by Eq. 8-10 for the loaded case and Eq. 8-11 for the empty case are 87 and 80%, respectively. These braking efficiencies would produce wheels unlocked decelerations of 22.4 ft/s² for the loaded vehicle and 20.6 ft/s² for the empty vehicle on a road surface having a tire-roadway friction coefficient of 0.8. These theoretical values, when computed to test data of 20 ft/s² unloaded and 23 ft/s² loaded, indicate that the braking system of the light truck was operating near or at an optimum condition. Changes in the brake force distribution or even a proportional braking system would yield no improvement in braking performance. This finding is in agreement with Eq. 8-24 indicating that solid-frame vehicles whose fixed brake force distribution was designed according to Eq. 8-14 are capable of achieving decelerations well within the requirement for safe braking, provided the vehicle experiences an increase in the relative static rear axle loading of not more than 12%, i.e., $\Delta\psi = \psi - \psi_0 \leq 0.12$.

Application of Eq. 8-14 to the school bus resulted in a brake force distribution $\phi = 0.50$ to 0.55. The vehicle was equipped with a brake force distribution $\phi = 0.42$. A brake force distribution of $\phi = 0.55$ would produce theoretical braking efficiencies of 72 and 93% for the empty and loaded vehicle, respectively, on slippery roadways with $\mu = 0.2$; and 92 and 96% for the empty and loaded vehicle, respectively on dry road surfaces with $\mu = 0.8$. For the empty vehicle a theoretical deceleration of 23.7 ft/s² may be expected on dry road surfaces. In the case of the school bus, a change in brake force distribution from 0.42 to 0.55 will improve braking performance for the vehicle on slippery road surfaces indicated by an increase in braking efficiency from 48 to 72%. Improvements in deceleration capability can be expected from a change in brake force distribution. However, a proportional braking system will yield only little increase in braking performance indicated by the small change in relative static rear axle loading of $\Delta\psi = 0.105$.

The design of the braking system for the medium truck is made difficult by a significant change in static axle loading indicated by $\Delta\psi = 0.29$. The brake system of this vehicle was designed to meet the braking requirements for the loaded driving condition indicated by an actual brake force distribution $\phi = 0.74$, i.e., 74% of the braking effort is concentrated on the rear axle. While this might produce desirable results for the loaded vehicle on slippery roads and hence little braking is done by the front brakes, and still acceptable results on dry road surfaces, the braking performance to be expected with the empty vehicle is unacceptable. Application of Eq. 8-14 resulted in the following inequalities for the brake force distribution:

$0.27 \leq \phi \leq 0.52$ for $\mu = 0.2$, empty
$0.12 \leq \phi \leq 0.36$ for $\mu = 0.8$, empty
$0.58 \leq \phi \leq 0.83$ for $\mu = 0.2$, loaded
$0.43 \leq \phi \leq 0.68$ for $\mu = 0.8$, loaded

Inspection of these results indicates that a brake force distribution $\phi = 0.74$ will produce acceptable braking performance only for the loaded vehicle on slippery road surfaces. Consider the second and third inequality as a compromise; a brake force distribution of $\phi = 0.47$ probably would yield better

braking performance for all road surface and loading conditions than can be expected from $\phi = 0.74$. The theoretical braking efficiencies with $\phi = 0.47$ are 67 and 90% for the empty and loaded vehicle, respectively, on road surfaces having a tire-roadway friction coefficient of $\mu = 0.8$. For the empty vehicle a deceleration of approximately 17.2 ft/s² therefore may be expected on dry pavement with $\mu = 0.8$. A deceleration of 23.2 ft/s² may be expected for the loaded vehicle with $\phi = 0.47$ provided the brake effectiveness is increased to such a level that wheel slide conditions can be approached (a condition not attainable by the loaded test vehicle). A further increase in braking capability only can be accomplished by means of a proportional braking system. This also is evident from the change in relative static rear axle loading of $\Delta\psi = 0.29$. A variable ratio braking system probably will increase the braking performance of the medium truck to 20 to 23 ft/s² for both the empty and loaded case.

The brake force distribution ϕ generally is not constant during braking. For low deceleration levels ϕ may be dependent upon the difference in pushout pressures on front and rear axle, whereas for higher decelerations ϕ may be affected by brake fade as discussed in Chapter 7. If the effects of pushout pressures are included in the analysis, the braking efficiency curves are altered, especially at low operating pressure, i.e., on slippery road surfaces, as illustrated in Fig. 8-8. If brake fade does not alter the design brake force distribution, it will have no effect on braking efficiency.

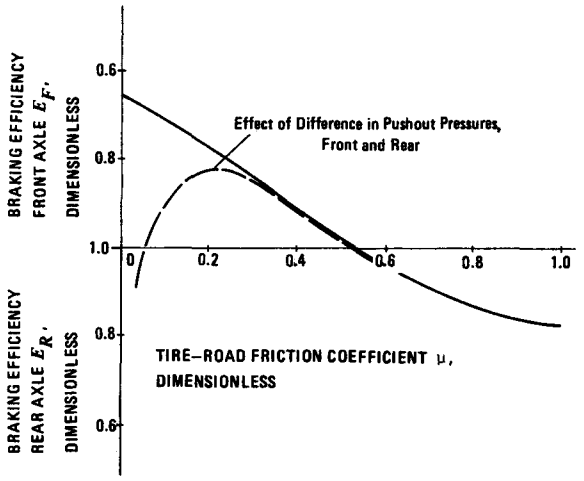

Figure 8-8. Braking Efficiency Affected by Pushout Pressures

8-1.6 STRAIGHT-LINE VERSUS CURVED PATH BRAKING PERFORMANCE

When braking in a turn, additional load transfer occurs due to the centrifugal force acting at the vehicle center of gravity resulting in increased normal forces at the outer wheels. In addition, the tires must produce side forces which reduce the friction available for braking.

Using the vehicle model shown in Fig. 8-9, a wheels-unlocked braking efficiency on rear and front axle may be derived (Refs. 6 and 7). The braking efficiency on the rear axle E_R is

$$E_R = \frac{-K_1\mu\chi}{K_2 - (\mu\chi)^2} + \left[\left(\frac{K_1\mu\chi}{K_2 - (\mu\chi)^2}\right)^2 + \frac{K_1^2 - K_3}{K_2 - (\mu\chi)^2}\right]^{1/2}, \text{ d'less} \quad (8\text{-}25)$$

where

$$K_1 = \psi - \chi\left[L(1-\psi) - x\right]\left(\frac{1}{g}\right)\left(\frac{V}{\rho_c}\right)^2, \text{ d'less} \quad (8\text{-}26)$$

$$K_2 = \phi^2, \text{ d'less} \quad (8\text{-}27)$$

$$K_3 = \left(\frac{\psi}{\mu g}\right)^2 V^2 \left(\frac{V}{\rho_c}\right)^2 \times \left[1 - \left(\frac{L(1-\psi) - x}{\rho_c}\right)^2\right], \text{ d'less} \quad (8\text{-}28)$$

where

L = wheel base, ft
V = vehicle speed, ft/s
x = displacement of center of rotation of vehicle due to tire creep, ft
ρ_c = radius of curvature, ft

The braking efficiency on the front axle E_F is

$$E_F = \frac{C_1\mu\chi}{C_2 - (\mu\chi)^2} + \left[\left(\frac{C_1\mu\chi}{C_2 - (\mu\chi)^2}\right)^2 + \frac{C_1^2 - C_3}{C_2 - (\mu\chi)^2}\right]^{1/2}, \text{ d'less} \quad (8\text{-}29)$$

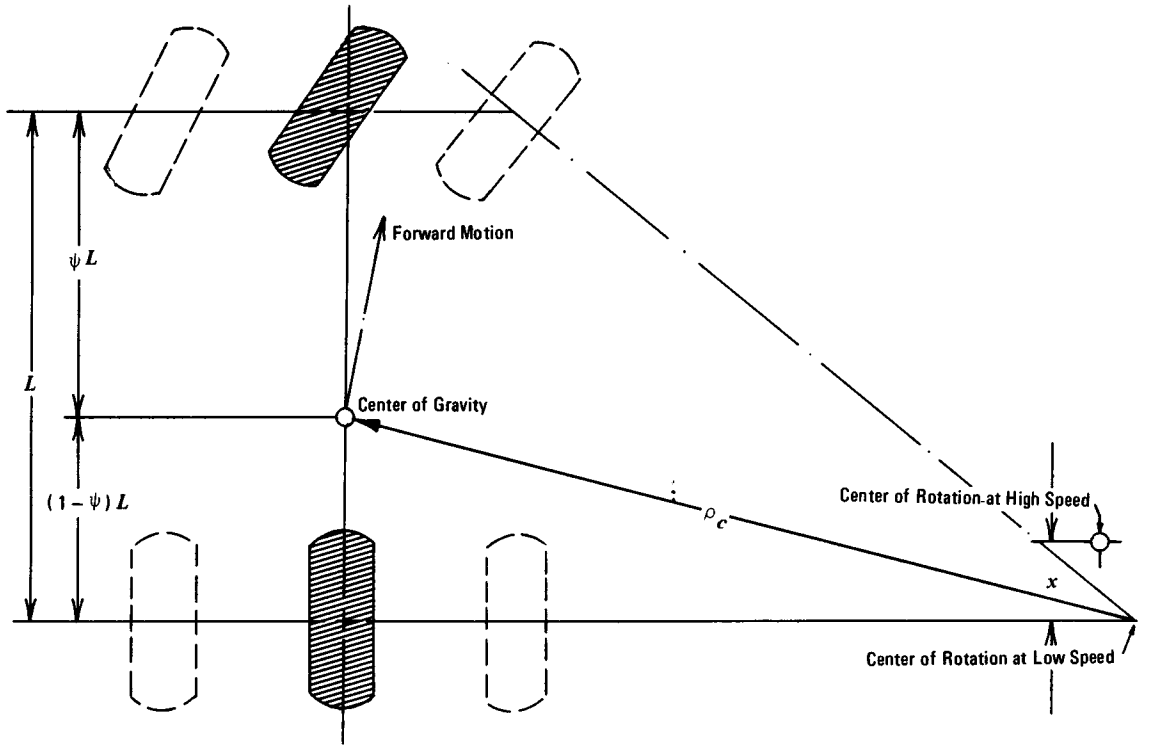

Figure 8-9. Simplified Vehicle Model

where

$$C_1 = (1-\psi) + \chi[L(1-\psi) - x] \times \left(\frac{1}{g}\right)\left(\frac{V}{\rho_c}\right)^2 \text{, d'less} \quad (8\text{-}30)$$

$$C_2 = (1-\phi)^2 \text{, d'less} \quad (8\text{-}31)$$

$$C_3 = \left(\frac{1-\psi}{\mu g}\right)^2 V^2 \left(\frac{V}{\rho_c}\right)^2 \times \left[1 - \left(\frac{L(1-\psi) - x}{\rho_c}\right)^2\right] \text{, d'less} \quad (8\text{-}32)$$

Eqs. 8-25 and 8-29 reduce to Eqs. 8-10 and 8-11 giving the braking efficiency for straight-line braking for $\rho_c = \infty$, i.e., a straight line. Inspection of Eqs. 8-25 and 8-29 indicates that the braking efficiency is now speed dependent for a given vehicle and road curvature. By using typical vehicle data, evaluation of Eq. 8-25 for the rear axle braking efficiency yields the graphical representation illustrated in Fig. 8-10.

A limiting condition similar to Eq. 8-14 on brake force distribution for optimum curved-line braking may be developed from Eqs. 8-25 and 8-29. The result is a lengthy algebraic relationship which is not presented here. Evaluation of the limiting relationship indicates clearly that braking systems optimized for straight-line braking do not result in optimum curved braking. Results indicate that a typical passenger car requires a brake force distribution of 30% for optimum straight-line braking, however, only 25% for optimum curved line braking (Ref. 7). The final choice of brake force distribution depends upon the intended vehicle function. Trucks equipped with dual tires on the rear axle generally permit somewhat larger relative rear axle brake forces than passenger cars.

To improve braking performance for a wide range of loading conditions for both straight and curved-line braking, automatic adjustable proportioning valves are used. A detailed discussion of proportional braking is presented in Chapter 9.

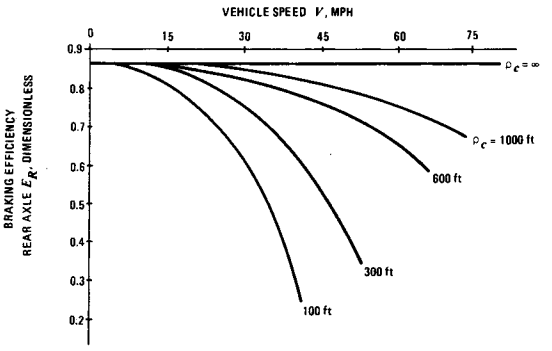

Figure 8-10. Rear Braking Efficiency as Function of Speed and Road Curvature for a Tire-Road Friction Coefficient of 0.6

In the derivation of the curved-path braking efficiency, i.e., Eqs. 8-25 through 8-32, a simple bicycle model is assumed where the vehicle center of gravity is considered to be in the plane of the road surface so as to rule out lateral load transfer effects. Only lateral tire forces are included along with the longitudinal load transfer stemming from the centrifugal force.

When braking in a turn, tires are required to produce both longitudinal or braking forces and side forces to hold the vehicle in the desired turn. The tire normal forces change due to the longitudinal deceleration of braking and the lateral acceleration or corner force as illustrated in Fig. 8-11. Additional longitudinal load transfer occurs due to the centrifugal force component F_{cx} in the direction of the longitudinal vehicle axis. The development of a combined braking and turning braking efficiency requires the determination of the tire normal forces, tire side forces, and braking forces.

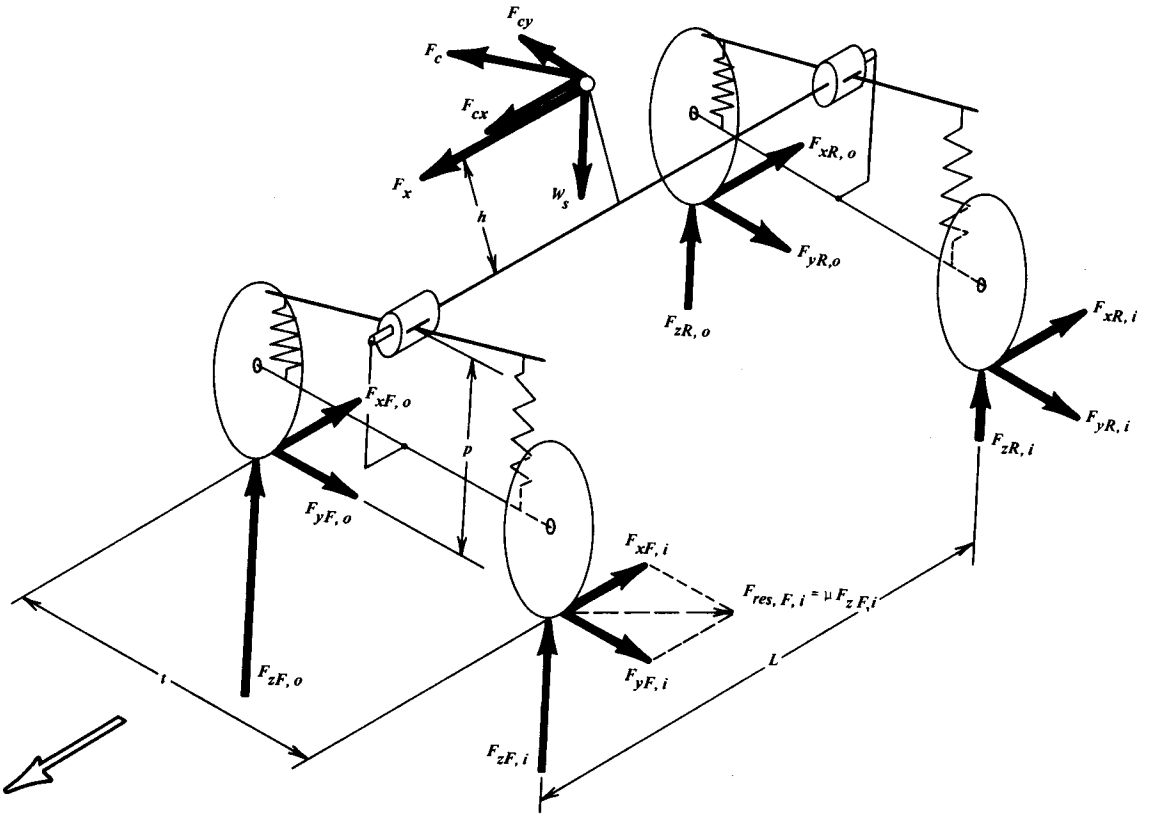

Figure 8-11. Forces Acting on a Braking and Turning Vehicle

For a four-wheel vehicle with its center-of-gravity located midway between the left and right wheels, the tire normal forces on the outer and inner front, and outer and inner rear wheels are

$$\left.\begin{aligned} F_{zF,o} &= \left(\frac{1}{2}\right)F_{zF,static} + \Delta F_{zF} \text{ , lb} \\ F_{zF,i} &= \left(\frac{1}{2}\right)F_{zF,static} - \Delta F_{zF} \text{ , lb} \\ F_{zR,o} &= \left(\frac{1}{2}\right)F_{zR,static} + \Delta F_{zR} \text{ , lb} \\ F_{zR,i} &= \left(\frac{1}{2}\right)F_{zR,static} - \Delta F_{zR} \text{ , lb} \end{aligned}\right\} \quad (8\text{-}33)$$

where

$F_{zF,i}$ = normal force of inner front wheel, lb
$F_{zF,o}$ = normal force of outer front wheel, lb
$F_{zR,i}$ = normal force of inner rear wheel, lb
$F_{zR,o}$ = normal force of outer rear wheel, lb
$F_{zF,static}$ = static normal force of front axle, lb
$F_{zR,static}$ = static normal force of rear axle, lb
ΔF_{zF} = load transfer of one front wheel due to turning, lb
ΔF_{zR} = load transfer of one rear wheel due to turning, lb

Including load transfer due to the distance between roll centers and the road surface, the centrifugal forces associated with unsprung axles, the suspension moment, and the longitudinal and lateral components of the centrifugal force, the tire normal forces are:

Front, inner wheel

$$F_{zF,i} = \left\{1-\psi + a_x \chi + \frac{\chi[L(1-\psi)-x]a_y}{\rho_c}\right\}\frac{W}{2} - a_y S_F W_s \text{ , lb} \quad (8\text{-}34)$$

Front, outer wheel

$$F_{zF,o} = \left\{1-\psi + a_x \chi + \frac{\chi[L(1-\psi)-x]a_y}{\rho_c}\right\}\frac{W}{2} + a_y S_F W_s \text{ , lb} \quad (8\text{-}35)$$

Rear, inner wheel

$$F_{zR,i} = \left\{\psi - a_x \chi - \frac{\chi[L(1-\psi)-x]a_y}{\rho_c}\right\}\frac{W}{2} - a_y S_R W_s \text{ , lb} \quad (8\text{-}36)$$

Rear, outer wheel

$$F_{zR,o} = \left\{\psi - a_x \chi - \frac{\chi[L(1-\psi)-x]a_y}{\rho_c}\right\}\frac{W}{2} + a_y S_R W_s \text{ , lb} \quad (8\text{-}37)$$

where

a_x = longitudinal acceleration, g-units
a_y = lateral acceleration, g-units
L = wheelbase, ft
S_F = front normalized roll stiffness, d'less
S_R = rear normalized roll stiffness, d'less
W = total vehicle weight, lb
W_s = unsprung weight, lb
ρ_c = radius of curvature of turn, ft

The normalized roll stiffness S_F on the front suspension is (Ref. 8).

$$S_F = \left(\frac{L_R}{L}\right)\left(\frac{p_F}{t_F}\right) + \left(\frac{K_F}{K_F + K_R - W_s h_r}\right)\left(\frac{h_r}{t_F}\right) + \left(\frac{w_F}{W_s}\right)\left(\frac{h_F}{t_F}\right), \text{ d'less} \quad (8\text{-}38)$$

where

h_F = center of gravity height of unsprung mass ft
h_r = distance between center of gravity and roll axis, ft
K_F = front roll stiffness, ft·lb/rad
K_R = rear roll stiffness, ft·lb/rad
L_R = horizontal distance between center of gravity and rear axle, ft
p_F = front roll center-to-ground distance, ft
t_F = front track width, ft
w_F = front suspension unsprung weight, lb

The rear normalized roll stiffness is obtained from Eq. 8-38 by replacing subscript F by R and using the appropriate vehicle data.

8-1.7 GENERAL BRAKING EFFICIENCY

For vehicles having a fixed brake force distribution between axles, the general braking efficiency equations are given by Eqs. 8-25 and 8-29. To achieve more flexibility in the analysis, a general approach

was developed to determine the braking efficiency of a brake system. This approach consists of the following eight steps:

1. Obtain brakeline pressures from proportioning characteristics — front and rear.
2. Compute brake forces F_x by Eq. 5-10 or 5-31 for individual wheels.
3. Compute total brake forces $F_{x,total} = \Sigma F_x$
4. Compute vehicle deceleration by

$$a_x = F_{x,total}/W \text{ , g-units} \qquad (8\text{-}39)$$

5. For a given lateral acceleration a_y compute the individual tire normal forces by Eqs. 8-34 through 8-37.
6. Compute tire side forces by the equations that follow.

Front, inner wheel

$$F_{yF,i} = (1-\psi)W\left(\frac{a_y}{\rho_c}\right)\left(\frac{F_{zF,i}}{F_{zF}}\right) \times \left\{\rho_c^2 - [L(1-\psi)-x]^2\right\}^{1/2} \text{ , lb} \qquad (8\text{-}40)$$

Front, outer wheel

$$F_{yF,o} = (1-\psi)W\left(\frac{a_y}{\rho_c}\right)\left(\frac{F_{zF,o}}{F_{zF}}\right) \times \left\{\rho_c^2 - [L(1-\psi)-x]^2\right\}^{1/2} \text{ , lb} \qquad (8\text{-}41)$$

Rear, inner wheel

$$F_{yR,i} = \psi W\left(\frac{a_y}{\rho_c}\right)\left(\frac{F_{zR,i}}{F_{zR}}\right) \times \left\{\rho_c^2 - [L(1-\psi)-x]^2\right\}^{1/2} \text{ , lb} \qquad (8\text{-}42)$$

Rear outer wheel

$$F_{yR,o} = \psi W\left(\frac{a_y}{\rho_c}\right)\left(\frac{F_{zR,o}}{F_{zR}}\right) \times \left\{\rho_c^2 - [L(1-\psi)-x]^2\right\}^{1/2} \text{ , lb} \qquad (8\text{-}43)$$

where

$F_{yF,i}$ = side force of inner front wheel, lb
$F_{yF,o}$ = side force of outer front wheel, lb
$F_{yR,i}$ = side force of inner rear wheel, lb
$F_{yR,o}$ = side force of outer rear wheel, lb

7. Compute the tire-road friction coefficient $\mu_{F,i,\,req}$ to prevent wheel lockup on the inner front wheel by

$$\mu_{F,i,req} = \left[\frac{(F_{xF,i})^2 + (m^2 F_{yF,i})^2}{(F_{zF,i})^2}\right]^{1/2} \text{ , d'less} \qquad (8\text{-}44)$$

where

$F_{xF,i}$ = brake force of inner front wheel, lb
m = tire factor, d'less

The tire factor m accounts for the difference in brake and side force produced by the tires. For $m = 1$ the so-called "friction circle" exists. The friction circle assumes that both longitudinal and lateral tire forces are related by the equation of a circle. A surface having a friction coefficient of $\mu = 1.0$ is capable of producing a maximum vehicle deceleration of 1.0g. The maximum lateral acceleration capability of the same vehicle is usually less than 1.0g. Reasons for this are caused by differences in mechanisms involved in producing braking and side forces. A tire-road surface having a braking friction coefficient of 0.9 and thus $a_x\ (max) = 0.9g$ tends to produce only about 0.7g lateral acceleration. The friction circle concept does not describe accurately the relationship between limit braking and turning performance for a given tire-road surface condition. To describe this behavior more accurately, Eq. 8-44 is proposed. The coefficient m is the ratio of a_{x0} to a_{y0} where a_{x0} designates the maximum braking in the absence of any lateral acceleration and thus is equal to the conventional tire-road friction coefficient μ, and a_{y0} designates the maximum lateral acceleration in the absence of any braking. The value of m for most tires and dry road surfaces ranges from 1.1 to 1.2.

8. Compute the braking efficiency by dividing deceleration a_x (step 4) by the required friction coefficient μ_{req}, e.g., for the inner front wheel

$$E_{F,i} = (a_x/\mu_{F,i,req}) \text{ , d'less} \qquad (8\text{-}45)$$

The computations were carried out using the geometrical and brake system data of a Fiat 124. Inspection of the results presented in Fig. 8-12 indicates that the inner rear wheel locks up first, the inner front second, the outer rear third, and the outer front last. A stable turn braking efficiency — limited by the outer rear — of 0.78 can be achieved with a tire-road friction coefficient of 0.8. This value corresponds to a deceleration of about 20 ft/s² at a lateral acceleration of 0.45g. For a tire-road friction coefficient of 0.45 no braking is possible since all friction is used for the turning maneuver.

Close inspection of Fig. 8-12 indicates that the inner wheels provide less braking while turning than the outer wheels. In attempting to modulate the brake forces, it should be remembered that the outer rear wheel is the most important contributor to directional stability during combined braking and turning maneuvers. If the outer rear wheel exceeds its side

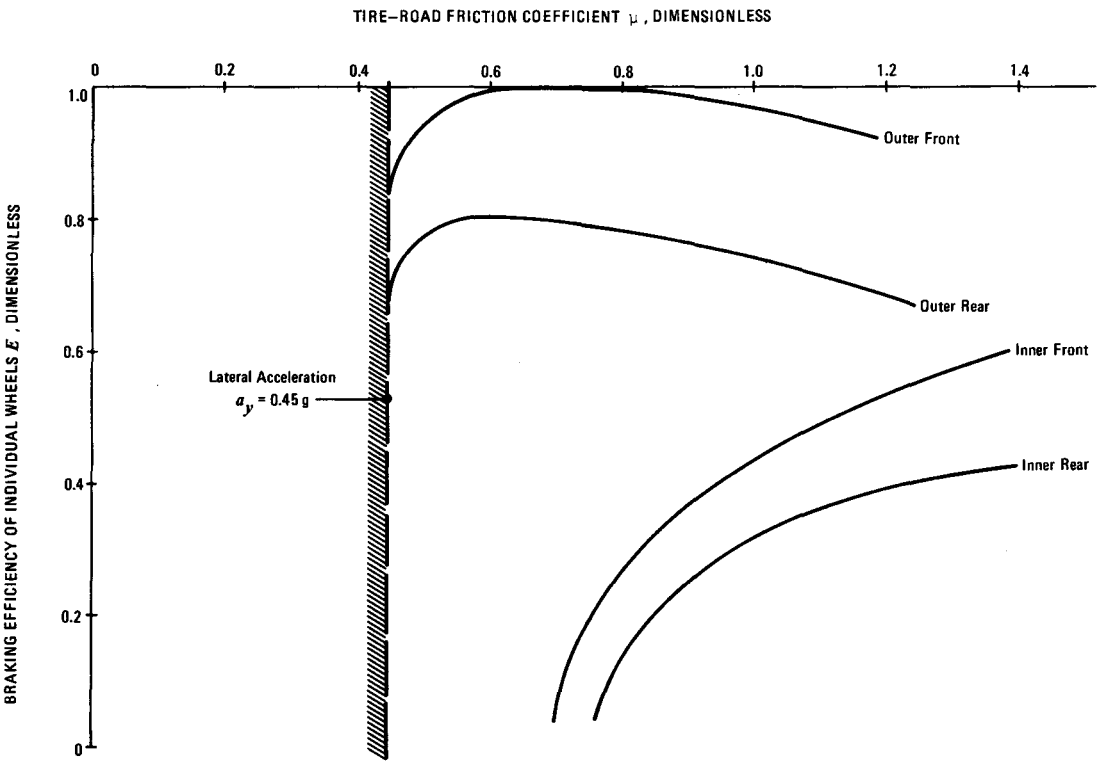

Figure 8-12. Braking Efficiency for Combined Braking and Turning (Fiat 124)

force limit, the vehicle tends to spin about its vertical axis creating a severe accident hazard.

8-1.8 VEHICLE STABILITY CONSIDERATIONS

Accident and vehicle test data, as well as basic engineering analysis, indicate that premature rear wheel lockup may result in violent vehicle instability, most frequently causing the vehicle to spin about its vertical axis. Investigations have shown that typical drivers when faced with an unexpected emergency maneuver apply large pedal forces causing wheel lockup to occur, and futhermore, no attempts are made to counteract the initial yaw motion of the vehicle. The development of vehicle instability due to wheel lockup is illustrated in Fig. 8-13. If it is assumed that the front wheels are still rolling or, have not yet approached sliding conditions and that the rear wheels are already sliding, any disturbance due to road grade or sidewind will produce a lateral component F_y at the vehicle center of gravity. The resultant force F_R, stemming from the inertia force F_x induced by braking and the lateral force F_y, is now oriented along angle α_V. Since the rear wheels are

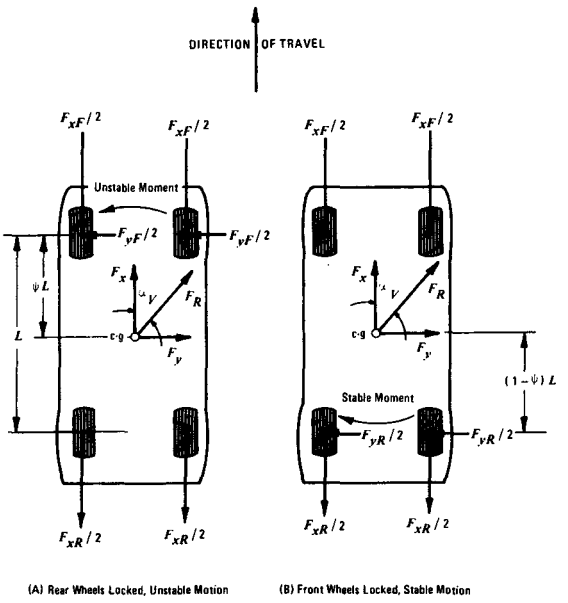

Figure 8-13. Vehicle Behavior With Rear and Front Wheels Locked

sliding, no tire side force can be produced at the rear and, consequently, the side forces developed by the front tires will produce a yawing moment of magnitude $F_{yF}\psi L$. This moment is directed so as to rotate the vehicle about its vertical axis in a manner that increases the initial angle α_V, caused by the external disturbance.

If the front wheels are locked, an identical disturbance will be reacted upon by a stabilizing moment $F_{yR}(1-\psi)L$ produced by the rear wheels. The direction of this moment is such as to rotate the longitudinal axis of the vehicle towards the direction of travel of the center of gravity of the vehicle, thus reducing the initial disturbance angle and rendering the vehicle completely stable.

Different brake forces on the front wheels generally cause a yawing motion of the vehicle about its vertical axis. The front suspension design has a significant effect upon the vehicle behavior when different brake forces are developed by the front wheels. The scrub radius r_s determines the degree to which a front wheel is forced to rotate about its vertical axis in the presence of front wheel brake force unbalance. Scrub radius is the distance between tire-to-road contact point and wheel assembly steering rotation relative to the ground. A positive scrub radius exists when the intersection A of the tire center plane (line 1 in Fig. 8-14) and wheel assembly steering line (line 2 in Fig. 8-14) is located below the road surface. A negative scrub radius exists when the intersection A is located above the road surface. The scrub radius is zero when the intersection A is located at the road surface.

A positive scrub radius has the effect of eliminating play in steering linkages during forward travel and wheel vibrations are reduced. Large values of positive scrub radius force the wheel to rotate towards the higher brake force in the event of front wheel brake unbalance. A negative scrub radius forces the wheel to rotate slightly in the direction of the lower brake force thus producing tire slip angles and tire side forces sufficiently large to hold the vehicle in a stable controlled stop. Inspection of Fig. 8-14 indicates that the space between wheel center line (1) and steering and suspension line (2) is small in the case of a negative scrub radius. It becomes difficult to provide the space sufficiently large to accept the brake rotor and caliper.

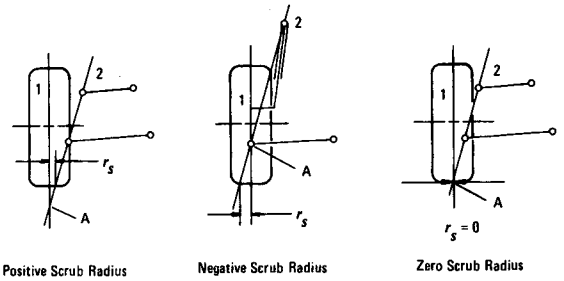

Figure 8-14. Definition of Scrub Radius

8-2 BRAKING OF TANDEM AXLE TRUCK

Tandem axles are used to increase the load carrying capacity of a vehicle and to distribute the load between both axles independent of road surface roughness. Tandem axle suspensions, as illustrated in Fig. 8-15, may be grouped according to basic designs, i.e., walking beam, elliptic leaf spring, and multiple leaf-multiple rod.

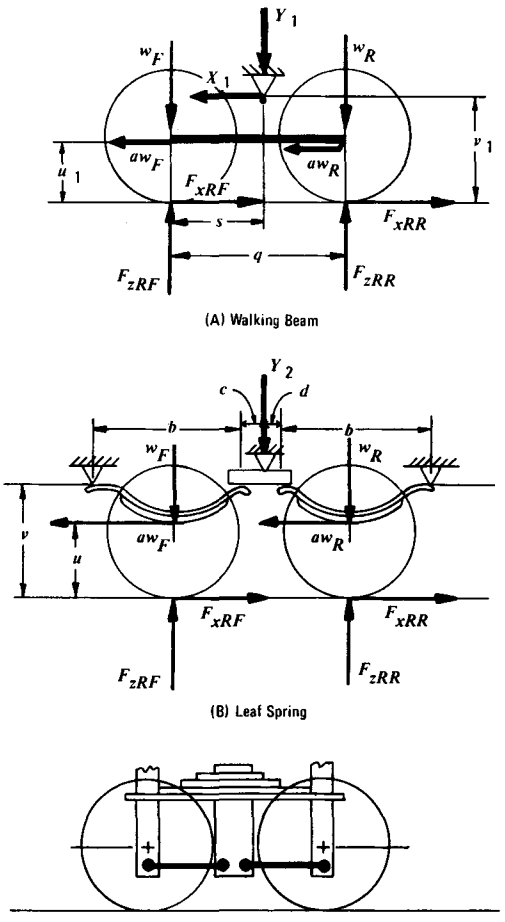

Figure 8-15. Tandem Axle Suspensions

In general, the reaction moments during braking cause a change in load distribution between both axles of the tandem suspension in addition to the dynamic load transfer to the front axle of the vehicle. Since load transfer on a tandem axle may lead to premature wheel lockup during braking, the particular axle suspension design has a pronounced effect upon braking performance. The particular type of tandem axle suspension must be included in the analysis and design of the vehicle brake system.

Many of the physical relationships presented in par. 8-1 may be applied directly to trucks equipped with tandem axle suspensions. For example, Eq. 8-14 will result in a basic brake force distribution between front axle and rear axles that will yield optimum braking performance. The brake force concentrated on the tandem axle must be matched to the dynamic axle loads of both individual axles of the tandem suspension.

The basic principles for the analysis of tandem axle suspensions can be applied to a variety of designs by using the general equations presented in Chapter 7. The equations are especially applicable to computer use. The braking analyses of a walking beam and two elliptic leaf spring suspension are presented in the next paragraphs.

As indicated by the discussion in Chapter 7, only the equations for the axle normal forces need be introduced in the braking analysis. The solution approach is as follows (see Chapter 7). The specified brake line pressure produces a brake torque and consequently a brake force at each braked axle. The appropriate equation for computing brake torque is Eq. 5-2 in which the brake factor relationships presented in Chapter 2 are used; the equation relating to brake system gain is presented in Chapter 5 (Eq. 5-9). The total brake force induces vehicle deceleration and hence an inertia force at the center of gravity. The inertia force produces dynamic load transfer from the rear axle(s) to the front. The tire-road friction coefficient required to prevent wheel slide conditions is computed by the ratio of axle brake force to axle normal force.

8-2.1 WALKING BEAM SUSPENSION

The forces acting on a decelerating tandem axle truck are illustrated in Fig. 8-16. The forces F_{xF}, F_{xRF}, and F_{xRR} which induce braking deceleration are obtained from the axle brake force and are considered to be known functions of brake line pressure. In the case of a hydraulic brake system, the brake forces are computed by Eq. 5-10; in the case of an air brake system the brake forces are computed by Eq. 5-31.

Use the notation from Figs. 8-15(A) and 8-16. The dynamic axle loads during braking on a tandem axle truck with walking beam rear suspension are

Tractor Front:

$$F_{zF} = W_s - Y_1 \text{ , lb} \qquad (8\text{-}46)$$

Tractor tandem forward:

$$F_{zRF} = Y_1 + w_F + w_R - F_{zRR} \text{ , lb} \qquad (8\text{-}47)$$

Tractor tandem rearward:

$$F_{zRR} = [Y_1 s - X_1 v_1 - (w_F + w_R)\, a u_1 + w_R q]/q, \text{ lb} \qquad (8\text{-}48)$$

The horizontal suspension force x_1 is given by

$$X_1 = aW_s - F_{xF} \text{ , lb} \qquad (8\text{-}49)$$

The vertical suspension force Y_1 is given by

$$Y_1 = (W_s \psi L - a W_s \chi L + X_1 v_1)/L \text{ , lb} \qquad (8\text{-}50)$$

where

a = deceleration, g-units
F_{xF} = actual front axle brake force determined by Eq. 5-10 or 5-31, lb
L = wheel base or distance between center of front wheels and center of tandem axle, in.
q = dimension, tandem axle, in.
s = dimension, tandem axle, in.
u_1 = dimension, tandem axle, in.
v_1 = dimension, tandem axle, in.

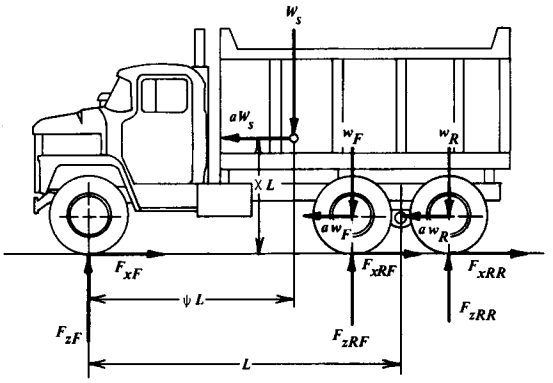

Figure 8-16. Forces Acting on a Tandem Axle Truck

W_s = weight of truck minus weight of tandem axle, lb
w_F = unsprung weight of tandem forward axle, lb
w_R = unsprung weight of tandem rearward axle, lb
χ = center of gravity height divided by wheel base L, d'less
ψ = static tandem axle load divided by vehicle weight, d'less

The forces X_1 and Y_1 are the forces transmitted by the suspension to the frame rails of the truck and are important in designing the suspension attachments.

The computed dynamic axle loads, using the data of a typical vehicle given in Table 8-1, are shown in Fig. 8-17. For a deceleration of 0.5g the axle load F_{zRR} on the tandem rearward axle has decreased to approximately 47% of its static value. The use of the tire-road friction coefficient by this suspension design is illustrated in Fig. 8-18 where the road friction coefficient required for wheels unlocked braking is shown as a function of vehicle deceleration. The braking of the tandem forward axle is close to optimum over a wide range of tire-road friction coefficients, whereas the front axle is largely underbraked and the tandem rearward axle overbraked. For example, on a $\mu = 0.6$ road surface wheels-unlocked decelerations of not greater than approximately 0.35g can be expected. In Fig. 8-19 the same physical relationships are demonstrated in the form of a braking efficiency diagram. The efficiencies on the rearward axle are about 74% and 53% on slippery ($\mu = 0.2$) and dry ($\mu = 0.6$) road surfaces, respectively. The friction utilization diagram in Fig. 8-19 gives a graphical representation of the "quality" of the vehicle/braking system match. Any improvement must come by increasing the brake force on the front axle with a corresponding decrease on the rearward axle of the tandem suspension.

TABLE 8-1
TANDEM AXLE TRUCK DATA

Truck	W_s	= 41,400 lb
	L	= 192 in.
	ψ	= 0.74
	χ	= 0.40
	Tire Radius R	= 20.25 in.
Suspension	w_F	= 2,300 lb
	w_R	= 2,300 lb
	q	= 50 in.
	s	= 24 in.
	u_1	= 20 in.
	v_1	= 14 in.

Brakes	Front Axle	Tandem Forward	Tandem Rearward
Type	Wedge	"S" Cam	"S" Cam
Drum radius r	7.5 in.	8.25 in.	8.25 in.
Brake Chamber Area A_C	20 in.^{2}	30 in.^{2}	30 in.^{2}
Wedge angle α	12 deg	—	—
Slack Adjuster Length l_s	—	5.5 in.	5.5 in.
Brake factor BF	4.3, d'less	2.7, d'less	2.7, d'less
Pushout pressure p_o	5.0 psi	2.5 psi	2.5 psi
Cam radius	—	0.5 in.	0.5 in.
Mechanical efficiency η_m	0.88	0.75	0.75

8-2.2 TWO-ELLIPTIC LEAF SPRING SUSPENSION

Use the notations from Figs. 8-15(B) and 8-16. The dynamic axle loads during braking on a tandem axle truck with two-elliptic leaf spring suspension are

Tractor front:

$$F_{zF} = W_s - Y_2 \left\{ \frac{d[(b/2) - av]}{(c+d)[(b/2) - av]} + \frac{c[(b/2) + av]}{(c+d)[(b/2) - av]} + 1 \right\} + \left[\frac{w_F u}{(b/2) + av} - \frac{w_R u}{(b/2) + av} \right], \text{ lb} \quad (8\text{-}51)$$

Tractor tandem forward:

$$F_{zRF} = \frac{Y_2 bd}{(c+d)[(b/2) + av]} + w_F - \frac{w_F ua}{(b/2) + av}, \text{ lb} \quad (8\text{-}52)$$

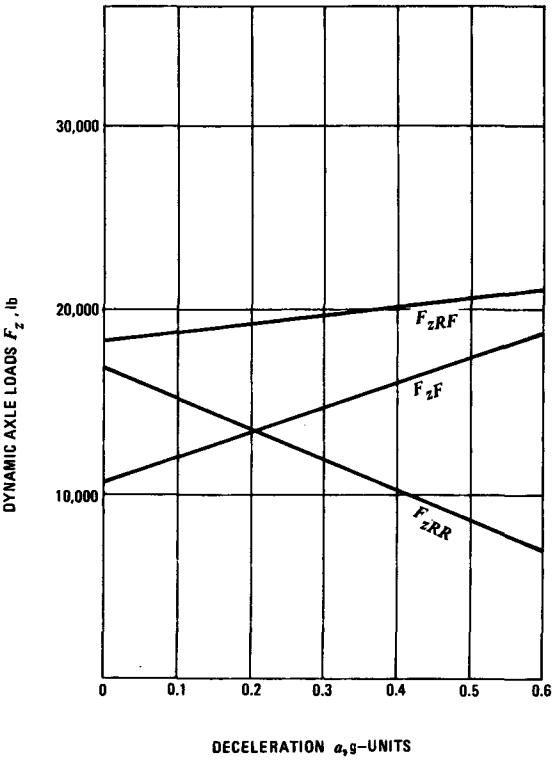

Figure 8-17. Dynamic Axle Loads for a Truck Equipped With Walking Beam Suspension

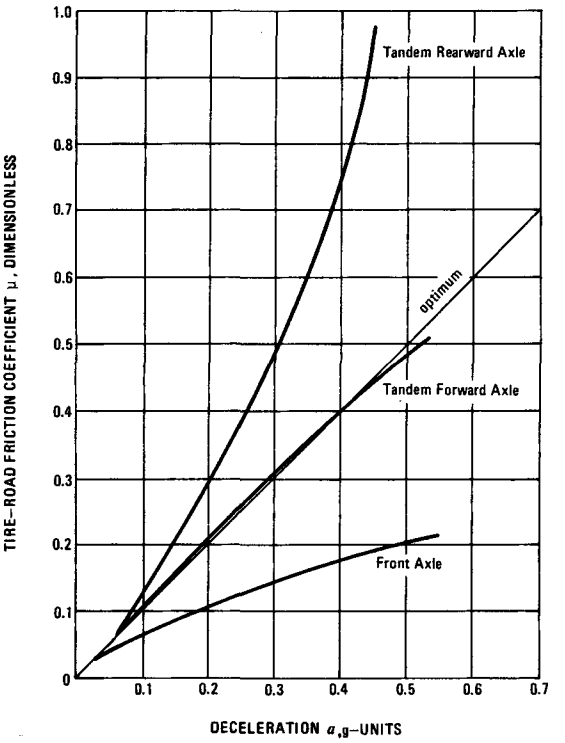

Figure 8-18. Tire-Road Friction Utilization for a Truck Equipped With Walking Beam Suspension

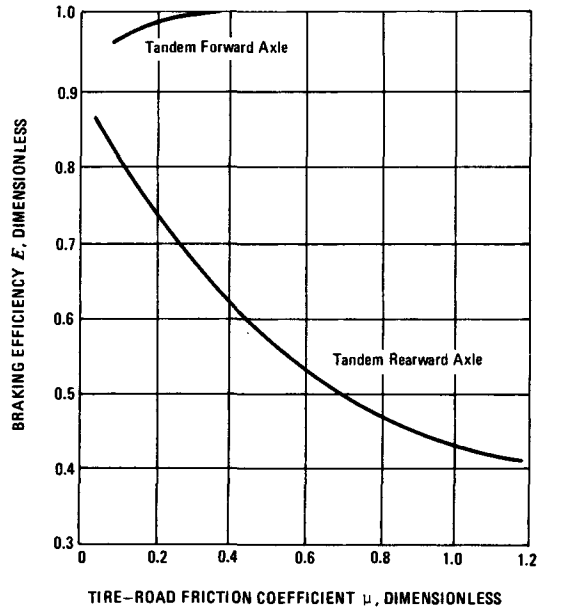

Figure 8-19. Braking Efficiency Diagram for a Truck Equipped With Walking Beam Suspension

Tractor tandem rearward:

$$F_{zRR} = \frac{Y_2 bc}{(c+d)[(b/2) - av]} + w_R + \frac{w_R ua}{(b/2) - av} \text{ , lb} \quad (8\text{-}53)$$

The vertical suspension force Y_2 at equalizing bar is given by

$$Y_2 = [W_s L(\psi - a\chi) + Ga]/H \text{ , lb} \quad (8\text{-}54)$$

where

$$G = \frac{w_F \mu}{(b/2) + av}(L - c - b - va) - \frac{w_R \mu}{(b/2) + av}(L + d + b - va) \text{ , in.-lb} \quad (8\text{-}55)$$

$$H = d/(c+d)\left[\frac{(b/2) - av}{(b/2) + av}\right](L - c - b - va) + c/(c+d)\left[\frac{(b/2) + av}{(b/2) - av}\right](L + d + b - va) + L - va \text{ , in.} \quad (8\text{-}56)$$

where

b = dimension, tandem axle, in.
c = dimension, tandem axle, in.
d = dimension, tandem axle, in.
u = dimension, tandem axle, in.
v = dimension, tandem axle, in.

For the example truck equipped with a two-elliptic leaf spring suspension, the dynamic axle loads are illustrated in Fig. 8-20. In addition to the data for the example truck given in Table 8-1, the tandem axle dimensions are b = 34 in., c = 7 in., d = 7 in., m = 21 in., v = 26.5 in. The dynamic axle load F_{zRF} approaches zero for a deceleration of approximately 0.55g. The friction utilization diagram, Fig. 8-21, indicates that a μ = 0.6 road surface allows wheels unlocked decelerations of only 0.25g. In this case the tandem rearward axle is slightly and the front axle greatly underbraked.

Some improvement in braking performance may be expected when the lever arms of the equalizer carrying the slip ends of the springs are made of unequal length. This change will alter the dynamic axle load distribution as illustrated in Fig. 8-22. The static load distribution also is changed giving the forward

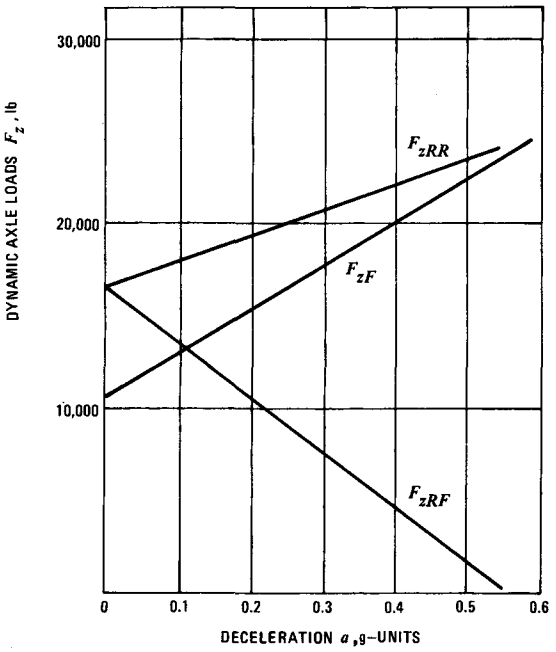

Figure 8-20. Dynamic Axle Loads for a Truck Equipped With Two-Elliptic Leaf Suspension

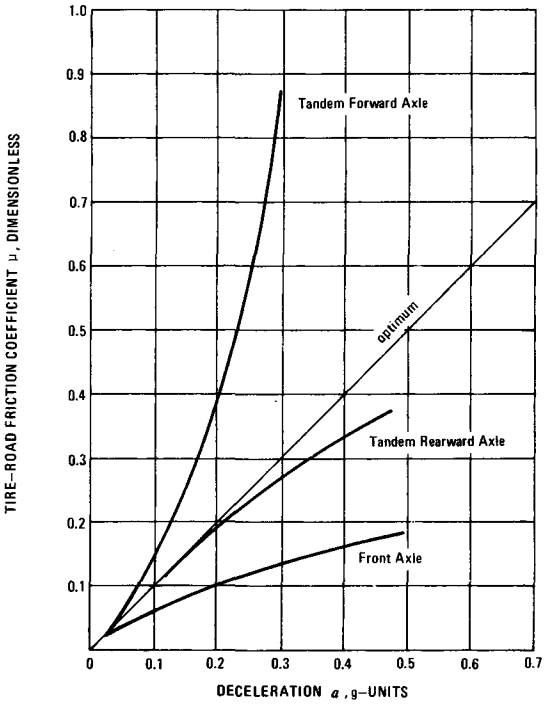

Figure 8-21. Tire-Road Friction Utilization for a Truck Equipped With Two-Elliptic Leaf Suspension

axle initially a higher load. The effects of unequal equalizer lever arms upon friction utilization is illustrated in Fig. 8-23.

An additional improvement can be achieved by changing the tandem axle design to include push rods as illustrated in Fig. 8-24. The improved friction utilization is shown in Fig. 8-25. The wheels unlocked deceleration has increased to 0.38g from an original value of 0.25g for $\mu = 0.6$. In terms of stopping distance from 50 mph, this means that the wheels unlocked stopping distance theoretically can be decreased from 347 ft to 233 ft using the simple design changes discussed so far.

No further major improvement in wheels unlocked deceleration may be expected from design changes on the tandem axle geometry. Any other improvement in braking performance must originate from a better matching of the individual brake forces to the dynamic axle loads. If the condition for an optimum brake force distribution, i.e., Eq. 8-14 is applied to this particular example, a baseline distribution of $\phi = 0.67$ will result. This change can be achieved by increasing the brake chamber on the front axle and correspondingly decreasing it on the rear axles. In this case, the wheels unlocked deceleration will increase to 0.43g. If the brake forces on both the forward and rearward axles of the tandem suspension are matched to the dynamic axle loads on these axles by decreasing the brake chamber size on the forward axle of the tandem suspension and increasing it on the rearward such that a brake force distribution ϕ — front to rear — of 0.33, 0.28, and 0.39 is obtained, the wheels unlocked deceleration will increase to approximately 0.48g on a $\mu = 0.6$ road surface. The friction utilization diagram

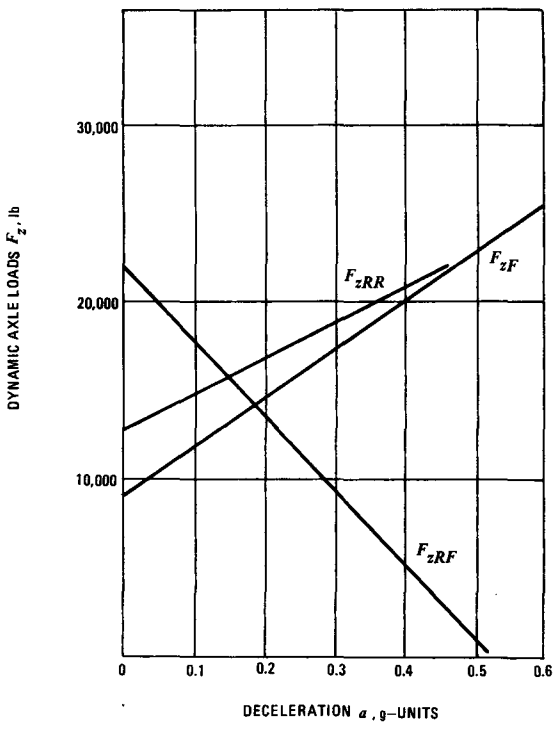

Figure 8-22. Dynamic Axle Loads for Improved Two-Elliptic Leaf Suspension

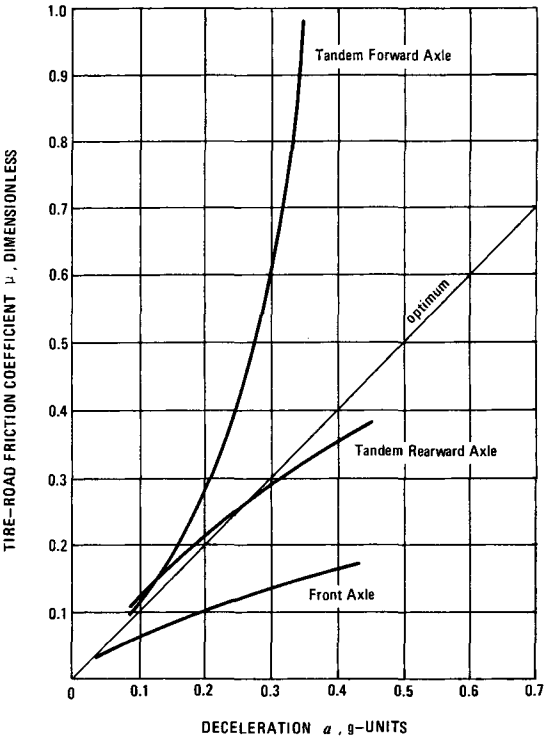

Figure 8-23. Tire-Road Friction Utilization for Improved Two-Elliptic Leaf Suspension

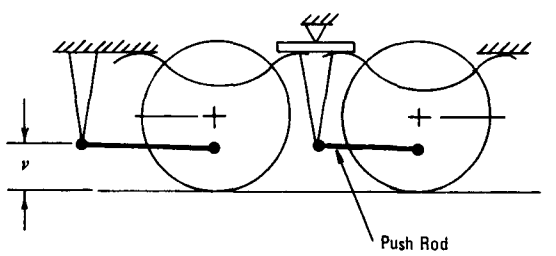

Figure 8-24. Two-Leaf-Two-Rod Suspension

shown in Fig. 8-26 indicates an almost optimum braking for decelerations less than 0.4g. The computed braking efficiencies are always greater than 80% on both slippery ($\mu = 0.2$) and dry ($\mu = 0.6$) road surfaces.

It can be concluded for a two-elliptic leaf spring suspension that considerable braking improvements may be expected through feasible changes on the tandem suspension design and brake chamber sizes. Any further improvement must come by means of load sensitive proportioning devices for each individual axle.

A two-elliptic leaf spring tandem axle suspension that has nearly equal axle loads on the forward and rearward axle during braking is illustrated in Fig. 8-27. In this case, either the two front or rear ends of the elliptic springs are connected by a compensating bar. The dynamic axle loads during braking are given by the following relationships:

Tractor front:

$$F_{zF} = W_s - [b(l_r+1)Y_4 + au_1(w_F+w_R)]/[(b/2)+av_1] \text{ , lb} \quad (8\text{-}57)$$

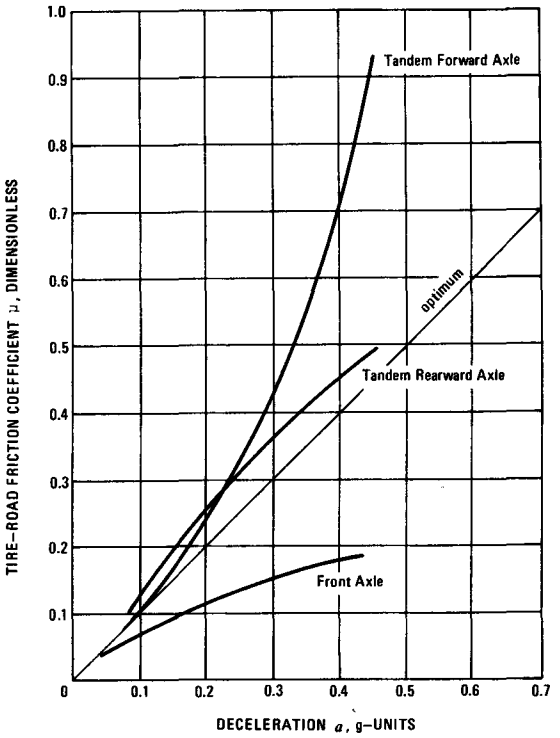

Figure 8-25. Tire-Road Friction Utilization for Truck Equipped With Two-Leaf-Two-Rod Suspension

Tractor tandem forward:

$$F_{zRF} = w_F + [bl_rY_4 - aw_Fu_1] \times [(b/2) + av_1]^{-1} \text{ , lb} \quad (8\text{-}58)$$

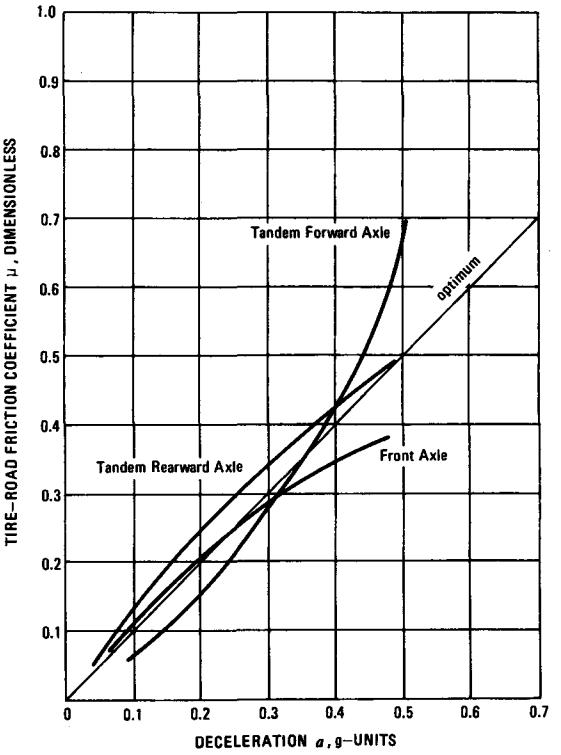

Figure 8-26. Tire-Road Friction Utilization for Optimum Brake Force Distribution

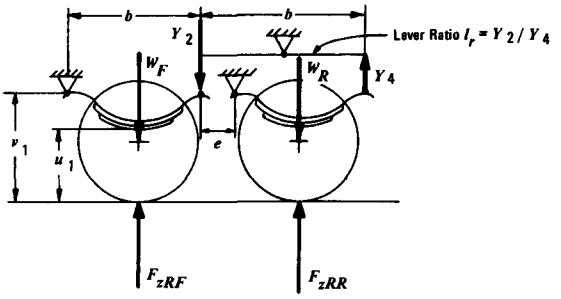

Figure 8-27. Two-Leaf Suspension With Equal Dynamic Axle Loads

Tractor tandem rearward:

$$F_{zRR} = w_R + [bY_4 - aw_R u_1] \times [(b/2) + av_1]^{-1}, \text{ lb} \quad (8\text{-}59)$$

where

$$Y_4 = T/D, \text{ lb} \quad (8\text{-}60)$$

$$T = W_s[\psi L - a\chi L][(b/2) + av_1] + a\{w_F u_1 L + w_R u_1 [L + (b/2) + e]\} - a^2 u_1 v_1 (w_F + w_R), \text{ lb·in.}^2 \quad (8\text{-}61)$$

$$D = ([b/2) + av_1][l_r(L + b) + L + e + 2b] + [(b/2) + av_1][l_r L + L + b + e] - abv_1 (l_r + 1), \text{ in.}^2 \quad (8\text{-}62)$$

e = dimension, tandem axle, in.
$l_r = Y_2/Y_4$ = lever ratio, d'less

For a truck equipped with this tandem axle suspension, the dynamic axle load changes during braking — based on data from Table 8-1 and b = 34 in., e = 7 in., and l_r = 1 — are illustrated in Fig. 8-28. It is evident that the braking dynamics are identical to those of a two-axle truck. Consequently, the physical relationships discussed in par. 8-1 may be applied directly to this case.

8-2.3 AIR SUSPENSION

Air suspensions are designed as pure air suspensions or as hydro-pneumatic suspensions. In the case of the air suspension, elastic bellows are inflated with air to a pressure corresponding to the vehicle loading. One of the advantages of air suspensions is that the ground clearance can be regulated so that it is always at the same level regardless of loading conditions. The wheel position is kept constant even in the case of an independent wheel suspension.

Gas-hydraulic or hydropneumatic suspensions use pressurized gas, often nitrogen, as spring element. The gas is separated from the suspension hydraulic oil by a membrane. As the suspension components move due to relative motion between body and wheel, the hydraulic fluid compresses the gas in the gas chamber. The hydraulic elements of the suspension also serve to dampen body vibrations. In some cases the hydraulic chambers of the left front and left rear wheel as well as the right front and right rear wheel are connected by hydraulic lines in order to reduce pitch vibrations.

Since air suspensions are not widely used, no analyses of particular designs are presented. The axle normal force can be derived by applying principles of mechanics such as the laws of force and moment equilibrium to the suspension system.

8-3 BRAKING OF TRACTOR-SEMITRAILER COMBINATION WITHOUT TANDEM AXLES

An approach similar to that of two-axle vehicles of par. 8-1 will be used in the braking analysis of tractor-semitrailers. Some simplifying assumptions will be made which yield analytical relationships important for the understanding of the factors affecting braking performance.

8-3.1 DYNAMIC AND ACTUAL BRAKE FORCES

For the correct design of a vehicular brake system, it is essential that the optimum brake force distributions among the individual axles are known for the empty and loaded vehicle. For a tractor-semitrailer the analysis is more complicated than for a

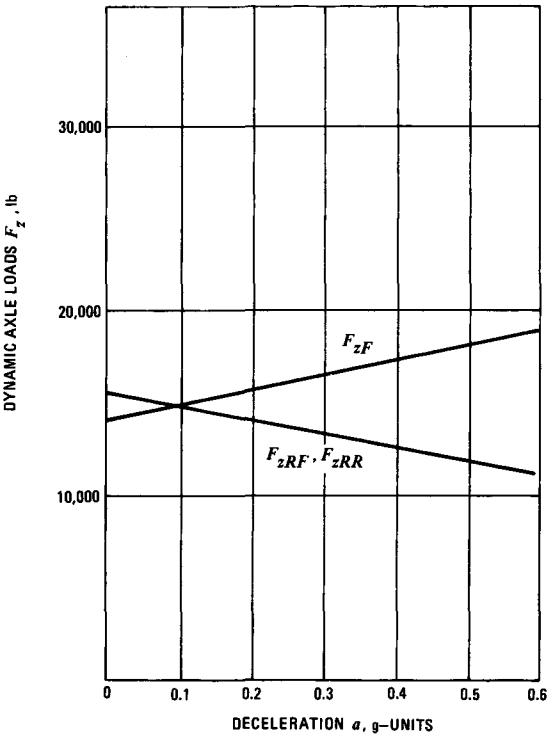

Figure 8-28. Dynamic Axle Loads for a Two-Leaf-Equal-Axle Load Suspension

two-axle vehicle because the summation of the axle loads of the tractor are not equal to the tractor weight. The tractor axle loads are also a function of the loading and braking of the trailer.

In the optimum condition, i.e., $a = \mu$, all road friction available is used, and the brake forces are directly related to the dynamic axle loads. Use the terminology shown in Fig. 8-29. The equations of force and moment equilibrium yield as the normalized dynamic braking forces on each axle (Ref. 9):

Tractor rear axle:

$$\frac{F_{x1R,dyn}}{W_1} = a(\psi_1 - a\chi_1) + a\left(\frac{W_2}{W_1}\right)(y - az_1) \times \left(\frac{1 - \psi_2 + a\chi_2}{1 + az_2}\right), \text{ d'less} \quad (8\text{-}63)$$

Tractor front axle:

$$\frac{F_{x1F,dyn}}{W_1} = a(1-\psi_1+a\chi_1) + a\left(\frac{W_2}{W_1}\right)(1-y+az_1) \times \left(\frac{1-\psi_2 + a\chi_2}{1 + az_2}\right), \text{ d'less} \quad (8\text{-}64)$$

Trailer axle:

$$\frac{F_{x2R,dyn}}{W_2} = a\left[\frac{\psi_2 + a(z_2 - \chi_2)}{1 + az_2}\right], \text{ d'less} \quad (8\text{-}65)$$

where

a = deceleration, g-units
L_1 = tractor wheel base, in.
L_2 = distance between fifth wheel and semitrailer axle, also called semitrailer base, in.
W_1 = tractor weight, lb
W_2 = semitrailer weight, lb
y = horizontal distance between front wheels and fifth wheel divided by tractor wheel base L_1, d'less
z_1 = fifth wheel height divided by tractor wheel base L_1, d'less
z_2 = fifth wheel height divided by semitrailer base L_2, d'less
ψ_1 = empty tractor rear axle load (without semitrailer) divided by tractor weight, d'less
ψ_2 = static semitrailer axle load divided by semitrailer weight, d'less
χ_1 = tractor center of gravity height divided by tractor wheel base L_2, d'less
χ_2 = semitrailer center of gravity height divided by semitrailer base L_2, d'less

If $W_2 = 0$, Eqs. 8-63 and 8-64 may be rearranged to yield the equations applicable to a straight truck.

The dynamic braking forces normalized by dividing by the total weight ($w_1 + w_2$) are shown in Fig. 8-30. Examination of these curves shows that it will be difficult to design a fixed ratio braking system that will produce actual brake forces which come close to the dynamic brake forces for the loaded and unloaded vehicle on both slippery and dry road surfaces.

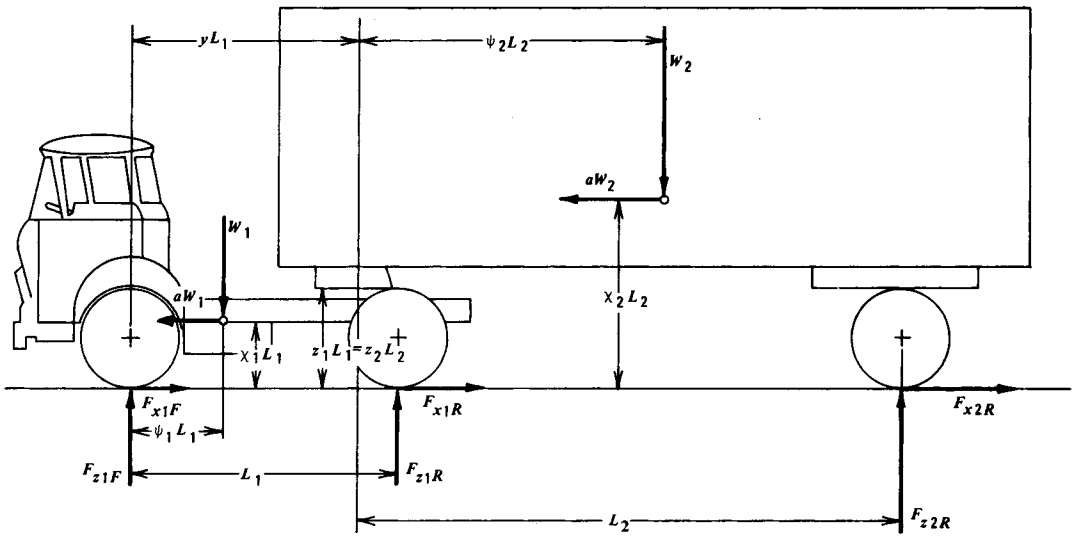

Figure 8-29. Forces Acting on a Decelerating Tractor-Semitrailer

Eqs. 8-63, 8-64, and 8-65 may be rewritten to yield the dynamic tractor brake forces as a function of trailer loading condition and brake force levels.

$$F_{x1F,dyn} = aW_1(1 - \psi_1 + a\chi_1) + (aW_2 + F_{x2R})(1 - y + az_1)\ ,\text{lb} \quad (8\text{-}66)$$

$$F_{x1R,dyn} = aW_1(\psi_1 - a\chi_1) + (aW_2 - F_{x2R})(y - az_1)\ ,\text{lb} \quad (8\text{-}67)$$

where

F_{x2R} = actual brake force of semitrailer axle, lb

The last term of each of the Eqs. 8-66 and 8-67 represents the influences of the trailer on the tractor. A graphical representation of Eqs. 8-66 and 8-67 is shown in Fig. 8-31 for a typical vehicle and several loading conditions.

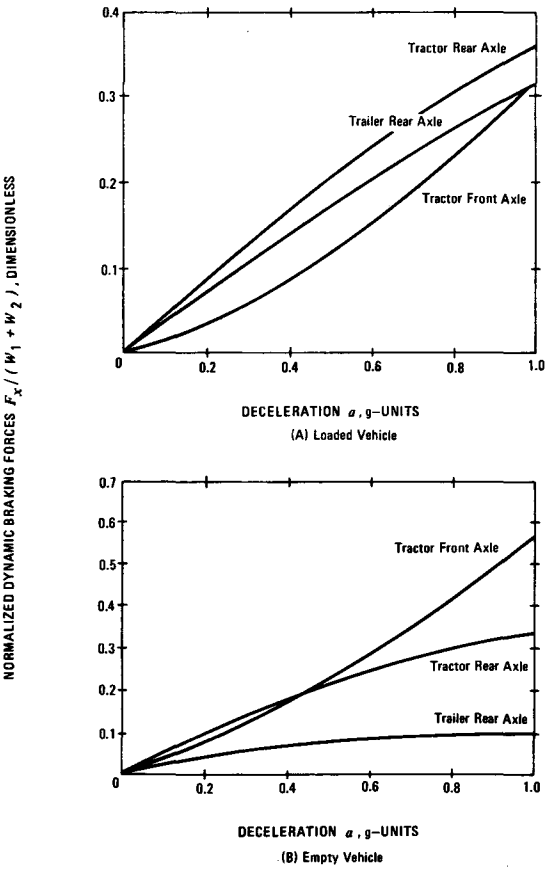

Figure 8-30. Normalized Dynamic Braking Forces of a Tractor-Semitrailer

The actual brake forces generated at each axle are determined by the brake line pressure supplied to the brakes, the brake geometry, the lining friction coefficient, and the effective tire radius. The brake force on each axle, e.g., for air brakes, may be computed from Eq. 5-31 with brake fade as discussed in Chapter 7 included. However, in order to simplify the analysis, an average brake factor is assumed here. A fixed ratio brake force distribution is presented in Fig. 8-31 as a straight line. The location of this line relative to the dynamic braking forces determines the utilization of the given road friction by the brake system and hence the overall braking performance of the vehicle combination.

8-3.2 OPTIMUM BRAKE FORCE DISTRIBUTION

The optimum brake force distribution is that fixed ratio of brake force distribution among the axles which will result in maximum decelerations prior to wheel lockup on dry and wet roadways for both the empty and loaded conditions. In this paragraph an approach, similar to that developed for the two-axle vehicle, that allows the determination of the approximate optimum tractor brake force distribution for a given trailer brake system will be outlined.

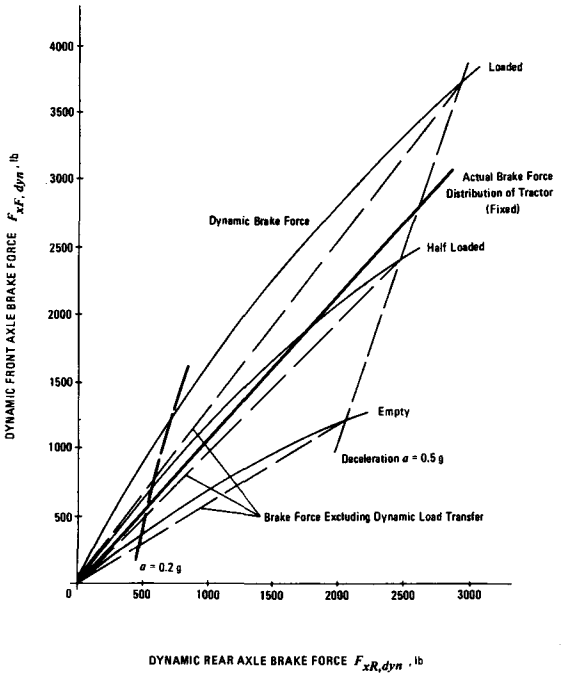

Figure 8-31. Dynamic Braking Forces of the Tractor of a Tractor-Semitrailer Combination

The tire-road friction coefficient required to prevent wheel lockup on a particular axle during braking can be computed by dividing the axle brake force by the instantaneous axle load. To simplify the analysis, the influence of dynamic weight transfer during braking is neglected; this is equivalent to replacing the curves of dynamic forces in Fig. 8-31 by straight lines — indicated by the broken lines. This procedure will yield a small error; however, the influence of the braking forces through the fifth wheel connection is retained. It should be noted that this simplification is introduced only to aririve at simple relationships considered important in designing a brake system for a combination vehicle. The design parameters hereby obtained subsequently should be checked and evaluated by means of the braking performance calculation program outlined in Chapter 7.

The tire-road friction coefficient μ_{1F} required to prevent wheel lockup on the tractor front axle is

$$\mu_{1F} = \frac{F_{x1F}}{F_{z1F}} = \frac{\phi_{1F} aW}{F_{z1F}} \text{ , d'less} \qquad (8\text{-}68)$$

where

$$\phi_{1F} = \frac{F_{x1F}}{F_{x1F} + F_{x1R} + F_{x2R}} \text{ , d'less}$$

F_{x1F} = actual brake force of tractor front axle, lb
F_{x1R} = actual brake force of tractor rear axle, lb
F_{x2R} = actual brake force of semitrailer axle, lb
W = total combination weight, lb

The brake force for each axle is determined from Eq. 5-10 or 5-31 with an average lining friction coefficient (values given in par. 14-2) used to compute the brake factor. The effect of pushout pressures on the brake force distribution is neglected in this analysis.

The approximate normalized axle loads of the combination can be computed and are

Tractor front axle:

$$\frac{F_{z1F,ap}}{W_1} = 1 - \psi_1 + \left(\frac{W_2}{W_1}\right)(1-\psi_2)(1-y) + \left(\frac{F_{x1F}+F_{x1R}}{W}\right)\left[\chi_1 + \left(\frac{W_2}{W_1}\right)z_1 + \left(\frac{W_2}{W_1}\right)(\chi_2 - z_2)(1-y)\right] + \left(\frac{F_{x2R}}{W}\right)\left[z_2(1-y) - (z_1 - \chi_1) + \left(\frac{W_2}{W_1}\right)\chi_2(1-y)\right], \text{ d'less} \qquad (8\text{-}69)$$

Tractor rear axle:

$$\frac{F_{z1R,ap}}{W_1} = \psi_1 + \left(\frac{W_2}{W_1}\right)(1-\psi_2)y - \left(\frac{F_{x1F}+F_{x1R}}{W}\right)\left[\chi_1 + \left(\frac{W_2}{W_1}\right)z_1 - \left(\frac{W_2}{W_1}\right)(\chi_2 - z_2)y\right] + \left(\frac{F_{x2R}}{W}\right)\left[z_2 y + z_1 - \chi_1 + \left(\frac{W_2}{W_1}\right)\chi_2 y\right], \text{ d'less} \qquad (8\text{-}70)$$

Trailer axle:

$$\frac{F_{z2R,ap}}{W_2} = \psi_2 - \left(\frac{F_{x1F}+F_{x1R}}{W}\right)(\chi_2 - z_2) - \left(\frac{F_{x2R}}{W}\right)\left[\chi_2 + \left(\frac{W_1}{W_2}\right)z_2\right] \text{ , d'less} \qquad (8\text{-}71)$$

where

F_{x1F} = actual brake force of tractor front axle, lb
F_{x1R} = actual brake force of tractor rear axle, lb
F_{x2R} = actual brake force of semitrailer axle, lb

Eqs. 8-69, 8-70, and 8-71 may be rewritten to be a function of the trailer axle brake force F_{x2R} only by using the relationship $F_{x1F} + F_{x1R} + F_{x2R} = aW$. The following expressions are obtained for the approximate axle loads on the tractor-semitrailer combination.

Tractor front axle:

$$F_{z1F,ap} = W_1(1-\psi_1) + W_2(1-\psi_2)(1-y) + F_{x2R}(z_2 - z_2 y - z_1) + a[W_1\chi_1 + W_2 z_1 - W_2(\chi_2 - z_2)(\chi_1 - y)], \text{ lb} \qquad (8\text{-}72)$$

Tractor rear axle:

$$F_{z1R,ap} = W_1\psi_1 + W_2(1-\psi_2)y + F_{x2R}(z_2 y + z_1) - a[W_1\chi_1 + W_2 z_1 - W_2(\chi_2 - z_2)y], \text{ lb} \qquad (8\text{-}73)$$

Trailer axle:

$$F_{z2R,ap} = W_2\psi_2 - F_{x2R}z_2 - aW_2(\chi_2 - z_2) \text{ , lb} \quad (8\text{-}74)$$

With the expressions for the approximate axle loads substituted into the friction relationship, Eq. 8-68, the decelerations achievable on an axle prior to wheel lockup for a particular tire-road friction coefficient, vehicle geometry, and trailer brake force level may now be computed by the following expressions.

Tractor front axle:

$$a_{1F} = \frac{\mu_{1F}[\lambda(1-\psi_1) + (1-\lambda)(1-\psi_2)(1-y) + \rho(z_2 - z_2 y - z_1)]}{\phi_{1F} - \mu_{1F}[\lambda\chi_1 + (1-\lambda)z_1 + (1-\lambda)(\chi_2 - z_2)(1-y)]}, \quad \text{d'less} \quad (8\text{-}75)$$

Tractor rear axle:

$$a_{1R} = \frac{\mu_{1R}[\lambda\psi_1 + (1-\lambda)(1-\psi_2)y + \rho(z_2 y + z_1)]}{\phi_{1R} + \mu_{1R}[\lambda\chi_1 + (1-\lambda)z_1 - (1-\lambda)(\chi_2 + z_2)y]}, \quad \text{d'less} \quad (8\text{-}76)$$

Trailer axle:

$$a_{2R} = \frac{\mu_{2R}[(1-\lambda)\psi_2 - \rho z_2]}{\phi_{2R} + \mu_{2R}(1-\lambda)(\chi_2 - z_2)}, \quad \text{d'less} \quad (8\text{-}77)$$

where

$\lambda = W_1/W$, d'less
μ_{1F} = tire-road friction coefficient on tractor front wheels, d'less
μ_{1R} = tire-road friction coefficient on tractor rear wheels, d'less
μ_{2R} = tire-road friction coefficient of trailer wheels, d'less
$\rho = F_{x2R}/W$, d'less
$\phi_{1F} = F_{x1F}/F_{x,total}$, d'less
$\phi_{1R} = F_{x1R}/F_{x,total}$, d'less
$\phi_{2R} = F_{x2R}/F_{x,total}$, d'less

For $\rho = 0$ and $\lambda = 1$, i.e., no trailer is connected to the tractor, Eqs. 8-75, 8-76, and 8-77 reduce to those for a two-axle truck.

A graphical representation of Eqs. 8-75, 8-76, and 8-77 is shown in Figs. 8-32 and 8-33 for the loaded and empty driving condition, respectively. In this example the brake forces were distributed to match the dynamic brake forces existing during the loaded driving condition. Consequently, for the empty vehicle the trailer axle is always overbraked compared to the two other axles. For example (Fig. 8-33) a deceleration of 0.4g requires a coefficient of friction μ = 0.6 on the trailer axle to prevent wheel lockup. The

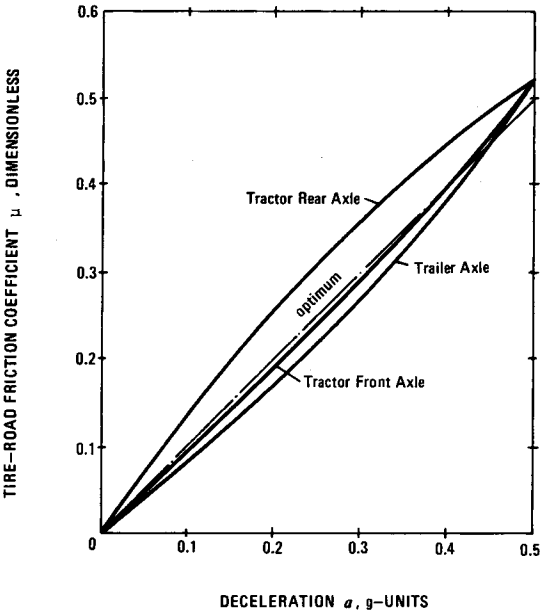

Figure 8-32. Tire-Road Friction Utilization for a Loaded Tractor-Semitrailer

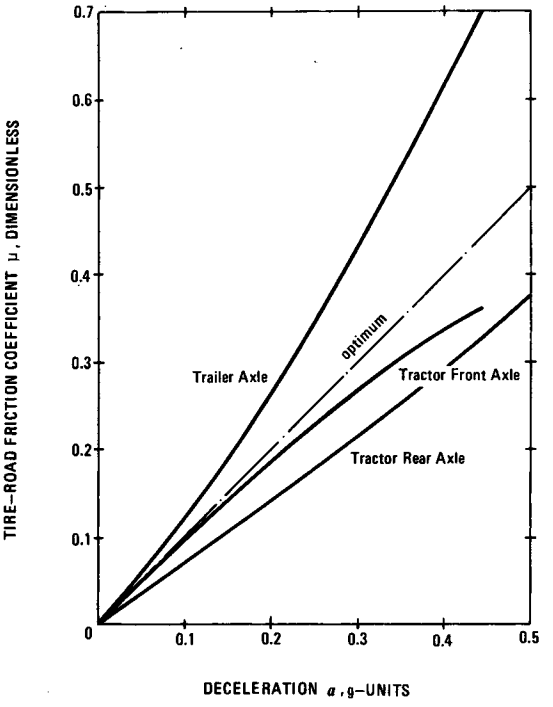

Figure 8-33. Tire-Road Friction Utilization for an Empty Tractor-Semitrailer

required friction coefficients for the loaded condition shown in Fig. 8-32 indicate an almost optimum braking of the vehicle with the rear tractor axle slightly overbraked.

Eqs. 8-75 and 8-76 may be used to develop limiting relationships on the relative rear axle brake force of the tractor. With the braking efficiency $E = a/\mu$ this results in the expression (Ref. 5)

$$\phi_{1R} = \frac{A}{E_{min}} - (\mu_{1R})B \text{ , d'less} \qquad (8\text{-}78)$$

where

$$A = \lambda\psi_1 + (1-\lambda)(1-\psi_2)y + \rho(z_2 y + z_1) \text{ , d'less} \qquad (8\text{-}79)$$

$$B = \lambda\chi_1 + (1-\lambda)z_1 - (1-\lambda)(\chi_2 - z_2)y \text{ , d'less} \qquad (8\text{-}80)$$

E_{min} = minimum braking efficiency to be achieved by vehicle, d'less

The relative brake force ϕ_{2R} on the trailer axle can be computed from $\phi_{2R} = \rho/a$ where a is equal to the deceleration of the combination in g-units. The relative front axle brake force is determined from $1 = \phi_{1F} + \phi_{1R} + \phi_{2R}$. For $\rho = 0$ and $\lambda = 1$, i.e., no trailer is connected to the tractor, Eq. 8-78 reduces to that for a two-axle vehicle.

The relative tractor rear axle brake force ϕ_{1R} for most cases should not exceed 0.50. A relatively small value of ϕ_{1R} and hence moderate utilization of the friction in longitudinal direction on the tractor rear axle means that still a considerable lateral tire force is available for directional stability. This is of importance since the danger of jackknifing is related directly to the lateral friction forces available at the tractor rear axle.

The decelerations achievable with a fixed brake force distribution on slippery ($\mu = 0.2$) and dry ($\mu = 0.8$) road surfaces must be checked with Eqs. 8-75, 8-76, and 8-77 for the empty and loaded driving condition. If the results indicate too low a performance for one loading condition, the distribution must be altered until an acceptable value between empty and loaded brake force distribution has been found.

For a typical tractor-semitrailer geometry with the vehicle data given in Table 8-2, the optimum brake force distribution was determined for $\rho = 0.23$ — i.e., a brake force of 23% of the total vehicle weight is acting on the trailer axle at maximum reservoir pressure — to be equal to $\phi_{1F} = 0.17$, $\phi_{1R} = 0.47$, and $\phi_{2R} = 0.36$ for a braking efficiency of 75%. When checked with Eqs. 8-75, 8-76, and 8-78, this brake force distribution yielded braking efficiencies of 75% for the empty and loaded vehicle on both slippery ($\mu = 0.2$) and dry ($\mu = 0.8$) road surfaces. This theoretical result is supported by actual road tests of a combination vehicle (Ref. 5). The brake force distribution originally was equal to 0.12, 0.44, 0.44 — front to rear — resulting in trailer axle lockup for the empty driving condition at approximately 0.53g indicating a braking efficiency of about 60%. No tractor axle lockup was observed for the loaded case. Changing the basic brake force distribution by means of Eq. 8-78 to 0.17, 0.44, and 0.39 — front to rear — increased the braking efficiency to approximately 70%.

8-3.3 STRAIGHT-LINE VERSUS CURVED PATH BRAKING PERFORMANCE

An analysis similar to that of solid frame vehicles can be developed which includes the effects of lateral acceleration on the braking efficiency and optimum brake force distribution. The resulting equations are lengthy and are normally evaluated only by means of computer programs (Refs. 10 and 11). Lateral acceleration values of trucks and truck-trailer combinations generally are limited to values significantly lower than those achievable by passenger cars. Tests have shown that proper brake system designs in terms of a brake force distribution causing a sequence of tractor front, trailer, and tractor rear axle lockup will yield minimum stopping distances for both straight and curved braking. A proper brake system design requires consideration of brake torque and wheel lockup sequence. For purposes of "stretching" the combination, the trailer brakes should be applied prior to the tractor brakes. In terms of wheel

TABLE 8-2
VEHICLE DATA FOR TRACTOR-SEMITRAILER CALCULATIONS

	Empty	Loaded
ψ_1	0.52	0.52
ψ_2	0.738	0.51
χ_1	0.22	0.22
χ_2	0.12	0.26
λ	0.6	0.21
ρ	0.23	0.23

($z_1 = 0.193, z_2 = 0.12; y = 0.93$)

lockup, stability requires that the tractor front axle lock first, the trailer axle second, and the tractor rear axle last.

8-3.4 VEHICLE STABILITY CONSIDERATIONS

Test results have shown that three different types of loss of control of a tractor-semitrailer combination may occur. In the event of front wheel lockup, steering control is lost and the vehicle continues in a straight and stable path. Steering control can be regained by simply lowering the pedal force sufficiently to release the front brakes. In the event of trailer wheel lockup trailer swing occurs (Refs. 12, 13,14,15, and 16). This instability can be overcome by releasing the brakes and stretching the combination by slight acceleration. The reason for trailer swing occurring is the same that causes a passenger car to spin around its vertical axis due to loss of side force on the rear wheels in the event of rear wheel lockup. Violent instability, including jackknifing, occurs when the tractor rear wheels lock prior to any others. In this case the side forces at the tractor rear wheels are nearly zero and in the event of braking in a turn the side forces on the front tires tend to support the jackknifing action by keeping the tractor front in the intended turn, whereas the tractor rear axle slides sideways causing the tractor to yaw violently.

Antijackknifing devices have been proposed that would affect the friction at the fifth wheel location (Refs. 17 and 18). Some extreme devices have been proposed that would lock the tractor rigidly in position relative to the trailer in the event of jackknifing. Such a device could change the articulated vehicle to that of a rigid system without steerability.

Any device affecting the fifth wheel friction would shift the side force requirements lost by the locked tractor rear axle to the front and trailer wheels (Ref. 19). This change may cause tire side force saturation at those wheels. In addition, the resulting combination vehicle motion may be more severe than the jackknifing alone.

Since the causes of jackknifing are loss of tire-side force at the tractor-rear wheels, a proper brake force distribution to ensure front wheel lockup first, then trailer wheels, and last tractor rear wheels appears to be a proper engineering approach for avoiding jackknifing (Refs. 20, 21, 22, and 23). Furthermore, with the advances made in antiskid controls for heavy vehicles, tractor rear and trailer wheel lockup is prevented for all loading and road conditions as well as driver skill levels.

8-4 BRAKING OF TRACTOR-SEMITRAILER COMBINATIONS EQUIPPED WITH TANDEM AXLES

First, only the trailer with a tandem axle suspension will be connected to a two-axle tractor. Later, both tractor and trailer will be equipped with tandem axle suspensions.

8-4.1 TWO-AXLE TRACTOR COUPLED TO A TRAILER EQUIPPED WITH A TWO-ELLIPTIC LEAF SPRING SUSPENSION

The forces acting on a decelerating tractor-semitrailer are shown in Fig. 8-34. Use the terminology of Fig. 8-34. The equilibrium equations applied to the free body of the tractor, sprung semitrailer, forward trailer axle, and rearward trailer axle yield a set of equations that may be solved for the individual axle loads. When aerodynamic drag, rotational energies, and rolling resistance are neglected, the equilibrium equations are:

Tractor:

$$Xz_1L_1 + Y(1-y)L_1 - F_{z1F}L_1 + W_1(1-\psi_1)L_1 + W_1a\chi_1L_1 = 0 \text{ , lb·in.} \quad (8\text{-}81)$$

$$F_{z1F} + F_{z1R} - W_1 - Y = 0 \text{ , lb} \quad (8\text{-}82)$$

Sprung semitrailer:

$$W_{s2}a - X - X_1 - X_3 = 0 \text{ , lb} \quad (8\text{-}83)$$

$$Y + Y_1 + Y_2 + Y_3 - W_{s2} = 0 \text{ , lb} \quad (8\text{-}84)$$

$$W_{s2}a(\chi_2 - z_2)L_2 + (X_1+X_3)(z_1L_1 - v) + Y_1(L_2 - c - b) + Y_2L_2 + Y_3(L_2 + d + b) - W_{s2}\psi_2L_2 = 0 \text{ , lb·in.} \quad (8\text{-}85)$$

Trailer forward axle:

$$X_1 - F_{x2RF} + w_Fa = 0 \text{ , lb} \quad (8\text{-}86)$$

$$F_{z2RF} - Y_1 - Y_2\,d/(c+d) - w_F = 0 \text{ , lb} \quad (8\text{-}87)$$

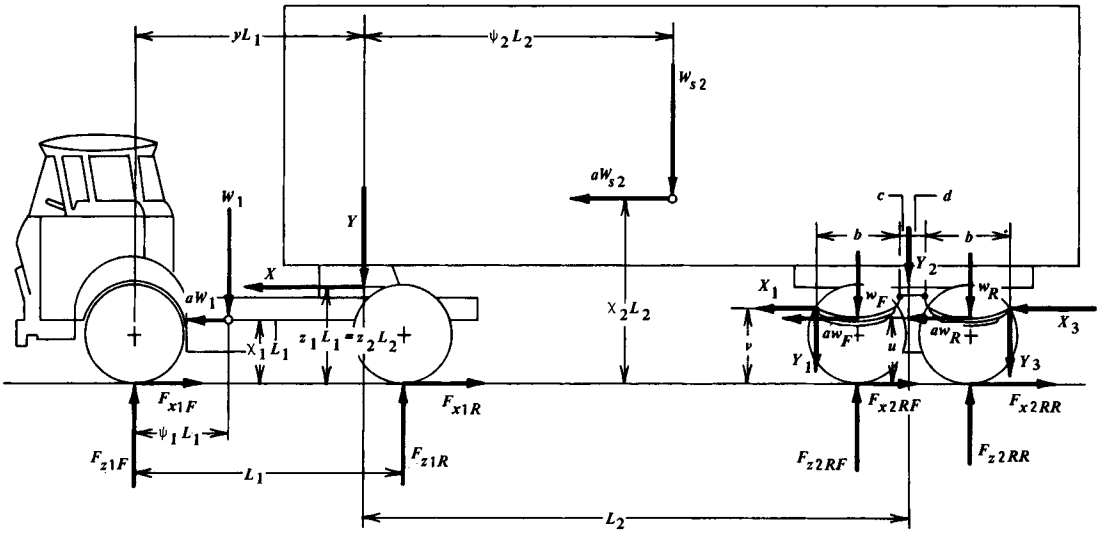

Figure 8-34. Forces Acting on a Tractor-Semitrailer Equipped With Two-Leaf Suspension

$$X_1 v + [Y_1 - Y_2\, d/(c+d)]\,(b/2) + aw_F\mu = 0 \text{ , lb·in.} \quad (8\text{-}88)$$

Trailer rearward axle:

$$X_3 - F_{x2RR} + aw_R = 0 \text{ , lb} \quad (8\text{-}89)$$

$$F_{z2RR} - Y_3 - Y_2 c/(c+d) - w_R = 0 \text{ , lb} \quad (8\text{-}90)$$

$$X_3 v + [Y_2 c/(c+d) - Y_3]\,(b/2) + aw_R\mu = 0 \text{ , lb·in} \quad (8\text{-}91)$$

where

F_{x2RF} = actual brake force of trailer tandem forward axle, lb
F_{x2RR} = actual brake force of trailer tandem rearward axle, lb
F_{z2RF} = normal force of trailer tandem forward axle, lb
F_{z2RR} = normal force of trailer tandem rearward axle, lb
W_{s2} = semitrailer weight minus weight of tandem axle, lb
X = horizontal fifth wheel force, lb
X_1 = horizontal suspension force, forward axle, lb
X_3 = horizontal suspension force, rearward axle, lb
Y = vertical fifth wheel force, lb
Y_1 = vertical suspension force, forward axle, lb
Y_2 = vertical suspension frame force, lb
Y_3 = vertical suspension force, rearward axle, lb
a = deceleration, g-units
b = dimension, tandem axle, in.
c = dimension, tandem axle, in.
d = dimension, tandem axle, in.
u = dimension, tandem axle, in.
v = dimension, tandem axle, in.

This system of eleven equations contains thirteen unknowns. Two additional equations can be obtained when optimum braking conditions are considered in which the deceleration in g-units equals the tire-road friction coefficient, i.e., $a = \mu$. Then the braking forces F_{x2RF} and F_{x2RR} are replaced by aF_{z2RF} and aF_{z2RR} and a system of eleven equations with eleven unknowns is obtained which can be solved by successive substitution.

The individual axle loads are:

Tractor front axle:

$$F_{z1F} = W_1(1-\psi_1 + a\chi_1) + Y(1-y + az_1) \text{ , lb} \quad (8\text{-}92)$$

where

$X = aY$, lb

Tractor rear axle:

$$F_{z1R} = W_1(\psi_1 - a\chi_1) + Y(y - az_1) \text{ , lb} \quad (8\text{-}93)$$

Trailer forward axle:

$$F_{z2RF} = \frac{Y_2 bd}{(c+d)[(b/2)+av]} + w_F - \frac{w_F ua}{(b/2)+av}, \text{ lb} \quad (8\text{-}94)$$

Trailer rearward axle:

$$F_{z2RR} = \frac{Y_2 bc}{(c+d)[(b/2)-av]} + w_R + \frac{w_R ua}{(b/2)-av}, \text{ lb} \quad (8\text{-}95)$$

The vertical loads on the kingpin of the fifth wheel and on the tandem suspension are given by

$$Y = W_{s2} - Y_2\left\{\frac{d[(b/2)-av]}{(c+d)[[b/2]+av]} + \frac{c[(b/2)+av)}{(c+d)[(b/2)-av)]} + 1\right\} + \left[\frac{w_F\mu}{(b/2)+av} - \frac{w_R\mu}{(b/2)-av}\right]a, \text{ lb} \quad (8\text{-}96)$$

$$Y_2 = \frac{W_{s2} L_2 [\psi_2 - a(\chi_2 - z_2)] + G_1 a}{H_1}, \text{ lb} \quad (8\text{-}97)$$

where

$$G_1 = \frac{w_F u}{(b/2)+av}[(z_1 L_1 - v)a + L_2 - c - b] - \frac{w_R u}{(b/2)-av}[(z_1 L_1 - v)a + L_2 + d + b], \text{ lb·in.} \quad (8\text{-}98)$$

$$H_1 = \frac{d}{c+d}[(z_1 L_1 - v)a + L_2 - c - b] \times \left[\frac{(b/2)-av}{(b/2)+av}\right] + \frac{c}{c+d}[(z_1 L_1 - v)a + L_2 + d + b] \times \left[\frac{(b/2)+av}{(b/2)-av}\right] + (z_1 L_1 - v)a + L_2, \text{ in.} \quad (8\text{-}99)$$

Introduction of Eqs. 8-92 through 8-99 in the braking performance calculation program resulted in the dynamic axle load diagram and the braking performance diagram presented in Figs. 8-35 and 8-36, respectively.

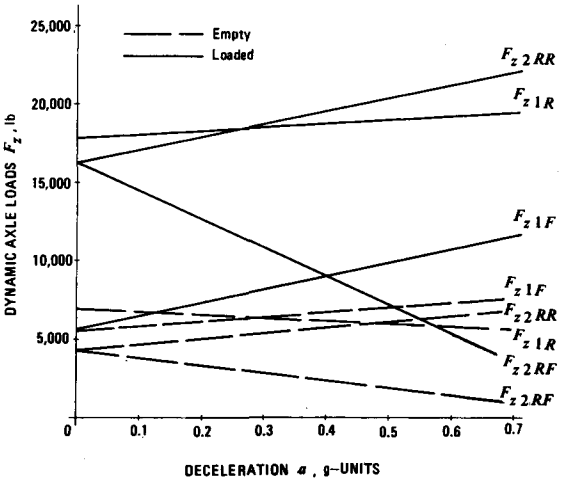

Figure 8-35. Dynamic Axle Loads for a Tractor-Semitrailer Combination

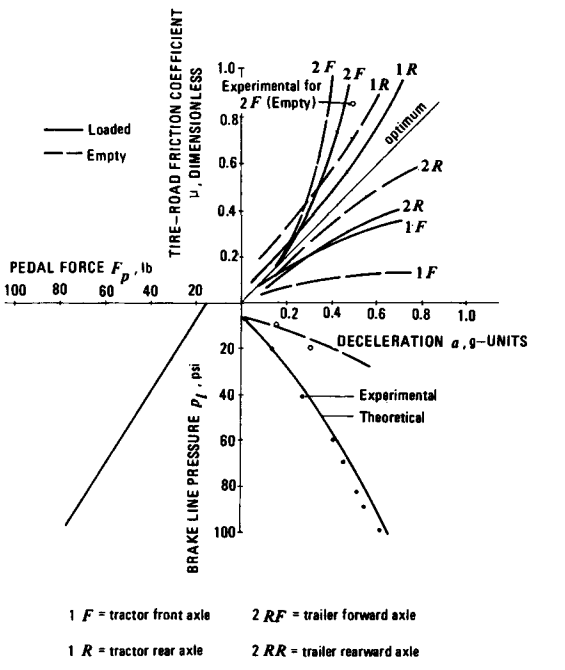

Figure 8-36. Braking Performance Diagram for a Tractor-Semitrailer Combination

8-4.2 TWO-AXLE TRACTOR COUPLED TO A TRAILER EQUIPPED WITH A WALKING BEAM SUSPENSION

Use the terminology shown in Fig. 8-37. The application of the equilibrium equations to the combination vehicle results in the following dynamic axle loads:

Tractor front axle:

$$F_{z1F} = W_1(1 - \chi_1 + a\chi_1) + Y(1 - y + az_1) \text{ , lb} \quad (8\text{-}100)$$

Tractor rear axle:

$$F_{z1R} = W_1 + Y - F_{z1F} \text{ , lb} \quad (8\text{-}101)$$

Trailer rearward axle:

$$F_{z2RR} = [Y_2 s_2 + w_R q_2 - au_2 (w_F + w_R) - X_2 v_2]/q_2 \text{ , lb} \quad (8\text{-}102)$$

Trailer forward axle:

$$F_{z2RF} = Y_2 + w_F + w_R - F_{z2RR} \text{ , lb} \quad (8\text{-}103)$$

where

$$X_2 = F_{x2RF} + F_{x2RR} - a(w_F + w_R) \text{ , lb} \quad (8\text{-}104)$$

$$X = W_{s2}\, a - X_2 \text{ , lb} \quad (8\text{-}105)$$

$$Y_2 = [W_{s2}\psi_2 L_2 - W_{s2}a(\chi_2 - z_2)L_2 - X_2 z_1 L_1 v_2]/L_2 \text{ , lb} \quad (8\text{-}106)$$

$$Y = W_{s2} - Y_2 \text{ , lb} \quad (8\text{-}107)$$

F_{x2RF} = actual brake force of semitrailer tandem forward axle, lb
F_{x2RR} = actual brake force of semitrailer tandem rearward axle, lb
q_2 = dimension, tandem axle, in.
s_2 = dimension, tandem axle, in.
u_2 = dimension, tandem axle, in.
v_2 = dimension, tandem axle, in.
x_2 = horizontal suspension force, lb

8-4.3 THREE-AXLE TRACTOR EQUIPPED WITH A WALKING BEAM SUSPENSION COUPLED TO A TRAILER EQUIPPED WITH A TWO-ELLIPTIC LEAF SPRING TANDEM SUSPENSION

Use the terminology shown in Fig. 8-38. The individual dynamic axle loads are

Tractor front axle:

$$F_{z1F} = W_{s1} + Y - Y_4 \text{ , lb} \quad (8\text{-}108)$$

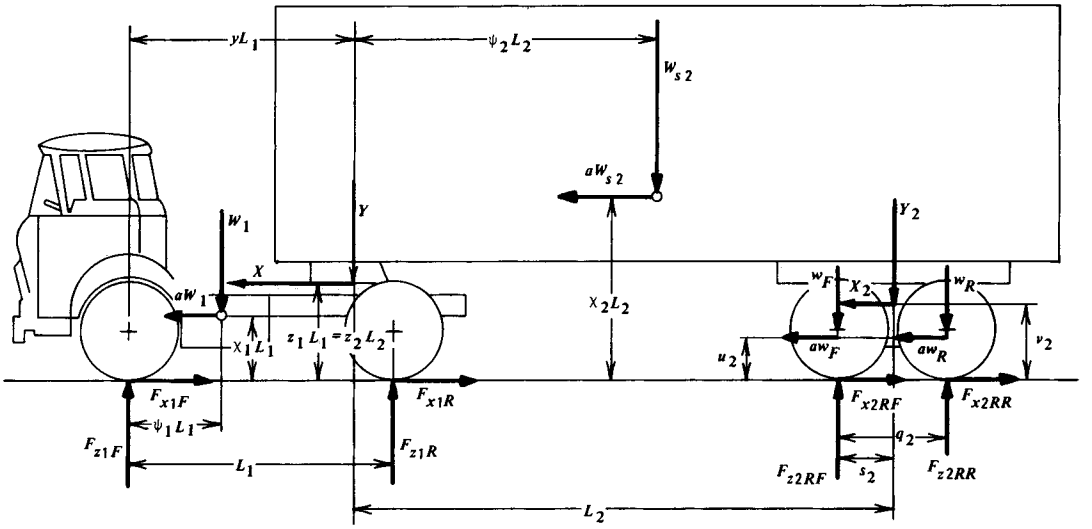

Figure 8-37. Forces Acting on a Tractor-Semitrailer Equipped With Walking Beam Suspension

Tractor tandem rearward axle:

$$F_{z1RR} = [Y_4 s_1 - X_4 v_1 + (w_{1F} + w_{1R}) a u_1 + w_{1R} q_1]/q_1 \text{ , lb} \quad (8\text{-}109)$$

Tractor tandem forward axle:

$$F_{z1RF} = Y_4 + w_{1F} + w_{1R} - F_{z1RR} \text{ , lb} \quad (8\text{-}110)$$

where

$$X_4 = F_{x1RF} + F_{x1RR} - a(w_{1F} + w_{1R}) \text{ , lb} \quad (8\text{-}111)$$

$$Y_4 = (W_{s1}\psi_1 L_1 + y Y L_1 - (a W_{s2} - F_{x2RF} - F_{x2RR}) z_1 L_1 - a W_{s1} \chi_1 L_1 + X_4 v_1]/L_1 \text{ , lb} \quad (8\text{-}112)$$

q_1 = dimension, tandem axle, in.
s_1 = dimension, tandem axle, in.
W_{s1} = tractor weight minus weight of tandem axle, lb
w_{1F} = unsprung weight of tractor tandem forward axle, lb
w_{1R} = unsprung weight of tractor tandem rearward axle, lb

The vertical force Y on the fifth wheel kingpin is obtained from Eq. 8-96. The trailer axle loads are identical to those derived in par. 8-4.1 for a two-axle tractor coupled to a tandem axle trailer and may be determined from Eqs. 8-94 and 8-95.

The application of the braking performance calculation program to a vehicle combination consisting of a tractor equipped with a walking beam suspension and a trailer equipped with a two-elliptic leaf spring tandem axle resulted in the dynamic axle loads, braking performance diagram, and braking efficiencies as presented in Figs. 8-39 through 8-41. Experimental results obtained for the vehicle are indicated in the braking performance and braking efficiency diagrams.

The individual axle brake forces as well as the total brake force computed for a 77,000 lb, 3-S2 tractor-semitrailer are presented in Fig. 8-42 as a function of brake line pressure. Inspection of the curves shows clearly the brake fade — indicated by a decreasing slope with increasing pressure. The brake forces associated with the tractor rearward axle and the trailer forward axle attain a maximum of about 6,000 lb for a line pressure of approximately 60 psi. Test data demonstrated that the aforementioned axles did lock-up at line pressures between 40 to 60 psi. The faster decrease in total brake force for line pressures above 60 psi is caused mainly by dynamic load transfer off

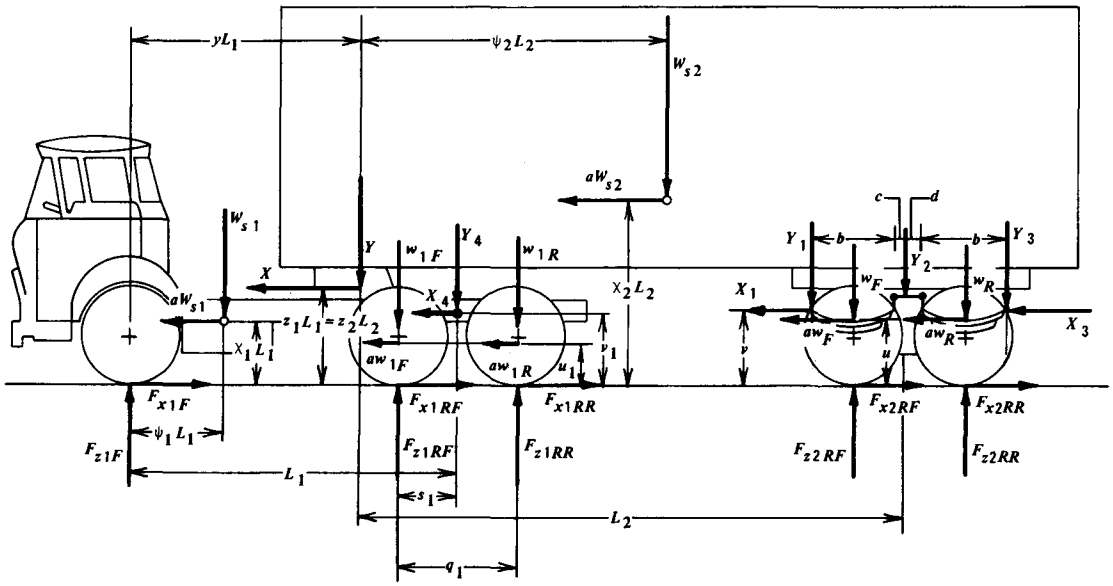

Figure 8-38. Forces Acting on a Tandem Axle Tractor — Tandem Axle Semitrailer Combination

the rearward axle of the tractor and forward axle of the trailer and not by brake fade.

The theoretical results demonstrate that a considerable dynamic load transfer occurs on tandem axles without equalization, i.e., the two axles of a tandem suspension in many cases cannot be lumped into one axle. The study has shown that for tandem axle designs as indicated in Fig. 8-15(B) the load transfer occurring between the forward and rearward axle can be reduced by decreasing the design measurement "v" as illustrated in Fig. 8-24. For example, a change of v from 32 in. to 16.8 in. will cause a decrease of the load on the forward axle to about 47% of its static value for a deceleration of 0.5g as compared to approximately 5% for v = 32 in. This also means that the wheels unlocked deceleration on the forward axle can be increased to about 0.45g, instead of 0.34g.

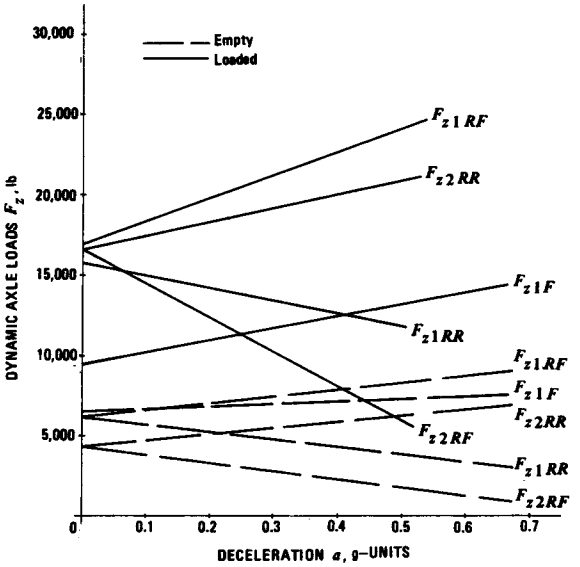

Figure 8-39. Dynamic Axle Loads for a Tandem Axle Tractor — Tandem Axle Semitrailer Combination

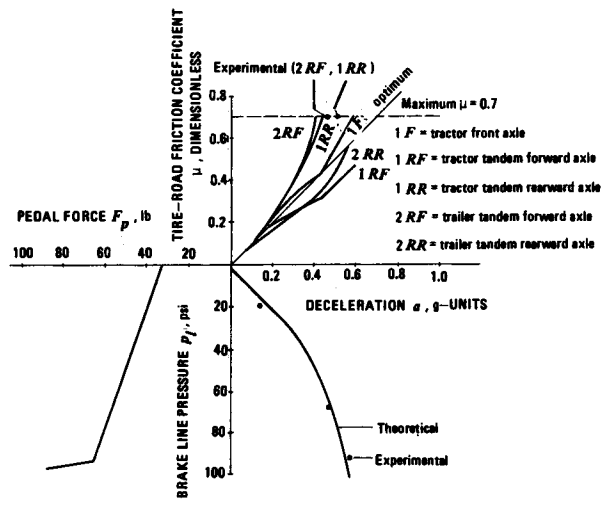

Figure 8-40. Braking Performance Diagram for a Loaded Tandem Axle Tractor — Tandem Axle Semitrailer Combination

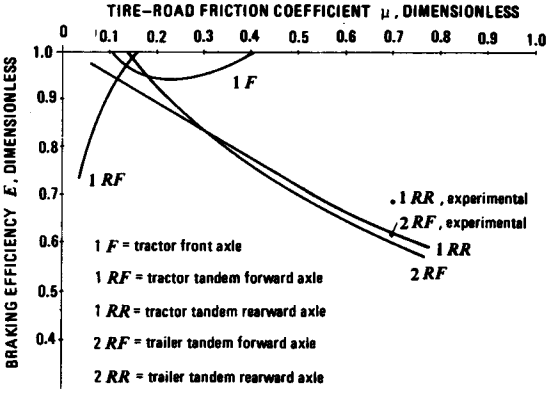

Figure 8-41. Braking Efficiency Diagram for a Tandem Axle Tractor — Tandem Axle Semitrailer Combination

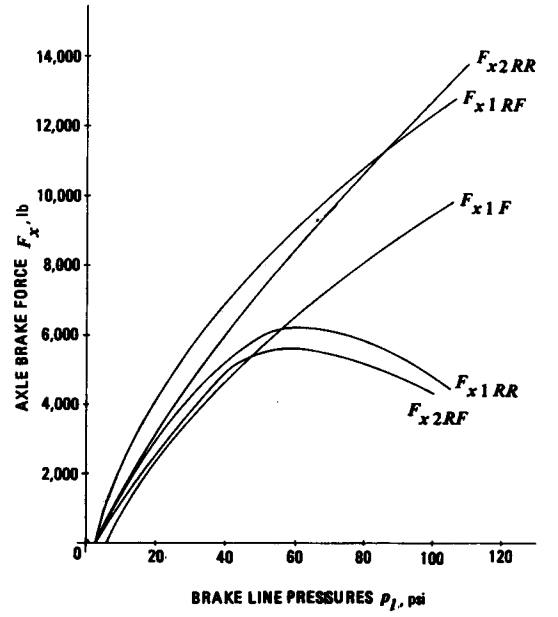

Figure 8-42. Axle Brake Forces

8-5 BRAKING OF A TWO-AXLE TRACTOR COUPLED TO A SINGLE AXLE SEMI-TRAILER AND A DOUBLE AXLE TRAILER

Use the terminology shown in Fig. 8-43. The dynamic axle loads are

Tractor front axle:

$$F_{z1F} = W_1(1 - \psi_1) + W_1 a(\chi_1 - z_1 - z_4 + z_2 + z_4 y - z_2 y) + W_2(1 - \psi_2)(1 - y) - W_2 a(z_4 - \chi_2)(1 - y) + (F_{x1F} + F_{x1R})(z_1 - z_2 + z_4 + z_2 y - z_4 y) + F_{x2R} z_4 (1 - y) \text{ , lb} \quad (8\text{-}113)$$

Tractor rear axle:

$$F_{z1R} = W_1\psi_1 - W_1 a(\chi_1 - z_1 + z_4 y - z_2 y) + W_2(1 - \psi_2)y - W_2 a(z_4 - \chi_2)y - (F_{x1F} + F_{x1R})(z_1 + z_2 y - z_4 y) + F_{x2R} z_4 y \text{ , lb} \quad (8\text{-}114)$$

Semitrailer axle:

$$F_{z2R} = W_1 a(z_4 - z_2) + W_2\psi_2 + W_2 a(z_4 - \chi_2) + (F_{x1F} + F_{x1R})(z_2 - z_4) - F_{x2R} z_4 \text{ , lb} \quad (8\text{-}115)$$

Double trailer front axle:

$$F_{z3F} = (W_1 + W_2)a z_3 + W_3(1 - \psi_3) + W_3 a\chi_3 - (F_{x1F} + F_{x1R} + F_{x2R})z_3 \text{ , lb} \quad (8\text{-}116)$$

Double trailer rear axle:

$$F_{z3R} = -(W_1 + W_2)a z_3 + W_3\psi_3 - W_3 a\chi_3 + (F_{x1F} + F_{x1R} + F_{x2R})z_3 \text{ , lb} \quad (8\text{-}117)$$

where

F_{x3F} = actual brake force of double trailer front axle, lb
F_{x3R} = actual brake force of double trailer rear axle, lb
F_{z3F} = normal force of double trailer front axle, lb
F_{z3R} = normal force of double trailer rear axle, lb
L_3 = wheel base of double trailer, in.
W_3 = double trailer weight, lb
z_3 = double trailer hitch height divided by double trailer wheel base L_3, d'less

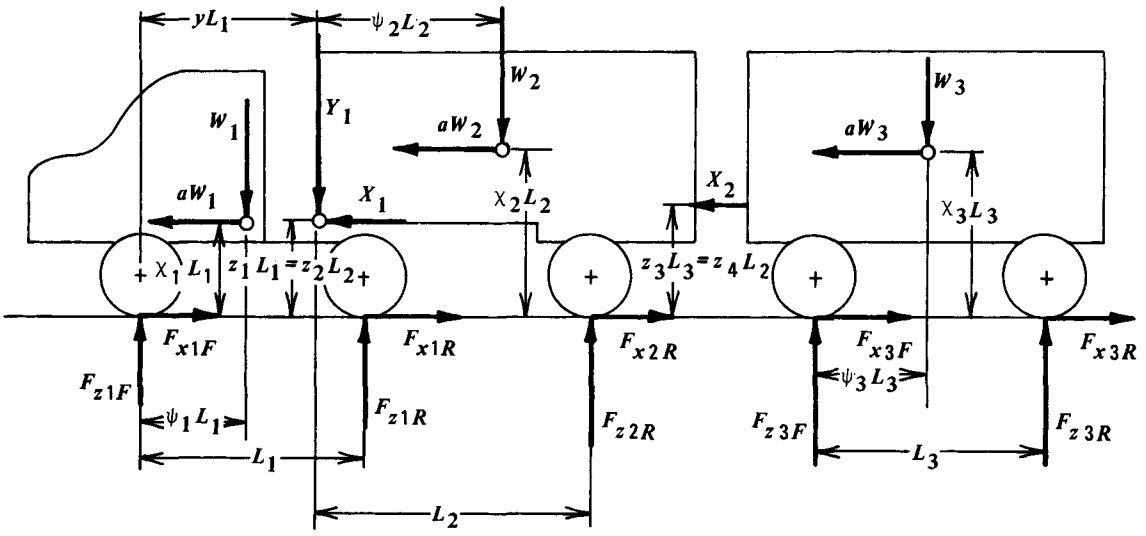

Figure 8-43. Forces Acting on a Tractor-Semitrailer-Double-Trailer Combination

z_4 = double trailer hitch height divided by semitrailer base L_2, d'less

χ_3 = double trailer center of gravity height divided by double trailer base L_3, d'less

ψ_3 = static double trailer rear axle load divided by double trailer weight W_3, d'less

The braking performance data obtained from the braking performance calculations program are presented in Fig. 8-44 for the loaded vehicle combination and are compared to actual road test data.

8-6 BRAKING OF COMBAT VEHICLES

The major factors in the braking analysis of combat vehicles stem from the moments of rotational energies to be absorbed by the brakes and the significantly increased rolling resistance associated with the full or half-trucks.

8-6.1 EFFECTS OF ROTATIONAL ENERGIES

The deceleration of a vehicle consists of the translatory and rotational inertias of the masses. So far, only the translatory effects were considered in the braking analysis. Rotational inertias include those of wheels, tracks, shafts, brake drums, and engine parts. The analysis is further complicated because the particular components rotate at different revolutions per minute as illustrated in Fig. 8-45.

Following fundamentals of mechanics, it becomes convenient to express mass moments of inertia relative to the shaft carrying the brake used for retarding the rotating components. For a rear-wheel-driven vehicle these rotational inertias consist of those associated with the rear wheels, drive shaft, and engine giving the total equivalent rear wheel mass moment of inertia I_{TR}

$$I_{TR} = I_R + \rho_t^2 I_d + \rho_t^2 \rho_d^2 I_e \text{ , in.·lb·s}^2 \quad (8\text{-}118)$$

where

I_d = mass moment of inertia associated with drive shaft, in.·lb·s²

I_e = mass moment of inertia associated with engine, in.·lb·s²

I_R = rotational inertias of rear wheels and connected shafts, in.·lb·s²

ρ_d = differential ratio, d'less

ρ_t = transmission ratio, d'less

An equation similar to Eq. 8-118 may be derived for front wheel driven vehicles. For full track vehicles, the effects of all driven wheels need to be considered. For the evaluation of rotational inertias

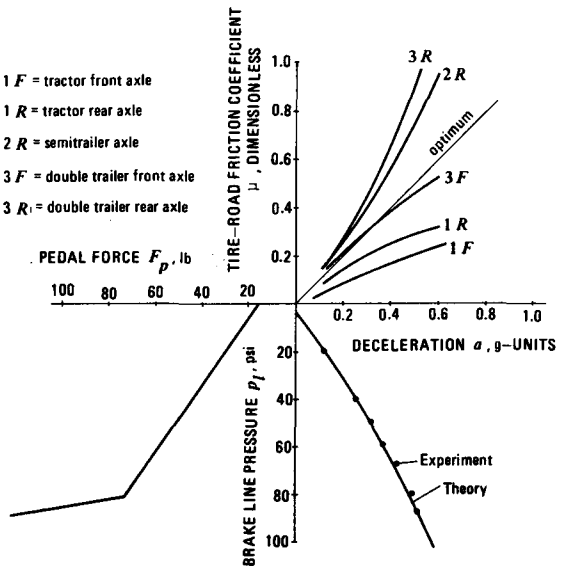

Figure 8-44. Braking Performance Diagram for a Tractor-Semitrailer-Double-Trailer Combination

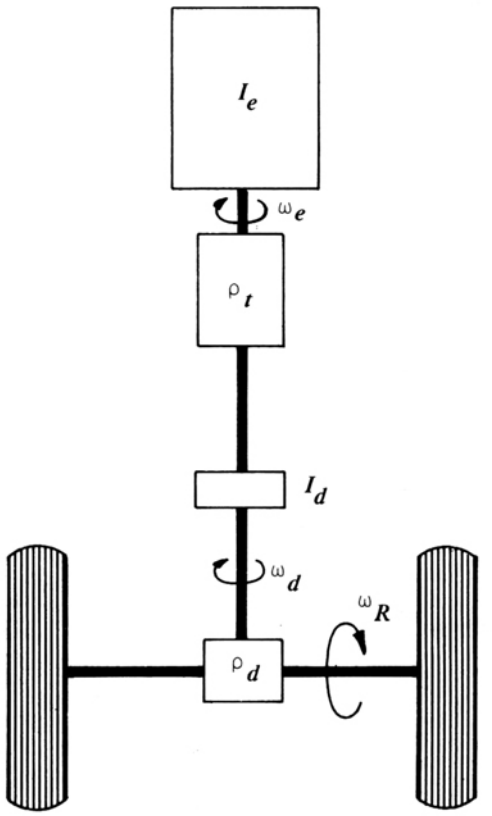

Figure 8-45. Rotational Inertias of a Rear Wheel Driven Vehicle

associated with heavy trucks, inertias for single wheels of 110 in.·lb·s² and 250 in.·lb·s² for dual wheels may be used. For other vehicles such as tanks no general inertia data can be given. The mass moments of inertia can normally be computed by basic laws of mechanics.

For the actual braking analysis, it becomes convenient to express the effects of rotational inertia by an increased translational inertia $(Wa)_{total}$ as (Ref 8)

$$(Wa)_{total} = \delta Wa \text{ , lb} \qquad (8\text{-}119)$$

where

$$\delta = 1 + (I_{TF} + I_{TR})g'/(R^2 W) \text{ , d'less} \qquad (8\text{-}120)$$

I_{TF} = mass moment of inertia of front wheels and brakes, in.·lb·s²

R = distance between wheel center and roadway, in.

W = vehicle weight, lb

g' = gravitational constant, 386 in./s²

The value of δ is a function of the transmission gear used during the braking process. Typical values for passenger cars range from 1.05 to 1.15 in high gear to 1.3 to 1.5 in low gear. Corresponding typical values for trucks range from 1.03 to 1.06 for high gear and from 1.25 to 1.6 for low gear.

The braking energy to be absorbed by the brakes consists of the translational and rotational components. For a braking process from speed v_1 to v_2 the total braking energy E_T is

$$E_T = [W/(2g)](V_1^2 - V_2^2) + \left(\frac{I}{2\times 12}\right)(\omega_1^2 - \omega_2^2) \text{ , ft·lb} \qquad (8\text{-}121)$$

where

g = gravitational constant, ft/s²

I = mass moment of inertia of rotating components decelerated by brakes, in.·lb·s²

V_1 = initial vehicle speed, ft/s

V_2 = final vehicle speed, ft/s

ω_1 = initial angular velocity of brake rotor, rad/s

ω_2 = final angular velocity of brake rotor, rad/s

8-6.2 TRACK ROLLING RESISTANCE

The rolling resistance of wheeled vehicles was discussed in Chapter 6. The rolling resistance associated with track vehicles stems mainly from road surface deformations, frictional losses of track elements at their connecting points, and friction at the track side walls pressing into the ground. The rolling resistance coefficient is affected greatly by the resistance of the ground to deformation and no specific values can be assigned to a road surface. For approximate design evaluation, the following rolling resistance coefficients for wheeled and track equipped vehicles may be used:

Road surfaces that are rigid
Tires: 0.01 to 0.015, tracks: 0.02 to 0.035
Road surfaces that deform
Dirt roads
Tires: 0.05 to 0.02; tracks 0.035 to 0.045
Loose sand, off road
Tires: 0.02 to 0.30, tracks 0.045 to 0.075

8-6.3 BRAKING OF HALF-TRACK VEHICLE

With the engineering relationships presented in previous chapters, it becomes possible to determine the braking performance of vehicles equipped with pneumatic tires on the front and track of the rear. For vehicles using rear brakes mounted on the drive wheels, the braking analysis of tandem axle trucks may be used as a base for computing braking performance. The effects of track rolling resistance must be included. For drive shaft mounted brakes the transmission ratio must be considered in the analysis.

8-6.4 BRAKING OF FULL-TRACK VEHICLES AND SPECIAL CARRIERS

The prediction of braking performance and brake temperature for full-track vehicles and special carriers becomes possible with the engineering relationships presented in previous chapters. Important design considerations are brake torque and hence braking effectiveness and brake cooling. Factors such as brake force distribution are eliminated since no individual load carrying axles are identified. A design example of a full-track vehicle is presented in Chapter 14. The brake analysis of special carriers does not present any difficulties. Since in most cases individual designs are used, no specific design solutions are suggested here.

8-7 CONCLUDING REMARKS ON VEHICLES EQUIPPED WITH FIXED RATIO BRAKING SYSTEMS

For the correct design of a vehicular brake system, it is essential that the optimum brake force distributions among the individual axles be known for the empty and loaded vehicle. In the case of a two-axle vehicle, these expressions are simple and can be given in terms of the deceleration or the rear axle brake force as a function of the front axle brake force. For a tractor-semitrailer vehicle, however, the

analysis is more complicated since the dynamic axle loads and hence the dynamic brake forces of the tractor are affected by the loading and brake force levels of the trailer. An improvement in braking performance can be expected by optimizing the brake force distribution among the axles of a solid frame and combination vehicle. However, no braking efficiencies much higher than 70 to 75% may be expected for heavy commercial vehicles that show a significant difference in the center of gravity location between the loaded and unloaded cases. Often front axle braking of heavy tractor-semitrailer combinations is eliminated under the erroneous notion that the danger of jackknifing or trailer swing is thereby reduced. Elimination of the front axle brakes has a pronounced effect on the baseline distribution in terms of reduced braking performance.

For track vehicles important design considerations are brake torque, brake system gain, space limitations, and brake cooling. Factors such as brake force distribution and dynamic brake forces are not major parts of a track vehicle braking analysis.

In some cases light weight-unbraked trailers are towed by a truck. The deceleration of the combination is reduced since the braking system of the tow vehicle must retard the entire weight. In most applications the hitch point is located at approximately the same vehicle distance from the ground as the center of gravity of the tow vehicle. With this assumption, the dynamic axle loads of the tow vehicle may be obtained from Eqs. 7-3a and 7-3b modified to yield

Truck Front Axle:

$$F_{zF,dyn} = (1 - \psi)W_{Truck} + \chi a(W_{Truck} + W_{Tr}) \text{ , lb} \quad (8\text{-}122a)$$

Truck Rear Axle:

$$F_{zR,dyn} = \psi W_{Truck} - \chi a(W_{Truck} + W_{Tr}) \text{ , lb} \quad (8\text{-}122b)$$

where

a = deceleration, g-units
W_{Truck} = truck weight, lb
W_{Tr} = trailer weight, lb

REFERENCES

1. J. A. Rouse, *The Distribution of Braking on Road Vehicles,* Instn. Mech. Engrs., Symposium on Control of Vehicles, Paper 9, March 1963.
2. R. Limpert, *An Experimental Investigation of Proportional Braking,* M.S. Thesis (unpublished) Brigham Young University, Provo, Utah, 1968.
3. R. Limpert and Ch. Y. Warner, *Proportional Braking of Solid-Frame Vehicles,* SAE Paper No. 710046, January 1971.
4. R. Murphy, R. Limpert and L. Segel, *Development of Braking Performance Requirements for Buses, Trucks, and Tractor/Trailers,* SAE Paper No. 710046, January 1971.
5. R. Murphy, R. Limpert and L. Segel, *Bus, Truck, Tractor-Trailer Braking Performance,* Volume 1 of 2: Research Findings, Final Report Contract FH-11-7290, prepared for the U.S. Department of Transportation, March 1971.
6. M. Wolf, "Braking Efficiency and Degree of Safety for Stationary and Nonstationary Braking in a Turn", *Automobiltechnische Zeitschrift* 59, No. 6, 1957.
7. R. Limpert, F. Gamero and R. Boyer, *An Investigation of the Brake Force Distribution for Straight and Curved Braking,* SAE Paper No. 741086, October 1974.
8. M. Mitschke, "Dynamics of Motor Vehicles", *Springer Publisher,* Berlin-Heidelberg-New York, 1972.
9. R. Limpert, *An Investigation of the Brake Force Distribution on Tractor-Semi-Trailer Combinations,* SAE Paper No. 710044, January 1971.
10. R. Murphy, et al., *A Computer Based Mathematical Method for Predicting the Braking Performance of Trucks and Tractor-Trailers,* Phase I Report, Highway Safety Research Institute, University of Michigan, September 15, 1972.
11. J. E. Bernard, et al., *A Computer Based Mathematical Method for Predicting the Directional Response of Trucks and Tractor-Trailers,* Phase II Technical Report, Highway Safety Research Institute, University of Michigan, June 1, 1973.
12. G. Fritzsche, "Brake Force Distribution in Tractor-Semitrailers", *Automobiltechnische Zeitschrift,* Vol. 63, No. 1, 1961, pp. 13-18.
13. O. Bode and W. George, "Analytical Investigation of the Brake Behavior of Tractor-Semitrailer Combinations", *Deutsche Kraftfahrtforschung und Strassenverkehrstechnik,* No. 159, 1961.
14. R. J. Morse, "Brake Balance — It Can Be Improved", *Society of Automotive Engineers,* Publication No. 660398, June 1966.
15. E. Stump, "Brake Force Distribution on Tractor-Semitrailers" *Automobiltechnische Zeit-*

schrift, Vol. 64, No. 7, 1962, pp. 203-207.

16. O. Bode and W. George, "Brake Tests with Tractor-Semitrailer Combinations", *Deutsche Kraftfahrtforschung und Strassenverkehrstechnik,* No. 150, 1961.
17. E. Ch. Mikulick, *The Dynamics of Tractor-Semitrailer Vehicles — The Jackknifing Problem,* A thesis presented to the faculty of the Graduate School of Cornell University for the Degree of Doctor of Philosophy, June 1968.
18. H. A. Wilkins, *Assessment of the Hope Anti-Jackknife Device,* Road Research Laboratory, Crowthorne, Bershire, England.
19. P. Leucht, *The Directional Dynamics of the Commercial Tractor-Semitrailer Vehicle During Braking,* SAE Paper No. 700371, 1970.
20. D. Runge, "Matching of the Trailer Brake Forces to the Loading of the Combination", *Automobiltechnische Zeitscrift,* Vol. 69, No. 7, 1967, pp. 211-17.
21. P. E. Nelson and J. W. Fitch, *Optimum Braking, Stability and Structural Integrity for Long Truck Combinations,* SAE Paper No. 680547, August 1968.
22. O. Bode, "Truck-Trailer Braking and Load Matching", *Automobiltechnische Zeitschrift,* Vol. 60, No. 3, 1958, pp. 79-85.
23. I. Schmidt, *The Directional Stability of Two- and Three Unit Vehicle Trains,* Dissertation, Technische Hochschule, Stuttgart, Germany, 1964.

CHAPTER 9
BRAKING OF VEHICLES EQUIPPED WITH VARIABLE RATIO BRAKING SYSTEMS

In this chapter the braking analysis of vehicles equipped with braking systems that change the brake force distribution among the axles is discussed. Analytical procedures are presented that allow the determination of the optimum variable ratio of proportioning. A detailed example demonstrates the proportional braking analysis of three-axle tractor-semitrailers.

9-0 LIST OF SYMBOLS

A_C = brake chamber area, in.^{2}
A_{WC} = wheel cylinder area, in.^{2}
a = deceleration, g-units
a_x = longitudinal deceleration, g-units
a_y = lateral acceleration, g-units
BF = brake factor, d'less**
C = vertical normalized distance between origin and intercept of proportional distribution and vertical axis, d'less
E_F = front axle braking efficiency, d'less
$E_{F,ab}$ = front axle braking efficiency above shift point, d'less
$E_{F,bel}$ = front axle braking efficiency below shift point, d'less
E_{min} = minimum braking efficiency, d'less
E_R = rear axle braking efficiency, d'less
$E_{R,ab}$ = rear axle braking efficiency above shift point, d'less
$E_{R,bel}$ = rear axle braking efficiency below shift point, d'less
F_p = pedal force, lb
$F_{x,dyn}$ = dynamic brake force, lb
F_{x1F} = front axle brake force, lb
F_{x1R} = rear axle brake force, lb
F_{x2R} = trailer axle brake force, lb
$F^*_{xF,dyn}$ = dynamic front axle brake force divided by vehicle weight, d'less
$F^*_{xR,dyn}$ = dynamic rear axle brake force divided by vehicle weight, d'less
L = wheel base, in.
L_1 = tractor wheel base, in.
L_2 = horizontal distance between fifth wheel and trailer axle or trailer base, in.
N = parameter, d'less
p_l = brake line pressure, psi
p_{lF} = front brake line pressure, psi
p_{lR} = rear brake line pressure, psi
$p_{l,dyn}$ = dynamic brake line pressure, psi
$p_{lR,dyn}$ = dynamic rear axle brake line pressure,psi
$p_{lF,dyn}$ = dynamic front axle brake line pressure, psi
p_{l1F} = brake line pressure on tractor front axle, psi
p_{l1R} = brake line pressure on tractor rear axle, psi
$p_{l1F,dyn}$ = dynamic brake line pressure on tractor front axle, psi
$p_{l1R,dyn}$ = dynamic brake line pressure on tractor rear axle, psi
$p_{l2R,dyn}$ = dynamic brake line pressure on trailer axle, psi
p_{oF} = pushout pressure, front brakes, psi
p_{oR} = pushout pressure, rear brakes, psi
p_{o1F} = pushout pressure, tractor front brakes, psi
p_{o1R} = pushout pressure, tractor rear brakes, psi
p_{o2R} = pushout pressure, trailer brakes, psi
R = effective tire radius, in.
r = effective drum or rotor radius, in.
W = vehicle weight, lb
W_o = empty vehicle weight, lb
W_1 = tractor weight, lb
W_2 = trailer weight, lb
y = horizontal distance between tractor front wheels and fifth wheel divided by tractor wheel base L_1, d'less
z_1 = fifth wheel height divided by tractor wheel base L_1, d'less
z_2 = fifth wheel height divided by trailer base L_2, d'less
α = angle between base line distribution and horizontal axis, deg
β = angle between proportional distribution and horizontal axis, deg
η_c = wheel cylinder efficiency, d'less
η_m = mechanical efficiency between brake chamber and brake shoe, d'less
μ = tire-road friction coefficient, d'less
ρ = displacement gain between brake chamber and brake shoe, d'less
ϕ = rear axle brake force divided by total brake force, d'less

**d'less = dimensionless

ϕ_i = brake force of ith axle divided by total brake force, d'less
ϕ_{1R} = tractor rear axle brake force divided by total brake force, d'less
χ = center of gravity height divided by wheel base L, d'less
χ_1 = tractor center of gravity height divided by tractor wheel base L_1, d'less
χ_2 = trailer center of gravity height divided by trailer base L_2, d'less
ψ = static rear axle load divided by vehicle weight, d'less
ψ_1 = static tractor rear axle load divided by tractor weight (without trailer), d'less
ψ_2 = static trailer axle load divided by trailer weight, d'less

Subscripts: 1 = tractor
2 = trailer
F = front or tandem front axle
R = rear or tandem rearward axle

9-1 TWO-AXLE VEHICLES

If for a given vehicle the deceleration levels achieved prior to wheel lockup as a result of fixed ratio braking are considered to be insufficient, a variable or proportional brake force distribution may be employed. The object of proportional braking is to bring braking efficiencies closer to unity over a wide range of loading and road surface conditions, encompassing summer and most winter driving situations. This is done by employing a variable braking force distribution. Through a proportioning valve the actual braking forces are brought closer to the dynamic (Refs. 1,2,3,4,5,6, and 7).

9-1.1 DYNAMIC AND ACTUAL BRAKE FORCES

The optimum brake force distribution of a two-axle vehicle equipped with a bilinear proportional brake system is shown in Fig. 9-1. For decelerations $a < 0.4g$ the rear line pressure is not proportioned relative to the front axle, resulting in a baseline distribution ϕ larger than for typical fixed distribution braking. This also has the advantage that in the range of most decelerations: (a) the rear axle brakes carry a greater portion of the total brake force and the wear life of the front brakes may be expected to increase, and (b) the pedal force required for decelerations below the shift point ($a = 0.4g$ in the example of Fig. 9-1) will be smaller. For $a \geq 0.4g$ the rear line pressure is proportioned in such a manner that the danger of overbraking the rear axle is prevented for all decelerations less than 1.0g, provided the tire-roadway

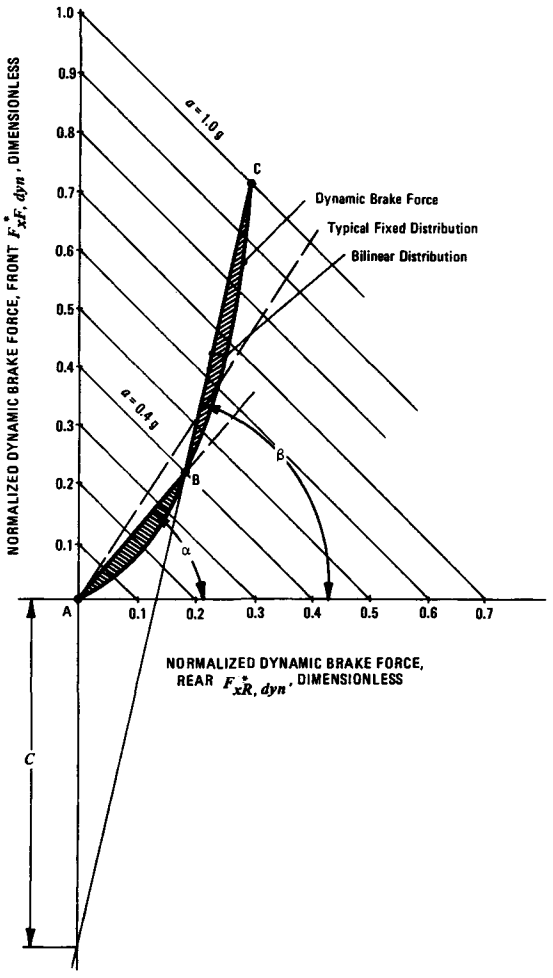

Figure 9-1. Dynamic and Actual Bilinear Brake Forces of Two-Axle Vehicle

friction coefficient is equal to or greater than the deceleration measured in g-units. In order to approximate the different load conditions between unloaded and loaded cases, the proportioning valve may be designed such that the displacement of the vehicle body relative to the rear axle controls the shifting point of the valve. Since the displacement is a function of the rear axle load, the proportional system is made automatically load-dependent. This means that in Fig. 9-1 the shifting point is moved between points A and B according to the current rear axle load.

Use the notation shown in Fig. 9-1. The angle α measures the brake force distribution before proportional braking occurs; the angle β measures the

proportional brake force distribution; the distance C measures the location of the shift point B. The braking efficiencies on the front and rear axle obtained with the variable brake force distribution illustrated in Fig. 9-1 for braking forces below the shift point B are
Front axle:

$$E_{F,bel} = \frac{(1 + \tan\alpha)(1 - \psi)}{\tan\alpha - (1 + \tan\alpha)\mu\chi}, \text{ d'less} \quad (9\text{-}1)$$

Rear axle:

$$E_{R,bel} = \frac{(1 + \tan\alpha)\psi}{1 + (1 + \tan\alpha)\mu\chi}, \text{ d'less} \quad (9\text{-}2)$$

For braking forces above shift point B the braking efficiencies of the front and rear axle are
Front axle:

$$E_{F,ab} = \frac{(1 - \psi) + \dfrac{C}{\mu(1 + \tan\beta)}}{\left(\dfrac{\tan\beta}{1 + \tan\beta}\right) - \mu\chi}, \text{ d'less} \quad (9\text{-}3)$$

Rear axle:

$$E_{R,ab} = \frac{\psi - \dfrac{C}{\mu(1 + \tan\beta)}}{\left(\dfrac{1}{1 + \tan\beta}\right) + \mu\chi}, \text{ d'less} \quad (9\text{-}4)$$

where

- C = vertical normalized distance between origin and intercept of proportional distribution and vertical axis, d'less
- α = angle between base line distribution and horizontal axis, deg
- β = angle between proportional distribution and horizontal axis, deg
- μ = tire-road friction coefficient, d'less
- χ = center of gravity height divided by wheel base L, d'less
- ψ = static rear axle load divided by vehicle weight, d'less

The braking efficiencies obtained with the bilinear brake force distribution shown in Fig. 9-1 are illustrated in Fig. 9-2. The braking efficiencies achievable with a typical fixed distribution are indicated by the broken line.

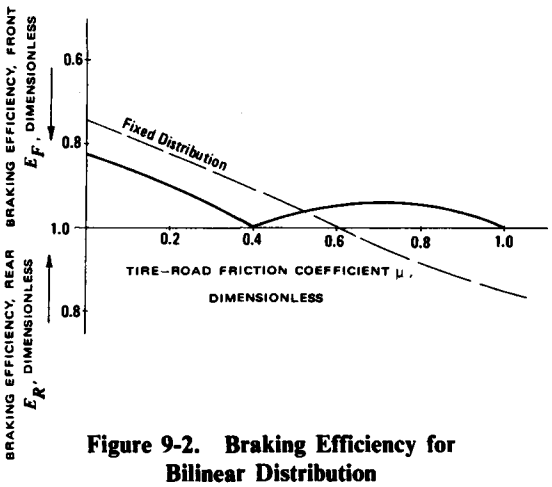

Figure 9-2. Braking Efficiency for Bilinear Distribution

9-1.2 OPTIMUM VARIABLE RATIO BRAKING DISTRIBUTION

For a solid frame vehicle Eqs. 9-1 through 9-4 may be used to develop limiting relationships on the baseline and proportional brake force distribution. In Fig. 9-1 the baseline distribution and variable ratio distribution are identified by the angles α and β, and distance C, respectively. Application of Eqs. 9-1 through 9-4 results in the inequalities for the two regimes
1. Between A and B (baseline distribution):

$$\frac{1 + \mu\chi - \left(\dfrac{\psi}{E_{min}}\right)}{\left(\dfrac{\psi}{E_{min}}\right) - \mu\chi} \leq \tan\alpha \leq \frac{\left(\dfrac{1 - \psi}{E_{min}}\right) + \mu\chi}{1 - \mu\chi - \left(\dfrac{1 - \psi}{E_{min}}\right)}, \text{ d'less} \quad (9\text{-}5)$$

2. Above B (proportional distribution):

$$\frac{1 + \mu\chi + \left(\dfrac{C}{\mu E_{min}}\right) - \left(\dfrac{\psi}{E_{min}}\right)}{\left(\dfrac{\psi}{E_{min}}\right) - \mu\chi} \leq \tan\beta \leq \frac{\left(\dfrac{1 - \psi}{E_{min}}\right) + \mu\chi + \left(\dfrac{C}{\mu E_{min}}\right)}{1 - \mu\chi - \left(\dfrac{1 - \psi}{E_{min}}\right)}, \text{ d'less} \quad (9\text{-}6)$$

For the case in which the shift point B is located on the dynamic brake force curve (see Fig. 9-1), the actual brake force is equal to the dynamic brake force existing at the shift point conditions. For this condition the distance C is determined by the angles α and β. Application of Eqs. 9-5 and 9-6 for this case and tire-road friction coefficients $0.2 \leq \mu \leq 0.8$ and a specified minimum braking efficiency E_{min} will define an envelope of acceptable values of α and β. Values of α and β within this envelope may be used for design evaluation.

For example, for $\psi = 0.55$, $\chi = 0.22$, $E_{min} = 0.80$, and $C = 0.5$, Eqs. 9-5 and 9-6 yield

29 deg $\leq \alpha \leq$ 57 deg, $\mu = 0.2$
43 deg $\leq \alpha \leq$ 55 deg, $\mu = 0.8$
79 deg $\leq \beta \leq$ 83 deg, $\mu = 0.2$
68 deg $\leq \beta \leq$ 80 deg, $\mu = 0.8$

Inspection of these values indicates that the angle α must be between 43 and 55 deg, the angle β between 79 and 80 deg in order for the vehicle to have a braking efficiency of 80%. In general, a trial and error solution must be sought in which different C-values are assumed until the values of α and β yield the desired braking efficiency.

If the shift point B is not located on the dynamic brake force curve, the actual brake forces do not optimally approach the dynamic braking forces and the associated braking performance is below the maximum possible. For these conditions the braking efficiencies may be computed by the use of the equations presented in Chapter 7 in connection with the braking performance calculation program.

9-1.3 DYNAMIC BRAKE LINE PRESSURES

In the design of proportioning brake systems it is convenient to work with the brake line pressure directly and not with the forces generated by them. The dynamic pressures are those which produce the dynamic braking forces. For a particular vehicle the dynamic pressure may be computed from the actual braking forces, i.e., Eq. 5-10 for hydraulic brake systems or Eq. 5-31 for pneumatic brake systems; and the dynamic brake force, i.e., Eqs. 8-1 and 8-2. By equating dynamic and actual brake forces and solving for brake line pressures, the dynamic brake line pressures $p_{l,dyn}$ for hydraulic brake systems are (Ref. 8):

Front axle:

$$p_{lF,dyn} = \frac{(1 - \psi + \chi a)\, a\, W}{2\, A_{WC}\, \eta_c\, BF\, (r/R)} + p_{oF} \text{ , psi} \qquad (9\text{-}7)$$

Rear axle:

$$p_{lR,dyn} = \frac{(\psi - \chi a)\, a\, W}{2\, A_{WC}\, \eta_c\, BF\, (r/R)} + p_{oR} \text{ , psi} \qquad (9\text{-}8)$$

where

A_{WC} = wheel cylinder area, in.^{2}
a = deceleration, g-units
BF = brake factor, d'less
p_{oF} = pushout pressure, front brakes, psi
p_{oR} = pushout pressure, rear brakes, psi
R = effective tire radius, in.
r = effective drum or rotor radius, in.
W = vehicle weight, lb
η_c = wheel cylinder efficiency, d'less

The dynamic brake line pressures for pneumatic brake systems are obtained in a fashion similar to a hydraulic brake system. In this case the brake shoe actuation force per unit brake line pressure $A_{WC}\eta_c$ is replaced by the corresponding term for the air brake system $A_C \eta_m \rho$, where A_C = brake chamber area, in.^{2}; η_m = mechanical efficiency between brake chamber and brake shoe, d'less; ρ = displacement gain between brake chamber and brake shoe, d'less. It is evident from Eqs. 9-7 and 9-8 that all information on the individual brakes must be known in order to determine the dynamic brake line pressures. Eqs. 9-1 through 9-5 however require no specific information on the brakes, and therefore, it seems advisable for the determination of the optimum design of proportional systems in a vehicle to apply the conditions discussed in pars. 9-1.1 and 9-1.2. For the actual design and determination of dimensions of the hardware, the relationships presented in par. 9-1.3 are more useful.

The dynamic brake line pressures for a light truck are illustrated in Fig. 9-3 (Ref. 9). In this case different deceleration scales are necessary for the empty and loaded driving condition. As indicated, the design pressure ratio front to rear is 2.5 to 1, and the shift point for the loaded case corresponds to a line pressure 750 psi. When the vehicle was actually tested, the brake line pressure and braking efficiencies for the empty driving condition as shown in Figs. 9-4 and 9-5, respectively, were achieved.

The braking performance calculation program discussed in Chapter 7 can be adapted easily to calculate the braking performance of a vehicle equipped with a proportioning brake system. The only change in the program is introduced by making the brake line pressure on the controlled axle a specific function of the master cylinder brake line pressure, i.e, the brake line pressure on each axle may be different depending upon the proportioning used. The particular functional relationship $p_{lR} = f(p_{lF})$ can be read directly off the dynamic line pressure diagram with the actual line pressure distribution shown. In the example of Fig. 9-1 this functional relationship is reflected

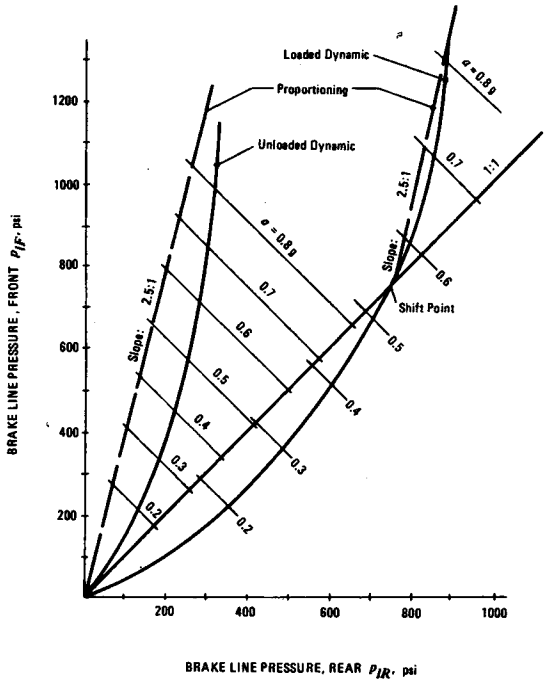

Figure 9-3. Dynamic and Actual Brake Line Pressures

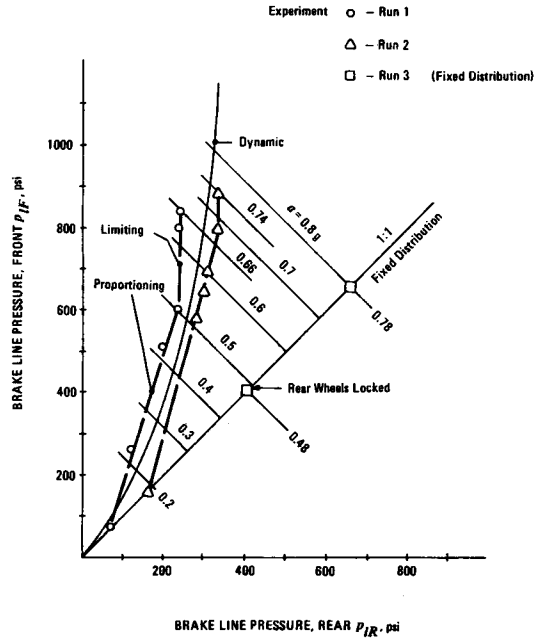

Figure 9-4. Brake Line Pressures for a Vehicle Weight of 4742 lb

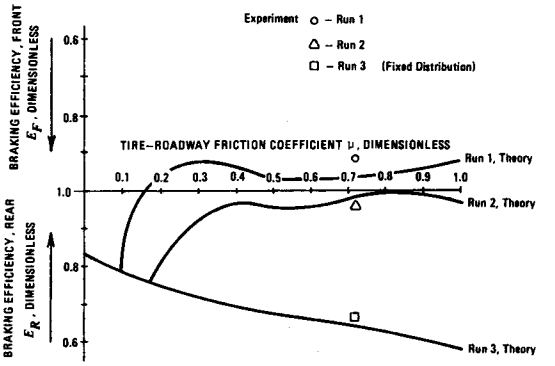

Figure 9-5. Braking Efficiency Diagram for a Vehicle Weight of 4742 lb

by the bilinear characteristic of the actual line pressure distribution.

Proportioning valves have been designed that modulate line pressure as a function of the static or dynamic axle loads. In the case of static modulation of the brake forces, the valve setting is not affected by any suspension movement during the braking process. However, the proportioning system can be made sensitive to deceleration by using the suspension deflection during braking as the parameter controlling the modulation of the individual brake line pressures. A problem associated with this type of proportioning is the filtering out of any suspension noise while still retaining an adequate signal.

9-1.4 PEDAL FORCE REQUIREMENTS

The pedal force required to achieve a given deceleration level is greater at all levels above the shift point with proportioning than without it; however, the wheels-unlocked decelerations achieved are increased for all tire-road friction coefficients as shown in Fig. 9-6. This means that a shorter, stable stop is possible at the expense of slightly increased pedal forces. This improvement in efficiency may be expected to be reflected in better distribution of tire and brake lining wear between front and rear wheels.

9-1.5 PRESSURE REGULATING VALVES

Brake line pressure regulating valves are designed to modulate the pressure applied to a particular axle or wheel brake in relationship to the supply pressure at the master cylinder or application valve. The regulating valves can be divided into three basic groups: (a) brake force limiting valve; (b) brake force proportioning valve with fixed shift point; (c) brake force

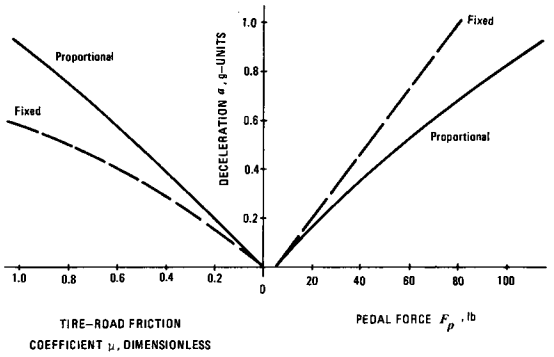

Figure 9-6. Pedal Force Required for Fixed and Variable Ratio Braking

proportioning valve with load or deceleration sensitive shift point adjustment. Each is discussed.

1. Brake force limiting valve. The valve closes off one brake line at a certain brake line pressure and holds the brake line pressure in the brake line constant regardless of increases in supply pressures to the valve. Increases in brake fluid requirement in the closed-off brake line due to thermal or elastic deformations of the brake drum or caliper are automatically adjusted by the valve through a brief reopening of the valve to the supply pressure. Once the pressure adjustment is completed, the valve automatically closes off the brake line with the limited pressure.

2. Brake force proportioning valve with fixed shift point. The valve permits the brake line pressure to increase in equal amounts in the supply line and brake line leading to the modulated axle. When the supply pressure has reached the shift point pressure, the valve closes and only a reduced brake line pressure reaches the modulated axle. Some valves use differential or stepped bore piston with the effective area ratio determining the proportioning between supply and exit pressure of the valve.

3. Brake force proportioning valve with load or deceleration sensitive shift point adjustment. The pressure proportioning (and pressure limiting) valve can be made more effective for different loading conditions or deceleration levels if the shift point is moved in proportion to the loading or deceleration of the vehicle. Load sensitive valves function in a fashion similar to proportioning valves with a fixed shift point. An additional mechanism is installed by which the force acting against the stepped bore piston can be varied according to the axle load. The shift point location is changed in proportion to the force acting on the stepped bore piston. Since axle load is a function of both static and dynamic axle load changes, the shift point location is sensitive to loading and load distribution, and deceleration level. The variation of the force against the stepped bore piston of the valve is achieved by an adjustable linkage installed between vehicle body and axle.

Deceleration sensitive brake force proportioning devices use inertia valves in which a steel ball rolls up an inclined ramp at a certain deceleration. The movement of the ball causes a spring loaded valve to close which disconnects the modulated axle from the supply pressure. In some applications a pendulum controlling the brake line pressure to the modulated axle as a function of vehicle decelerations has been used.

Brake line pressure regulating valves of hydraulic brake systems often are combined with other valves to a single unit generally called a combination valve. Most combination valves serve three functions: (a) to function as brake force regulator; (b) to reduce the brake line pressure to the front disc brakes until the return spring force of the rear drum brakes is overcome; (c) to actuate a switch in the event of a hydraulic leak in the brake system. Most combination valves are designed to bypass the proportioning function of the valve in the case of a front brake circuit failure. This feature becomes necessary to provide sufficiently large braking forces at the rear brakes with the front brakes failed.

9-1.6 STRAIGHT-LINE VERSUS CURVED LINE BRAKING PERFORMANCE

The discussion of straight versus curved line braking of vehicles equipped with fixed ratio braking presented in par. 8-1.6 applies to variable ratio braking also.

Experimental results indicate that fixed shift point proportioning valves and static load sensitive proportioning achieve nearly identical straight line braking performance, when tested for the design load condition. When significant load changes occur, the load sensitive brake force regulating system yields better braking performance over a wide range of load conditions. Proportioning systems that adjust the brake force distribution as function of the dynamic-load changes generally do not yield significant improvements over static load sensitive proportioning systems.

When braking in a turn on a low friction road surface, the fixed shift point proportioning valve tends to produce overbraking of the rear axle. For these conditions the brake line pressures induced by the pedal force are not sufficiently high to exceed the shift point pressure beyond which reduced brake line pressures are supplied to the rear axle. Under those

circumstances the large rear brake force is sufficient to cause premature rear wheel lockup and subsequent vehicle instability. Dynamic and load sensitive proportioning valves generally do not exhibit this undesirable behavior. When braking on high friction road surfaces, fixed shift point proportioning valves generally do not cause vehicle instability.

Some improvements have been achieved by making the brake force distribution both longitudinal and lateral acceleration sensitive. Feasibility studies have shown that two-way proportioning increased the curved-line braking performance by as much as 20% when compared with fixed ratio braking (Ref. 10).

The braking in-a-turn analysis presented in Chapter 8 may be used to determine the dynamic brake line pressures for each individual wheel. The dynamic brake line pressures supplied to each wheel take braking deceleration and level of lateral acceleration into account and provide the brake forces for an optimum stop. The detailed calculations were carried out for a Fiat 124 passenger car and the results are illustrated in Fig. 9-7. Front and rear as well inner and outer brake line pressures are indicated for different longitudinal deceleration a_x and lateral acceleration a_y. The combination of deceleration and lateral acceleration values defining a performance point are a function of the particular tire characteristics. Inspection of Fig. 9-7 indicates a brake line pressure of approximately 850 psi on both rear wheels and 1400 psi on the front wheels for a straight stop. The same values of dynamic brake line pressures also could have been determined from Eqs. 9-7 and 9-8. For braking in a turn, e.g., at 0.4g lateral acceleration and 0.89g braking, the individual brake line pressures are approximately 900 psi at the outer rear wheel, 400 psi at the inner rear wheel, 1625 psi at the outer front wheel, and 1020 psi at the inner front wheel. These numbers show the outer front wheel to be the most critical one for producing both braking and turning forces. As the discussion of vehicle stability during braking has shown (Chapter 8), the outer rear wheel is the most critical wheel for producing stabilizing forces during a combined braking and turning maneuver. Two-way proportioning should be designed such that no outer wheel can be locked prior to any inner wheel.

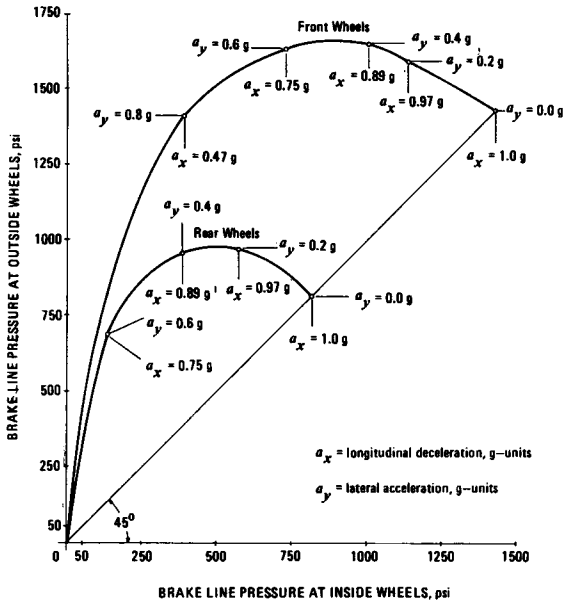

Figure 9-7. Dynamic Brake Line Pressures for Combined Braking and Turning

9-1.7 VEHICLE STABILITY CONSIDERATIONS

The stability factors presented in par. 8-1.7 for fixed ratio braking apply directly to vehicles equipped with variable ratio braking systems. Important considerations are again the prevention, by a proper brake force distribution, of premature rear-wheel lockup.

9-2 BRAKING OF TRACTOR-SEMITRAILER VEHICLE

An approach similar to that of two-axle vehicles is presented.

9-2.1 DYNAMIC AND ACTUAL BRAKE FORCES

The normalized dynamic brake forces of a typical tractor-semitrailer vehicle for the empty and loaded driving conditions are shown in Fig. 9-8. These curves show that the dynamic brake forces are heavily influenced by the vehicle loading. If the brake system is designed to operate near optimum conditions for the loaded vehicle, it will perform poorly for the empty case unless a proportional brake system is provided that will vary the brake force distribution according to the loading condition of the vehicle combination.

An additional difficulty arises from the fact that a particular tractor may be used with different trailers, each having a variety of loading configurations and brake force levels. It appears, therefore, necessary to distinguish between the brake system design of a tractor-semitrailer whose tractor and semitrailer will

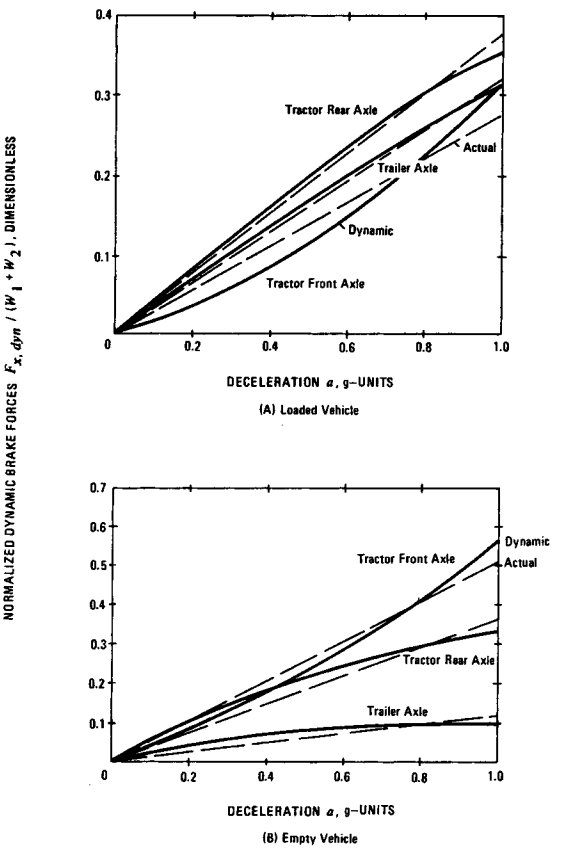

Figure 9-8. Normalized Dynamic Braking Force Distribution

always operate together, and the brake system design of a tractor that will operate with semitrailers having a range of brake force levels.

The fundamental relationships discussed in par. 8-3 apply to proportional braking of tractor-semitrailers. Eqs. 8-49 through 8-51 may be used to determine the dynamic brake force distribution among the individual axles of the combination. The dynamic brake forces of a typical combination vehicle are shown in Fig. 9-8. The actual brake forces for the empty and loaded cases which would best approximate the dynamic forces are illustrated by the broken lines. The curves indicate that for a deceleration of 0.8g the actual brake forces — front to rear — are equal approximately to $0.22W$, $0.30W$, $0.24W$ for the loaded vehicle, and $0.40W_o$, $0.30W_o$, and $0.10W_o$ for the empty vehicle. With a loaded and empty vehicle weight of W = 44,000 lb and W_o = 20,000 lb, respectively, the brake forces for optimum braking at a = 0.80g must be proportioned between 8,000 lb to 9,700 lb on the tractor front axle, 6,000 lb to 13,200 lb on the tractor rear axle, and 2,000 lb to 10,500 lb on the trailer axle to best adjust to the empty and loaded condition. The numbers indicate that, whereas, the dynamic brake force on the front axle varies little with change in vehicle loading, the dynamic brake force on the rear axle of the tractor and on the trailer axle is heavily influenced by the loading condition.

It has been found convenient to implement a variable brake force distribution in articulated vehicles in the manner described here (Refs. 11, 12, and 13). The front axle brake force of the tractor is designed to be proportional to the application valve exit pressure. The application valve is the device by which the driver controls the brake line pressure in the brake system. The brake force at the rear axle of the tractor is determined by the load sensitive proportioning valve. Depending on the design of the proportioning valve of the tractor, the brake torque on the tractor rear axle may vary, e.g., from 60 to 140% of the tractor front axle brake torque. The brake torque on the trailer axle is determined by either a proportioning or limiting valve. Depending on the design of the proportioning valve of the trailer, the brake torque on the trailer axle may vary from 20 to 100% of the front brake torque. It may be sufficient to control the brake force of the trailer axle by a manually or automatically positioned limiting valve which has settings for the empty, half-loaded, and loaded conditions resulting in different limiting brake torque/line pressure relationships on the trailer axle.

The results of the friction utilization calculations carried out for several loading and proportioning valve settings are presented for a 2-S1 tractor-semitrailer combination, i.e., the tractor has two axles, the trailer one axle. The vehicle combination having the baseline friction utilization shown in Figs. 8-31 and 8-32 was analyzed by employing the braking performance calculation program discussed in Chapter 7. The different valve settings corresponding to the following cases were introduced into Eq. 5-31:

1. Case 1. The vehicle combination was loaded to full capacity, and the proportional valve setting on the tractor rear axle and the limiting valve setting on the trailer axle are as shown in Fig. 9-9. The tire-road friction coefficient required to prevent wheel lockup, illustrated in Fig. 9-10, indicates an almost optimum braking of the vehicle.

2. Case 2. Identical to Case 1, except the trailer setting is wrong as indicated by the broken lines in Fig.

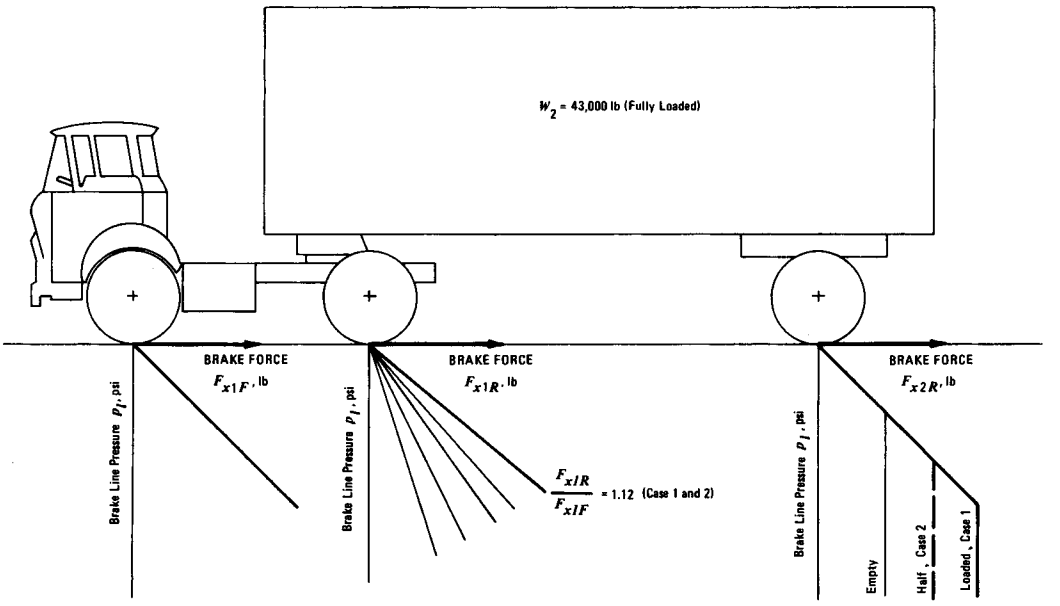

Figure 9-9. Schematic Brake Force Distribution, Cases 1 and 2

9-9. As an inspection of Fig. 9-10 indicates, up to a deceleration of 0.36g the same tire-road friction utilizations exist as in Case 1. For decelerations greater than 0.42g the danger of locking the tractor rear axle first exists resulting in a possible instability of the combination.

3. Case 3. The combination is half-loaded with the proportioning valve settings of the tractor as indicated in Fig. 9-11. The trailer valve setting is for the half-loaded case also. The danger of first wheel lockup of the tractor rear axle exists for decelerations greater than 0.49g below which the front axle is overbraked as illustrated in Fig. 9-12. The trailer tends to lock up for decelerations greater than about 0.32g.

4. Case 4. Identical to Case 3, except the trailer valve is mistakenly set to the empty position as illustrated in Fig. 9-11. As noted from Fig. 9-12, now the tractor rear axle tends to overbrake at decelerations of 0.36g and greater, requiring relatively high coefficients of friction between tire and road.

5. Case 5. For the empty vehicle combination the valve settings are indicated in Fig. 9-13. The tire-road friction utilization is illustrated in Fig. 9-14. The trailer axle tends to overbrake compared to the two other axles for decelerations below 0.53g. For decelerations above 0.53g the tractor rear axle begins to lockup.

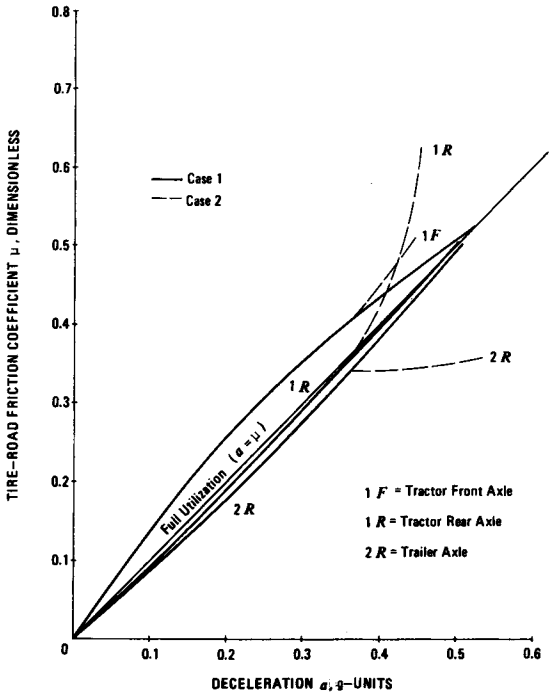

Figure 9-10. Tire-Road Friction Utilization, Cases 1 and 2, W_2 = 43,000 lb

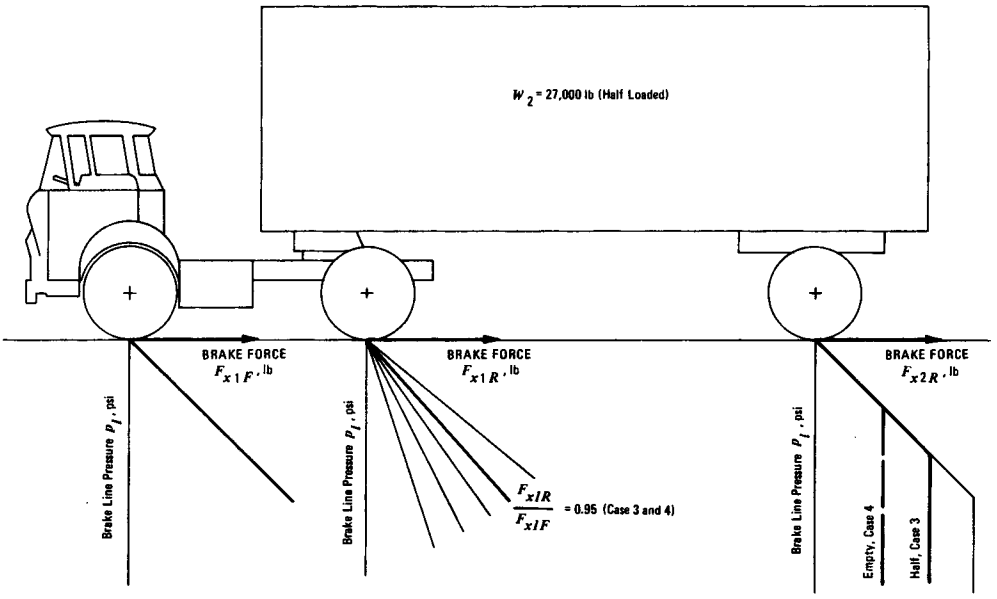

Figure 9-11. Schematic Brake Force Distribution, Cases 3 and 4

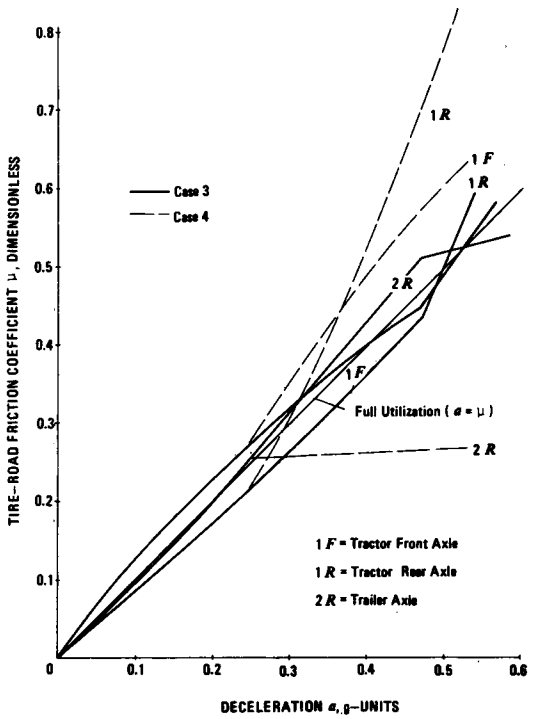

Figure 9-12. Tire-Road Friction Utilization, Cases 3 and 4, W_2 = 27,000 lb

6. Case 6. The empty vehicle combination is braked with valve settings as indicated in Fig. 9-15. The tractor rear axle brake force is set for the loaded condition. The trailer brake force is set for the empty condition. This case illustrates the importance of automatic load-dependent and driver-independent brake torque variation of the tractor rear axle. Examination of the friction utilization diagram shown in Fig. 9-16 indicates that a deceleration of approximately 0.4g tends to be critical with respect to vehicle stability since the tractor rear axle is always overbraked.

7. Case 7. The empty combination vehicle is equipped with the tractor proportioning valve automatically set to the empty position as indicated in Fig. 9-17. The trailer brake force is no longer limited as in previous cases. The trailer brake force is not controlled by a valve. The results of the friction utilization calculations shown in Fig. 9-18 demonstrate an almost optimum braking indicated by the fact that all three curves are close to the optimum or full utilization line.

8. Case 8. The loaded vehicle is braked with the tractor rear axle valve set to the loaded condition. The trailer rear axle is not controlled and produces the brake force illustrated in Fig. 9-19, i.e., the same brake force as in the previous case. As illustrated in Fig. 9-20, the front axle tends to overbrake first for

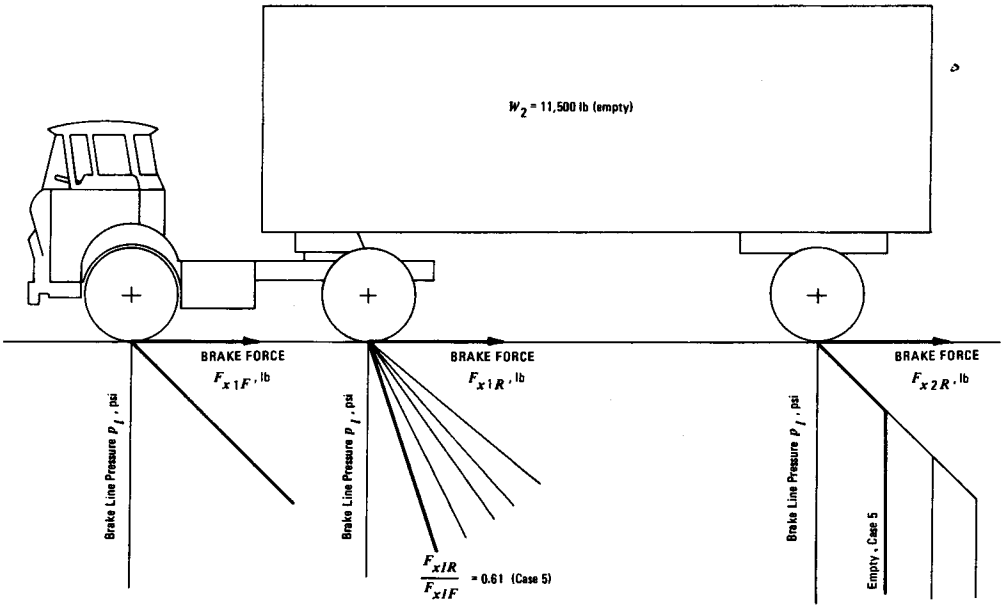

Figure 9-13. Schematic Brake Force Distribution, Case 5

decelerations below 0.43g. Above 0.43g there is a danger of overbraking the tractor rear axle.

Cases 7 and 8 demonstrate that optimum braking conditions (Case 7) for one loading configuration does not necessarily yield acceptable braking conditions for another loading configuration (Case 8). Although the trailer rear axle brake force appears to be optimum for the loaded vehicle combination as illustrated in Fig. 9-19, the tire-road friction utilization is greatly degraded (Fig. 9-20) when compared with the friction utilization for the empty case (Fig. 9-18). The reasons for this are as follows. The trailer brake force for the loaded case is insufficient, resulting in a lower deceleration of the vehicle combination and less dynamic load transfer to the tractor front axle. This condition, however, causes the front wheels to lock prematurely. As deceleration increases, the largest portion of braking is provided by the tractor rear wheels. Since the normal force of the tractor rear axle does not change as much as that of the tractor front axle or trailer axle, the tractor rear axle tends to lockup for higher decelerations (above 0.43g).

The tractor front axle normally is equipped with a brake line pressure regulating valve. Improvement in braking performance can be achieved by means of modulating the brake force of the tractor front axle if

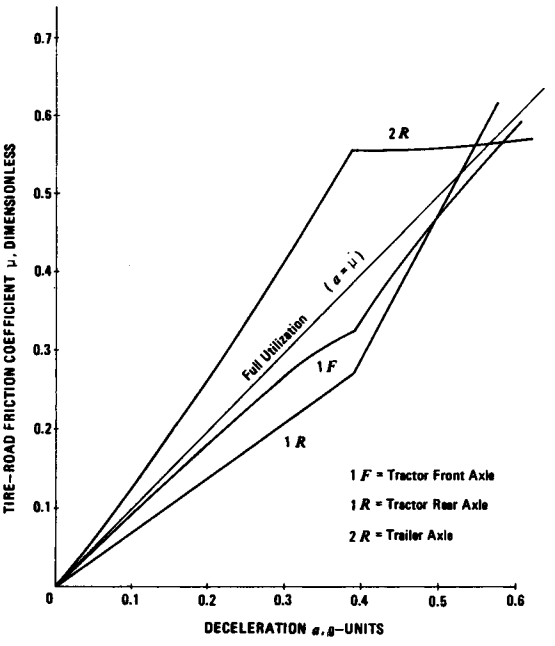

Figure 9-14. Tire-Road Friction Utilization, Case 5, W_2 = 11,500 lb

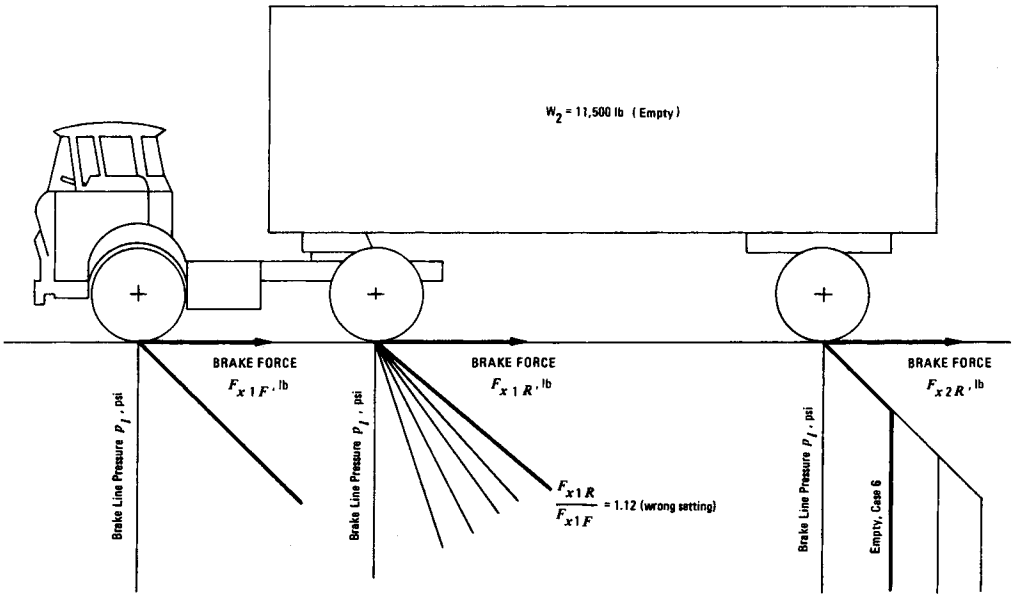

Figure 9-15. Schematic Brake Force Distribution, Case 6

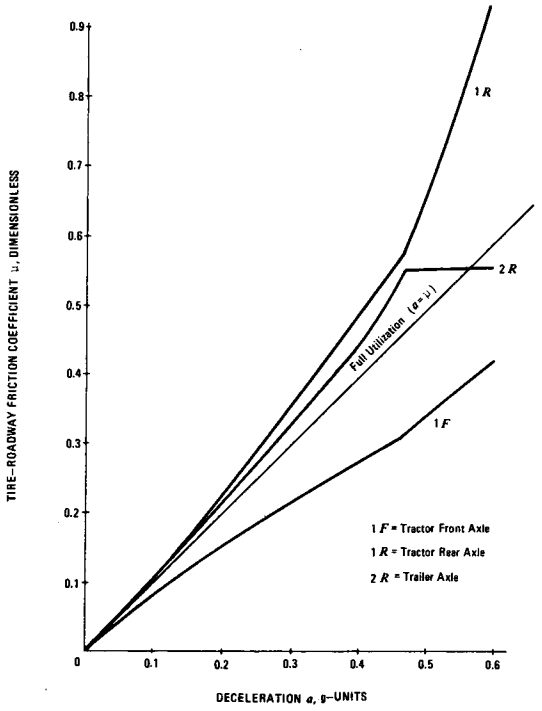

Figure 9-16. Tire-Road Friction Utilization, Case 6, W_2 = 11,500 lb

the static loaded-to-empty axle load ratio of the tractor front axle is greater than 1.4. If the loaded-to-empty ratio is less than 1.4, then only the tractor rear axle must be modulated along with the trailer axle.

Road tests have shown that a proper brake force distribution among the axles of a tractor-semitrailer combination has been achieved when no wheels lock below decelerations of 0.5g with the loaded combination braking on a dry road surface. This brake force distribution generally yields acceptable braking performance with the empty combination. However, if some axle(s) lock below 0.5g, the advantages of load dependent brake force distribution are not fully utilized.

9-2.2 DYNAMIC BRAKE LINE PRESSURES

For a particular vehicle combination, the dynamic brake line pressures may be computed from Eqs. 5-10 or 5-31 and 8-49 through 8-51 when the brake forces of each axle including the trailer are optimized. This results in the following expressions for the dynamic brake line pressures $p_{l,dyn}$ on each axle given here for an air brake system

1. Front axle:

$$p_{l1F,dyn} = \{a[(1 - \psi_1 + a\chi_1) W_1 + (1 - y + az_1) W_2 N]\} \times \{2[A_C \eta_m (BF)(r/R) \rho]_{1F}\}^{-1} + p_{o1F}, \text{ psi} \quad (9\text{-}9)$$

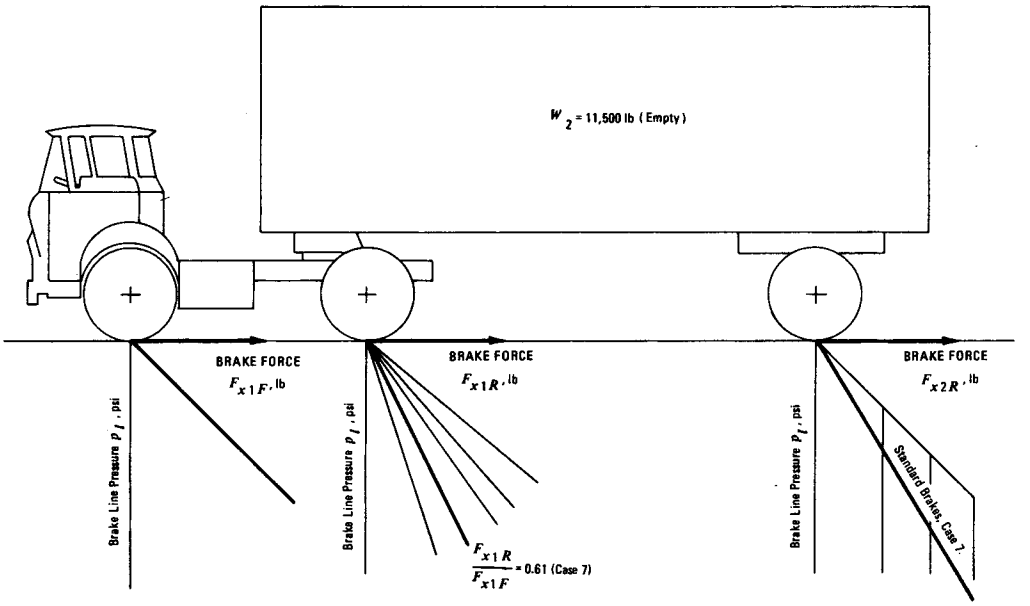

Figure 9-17. Schematic Brake Force Distribution With Proportioning Valves on Tractor Rear and Standard Brakes on Trailer Axle

2. Tractor rear axle:

$$p_{l1R,dyn} = \{a[(\psi_1 - a\chi_1) W_1 + (y - az_1) W_z N]\} \times \{2[A_c \eta_m (BF)(r/R)\rho]_{1R}\}^{-1} + p_{o1R}, \text{ psi} \quad (9\text{-}10)$$

3. Trailer axle:

$$p_{l2R,dyn} = \frac{a(1 - N) W_2}{2[A_C \eta_m (BF)(r/R)\rho]_{2R}} + p_{o2R}, \text{ psi} \quad (9\text{-}11)$$

where

$N = \dfrac{1 - \psi_2 + a\chi_2}{1 + az_2}$, d'less

A_C = brake chamber area, in.^{2}

L_1 = tractor wheel base, in.

L_2 = distance between fifth wheel and trailer axle or trailer base, in.

p_{o1F} = pushout pressure, tractor front brakes, psi

p_{o1R} = pushout pressure, tractor rear brakes, psi

p_{o2R} = pushout pressure, trailer brakes, psi

W_1 = tractor weight, lb

W_2 = trailer weight, lb

y = horizontal distance between tractor front wheels and fifth wheel divided by tractor wheel base L_1, d'less

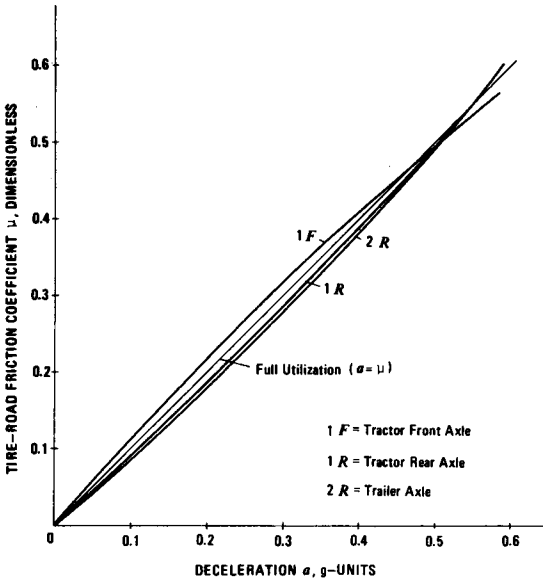

Figure 9-18. Tire-Road Friction Utilization, Case 7, W_2 = 11,500 lb

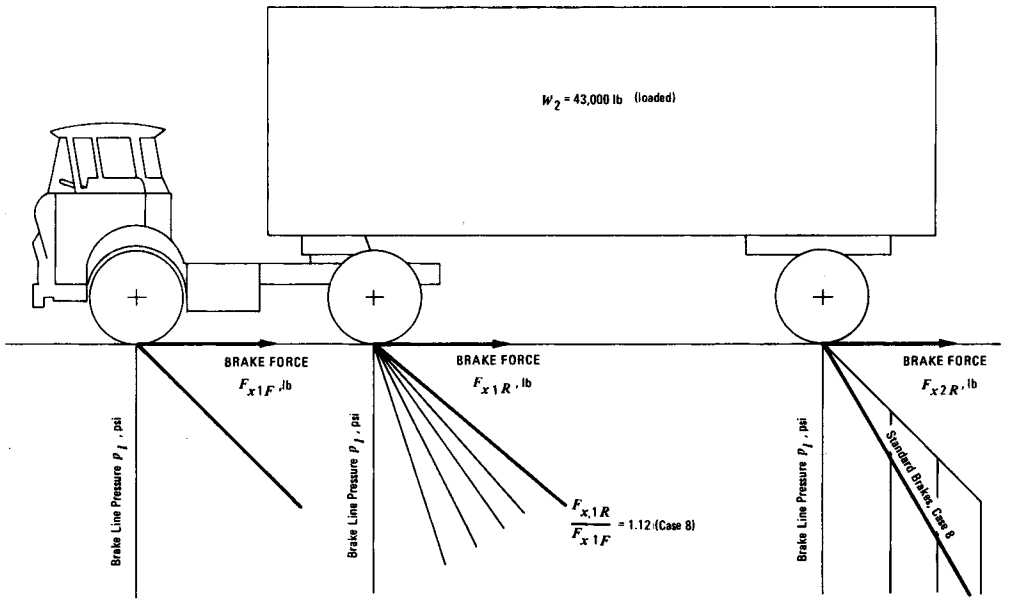

Figure 9-19. Schematic Brake Force Distribution, Case 8

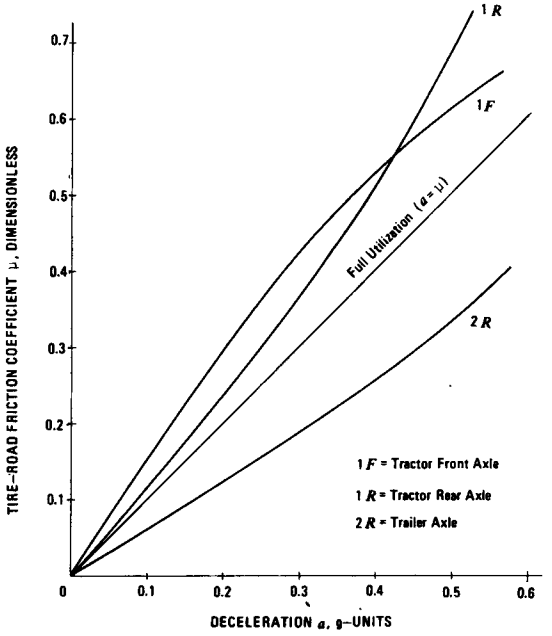

Figure 9-20. Tire-Road Friction Utilization, Case 8, W_2 = 43,000 lb

z_1 = fifth wheel height divided by tractor wheel base L_1, d'less

z_2 = fifth wheel height divided by trailer base L_2, d'less

η_m = mechanical efficiency between brake chamber and brake shoe, d'less

ρ = application gain (lever ratio) between brake chamber and brake shoe, computed from Eqs. 5-32 or 5-33, d'less

χ_1 = tractor center of gravity height divided by tractor wheel base L_1, d'less

χ_2 = trailer center of gravity height divided by trailer base L_2, d'less

ψ_1 = static tractor rear axle load divided by tractor weight (without trailer), d'less

ψ_2 = static trailer axle load divided by trailer weight, d'less

Eqs. 9-9 through 9-11 either may be represented in terms of dynamic pressure versus deceleration or in terms of individual dynamic pressures versus application valve exit pressure. The latter is probably more suited for design purposes. The graphical relationships representing the actual brake line pressures delivered to the brake chambers of different axles are an effective means for obtaining the desired proportioning valve control range on each axle.

If a proportioning device is to be installed into a tractor brake system and if the loading and brake force levels of the trailer are specified, i.e., a given

trailer is to be connected to a tractor, the dynamic brake line pressures on the tractor may be obtained by means of Eqs. 5-31, 8-52, and 8-53 yielding the following expressions

1. Tractor front axle:

$$p_{l1F,dyn} = [a\,W_1(1 - \psi_1 + a\chi_1) + (a\,W_2 - F_{x2R})(1 - y + az_1)] \times \{2[A_c\,\eta_m\,(BF)\,(r/R)\,\rho]_{1F}\}^{-1} + p_{o1F}\ , \text{psi} \quad (9\text{-}12)$$

2. Tractor rear axle:

$$p_{l1R,dyn} = [a\,W_1\,(\psi_1 - a\chi_1) + (a\,W_2 - F_{x2R})\,(y - az_1)] \times \{2[Ac\,\eta_m\,(BF)\,(r/R)\,\rho]_{1R}\}^{-1} + p_{o1R}\ , \text{psi} \quad (9\text{-}13)$$

where

F_{x2R} = trailer axle brake force, lb

The graphical representation of Eqs. 9-12 and 9-13 for typical tractor and trailer data is shown in Fig. 9-21 for several loading conditions. The curves presented in Fig. 9-21 may be used to design the variable brake force distribution of the tractor. When a proportional ratio between front and rear is decided upon for a given trailer brake force level, the braking performance calculation program of Chapter 7 may be employed as a final check on the adequacy of the variable braking ratio chosen.

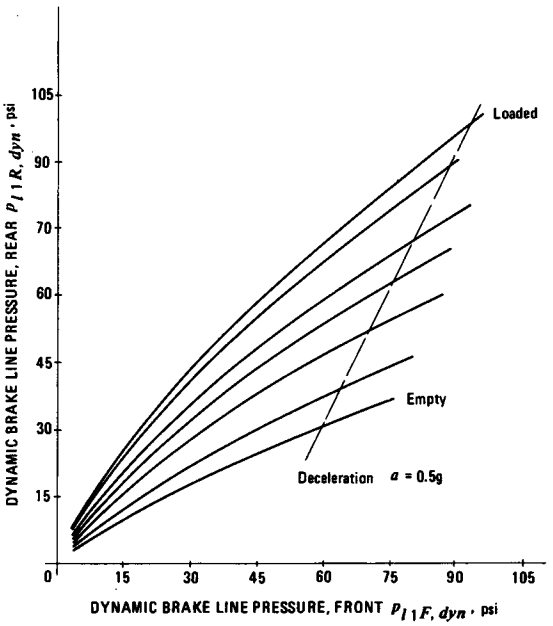

Figure 9-21. Dynamic Brake Line Pressures for the Tractor of a Tractor-Semitrailer Combination

9-2.3 PRESSURE VARIATION AS A FUNCTION OF SUSPENSION DEFLECTION

The load sensitive variation of the ratio of the brake line pressures — tractor rear axle to tractor front axle — i.e., p_{l1R}/p_{l1F} or the variation of the relative tractor rear axle brake force ϕ_{1R} with respect to the total brake force of the combination may be obtained directly as a function of the tractor rear axle suspension deflection which is a direct measure of tractor axle loads. The values for the variation of p_{1R}/p_{1F} and the relative tractor rear axle brake force ϕ_{1R} are shown in Fig. 9-22 as a function of the rear suspension deflection for a standard and heavy duty suspension.

9-2.4 TWO-AXLE TRACTOR COUPLED TO A TRAILER EQUIPPED WITH TWO-ELLIPTIC LEAF SPRING SUSPENSION

Two-elliptic leaf spring suspensions commonly in use on heavy trailers distribute the tandem axle loads during braking by decreasing the normal force on the forward axle and increasing the normal force on the rearward axle of the tandem suspension. Road tests and computations have shown that the axle load on the tandem forward axle of two-elliptic leaf spring suspension for the empty vehicle may decrease to zero for decelerations between 0.5 and 0.6g. The axle load of the tandem rearward axle decreases due to the load transfer to the tractor but increases again due to load transfer within the tandem suspension. For example, a static tandem axle forward load of 5,255 lb may decrease to 3,344 lb at a deceleration of 0.3 g; the static tandem axle rearward load of 5,255 lb may increase to 6,536 lb for 0.3g. Examination of these numbers indicates that a load of 630 lb was transferred to the tractor; that the tandem forward axle load decreased by 1,911 lb; and the tandem rearward axle load increased by 1,281 lb. In designing the proportioning characteristic for individual axles, the change in axle loads within a tandem axle as well as

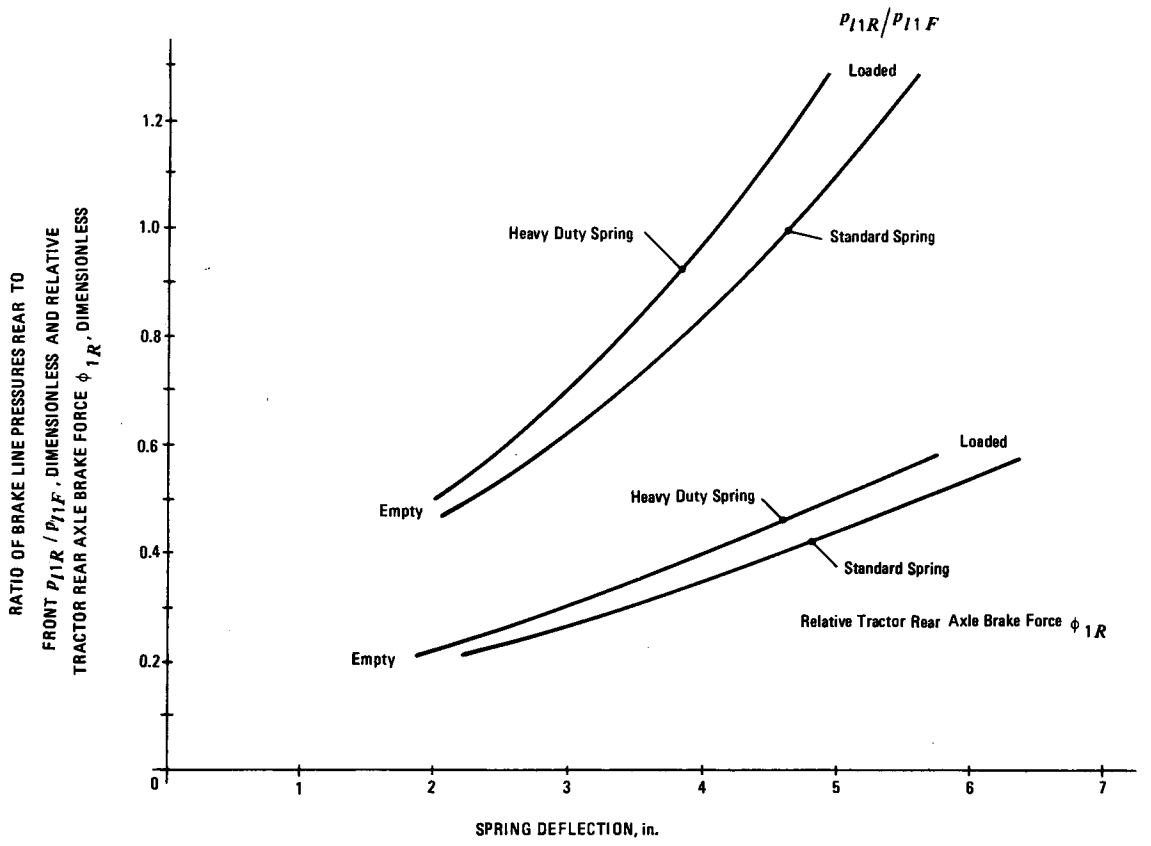

Figure 9-22. Brake Line Pressure Variation as Function of Spring Deflection on Trailer Axle

load transfer from a tandem axle must be considered. The variable brake force distribution analysis of a 2-S2 tractor-semitrailer combination with the trailer equipped with a two-elliptic leaf spring suspension is in large part identical to the analysis presented in par. 9-2.1 for single axle trailers connected to two-axle tractors. The only difference is the additional proportioning of the brake line pressures supplied to the tandem forward and rearward axles in accordance with the different dynamic axle loads of those axles. No detailed discussion of this facet of proportional braking is presented here. The paragraph that follows will present the results of a proportional braking analysis of a trailer equipped with a two-elliptic leaf spring suspension coupled to a tandem axle tractor.

9-2.5 THREE-AXLE TRACTOR EQUIPPED WITH WALKING BEAM SUSPENSION COUPLED TO A TRAILER EQUIPPED WITH TWO-ELLIPTIC LEAF SPRING SUSPENSION

The tire-road friction utilization calculations were carried out by means of the braking performance calculation program described in Chapter 7. The equations for the axle loads as a function of vehicle deceleration — described in Chapter 8 — were used in the computations. The important vehicle data are presented in Table 9-1.

The results of the tire-road friction calculations for the vehicle combination equipped with standard brakes (Table 9-1 data) are presented in Figs. 9-23

TABLE 9-1
TRACTOR-SEMITRAILER DATA

Tractor:	W = 16,180 lb
	L_1 = 160 in.
	χ_1 = 0.22, d'less
	ψ_1 = 0.40, d'less
Trailer:	W_2 = 15,950 lb (empty); 62,820 lb (loaded)
	L_2 = 391 in.
	χ_2 = 0.154 (empty and loaded), d'less
	ψ_2 = 0.58 (empty); 0.57 (loaded), d'less
Brakes:	No brakes on tractor front axle
	Tractor tandem axle
	A_C = 30 in.^{2}; BF = 2.3, d'less (unfaded)
	ρ = 5.5, d'less
	r = 8.25 in.
	η_m = 0.70, d'less
	Trailer tandem axle
	Identical to tractor brakes except
	BF = 1.9, d'less (unfaded)
Tire Radius:	R = 21 in.

and 9-24 for the empty and loaded vehicle, respectively. Examination of the curves for the empty case shown in Fig. 9-23 indicates that the tandem forward axle of the trailer overbrakes for deceleration below 0.32g. The tandem forward axle of the tractor (1*RF*) shows good friction utilization values over a wide range of decelerations. The tandem forward axle of the trailer (2*RF*) and the tandem rearward axle of the tractor (1*RR*) behave in an almost identical fashion. The tandem rearward axle of the trailer is slightly overbraked.

The results of the tire-road friction calculations obtained with the loaded vehicle combination are presented in Fig. 9-24. Inspection of Fig. 9-24 indicates that the tandem rearward axle of the tractor is overbraked for decelerations below 0.30g. For higher decelerations the tandem forward axle of the trailer is overbraked. The tractor tandem forward axle shows good friction utilization values. The tandem rearward axle of the trailer is underbraked for all deceleration levels.

Major portions of braking and tire side forces must be produced by the tandem forward axle of the tractor and the tandem rearward axle of the trailer due to decrease in axle loading on the other tandem axles. A comparison of the tire-road friction curves of Fig. 9-24 of the loaded vehicle with the curves of Fig. 9-23 of

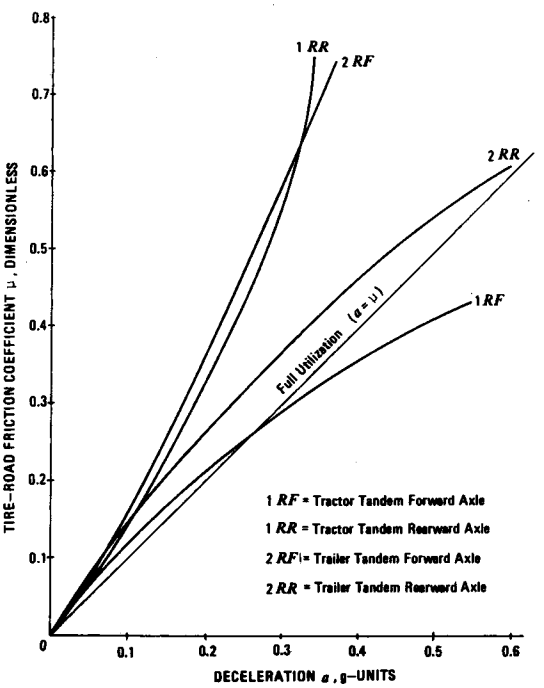

Figure 9-23. Tire-Road Friction Utilization for 3-S2 Tractor-Semitrailer Combination (Empty) With Standard Brakes (No Front Brakes)

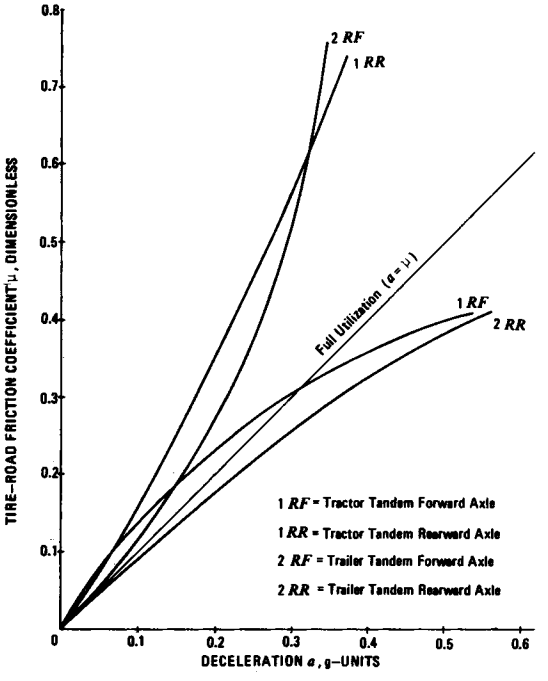

Figure 9-24. Tire-Road Friction Utilization for 3-S2 Tractor-Semitrailer Combination (Loaded) With Standard Brakes (No Front Brakes)

the empty vehicle indicates that the tandem rearward axle of the trailer is overbraked in the empty condition. To avoid possible trailer swing due to premature wheel lock of the critical tandem rearward axle of the trailer, load sensitive proportioning must reduce the brake force concentrated on the tandem rearward axle of the trailer. The relative brake force distribution ϕ_i of the standard brake system — front to rear — is 27%, 27%, 23%, and 23%. The results of the proportioning analysis for the empty vehicle are illustrated in Fig. 9-25. The proportional brake force distribution ϕ_i — front to rear — is 40%, 20%, 20%, and 20%. Inspection of Fig. 9-25 indicates that the tandem forward axle of the tractor is overbraked for decelerations below 0.17g. However, the tandem rearward axle of the tractor is slightly underbraked for decelerations below 0.17g resulting in sufficient side force capacity on the tractor tandem axle to prevent jackknifing. The tandem rear axle of the trailer is braked near optimum over a wide range of deceleration values providing sufficient trailer axle side forces to prevent trailer swing. The tandem forward axle of the tractor shows improved friction utilization values with the proportioning chosen in the example.

No major improvements in tire-road friction utilization may be expected from a different proportional brake force distribution without installing brakes on the tractor front axle. The effects of tractor front axle braking for a proportional brake force distribution ϕ_i = 17%, 25%, 20%, 19%, and 19% are illustrated in Fig. 9-26 for the empty vehicle. Examination of Fig. 9-26 indicates that the tandem forward axle of the tractor and tandem rearward axle of the trailer — both critical to vehicle combination stability — are near optimum for deceleration below 0.3g and are slightly (2*RR*) and moderately (1*RF*) underbraked for greater decelerations. The tractor front axle always is underbraked.

9-3 CONCLUDING REMARKS ON VEHICLES EQUIPPED WITH VARIABLE RATIO BRAKING SYSTEMS

Variable ratio braking systems represent an improvement over those with a fixed ratio brake force distribution for vehicles which experience a significant shift in center of gravity location due to loading. If the center of gravity location remains the

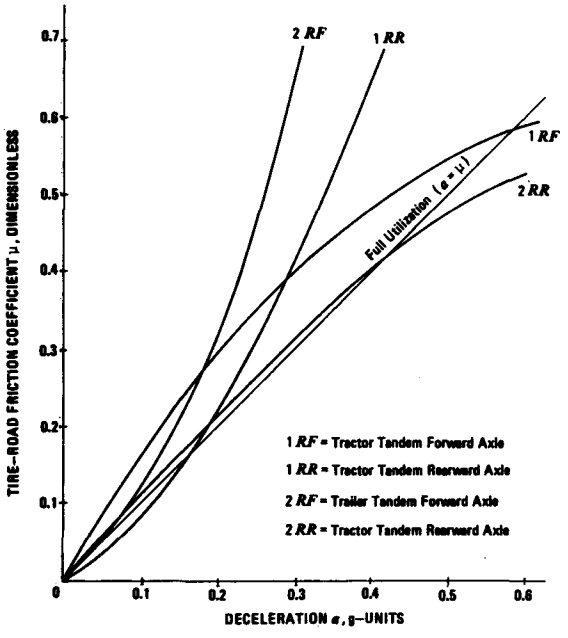

Figure 9-25. Tire-Road Friction Utilization for 3-S2 Tractor-Semitrailer (Empty) With Proportioning (No Front Brakes)

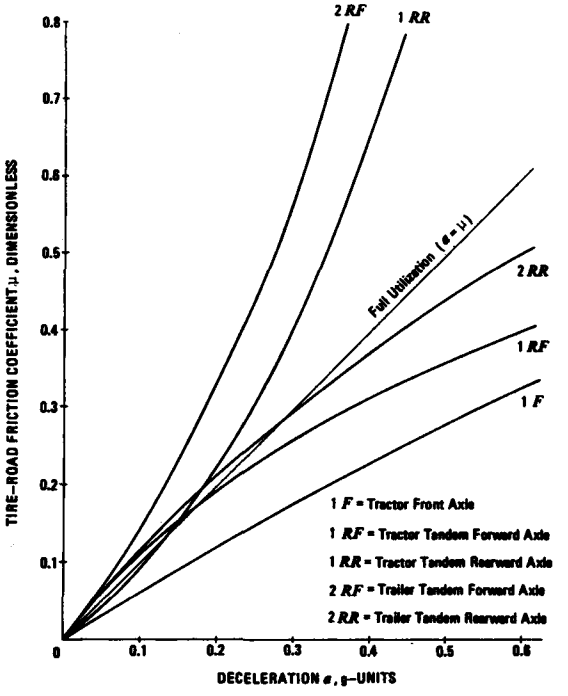

Figure 9-26. Tire-Road Friction Utilization For 3-S2 Tractor-Semitrailer (Empty) With Front Brakes and Proportioning

same for the empty and loaded case, then no increased tire-road friction utilizations can be achieved through a variable ratio braking. Since proportioning systems involve the reduction in brake line pressure for a given pedal force, the pedal force/deceleration gains for the empty and loaded conditions are not changed significantly. Constant or near constant pedal force/deceleration gains, however, mean better braking without requiring increased driver skills.

In general, the advantages of a load sensitive variable ratio braking system in good mechanical condition are:

1. Shorter stopping distance
2. Less driver fatigue
3. Less tire wear
4. Improved wheel lock sequence and vehicle stability
5. Smaller tongue or kingpin forces regardless of loading condition.

Because proportional systems are implemented by making the brake line pressure a nonlinear function of the pedal force rather than a function of the actual wheel angular rotation or the friction coefficient between tire and road, it is still possible to lock the wheels, especially on low friction road surfaces. Proportional systems provide a brake force distribution that matches a wide range of load and road surface conditions, but they are still subject to some of the basic limitations of systems with fixed brake force distribution.

REFERENCES

1. "Braking Proportional to Load", *Automobile Engineer*, Vol. 55, No. 12, November 1965, pp. 491-93.
2. H. Strien, "Brake Force Distribution on Passenger Cars", *Automobiltechnische Zeitschrift*, Vol. 67, No. 8, pp. 240-45.
3. R. T. Eddy and R. A. Wilson, *An Approach to Load Sensing Brake Proportioning for Passenger Cars and Light Trucks*, SAE Paper No. 660411.
4. E. L. Cornwell, "Automatic Load-Sensitive Air Brake Control", *Mod. Transp.*, Vol. 94, No. 2416, 1965, pp. 8-9.
5. A. Furia, S. Chachter, and P. Gancel, *Trends in Braking Techniques of European Vehicle*, SAE Paper No. 670505, May 1967.
6. C. Eaton and J. Schreur, *Brake Proportioning Valve*, SAE Paper No. 660400, June 1966.
7. F. E. Lueck, W. A. Gartland, and M. J. Denholm, *Proportioning Valve to Skid Control – A Logical Progression*, SAE Paper No. 690456, 1969.
8. H. Oberthuer and F. Baum, "Brake Force Distribution on Hydraulic Vehicle Brakes", *Automobiltechnische Zeitschrift*, Vol. 66, No. 8, 1964, pp. 222-225.
9. R. Limpert and Ch. Y. Warner, *Proportional Braking of Solid Frame Vehicles*, SAE Paper No. 710046, January 1971.
10. R. Limpert, et al., *Analysis, Design and Testing of Two-Way Proportioning for Improved Braking in a Turn*, SAE Paper No. 760347, February 1976.
11. M. Mitschke and D. Runge, "Load Dependent Brake Force Modulation on Tractor-Semitrailers", *Automobiltechnische Zeitschrift*, Vol. 68, No. 2, pp. 50-55 and Vol. 68, No. 7, pp. 253-56.
12. G. Mueller, "Improved Safety in Braking of Tractor-Semitrailers and Truck-Trailer Combinations", *Automobiltechnische Zeitschrift*, Vol. 62, No. 7, 1960, pp. 194-95.
13. G. Fritzsche, "Static Modulation of the Brake Forces on Motor Vehicles and Trailers According to Load and Deceleration", *Automobiltechnische Zeitschrift*, Vol. 61, No. 8, 1959, pp. 219-24.

CHAPTER 10
WHEEL-ANTILOCK BRAKE SYSTEMS

In this chapter the fundamentals of wheel-antilock brake systems are presented. Antilock brakes of hydraulic and pneumatic brake systems are discussed. Typical test results are presented.

10-0 LIST OF SYMBOLS

c_1 = time constant indicating pressure decrease characteristic, s^{-1}
c_2 = time constant indicating pressure increase characteristic, s^{-1}
c_3 = time constant indicating pressure increase characteristic, s^{-1}
F_z = tire normal force, lb
I_W = mass moment of inertia of wheel, lb·in.·s^2
k = brake torque versus time, slope, lb·in./s
m = factor characterizing deceleration increase with time, ft/s^3
p_a = applied pressure, psi
p_l = brake line pressure, psi
p_{max} = maximum brake line pressure, psi
p_z = brake line pressure just below wheel lockup pressure, psi
R = tire radius, in. or ft
s = tire slip, d'less*
s_P = tire slip at peak friction, d'less
T = brake torque, lb·in.
T_4 = difference between time t_4 and time associated with a pressure increase from zero pressure, s
T_5 = difference between t_5 and time associated with a pressure increase from zero pressure, s
t = time, s
t_h = hold time during which pressure is held constant, s
t_P = time required by wheel to attain maximum friction force, s
t_S = time required by wheel to move from maximum friction to sliding friction conditions, s
t_1 = time at which antiskid signal is received by brake pressure modulator, s
t_2 = time at which maximum brake line pressure is reached and pressure decrease begins, s
t_3 = time at which wheel speed attains specified value, s
t_4 = time at which pressure increase begins, s
t_5 = time at which pressure increase begins, s
V = vehicle speed, ft/s
α_r = specified angular deceleration, rad/s^2
α_P = wheel angular deceleration at which maximum braking force is attained, rad/s^2
μ = tire-road friction coefficient, d'less
μ_P = peak tire-road friction coefficient, d'less
μ_S = sliding tire-road friction coefficient, d'less
τ_1 = response time, s
τ_2 = response time, s
ω = angular velocity, rad/s
ω_c = specified angular velocity, rad/s
ω_o = initial wheel angular velocity, rad/s
ω_P = angular velocity of wheel at peak friction, rad/s

*d'less = dimensionless

10-1 FUNDAMENTALS ASSOCIATED WITH ANTILOCK BRAKE SYSTEM ANALYSIS

Wheel-antilock brake systems prevent the wheels from locking up during braking by adjusting the braking effort to the traction force available at the tire-roadway interface. Under normal braking conditions the driver operates the brakes as usual; however, on slippery roadways or during severe braking, as the driver causes the wheels to approach lockup, the device takes over and modulates the brake force independent of pedal force.

In general, wheel-antilock brake systems should provide the following:

1. Prevention of wheel lockup for all braking, loading, and road surface conditions
2. Minimum stopping distance
3. Vehicle stability and retention of steering and controllability.

Tests using wheel-antilock devices on dry pavement have demonstrated that, in some instances, a slight increase in stopping distance results, while in other cases a slight decrease in stopping distance is noted. However, wheel-antilock braking systems contribute considerably to the improvement of vehicle directional stability during braking. Skidding in normal cornering maneuvers is prevented by the lateral friction forces in the tire-road contact area. During

braking, the capability of the tire to produce lateral friction forces is somewhat decreased, as is shown for a typical tire in Fig. 6-1. Note that this capability to produce lateral forces is a minimum when the wheel is locked. The antilock system keeps the tire slip at relatively low values during braking, which in turn allows the tire to produce lateral forces adequate to maintain vehicle directional stability.

The design of a wheel-antilock system begins with a complete understanding of the tire-roadway friction characteristic. The braking process would be optimum if the slip of the braked wheel could always be kept at values corresponding to maximum friction forces. Ideally then, a sensor would detect the magnitude of the coefficient of friction at the tire-roadway interface under all possible conditions, and the rest of the brake system will use this signal to modulate the brake torque in such a manner that the maximum friction coefficient is used throughout the braking process.

In general, the following methods have been suggested as modulating parameters for the automatic control of brake torque:

1. Angular velocity of the wheel
2. Brake slip of the wheel
3. Velocity difference between wheel and vehicle
4. Velocity difference between the wheel and the other wheels of the vehicle.

In practice, it is not feasible to detect directly the friction coefficient or the relative slip since this would require a fifth wheel as employed in road-friction measuring equipment. Practical sensors attempt to measure wheel angular velocity. The relative tire slip ratio then is estimated by comparing a measured wheel velocity with a "memory" of the vehicle velocity before initiation of braking.

The memory usually consists of a flywheel in the case of mechanical systems or a capacitor for electrical systems. The design of the memory requires extensive knowledge on the friction-slip curve expected during braking. If the expected friction-slip characteristics are different from those actually occurring at the tire-roadway interface, the braking process may not result in minimum stopping distance.

In most antilock braking systems the brake line pressure is regulated to prevent wheel lockup and the standard brake system remains intact. For practical cases, the wheel angular velocity is measured and from this the angular deceleration is determined electronically. If the wheel approaches lockup conditions, the angular velocity beings to decrease sharply and the angular deceleration to increase. At the instant the wheel angular deceleration exceeds a predetermined threshold value, the electronic unit causes the brake line pressure regulating valve after a response time of the electronic unit as well as the regulating valve has elapsed to decrease line pressure. The decrease in brake line pressure causes the angular velocity of the wheel to increase again, accompanied by a decrease of angular deceleration below the threshold value. In the next phase the electronic unit causes the brake line pressure to be reapplied with subsequent decrease in angular velocity of the wheel and the cycle repeats itself.

For the basic understanding of the factors associated with a locking wheel, some important equations are discussed next.

The analysis and evaluation of wheel-antilock brake systems presents a certain challenge to the automotive engineer. Other vehicle parameters — such as tire and driver characteristics, road surface, and type of maneuver — may affect significantly the performance of the antiskid system. However, certain physical aspects are common to all designs. For this reason, a somewhat simplified approach is discussed that will indicate the importance of the individual parameters affecting antiskid performance (Ref. 1).

The following relationships must be considered in the analysis of a locking wheel:

1. The equations of motion of the wheel which include rotational inertias of wheel and connected components, brake torque, circumferential force at the tire-road interface, and normal tire force
2. The circumferential force determined by the friction slip characteristics which contain the relationship between translatory and rotational motions of the wheel, as well as the tire and road design factors
3. The pedal force or brake torque time histories affecting antiskid performance
4. The equations of motion of the entire vehicle yielding the time dependent vehicle and wheel decelerations
5. As a result of vehicle decelerations, the tire normal force that changes as a function of time.

The listing indicates the mathematical process to be a complicated matter. For purposes of evaluating the requirements of antiskid control systems, certain simplifications may be introduced without limiting the analysis too much, namely:

1. Since the locking of a wheel occurs during a relatively short period of time, the translatory deceleration may be assumed to be zero, i.e., vehicle velocity equals a constant.
2. The tire normal force remains constant.
3. The friction slip curve may be expressed by a bilinear relationship as shown in Fig. 10-1. The

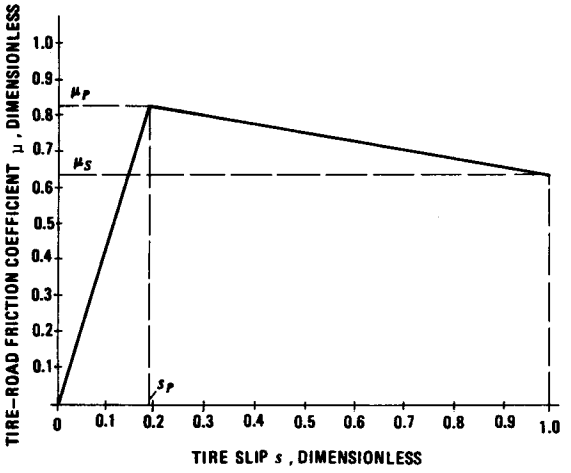

Figure 10-1. Idealized Tire-Road Friction Slip Characteristics

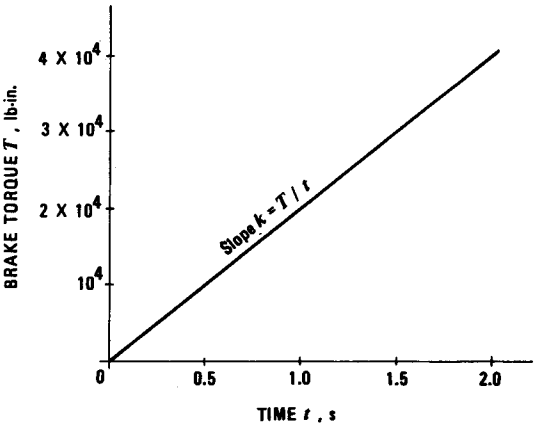

Figure 10-2. Brake Torque Rate — Induced by Driver

solutions to the problem are then given for each linear region of tire slip.

4. Tire transient effects are neglected. This is to say that tire forces are produced instantaneously and do not require a certain fraction of wheel rotation before forces are produced.

5. Brake torque rate is idealized as shown in Fig. 10-2.

An important consideration in the design of antilock brake systems is the determination of the time required by the braked wheel to attain its maximum braking force and the determination of the angular deceleration of the wheel operating at maximum brake force. Furthermore, it is necessary to determine the time required by the wheel to move from maximum brake force conditions at optimal slip to sliding conditions or 100% slip. In order for an antilock device to prevent wheel lock, the system must respond and regulate brake line pressure in a time less than that required for wheel lockup to occur.

The time t_P required to attain the peak tire friction value — a function of wheel inertia, initial wheel velocity, peak friction value and associated tire slip level, tire normal force, effective tire radius, and brake torque rate — may be expressed as (Ref. 1)

$$t_P = \frac{s_P I_W \omega_o}{\mu_P F_z R} + \frac{\mu_P F_z R}{k}, \text{s} \qquad (10\text{-}1)$$

where

F_z = tire normal force, lb
I_W = mass moment of inertia of wheel, lb·in.·s²
k = brake torque versus time, slope, lb·in./s
R = tire radius, in.
s_P = tire slip at peak friction, d'less
μ_P = peak tire-road friction coefficient, d'less
ω_o = initial wheel angular velocity, rad/s

The wheel angular deceleration α_P at which maximum braking forces are produced is called threshold deceleration and may be computed by

$$\alpha_P = \frac{\omega_o k s_P}{\mu_P F_z R}, \text{rad/s}^2 \qquad (10\text{-}2)$$

For the second linear region of Fig. 10-1 during which the wheel approaches lockup, the tire-road sliding friction coefficient μ_S affects the time required for the wheel to attain lockup. The time t_S required by the wheel to approach lockup, i.e., for the tire slip to move from peak value s_P to sliding value (100% slip) is determined approximately by (Ref. 1)

$$t_S = \left\{ \left[\frac{s_P I_W \omega_P}{(\mu_P - s_P \mu_S) F_z R} \right]^2 + \frac{2 \mu_P I_W \omega_P}{k(\mu_P - s_P \mu_S)} \right\}^{1/2} - \frac{s_P I_W \omega_P}{(\mu_P - s_P \mu_S) F_z R}, \text{s} \qquad (10\text{-}3)$$

where

μ_S = sliding tire-road friction coefficient, d'less
ω_P = angular velocity of wheel at peak friction, rad/s

As mentioned earlier, most antiskid control systems use a specific wheel angular deceleration threshold value beyond which the system automatically reduces the brake torque in order to prevent wheel lockup. Consequently, two significant parameters may be considered, namely, (a) the wheel angular deceleration α_P as determined by Eq. 10-2 at which time the maximum tire friction level is attained, and (b) the time t_S required by the wheel to attain lockup conditions. In order to prevent wheel lockup, the antiskid control system has to respond in a time less than the lockup time as determined by Eq. 10-3.

The threshold angular deceleration is a function of tire normal force, effective tire radius, initial vehicle velocity, increase in friction force as determined by the tire-slip curve, and the brake torque rate as determined by the pedal force application rate and brake system dynamics.

It is obvious that the design threshold value may vary widely depending upon the operating conditions. For example, for a tire-normal force of 1,000 lb and tire radius of 1 ft, the following ranges may be obtained for automotive brakes: initial vehicle forward speed between 30 and 150 ft/s, brake torque rate between 8,000 and 40,000 lb·in./s, friction slip curves having between 1 and 7 for the ratio of peak friction coefficient to associated slip value for icy and dry road surfaces, respectively. If these extreme values are used in Eq. 10-2, a ratio of maximum-to-minimum angular deceleration threshold values of 175 is possible. This indicates that the optimum threshold value for one set of driving conditions may be as much as 175 times greater than the optimum value for another set of conditions. In order to reduce this large difference, certain reasonable and practical operational constraints may be introduced. For example, when braking on dry or wet roads at high speeds, a careful and hence slower pedal force application rate yields a decreased range of threshold values. Similarly, when braking on icy roads, lower speed as well as careful braking also will reduce the difference between maximum and minimum threshold values. For these conditions of practical constraints the design threshold angular deceleration as computed by Eq. 10-2 is approximately equal to 40 rad/s^2 (Ref. 1).

As an inspection of Eq. 10-3 indicates, the time for a given wheel operating under certain conditions to move from peak to sliding friction varies with the angular velocity ω_P existing at peak tire-road friction. The time typically ranges between a few hundredths to a tenth of a second.

It is apparent from the previous discussion that the operating conditions significantly affect braking performance, especially in terms of the design threshold values of wheel angular deceleration. However, the driver controlled inputs to the braking system and the initial speed are to a large measure outside the control of the brake system design engineer. Consequently, control systems designed for optimum operation in one situation may result in below optimum performance in a different situation. This performance difference is more pronounced for control systems having a low cycle rate as exhibited by vacuum-assisted brake systems. This mismatch of control rate is more pronounced when braking on split-coefficient or intermittently changing friction surfaces (Refs. 2, 3, 4, and 5). Split-coefficient surfaces involve different friction coefficients under the left tires than under the right. This condition may exist when portions of roadway are covered with ice and others are dry. Intermittently changing friction surfaces involve different tire-road friction coefficients in the direction of vehicle travel.

It is apparent from the previous discussion that wheel-antilock brake systems must be designed to respond within the time limits set by the braked tire. Research studies have shown that vacuum power sources for brake-valve actuation nearly always lead to less than optimum performance when braking on dry road surfaces (Refs. 5, 6, and 7). Reasons for this are related to the slow response generally exhibited by vacuum-actuated valves. Actual wheel-antilock systems can only approach the friction slip curve existing at the tire-road interface. In addition, the pressure regulating valve and associated components possess certain response times that affect system performance.

Some details associated with the analysis of the wheel-antilock control of an air brake system and in particular the brake line pressure regulation as a function of time $p_l = f(t)$ will be discussed next.

The time dependent behavior of vehicle speed V and tire circumferential speed $R\omega$ are illustrated schematically for an air brake system in Fig. 10-3(A). The angular velocity of the wheel is designated by ω, the tire radius by R measured in ft. Shown in Fig. 10-3(B) are the characteristics of brake line pressure p_l as a function of time during the wheel-antilock control process.

As the angular velocity and thus tire circumferential speed $R\omega$ begins to decrease more than the vehicle forward speed V and reaches a point corresponding to the design threshold angular deceleration α_P, the brake line pressure regulating valve receives a signal at time t_1, to reduce the pressure. After the response time τ_1 has elapsed, the pressure

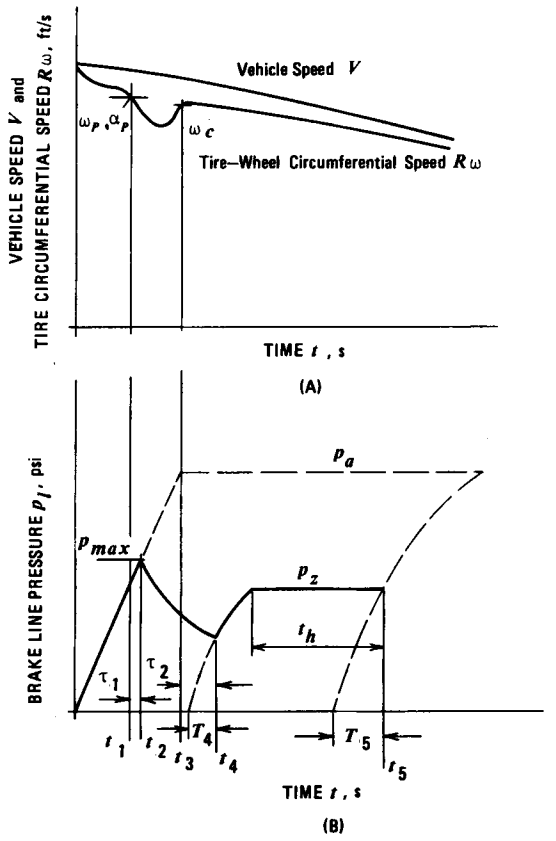

Figure 10-3. Wheel-Antilock Control for an Air Brake System

begins to decrease at time t_2 according to the functional relationship (Ref. 8)

$$p_l = p_{max}\exp[-c_1(t-t_2)] \text{ , psi} \qquad (10\text{-}4)$$

where

c_1 = time constant indicating pressure decrease characteristic, s^{-1}
p_{max} = maximum brake line pressure, psi
t = time, s
t_2 = time at which maximum brake line pressure is reached and pressure decrease begins, s

The decrease in brake pressure causes the angular velocity of the wheel to increase again (Fig. 10-3(A)). Parallel to this process an angular velocity ω_c is computed from a specified angular deceleration α_r and from the angular velocity ω_P of the wheel at the instant the threshold value α_P was exceeded as

$$\omega_c = \omega_P + \alpha_r(t - t_1) \text{ , rad/s} \qquad (10\text{-}5)$$

where

t_1 = time at which antiskid signal is received by brake pressure modulator, s
α_r = specified angular deceleration, rad/s^2
ω_P = wheel angular velocity at peak friction value, rad/s

When the actual angular speed of the wheel has attained the computed value ω_c at time t_3, the brake line pressure regulating valve receives the signal to increase pressure again. After the response time τ_2 has elapsed, the brake line pressure begins to increase at time t_4 according to

$$p_l = p_a\{1 - \exp[-c_2(t - t_4 + T_4)]\} \text{ , psi} \qquad (10\text{-}6)$$

where

c_2 = time constant indicating pressure increase characteristic, s^{-1}
p_a = applied pressure, psi
T_4 = difference between time t_4 and time associated with a pressure increase from zero pressure, s
t_4 = time at which pressure increase begins, s

The brake line pressure p_l is increased only to a pressure p_z and always remains below the applied pressure p_a. The brake line pressure p_z is generally somewhat smaller than the pressure that causes lockup to occur. However, if the wheel tends to lock up again at a pressure equal to or lower than p_z, the previous pressure decreasing and increasing processes are repeated until a pressure p_z is produced that does not cause wheel lockup to occur. This brake line pressure is kept constant until the hold time t_h has elapsed after which the pressure is increased again toward the applied pressure p_a to allow the wheel-antilock braking system to adjust the braking effort to a different tire-road friction situation that might have developed during the hold time t_h. The pressure increases toward p_a according to the approximate relationship

$$p_l = p_a\{1 - \exp[-c_3(t - t_5 + T_5)]\} \text{ , psi} \qquad (10\text{-}7)$$

where

c_3 = time constant indicating pressure increase characteristic, s^{-1}
T_5 = difference between time t_5 and time associated with a pressure increase from zero pressure, s
t_5 = time at which pressure increase begins, s

The introduction of an adjustable "hold time" t_h has the advantage that the control frequency is

adjustable. This allows the prevention of control frequencies near the natural frequencies of suspension and steering components which otherwise may cause undesirable vibrations and damage to suspension components. The air consumption also may be kept low as a result of an adjustable hold time.

Summarizing, the type of modulation described lowers the brake pressure when the critical brake slip is exceeded and in general elevates it again when the brake slip is smaller than the critical, independent of momentary critical slip values. The brake force fluctuates near its maximum value and is kept at a constant value during an adjustable time interval. The force level is only a little smaller than the maximum value of the brake force, provided the friction conditions between tire and road surface have not improved considerably in the meantime.

10-2 HYDRAULIC VACUUM POWERED SYSTEMS

10-2.1 WHEEL-ANTILOCK CONTROL SYSTEMS

A schematic of a typical wheel-antilock brake is illustrated in Fig. 10-4 (Ref. 7). A wheel speed sensor transmits the signal of impending wheel lockup to the logic control which in turn signals a modulator to release brake line pressure which causes the wheel rotational speed to increase again. The operation of a typical vacuum-assisted modulator is shown in Fig. 10-5. In the normal position during which no wheel-antilock braking occurs, a vacuum is maintained on both sides of the diaphragm with the displacement plunger holding the hydraulic shutoff valve open. If wheel lockup is imminent, the logic controller sends a signal to the solenoid valve, closing off the vacuum to the front side of the diaphragm. At the same time, the air valve is opened, producing a pressure differential across the diaphragm and movement of the plunger to the right. This closes the hydraulic shutoff valve which isolates that particular brake from the system. As the diaphragm and plunger move to the right, the brake line volume is increased, reducing brake line pressure. When the wheel begins to accelerate, the solenoid valve is closed, and the spring returns the diaphragm. Modulators may be a two stage type that allows the brake line pressure to be reapplied at a slow or fast rate. Vacuum-powered modulators can be cycled between three to five times per second.

Ideally, an antiskid brake system would modulate all four wheels independently so that maximum longitudinal as well as lateral tire forces are produced. Furthermore, such a system would allow panic brake applications even while operating near or at the limit turning speed of the vehicle. Limit turning speed is defined as the maximum speed the vehicle can maintain in the absence of braking without losing front or rear wheel lateral traction. Obviously, these specifications require brake system designs with sophisticated electronic and hydraulic hardware.

The performance characteristics of these systems are such that the longitudinal slip or brake force increases less rapidly — approximately 0.3 s is required to reach maximum value; consequently, the lateral

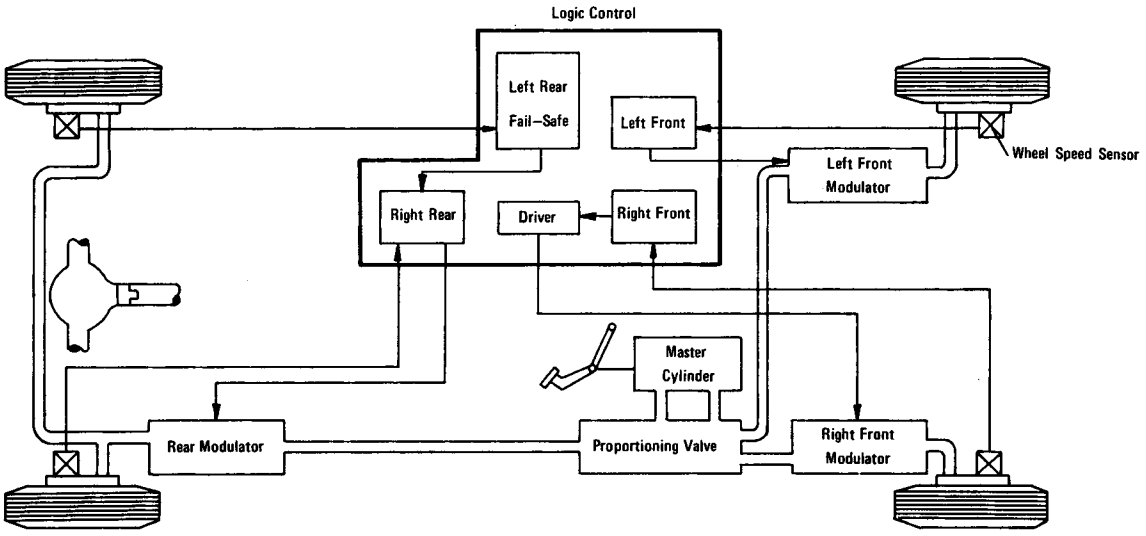

Figure 10-4. Independent Front, Select-Low Rear, Control Method Wheel-Antilock Brake System

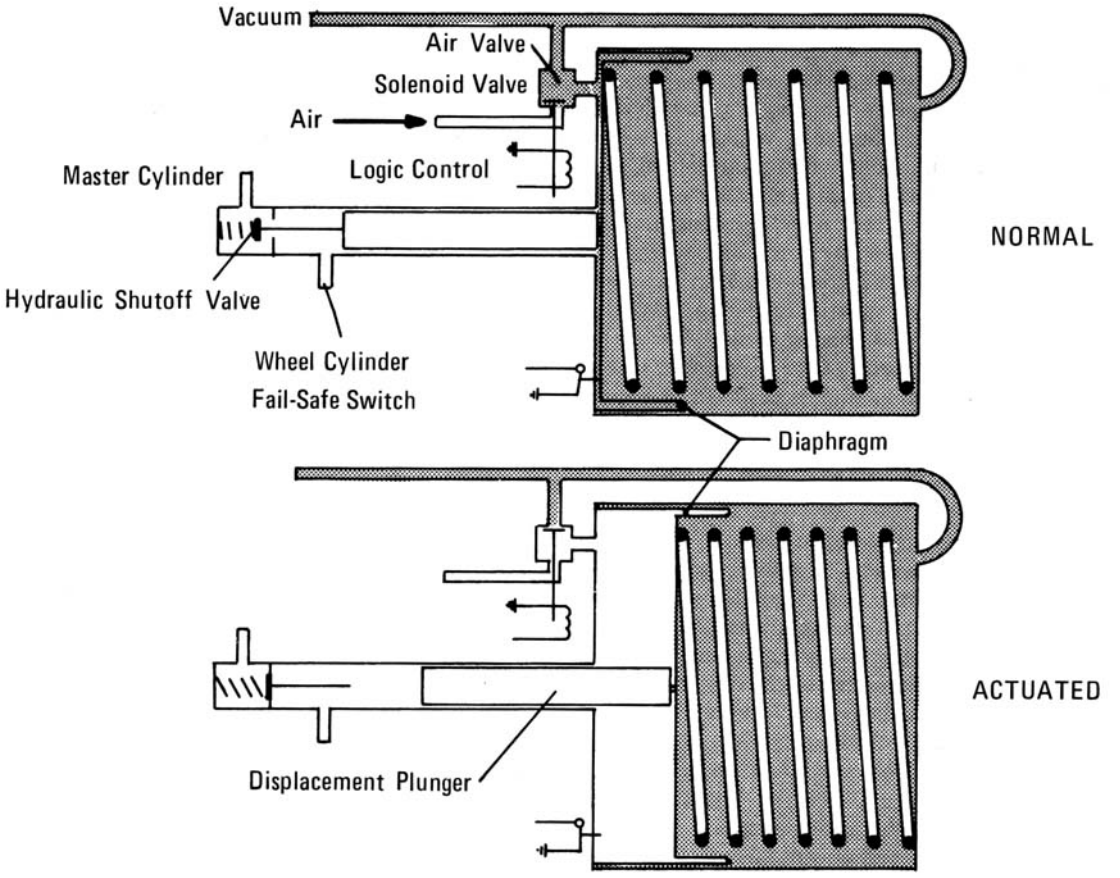

Figure 10-5. Typical One-Stage Vacuum-Assisted Modulator

tire force is not degraded appreciably. Also, the vehicle speed has decreased during the buildup of the brake force, causing a decrease in tire side forces required to continue a stable turn. As the brake force is increased, the lateral tire force demand also continues to decrease to the point that corresponds to the controlled longitudinal tire slip design threshold. However, now the vehicle speed has decreased to the extent that the lateral tire forces available exceed the demand required by the turning vehicle, and a totally stable braking maneuver results.

A system, less expensive than the four-wheel independent system, uses independent front wheel modulation and select-low, rear axle control as shown in Fig. 10-4. Here, select-low refers to the fact that the rear wheel operating on the low coefficient surface controls that modulation of both rear wheels. Some performance degradation from the optimum braking on the rear axle is suffered when operating on split coefficient surfaces. Braking in a turn, as well as straight-line braking performance, approximates that of four-wheel control systems when operating on typical highways including wet and dry road surfaces.

A further decrease in costs is obtained through systems modulating only the rear axle, either each wheel independently, or the rear axle by sensing the propeller shaft angular rotation. In a panic brake application or while operating on slippery road surfaces, the front wheels can lock, thus rendering the vehicle unsteerable. Although this provides a stable stop, the accident avoidance characteristics of such a system may not prove to be cost beneficial. When braking in a turn, a rear wheels or axle controlled vehicle will leave the curved path when the front wheels are locked.

Rear axle controlled antiskid systems employing propeller shaft sensors have several shortcomings, both from a theoretical as well as a practical point of

view. This type of inexpensive modulation device apparently was designed to circumvent problems associated with large rear-brake-torque bias typically found on large and medium domestic passenger cars. However, when operating such vehicles in a turn without locking the front wheels, the lateral load transfer on the rear axle causes a decrease of the normal force on the inner rear wheel resulting in wheel lockup for that wheel. In this condition the propeller shaft sensor averaging the signal it receives may cause the outer wheel to lock up also, rendering the vehicle unstable. The cause of this instability lies in the operational characteristics of the differential sensor. If the brake force modulation is designed to achieve minimum stopping distances in straight-line stops, the modulation signal will be selected for that condition. For straight-line braking the propeller shaft speed changes proportionally with the changes of wheel speed, assuming uniform tire-road friction for each wheel. In a turning maneuver, however, the differential housing speed with the inner wheel locked will be half the speed of the outer wheel. The propeller shaft speed will decrease correspondingly. This information will be interpreted by the sensor as if both wheels were approaching wheel lockup. The system responds with a rapid decrease in brake line pressure and, thus, near-zero brake torques on both wheels and nearly free-rolling wheels. At this instant, the sensor may over-react, causing excessive brake line pressure buildup and subsequent lockup of both rear wheels for a time period which, although short, is sufficient to cause the rear wheels to lose lateral stability.

It is obvious that a poorly designed antilock brake system may not yield any safety benefits. Properly engineered conventional or proportional brake systems will produce equal or even better results. Furthermore, rear wheel antilock brake systems still render the vehicle nonsteerable during panic brake application with the front wheels locked. Investigations of accident studies indicate that no significant safety benefits may be expected with stable yet nonsteerable rear antiskid vehicles, especially in intersection type accidents. Similar or even improved, yet less costly, braking performance is available with a properly designed brake system exhibiting sufficiently low values of rear brake bias.

10-2.2 ANALYSIS OF VACUUM-POWERED SYSTEMS

Test results of passenger cars using engine vacuum as the power source for the brake pressure modulator have shown consistently that when tested in the wheel-antilock mode no shorter or even longer stopping distance resulted as compared to a stop involving some or all wheels locked.

Experimental data revealed that vehicles equipped with 1971 production or experimental four-wheel antilock systems can achieve brake system efficiencies in the range of 60 to 70% on a dry surface and 75 to 98% on a wet, slippery surface (Ref. 5).

A friction utilization as low as 60% on a dry road surface appears to be unnecessarily low. Detailed inspection of the stopping distance data reveals that the distances for antilock were always longer compared to those obtained with the control system off when operating on a dry road surface. A reason for this undesirable behavior may be found from inspection of the actual pedal force and deceleration time histories shown in Figs. 10-6 and 10-7. Although the brake line pressure rises rapidly, the deceleration developed by the vehicle-braking system shows a significant time lag. The braking performance with the antiskid system operational as illustrated in Fig. 10-7 shows a slower deceleration response than with the control system disabled as indicated in Fig. 10-6.

If one approximates the deceleration-time history in Fig. 10-6 by four linear sections, simple integration yields the stopping distance and mean deceleration. For a stop from 60 mph, a stopping distance of 244 ft at a mean deceleration of 16.2 ft/s^2 and a maximum deceleration of 20.4 ft/s^2 results. The ratio of mean-to-maximum decelerations is 0.795. Furthermore, if one assumes a linear rise — characterized by the factor m measured in ft/s^3 — of the deceleration to the maximum values, one obtains — on wet road surfaces with low levels of maximum deceleration — low values of rise times as compared to those associated with braking on dry road surfaces. Inspection of the deceleration time history of Figs. 10-6 and 10-7 indicates a deceleration delay time of approximately 0.1 s. By the use of the foregoing assumptions and data, Table 10-1 may be constructed for a stop from 30 mph. Inspection of the table indicates that the ratio of mean-to-maximum deceleration for stops on slippery surfaces is fairly close to unity; whereas, the ratio value for braking on dry surfaces is significantly lower. Since a low ratio of mean-to-maximum deceleration indicates a brake system operation below maximum capability over extended periods of time, no improvements in dry road surface stopping distance may be expected from an antiskid control system exhibiting the performance characteristics shown in Figs. 10-6 and 10-7. The comparison of the ratio values reveals that the vacuum power source characteristics and possibly the cold sensitivity of the lining material significantly affect the brake system efficiency.

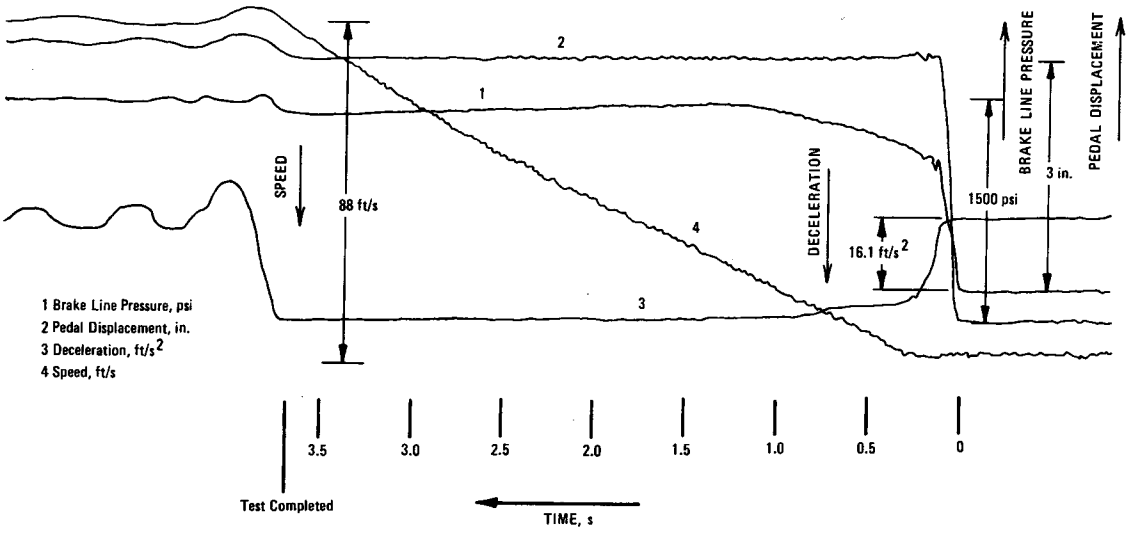

Figure 10-6. Oscillograph Record for Stop With Antilock System Disabled, Dry Road Surface

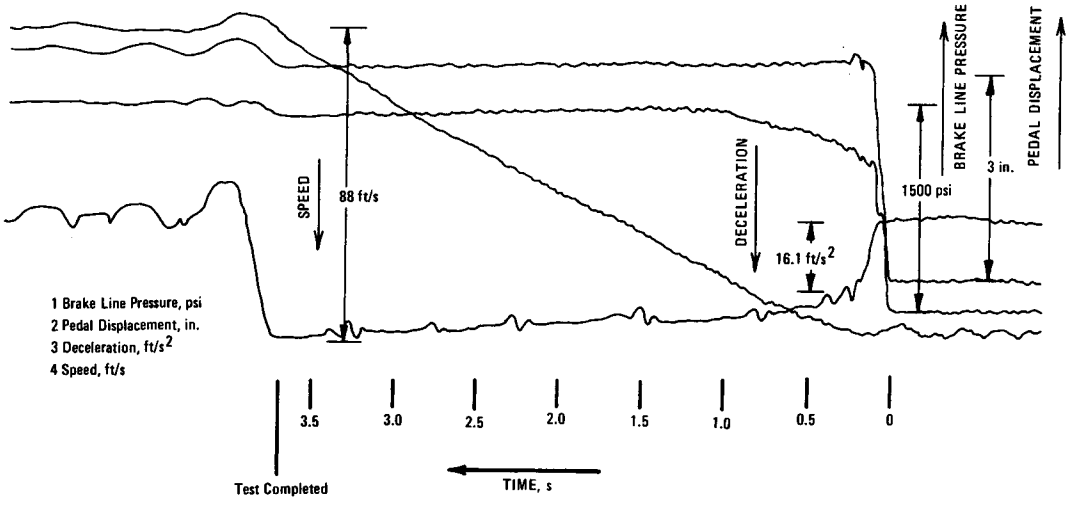

Figure 10-7. Oscillograph Record for Stop With Antilock, Dry Road Surface

10-3 HYDRAULIC PUMP PRESSURIZED SYSTEMS

Pump pressurized or full hydraulic brake systems use high fluid pressure as the energy source for brake line pressure regulation rather than engine vacuum. High pressure permits the design of compact components and the operation at higher frequencies than vacuum-powered systems. If the pressure regulator possesses a sufficiently large frequency range and adaptive capability, the pressure regulating frequency may be varied with changing conditions at the tire-road interface. Some full hydraulic pressure regulators have frequencies that vary between 2 and 8 cycles per s and may go as high as 12 or 15 cycles per s. Higher frequencies will cause the wheel brakes to be applied and released near the natural frequency of vehicle suspensions. This condition, however, leads to undesirable suspension and vehicle body vibrations. Pressure regulating frequencies below 2 cycles per s are not capable of adapting sufficiently fast to

TABLE 10-1
EVALUATION OF VACUUM POWERED WHEEL-ANTILOCK BRAKE

Deceleration Rise		Road Surface and Antiskid System (On or Off)				
		Wet (Slippery)		Dry		
		Off	On	Off	On	Units
m = 40 ft/s³	Maximum Deceleration	6.65	10	25	28	ft/s²
	Stopping Distance	155	106	48.6	44.5	ft
	Mean Deceleration	6.4	9.3	20.4	22.4	ft/s²
	Ratio of $\frac{\text{mean}}{\text{max.}}$ deceleration	0.96	0.94	0.82	0.79	
m = 12.5 ft/s³	Stopping Distance	157.5	109	57.5	54.7	ft
	Mean Deceleration	6.3	9.05	17.2	18.1	ft/s²
	Ratio of $\frac{\text{mean}}{\text{max.}}$ deceleration	0.95	0.91	0.69	0.64	

changing frictional conditions at the tire-road interface.

The functioning and components of a first generation full power pressure regulating system and valve are discussed next (Ref. 9).

A pump pressurized antilock system is illustrated in Fig. 10-8. The system shown is of the independent front, select low on the rear axle, control type. The brake system consists of the pressure boosted master cylinder (1) with the reservoir (2), the accumulator (3), the combination unit of pressure modulator and energy source (4), the logic control (5), the wheel sensors (6), and the wheel brakes (7). If the standard brake system is full power hydraulic, then only the logic control, pressure modulator, and wheel speed sensors must be added. The details of the pressure modulator and energy source are illustrated in Fig. 10-9. The electric motor driven pump (1) charges the diaphragm accumulator (2) as well as the piston accumulator (3) in the modulator which is preloaded by a coil spring (4). The charge pressure is transmitted past the open solenoid valves (5) and passage (6) to the plungers (7) which are held against their stops, thus forcing the cutoff valves (8) open and allowing the brake line pressure produced by the master cylinder (9) to be transmitted to the wheel brakes (10). If a wheel antilock signal is received from the logic control, the solenoid valves (5) close and (11) open. This condition results in separating the chamber (12) from the piston accumulator (3) and

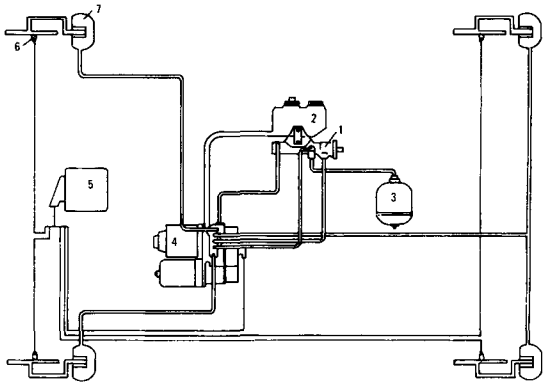

Figure 10-8. Schematic of Pump Pressurized Wheel Antilock System

allowing the fluid to return to the reservoir (13). The line pressure in the wheel cylinder (10) forces the plunger (7) to the left and the cut-off valve (8) closes off the return to the master cylinder. The space vacated by the plunger is occupied by the brake fluid coming from the wheel cylinder, resulting in a decrease in brake force of the modulated wheel. Reapplication of the brakes occurs after the solenoid

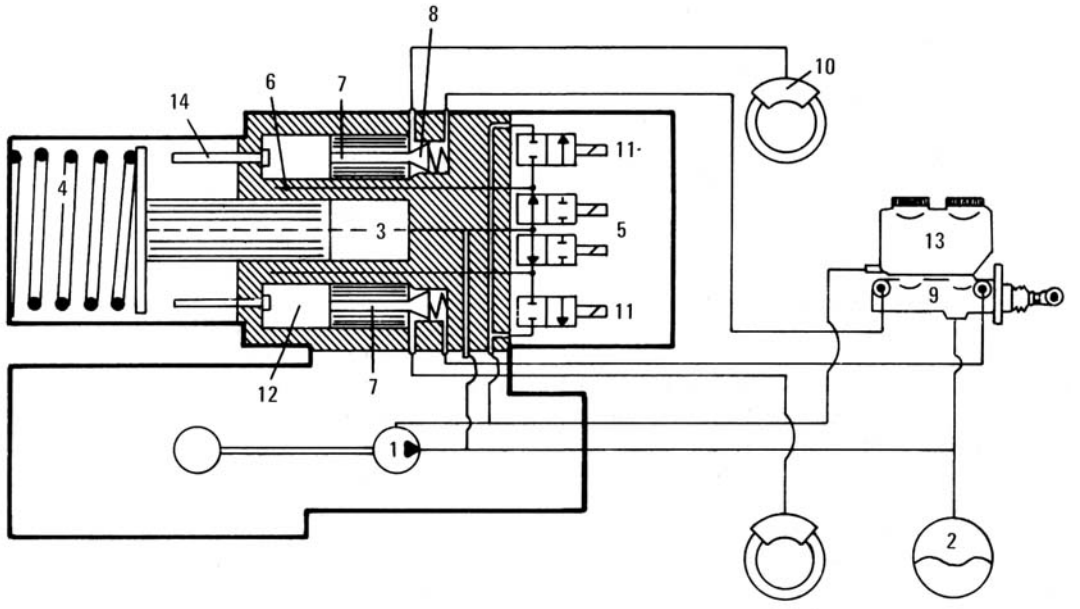

1 Electric Motor Driven Pump
2 Accumulator
3 Piston Accumulator
4 Coil Spring
5 Solenoid Valve
6 Flow Passage
7 Plunger
8 Cutoff Valve
9 Master Cylinder
10 Wheel Brakes
11 Solenoid Valve
12 Chamber
13 Brake Fluid Reservoir
14 Tappet

Figure 10-9. Schematic of Wheel-Antilock Modulator

valves have returned to their original position and accumulator pressure is reintroduced to chamber (3). If the accumulator fails, the vehicle can be braked manually since the spring (4) forces the tappets (14) to the right and mechanically holds the cut-off valve open all the time.

10-4 PNEUMATIC SYSTEMS

Wheel-antilock control systems for air brakes use concepts similar to those found in hydraulic brake systems. Major components are: wheel sensors, usually one for each wheel on the axle; an electronic control, which collects the sensor information, processes it, and sends control signals to the air pressure control valve; and an air pressure control valve which accomplishes the air pressure modulating function by the use of electrical solenoids. The air pressure application and release cycle may be varied between 1 to 5 cycles per second for most current systems.

In the event of malfunction of the major elements in the antiskid control system, the brake system will revert to the standard service brake operation. For tractor-trailer combination the trailer antiskid control system generally is powered through the brake light signal going from the tractor to the trailer. This condition allows also the intermixing of antiskid equipped tractors with trailers having standard brakes and conversely.

In the case of a hydraulic brake system, the brake fluid must be conserved during the period of pressure decrease as contrasted with air brake systems where air is ventilated from the brake chamber through the

control valve into the ambient. However, due consideration must be paid to the fact the air consumption must remain within the reservoir capacity of the brake system. This is of significance when braking on slippery roadways requiring long stopping distances and continued brake force modulation.

The functioning and components of a typical air brake wheel-antilock system are discussed next (Ref. 10).

The wheel-antilock system is designed to prevent any regulated axle from locking up during braking for speeds above approximately 5 mph. The system consists of the modulator assembly, the wheel speed sensor assembly, the rotor assembly, and the fail-safe monitor unit. A tractor wheel-antilock control system includes a modulator consisting of an antilock control/relay valve and electronic controller for each braked axle, a wheel speed sensor and rotor assembly at each braked wheel, and a fail-safe monitor assembly. Each is discussed.

1. Modulator Assembly. The modulator assembly consists of the wheel-antilock control/relay valve and an electronic controller. The modulator assembly is connected to the brake system plumbing system through the supply, service, and deliver ports. In normal operation the modulator valve supplies air pressure to the brake chambers at a pressure equal to that demanded by the vehicle driver with the application valve. When wheel-antilock action is required by signals from the controller, pressure to the brake is reduced, either partially or completely, by two solenoids which actuate a small valve. The solenoids operate either independently as in the case of individual wheel control or simultaneously as in the case of an axle control to regulate the air pressure to the brake chambers. This pressure reduction to the brakes occurs in steps of 33%, 67%, or 100%.

2. Controller. The controller is a small computer which contains the circuits necessary to control the vehicle wheel rotational speed. The electronic unit is totally enclosed and protected from the ambient effects. The controller circuitry is fully solid state and receives electrical signals from the wheel speed sensors, interprets the signals in terms of existing conditions, and sends corresponding signals to the wheel-antilock control relay valve to regulate brake pressure.

3. Fail-safe Monitor Unit. The fail-safe monitor is an electronic warning unit which processes signals from the controller and energizes an indicator light, mounted on the instrument panel, if an electrical or electronic malfunction occurs. The fail-safe indicator light will come on and remain on if any of the following occurs on any axle with wheel-antilock control:

a. An open or short in a wheel sensor or wiring harness
b. An open or shorted power lead
c. An open or shorted fail-safe lead
d. A shorted fail-safe monitor unit
e. A blown fail-safe unit fuse
f. A continuous solenoid signal
g. An open or shorted solenoid lead
h. A malfunctioning controller
i. On very slippery roads with patches of ice, the indicator light may come on due to one drive wheel accelerating at a very high rate when starting to move the vehicle. Reset the fail-safe light by turning key off and back on.

4. Wheel Speed Sensor Assembly. The wheel speed sensor is a self-generating electromagnetic device which generates a signal whose frequency is directly proportional to wheel rotational speed. The sensor generates a pulse each time a gear tooth travels past it; 60 pulses are generated per revolution. The speed sensor consists of a stationary permanent magnet assembly, a coil, and an output cable assembly. The speed sensor is attached to a mounting bracket and the speed sensor assembly is mounted to the brake backing plate. The rotor assembly is attached to the hub and drum and rotates with the wheel.

10-5 STRAIGHT-LINE VERSUS CURVED PATH PERFORMANCE

Some differences of braking performance existing in vehicles when braking in a straight line or curved path have been discussed in par. 10-2.1 in connection with drive shaft controlled rear axle antilock systems.

When braking in a turn, the tires must produce braking and side forces to hold the vehicle in the desired path. The relationships between longitudinal and side slip of a tire are a function of a great number of variables. As discussed in par. 10-1, wheel lockup may be the result of excessive braking or turning, or both. Wheel-antilock systems which operate at a constant longitudinal slip value, e.g., 15%, will cause a reduction in side force when turning under certain conditions with subsequent wheel lockup to occur. Considerable improvement in braking performance while holding the vehicle in a stable turn can be accomplished by control systems that use the angular deceleration of the braked wheel to derive a logic signal. Latest experimental designs use the steering wheel rotation provided by the driver as an input to alter the sensitivity of the controller to improve

braking in a turn (Ref. 11). Finally, the fundamentals involved in designing the optimum brake force distribution of a standard brake system must be applied to the design of a wheel-antilock brake system. Since high values of tire-road friction utilization result in high decelerations and hence shorter stopping distances, the fundamentals presented in Chapters 8 and 9 must be applied. The consequence of poor tire-road friction utilization is premature wheel lockup of a particular axle and in the presence of a wheel-antilock system the premature application of the automatic brake force modulation at a friction level that may be less than what the tire-road friction could provide if utilization were optimized.

10-6 THEORETICAL AND EXPERIMENTAL RESULTS

The prediction of the dynamic performance of a wheel-antilock brake system is a difficult task. To accomplish the analysis, mathematical models of vacuum-assist units or full power pressure regulating devices, master cylinder, brake line, wheel cylinders or brake chambers, and mechanical friction brakes must be developed. Furthermore, the tire-road friction characteristics must be described by a mathematical expression that includes the effects of normal force, turning forces, and road surface contamination. Finally, suspension and vehicle dynamic effect must be described by mathematical equations. Although the development of the mathematical expressions does not present basic difficulties, the measurement of a large number of parameters, such as friction coefficients, damping values, brake fluid viscosity changes, and nonlinear spring stiffnesses may significantly affect the outcome of the analysis. Due to this difficulty, mostly experimental data have been published. Comparisons of theoretical and experimental results generally cannot be transferred to other vehicles or operating conditions, unless the mathematical model is formulated to include different operating conditions.

A comparison of theoretical and experimental results for a pneumatic wheel-antilock system is illustrated in Fig. 10-10 (Ref. 8). The data shown were obtained from road testing a tractor-semitrailer combination. In general, good agreement is noted. The accuracy of predicting vehicle deceleration generally becomes poor for vehicle speeds below 10 mph due to the significant change in tire-road friction coefficient with speed. However, at higher speeds the acceptable prediction capability allows the study of the effects of brake force modulation on the fifth wheel kingpin forces, dynamic axle loads, directional stability, and

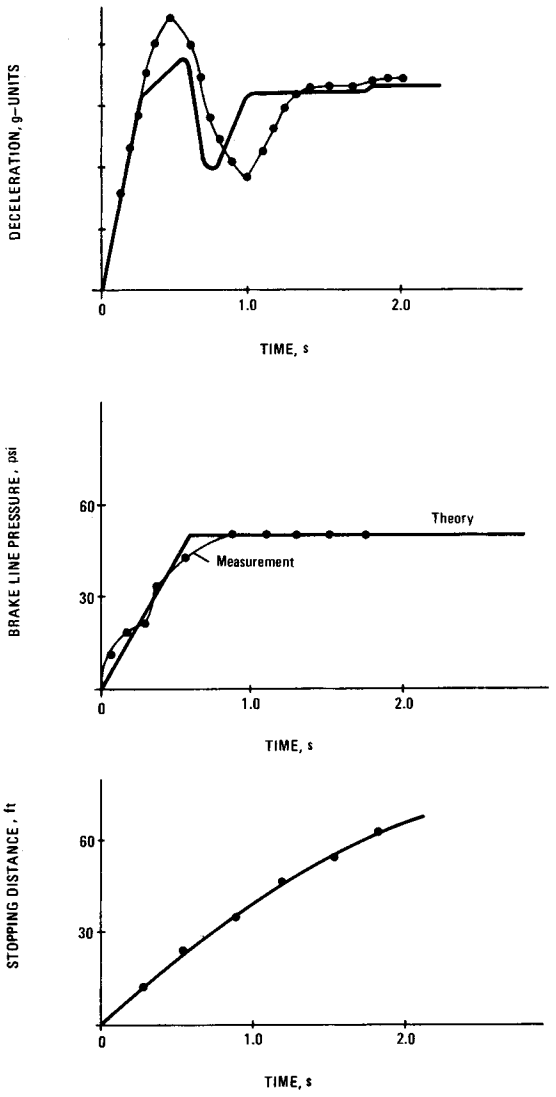

Figure 10-10. Measured and Computed Performance for Pneumatic Wheel Antilock System

other parameters difficult and expensive to determine experimentally.

Test data obtained with passenger cars equipped with vacuum-assisted and full power hydraulic brake force modulation have been published (Refs. 12, 13, and 14). Test results obtained with a vacuum-assisted wheel-antilock brake system are presented in Table 10-2. Test conditions are shown in Tables 10-3 and 10-4 (Ref. 7). Inspection of the data in Table 10-2 indicates that shorter stopping distances may be achieved when braking in the no-antilock mode on a

TABLE 10-2
PASSENGER CAR WHEEL-ANTILOCK BRAKE SYSTEM TEST DATA

System	Path	Wheel Condition	Maintained Steering Control	Stability	Stopping Distance, ft High	Medium	Low
No antilock	Curve	Incipient	Yes	(1)	196	187	207
		Locked	No	(2)	117 (3)	180 (3)	203 (3)
	Straight	Incipient	Yes	(1)	123	140	155
		Locked	No	(2)	115	128	152
Drive shaft controlled rear	Curve	Incipient	Yes	(1)	142	167	197
		Locked	No	(2)	120 (3)	150 (3)	204 (3)
	Straight	Incipient	Yes	(1)	124	133	146
		Locked	No	(1)	110	139	163
Select-low rear	Curve	Incipient	Yes	(1)	145	148	224
		Locked	No	(1)	124 (3)	127 (3)	136 (3)
	Straight	Incipient	Yes	(1)	111	123	197
		Locked	No	(1)	124	126	159
Select-low front,	Curve	Incipient	Yes	(4)	159	140	165
Select-low rear	Straight	Incipient	Yes	(4)	115	155	142
Independent front,	Curve	Incipient	Yes	(4)	126	127	153
Select-low rear-wheel	Straight	Incipient	Yes	(4)	118	122	135
Four-wheel independent	Curve	Incipient	Yes	(4)	124	116	140
	Straight	Incipient	Yes	(4)	115	126	141

(1) Occasional yaw less than 20 deg
(2) Unpredictable with yaw more than 20 deg
(3) Vehicle left 12-ft lane and entered a higher coefficient surface
(4) No yaw

TABLE 10-3
PASSENGER CAR TEST SPEEDS, MPH

	Dry Asphaltic Concrete	Wet Asphaltic Concrete	Wet "Jet Seal"
Straight Path	78.3	67.4	25.0
Curved	78.6	67.6	20.6

TABLE 10-4
TIRE-ROAD FRICTION COEFFICIENTS

High	Medium	Low
0.46	0.45	0.40

high friction road surface. For example, on a straight path the no-antilock mode required 115 ft wheels locked stopping distance as compared with 124 ft with the select-low rear wheel-antilock mode.

Measured stopping distances for full power hydraulic systems on passenger cars traveling at an initial speed of 62.5 mph were 138 ft for dry and 208 ft for wet road surfaces (Ref. 15). The equivalent dry peak and sliding friction values of the test surface are 1.05 and 0.85, respectively. The stopping distances without four wheel antiskid system were 166 ft and 332 ft on the dry and wet surfaces, respectively. Tests conducted with independent rear-wheel control resulted in 60% longer stopping distances than those obtained with the four-wheel control system. This significant difference was caused by the additional stopping distance accumulated during careful brake force buildup to avoid front-wheel locking. Test data for braking in a turn maneuver indicate an initial value of lateral acceleration of 0.5g and an average

longitudinal deceleration of 0.7g. Since the wet peak tire-road friction is limited to about 0.75, this limit braking-turning performance is only possible by delaying the maximum braking force by approximately 0.3 s, a value sufficiently long to allow the side-force requirement to decrease. Once the side-force demand is lowered due to decreased speed, the braking force is modulated near or at the maximum available.

Experimental results for a tractor-semitrailer combination with a total weight of 77,780 lb obtained on a wet road surface having a tire-roadway friction coefficient of approximately 0.25 are presented in Fig. 10-11 (Ref. 16). Again, the significant decrease in stopping distance with the wheel-antilock system operational compared to the baseline brake system is noted. Inspection of Fig. 10-11 also indicates that an optimum distribution of the brake forces among the axles will yield a decrease in stopping distance of 100 ft as compared to the original brake system.

10-7 DIFFERENT ANTISKID SYSTEM DESIGNS

The earliest wheel-antiskid system appeared in 1928 (Ref. 17). It involved mechanical controllers in form of fly wheels. No practical tests were ever conducted. The application of wheel-antilock systems to trains and airplanes preceded the application to automobiles and trucks. Most of the train antilock systems also use mechanical controllers.

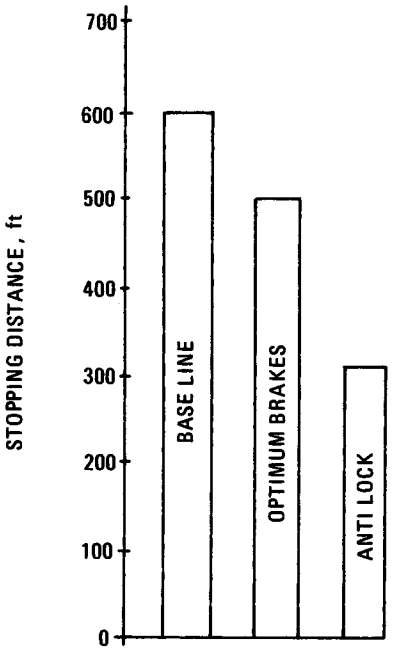

Figure 10-11. Comparison of Stopping Distance on Slippery Road Surface for a Tractor-Semitrailer Combination

For automotive use, a great number of different manufacturers have been involved in the research, development, and manufacture of wheel-antilock systems, both for hydraulic and pneumatic application. Some systems are discussed briefly (Ref. 18).

1. Bendix Braking Control System. An electromagnetic wheel velocity pickup is used and the signal is differentiated electronically after appropriate processing. Vacuum-operated brake pressure modulators controlled by solenoid valves provide the brake pressure control. At vehicle speeds below 5 mph, the system is disengaged to permit normal braking in slow moving traffic.

2. Dunlop Maxaret Hydraulic Control System. The system is a wheel-antilock system which is sensitive to wheel or shaft deceleration. The controller is a flywheel and acts as a memory for determining the point of pressure reapplication. Vacuum is used as energy source for modulating brake line pressure. The system operates between 5 to 10 cycles per second.

3. Dunlop Maxaret Pneumatic Control System. The system has been designed for trucks and trailers equipped with air brakes. The propeller shaft rotational speed is sensed to detect the onset of wheel lockup on one or both wheels of the rear axle.

4. Hydro-Aire Hytrol Control System. The system is designed for truck application. Wheel angular deceleration detectors are mounted on the hub of each wheel to be controlled and a regular solenoid valve in the brake circuit accomplishes the pressure control function. The sensor is a flywheel. Operating frequency can be up to 4 cycles per second.

5. Jacobs Automatic Control System. The system designed for trucks and trailers uses a flywheel to detect critical wheel deceleration. The inertia of the flywheel is used to produce an axial displacement which operates the antiskid air control valve.

6. Kelsey-Hayes Sure-Track System. The system senses wheel rotational speed, differentiates the signal to obtain wheel deceleration, and uses a comparison with a preset deceleration valve to trigger a brake pressure release unit. The brake pressure regulator is a vacuum-assisted unit.

7. Kerr Braking-Control System. The system is designed for cars and light trucks and uses changes in braking reaction in the suspension to control hydraulic brake line pressure. To accomplish this, a hydraulic valve is located in the line to each brake of the vehicle. During wheel-antilock operation, the master

cylinder is isolated from the wheel cylinder, and the brake line pressure is regulated in proportion to the dynamic force stemming from the changes in braking reaction of the suspension system.

8. Lockheed Antilock Hydraulic Control System. The system uses a flywheel and vacuum-assisted brake pressure regulators to accomplish the wheel-antilock function. The flywheel is located to sense the rotational deceleration of the transmission shaft. The system is designed for rear wheel-antilock control. A system using components of the hydraulic system has been designed for pneumatic application.

9. Ate Braking Control System. The system uses wheel sensors to measure rotational wheel speed. Wheel angular deceleration is computed and a full power pressure regulator is used to accomplish the wheel-antilock function.

10. Teldix Braking Control System. The system uses wheel sensors to measure angular speed of the wheels. Wheel angular deceleration is computed and high frequency pressure regulator valves are used to accomplish the wheel-antilock function. The system is a full power hydraulic system.

11. Girling Braking Control System. The system uses wheel sensors to measure wheel speed. The wheel speed signal is differentiated to give wheel deceleration. The pressure regulators are actuated by a pressurized system operating at 300 psi (Ref. 19).

Due to Federal performance requirements for trucks and trailers equipped with air brakes, the design and manufacture of pneumatic wheel-antilock control systems has progressed rapidly and several other manufacturers are producing pneumatic wheel-antilock systems.

REFERENCES

1. M. Mitschke, "Dynamics of Motor Vehicles", *Springer Publisher*, Berlin-Heidelberg-New York, 1972.
2. W. D. Limpert and H. Leiber, "A New Method for Prevention of Wheel Locking on Motor Vehicles by Automatic Control of Tire Slip", *Automobilisimo and Automobilisimo Industriale*, Vol. 16, No. 2, March-April 1968, pp. 67-81.
3. H. Leiber and W. D. Limpert, "The Electronic Brake Modulator", *Automobiltechnische Zeitschrift*, Vol. 71, No. 6, 1969, pp. 181-89.
4. R. H. Madson and H. E. Riordan, *Evolution of Sure-Track Brake System*, SAE Paper No. 690213, January, 1969.
5. R. Murphy, *A Procedure for Evaluating Vehicle Braking Performance*, Contract No. DOT-HS-031-1-051, October 1971, prepared for U.S. Department of Transportation.
6. E. Hoerz, "Requirements on Brake Force Modulation for Passenger Cars", *Automobiltechnische Zeitschrift*, Vol. 71, No. 7, 1969, pp. 238-44.
7. R. Limpert, et al., *An Investigation of the Brake Balance for Straight and Curved Braking*, SAE Paper No. 741086, October 1974.
8. H. J. Neu and J. Helling, "Braking Force Control for a Light Truck", *Automobiltechnische Zeitschrift*, Vol. 71, No. 3, 1969.
9. O. Depenheuer and H. Strien, "Hydraulic Brake Actuation Systems under Consideration of Antilock Systems and Disc Brakes", *Alfred Teves GmbH*, Frankfurt, Germany, March 1973.
10. B. F. Goodrich, *Skid Control System*, Maintenance Manual OH574, November 1974.
11. M. Mitschke and P. Wiegner, "Simulation of Panic Braking with Various Anti-Lock Devices on Roads with Split Friction Coefficient", *Automobiltechnische Zeitschrift*, Vol. 77, No. 11, 1975.
12. J. L. Harned and L. E. Johnson, *Anti-Lock Brakes*, General Motors Automotive Safety Seminar, July 1968.
13. T. C. Schafer, et al., *Design and Performance Considerations for a Passenger Car Anti-Skid System*, SAE Paper No. 680458, May 1968.
14. G. B. Hickner, et al., *Development and Evaluation of Anti-Lock Brake Systems*, SAE Paper No. 760348, February 1976.
15. "The Brake Control System ABS of Daimler Benz/Texdix", *Automobiltechnische Zeitschrift*, Vol. 73, No. 3, 1971, pp. 104-07.
16. R. Murphy, R. Limpert, and L. Segel, *Development of Braking Performance Requirements for Buses, Trucks, and Tractor/Trailers*, SAE Paper No. 710046, January 1971.
17. F. Ostwald, "Development of Wheel-Antilock Systems for Motor Vehicles", *Automobil Revue*, No. 40, Bern, September 1964.
18. "Phase II Report on the Study of Applicability of Anti-Skid and Load Proportioning Systems for Highway Vehicles", for U.S. Department of Transportation, Contract No. FH-11-6859, prepared by Booz-Allen Applied Research, Inc., July 1969.
19. D. Brown and C. Harrington, *Brake Fluid Functionability in Conventional and Anti-Skid Systems in Arctic Conditions*, SAE Paper No. 750383, February 1975.

CHAPTER 11
DYNAMIC ANALYSIS OF BRAKE SYSTEMS

In this chapter some fundamentals of brake system dynamics are discussed. Practical relationships for predicting response times of pneumatic brake systems are introduced.

11-0 LIST OF SYMBOLS

c = speed of sound in brake fluid, ft/s
F_p = pedal force, lb
l_1 = brake line length between reservoir and brake application valve, ft
l_2 = brake line length between brake application valve and brake chamber, ft
p_l = brake line pressure, psi
t_{total} = total time lag of brake system, s
t_v = total lag of application valve, s
t_1 = time required by brake line pressure wave to travel between the brake application valve and brake chamber, s
t_2 = time required by brake line pressure to overcome brake chamber piston slack, s
t_3 = time required by brake line pressure to attain 90% of reservoir pressure, s
V_o = brake chamber volume to be filled prior to any piston displacement, ft³
V_s = brake chamber volume to be filled to take up slack, ft³
V_2 = volume of brake line connecting brake application valve and brake chamber, ft³

11-1 FUNDAMENTALS OF RESPONSE TIME ANALYSIS

In Chapter 5 the performance of the brake system and brake system components is discussed in terms of quasi-static characteristics. The effect of response time of a brake system on stopping distance is treated in an idealized manner in Chapter 1 (Fig. 1-1). The deceleration rise is characterized by the buildup time t_b. The total stopping distance of a vehicle can be obtained by Eq. 1-3. The stopping distance of a vehicle consists of three parts. The first part is the distance traveled by the vehicle between the instant of pedal application and the instant at which brake force production begins. The second part is the distance traveled between the instant brake force production begins and the instant the sustained level of brake force is achieved. The third part is the distance traveled during the time interval the sustained brake force is acting on the vehicle and the vehicle comes to a stop. The reaction time of the driver is not included in the stopping distance calculation.

Relatively few publications have addressed the problem of brake system dynamics. In earlier attempts, the effect of brake-system response on stopping distance was calculated by considering friction at the pedal linkage, fluid compliance and fluid inertia in the brake lines, and drum brakes with negligible brake line pressure/torque response dynamics. The results of the analysis showed that the stopping distance may increase by as much as 15% due to the response time of the brake system in a 60 mph stop (Ref. 1).

In a different publication the differential equations governing the relationship between pedal force and brake line pressure at the wheel cylinders were solved (Ref. 2). In the analysis the brake pedal linkage was considered an inertialess system with a fixed mechanical efficiency. The master cylinder was shown to have negligible response times. The brake fluid in the brake line was analyzed by the wave equation. The wheel brake was assumed to be rigid. The solution to the differential equation indicated that the dynamics of the fluid of the brake line was of less importance. The major effect was associated with the compliance of the system. Based on experimental tests, it was shown that brake system dynamics may increase the overall stopping distance by as much as 10%.

With the introduction of wheel-antilock brake systems on passenger cars and trucks, an increased interest in the dynamic analysis of brake systems and components has developed. Most efforts involve the computer simulation of the entire brake system (Refs. 3,4 and 5).

The dynamic analysis of pneumatic brake systems for railroad trains has been carried out on a limited basis (Ref. 6). In an experimental program the effects of response time of an automotive air brake system on braking performance were measured and expressed in functional relationships (Ref. 7).

11-2 HYDRAULIC BRAKE SYSTEMS

A detailed analysis of the dynamic response characteristics of hydraulic brake systems is beyond the scope of this handbook. The dynamic analysis involves the solution of several differential equations

by means of an analog or digital computer. Some important facets of the dynamics of hydraulic brake systems are discussed.

Generally the response characteristics of hydraulic brake systems are such that the time lags between input and output variables are very small and are typically less than 0.1-0.2 s. The importance of each major component relative to system dynamics is discussed.

1. Brake Pedal Linkage. The dynamics of the brake pedal and linkage are of little importance to the dynamic response of a complete brake system. If desired, the equations of motion of the linkage system may be developed by means of basic fundamentals of mechanics.

2. Vacuum-Assist Unit. The vacuum-assist unit consists of several components such as pistons, valves, and pushrods all of which must be included in the mathematical equations describing the dynamic behavior of the assist device. Furthermore, certain assumptions must be made to simplify the thermodynamic relationships governing the pressure development in the vacuum and ambient pressure chambers (Ref. 5). Transient responses for the vacuum-assist unit of a station wagon were measured and are illustrated in Fig. 11-1. Inspection of Fig. 11-1 indicates the response characteristics for a slow pedal force application to be similar to the quasi-static behavior discussed in Chapter 5 (Fig. 5-4). The response of the brake line pressure produced at the master cylinder outlet to a rapid pedal force application shows a significant lag composed with the response associated with a slow application. The brake line pressures produced in the slow and rapid application do not approach being equal until a pedal force in excess of 230 lb is attained. Inspection of Fig. 11-1 indicates that significant differences exist between the actual (represented by the fast application curve) and the design (represented by the slow application curve) brake line pressures when a rapid application is attempted. The vacuum-assit unit contributes significantly to the response lag of the brake system.

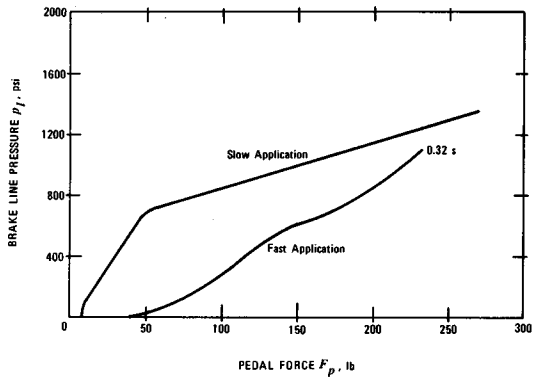

Figure 11-1. Measured Steady-State and Transient Brake-Line Pressure/Pedal Force Response

3. Master Cylinder. The dynamics of the master cylinder are relatively insignificant in comparison with those of the complete brake system. Major reasons for the small effect of the master cylinder on system dynamics are the small masses — that of the pistons — and high geometrical stiffness of the cylinder. By the application of fundamentals of mechanics, the differential equations governing the dynamics of the master cylinder may be derived (Ref. 5). In general, the equations describe the output flow of the master cylinder chambers as a function of the input force and the brake line pressure acting on the chambers.

4. Brake Line. In the past, hydraulic brake lines have been analyzed by means of the wave equation which describes the longitudinal vibrations of the fluid in the brake line. For small diameter hydraulic lines, it has been found that the viscosity of the brake fluid has a significant effect on response time. In the latest research, the column of brake fluid was represented by a distributed mass system. The model consisted of a rod representing the fluid, a spring at one end of the rod representing the stiffness of the wheel brake, and a pressure input at the other end of the rod (Ref. 5). Theoretical results computed by use of this model showed good correlations with experimental data. Analyses and test data indicate that the brake line contributes significantly to the response lag of a complete brake system.

5. Wheel Brake. The dynamic performance of the wheel brake may be analyzed by the use of several submodels, such as thermal submodel, friction coefficient submodel, static performance submodel, and dynamic performance submodel (Ref. 5). The static performance submodel predicts the brake torque as a function of brake line pressure and coefficient of friction between lining and rotor. The brake torque of the static submodel is determined by Eq. 5-2. The dynamic performance submodel calculates a dynamic brake torque by treating the brake as a mass-spring-damper system. The thermal submodel considers the brake as an energy-conversion and heat-dissipation device in predicting brake temperature. The friction material submodel considers the time-varying coefficient of friction between lining and rotor. The findings on the dynamic performance of wheel brakes

indicate that typical wheel brakes are a highly responsive component. Earlier research had led to the opposite conclusion (Ref. 4).

The dynamic response of a complete brake system consists of a quasi-static component and a transient component. The transient behavior is that associated with rapidly changing system variables, such as brake line pressure following a rapid pedal force input. The quasi-static behavior is associated with slowly changing variables, such as the change in coefficient of friction between lining and rotor due to a decrease in wheel speed during deceleration of vehicle.

The principal dynamic elements in a typical brake system are the vacuum-assist unit and the brake lines. The flow rate of brake fluid from the master cylinder to the wheel cylinder is a function of fluid viscosity, cross-sectional flow area, and brake line length. The elements determining the flow rate are the capacitance, resistance, and inertance of the section of brake line. The capacitance element accounts for fluid compressibility and wall compliance, while the resistance element introduces the pressure losses due to laminar or turbulent flow, i.e., frictional effects. Inertance effects are a result of the mass of the fluid in the lines. As fluid viscosity increases, the time interval between the application of force to the brake pedal and operation of the wheel brake increases and hence for a given input, time and distance required to stop the vehicle increase. Similarly, there is an increase in brake release time. On most vehicles, tubing to the left front brake is shorter than that leading to the right front brake because of the location of the junction block for the front system on the left side of the master cylinder. Because of the difference in tubing length in the front circuit, the left front brake is actuated before the right front brake. At low viscosity levels the difference is not perceptible. However, as viscosity increases, flow rates to each of the front brakes becomes significantly different and a noticeable unbalance in braking may exist. The amount of brake unbalance is affected by the rate of force application to the brake fluid to the brake. As fluid viscosity increases, the time required for fluid to return through the tubing from the brake to the master cylinder increases due to the slower flow rate, resulting in the brakes being applied for a longer time. Slow response, and thus longer stopping distances, is the most serious problem stemming from high brake fluid viscosity.

Pressurized hydraulic brakes employ a pump/accumulator system in which the hydraulic fluid is under pressure at all times. Since this system can be brought into operation by opening a valve, i.e., the hydraulic pressure does not have to buildup from zero, the time lag will be small and the stopping distance will be shorter compared to air or vacuum-assisted brake systems. Hydraulic full power brakes seem particularly suited for vehicle combinations since the length of the brake line has little effect upon the time lag, and the system can be easily designed for a dual circuit brake system.

11-3. PNEUMATIC BRAKE SYSTEMS

Air brakes have relatively long response times and high pressure losses. The time lag can be kept small through adequate pneumatic piping design.

A detailed investigation of the dynamic behavior of an air brake system indicates that the time required to overcome clearance between the brake shoe and drum becomes smaller with increased line pressure and decreased brake chamber piston travel. The time required to buildup brake torque also decreases with increasing line pressure, increased reservoir pressure, decreased piston travel, and decreased brake line length. For example, increasing the brake line length between the brake application valve and the brake chamber from 6.5 to 35 ft increases the application time only a little, while the buildup time is nearly doubled. The application time is defined as the time elapsed between the instant of the first brake pedal movement and the instant the brake shoes are contacting the drum. The buildup time is defined as the time elapsed between the instant the brake shoes contact the drum and the instant a specified brake line pressure is obtained at the brake chambers. The optimum result therefore should be achieved with minimum volume and maximum brake line pressure. Experiments have shown that considerable time lags are associated with the control and flow processes in the brake application valve (Refs. 7 and 8). The time lag of application valves varies slightly from design to design and depends also on the volume to be pressurized. Typical time lags for application valves range from 0.05 s for a volume of 0.035 ft^3 to 0.25 s for a volume of 0.125 ft^3.

Experiments with scaled physical models representing actual pneumatic brake systems have shown that brake system response lags may be composed of three parts as illustrated in Fig. 11-2, each influenced by different factors (Ref. 7). In the first part, a time lag t_1 derives from the speed with which the pressure wave travels through a brake line of given length. The second time lag t_2 derives from the motion of the brake chamber piston required to overcome slack. This time lag is proportional to the volume of the brake chambers. The third time lag t_3 consists of the time required for the brake line pressure to reach 90%

of the reservoir pressure. This lag is proportional to both the total volume and the flow resistance of the brake system. The system schematic is shown in Fig. 11-3.

The time t_1 required for the pressure wave to travel between the brake application valve and the brake chamber is

$$t_1 = l_2/c \ , \ s \qquad (11\text{-}1)$$

where

l_2 = length of brake line between application valve and brake chamber, ft

c = speed of sound in brake fluid, ft/s

The time t_1 is little affected by typical curves and fittings found in air brake systems. The time required by the pressure wave to travel between the brake application valve and the brake chambers located farthest away is approximately 0.01 s for a tractor-trailer combination.

The time lag t_2, required by the brake line pressure of a typical air brake system in good mechanical condition to overcome brake chamber piston slack and shoe return springs, is determined by the volume v_o to be filled prior to any brake chamber piston movement, the volume v_s to be filled to overcome brake chamber piston slack, and the brake line length l_1 between reservoir and application valve as well as the line length l_2 between application valve and brake chamber(s). An approximate expression determined from experiment for typical air brake lines is (Ref. 7)

$$t_2 = (V_o + V_s)(0.007\, l_1 + 0.025 l_2) \ , \ s \qquad (11\text{-}2)$$

where

l_1 = brake line length between reservoir and brake application valve, ft

l_2 = brake line length between brake application valve and brake chamber, ft

V_o = brake chamber volume to be filled prior to any piston displacement, ft³

V_s = brake chamber volume to be filled to take up slack, ft³

The time t_3, required for the brake line pressure to attain 90% of the maximum reservoir pressure, is determined by the total volume between brake valve and brake chamber including the brake line and is given by

$$t_3 = 0.042(l_1 + l_2)(V_s + V_o + V_2) \ , \ s \qquad (11\text{-}3)$$

where

V_2 = volume of brake line connecting brake application valve and brake chamber, ft³

The total time lag is increased by the time lags of the brake application valve associated with each of the three phases. The valve time lag can only be determined conveniently by experiment for the particular brake application valve installed in the brake system. The total time lag t_{total} is

$$t_{total} = t_1 + t_2 + t_3 + t_v \ , \ s \qquad (11\text{-}4)$$

where

t_v = time lag of application valve, s

For example, a tractor-semitrailer combination may have the brake system data that follow: l_1 = 10 ft, l_2 = 30 ft, $V_o + V_s$ = 0.10 ft³, and V_2 = 0.03 ft³. The total time lag computed by Eq. 11-4 is

t_{total} = 0.010 + 0.082 + 0.220 + 0.25 = 0.562 s

In the calculations t_1 = 0.01 s, t_2 = 0.082 s, t_3 = 0.220 s, and t_v = 0.25 s were either assumed or computed.

The time lag due to the long brake line length associated with the brakes of articulated vehicles can become critical at higher speeds. Studies have shown that a time lag of one second or more between the brakes of the empty semitrailer and the tractor brakes

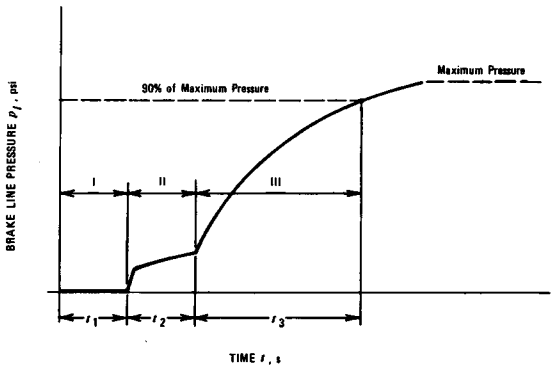

Figure 11-2. Schematic of Pressure Rise in Air Brake System

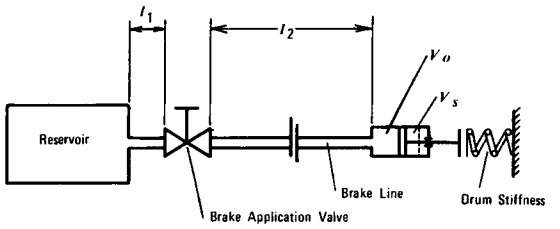

Figure 11-3. Air Brake System Schematic

may cause instability for speeds in excess of 60 mph due to the increased horizontal forces at the kingpin of the fifth wheel and the premature wheel lock up associated with an empty combination (Ref. 9).

In vehicle combinations it is essential that the brakes of the rear axle of the trailer are applied first and then the brakes applied progressively forward to the front axle of the tractor in order to avoid too large fifth wheel kingpin or hitch forces. Large kingpin or hitch forces may cause jackknifing or trailer swing even if the wheels have not yet attained sliding conditions.

In the United States, it is common practice to define the response time of a pneumatic brake system as the time required from the instant of brake pedal movement until a pressure of 60 psi is attained in the brake chamber having the longest brake line distance from the brake valve. Results of road tests have shown that it takes considerably more time to reach maximum brake line pressure and hence maximum deceleration than that required to reach 60 psi. Vehicle tests also have demonstrated that time lags are greater for the empty vehicle than for the loaded when wheels unlocked stops are required. This is caused mainly by the lower line pressure in the case of the empty vehicle resulting in lower pressure differentials and consequently slower brake chamber fill characteristics. In Europe it is the practice to define the total time delay as the time elapsed between the beginning of depression of the brake pedal and the instant when 90% of the maximum pressure is attained in the brake chamber located the longest distance away from the brake valve.

Brake response time tests are conducted to determine the time required by the individual brake chamber pressures to reach a specified value. To measure the brake response time of a tractor-trailer combination, pressure transducers are fitted to the output of the brake application valve, and at each axle of the vehicle on which brakes are mounted. In Fig. 11-4 brake response times measured on a tractor-semitrailer are presented (Ref. 10). Improvements of brake response times of pneumatic brake systems can be achieved through the use of larger cross section hoses and pipes, improved connectors and fittings, quick release valves, relay valves on the tractors, and trailer brake synchronization. Quick release valves provide a large exit opening for the air to vent to the atmosphere at the moment the driver releases the brake pedal. The quick release valve is located near the axle so that the air is not required to travel to the application valve exit. Relay valves serve the function of decreasing the response times of brake chambers during brake application and brake release. Their

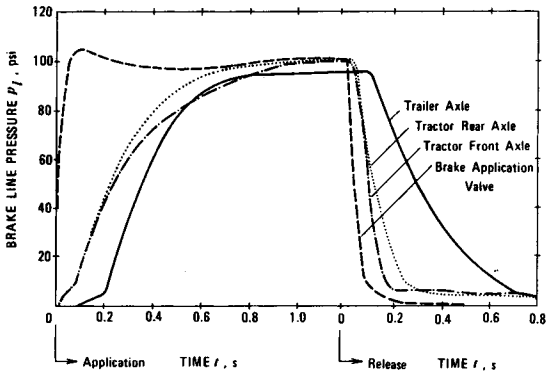

Figure 11-4. Brake Response Times For Tractor-Semitrailer Combination

operation is similar to that of the brake application valve of the driver, however remotely controlled by the brake line pressure from the application valve. Trailer brake synchronization involves the application of the trailer brakes by means of an electrical signal. Tests have shown that brake synchronization improves, i.e., decreases trailer brake application time by about 25% and the release time by more than 40% (Ref. 10). The installation of proportioning valves and/or wheel-antilock brake systems does not seem to affect either application or release times (Ref. 10).

REFERENCES

1. F. A. G. Fazekas, "Brake Torque", *Automobil Engineer*, May 1951, pp. 185-191.
2. G. Fritzsche, "Investigations Concerning the Interrelation of the Application and Effect of Motor Vehicle Brakes, Part 5: The Relation Between Brake Actuation and Brake Force for Hydraulic Brake Systems", *Deutsche Kraftfanrtforschung and Strassenverkehrstechnik*, Report No. 116, 1958.
3. G. B. Hickner and D. W. Howard, *Analog Simulation as a Design Tool for Advanced Braking Concepts*, SAE Paper No. 700157, January 1970.
4. T. S. Scafer, et al., *Design and Performance Considerations for Passenger Car Anti-Skid Systems*, SAE Paper No. 680458, May 1968.
5. D. K. Fisher, *The Dynamic Characteristics of Vehicle Braking Systems*, Ph.D. Dissertation, University of Michigan, Ann Arbor, Michigan, 1970.

6. H. Buehler, "The Dynamic Characteristics of Pneumatic Brakes and Their Simulation by the Analog Computer", *Glaser Annalen*, Vol. 90, No. 5, May 1966.
7. F. Sido, "Analysis of the Response Characteristics of Pneumatic Brake Systems Through Model Test", *Automobiltechnische Zeitschrift*, Vol. 71, No. 3, 1969.
8. J. P. C. Guerana, *The Influence of Time Lag in the Braking of Commercial Vehicles*, 12th F.I.S.I.T.A. Congress, Paper No. 2-08.
9. A. Slibar and H. Troger, "Unsteady Behavior of the Tractor-Semitrailer during Delayed Trailer Braking", *Automobiltechnische Zeitschrift*, Vol. 75, No. 4, 1973.
10. R. W. Murphy, et al., *Bus, Truck, Tractor-Trailer Braking Performance*, Final Report, Contract FH-11-7290, prepared for U.S. Department of Transportation, March 1971.

CHAPTER 12
BRAKE SYSTEM FAILURE

In this chapter basic relationships presented in previous chapters are applied to the analysis of braking with the system in a partially failed condition. Brake circuit and power boost failure and brake fade are investigated.

12-0 LIST OF SYMBOLS

A_C = brake chamber area, in.^{2}
A_{MC} = master cylinder area, in.^{2}
A_{WC} = wheel cylinder area, in.^{2}
a = deceleration, g-units
a_F = front wheels unlocked deceleration, g-units
a_R = rear wheels unlocked deceleration, g-units
BF = brake factor, d'less**
BF_{left} = brake factor of left brake, d'less
BF_{right} = brake factor of right brake, d'less
B^* = power assist gain, d'less
F_a = application force, lb
F_p = pedal force, lb
i = identifies location of wheel, d'less
K = steering stiffness, lb·in./deg
k = ratio of push rod piston travel S_3 to available travel of the pistons of tandem master cylinder S_{av}, d'less
l_o = tire offset, in.
l_p = pedal lever ratio, d'less
n = number of braked wheels, d'less
p_l = brake line pressure, psi
p_o = pushout pressure, psi
R = effective tire radius, in.
r = effective drum or disc radius, in.
S_{av} = $S_3 + S_4$, travel of pistons associated with tandem master cylinder available for pressure buildup, in.
$S_{p,failed}$ = pedal travel with circuit failure, in.
$S_{p,front}$ = pedal travel with front brakes operational, in.
$S_{p,max}$ = maximum pedal travel, in.
$S_{p,nor}$ = normal pedal travel, in.
$S_{p,rear}$ = pedal travel with rear brakes operational, in.
S_1 = travel to overcome push rod play, in.
S_2 = travel to overcome hole connecting chamber with reservoir, in.
S_3 = possible push rod piston travel, in.
S_4 = possible floating piston travel, in.
W = vehicle weight, lb

**d'less = dimensionless

δ = front wheel steering angle, deg
η_c = wheel cylinder efficiency, d'less
η_p = pedal lever efficiency, d'less
μ = tire-road friction coefficient, d'less
ρ = ratio of actual travel used for pressure build up by pushrod piston and floating piston to available travel of pushrod piston and floating piston, d'less
ϕ = rear brake force divided by total brake force, d'less
χ = center of gravity height divided by wheel base, d'less
ψ = static rear axle load divided by vehicle weight, d'less

12-1 BASIC CONSIDERATIONS

Motor vehicle brake systems are designed to decelerate the vehicle safely. A review of the approximately 8000 multidisciplinary accident investigation studies reveals that brake malfunctioning was noted as accident causation factor in less than 2% of all accidents (Ref. 1). The brake malfunctioning involved brake failures such as brake line failure, wheel cylinder failure, brake hose failure, defective lining attachment, and lining mismatch. A review of the individual case reports revealed that most brake malfunctionings were caused by faulty maintenance or repair. Based on the accident data available, it appears that present brake system designs are sufficient and a reduction of braking accident causation may be expected only from design changes that affect maintainability.

12-2 DEVELOPMENT OF BRAKE FAILURE

Failure of braking system components under ordinary driving conditions is likely to occur only if:

1. Parts are defective
2. Parts become severely worn
3. Parts become degraded.

A part becomes degraded, e.g., through oil contamination of brake linings. A part becomes severely worn through long-time use, e.g., in the case of cups

or seals of master cylinders and wheel cylinders. A part is defective when it is designed defectively or manufactured defectively.

In friction brakes the linings are designed to take most of the wear. Since wear will increase with time of rubbing, linings and drums in use over a longer period of time are more likely to fail than new ones. Also, master and wheel cylinder housings, pistons, and seals will show increasing wear with time of operation. Excessive wear may cause brake failure. In general, brake or automobile manufacturers will specify permissible wear dimensions of cylinders and drums. Under normal driving conditions failure of brake components of new vehicles is not likely to occur. In most cases brake system failures occur during severe brake application, i.e., during driving maneuvers requiring large pedal forces that severely stress the entire brake system.

Degradation of brake components because of corrosion, aging, or environmental factors may also cause brake failure. Investigations have shown that steel and copper coated steel hydraulic brake tubing used on cars and trucks can be a safety hazard (Ref. 2). The performance of steel tubing becomes highly erratic after four to six years in service. The age of the vehicle appears to be more significant than mileage relative to brake tube corrosion (Ref. 2). Visual inspection of brake tubing does not always give an accurate indication of its performance. Improvements in brake tubing performance is accomplished through different materials, specifically copper alloy (Ref. 3). The results showed that copper alloy tubing material exhibited no significant decrease of tensile strength after 180 days' exposure to salt spray, whereas copper coated steel tubing showed no tensile strength, indicating complete corrosion.

Prior to the development of a partial or complete brake failure, certain conditions exist that may indicate the beginning of brake failure. These conditions are different for drum brakes and disc brakes in several points. Major causes of brake failure are discussed.

1. Drum Brake System

Defect	Cause
a. Brake pedal travel too long; brake pedal touching floor.	Worn linings; leaking brake system.
b. Brake pedal travel long and spongy	Air in brake system; low on brake fluid
c. Brake pedal travel long (after bleeding of brake)	Check valve of master cylinder defective
d. Brake pedal travel long but may be reduced by "pumping"	Check valve of master cylinder not closing; check valve spring too weak
e. Brake pedal can be pushed to the floor after holding initially	Leaking brake lines or seals in master or wheel cylinder
f. Brakes heat up while driving	Compensating port connecting reservoir and master cylinder not open when master cylinder piston is in released position; brake shoe return springs too weak due to aging; rubber seals have "grown" due to use of wrong fluid in brake system; tight wheel bearing or wheel adjustment
g. No or low braking performance, hard pedal	Brake linings contaminated with oil or water; wrong brake linings; assist unit defective; leak in brake system; defective seals in master cylinder
h. Brake applies without being operated by driver	Same cause as 1f and outboard, rear axle ball bearing cage disintegrated
i. Brakes develop brake imbalance (left-to-right)	Brake drum not round; brake linings contaminated by oil
j. Brakes grab and perform erratically; brakes tend to lock up	Brake linings are not attached securely to shoes; lining rivets contact brake drum; brake drum not round; brake shoe return springs too weak
k. Brakes make noise while braking	Brake drum not round; dirt contamination of linings; lining rivets not securely attached; metal shoe contacting drum
l. Brake grabs in spite of low pedal force	Improperly adjusted brake; brake backing plate not securely attached

m. Brake(s) do not release	Frozen master cylinder piston; weak or broken shoe return springs, frozen wheel cylinder piston(s)

2. Disc Brake System

Defect	Cause
a. Excessive pad wear	Pads do not move freely in pad support; caliper pistons do not move freely in wheel cylinder housing; contaminated brake rotor; rotor surface rough; rear brakes (if drum brakes) out of adjustment
b. Excessive brake pedal travel	Brake rotor has excessive axial tolerance; air or not enough brake fluid in brake system; leak in brake system; defective seals in master cylinder
c. Low or no brake force	Same as 1g; caliper pistons pushed too far back during repair

3. Brake Failures Common to Drum and Disc Brake Systems

Defect	Cause
a. Soft pedal	Caused by air in the brake system or by vaporization of brake fluid due to excessive temperatures at wheel cylinders
b. Hard pedal and excessive pedal force	Defective vacuum assist unit, wheel cylinder pistons not moving freely, wrong or oily linings
c. Brake pedal vibrations	Caused by waves in brake fluid due to wheel cylinder vibrations which are caused by excessive axial play of disc brake rotors, excessive wheel bearing looseness, or drum not round
d. Brake fade	Caused by a reduction in gain or brake factor of wheel brakes; poor lining; excessive brake temperatures or vehicle speed; fading is more pronounced in drum brakes than in disc brakes due to the greater sensitivity of drum brakes to lining friction coefficient
e. Slow braking response	Defective vacuum assist unit

4. Brake Failures of Air Brake Systems

Defect	Cause
a. No brake force	No air supply pressure; restricted tubing or hose; defective application valve
b. Low brake force	Low brake line pressure; too much push rod travel at brake chambers due to excessive lining wear; worn linings or drums; leaking chamber diaphragm; slack adjuster out of adjustment; oil on brake linings
c. Slow brake response	Low brake line pressure; linkage binding; too much push rod travel; leaking application valve; leaking brake chamber diaphragm; brake shoe anchor pins frozen, application valve control linkage improperly adjusted
d. Slow brake release	Linkage binding; restriction in brake line; too much push rod travel; defective application valve; binding cams or wedges at wheel brakes, weak brake shoe return springs

e. Grabbing brakes	Uneven slack adjuster setting; linkage bindings at one or more wheels; linings worn unevenly; brake shoe return spring weak or broken; defective brake chamber; unequal springs in brake chambers or between brake shoes
f. Slow pressure buildup in reservoir	Clogged air cleaner; air leak; defective compressor; open or leaking reservoir drain cocks; defective compressor governor.

The brake failures identified in the previous list can be grouped into failures causing (a) insufficient brake force; (b) excessive component wear; and (c) inconvenience to driver. Of these, the category dealing with insufficient brake force will be discussed in par. 12-4.

12-3 DEVELOPMENT OF DRUM AND ROTOR FAILURE

Drums and disc brake rotors can fail, e.g., due to excessive wear, cracking, and surface rupture. Excessive wear can be reduced through proper sizing of the drum or rotor, selection of improved drum and rotor materials, and brake designs that prevent the grinding effect of contaminants such as dust and mud. Sealed brakes are used in applications where vehicles are required to operate in adverse environment (par. 3-1.8). Some details relating to surface rupture of disc brake rotors are discussed next.

Before an objective assessment of the conditions leading to rotor failure by rupture can be attempted, a summary of the factors influencing surface rupture is appropriate.

Rupture will occur when the stress exceeds the strength of the material. The occurrence of surface rupture is affected mainly by the following factors: thermal stress, number and frequency of braking cycles, surface conditions due to machining and corrosion, and material strength.

The thermal stresses are affected by:

1. Temperature gradient
2. Thermal expansion coefficient as a function of temperature
3. Elastic modulus as a function of temperature
4. Particular rotor geometry.

The temperature distribution in the rotor is affected by:

1. Heat flux absorbed by the rotor
2. Thermal conductivity as a function of temperature
3. Specific heat as a function of temperature
4. Rotor density
5. Initial rotor temperature
6. Rotor thickness
7. Duration of brake application
8. Heat transfer coefficient
9. Ambient temperature.

The strength of the rotor material is affected by:

1. Chemical composition
2. Melting practice
3. Microstructure and heat treatment
4. Temperature
5. Type of stress loading.

It is apparent that surface failure is affected by a combination of factors. However, for a given rotor material having a certain strength associated with thermal loading, the tendency of the surface to rupture will be decreased if for a given heat flux the temperature gradient at the surface assumes small values, the thermal expansion coefficient and the elastic modulus are decreased, and the rotor is designed so that thermal expansion is maximally unconstrained. The temperature gradient, again for a given heat flux, depends during the first few brake applications upon the thermal properties of the rotor material.

For example, a high thermal conductivity results in a less marked temperature gradient. The rate of change of temperature at a given location in the rotor will be less pronounced for increased values of specific heat and material density. The rotor thickness has a twofold effect upon the stress state; a thicker rotor produces higher temperature gradients and tends to be more rigid, thus producing more marked constraints on free thermal expansion.

Careful examination of the rotors used in a study showed that surface rupture occurred after only one brake stop from 60 mph (Ref. 4). This observation indicated that the temperature gradients were sufficiently large to cause the thermal stresses to exceed the yield strength of the material existing at that temperature. The thermal stress computation yielded compressive stresses up to 26,000 psi. Since the nominal yield strength of cast iron grade 32510 is listed as 32,500 psi at room temperature, it is deemed highly likely that plastic deformation occurred at the rotor surface, considering that the yield strength is strongly temperature dependent (Ref. 5).

The test results indicated that to a large measure the number of surface cracks was little affected by the number of brake applications. The reason for this behavior is that surface rupture will occur after one brake application, provided the conditions previously described are met. Test results have shown that the average crack length is approximately proportional to the energy absorbed by the rotor. Since the surface temperatures of the rotor may easily reach 1,400°-1,500°F after only a few brake applications, metallurgical considerations have a significant effect upon any localized stress pattern.

Careful examination of a rotor surface after 60 brake applications showed the surface cracks were generally oriented in a radial direction and furthermore indicated a significant deterioration of material, such as attachment of metal particles from the brake pad onto the rotor surface. Rotor surfaces examined also showed severe plastic flow and, to a certain extent, brittle fracture in the generally highly loaded friction surface. During severe braking, the surface layer easily may attain temperatures 400°-800°F higher than the interior. Upon releasing the brakes, sudden heat transfer from the outside layer to the inside may occur. This sudden quenching of the rotor surface may result in the formation of martensite, accompanied by an expansion above the original rotor surface. Since the surrounding material provides a restraint, the stress pattern developed may not be radially oriented. A fine rupture is produced at the surface and this may later develop into major cracks oriented in a radial direction.

Inspection of severely loaded friction surfaces also has shown that fine cracks may result from marked stress concentration due to surface porosity. Here the cracks originated from edges of places where either particles of the base material had been torn out by the friction process or where subsurface porosities had been torn open. Although the original cracks were not necessarily located in a radial direction, the further development of the crack tended to be oriented radially.

Two basic modes of surface rupture have been observed. In single brake applications wherein the rotor surface was subjected to excessive temperature gradients, surface cracks, if they occurred, developed generally in a radial direction. A condition involving surface temperature gradients causing surface rupture is commonly referred to as thermal shock. Subsequent braking cycles with the brake operating below certain maximum temperatures produced a stress pattern that was mainly a further development of the original cracks caused by thermal shock. The other failure mode appears to be associated with severe surface temperatures, resulting in partial surface melting and dislocation of particles at the surface. This condition might produce hot spots, resulting in a randomly oriented localized stress pattern. Stress patterns of this type also may be caused by localized interference of heat transfer, resulting from subsurface porosities. The surface porosities may be produced by material tearing or opening of subsurface porosities. Radially oriented cracking can be an extension of randomly oriented fine cracks that are developed, i.e., from subsurface porosities, but it may also be the sole cause of surface rupture. This statement has important implications concerning the design and testing of brake rotors.

12-4 BRAKE FAILURE ANALYSIS

The purpose of a failure analysis is to determine how the design effectiveness of the brake system, i.e., the deceleration/pedal force relationship, is modified if a partial failure should occur within the system.

Three basic categories of failure are considered in this failure analysis:

1. Loss of line pressure in dual braking system
2. Loss of vacuum boost in a power boost element
3. Loss of effectiveness exhibited by an overheated brake commonly called fade.

Each of these partial failure modes is considered and evaluated with respect to its influence on vehicle braking performance and with respect to the resulting consequences for safety — namely, the ability of drivers to achieve the desired levels of deceleration.

12-4.1 BRAKE LINE FAILURE

A hydraulic brake system is a dual system when the transmission of braking effort from the master cylinder to the wheel brakes consists of two independent circuits. Any power assist unit installed in the system does not have to consist of two circuits.

Any brake system contains the mechanism for pedal force application, pedal force transmission, and brake force production. The mechanism for application of pedal force F_p involves a pedal lever ratio l_p such that a pedal effort $F_p l_p$ is applied to the master cylinder push rod. The pedal force transmission involves a dual circuit master cylinder, generally termed tandem master cylinder and the hydraulic brake lines between master cylinder and wheel brakes. Connected into the brake lines can be special devices such as metering or proportioning valves. The wheel brakes may be divided into those involving one or two actuating mechanisms. The first category includes leading-trailing type drum brakes and single caliper type disc brakes with one wheel cylinder. In

the event of a circuit failure no braking action can be developed by this brake. Brakes involving two actuating mechanisms or two wheel cylinders may be connected to both brake circuits. In the case of one circuit failure the wheel brakes produce a reduced brake force, in most cases a braking action equal to 50% of the nonfailed case.

The six basic possibilities for installing brake lines between master cylinder and wheel brakes to form two independent brake line circuits are shown in Fig. 12-1. System 1 is the design generally used by vehicles of US manufacture. Systems 2, 4, 5, and 6 exhibit equal braking force for each circuit. In the case of systems 1 and 3, a failure of circuit 1 or 2 will result in different braking force. The braking force achievable with systems 2 and 6 are identical in the failed mode for either circuit. The effects upon vehicle stability while braking under partial failure mode, i.e., a failure of circuit 1 or 2 will be different, with system 6 showing an undesirable side-to-side brake unbalance. Since it is obvious that a dual system of type 6 is undesirable, it is not included in any further analysis.

Three measures of braking performance for dual brake systems may be identified.

1. Reduced braking force of the vehicle in the partial failure mode due to a decreased brake system gain between master cylinder exit and wheel brake.
2. Changes in brake force distribution front to rear and hence reduced braking efficiency.
3. Increased application times due to longer brake pedal travel.

All three measures will cause an increase in stopping distance. In addition to these measures relative to brake force production, the effects of brake force unbalance on vehicle stability must be considered.

12-4.1.1 Vehicle Deceleration

The deceleration of a vehicle with nonfailed brakes may be computed by Eq. 5-3. The deceleration *a*

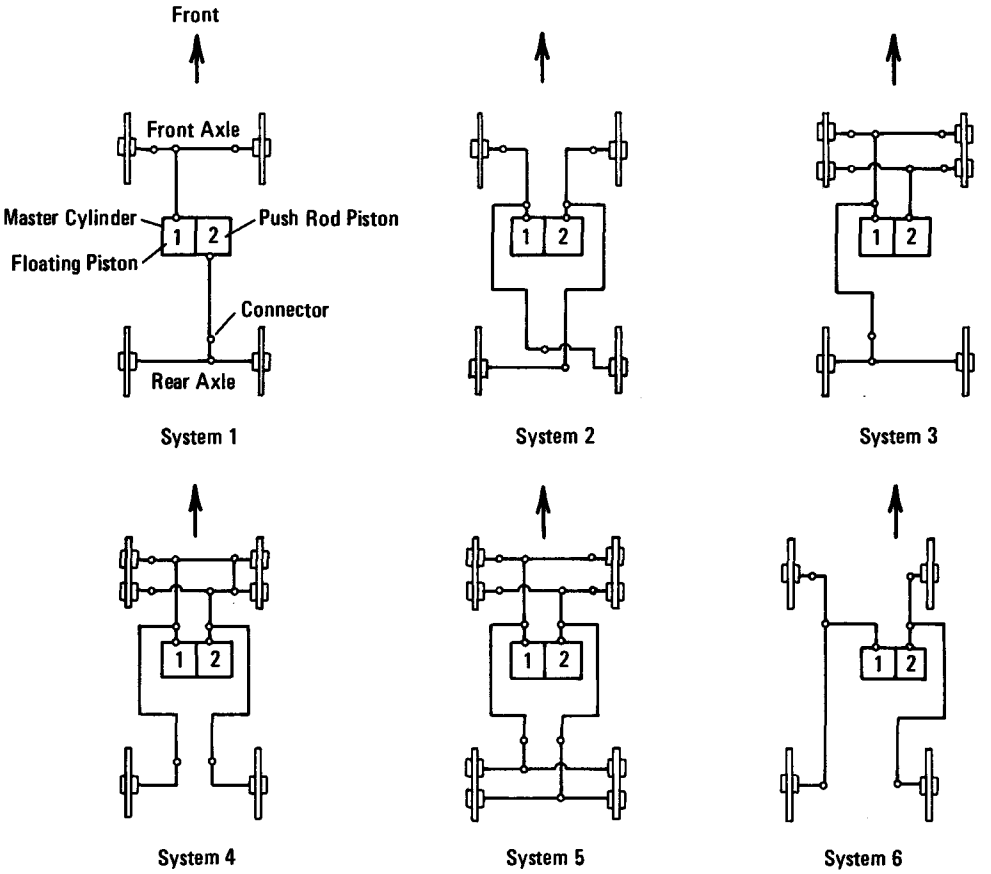

Figure 12-1. Different Dual Circuit Brake Systems

achievable with a complete brake system may be rewritten as

$$a = \frac{1}{W} \sum^{n} [(p_l - p_o) A_{WC}\, BF\, \eta_c\, r/R]_i \text{, g-units} \quad (12\text{-}1)$$

where

A_{WC} = wheel cylinder area, in.^{2}
BF = brake factor, defined as ratio of brake drag to actuating force of one shoe, d'less
i = identifies location of wheel, i.e., front or rear, left or right, d'less
n = number of wheels braked, d'less
p_l = brake line pressure, psi
p_o = pushout pressure, psi
R = effective tire radius, in.
r = effective drum or disc radius, in.
W = vehicle weight, lb
η_c = wheel cylinder efficiency, d'less

Eq. 12-1 may be used to compute the vehicle deceleration with a partially failed system by summing only the brake forces of the wheels not affected by a system failure.

12-4.1.2 Pedal Force

The pedal force F_p is

$$F_p = \frac{p_l A_{MC} B^*}{l_p \eta_p} \text{, lb} \quad (12\text{-}2)$$

where

A_{MC} = master cylinder area, in.^{2}
B^* = power assist gain, d'less
l_p = pedal lever ratio, d'less
η_p = pedal lever efficiency, d'less

The pedal force/brake line pressure gain is not affected by a circuit failure as indicated by Eq. 12-2. The pedal force/deceleration gain is affected by a circuit failure as an evaluation of Eqs. 12-1 and 12-2 indicates. As shown in par. 12-4.2, a loss of vacuum assist results in decreased values for the power assist gain B^* and thus causes increased pedal force requirements.

12-4.1.3 Braking Efficiency

Braking efficiency is a measure of the capability of the vehicle to use a given tire-road friction coefficient for vehicle deceleration. The maximum wheels unlocked deceleration a_R or a_F that can be obtained with the partially failed system on a road surface with a specified tire-road friction coefficient μ can be expressed for system 1 (Fig. 12-1) as

1. Front failed:

$$a_R = \frac{\psi\mu}{1 + \mu\chi} \text{, g-units} \quad (12\text{-}3)$$

2. Rear failed:

$$a_F = \frac{(1 - \psi)\mu}{1 - \mu\chi} \text{, g-units} \quad (12\text{-}4)$$

where

μ = tire-road friction coefficient, d'less
χ = center of gravity height divided by wheel base, d'less
ψ = static rear axle load divided by vehicle weight, d'less

Braking efficiency may be computed by dividing the decelerations computed by Eqs. 12-3 and 12-4 by the tire-road friction coefficient μ. Similar relationships may be derived for most of the system indicated in Fig. 12-1. An alternative method for computing wheels unlocked deceleration levels in the failed condition for any type of brake systems uses the steps that follow which are similar to those of the braking performance calculation program discussed in Chapter 7:

1. Set increased levels of brake line pressure.
2. Compute wheel braking forces.
3. Compute total brake force.
4. Compute vehicle deceleration.
5. Compute tire-normal forces.
6. Compute individual values of tire-road friction coefficient μ required to prevent wheel lock up.
7. Draw a graph showing μ required as function of vehicle deceleration.
8. Obtain vehicle deceleration a achievable for a specified μ from Step 7.
9. Compute braking efficiency by dividing deceleration a by μ.

12-4.1.4 Pedal Travel

The increased pedal travel is a significant factor when braking with one circuit failed. Reasons for this are longer times required to apply the brakes and possible undesirable driver reaction to the unfamiliar pedal position. Since pedal travel is determined by the master cylinder piston travel, the functioning of a master cylinder used in dual circuit brake systems is discussed next for normal and failed operation. A

typical dual circuit or tandem master cylinder is illustrated in Fig. 12-2. The operation is in principle the same as a single circuit master cylinder. When the push rod piston is moved toward the floating piston, the hole (1) connecting chamber (2) with the reservoir (3) is closed. The resulting pressure buildup in chamber (2) is transmitted by the floating piston to chamber (4). The floating piston moves forward and hole (5) connecting chamber (4) with the brake fluid reservoir (6) closes. At this instant the same pressure exists in both chambers and the respective brake lines.

If the circuit connected to chamber (2) fails, i.e., develops a hydraulic leak, no brake line pressure can be developed in chamber (2). This condition causes the pin (7) of the push rod piston to contact the pin (8) of the floating piston. The push rod force is transmitted directly upon the floating piston and pressure buildup in chamber (4) results.

Similarly, a leak in the circuit connected to chamber (4) causes the floating piston pin (9) to come in contact with the stop (10). At this instant brake line pressure can be developed in chamber (2) by the push rod piston. The pedal travels in either failure mode are longer than in the unfailed condition. Longer pedal travels result in increased time before the brakes are applied and hence longer stopping distance. Measurements of pedal displacement indicate that a pedal travel of 5 in. requires approximately 0.25 s for the 90th percentile male driver.

The pedal travel is determined by the travel of the push rod piston. Since the push rod piston travel is affected by the travel of the floating piston, the following travels are identified and illustrated in Fig. 12-2:

1. Travel to overcome push rod play

$$S_1 \approx 0.02\, S_{av} \text{ , in.}$$

2. Travel to overcome hole connecting chamber (2) or chamber (4) with reservoir

$$S_2 \approx 0.06\, S_{av} \text{ , in.}$$

3. Possible travel of push rod piston available for pressure buildup

$$S_3 = kS_{av} \text{ , in.}$$

4. Possible travel of floating piston available for pressure buildup

$$S_4 = (1 - k)S_{av} \text{ , in.}$$

where

$S_{av} = S_3 + S_4$, travel of pistons associated with tandem master cylinder, available for pressure buildup, in.

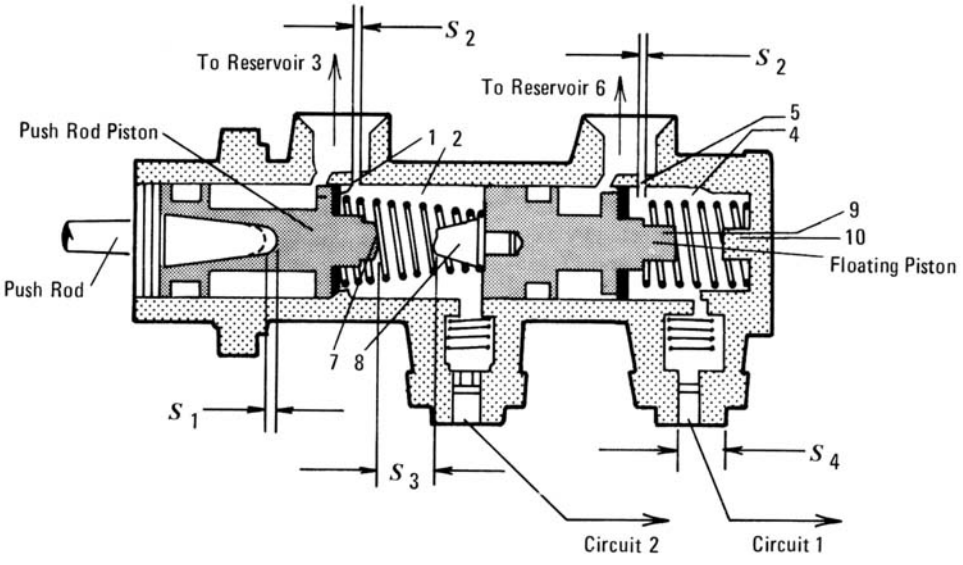

Figure 12-2. Tandem Master Cylinder

k = ratio of push rod piston travel S_3 to available travel of the pistons of the tandem master cylinder S_{av}, d'less

The factor k generally assumes values between 0.9ϕ to 1.25ϕ, where ϕ is the ratio of rear axle brake force divided by total brake force, dimensionless.

The maximum pedal travel $S_{p,\,max}$, determined by the maximum travel of the pistons of the master cylinder, the push rod play, and the pedal lever ratio is

$$S_{p,\,max} = l_p(S_1 + S_2 + S_3 + S_4) \text{ , in.} \qquad (12\text{-}5)$$

Eq. 12-5 can be rewritten with the previous expression for the individual travels as

$$\begin{aligned} S_{p,\,max} &= l_p S_{av}(0.02 + 0.06 + k + 1-k) \\ &= 1.08\, l_p S_{av} \text{ , in.} \end{aligned} \qquad (12\text{-}6)$$

where

l_p = pedal lever ratio, d'less

The travel of the push rod piston and floating piston actually used in a normal braking situation is less than the maximum design values S_3 and S_4. Let ρ be the ratio of the actual travel used for pressure build-up by the push rod piston and floating piston to the available travel of the push rod piston and floating piston. The brake pedal travel for normal braking for the nonfailed and failed brake system may then be represented by the expressions that follow

1. Service brake not failed:

$$\begin{aligned} S_{p,\,nor} &= l_p S_{av}[0.08 + \rho k + \rho(1-k)] \\ &= l_p S_{av}(0.08 + \rho) \text{ , in.} \end{aligned} \qquad (12\text{-}7)$$

2. Circuit failure, system 1 (Fig. 12-1):

a. Circuit No. 1 failed, i.e., the front brakes are failed and the rear brakes are operative, and the floating piston develops no brake line pressure

$$\begin{aligned} S_{p,\,rear} &= l_p S_{av}(0.08 + \rho k + 1 - k) \\ &= l_p S_{av}[1.08 - k(1-\rho)] \text{ , in.} \end{aligned} \qquad (12\text{-}8)$$

Eq. 12-8 is obtained from Eq. 12-7 by substituting the entire travel of the floating piston available into Eq. 12-7, i.e., $l_p S_{av}(1-k)$ and not $l_p S_{av}\rho\,(1-k)$ as used in normal braking without brake failure.

b. Circuit No. 2 failed, i.e., the rear brakes are failed and the front brakes are operative, and the push rod piston (Fig. 12-2) develops no brake line pressure

$$\begin{aligned} S_{p,\,front} &= l_p S_{av}[0.08 + k + \rho(1-k)] \\ &= l_p S_{av}[0.08 + \rho + k(1-\rho)] \text{ , in.} \end{aligned} \qquad (12\text{-}9)$$

3. Circuit failure, system 2 (Fig. 12-1):
Any circuit failed:

$$S_{p,\,failed} = l_p S_{av}[0.58 + 0.5\rho] \text{ , in.} \qquad (12\text{-}10)$$

4. Circuit failure, system 3 (Fig. 12-1)

a. Circuit No. 1 failed, i.e., the floating piston develops no brake line pressure

$$S_{p,\,failed} = l_p S_{av}[1.08 - k(1-\rho)] \text{ , in.} \qquad (12\text{-}11)$$

b. Circuit No. 2 failed, i.e., the push rod piston develops no brake line pressure

$$S_{p,\,failed} = l_p S_{av}[0.08 + \rho + k(1-\rho)] \text{ , in.} \qquad (12\text{-}12)$$

5. Circuit failure, system 4 (Fig. 12-1)
Any circuit failed:

$$S_{p,\,failed} = l_p S_{av}(0.58 + 0.5\rho) \text{ , in.} \qquad (12\text{-}13)$$

6. Circuit failure, system 5 (Fig. 12-1)
Any circuit failed:

$$S_{p,\,failed} = l_p S_{av}(0.58 + 0.5\rho) \text{ , in.} \qquad (12\text{-}14)$$

12-4.1.5 Performance Calculation

The three performance measures were applied to a particular case. No attempts were made to express longer pedal travels in terms of increased application times. It may be assumed that application time increases linearly with pedal travel.

The decelerations achievable by a passenger vehicle with different circuit failures were computed and are shown in Fig. 12-3. A maximum tire-road friction coefficient of $\mu = 1.0$ was assumed for columns 1 and 4. The tire-road friction coefficient for the computations of columns 2 and 3 was assumed to be large enough to prevent wheel lockup. The column identified by "Wheels Unlocked" (1) represents the maximum decelerations that can be attained by the

	1		2		3		4		5
	Wheels Unlocked		No Proportioning, Pedal Force 110 lb		Proportioning Pedal Force 110 lb		Wheels Locked		Vehicle Side to-Side Stability
No Failure	0.801		1.23		1.23		1.00		Stable
Circuit Failed	1	2	1	2	1	2	1	2	
System 1	0.41	0.64	0.50	0.73	0.25	0.73	0.41	0.64	Stable
System 2	0.48	0.48	0.62	0.62	0.49	0.49	0.50	0.50	Unstable
System 3	0.64	0.61	0.37	0.86	0.37	0.62	0.64	1.00	Stable
System 4	0.48	0.48	0.62	0.62	0.49	0.49	0.84	0.84	Unstable
System 5	0.80	0.80	0.62	0.62	0.49	0.49	1.00	1.00	Stable

Figure 12-3. Calculated Deceleration in g-Units for Partial Failure

different systems with either circuit No. 1 or No. 2 failed. The deceleration achievable with the nonfailed system is indicated also. The column identified by "No Proportioning" (2) gives the decelerations that can be achieved with a brake system with fixed ratio braking and a pedal force of 110 lb with either circuit No. 1 or No. 2 failed. The column identified by "Proportioning" (3) represents the decelerations that can be achieved by a vehicle having a variable brake force distribution. In this case the proportioning valve is not affected by the circuit failure of the front wheels, i.e., the proportioning valve is not bypassed when the front brakes are failed. The column identified by "Wheels Locked" (4) gives the maximum decelerations achievable on a $\mu = 1.0$ friction surface without regard to pedal force and lock up. Column 5 provides information on braking stability.

Inspection of Fig. 12-3 indicates that the performance of system 1 is limited to a deceleration of 0.25g with circuit No. 1 failed, i.e., the front brakes inoperative, when a proportioning valve is installed which is not bypassed when the front brakes are failed. If the proportioning valve is bypassed, the deceleration achievable with a pedal force of 110 lb is 0.5g with the front brakes failed. Inspection of the deceleration values reveals whether the pedal force and brake system gain or tire-road friction determines the deceleration available. For example, a system with proportioning and a pedal force of 110 lb produces a deceleration of 0.25g for system 1 with circuit No. 1 failed. If no pedal force limit were set, the tire-road friction coefficient permits deceleration of 0.41g which indicates that either the pedal force must exceed 110 lb, or if that is undesirable, the brake system gain must be increased.

Indicated in Fig. 12-3 are also the effects of side-to-side brake unbalance on vehicle stability. Only systems 2 and 4 exhibit a measure of vehicle instability upon occurrence of circuit failure. The influence of an unbalance on the front wheels such as experienced by system 2 could, to a large extent, be counteracted by a negative scrub radius. A negative scrub radius forces the wheel to rotate slightly in the direction of the lower brake force thus producing tire slip angles sufficiently large to hold the vehicle in a stable controlled stop (par. 8-1.7).

The pedal travel analysis was applied in detail to the common front-to-rear circuit split identified as system 1. Brake system data of a large domestic automobile were used as a base for computing the pedal travels required to perform a stop under partially failed conditions. The results are shown in Fig. 12-4 in terms of pedal travel ratios. The pedal travel ratios shown in Fig. 12-4 are the pedal travel for normal braking to maximum travel available; the pedal travel with the front brakes failed to maximum travel available; and the pedal travel with the rear brakes failed to maximum travel available. The values were computed for $\rho = 0.5$, i.e., 50% of the available master cylinder piston travel is required for a service brake stop. Inspection of Fig. 12-4 indicates that in the case of a failure of the front brakes the ratio of pedal travel required to apply the rear brakes to the maximum pedal travel is nearly twice the ratio for unfailed or normal brakes for brake force distribution values ϕ less than 0.3.

The ratios of pedal travel under failed conditions to those required under normal conditions may be a more meaningful indicator to the driver. These ratios are presented in Fig. 12-5. Inspection of Fig. 12-5 again clearly indicates that the standard front-to-rear split is of rather questionable safety benefit in the case of front circuit failure due to the significantly increased pedal travels for small values of ϕ. This condition exists in spite of a rather long master cylinder piston travel as indicated by $\rho = 0.50$, used in the calculations.

To show the effect of long versus short master cylinder piston travel for the front-to-rear split design, the pedal travel ratios failed/normal are plotted in Fig. 12-6 as a function of ρ, i.e., versus utilization of effective master cylinder piston travel required for a normal stop. A ratio of floating piston travel to push rod piston travel of 74:26 and a brake

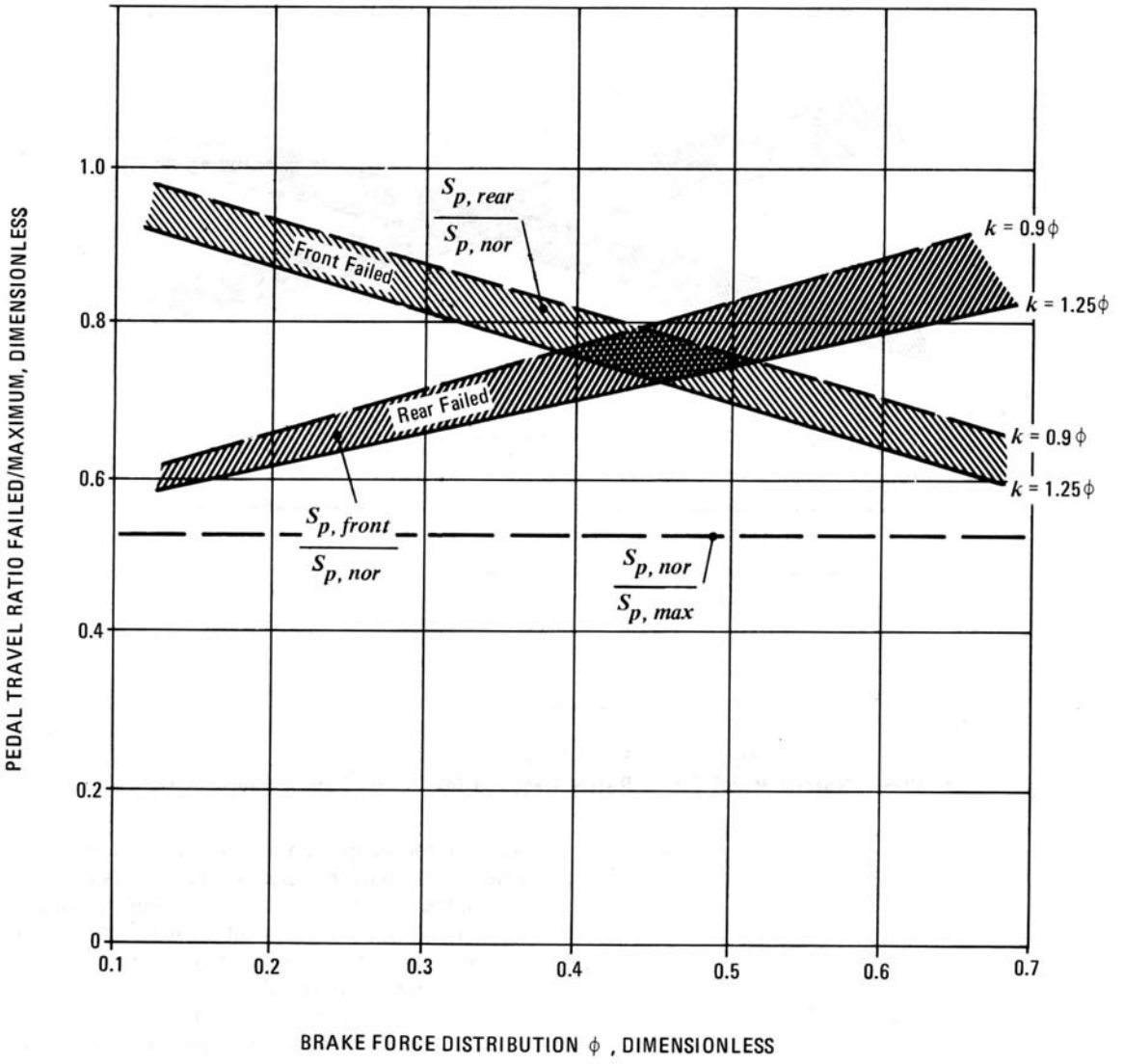

Figure 12-4. Maximum Pedal Travel Ratios Required for Partial Failure Stops, System 1

force distribution $\phi = 0.32$ were used in the calculations. Inspection of the curve representing front brake failure indicates that long master cylinder or large pedal travel reserves, i.e., low values of ρ result in undesirably long pedal travels in case of front brake failure. This condition exists in spite of the highly acceptable normal-to-maximum pedal travel ratio.

12-4.1.6 Improved Dual Brake System Design

Significant improvements in minimizing the effects of partial failure on pedal effort and pedal travel have been accomplished by means of the stepped bore tandem master cylinder (Ref. 6). The brake line pressures achieved under failed conditions are double the pressure achieved under normal conditions. The change in effective piston area is accomplished by

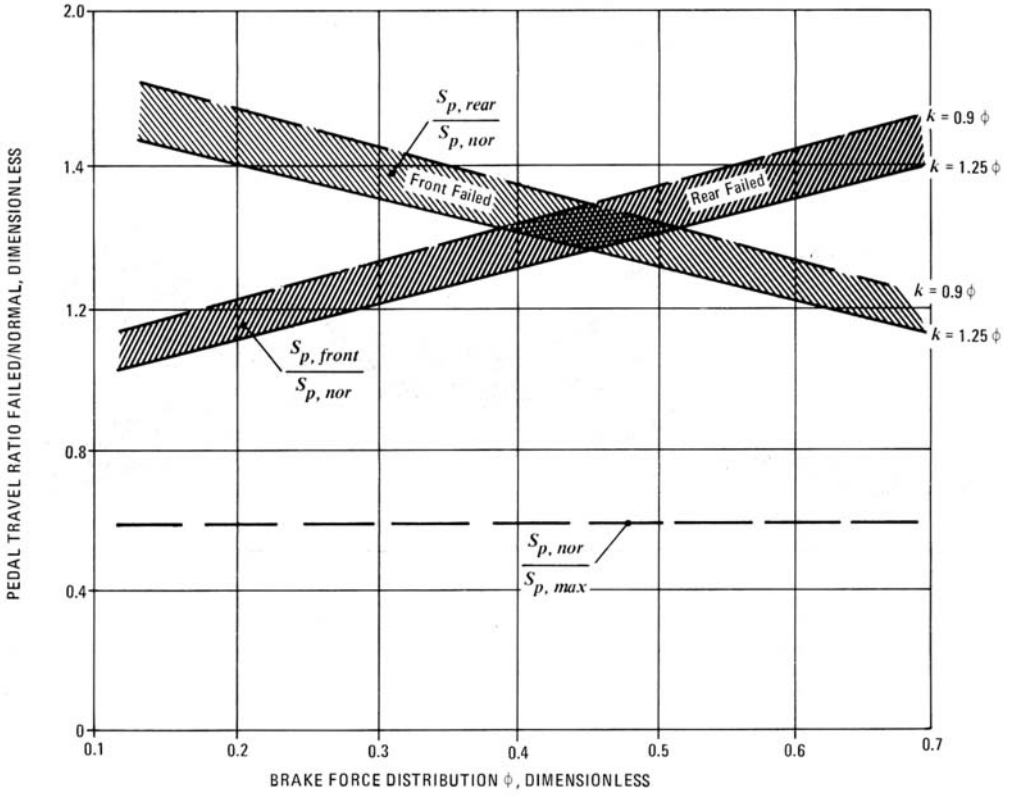

Figure 12-5. Normal Pedal Travel Ratios Required for Partial Failure Stops, System 1

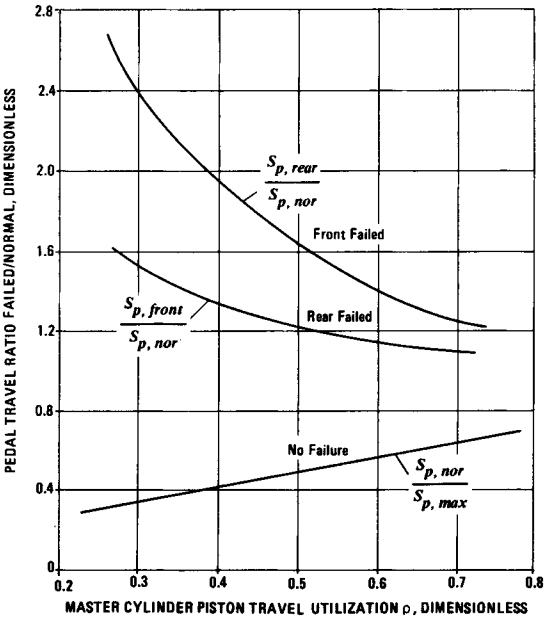

Figure 12-6. Pedal Travel Ratio as a Function of Piston Travel Utilization

means of the stepped bore as illustrated in Fig. 12-7. Whereas, the larger master cylinder feeds both circuits in the case of an intact brake system; the smaller diameter master cylinder is utilized in the event of circuit No. 1 failure, and doubled brake line pressure is produced due to the fact that the smaller piston area is one half the area of the larger piston. If circuit No. 2 fails, the differential area between larger and smaller bore, i.e., one-half of the standard area, becomes the effective brake line pressure producing area. The result is a brake line pressure under failed conditions that is twice as large as under normal conditions. Since under circuit failure conditions not all wheel brakes are actuated, a nearly constant deceleration results with the same pedal effort. The pedal travel in the failed condition exceeds the pedal travel in the unfailed condition by not more than approximately 30%. Thus, pedal forces and pedal travel are no longer the limiting factors in the case of partial failure braking. Brake system splits using unequal volume distribution between circuits and hence significantly different cross-sectional areas for the floating and push rod piston may lead to excessively high brake line pressures in case of partial failure.

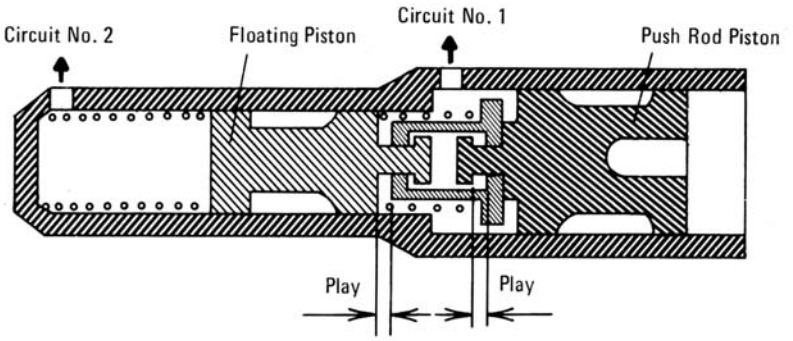

(A) Stepped Bore Master Cylinder, Normal Brake Application

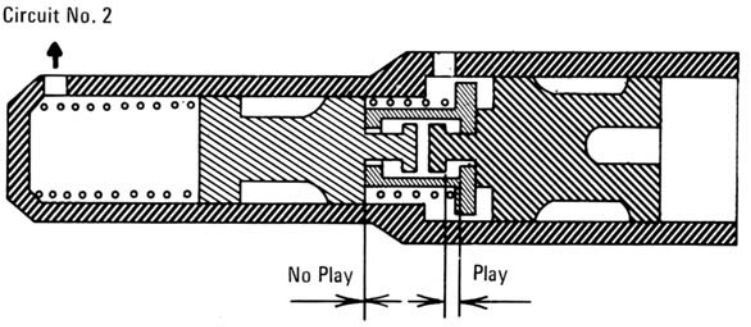

(B) Stepped Bore Master Cylinder, Brake Application With Leakage in Circuit Number 1

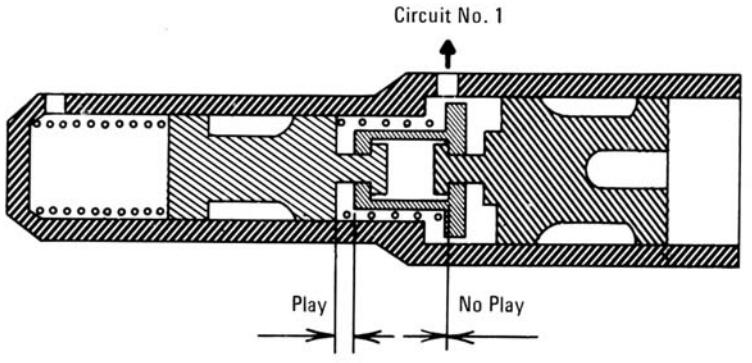

(C) Stepped Bore Master Cylinder, Brake Application With Leakage in Secondary Circuit Number 2

Figure 12-7. Stepped Bore Tandem Master Cylinder

12-4.1.7 Comparison of Dual Brake Systems

A comparison of the dual brake systems represented in Fig. 12-1 indicates a different number of connectors and flexible hoses is required for the different systems. For example, system 1 requires 17 connections compared with 34 for system 5.

A leak is more likely to develop in a hydraulic circuit that contains more removable connections, wheel cylinder seals, and other devices such as valves, and control elements. A comparison of the complexity of the different dual circuit splits is shown in Fig. 12-8. All removable connections, such as T-fittings, are included in Fig. 12-8. The data indicate system 5 to have a higher failure probability than the remaining systems. Difficulties also may arise in installing properly the flexible hoses near the wheels.

Brake System	Single Circuit System	System No.				
		1	2	3	4	5
Wheel Cylinder	8	8	8	12	12	16
Removable Connections	17	15	16	25	26	34

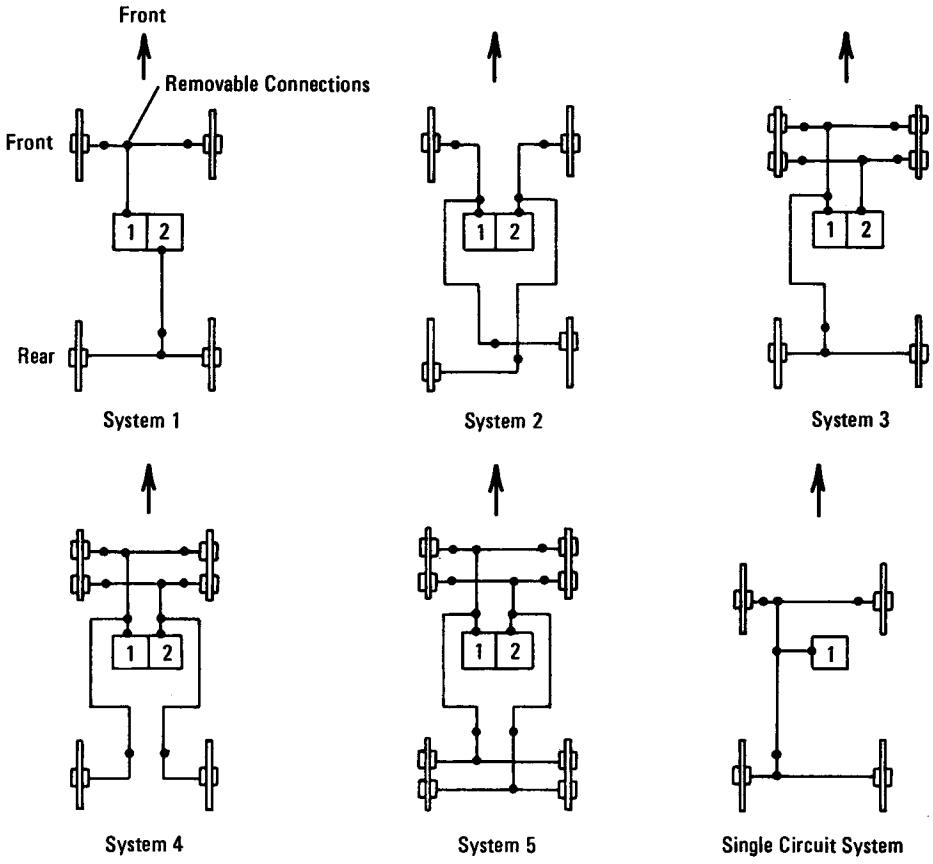

Figure 12-8. Comparison of System Complexity

Not included in the number of removable connections is the third bleeder screw required for double caliper disc brakes if they are designed as one unit.

The maximum temperature of a brake should be kept below certain limits. High brake temperature will result in: (a) brake fade and increased lining wear, (b) high tire bead temperatures, and (c) increased temperature of the brake fluid in wheel cylinders. High brake fluid temperature may cause brake fluid boiling and vaporization. Modern brake fluids boil at approximately 450°F. Consequently, continued brake applications, as experienced in prolonged downhill travel, may cause the brake fluid to boil and vapor to develop, and the brake system to fail.

One effect of thermal overloading on circuit failure of the different dual splits is indicated in Fig. 12-9. It is assumed that the front brakes are experiencing excessive temperatures leading to vaporization of brake fluid and hence failure of the circuits connected to the front wheels. Inspection of Fig. 12-9 indicates that only system 1, the front-to-rear split, provides a partial braking capability on the rear wheels with the front brakes failed due to vaporization. If on the

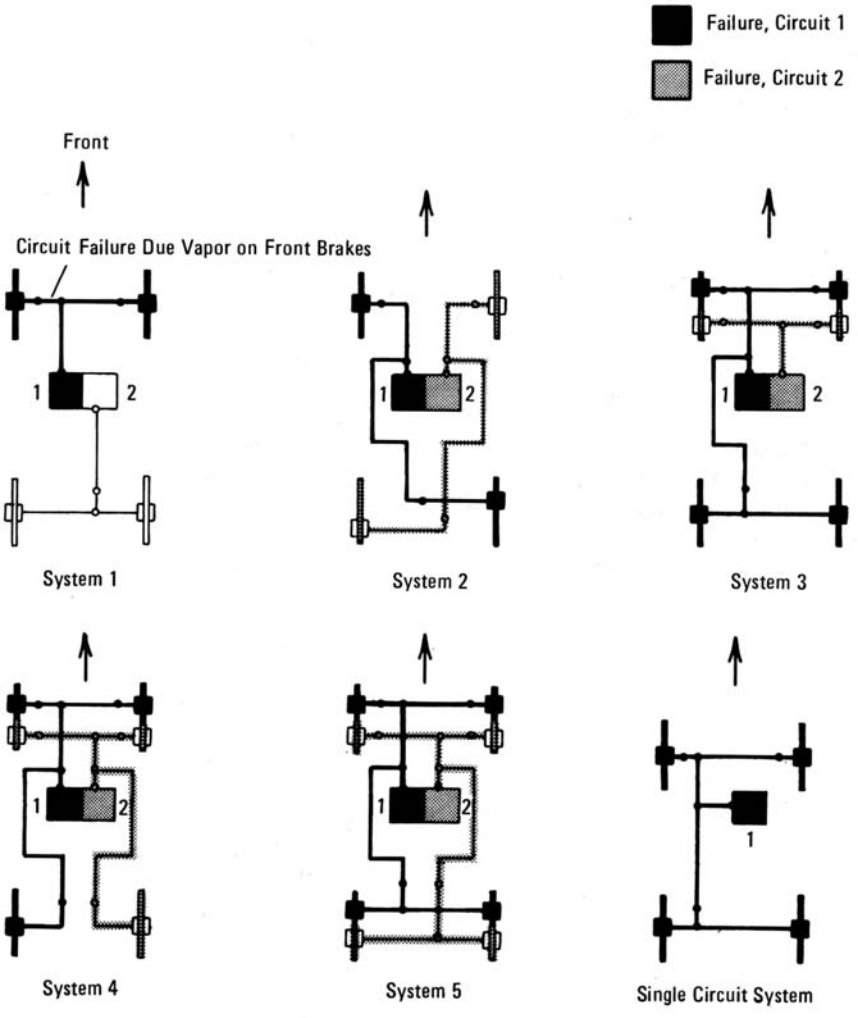

Figure 12-9. Dual Systems, Front Brake Failure Due to Brake Fluid Vaporization

other hand the rear wheels exhibit vaporization and hence circuit failure, all but systems 1 and 3 will fail completely.

12-4.2 VACUUM ASSIST FAILURE

Vacuum assist failure exists when the assist function of the vacuum assist unit is degraded through insufficient vacuum or complete loss of vacuum.

With the complete or partial failure of the vacuum assist unit the reduced brake line pressure may be obtained from Eq. 12-2 with the assist gain B^* reduced accordingly. The lower brake line pressure may then be used in Eq. 12-1 to compute the vehicle deceleration under a power failure condition. Typical results of such an analysis are presented in Fig. 12-10 in form of a braking performance diagram. Typical dimensions were assumed for the elements in a brake system. The observations that follow can be made with respect to various levels of power boost failure:

1. No assist. To produce a deceleration of 0.9g, a pedal force of approximately 270 lb is required. A deceleration of only 0.32g is produced by a pedal force of 100 lb.

2. Thirty-two % assist. The deceleration — produced by a pedal force of 100 lb — is 0.52g. A deceleration of 0.90g requires a pedal force of about 215 lb.

3. Sixty % assist. The deceleration — produced by a 100 lb pedal force — is 0.76g. A deceleration of 0.90g requires a pedal force of about 150 lb.

12-4.3 FAILURE OF FULL POWER HYDRAULIC BRAKE SYSTEMS

Full power hydraulic brake systems use a tandem master cylinder in conjunction with a pressurized accumulator or circulating pump system. Dual circuit

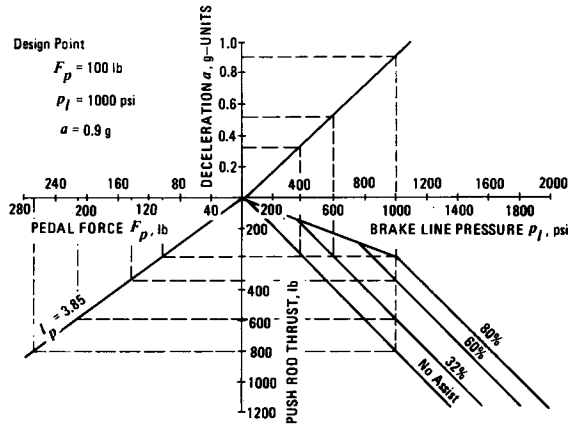

Figure 12-10. Braking Performance Diagram for a Vacuum Assisted Brake System

failure analysis is identical to that of unassisted or vacuum power assisted brake systems. In the event of a power source failure, a sufficient level of energy is stored in the accumulator to produce a certain number of successive emergency stops. Furthermore, the design provides that a "push through" capability exists, i.e., the driver developed pedal force will produce a small retarding effect.

12-4.4 FAILURE OF PNEUMATIC BRAKE SYSTEMS

Pneumatic brake systems are designed to provide an emergency brake application in the event the service brake or primary brakes of the vehicle become partially or completely failed. The system is designed to apply the brakes automatically when the truck or tractor brake system pressure falls below 45 psi. Whenever the emergency or secondary brakes are actuated, either manually or automatically, truck air system pressure must be increased above 45 psi to charge the trailer (or truck in case of single vehicle) emergency line and release the brake. The secondary or emergency brake system may be actuated by air pressure or by a spring located in the brake chamber. The brake force produced by the axle(s) actuated during emergency braking may be computed by Eq. 5-31. In the case of spring actuated wheel brakes the shoe actuating force $(p_l - p_o)A_C$ is replaced by the spring force.

The emergency or secondary brake of an air brake system becomes the parking brake when the vehicle is stationary. During normal operation the air pressure in the system compresses the spring and prevents contact between brake shoe and drum. As the parking brake is applied, the air is released from the brake chamber and the spring forces the brake shoe against the drum. Parking brakes generally are designed to hold the vehicle stationary on a 20% grade.

The air brake system of a tractor-trailer combination may be designed so that only one brake line connects the brake system of the tractor with the trailer brake system. During nonbraking, the line is used to charge the air tank of the trailer from the compressor of the tractor. During braking, the brake line between tractor and trailer serves as the control line transmitting the pressure signal from the brake application valve to the trailer brake valve. During braking the air tank of the trailer is not charged.

In a different system, two air lines are installed between tractor and trailer. During braking the air tank of the trailer is charged by the compressor and thus provides an inexhaustable energy source for brake application of the trailer brakes.

Pneumatic brake systems may be designed to provide two independent circuits identical to hydraulic brake systems.

12-4.5 BRAKE FADE

If a vehicle is subjected to a series of severe stops in rapid succession, in most cases for each successive stop a higher pedal force is necessary to maintain a specified deceleration level. This phenomenon is called brake fade. The phenomenon can be analyzed and predictions of the increase in pedal force can be made provided the variation of the brake factor as a function of the friction coefficient of the lining and the variation of lining friction coefficient with vehicle speed, pressure between lining and drum, and brake temperature are known. An illustration of brake fade is presented in Fig. 8-42 where the individual brake forces produced by the axles of a tractor-semitrailer combination are plotted. Fade is indicated by a decrease in slope. An approximate relationship for the decrease in lining friction coefficient is presented in Chapter 7, Eq. 7-1. Eq. 7-1 may be used to compute the decrease in lining friction coefficient during braking.

To illustrate the change in brake effectiveness due to fade, experimental results obtained with a passenger car in three successive high speed stops at a deceleration of 0.8g are presented in Fig. 12-11. The 2000-lb vehicle was equipped with disc brakes on the front and rear axle. Fig. 12-11 shows the hydraulic pressures and the pedal forces measured in the nonfaded condition and in each of the three high speed stops. The variations in brake factor as exhibited by the change in slope of line pressure versus deceleration is due to temperature increase which ranged from 212° to 1100°F measured on the surface of the front discs. Inspection of Fig. 12-11 shows that the pedal force decreased after making the first stop; examination of the test vehicle showed this to be the result of an increase in the rear disc brake factor. In the successive high speed stops the pedal force required for an 0.8g stop increases to 125 lb compared to the 80 lb required for the first high speed stop.

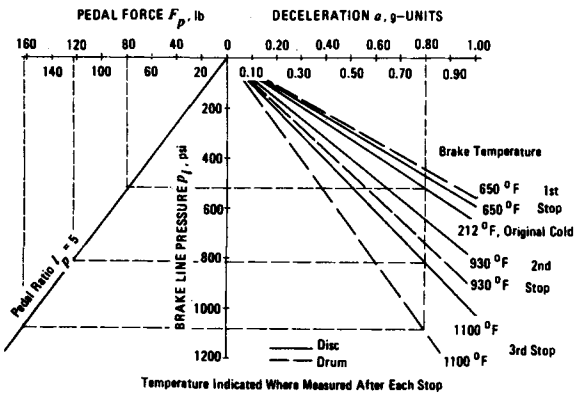

Figure 12-11. Fade Effectiveness Diagram

When the same vehicle was equipped with drum brakes, road tests indicated that the fade effects were greater, as is shown in Fig. 12-11. The pedal force required for an 0.8g stop increased from 68 lb to 165 lb after completing three high speed stops.

Of significance is the change in brake force distribution from the design point due to a differential fade — front to rear — as was observed for the disc brakes during the stop in which the temperature increased to 650°F. This condition may result in premature rear wheel lockup and subsequent vehicle instability.

12-4.6 BRAKE ASSEMBLY FAILURE DUE TO EXCESSIVE TEMPERATURE

Brake assembly failure will occur when excessive temperatures are allowed to exist over prolonged periods of time. The thermal capacity of a brake is a function of the allowable temperature of the brake and the surrounding components such as wheel cylinders and brake fluid, tire, and wheel bearings. The temperature of the surrounding components is increased by means of heat transfer through conduction, convection, and radiation. The allowable temperature assumes different values for the individual components. Furthermore, the operating mode of the braking process affects the thermal performance. For an effectiveness stop the surface temperature and the associated temperature gradient are the limiting thermal performance measures. In the case of a continuous brake application, the brake and components limit the thermal performance. For repeated brake applications or continued braking, the thermal performance measure is given by the limiting temperature of the brake rotor and brake lining, the wheel cylinder cup and brake fluid, and the tire bead temperature. Maximum allowable temperatures of the linings are about 800°F for drum brakes and 1000°F for disc brakes. Special linings may permit higher temperatures, e.g., Abex P 336 GG disc brake pads that show little or no fading at temperatures even as high as 1400°F. The maximum allowable temperature of the wheel cylinder is approximately 350°F. Higher temperatures tend to cause damage to seals and vaporization of the brake fluid. The tire bead temperature generally is limited to temperatures near 200°F. If tire bead temperatures are in excess of

200°F, tire unseating may occur during severe braking.

12-5 CONSEQUENCES OF BRAKE FAILURE

The major effect of the three failure modes (line failure, booster failure, brake fade) is an increase of the pedal force/deceleration gain from the design point. Longer stopping distances are likely to occur since the driver may not be able to produce the large pedal forces that are necessary to generate the braking forces normally achieved under nonfailure conditions.

In the case of a hydraulic line failure and a standard front to rear split, the remaining brakes available for braking must convert the entire kinetic energy of the vehicle into thermal energy which will most likely result in an excessive temperature rise in the friction surfaces or the entire brake assembly. Excessive heating of the brakes, however, may cause a decrease in brake effectiveness due to fading thus compounding the change in pedal force/deceleration gain. The effect of fading due to excessive thermal loading will be more pronounced if the driver tends to achieve high deceleration rates under brake line failure conditions. Another disadvantage of a standard split front to rear is that in the case of a line failure the braked axle is likely to overbrake — especially on road surfaces with a low coefficient of friction — rendering the vehicle directionally unstable in the case of rear wheel lock up.

Changes in brake factor due to fading may not be identical for the left and right brakes of the vehicle, possibly resulting in directional instability of the vehicle. It is even possible that an increase in lining friction occurs on the brakes of one side of the vehicle, whereas the other side experiences a decrease in the coefficient of lining friction due to different temperatures attained by the individual brakes. As is discussed in Chapter 2, this may result in an appreciable difference in brake torque developed on each side.

A difference in braking forces at the left and right front wheel, for example, will cause a deflection δ of one front wheel as indicated in Fig. 12-12. With a steering stiffness K and tire offset l_o as indicated in Fig. 12-12 the front wheel steering angle δ is

$$\delta = (r/R)(l_o/K)F_a(BF_{left} - BF_{right}) \text{ , deg} \quad (12\text{-}15)$$

where

BF_{left} = brake factor of left brake, d'less
BF_{right} = brake factor of right brake, d'less
F_a = application force, lb
l_o = tire offset, in.
K = steering stiffness, lb·in./deg

From Eq. 12-15 the following can be concluded:

1. Angle δ, and hence directional instability, will increase with increasing application force F_a, i.e., deceleration and therefore speed.

2. Angle δ will be large for a steering with small stiffness K.

3. Angle δ will be large for more sensitive brakes, i.e., high gain brake such as duo-servo brakes due to larger difference between brake factor on the left and right brakes.

12-6 BRAKE SYSTEM COMPONENT DETERIORATION

Brake system components that are likely to deteriorate during the life of the motor vehicle generally are designed such that critical elements are replaced periodically. These elements include brake linings, seals, dust boots, and brake fluids. Until approximately 1950 to 1955, the brake lines of hydraulic brake systems significantly limited the overall life of a brake system. Today, this problem has been solved by the use of copper alloy tubing. Tests have shown that the resistance in terms of a decrease in tensile strength of copper alloys remained almost unaffected by a 180 d exposure to salt spray (Ref. 3). The tensile strength of copper coated steel tubes rapidly deteriorated after 90 d with essentially no tensile properties remaining after 180 d of exposure to the salt spray. Hydrostatic pressure tests confirm these results. Before the pressure tests, the bursting pressure of the copper alloy tubes ranged from 8500 psi for tubes 3/8 in. diameter to 1700 psi for 3/16 in. diameter tubes. Steel tubes (as received) were generally 10% stronger in burst tests than copper alloy tubes. When the steel tubes were exposed to salt spray for 90 d they reduced

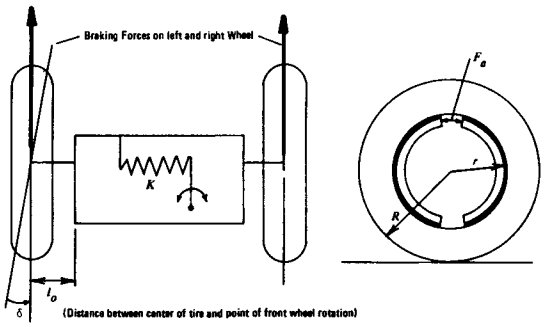

Figure 12-12. Steering Schematic

in their burst strength to about 50%; after 180 d, nearly 90% of their initial burst strength. It is obvious that steel tubing when used in a driving environment subjected to salt sprays could reduce its ability to withstand brake line pressures of 1,500-2,000 psi — commonly obtained in panic brake stops.

Fatigue and impact tests conducted with steel and copper alloy tubes indicated a superior performance of the copper alloy when exposed to a salt spray over an extended period of time.

Specific tests, recommended by the Society of Automotive Engineers, determine the allowable weight loss of tubing material when exposed to hydraulic brake fluid. Test results show that copper alloys are well within specified ranges (Ref. 3).

Other recommended standards published by the Society of Automotive Engineers deal with the minimum performance required, e.g., for air brake hoses, vacuum hoses, hydraulic brake hoses, brake fluid, brake linings and brake pads, and structural integrity of the service brake (Ref. 7). Of the components mentioned, hydraulic brake fluid deserves further detail. The performance requirements of brake fluid include:

1. Low tendency to absorb water; water in the brake fluid leads to corrosion and decrease boiling temperatures of the fluid and hence brake fluid vaporization during continued braking. For example, motor vehicles operating near large bodies of water such as oceans may absorb enough water to reduce the boiling temperature of the brake fluid from 450°F to 300°F within one year.
2. High boiling temperature
3. Insensitive to temperature changes; must operate at arctic conditions
4. Lubrication must be provided for seals and cups under high pressures and temperatures
5. No corrosion of system components caused by the brake fluid
6. Properties of brake fluid should not be affected by storage time, and high and low temperatures.

Concerning the effect of aging on brake system components, storage time should not be too long. Components such as master cylinders, wheel cylinders, and brake hoses may be stored for three years without exhibiting deterioration. Components such as vacuum assist units and proportioning valves should not be stored for more than two years. Excessive storage times may cause malfunctioning of the brake component due to frozen pistons and hardened seals or cups (Ref. 8).

12-7 VEHICLE STABILITY AND CONTROLLABILITY

Vehicle stability during braking is affected most by a change of brake force distribution. Partial failure of a brake system may cause a larger brake force concentration on the rear axle than the design brake force distribution ϕ. Large values of ϕ may result in premature rear wheel lockup and subsequent vehicle instability (par. 8-1.7). Increases in brake force distribution ϕ may be caused by front-brake failure, differential fade in which the front brakes fade more than the rear brakes, or defective proportioning valve. Differential fade has been reduced by the use of disc brakes on both front and rear axles. The general design practice of installing disc brakes on the front axle and drum brakes on the rear axle is likely to increase differential fade due to the difference in brake sensitivity of disc and drum brakes (Fig. 7-1).

Brake controllability is defined in par. 7-1.4 and relates to the ability of the driver to modulate brake force under a wide variety of loading and road surface conditions to minimize stopping distance while preventing wheel lockup. During a partial failure in which the pedal force/deceleration characteristics are altered from the design point, brake controllability is affected in terms of a brake pedal feel "unfamiliar" to the driver in addition to the increased pedal travel. Furthermore, pedal forces during failure may exceed the capability of the driver. This situation exists especially in cases where a high gain vacuum assist unit failed. During the nonfailed condition only small pedal forces are required to produce high decelerations; during failure the manual effort is not sufficient to produce acceptable values of deceleration.

12-8 HUMAN FACTORS CONSIDERATIONS

In manual brake systems the driver provides the pedal effort required to press the brake shoes against the drums. Increased pedal forces will result in increased deceleration, provided fade is ignored for the moment. Brake systems using assist devices are designed so that the pedal effort is used to control the assist force in addition to providing the manual pedal effort which produces brake line pressure. Full power hydraulic and pneumatic brake systems use the pedal effort to operate a valve which controls the brake line pressure. The work required for pressing the brake shoes against the drums is stored and not affected by pedal effort. For manual systems the pedal force limits braking performance. For this reason it is important to know the foot force capabilities of individuals comprising the driving population.

The maximum force exerted with the right foot for the 5th percentile female is approximately 100 lb; for the male approximately 185 lb (Ref. 9). These data were obtained in controlled laboratory conditions. It

has been argued that the stress of an emergency situation may enable the drivers to exert higher pedal forces. Satisfactory driver braking performance has been observed in controlled road tests when the lower value of pedal force/deceleration gains is 4.76 lb/g; whereas, the upper value of pedal force/deceleration gain is 83 lb/g (Ref. 9). These numbers indicate that not less than approximately 5-lb pedal force should be required to produce a deceleration of 1g, and that not more than approximately 80-lb pedal force should be required to produce a deceleration of 1g. Too large gain values result in a sensitive brake system where the driver may have difficulty in applying the brakes carefully. Too low gain values result in ineffective brakes; the pedal force of the driver may not be sufficiently large to produce an acceptable deceleration.

12-9 EFFECT OF MAINTENANCE ON BRAKE FAILURE

Maintenance has been defined as follows. All actions necessary for retaining an item in or restoring it to a serviceable condition. Maintenance includes servicing, repair, modification, modernization, overhaul, inspection, and condition determination (Ref. 10). Problems associated with maintenance are:

1. Accessibility
2. Complexity
3. Durability
4. Diagnosis.

While accessibility and complexity are not addressed directly in physical formulations of the decelerating mechanisms, they certainly are of importance. Critical performance limits of components as well as systems obtained in the braking analysis may be used in assessing critical aspects of durability and diagnosis.

Methods for detecting component defects or degradation that affects brake system performance can be devised. Such techniques use the results of laboratory type brake dynamometers or performance data obtained in actual road tests. These performance related degradations and defects include system gain, system response, front-to-rear brake force distribution, side-to-side brake balance, brake fade, and pedal travel. Some brake system components can be efficiently and objectively inspected, visually or manually. These components include linkages, brake lines and hoses, and other related mechanisms. Although a diagnosis indicating partial loss of system gain clearly means a loss in braking performance capability, present diagnostic techniques do not identify the source of malfunctioning in all cases. A decrease in system gain could be caused by a change in brake factor, i.e., a change in brake lining/drum friction coefficient, by a loss in power assist performance, or by a decrease in mechanical or hydraulic efficiency. The latter could be caused by frozen wheel cylinder pistons, cams, or wedges. Insufficient system gain in the case of rapid brake applications could indicate severe brake line restrictions or power boost malfunctioning. Excessive pedal travel without evidence of external leakage could indicate large brake shoe travel due to severely worn linings, or internal master cylinder leakage caused by a leaking primary cup in the master cylinder. Excessive pedal travel also could be attributed to large elastic deformation of brake shoes, to soft pad or lining material, and excessive elastic deformations of drums or calipers. However, most of these outages can be monitored with relatively inexpensive gages so that the cause of any performance related defect or degradation can be identified.

Defects and degradations that do not affect system performance are not easily detectable. In some cases, however, the anticipated failure mode can be categorized in terms of intended or actual vehicle functions. Vehicles operating in typical highway environment will exhibit different wear and hence failure modes than vehicles operating over extended periods of time on unpaved dirt roads. This observation was made in the case of school buses operating in urban and rural environments. Their respective maintenance requirements showed significant differences. In general, basic mechanical engineering considerations may be utilized in assessing the safety criticality of different brake system components. One such application is the prediction of the life expectancy of honed versus rolled master cylinder sliding surfaces as a function of primary seal friction. Furthermore, fixed-in-place or periodically introduced sensors may be used efficiently to obtain information on the expected safety performance of components, information for maintenance purposes, and other related aspects of vehicle inspection. It should be emphasized that this must be done in connection with a proper combination of analysis and parameter evaluation of the braking system. For example, it appears rather useless to measure brake line pressure versus torque in order to determine the safety performance of the brake shoe applicator (wheel cylinder piston, cam, or wedge) without accurate knowledge of the brake factor or internal gain of the foundation brake. Also, a determination must be made if a brake factor decrease is caused by a drop in lining friction, or geometry change of the brake drum or shoe due to permanent drum distortion.

12-10 MINIMIZING BRAKE FAILURE THROUGH PROPER DESIGN

Redundant brake system design offers one solution for minimizing brake failure through design. However, such an approach generally is expensive and shows an undesirable ratio of system cost and expected benefits. At present, no general approach can be suggested that would justify a certain level of brake system hardware. A bus, for example, may justify a more involved brake system design than an off-road forklift truck. The degree to which motor vehicles used for civilian application must be designed for performance under brake systems failure has been specified by the US Department of Transportation in the Federal Motor Vehicle Safety Standards 105 for hydraulic and 121 for air brakes. Although not directly specified in terms of design requirements, the performance levels and requirements make the use of a certain level of brake system design necessary from a failure viewpoint.

REFERENCES

1. R. Limpert, *A Critical Review of FMVSS105,* SAE Paper No. 760217, February 1976.
2. A. G. Imgram and D. K. Miner, *Hydraulic Brake Line Corrosion: An Initial Investigation of the Problem,* SAE Paper No. 690530, May 1969.
3. B. J. Sirois, "New Copper Alloy for Hydraulic Brake Lines", *Material Progress,* November 1965, pp. 64-66.
4. R. Limpert, *An Investigation of Thermal Conditions Leading to Surface Rupture of Cast Iron Rotors,* SAE Paper No. 720447, May 1972.
5. *Metals Handbook,* Vol 1, 8th Edition, American Society for Metals, Metals Park, Ohio, pp. 366-76.
6. A. Larsson and L. Larsson, *Stepped Bore Master Cylinder – A Way of Improving Dual Brake Systems,* SAE Paper No. 750385, February 1975.
7. *Motor Vehicle Braking Systems and Components,* Handbook Supplement HS24, 1974 Edition, Society of Automotive Engineers, Inc., Two Pennsylvania Plaza, New York, New York 10001.
8. H. J. Leyhausen, "The Master Mechanic for Automobiles", *Vogel Publisher,* Wurzburg, Germany, 1975.
9. R. G. Mortimer, et al., *Brake Force Requirement Study: Driver-Vehicle Braking Performance as a Function of Brake System Design Variables,* Final Report Contract FH-11-6952, prepared for U.S. Department of Transportation by University of Michigan, 1970.
10. AMCP 706-132, Engineering Design Handbook, *Maintenance Engineering Techniques.*

CHAPTER 13
TESTING OF VEHICLE BRAKE SYSTEMS

In this chapter important considerations for brake system testing are discussed. The basic elements of a braking standard are introduced and the effects of brake inspection and maintenance on brake testing are discussed. Major elements of test procedures used for wheeled and track vehicles are presented.

13-0 LIST OF SYMBOLS

a = deceleration of truck-trailer combination, g-units
a_1 = deceleration of truck or tractor, g-units
a_2 = deceleration of trailer (if considered alone) g-units
E_{min} = minimum braking efficiency, d'less*
W_1 = truck or tractor weight, lb
W_2 = trailer weight, lb
μ = tire-road friction coefficient, d'less
ϕ_{max} = maximum brake force distribution, d'less
ϕ_{min} = minimum brake force distribution, d'less
χ = vehicle center of gravity height divided by wheel base, d'less
ψ = vehicle rear axle load divided by vehicle weight, d'less

13-1 BASIC TESTING REQUIREMENTS

The testing of the vehicle brake system and its performance is essential for safe vehicle operation. The braking system should be capable of stopping the vehicle when loaded and unloaded, on slippery and dry roads without skidding and losing directional stability. The brakes must show no or little loss of effectiveness after severe usage, i.e., the linings and drums should not fade. If fade has occurred, the lining friction should return to the design performance level quickly. Linings should not show excessive wear, drums and disc brake rotors should not become distorted. Other factors relating to the performance of brake systems include safe and gradual pedal force modulation of power assisted or full power brake systems, pedal force and pedal travel requirements based on human factors consideration, and air brakes that do not freeze at cold temperatures. Although this list of factors relating to the performance of braking systems is not complete, it points to the complex and comprehensive procedures required for testing motor vehicle brake systems.

*d'less = dimensionless

In general, testing serves the purpose of either verifying theoretically predicted performance and determining presently unknown functional relationships among certain variables or establishing compliance with existing braking standards, such as Federal Motor Safety Standard 105 or 121.

13-2 GENERAL OUTLINE OF A BRAKE TEST STANDARD

The braking system of a motor vehicle must perform acceptably both during a service brake application and during partial failure conditions. Performance requirements and compliance test procedures must be objective, practical, and safety related.

Statistics indicate that most passenger vehicles carry less than two occupants over a large percentage of their operational life. Accident statistics show that most automobiles involved in accidents are lightly loaded. Based on this information it appears desirable to design a motor vehicle braking system so that it achieves maximum braking performance, i.e., shortest stopping distance, when the vehicle is lightly loaded. Consequently, in either designing a braking system or in developing test procedures, braking performance achieved in the lightly loaded condition receives first priority. Testing vehicles in the lightly loaded condition is generally done by an effectiveness stop where the vehicle is required to stop in a specified distance from a given speed.

A justifiable case can be made for assigning brake fade performance the second priority. Consequently, the performance requirements of a brake test standard must be such that:

1. Effectiveness stopping performance on both low- and high-friction road surfaces is not degraded.
2. Reasonable fade performance is achieved.

Accident statistics reveal little about the accidents precipitated by partial brake system failure. Basic engineering and safety considerations, however, suggest that braking performance with partial brake failure should be assigned third priority. The performance

requirements of this element of the brake test standard must be designed such that:

1. Effectiveness stopping performance on both low- and high-friction road surfaces is not degraded.
2. Fade performance is not affected significantly.
3. Reasonable braking performance is achieved with partial failure of the brake system.

If, for example, the partial failure performance requirements were designed such that the requirements only could be met by a vehicle with the brakes designed for this particular element of the standard, then the braking performance in the effectiveness stopping category very likely would not be the optimum possible. Consequently, a brake test standard must be designed such that a vehicle which complies with the standard exhibits performance priorities that are safety oriented.

The parking brake performance should be assigned fourth priority. The test standard requirements for the parking brake should be such that the particular design of the parking brake — which meets the test requirements — does not cause a:

1. Decrease in effectiveness stopping performance
2. Significant decrease in fade performance
3. Significant decrease in partial failure performance.

The list of priorities may be extended to include all elements of the braking standard. For each element, due consideration must be paid to such things as lining wear, brake noise caused by vibrations, pedal effort in terms of force and displacement, brake sensitivity, braking stability, effect of driver skill on test results, manufacturing tolerances, and braking-in-a-turn performance.

Test procedures used for compliance testing need to be practical, simple, and as inexpensive as possible. It is desirable for increasing traffic safety that the entire or major elements of a braking standard be applied to both new and vehicles-in-use. Furthermore, the elements of a braking standard should allow both hydraulic and pneumatic brake actuation to be included in a consolidated standard.

As discussed in Chapter 7, there are five measures of braking performance — namely, effectiveness, efficiency, response, controllability, and thermal effectiveness. All five measures must be addressed in the brake test standard for each element of the standard. For example, in a stopping distance test significant measures are effectiveness, efficiency, response, and controllability. Thermal effectiveness normally is of little concern in an effectiveness stop. For the parking brake, for example, effectiveness and controllability are important measures of performance.

13-3 MEASUREMENT OF BRAKING PERFORMANCE

13-3.1 EFFECTIVENESS

Dynamometer testing for purposes of determining braking effectiveness is straightforward and done routinely for vehicles-in-use evaluation. In this case, each axle may be tested individually. The effectiveness of an individual axle depends on the design brake force distribution or front-to-rear brake balance. A number of tests may be conducted with increasing levels of pedal force to determine the sensitivity of the brake factor as brake temperature and/or vehicle speed is increased.

Road tests may be used to determine braking effectiveness. Since effectiveness as defined earlier is not affected by brake application and response times, only deceleration measurements as functions of induced pedal forces are required for effectiveness evaluations. Deceleration serves as effectiveness performance measure. Furthermore, deceleration levels must stay sufficiently below wheel lockup conditions to prevent any complication of test data interpretation.

Pedal force/deceleration gains for passenger cars equipped with disc brakes are usually not subject to significant fade during an effectiveness stop. Consequently, pedal force/deceleration gain values are nearly constant for one set of conditions. Of course, as indicated earlier, performance requirements on pedal force/deceleration gain must be based to some extent on the more severe condition to challenge the brake system capability to produce sufficient gain.

The heat generation at the interface between lining and drum or pad and rotor is proportional to the product of (lining friction coefficient) $\times$ (mechanical pressure between shoe and drum) $\times$ (sliding velocity between both friction partners). Thus, thermal effects can be evaluated in terms of high mechanical pressure and hence deceleration and low or high levels of speed. This may lead to a special requirement on vehicles capable of traveling in excess of certain upper speeds.

Brake fade is defined as a decrease in effectiveness relative to a specified pedal force. The effect of speed on fade can be determined on the dynamometer or in a road test by measuring the change in baseline effectiveness. A requirement may state that vehicles capable of traveling in excess of 70 mph may not experience a decrease in baseline effectiveness of more than 20% when tested at maximum speed.

13-3.2 EFFICIENCY

Braking efficiency involves the capability of ve-

hicle braking system to use a portion of a certain level of tire road friction. This level may be specified in terms of a tire-road friction characteristic or in terms of a stopping distance. It appears that in light of the great number of variables involved in assessing a coefficient of friction between tire and road, practicality and usefulness should be the guiding factors in developing a braking efficiency measure.

The braking efficiency measure differs from braking effectiveness to the extent that now the braking process occurs near the limit of tire-road friction associated with either the front or rear axle(s). It is solely a brake force distribution or brake balance problem.

For solid-frame vehicles Eq. 8-10 may be used to develop a limiting relationship on the upper level of brake force distribution ϕ_{max}

$$\phi_{max} < \frac{\psi}{E_{min}} - \mu\chi \quad \text{, d'less} \qquad (13\text{-}1)$$

where

E_{min} = minimum value of braking efficiency, d'less
μ = tire-road friction coefficient, d'less
χ = vehicle center of gravity height divided by wheel base, d'less
ψ = vehicle rear axle load divided by vehicle weight, d'less

The value for E_{min} would be specified in the standard. Furthermore, since the lightly loaded vehicle condition is most challenging relative to rear wheel lockup, ψ and χ values for the empty condition must be used for determining the allowable rear brake balance. For the loaded condition and low friction surface, the requirement for the lower level of brake force distribution ϕ_{min} is

$$\phi_{min} > 1 - \mu\chi - \frac{1-\psi}{E_{min}} \quad \text{, d'less} \qquad (13\text{-}2)$$

The brake force distribution actually installed may be determined easily by conducting partial system, i.e., rear or front axle, effectiveness tests. These tests may be conducted on a dynamometer which probably is a preferred procedure since ambient conditions and effects are easily controlled, or by means of actual road tests. Since for many motor vehicles the design brake force distribution can be computed within certain small tolerances, braking efficiency may be determined analytically. However, for compliance testing purposes a dynamometer test may prove to be more desirable since it requires only effectiveness type tests in addition to a minimum amount of computation to determine vehicle braking efficiency.

The equations determining the allowable brake force distribution for articulated vehicles are more lengthy and are not presented here. A detailed discussion is given in Chapter 8 in connection with Eq. 8-78.

13-3.3 RESPONSE TIME

Application and buildup times are defined as the time required for a brake to reach a given level of effectiveness from the time that the brake control or pedal is activated. The effects of application and buildup times on stopping distance are discussed in Chapter 1. Empirical relationships for determining the response times of pneumatic brake systems are shown in Chapter 11. A major contributor to time delays of the hydraulic brake system is associated with the vacuum-assist unit. The distances traveled during response and application time are a significant parameter in accident avoidance. Response times have been measured (Ref. 1). The results indicate a reaction time including movement of foot from accelerator pedal to brake pedal for the 90th percentile male between 25 and 40 years of age, of 0.67 s. The pedal force buildup times for severe, moderate, and "soft" application are 0.36, 0.35, and 0.36 s, respectively. The corresponding values for the 10th percentile male are 0.06, 0.05, and 0.065. It is apparent that large increases in stopping distance are associated with the 90th percentile driver. In order to eliminate the influence of test driver on braking performance, an objective brake system response time measure, both in terms of application as well as deceleration buildup, becomes necessary. No useful purpose is served by exceeding pedal force application rates of 0.1 s to achieve maximum pedal force as repeated application may result in damage to the brake system. Brake system response times ideally may be measured in dynamometer tests. In road tests the longitudinal dynamic and suspension effects may significantly complicate the interpretation of test data. A response time performance measure could include wheel angular velocity-time histories or deceleration-time histories.

13-3.4 CONTROLLABILITY

Brake controllability is the ability of the driver to modulate brake force under a wide variety of loading and road surface conditions to minimize stopping distance while preventing wheel lockup. Four-wheel antiskid brake systems automatically provide a high measure of controllability not provided by manual

brakes. For standard brakes, controllability requirements are vehicle stability and sufficient modulating performance in terms of brake system sensitivity.

System controllability will be established automatically if the design brake force distribution is kept between the ranges established by Eqs. 13-1 and 13-2. Values within this range will yield a front brake force balance sufficiently large to cause front-before-rear wheel lockup. A compliance test is simply carried out in the form of a road test.

Brake system sensitivity is established automatically in the brake effectiveness tests by the slope of the curve relating deceleration to pedal force (par. 12-8).

13-3.5 THERMAL EFFECTIVENESS

The thermal effectiveness of a brake can be characterized by the ability of the brake to absorb heat generated in a single stop and to conduct, convect, and/or radiate heat generated in a series of stops. Thermal capacity or resistance to fade is measured in terms of the level of braking effectiveness that can be maintained during a series of rapidly repeated snubs or the number of snubs which can be accomplished in a given time interval, or the decrease in tow bar force in a towing test.

13-4 BRAKE USAGE AND MAINTENANCE

The usage and maintenance of a vehicular braking system affect, to a large extent, its performance. Testing procedures should be directed at determining any undesirable effects of previous use or maintenance upon the braking performance of a vehicle. Testing procedures should reveal if too large stopping distances are caused by faded brakes, long time delays due to poor maintenance, or if the basic stopping ability designed into the vehicle is unsatisfactory.

The brake usage of passenger cars has been studied by several investigators. Only recently have these studies been extended to investigation of brake usage of trucks and trailers (Ref. 2). European studies of Alpine descents indicate a maximum deceleration of 0.14g (Ref. 3). The brakes were applied for a longer time and more frequently than during driving on a flat road. In general, the results indicate that a heavy vehicle travels descents at nearly uniform speed with the speed determined by factors such as type of road and size of vehicle. The work done by the brakes depends on the slope of the descent and the gear used. For a particular Alpine route, the mean value of the work done by the brakes was 41% of the total energy dissipated.The results of brake usage investigations on heavy trucks seem to correlate well with earlier results obtained for passenger cars. Other investigations show that on flat roads only few decelerations exceed 0.35g. A public service vehicle, e.g., rarely exceeds 0.25g in city traffic; however, it has a large number of decelerations at values below 0.2g.

For passenger cars it appears that the decelerations during routine driving depend on the driver and the top speed performance of the car. For commercial vehicles the four-main controlling variables on brake usage seem to be engine horsepower output, driver and route type, and energy transfer — a factor determined experimentally on the brakes of the vehicle.

Before testing a vehicle, the brake system including tires should be brought to a mechanical condition corresponding to the manufacturer's specifications. Even small factors such as balancing shoe return springs may have a pronounced effect when braking at relatively low line pressures on slippery road surfaces.

A brief description of the more important maintenance requirements follows:

1. The brakes should be relined with the lining material specified by the vehicle or brake manufacturer. Complete sets of brake blocks should be installed even when one lining does not show any apparent wear.

2. The brake drum or disc brake rotor surface should be smooth and concentric. If the drum or rotor is scarred or worn unevenly, it should be reconditioned by reboring the friction surface. Reboring should be a preferred practice at each brake relining.

3. Shoe return springs should be balanced to insure specified distribution of braking forces at low brake line pressures.

4. Brake chambers and wheel cylinders should be in good mechanical condition in order to guarantee good brake balancing.

5. Worn or loose slack adjusters should be replaced since they may affect unfavorably time lag and force transmission.

6. With all brake components in good mechanical condition, a carefully conducted brake balancing test should be carried out. It will reveal if the individual axles produce the brake force levels specified by the manufacturer.

13-5 BRAKE SYSTEM INSPECTION AND DIAGNOSIS

The intent of an inspection program is to determine if a brake system has the ability to perform in

a safe manner for a reasonable length of time. Fundamental to the successful development of any inspection program is a clear definition of the criteria by which items will be inspected and the rationale by which these criteria are developed. The program must be able to establish immediate brake system performance capabilities and determine if there are any defects or degradation that will lead to near-future failure or sublevel performance.

As goals, the inspection system developed should have the following capabilities (Refs. 4 and 5):

1. Ascertaining brake system performance capabilities in severe, safety-related maneuvers, and duty cycles
2. Detecting defects and states of deterioration that will lead to eventual sublevel performance or catastrophic failure
3. Identifying components or areas of the brake system which are defective when brake system outages occur
4. Displaying inspection results in a manner commensurate with capabilities of personnel manning the system
5. Sufficient flexibility to allow for changes in vehicle design and the incorporation of new techniques of inspection as they occur.

Effective vehicle brake system inspection will involve a combination of component inspection and system performance testing. Component inspection should be directed toward critical modes of brake degradation that do not affect current system performance. Based on current technology, component inspection must be performed visually to identify items such as missing or broken parts or small hydraulic leaks; and, with the aid of appropriate gauges, inspect for items such as oversize drums, undersize discs, and thin friction material.

The large number of brake degradation modes can be grouped into the four basic brake subsystems where they originate. The subsystems are brake pedal linkage, power booster hydraulic system, antiskid brake control, and wheel brakes. A summary of all the major modes of hydraulic brake degradation is presented in Chapter 12 in connection with discussion on brake failure development.

In addition to the component inspection required for safety such as leaking wheel cylinders and broken return springs, components must be inspected to ensure adequate performance. The components that follow must be inspected and performance measured (if necessary):

1. Engine vacuum to determine the effectiveness of vacuum assist unit
2. Hydraulic pump pressure and accumulator pressure of full power hydraulic brake systems
3. Adjustment of belts which are used to drive hydraulic pumps or air compressors
4. Pressure regulators which control the maximum pressure in air or full hydraulic brake systems
5. Reservoir tanks of pneumatic brake systems should contain no moisture
6. Brake application valve; brake pressure gauge must reach reservoir pressure within one second after brake pedal application
7. Valves such as quick release valves, proportioning valves, trailer emergency control valves must be checked and, if required, tested in special tests specified by the manufacturer.

Special sensors are used to aid in the inspection and diagnosis process. Brake line failures are indicated by lamps that are lit when the brake fluid level in the reservoir falls below a certain level, and by a differential switch that actuates an indicator lamp when the difference in brake line pressure of a dual circuit exceeds a certain value. An electrical failure in the antilock system is indicated by a lamp. Wear indicators are used to warn the driver when excessive pad or lining wear exists. These indicators are mechanical causing a squealing noise when the pads should be replaced, or electrical with a warning lamp. Other sensors are used on air brake systems which indicate low reservoir air pressure by means of a buzzer.

13-6 BRAKE SYSTEM TESTING

With the brake system in good mechanical condition, the vehicle may be tested. Testing of the entire braking system and its braking performance are essential from a safety viewpoint. Vehicle braking tests may be conducted with the vehicle stationary as in the case of roller dynamometers and platform testers, or nonstationary as in the case of road testing.

13-6.1 ROLLER DYNAMOMETER

Roller dynamometers permit the measurement of the brake torque produced by individual wheels or axles. Roller dynamometers do not require a large test facility. The vehicle is driven onto a pair of rollers, which either are powered by an electric motor or have a mass moment of inertia corresponding to the vehicle weight carried by the braked wheel. The rollers replace the function of the road and as such attempt to rotate the wheel against the braking action of the brakes. In the case of the electric motor driven rollers, the torque produced by the motor is a direct

measure of the brake force. The brake force measurement is slightly affected by the tire-to-roller rolling resistance. In the case of the inertia dynamometer, commonly called inertia wheel brake dynamometer, the brake torque is measured by load cells.

Advantages of roller dynamometers are:

1. Measurement of brake force as a function of time
2. Measurement of brake force as a function of pedal force
3. Out-of-round drums are detected.

Disadvantages are:

1. Dynamic load transfer from rear to front is not evaluated
2. Actual tire-road friction coefficients are not easily represented.

13-6.2 PLATFORM TESTER

The platform tester serves as a device to determine brake force of passenger cars and motorcycles. Only in rare cases are platform testers used for brake testing of heavy vehicles. The platform tester consists of four movable plates located a distance equal to the track width apart and long enough so that each plate supports one wheel. The vehicle is driven on the plates at low to moderate speed and the brakes are applied. The four plates are restrained in their longitudinal motion by force transducers. The forces measured on each plate are equal to the brake forces between tire and plate and are a direct indication of the braking performance of the vehicle.

Advantages of the platform tester are:

1. Short test duration with little or no preparation
2. Dynamic load transfer effects can be considered.

Disadvantages are:

1. Brake force data are affected by the speed at which the vehicle is driven onto the platforms
2. Incorrect measurement of brake forces due to wheel lockup
3. Only one value of braking force is obtained
4. Degraded component performance not easily determined.

13-6.3 BRAKE ROAD TESTING

In brake road testing, the vehicle is tested under conditions which are close to the conditions encountered during braking on the highway. Usually, detailed test schedules are arranged so as to test the brakes according to their expected usage. The amount and type of experimental data desired determines the amount of instrumentation required. Test and rating procedures in current usage in the United States were established by the Society of Automotive Engineers with the automotive industry and are used to some degree in Federal Braking Standards. Federal Motor Vehicle Safety Standard (FMVSS) 105 contains test procedures and performance requirements for motor vehicles equipped with hydraulic brake system. FMVSS 121 contains test procedures and performance requirements for motor vehicles equipped with pneumatic brake systems including air-over-hydraulic brake systems. Brake systems that use compressed air or vacuum only to assist the driver in applying muscular force to produce brake line pressure are not included in FMVSS 121 but are regulated by FMVSS 105. The discussion that follows constitutes a synopsis of the Federal Braking Standards FMVSS 105 and 121.

1. FMVSS 105. This standard applies to passenger cars and trucks equipped with hydraulic brake systems. The major requirements are:

a. Vehicles must be equipped with a dual circuit service brake which meets certain performance requirements contained in the standard.

b. Service brake system must be capable of stopping the vehicle in four effectiveness tests within specified distances and from specified speeds under a variety of test conditions. The most stringent stopping distance requirements for passenger cars are from a speed of 60 mph: (1) 216 ft in the first and fourth effectiveness stop; (2) 204 ft in the second effectiveness stop; (3) 194 ft in the third effectiveness stop.

c. Brake system must stop the vehicle within specified distances in the event a partial system failure occurs.

d. Brake system must stop the vehicle within specified distances in the event a power assist failure occurs.

e. Brake system must be capable of producing specified deceleration levels during ten fade stops and fifteen recovery stops.

f. Brake system must be capable of producing specified deceleration levels within specified pedal force limits after the vehicle was driven through water having a depth of 6 in.

g. Brake system must be capable of making ten spike stops in which a rapid pedal force application occurs.

h. Parking brake system must be capable of holding the vehicle on a specified slope within specified application forces.

i. Brake system must be equipped with several indicators which indicate: (1) hydraulic leaks; (2) low brake fluid level in the reservoir; (3) a total functional electrical failure in a wheel-antilock or variable pro-

portioning system; and (4) parking brake application.

2. FMVSS 121. This standard applies to motor vehicles equipped with air brakes. Each vehicle must be equipped with:

a. Air compressor of specified capacity

b. One or more service brake reservoirs of a size which is twelve times the combined volume of all service brake chambers at maximum travel of the pistons or diaphragms.

c. Towing vehicle protection system to protect a tractor brake system from air loss in the event the trailer has a defective brake system.

d. Pressure gauge that indicates the service reservoir air pressure.

e. Warning system in addition to pressure gauge to indicate a low air pressure in the service reservoir.

f. Wheel-antilock warning signal to indicate total electrical failure of the antilock system.

g. Service brake lamp switch to actuate stop lights in the event brake line pressure reaches 6 psi.

h. Service brake system of trucks and buses must be capable of stopping vehicle within specified distances for different conditions.

i. Trailer brakes must be capable of stopping the tractor-trailer combination without the help of the brakes of the tractor without leaving a 12-ft wide lane.

j. Brake actuation times must be within specified ranges for specified conditions.

k. Brake release times must be within a specified range for specified conditions.

l. Service brake assembly must be certified by dynamometer testing.

m. Parking brake system must hold vehicle on specified slope under specified conditions.

n. Brake system must be capable of stopping vehicle under a variety of emergency conditions.

Although not part of FMVSS 121, frequently it becomes necessary to determine the braking performance of a trailer brake system from road test data. The deceleration of the trailer a_2, if it were braked alone, can be computed by

$$a_2 = \frac{a(W_1 + W_2) - W_1 a_1}{W_2}, \text{ g-units} \quad (13\text{-}3)$$

where

a = measured deceleration of tractor-trailer combination, g-units

a_1 = measured deceleration of tractor, g-units

a_2 = computed deceleration of trailer (if considered alone), g-units

W_1 = tractor weight, lb

W_2 = trailer weight, lb

13-7 BRAKE TEST PROCEDURES FOR MILITARY VEHICLES

Brake road test procedures developed for military vehicles differ from those for civilian vehicles. The discussion that follows presents the important elements of the test procedures applicable to wheeled and tracked vehicles.

13-7.1 ROAD TEST PROCEDURES FOR WHEELED VEHICLES

The major procedures and requirements are (Ref. 6):

1. Preparation of test vehicle and instrumentation consist of:

a. The vehicle power train, braking, steering, and electrical systems are prepared for optimum operation.

b. Proper vehicle weight distribution, lubrication, and tire inflation pressures are assured.

c. For mountain highway brake tests a yellow and black diagonally striped signboard is mounted at the rear of the vehicle, displaying 6-in. diameter stoplights and turning signals.

d. All instruments are calibrated before and after a test and, if necessary, during the test.

2. Restrictions. Tests are not conducted at night, during inclement weather, in congested traffic, or when the road surface may introduce a hazard to the test vehicle or other traffic on the road. Dry, unobstructed surfaces are used unless the test plan introduces a specific requirement.

3. Safety evaluation. Prior to the conduct of other wheeled vehicle braking system tests, tests will be conducted to accumulate data on which to base a recommendation for the issuance of a safety release.

4. Performance tests. Brake performance will be evaluated in terms of adequacy of the vehicle braking system to perform at the required level for each test phase.

a. Brake Burnish. Friction material burnishing is accomplished by specified procedures. The criterion for friction material burnishing is that not less than 90% of the friction material surface area be in contact with the swept area of the rotating brake member (drum or disc).

b. Brake Holding Ability. The vehicle is parked on dry, paved, longitudinal slopes in both ascending and descending attitudes. Service and parking brake

systems are engaged individually to assure their individual capability to hold the vehicle stationary.

c. Brake Stopping Ability. Brake stopping distances are obtained from 20 to 40 mph and from additional road speeds if specifically requested. Stopping distances are measured over the input pressure range up to the point of wheel locking. The criteria for brake stopping ability are as follows: (1) Wheeled vehicles of gross vehicle weights up to and including 50,000 lb will be capable of making a straight line full stop from a road speed of 20 mph within a distance of 30 ft; they will be capable of making a full stop from a vehicle speed of not less than 40 mph at an average deceleration rate of 14.4 ft/s^2; (2) wheeled vehicles of gross vehicle weights exceeding 50,000 lb will be capable of making a straight line full stop from a road speed of 20 mph within a distance of 40 ft; they will be capable of making a full stop from a vehicle speed of not less than 40 mph at an average deceleration rate of 11 ft/s^2; (3) during all braking stops, vehicle slew shall not exceed the limits of a roadway lane width equal to 1-1/2 times the overall width of the test vehicle.

5. Brake Recovery After Immersion in Water. Wheeled vehicle braking systems will be completely submerged in water for a period of 15 to 30 min. After immersion, recovery is determined by making brake applications from a vehicle speed of 20 mph at a pre-selected input pressure at 1-min intervals. The criterion for brake recovery is that after immersion in water for a period of 15 to 30 min, brake stopping ability shall have achieved complete recovery after 10 brake applications over a period of 12 min.

6. Trailer Breakaway Holding Ability. This test phase will be performed in both ascending and descending attitudes on paved, longitudinal slopes. The trailers will be parked on the grade and brake lines disconnected to actuate the breakaway feature. The criterion for trailer breakaway holding ability is that the safety brake feature be capable of holding the vehicle stationary in both ascending and descending attitudes on the maximum slope over which the vehicle is designed to operate for a period of 30 min.

7. Maximum Pedal Effort Braking. Maximum pedal effort brake stops will be made in the forward vehicle direction on a dry, level, paved surface at 5-mph road speed increments over a speed range span of 20 mph to maximum vehicle speed (or to the highest speed where safe maximum pedal effort braking can be achieved). The criterion for maximum safe speed at maximum pedal effort is that vehicle slew shall not exceed the limits of a roadway lane width equal to 1-1/2 times the overall width of the test vehicle.

8. Brake Actuation and Release Time. The time lapse between brake application, actuation, and release will be determined by means of a recording device triggered by switches installed at the application mechanism and at the point where the brake friction material contacts the rotating member. Brake input pressure will be measured at the input source and at the brake location farthest from the input source.

9. Low Temperature Effects. This test is conducted to assure satisfactory operation of the moving components of the braking system under extreme cold environmental conditions. Testing is accomplished by actuating the brake system while the vehicle is stationary. The criterion for this test is that braking system components function satisfactorily at ambient air temperature designated in the plan of test for each specific vehicle without damage to seals, gaskets, or moving parts. In the absence of a specific standard, −50°F will be used.

10. Brake Fade Test. Brake fade characteristics will be determined during repeated braking operation over a downhill roadway of approximately 9 to 11% grade over a distance of approximately 2 mi and a 40 mph full stop at the bottom of the grade. The tests are designed to be conducted over a 25-mi section of US Route 30 in the Jennerstown area of western Pennsylvania. The criteria for brake fade are:

a. Immediately following the downgrade brake snubbing procedure, the test vehicle must demonstrate the capability of making a full stop at the bottom of the grade as indicated in the table that follows

Gross Vehicle Weight, lb	Deceleration Rate, ft/s^2	Initial Braking Speed, mph
Up to 12,000	14.4	40
12,000-50,000	14.4	40
Over 50,000	11.0	30

b. Vehicle slew shall not exceed roadway lane width limits equal to 1-1/2 times the overall width of the test vehicle.

11. High Temperature Endurance Test. A high temperature highway brake test is conducted for the purpose of evaluating the performance, fade, wear, and endurance characteristics of wheeled vehicle braking systems under conditions where elevated brake system temperatures and braking torques are a factor. The criteria are:

a. After the complete brake fade test, brake component deterioration shall not have reduced vehicle stopping ability.

b. Damage to brake, wheel, and suspension system components, such as bending, twisting, or breakage, shall not occur as a result of test operation.

12. Brake Endurance Test. The mileages accumulated during specified tests will be used for brake endurance evaluation as applicable for off-highway and general operation. The criteria for off-highway braking system endurance are:

a. Brake component wear attributable to abrasives accumulated during normal vehicle endurance testing shall not reduce vehicle stopping ability over an accumulated span of 500 mi when test course surfaces are in a wet, muddy condition.

b. Damage to brake, wheel, and suspension system components such as bending, twisting, or breakage, shall not occur as a result of test operation.

13-7.2 ROAD TEST PROCEDURES FOR TRACKED VEHICLES

The major procedures and requirements are (Ref. 7):

1. Operation Safety. The dangers of operational hazards during the various phases of the braking tests must be identified and understood to assure that the dangers to personnel and equipment are kept to a minimum. The operational details to survey include vehicle stability, braking and steering control, brake sensitivity, course conditions, vehicle condition, use of safety cables, and the imposing of operational limitations.

2. Safety Evaluation. Every phase of the brake test is a safety test and therefore considered to be part of the safety evaluation of the vehicle. Those factors considered most critical are:

a. Holding ability of parking and service brakes on 60% slope

b. Stopping ability from 20 mph

c. Stability and control when braking.

3. Test Instrumentation. Adequate measurements depend upon the use of appropriate instrumentation, calibrated before and after a test and, if necessary, during the test. Calibrations are required on all instrumentation.

4. Test Procedure. The collection of valid test data requires that an individual test be repeated a sufficient number of times to provide a reliable average value. A suitable time must elapse between measurements to assure stable conditions. Any failed parts are reported. Samples of expendable supplies used during brake testing, such as lubricants, hydraulic fluid, and worn lining materials, are retained until completion of the vehicle test project.

5. Weight. The tracked vehicle is loaded with properly distributed test weight, and the vehicle weight at each road wheel position is recorded. If a towed load is prescribed for the vehicle, weight distribution is taken with and without the prescribed towed load.

6. Dimensions. Dimensional checks are made on the braking system for comparison before and after the tests. Name of manufacturer and characteristics of critical components are recorded.

7. Adjustments. Suspension and braking systems are carefully checked and adjusted in accordance with technical manuals, manufacturer's specifications, or standard practice. All components are required to be in new, near perfect condition.

8. Wear Measurements. If stipulated in the test plan, all friction surfaces are measured before and after the endurance test to determine rates of wear.

9. Free Roll Deceleration. The normal free roll deceleration of a tracked vehicle is determined by allowing the vehicle to coast to a stop without steering, with the transmission in neutral and in highest gear, and with the engine idling.

10. Human Application Force vs Braking System Pressure. The input of human force versus resultant braking system pressure is measured and a characteristic curve defined.

11. Burnishing. Break-in operation is conducted to burnish the brake surfaces. If the brake surfaces are accessible, they are inspected to assure that proper burnishing has been accomplished.

12. Slope Tests of Parking Brakes. Parking brakes are tested for stopping effectiveness and for holding ability on longitudinal slopes. These tests are conducted progressively up to 60% slope, operating the vehicle up and down the slope. Parking brakes must hold for a 15-min period without creep.

13. Wet and Freezing Effects. For vehicles not having internal power train braking (usually only foreign vehicles), tests are performed to determine whether wet and freezing conditions will affect the functioning of the service and parking brake systems. Degradation of braking is determined by measuring the input pressure required to maintain a deceleration rate of 6 to 8 ft/s^2 during successive stops from specified speeds. Effects of frost and ice forming on vital parts of the service and parking brake systems are evaluated in cold chamber testing.

14. High Temperature Effects. Influence of high temperatures is tested during the service brake effectiveness test and the fade and recovery tests.

15. Stopping Distance. Specified stopping distance should be obtained at even 10 mph increments at approximately 50, 75, and 100% of maximum speed, starting at a speed of not less than 20 mph.

16. Braking Potential. Parking brake potential is determined by measuring the breakaway towing force, using a towing dynamometer, when brake lever

forces ranging from 75 to 150 lb are applied. Braking potential of service and steering brakes is determined as follows:

a. The application force required to provide the necessary brake force is measured under both static and dynamic conditions over the range of minimum to maximum apply effort.

b. With friction material at "cold lining" temperature (under 200°F) the breakaway force is measured over the brake apply force range by means of a towing dynamometer.

17. Service Brake Effectiveness. The effectiveness defines the relationship between input force applied to the hydraulic system through the pedal linkage and vehicle deceleration from a coasting condition to a point of track lockup. The following tests are conducted:

a. An effectiveness spot check is made at 20 mph, 30 mph, and at 5 mph below maximum vehicle speed, utilizing maximum pedal input force.

b. Effectiveness tests are conducted with the hottest brake under 200°F over the pedal input force range of the braking system up to the point where a track locking condition occurs.

c. Effectiveness tests are conducted with the brake friction material at 350°F or an oil temperature of 230°F at the hottest brake over the pedal input force range of the braking system up to the point where a track locking condition occurs.

18. Fade and Recovery Test. The purpose of fade and recovery tests is to evaluate service and steering brakes during multiple applications. These tests may require modifications for certain braking systems because of the variety of tracked vehicle configurations. The service brake is evaluated according to the tests that follow:

a. A base line check is performed at 20 mph and two-thirds maximum speed or a specified speed with an initial temperature as specified using a normal deceleration of 8 ft/s^2.

b. Immediately after the base line check, 10 stops are made from the base line speed under the same conditions, attempting to maintain 30 s between stops. Input pressure, stopping distance, and final friction material temperatures are recorded for the final (tenth) stop.

c. With the initial brake temperature the same as after the tenth stop, the vehicle is operated two additional miles after which a recovery test is made. Temperatures of the energy-absorbing components are recorded before and after operations. The base line check (a) is repeated after the brakes have cooled to less than 200°F. The fade and recovery tests are repeated if incipient or actual failures are detected.

19. Steering brakes. The vehicle is operated over a sine wave steering course consisting of a roadway 30 ft wide with center stakes placed 100 ft apart. Operation is conducted at progressively increasing approach speeds, continuing at wide open throttle for a distance of 2,000 ft. A maximum-effort brake stop is made from a speed of 20 mph at the end of the course.

20. Service Brake System Endurance Test. If specifications do not exist for the vehicle to be tested, the endurance test will consist of making 400 brake applications (snubs) from 20 to 10 mph (or two-thirds to one-third maximum speed) at 8 ft/s^2. Ten applications constitute a series, and a full stop is made on the tenth. In the series an attempt is made to maintain 30 s intervals between snubs. Deceleration is measured throughout the test while temperatures, stopping distance, input force and pressure, and pedal or level travel are recorded during full stops only.

21. Human Factors Evaluation. All of the observations on the human factors involved in brake applications are recorded. These include: effort required in brake application, accessibility of brakes to men of all sizes, danger to crew from sudden brake applications, and ease with which emergency brake applications can be made.

13-8 COMPONENT TESTING

Brake system components may be tested in road tests or laboratory tests. When evaluated in road test procedures, effects from, e.g., ambient conditions, and other vehicle and brake system components may affect significantly the performance of a component. Consequently, specific brake system components such as brake linings, switches, and brake application valves are certified or tested under laboratory conditions. Frequently, the application and release times of pneumatic brake systems are determined under laboratory conditions.

Of special importance to the brake engineer is the information on brake lining friction coefficients. Drum brake linings may be evaluated on inertia dynamometers in which a large flywheel — turning at speeds equivalent to the rotational speed of the wheel of the motor vehicle — is braked. Although this method provides torque vs application force data, the lining friction coefficient only can be computed by the brake factor equations presented in Chapter 2. Frequently, the coefficient of friction of a segment of brake lining is evaluated in a simple friction test in which the small lining segment is pressed against the drum friction surface. Although this test method does not represent actual conditions, good correlation of

results is obtained from machines that evaluate lining segments only and test data obtained from complete brake tests. For practical purposes a lining or pad friction coefficient may be stated in terms of an average friction value together with minimum and maximum values corresponding to low and high brake temperatures or sliding speeds. Good linings have limits of ± 15 - 20% of the base line friction value. Excellent linings may assume limits as high as ± 10%.

Test procedures and performance requirements for nearly all brake system components such as brake base, brake tubing, lining materials, and wheel-antiskid controls have been developed by the Society of Automotive Engineers (Ref. 8).

REFERENCES

1. M. Mitschke, "Dynamics of Motor Vehicles", *Spring Publisher,* Berlin-Heidelberg-New York, 1972.
2. R. T. Spurr and T. P. Newcomb, *Testing of Commercial Vehicle Brakes,* 12th International Congress, FISITA, Barcelona, Spain, 19-28 May, 1968.
3. D. M. Frood, D. K. Mackenzie, and T. P. Newcomb, *Brake Usage in a Heavy Vehicle,* Inst. Mech. Engrs. Auto. Div., December 28, 1961.
4. M. Cardon, *Development of Brake Inspection Criteria and Equipment,* Bendix Research Laboratories, Southfield, Michigan, 1973.
5. G. L. Parker, T. W. Keranen, and M. H. Cardon, *Determining the Effects of Brake Degradation,* SAE Paper No. 730190.
6. *Material Test Procedure 2-2-608,* US Army Test and Evaluation Command, 15 January 1971.
7. *Material Test Procedure 2-2-627,* US Army Test and Evaluation Command, 1 July 1971.
8. *Motor Vehicle Braking System and Components,* Handbook Supplement HS24, Society of Automotive Engineers, Inc., Two Pennsylvania Plaza, New York, New York, November 1974.

CHAPTER 14
DESIGN APPLICATIONS

In this chapter major concepts presented in previous chapters are applied to specific design examples. A design check list is presented at the end of this chapter.

14-0 LIST OF SYMBOLS

A_P = lining or pad rubbing area of leading or secondary shoe, or brake pad, ft²
A_{pp} = projected lining area, in.²
A_S = swept area of rotor or drum, ft²
A_{WC} = wheel cylinder area, in.²
$A_{WC,F}$ = front wheel cylinder area, in.²
$A_{WC,R}$ = rear wheel cylinder area, in.²
a = deceleration, g-units
a_b = brake dimension, in.
a' = brake dimension, in.
BF = brake factor, d'less**
BF_1 = brake factor of primary shoe, d'less
BF_2 = brake factor of secondary shoe, d'less
c = brake dimension, in.
D_o = outer diameter of rotor, ft
D_i = inner diameter of rotor, ft
d = wheel-cylinder piston displacement, in.
d_h = hydraulic diameter, in.
E_F = front axle braking efficiency, d'less
E_R = rear axle braking efficiency, d'less
E_T = kinetic energy, ft·lb
F_a = brake shoe application force, lb
F_{ax} = application force of secondary shoe, lb
F_{d1} = drag force due to primary shoe, lb
F_{d2} = drag force due to secondary shoe, lb
F_H = hand lever force, lb
F_p = pedal force, lb
F_{ret} = retarding force, lb
F_x = brake force, lb
F_{xF} = front axle brake force, lb
$F_{x,total}$ = total brake force, lb
$F^*_{xF,dyn}$ = normalized dynamic front axle brake force, d'less
$F^*_{xR,dyn}$ = normalized dynamic rear axle brake force, d'less
G = road gradient, d'less
h = brake dimension, in.
h_R = heat transfer coefficient of rotor, BTU/h·°F·ft²
IC = booster input characteristic, d'less
I_R = mass moment of rotational inertia, lb·in.·s²
$I_{t,Rotor}$ = equivalent mass moment of rotational inertia at the brake rotor, lb·in.·s²
k_a = thermal conductivity of air, BTU/h·°F·ft
l = vane length, in.
l_p = pedal level ratio, d'less
M_e = engine retarding torque, lb·ft
n_v = number of vanes per rotor, d'less
o = brake dimension, in.
P = pressure ratio, d'less
Pr = Prandtl number, d'less
P_A = accumlator pressure, psi
P_G = gas charge pressure of accumulator, psi
p_{lF} = front brake line pressure, psi
p_{lR} = rear brake line pressure, psi
p_l = brake line pressure, psi
p_m = mean pressure between lining and drum, psi
p_o = pushout pressure, psi
q_o = braking energy, BTU/h
$q_{(o)}$ = braking energy at onset of braking, BTU/h
q''_P = horsepower absorbed by lining or pad, hp/ft²
q''_R = heat flux absorbed by rotor, BTU/ft²·s
R = effective tire radius, in.
Re = Reynolds number, d'less
r = effective drum or rotor radius, in.
S_B = brake sensitivity, d'less
T = temperature, °F
T_B = brake torque, lb·ft
t_s = braking time, s
u = effective width of brake drum swept area, in.
v_e = engine displacement, in.³
V_{in} = inlet velocity, ft/s
V_{out} = outlet velocity, ft/s
V_{MC} = master cylinder volume, in.³
V_{Ratio} = volume ratio, d'less
v = ratio of hose expansion to master cylinder volume, d'less
W = vehicle weight, lb
W_o = empty vehicle weight, lb
Y = pedal travel, in.
α = road slope angle, deg
α_o = lining angle, deg
$\hat{\alpha}_o$ = arc of α_o, rad
α_1 = angular brake dimension, deg

**d'less = dimensionless

α_2 = angular brake dimension, deg
α_3 = $\alpha_1 + \alpha_2$, deg
β = angular brake dimension, deg
γ = angular brake dimension, deg
ΔBF = brake force change, d'less
ΔT = temperature increase per brake application, = deg F
$\Delta\mu_L$ = lining friction coefficient change, d'less
η_c = wheel cylinder efficiency, d'less
η_H = relative portion of braking energy absorbed by an individual brake shoe, d'less
η_p = mechanical efficiency of the pedal, d'less
η_T = efficiency of transmission, d'less
λ = relative portion of braking energy absorbed by an individual brake shoe, d'less
μ = tire-road friction coefficient, d'less
μ_L = lining or pad friction coefficient, d'less
μ_s = coefficient of friction between brake shoe and abutment, d'less
ρ = transmission ratio between engine and wheels, d'less
ρ_B = gain of emergency brake, d'less
ρ_H = displacement gain of emergency brake, d'less
ϕ = rear axle brake force divided by total brake force, d'less
ϕ_i = brake force of ith brake divided by total brake force, d'less
χ = center of gravity height divided by wheel base, d'less
χ_o = center of gravity height divided by wheel base for empty vehicle, d'less
ψ = static rear axle load divided by vehicle weight, d'less
ψ_o = static rear axle load divided by empty vehicle weight, d'less

14-1 BASIC CONSIDERATIONS

In most cases when the brake engineer is asked to determine the brake system layout, the data that follow are available:

1. Empty and loaded vehicle weight
2. Vehicle wheel base
3. Static weight distribution among axles
4. Center of gravity height
5. Tire and rim size
6. Intended vehicle function
7. Maximum speed
8. Braking performance that must be met such as Federal or European standards.

In many cases additional restrictions are placed upon the design in terms of what specific brake system components must be used such as drum brakes, low assist braking units, or disc brakes located inboard near the differential. In most practical cases, economic considerations require the use of mass production shelf items, and it is not possible always to optimize a braking system by using existing hardware. On the other hand, if the anticipated cost-benefit relationship is favorable, the production of an additional component size may be justified.

14-2 SPECIFIC DESIGN MEASURES

Several specific design measures have been developed that allow a proper design of major elements of a braking system. These design measures are related to the thermal and safety performance of a brake system.

In general, thermal cracking of the brake drum or rotor has not been observed when the heat flux q''_R into the swept area of the rotor or drum is kept below a certain value as defined by Eq. 14-1.

$$q''_R = \frac{q_o\,\phi_i}{3600\,A_S} < 150\ \text{BTU/ft}^2\cdot\text{s} \qquad (14\text{-}1)$$

where

A_S = swept area of rotor or drum, ft^2
q_o = braking energy, BTU/h (determined by Eq. 3-1)
ϕ_i = brake force of ith brake divided by total brake force, d'less

The brakes generally do not exhibit significant fade if the horsepower q''_P absorbed by the lining or pad is kept below a certain value as defined by Eq. 14-2.

$$q''_p = 1.41\,q_o\,\phi_i\,\lambda/(3600\,A_p) < \begin{cases} 460\ \text{hp/ft}^2, \text{drum} \\ 2300\ \text{hp/ft}^2, \text{disc} \end{cases} \qquad (14\text{-}2)$$

where

A_P = lining or pad rubbing area of leading or secondary shoe, or brake pad, ft^2
λ = relative portion of the braking energy absorbed by an individual brake shoe, d'less
λ = 0.5 for two-leading shoe brake
= 0.7 for leading-trailing shoe or duo-servo brake
= 1.0 for disc brake pad

Excessive wear generally has not been observed if the product of the mean pressure p_m between lining and drum, and lining friction coefficient μ_L is kept below a certain value as defined by Eq. 14-3.

$$\mu_L\,p_m = \lambda\,W\,a\,\phi_i\,(R/r)/A_{pp} < \begin{cases} 95\ \text{psi, drum} \\ 350\ \text{psi, disc} \end{cases} \qquad (14\text{-}3)$$

where

A_{pp} = projected lining area of leading or secondary shoe
= 1.62 ru, in.^{2}
a = deceleration, g-units
R = effective tire radius, in.
r = effective drum or rotor radius, in.
u = effective width of brake drum swept area, in.
W = vehicle weight, lb
μ_L = lining or pad friction coefficient, d'less

If no specific information is available on the coefficient of friction μ_L for the brake linings or pads, the values that follow may be used for design purposes:

Leading - trailing shoe brake μ_L = 0.35
Two-leading shoe brake μ_L = 0.45
Duo-servo brake μ_L = 0.35
Disc brake μ_L = 0.40

Safety considerations require that the wheel-cylinder piston displacement d produced by the master cylinder exceeds certain values. This condition may be expressed by an approximate relationship.

$$d = BF/25 \text{ , in.} \qquad (14\text{-}4)$$

where

BF = brake factor, d'less

Eq. 14-4 applies to drum and disc brakes.

Basic considerations of pedal force transmission yield the work output $F_p Y$ from the master cylinder and hence pedal force F_p for a manual brake system as

$$F_p Y = 0.53\, a\, W r/R \text{ , in.·lb} \qquad (14\text{-}5)$$

where

F_p = pedal force, lb
Y = pedal travel, in.

14-3 DESIGN OF RELATED COMPONENTS SUCH AS SUSPENSION, TIRES, AND RIMS

The limiting brake forces are determined by the normal forces between the tire and road, and the tire-road friction coefficient. The normal forces are a function of the load transfer occurring during braking. Transient dynamic forces caused by road surface roughness, oscillating pedal force applications, or cycling brake force modulations of antiskid systems also affect the instantaneous tire normal force. The vertical dynamics of the suspension systems is a function of the unsprung weight, spring stiffness, and damping characteristics. The vertical spring stiffness consists of that associated with the spring connecting body and axle, and of the tires. For vehicles equipped with tandem axles, the load transfer among individual axles must be considered as discussed in Chapters 8 and 9. The braking analysis provides force and moment data required for the design of suspension members and frame attachments. An important consideration is that the oscillating frequency of an antiskid system is such that it does not operate near or at the wheel hop or suspension natural frequency. The proper analysis and design of an antiskid system require tire brake force and side force data as a function of tire slip. Steady-state braking analyses require only tire size data, such as tire diameter and tire width. An increase in tire diameter, e.g., by 10% with otherwise unchanged conditions, will cause a 10% decrease in braking effectiveness. A wider tire may result in decreased cooling capacity of the brake because of the obstruction of air flow to the rotor or drum.

Rim data are essential in determining the maximum rotor or drum diameter that can be used in a particular wheel. Special passages in the rim may be used to increase the cooling of a wheel brake. Normally, these openings must be of elaborate design to produce a significant effect on the thermal capacity of the wheel brake.

14-4 BRAKE SYSTEM DESIGN CHECK

The objective of a design check is to ensure that braking performance levels and safety specifications are met. Furthermore, economic considerations must be included in a design check in form of optimum component size.

A design check can be divided into the tasks that follow:

1. Braking effectiveness analysis:
   a. Determination of brake factors from brake geometry and lining friction coefficient
   b. Determination of braking effectiveness, i.e., brake line pressure/deceleration characteristic
   c. Determination of pedal force/brake line pressure, and hence pedal force/deceleration characteristic
   d. If appropriate, determination of vacuum assist characteristic and increased braking effectiveness
   e. If appropriate, determination of full power characteristic.
2. Braking efficiency analysis:
   a. Determination of maximum straight line wheels unlocked deceleration for low and

high roadway friction
   b. If appropriate, determination of maximum curved line wheels unlocked deceleration for low and high roadway friction.
3. Response lag: For air brake systems, determination of time lags.
4. Emergency or parking brake:
   a. Determination of maximum deceleration by application of emergency brake on level and sloped roadways
4. b. Determination of maximum grade holding capacity.
5. Partial failure analysis:
   a. Determination of braking effectiveness with service system circuit failure
   b. Determination of braking effectiveness with partial or complete assist failure
   c. Determination of braking efficiency with service system circuit failure
   d. Determination of braking effectiveness with service brakes in faded condition
   e. Determination of increased pedal travels for circuit failure.
6. Thermal analysis:
   a. Determination of heat transfer coefficients
   b. Determination of brake temperatures during continued braking, repeated braking, and maximum effectiveness stop
   c. Determination of thermal surface stresses.
7. Volume analysis:
   a. Determination of wheel cylinder piston displacements
   b. Determination of master cylinder bore and master cylinder piston travel
   c. Determination of pedal travel.
8. Specific design measures:
   a. Determination of heat flux absorbed by rotor in an effectiveness stop
   b. Determination of horsepower absorbed by brake lining or pad
   c. Determination of wear measure expressed as product of lining friction coefficient and mean pressure between lining and drum
   d. Determination of wheel cylinder piston travel limit value.
9. Brake force distribution:
   a. Determination of optimum brake force distribution for straight line braking
   b. If appropriate, determination of optimum brake force distribution for curved line braking
10. Safety regulations: If appropriate and required, determination of level of compliance with existing safety standards.

14-5 BRAKE FACTOR CALCULATION

The objective is the computation of the brake factor and brake sensitivity of a duo-servo drum brake with sliding abutment on the primary shoe and pivot support on the secondary shoe. The schematic and geometrical information are illustrated in Fig. 2-16. The brake data that follow were measured on the brake:

Primary shoe:	Secondary shoe:
a = 4 in.	a = 4 in.
c = 4 in.	a' = 4 in.
o = 1.5 in.	h = 8 in.
r = 5 in.	o = 0 in.
α_o = 126 deg	r = 5 in.
$\hat{\alpha}_o$ = 2.2 rad	α_o = 126 deg
β = 3 deg	$\hat{\alpha}_o$ = 2.2 rad
μ_S = 0.2 (steel on steel)	α_1 = 24 deg
	α_2 = 150 deg

The total brake force BF may be computed by Eqs. 2-27, 2-29a, and 2-30 with the brake factor BF_1 of the primary shoe given by Eq. 2-29a and the shoe factor F_{d2}/F_{ax} of the secondary shoe given by Eq. 2-27. Substitution of the appropriate data of the primary shoe into Eq. 2-29a yields

$$BF_1 = \frac{F_{d1}}{F_a}$$

$$= \frac{\mu_L\,(1.67) + \mu_L^2\,(0.073)}{0.726 - \mu_L\,(1.01) + \mu_L^2\,(0.579)}\text{, d'less} \quad (14\text{-}6)$$

where

F_a = brake shoe application force, lb
F_{d1} = drag force due to primary shoe, lb
μ_L = friction coefficient between lining and drum, d'less

Eq. 14-6 presents the variation of the brake factor BF_1 of the primary shoe with lining friction coefficient μ_L. Eq. 2-29a is used to derive Eq. 14-6 since the primary shoe of the brake to be analyzed is supported by a parallel sliding abutment.

Eq. 14-6 may be evaluated for different values of μ_L giving the values listed in Table 14-1.

TABLE 14-1
BF_1 VS μ_L

μ_L	0.1	0.2	0.3	0.4	0.5	0.6
$BF_1 = F_{d1}/F_a$	0.266	0.616	1.068	1.639	2.332	3.131

The secondary shoe is actuated by the support force between primary and secondary shoes. Since the brake factor is defined by the ratio of drum drag to application force produced by the wheel cylinder, the brake factor of the secondary shoe must be computed in two steps. First the shoe factor is determined by Eq. 2-27 with the support force of the primary shoe used as actuation force of the secondary shoe. Then the shoe factor is modified by means of Eq. 2-30 to yield the brake factor of the secondary shoe. Substitution of the appropriate data into Eq. 2-27 with $\alpha_3 = \alpha_1 + \alpha_2 = 174$ deg yields

$$F_{d2}/F_{ax} = \mu_L(1.6)/[0.67535 - \mu_L(1.019)] \text{ , d'less} \quad (14\text{-}7)$$

where

F_{ax} = application force of secondary shoe, lb
F_{d2} = drag force due to secondary shoe, lb

The minus sign is used to determine the shoe factor of the secondary (or leading) shoe. Eq. 14-7 may be evaluated for different values of μ_L, yielding the values given in Table 14-2.

Since the brake factor is defined as the ratio of total drum drag to the application force F_a at the wheel cylinder, the shoe factor of the secondary shoe must be modified to yield the brake factor of the secondary shoe (Eq. 2-30)

$$BF_2 = (F_{d2}/F_{ax})(F_{ax}/F_a) \text{ , d'less} \quad (14\text{-}8)$$

The ratio F_{ax}/F_a is determined by Eq. 2-31.

$$F_{ax}/F_a = (c/a) + (F_{d1}/F_a)(r/a)$$
$$= 1.0 + (F_{d1}/F_a)(1.25) \text{ , d'less} \quad (14\text{-}9)$$

where

a = brake dimension, in.
c = brake dimension, in.

The ratio F_{ax}/F_a assumes different values for various values of μ_L. Using the values of F_{d1}/F_a from Table 14-1 in Eq. 14-9 gives the values of F_{ax}/F_a listed in Table 14-3.

The brake factor BF_2 of the secondary shoe can now be determined by Eq. 14-8. Values of BF_2 for various values of μ_L are given in Table 14-4.

TABLE 14-2
F_{d2}/F_{ax} VS μ_L

μ_L	0.1	0.2	0.3	0.4	0.5	0.6
F_{d2}/F_{ax}	0.279	0.679	1.299	2.390	4.824	15.012

The total brake force BF is obtained by adding the individual shoe brake factors, yielding the data in Table 14-5.

The brake factor characteristic is illustrated in Fig. 14-1. Inspection of the brake factor curves for the individual shoes indicates that both shoes produce nearly equal amounts of brake torque for friction coefficients below 0.3. For higher values of μ_L the secondary shoe is heavier loaded than the primary shoe indicated by a higher brake factor BF_2.

Brake sensitivity S_B is defined as the ratio of a change in brake factor to the associated change in lining friction coefficient. In some cases the brake sensitivity may be expressed by a mathematical equation (Eq. 2-24). Most drum brakes in use today require complicated relationships for the computation of brake sensitivity. For these cases, an approximate value of brake sensitivity may be obtained from the brake factor curve.

For the sample problem, the approximate slope of the brake factor curve at various values of lining-drum friction coefficient can be determined from Fig. 14-1. For example, for $\mu_L = 0.15$

$$S_B = \frac{\Delta BF}{\Delta \mu_L} = \frac{1.818 - 0.637}{0.2 - 0.1} = 11.8 \text{ , d'less}$$

where

ΔBF = brake factor change, d'less
$\Delta \mu_L$ = lining friction coefficient change, d'less

TABLE 14-3
F_{ax}/F_a VS μ_L

μ_L	0.1	0.2	0.3	0.4	0.5	0.6
F_{ax}/F_a	1.333	1.770	2.335	3.049	3.915	4.914

TABLE 14-4
BF_2 VS μ_L

μ_L	0.1	0.2	0.3	0.4	0.5	0.6
$BF_2 = \left(\frac{F_{d2}}{F_{ax}}\right)\left(\frac{F_{ax}}{F_a}\right)$	0.372	1.202	3.036	7.287	18.870	73.579

TABLE 14-5
BF VS μ_L

μ_L	0.1	0.2	0.3	0.4	0.5	0.6
BF	0.638	1.818	4.103	8.926	21.202	76.890

The brake sensitivities of Table 14-6 may be obtained by the same procedure. The S_B values for μ = 0.5 and 0.6 are too large to be determined from the brake factor curve shown in Fig. 14-1.

A graphical representation of the data from Table 14-6 is shown in Fig. 14-2. Brake sensitivity values normally should not exceed 30. Higher values could lead to severe side-to-side brake unbalance. Lower values of brake sensitivity are obtained by lowering the lining friction coefficient μ_L with a corresponding decrease in brake factor. The brake factor decrease causes the gain of the brake system to be lowered. The gain of the brake system can be increased again by increasing the drum or rotor radius or by installing (or increasing) an assist unit.

14-6 DESIGN OF LIGHT TRUCK BRAKE SYSTEM

The objective is the design of a brake system for a series of six vans using as many identical brake system components as possible. The loading and geometrical data are presented in Table 14-7, indicating a weight range from 2740-7200 lb for the empty and loaded case for the lightest and heaviest vehicle, respectively. The maximum pedal travel Y for the service brake is 8.25 in., the pedal lever ratio l_p is 5 to 1, the hand lever travel for the emergency or secondary brake is 8 in., and the hand lever ratio ρ_H is 5.6 to 1. The pedal force F_p should not exceed 150 lb for all six vehicles for a deceleration of 0.5g. The hand lever force F_H is limited to 90 lb for a deceleration of 0.25. Maximum speed is 60 mph.

The investigation resulted in two brake systems, one for vehicles 1 through 3 and one for vehicles 4 through 6. The component dimensions and performance measures of the brake systems of vehicles 3 and 6 are shown in Table 14-8. The brake system design and performance data were determined from the equations of previous chapters. A two-leading shoe

TABLE 14-6
S_B VS μ_L

μ_L	0.1	0.2	0.3	0.4	0.5	0.6
S_B	8	14	32	80	—	—

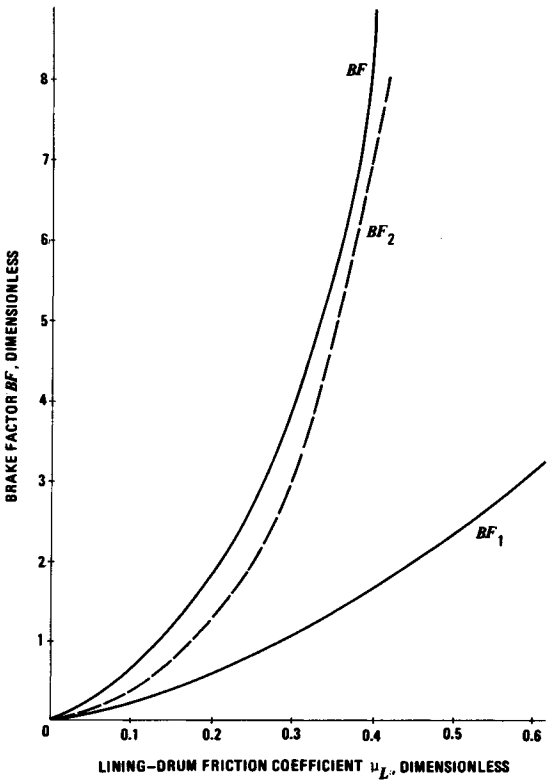

Figure 14-1. Brake Factor Characteristic of a Duo-Servo Brake

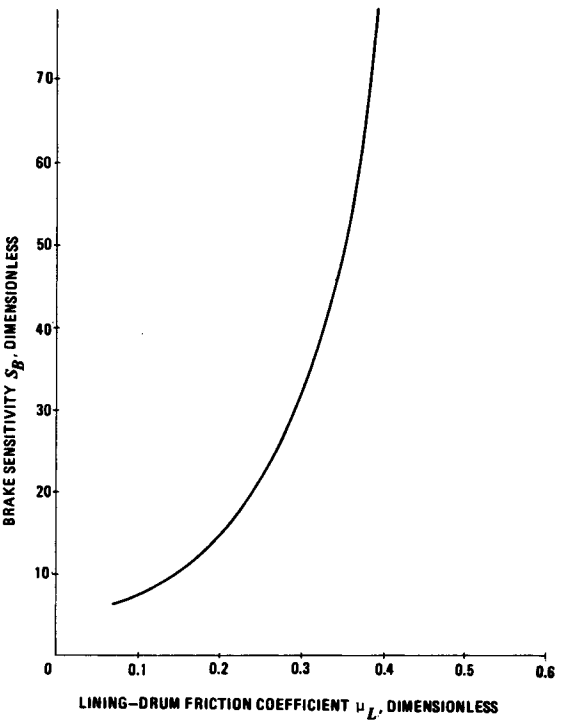

Figure 14-2. Brake Sensitivity

TABLE 14-7
LOADING AND GEOMETRICAL DATA

	Empty			Loaded			
Vehicle No.	Weight W_0, lb	ψ_0	χ_0	Weight W, lb	ψ	χ	Effective Tire Radius R, in.
1	2740	0.393	0.293	4050	0.546	0.353	12.2
2	2748	0.296	0.317	4600	0.583	0.359	12.5
3	2770	0.298	0.325	5200	0.614	0.364	12.8
4	3250	0.265	0.308	6000	0.663	0.328	12.2
5	3260	0.269	0.317	6600	0.684	0.335	12.5
6	3320	0.272	0.325	7200	0.702	0.337	12.8

TABLE 14-8
BRAKE SYSTEM DESIGN AND PERFORMANCE DATA

Vehicle No.	3		6	
Axle	Front	Rear	Front	Rear
Brake Diameter & Width, in.	10 × 2-5/8	10 × 1-3/8	10 × 2-3/4	10 × 2-5/8
Wheel Cylinder Diameter, in.	13/16	9/16	7/8	3/4
Brake Factor, d'less	4.35	4.35	4.35	4.35
Brake Force Distribution, %	67.5	32.5	58	42
Swept Drum Area, ft²	0.94	0.60	1.20	0.94
Lining Area, ft²	0.52	0.33	0.67	0.52
Heat flux into Drum, BTU/ft²·s	112	84	103	98
Horsepower into Lining, hp/ft²	326	244	200	285
Product of Lining Friction Coefficient & Mechanical Pressure, psi	75	56.5	69	65
Master Cylinder	11/16 in. diameter; 1-21/32 in. stroke			

drum brake with a brake factor equal to 4.35 was arbitrarily chosen. The drum brakes are identical for each vehicle except for the shoe width.

The important aspects of the brake system design are discussed in the paragraphs that follow.

14-6.1 EMERGENCY BRAKE ANALYSIS

Emergency or hand brakes may be designed to act on the rear or front axle. The braking analysis is identical to that of a front or rear axle brake circuit failure of the service brake.

The wheels unlocked deceleration achievable on a horizontal roadway with the emergency brake acting on the rear axle may be obtained by Eq. 12-3 for a specified tire-road friction coefficient. Similarly, when the emergency brake is acting on the front axle, the corresponding deceleration may be obtained by Eq. 12-4.

The results of Eqs. 12-3 and 12-4 are illustrated in Figs. 14-3 through 14-6 for vehicles 1, 3, 4, and 6, respectively. Inspection of the curves indicates that the lighter vehicles produce larger decelerations with the emergency brake acting on the front axle. For example, Fig. 14-3 shows that a tire-road friction coefficient $\mu = 0.7$ produces deceleration of approximately 0.55g for the empty vehicle 1 with the emergency brake on the front axle and only approximately 0.25g with the emergency brake on the

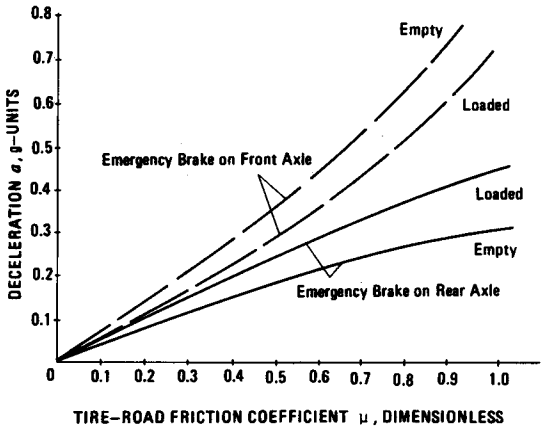

Figure 14-3. Emergency Brake Performance, Vehicle No. 1

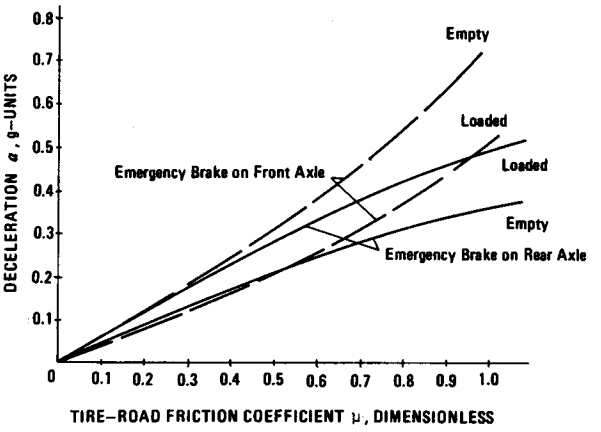

Figure 14-5. Emergency Brake Performance, Vehicle No. 4

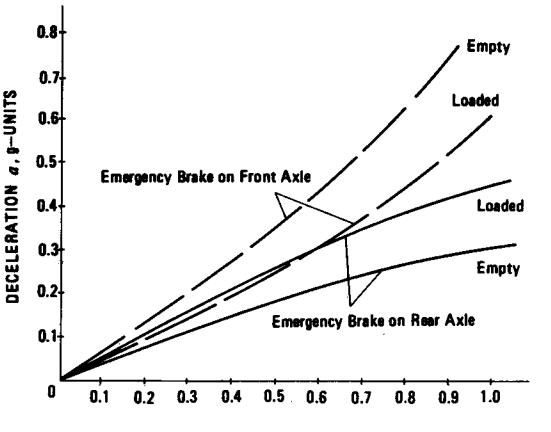

Figure 14-4. Emergency Brake Performance, Vehicle No. 3

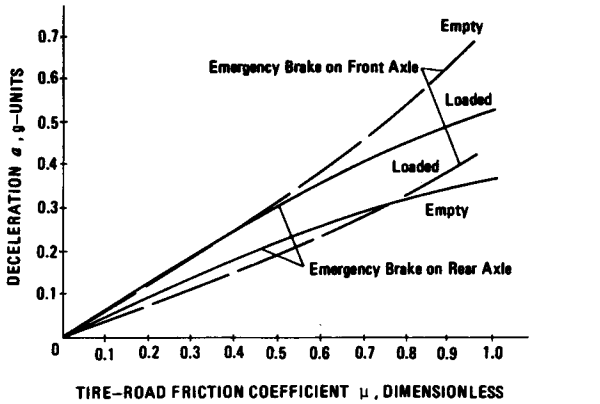

Figure 14-6. Emergency Brake Performance, Vehicle No. 6

rear axle. For the heavier vehicles front or rear axle location of the emergency brake produces near equal results when both the empty and loaded driving conditions are considered. A mechanical (emergency) brake located on the rear axle presents less problems for the installation of the cable with respect to the relative motion of the wheel. Front axle location of the brake requires special provisions to account for the steering angle of the front wheels.

In the paragraphs that follow the front and rear axle location of the emergency brake is analyzed for different conditions with the vehicle operating on a road gradient.

Of importance is the capability of an emergency brake to hold a vehicle stationary on an inclined roadway. Since the road gradient affects the static axle load distribution, the effect of the change of axle loading on the "parking" performance must be analyzed. Only the most severe condition must be investigated. In general, for a vehicle with the emergency brake acting on the front axle, the condition in which the vehicle is facing uphill is more severe. The road gradient G on which the vehicle can safely be held stationary is

$$G = \frac{\mu(1-\psi)}{1+\mu\chi} \text{ , d'less} \qquad (14\text{-}10)$$

where

μ = tire-road friction coefficient, d'less
χ = center of gravity height divided by wheel base, d'less
ψ = static rear axle load divided by vehicle weight, d'less

For a vehicle with the emergency brake acting on the rear axle and the vehicle facing downhill, the road gradient may be determined by Eq. 14-10 with $(1 - \psi)$ replaced by ψ.

The graphical representation of Eq. 14-10 is presented in Fig. 14-7 for vehicle 3 in the loaded condition. The loaded case is chosen since this condition is associated with a larger weight concentration on the rear axle than the empty case. Inspection of Fig. 14-7 indicates that a road gradient $G = 0.25$ requires a tire-road friction coefficient $\mu = 0.85$.

Finally, when applying the emergency brake to stop a vehicle going downhill, a rear axle location of the emergency brake presents the more severe condition. The wheels unlocked deceleration a for vehicles equipped with a rear axle emergency brake when going downhill is

$$a = \frac{\mu\psi\cos\alpha}{1+\mu\chi} \text{ , g-units} \qquad (14\text{-}11)$$

where

α = road slope angle, deg

The results of Eq. 14-11 obtained for vehicle 6 in the empty condition are illustrated in Fig. 14-8 with the road slope angle α expressed in terms of road gradient G. Inspection of Fig. 14-8 indicates that a deceleration of 0.20g on an 11% slope requires a tire-road friction coefficient of approximately 0.75.

The braking effectiveness or deceleration due to the emergency brake may be obtained by

$$a = F_x/W \text{ , g-units} \qquad (14\text{-}12)$$

where

F_x = braking force, lb (determined by Eq. 5-36)

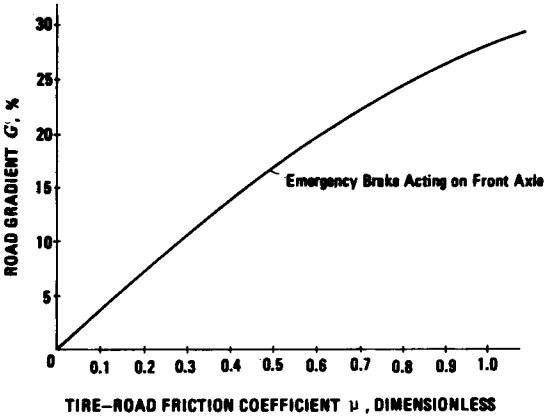

Figure 14-7. Road Gradient on Which Vehicle No. 3 Can Be Held Stationary

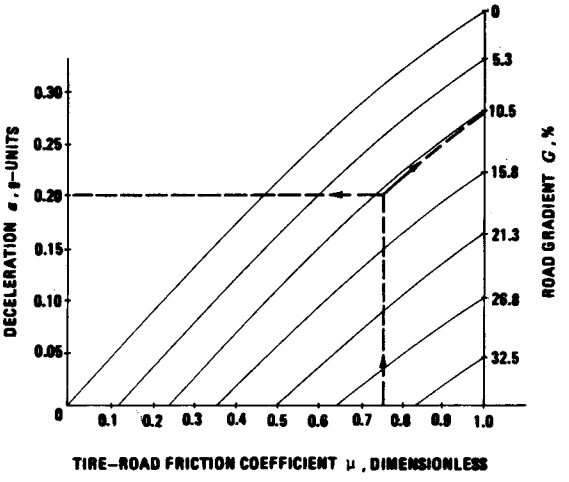

Figure 14-8. Downhill Emergency Braking Capability of Vehicle No. 6

The gain ρ_B of the emergency brake determined by Eq. 5-35 is equal to 3.1; the mechanical efficiency η_H is assumed to be equal to 0.7. Based on these data and a displacement gain ρ_H = 5.6, the braked wheels of vehicle 6 produce a braking force of (Eq. 5-36)

$$F_x = 90 \times 5.6 \times 3.1 \times 0.7 \times 4.35 \times 5/12.8$$
$$= 1858 \text{ lb}$$

The deceleration is a = 1858/7200 = 0.258 on a level roadway.

The emergency brake analysis results in two designs: for vehicles 1 through 3 front axle location, for vehicles 4 through 6 rear axle location of the emergency brake is used. The reasons for this solution follow. Inspection of Figs. 14-3 and 14-4 indicates that a front axle location of the emergency brake yields larger decelerations for the empty and loaded condition of vehicles 1 and 3. A rear axle location of the emergency brake would yield unnecessarily low decelerations for vehicles 1 through 3. Inspection of Fig. 14-7 indicates that a tire-road friction coefficient of 0.8 yields a slope holding of G equal to approximately 0.23 for a front axle location of the emergency brake. If this value is considered low, vehicle slope holding capacity may be increased by use of the transmission pawl or engine friction, provided the rear wheels are the driven wheels. If retardation due to pawl or engine friction is not permissible, the emergency brakes of vehicles 1 through 3 must be located on the rear axle. However, the level road wheels unlocked deceleration of vehicle 1 in the empty condition is then less than 0.25g. An inspection of Figs. 14-5 and 14-6 indicates similar or better braking performance with an emergency brake located on the rear axle for vehicles 4 through 6 as compared to a front axle location.

14-6.2 DYNAMIC BRAKE FORCES

An optimum distribution of the brake forces among the axles is obtained by bringing the actual brake forces close to the dynamic brake forces over a wide range of loading and roadway conditions. The condition expressed by Eq. 8-14 may be used to obtain a range of values for the brake force distribution ϕ that may be used for design evaluation. Substitution of the data for vehicle 1 for a minimum braking efficiency of 0.75 yields the following upper and lower limits on the brake force distribution:

$0.132 \leq \phi \leq 0.465$, μ = 0.2, empty
$0.0 \leq \phi \leq 0.290$, μ = 0.8, empty
$0.324 \leq \phi \leq 0.657$, μ = 0.2, loaded
$0.113 \leq \phi \leq 0.446$, μ = 0.8, loaded

where

ϕ = rear axle brake force divided by total brake force, d'less

Inspection of these values indicates that a braking efficiency of 0.75 requires a brake force distribution of 0.29 or less for the empty loading condition when braking on a road surface having a tire-road friction coefficient of 0.8. Similarly, when braking on a low friction road surface in the loaded condition the brake force distribution should not be less than 0.324. It is apparent that the actual brake force distribution must assume a value between 0.29 and 0.324 since this would satisfy the remaining requirements.

Application of Eq. 8-14 to vehicles 2 and 3 produced similar brake force distribution data. The actual brake force distribution chosen for vehicles 1 through 3 is ϕ = 0.324.

A graphical representation of the normalized dynamic brake forces computed by Eqs. 8-3 and 8-4 and the actual brake force distribution is shown in Figs. 14-9 and 14-10 for vehicles 1 and 3, respectively. Inspection of Figs. 14-9 and 14-10 indicates that the line of actual brake force intercepts with the dynamic brake force for the empty case at a approximately equal to 0.25g. This condition indicates overbraking of the rear axle for decelerations greater than 0.25g (also see Fig. 8-3). Conversely, lockup of

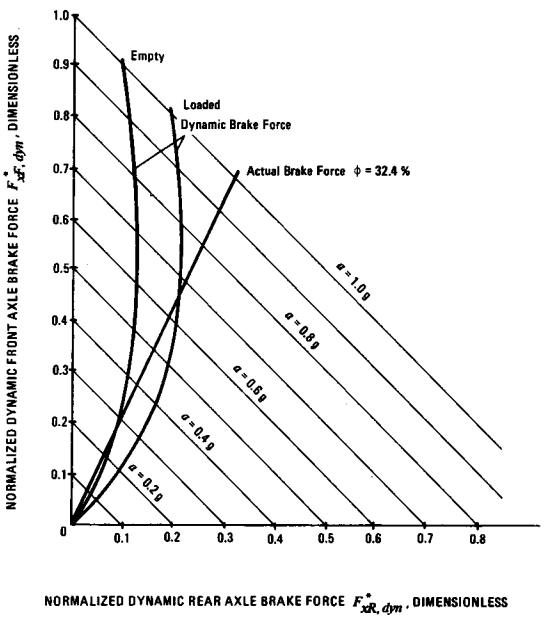

Figure 14-9. Normalized Dynamic and Actual Brake Forces, Vehicle No. 1

the rear wheels before the front wheels is avoided for decelerations less than 0.25g. This lockup condition is designed into the vehicle-braking system to decrease the danger of premature rear wheel lockup and hence decrease the probability of loss of directional braking stability for the empty case.

The brake force distribution for vehicles 4 through 6 may be obtained in a similar manner. The actual brake force distribution chosen for the heavier vehicles is $\phi = 0.42$. The graphical representation of dynamic and actual brake forces for vehicles 4 through 6 is illustrated in Figs. 14-11 and 14-12, respectively.

14-6.3 BRAKING EFFICIENCY

The braking efficiency is defined as the ratio of wheels unlocked deceleration to existing tire-road friction coefficient. With the design brake force distribution established, braking efficiency may be obtained by Eqs. 8-10 and 8-11. The results are presented in Figs. 14-13 and 14-14 for vehicles 1 and 3, respectively. Inspection of Fig. 14-14 indicates a braking efficiency of approximately 0.70 for the empty case and $\mu = 0.8$. It is apparent that a brake force distribution $\phi = 0.324$ is too large to produce a braking efficiency of 0.75. As the previous analysis

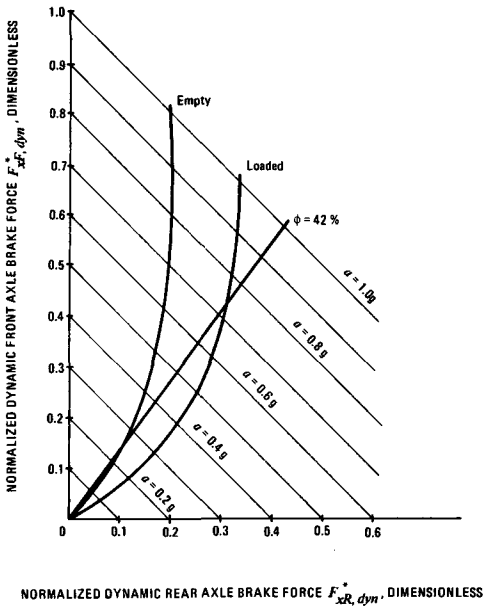

Figure 14-11. Normalized Dynamic and Actual Brake Forces, Vehicle No. 4

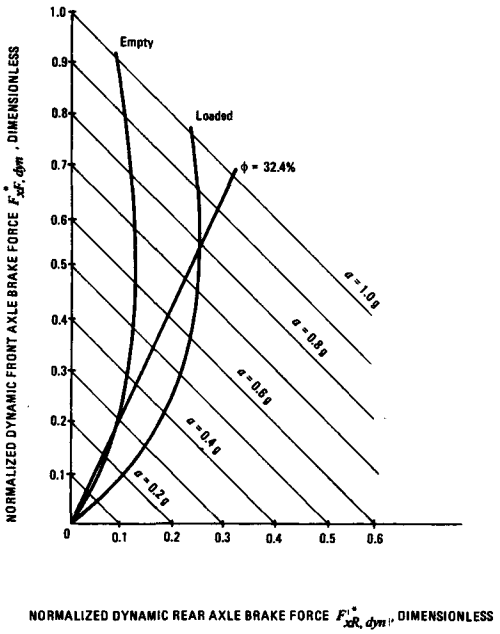

Figure 14-10. Normalized Dynamic and Actual Brake Forces, Vehicle No. 3

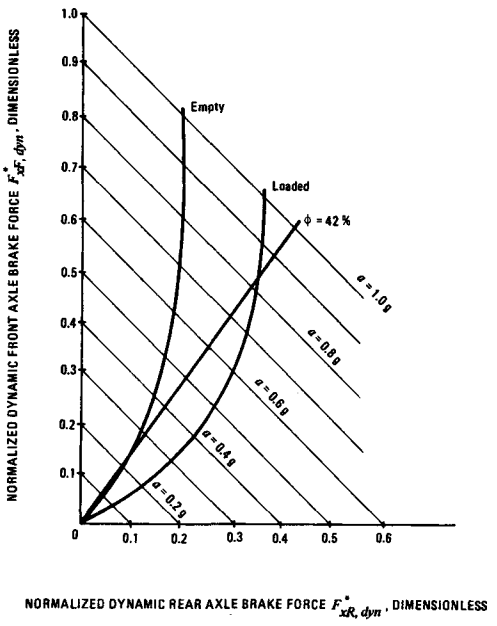

Figure 14-12. Normalized Dynamic and Actual Brake Forces, Vehicle No. 6

showed, the ϕ-value for the empty vehicle must be less than 0.29 to yield a braking efficiency of 0.75. A braking efficiency larger than 0.70 can be obtained by reducing the brake force distribution to a level below 0.324. Inspection of Fig. 14-14 indicates a braking efficiency of vehicle 3 of 0.65 associated with the loaded case and the low friction road surface. Lower levels of brake force distribution — as desired for vehicle 1 — would have increased the brake force concentrated on the front axle and hence would have further decreased the braking efficiency of vehicle 3 on the low friction surface due to premature front wheel lock-up. The variation of braking efficiency as a function of brake force distribution for the loaded vehicle 1 for dry road surfaces (μ = 0.8) is illustrated in Fig. 14-15. The curves are obtained by Eqs. 8-10 and 8-11. Inspection of Fig. 14-15 indicates that a ϕ-value of 0.26 yields a braking efficiency of unity. A ϕ-value of 0.113 (par. 14-5.2) yields a braking efficiency of 0.75 (with the front axle limiting any further increase in braking efficiency) and a ϕ-value of 0.446 yields a braking efficiency of 0.75 (with the rear axle limiting any further increase in braking efficiency). The same conditions had been obtained previously by the application of Eq. 8-14. As Fig. 14-15 shows, values of ϕ less than 0.26 concentrate too much brake force on the front axle and cause a decrease in braking efficiency of vehicle 1. Since the normalized geometrical and loading data of vehicles 1 and 3 (for the loaded case) are not much different (Table 14-7), similar conditions exist for vehicle 3.

The braking efficiencies computed for vehicles 4 and 6 are illustrated in Fig. 14-16. The minimum

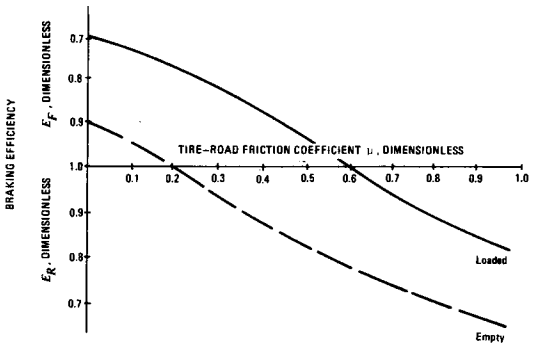

Figure 14-13. Braking Efficiency, Vehicle No. 1

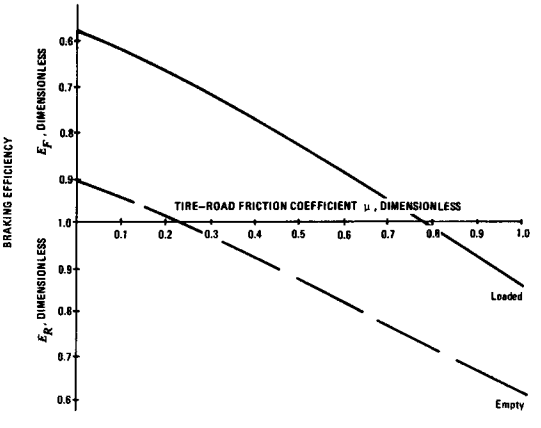

Figure 14-14. Braking Efficiency, Vehicle No. 3

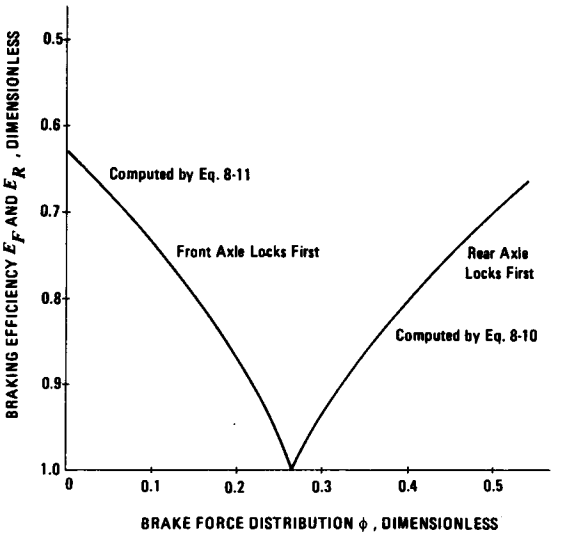

Figure 14-15. Braking Efficiency of Loaded Vehicle 1 as a Function of Brake Force Distribution ϕ for a Tire-Road Friction Coefficient of 0.8

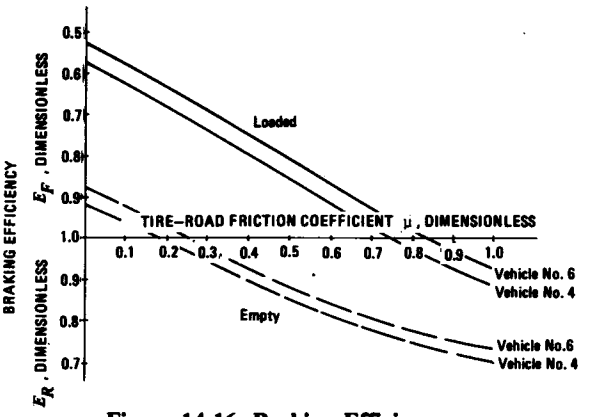

Figure 14-16. Braking Efficiency, Vehicles No. 4 and 6

values of braking efficiency are associated with the loaded cases and a low friction road surface.

14-6.4 BRAKING PERFORMANCE DIAGRAM

The braking performance of the brake system for vehicles 3 and 6 is illustrated in Figs. 14-17 and 14-18, respectively. The pedal force/brake line pressure relationship is obtained by Eq. 5-1. Typical value of mechanical efficiency η_p of the pedal is 0.80. Eq. 5-11 is used to determine the relationship between brake line pressure and deceleration. A typical value of wheel cylinder efficiency η_c is 0.96. Generally, the determination of brake system component size is obtained by a trial and error solution. Since both pedal force/deceleration relationships and safety requirements such as expressed by Eq. 14-4 must be met, the selection of component size may involve several iterations before a braking performance diagram can be constructed that satisfies pedal force, deceleration, and friction utilization requirements. Generally, the procedure that follows may be used for determining component size:

1. Determine an approximate master cylinder diameter and stroke from Eq. 5-17 for a maximum brake line pressure of 1500 psi.

2. Determine the brake line pressure for a given pedal force from Eq. 5-1.

3. Pick wheel cylinder sizes for front and rear brakes and check brake fluid volume requirement by means of Eq. 5-12 under consideration of Eq. 14-4. Use a volume loss v = 10-30%.

4. Compute deceleration from Eq. 5-11 with brake line pressure obtained in step 2.

5. Compute tire-road friction coefficient as function of deceleration by Eqs. 8-8 and 8-9.

The tire-road friction utilization of the rear and front axle are computed by Eqs. 8-8 and 8-9, respectively, and are illustrated in Figs. 14-17 and 14-18. Inspection of Fig. 14-18 indicates that for the fully loaded vehicle 6 a pedal force of 125 lb produces a brake line pressure of approximately 1260 psi, resulting in a deceleration of 0.61g. A deceleration of 0.61 requires a tire-road friction coefficient of 0.74 or more to prevent front wheel lockup in the loaded case, or 0.90 or more to prevent rear wheel lockup in the empty case. Also, inspection of Figs. 14-17 and 14-18 indicates nearly identical relationships between brake line pressure and deceleration in spite of the different wheel cylinder sizes for the light and heavy vehicles in the loaded condition. The reason for this is that the ratio of wheel cylinder area to vehicle weight of vehicles 3 and 6 is nearly identical.

14-6.5 BRAKE FLUID VOLUME ANALYSIS

The master cylinder volume V_{MC} may be determined by Eqs. 5-12 and 14-4. The wheel cylinder piston displacement required for an adequate braking operation is determined by Eq. 14-4 as 0.174 in. A

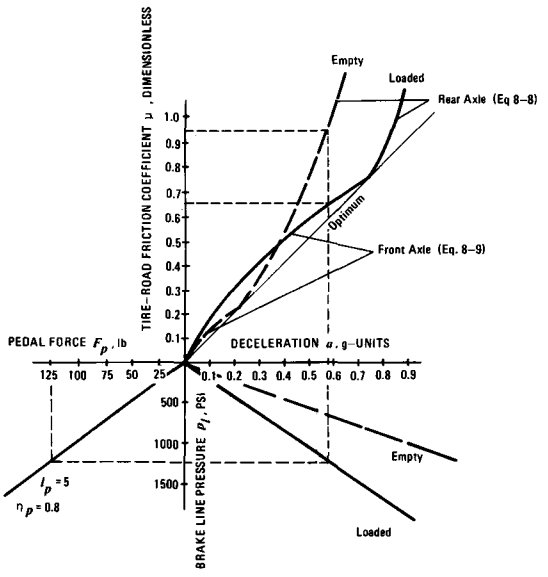

Figure 14-17. Braking Performance Diagram, Vehicle No. 3

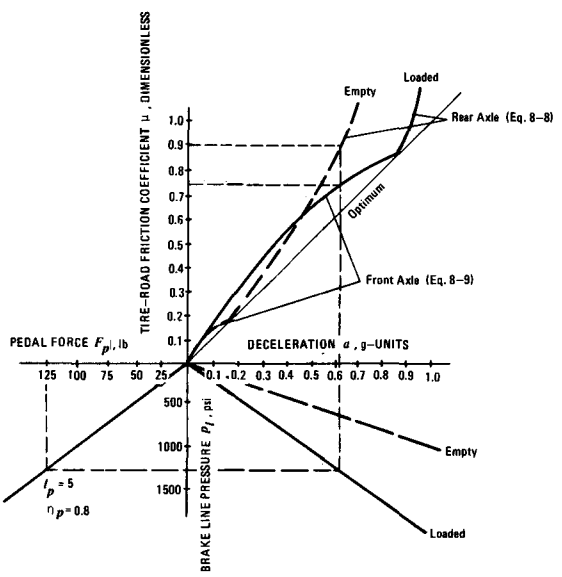

Figure 14-18. Braking Performance Diagram, Vehicle No. 6

value as low as 0.14 in. may be accepted if automatic brake shoe adjustment is provided. With the vehicle 3 wheel cylinder data of Table 14-8, d = 0.14 in. and v = 11% — the volume required by the master cylinder to overcome hose expansion — Eq. 5-12 yields a master cylinder volume of 0.45 in.^{3} The maximum volume delivered by a master cylinder having a bore of 11/16 in. and a stroke of 1-21/32 in. is 0.615 in.^{3} which indicates sufficient size. For vehicle 6, the wheel cylinder areas are larger than those of vehicle 3. The required master cylinder volume determined by Eq. 5-12 is 0.613 in.^{3} Since the required volume is less than the volume produced by the master cylinder, i.e., 0.613 < 0.615, the proposed master cylinder is adequate for vehicles 1 through 3 and vehicles 4 through 6. If the wheel cylinder piston travel of 0.14 in. is considered too small, the stroke of the master cylinder piston must be increased. However, such a change would require increased pedal travels.

A final check on the brake shoe displacement associated with the emergency brake must be carried out. The displacement gain ρ_B = 3.1 was determined from detailed geometrical data by use of Eq. 5-35. Upon substituting the appropriate brake system data into Eq. 5-37, a shoe displacement of d equal to 0.46 in. is obtained. The brake shoe displacement provided by the emergency brake exceeds that produced by the service brake, indicating an adequate emergency braking capacity in the event of a service brake failure caused by excessive wheel cylinder piston travel due to lining wear or drum distortion. Under these conditions the emergency brake is still capable of applying the brake shoes when the service brake fails.

14-6.6 SPECIFIC DESIGN MEASURES

The specific design measures obtained by Eqs. 14-1 through 14-3 are shown in Table 14-8. Inspection of the values indicates that the actual measures are below maximum allowable values.

14-7 DESIGN OF TRUCK PROPORTIONAL BRAKE SYSTEM

The objective is the design of a truck brake system for either drum or disc brakes. The brake system is to be designed for fixed ratio and variable ratio braking. The geometrical and loading data are presented in Table 14-9. The maximum pedal force is 100 lb for a deceleration of 0.75g. The maximum pedal travel is 5 in. The rim size permits 13-in. diameter drums to be installed. Two-leading shoe drum brakes with a brake force of 4.15 are to be used. The brake factor of the disc brake is 0.8; the effective disc radius is 4.75 in.

14-7.1 FIXED RATION BRAKING — DRUM BRAKES

The normalized dynamic brake force front and rear are computed by Eqs. 8-3 and 8-4 and are illustrated in Fig. 14-19 for the empty and loaded case. The use of Eq. 8-14 for the empty and loaded cases and low and high tire-road friction coefficients with a value of the minimum braking efficiency of 0.75 resulted in the ϕ-range that follows.

$0.289 \leq \phi \leq 0.623$, μ = 0.2, empty
$0.157 \leq \phi \leq 0.491$, μ = 0.8, empty
$0.538 \leq \phi \leq 0.871$, μ = 0.2, loaded
$0.352 \leq \phi \leq 0.685$, μ = 0.8, loaded

Inspection of the ϕ-values indicates that a ϕ-value greater than 0.491 and smaller than 0.538 would best

TABLE 14-9
GEOMETRICAL AND LOADING DATA

Empty	Loaded
W_o = 3500 lb	W = 8000 lb
ψ_o = 0.50	ψ = 0.70
χ_o = 0.22	χ = 0.31
Tire Radius	R = 15.2 in.

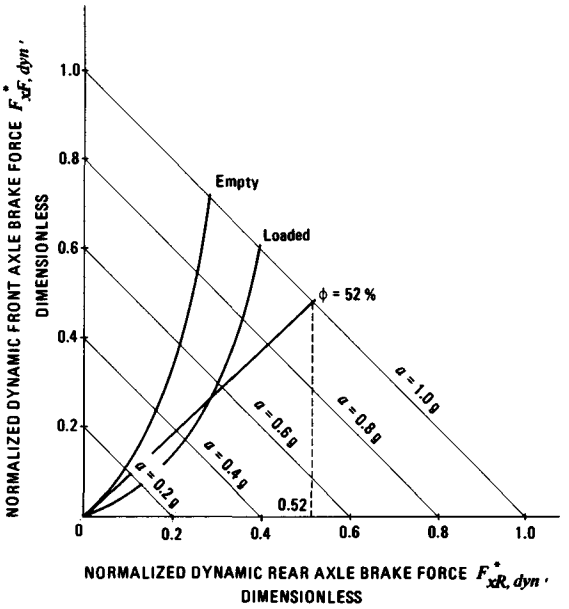

Figure 14-19. Normalized Dynamic and Actual Brake Forces

satisfy the requirements. A value $\phi = 0.52$ is chosen. The maximum wheels unlocked decelerations may now be determined by Eqs. 8-8 and 8-9. For a dry road surface with $\mu = 0.8$ the empty case presents the limiting condition for maximum wheels unlocked deceleration. The use of Eq. 8-8 yields a deceleration of 0.575g prior to rear wheel lockup. For a low friction road surface the loaded case is the limiting condition. Eq. 8-9 yields a deceleration of 0.144g prior to front wheel lockup. The braking efficiencies as a function of tire-road friction coefficient are computed as Eqs. 8-10 and 8-11 and are illustrated in Fig. 14-20. Inspection of Fig. 14-20 indicates a braking efficiency of 0.72 for a tire-road friction coefficient of 0.8 and 0.2.

The piston area of the wheel cylinder can now be determined from Eq. 8-7 in a trial and error approach. Upon assuming a front wheel cylinder diameter of 13/16 in., the rear wheel cylinder area becomes

$$A_{WC,R} = \frac{\phi A_{WC,F}}{1 - \phi} = \frac{(0.52)(0.518)}{0.48} = 0.562 \text{ in.}^2$$

Thus, the rear wheel cylinder diameter is 27/32 in. The master cylinder volume may be obtained by Eq. 5-12 as 0.572 in.^{3} A volume loss $v = 0.05$ in.^{3} and a minimum wheel cylinder piston travel of 0.126 in. are used. A master cylinder piston area of 0.375 in.^{2} and an effective master cylinder piston stroke of 1.53 in. satisfy the 0.572 in.^{3} volume requirement. Consequently, a master cylinder having an 11/16 in. diameter and 1.53 in. stroke may be used. The brake line pressure required to decelerate the loaded vehicle at 0.75g obtained by Eq. 5-11 is 1630 psi. A wheel cylinder efficiency of 0.96 is used. The pedal force required to produce a brake line pressure of 1630 psi computed by Eq. 5-1 is equal to 234 lb. A pedal ratio of 5/1.53 = 3.27 and a pedal efficiency of 0.8 are used. A pedal force of 234 lb is greater than the maximum allowable pedal force. It becomes necessary to install a vacuum assist unit to reduce pedal force. By the use of the booster design chart (Fig. 5-5) the pedal force required for a 0.75g stop is reduced to approximately 75 lb. The assist unit cylinder diameter is 7 in. with a relative vacuum of 0.8, i.e., 80% of the ambient pressure is used for the assist effort. The assist characteristic is equal to approximately 2.5.

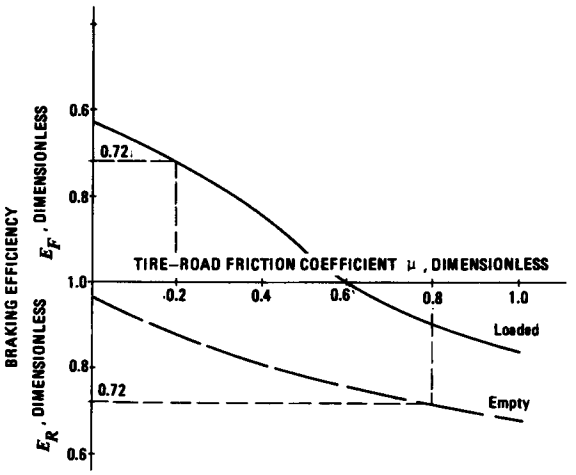

Figure 14-20. Braking Efficiency for Fixed Ratio Braking, $\phi = 0.52$

14-7.2 FIXED RATIO BRAKING — DISC BRAKES

The basic parameters such as maximum pedal force requirement, and pedal travel remain unchanged. The sizes of the wheel cylinders are again obtained by Eq. 8-7. Generally, several trial and error runs must be made before a final wheel cylinder can be selected. For a front wheel cylinder diameter of 2-1/4 in., Eq. 8-7 yields a rear wheel cylinder diameter of 2-11/32 in.

The master cylinder volume as determined by Eq. 5-12 is 0.869 in.^{3} for a wheel cylinder piston travel of 0.025 in. The master cylinder diameter is 13/16 in. for a master cylinder piston stroke of 1.6 in. The fluid volume delivered by the master cylinder is 0.829 in.^{3} and hence is slightly less than that required for a wheel cylinder piston displacement of 0.025 in. For common disc brakes with automatic adjustment, the master cylinder size yielding a slightly lower fluid volume is acceptable. The brake line pressure required for a 0.75g deceleration of the loaded vehicle is 1507 psi as determined by Eq. 5-11. A pedal force of 313 lb is computed by Eq. 5-1. A pedal lever ratio of 3.12 is used as determined by the ratio of pedal travel to master cylinder piston stroke (5/1.6 = 3.12). By the use of the vacuum booster design chart (Fig. 5-5) a pedal force of 80 lb is obtained for a vacuum booster diameter of 8.5 in., a relative vacuum of 0.8, and a booster characteristic of 3.0.

14-7.3 VARIABLE RATIO BRAKING — DRUM BRAKES

Examination of the braking efficiency curves of Fig. 14-20 indicates that the braking efficiencies for the empty vehicle are always less than 80% for medium to high friction road surfaces. The rear axle of the empty vehicle tends to overbrake for all road

conditions increasing the danger of vehicle skid and loss of directional stability during braking.

A variable ratio distribution is shown in Fig. 14-21. The bilinear distribution may be obtained from Eqs. 9-5 and 9-6 for a specified minimum value of braking efficiency or various C-values by trial and error solution. In a graphical procedure, a variable brake force distribution line may be drawn in the normalized dynamic brake force diagram such that the actual and dynamic brake force are as close as possible over a wide range of deceleration values as illustrated in Fig. 14-21. The empty and loaded vehicle braking efficiencies for the condition represented by Fig. 14-21 obtained by Eqs. 9-1 to 9-4 are illustrated in Fig. 14-22. The braking efficiencies associated with the variable brake force distribution are always greater than 85% for most loading and roadway conditions. A comparison of the curves of Figs. 14-20 and 14-22 demonstrates clearly the significant improvement in braking performance resulting from proportioning valves, especially for vehicles having a large change in center of gravity location caused by loading.

The wheel cylinder diameters for the base line distribution ϕ = 62% may be obtained by means of the same procedures used in the fixed ratio braking-drum brake analysis. The results are a 13/16 in. diameter wheel cylinder on the front axle and a 1-1/32 in. diameter wheel cylinder on the rear axle.

With the wheel cylinder sizes established, the dynamic brake line pressures may be obtained by Eqs. 9-7 and 9-8. A wheel cylinder efficiency of 0.96 is used in this analysis. The results obtained while neglecting the individual pushout pressures to overcome brake shoe return springs are presented in Fig. 14-23. The pressure ratio P — front to rear — is 2.6 to 1 and the shift point pressure is 430 psi. The shift

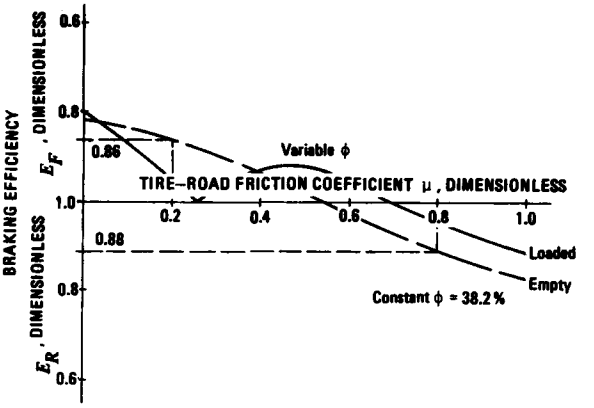

Figure 14-22. Braking Efficiency for Variable Ratio Braking

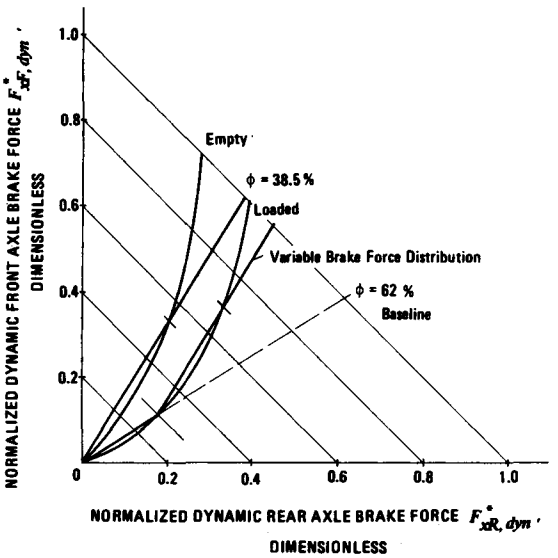

Figure 14-21. Normalized Dynamic and Actual Braking Forces for Variable Ratio Braking

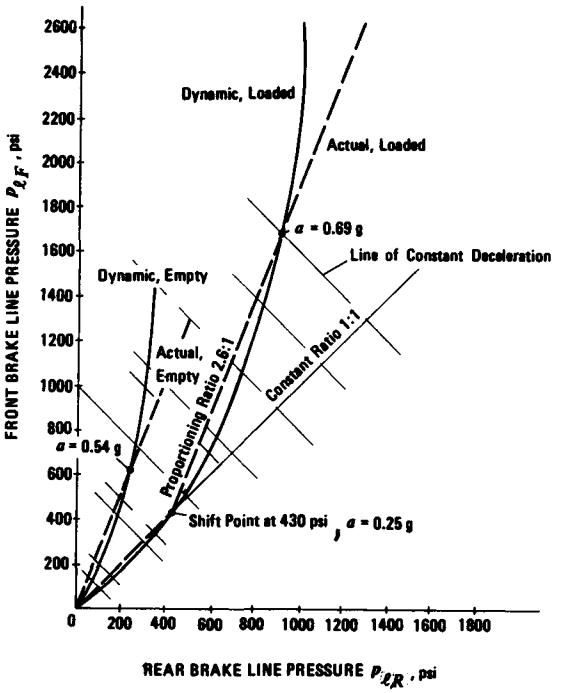

Figure 14-23. Dynamic and Actual Brake Line Pressures

point pressure may be obtained from Eqs. 8-1 and 5-10. If the variable ratio braking system is designed as shown in Fig. 14-23, the braking efficiency curves as presented in Fig. 14-22 are obtained.

The master cylinder volume determined by Eq. 5-12 is 0.72 in.^{3} An effective master cylinder piston stroke of 1.50 in. yields a master cylinder area of 0.48 in.^{2} or a diameter of 13/16 in. The brake line pressure required for a 0.75g deceleration is determined by Eq. 5-10 by trial and error or from Fig. 14-23. The lines in Fig. 14-23 drawn at 45 deg represent lines of constant deceleration. One point is identified as a = 0.69g or approximately 0.7g for the loaded vehicle condition. If the scale between the origin and 0.7g is extended to 0.75g, brake line pressures on the front and rear axle of approximately 1430 and 1000 psi, respectively, are obtained. A pedal force of 258 lb is computed by Eq. 5-1 with a pedal lever ratio of 5/1.5 = 3.33, a mechanical efficiency of 0.8, and a brake line pressure of 1430 psi. By the use of the booster design chart, Fig. 5-5, the pedal force may be reduced to 65 lb when a vacuum booster with a diameter of 8.5 in. and a relative vacuum of 0.8 is used. The booster characteristic is approximately 3.0.

14-7.4 VARIABLE RATIO BRAKING — DISC BRAKES

If the disc brake parameters are chosen in such a manner that the product of $(BF)(A_{wc})(r)$ on the front and rear axle are identical to those of the drum brake system, then the dynamic brake line pressure curves of Fig. 14-23 are applicable directly. Application of this condition results in wheel cylinder areas of 3.68 in.^{2} and 5.92 in.^{2} on the front and rear axle, respectively. The corresponding wheel cylinder diameters are 2-5/32 in. on the front and 2-3/4 in. on the rear wheels. The master cylinder volume as determined by Eq. 5-12 is equal to 0.98 in.^{3}, yielding a master cylinder cross-sectional area of 0.56 in.^{2} for a stroke of 1.75 in. The vacuum assist parameters obtained from Fig. 5-5 are a booster diameter of 10 in. with a relative vacuum of 0.8. The reduced pedal force is approximately 85 lb. The booster design chart shown in Fig. 5-5 must be expanded by an extension of the appropriate lines to determine the booster parameters and pedal force.

A comparison of the sizes of the vacuum assist units for all four braking systems indicates that larger assist units must be provided for vehicles with disc brakes and brake systems using variable ratio braking.

14-8 DESIGN OF TANK DISC BRAKES

The objective is the design check of a disc brake system for a tank. The following vehicle data are specified:

1. Weight 66,000 lb
2. Maximum speed 45 mph
3. Maximum deceleration 0.6g
4. Gear ratio between brake shaft and track drive sprocket 1:11
5. Track drive sprocket radius 16 in.
6. Track rolling resistance coefficient 0.045 for operation on smooth dirt road, 0.075 for operation on off road surface
7. Mass moment of inertia per track 1000 lb·in.·s^2.

The following disc brake data are specified:

1. Brake rotor weight 175 lb (ventilated rotor)
2. Outer brake rotor diameter 22.5 in.
3. Inner brake rotor diameter 12 in.
4. Maximum brake rotor revolutions, 4750 rpm at a vehicle speed of 45 mph.
5. Brake rotor revolutions, 1,825 rpm at 17 mph during continued downhill operation.
6. Effective brake rotor radius 8.5 in. (Eq. 2-22)
7. Number of wheel cylinders per rotor 2
8. Wheel cylinder diameter 2 in.
9. Brake factor 0.50.

14-8.1 MECHANICAL ANALYSIS

The maximum brake force $F_{x,total}$ may be obtained from Eq. 7-4c as

$$F_{x,total} = (66{,}000)(0.6) = 39{,}600 \text{ lb}$$

One track has to produce a braking force of 19,800 lb. Rolling resistance opposes vehicle motion (par. 6-4). Under consideration of the rolling resistance, the braking force per track becomes

$$F_x = 19{,}800 - \frac{(0.045)(66{,}000)}{2} = 18{,}315 \text{ lb}$$

The brake torque T_B at the rotor may be obtained by Eq. 4-2 where

$M_e = T_B, F_{ret} = F_x, R = 16$ in., $\eta = 0.95, \rho = 11$ is used.

$$T_B = \frac{(18315)(16)(0.95)}{(11)(12)} = 2109 \text{ lb·ft} \quad (14\text{-}13)$$

The kinetic energy E_T produced in the effectiveness stop by both rotors may be obtained by Eq. 8-121,

$$E_T = \frac{66{,}000}{(2)(322)}(66)^2 + \frac{(2)(44.36)}{(2)(12)}(497)^2$$

$$= 4{,}464{,}223 + 911{,}052 = 5{,}375{,}275 \text{ ft·lb}$$

The equivalent mass moment of rotational inertia $I_{t,Rotor}$ at the brake rotor was obtained by Eq. 8-118 as

$$I_{t,Rotor} = I_R + \frac{1000}{(11)^2} = 36 + 8.26$$

$$= 44.26 \text{ lb·in·s}^2 \qquad (14\text{-}14)$$

In Eq. 14-14 the track mass moment of inertia of 1000 lb·in·s² and the mass moment of inertia of the brake rotor of 36 lb·in·s², estimated from rotor weight and inner and outer diameter, are used.

The kinetic energy absorbed by the rotor is equal to the kinetic energy of the vehicle minus the work due to rolling resistance. The total rolling resistance work is equal to the product of rolling resistance and stopping distance, giving 335,610 lb·ft when a stopping distance of 113 ft is used. Consequently, the kinetic energy absorbed by one brake rotor becomes 2,519,832 lb·ft.

Use the value of brake torque from Eq. 14-13 in Eq. 5-12 to determine brake line pressure required for an effectiveness stop without consideration of the pushout pressure as

$$p_l - p_o = \frac{(2109)(12)}{(8.5)(0.5)(2)(3.14)(0.92)} = 1031 \text{ psi}$$

The "2" in the denominator indicates that two separate wheel cylinders are used in the caliper, each having a wheel cylinder area of 3.14 in.² A brake factor of 0.50 and a wheel cylinder efficiency of 0.92 are used.

The pad friction area may be obtained from Eq. 14-2. Eq. 14-2 requires the use of Eq. 3-1. The tire slip is replaced by the track slip which is assumed to be zero. Eq. 3-1 yields a braking energy per rotor friction surface of 1,511,722 BTU/h. The minimum pad area A_p per rotor friction surface — determined by Eq. 14-2 with $q''_p = 2300$ hp/ft² and $\phi_i = 1$ — is 37 in.²

The requirement of the secondary brake system is to hold the vehicle on an 80% slope on off-road surfaces. The track rolling resistance coefficient is approximately 0.075.

The braking force per track becomes

$$F_x = (W/2)\sin\alpha - (W/2)(0.075)$$

$$= (33{,}000)(0.625) - 2475 = 18{,}150 \text{ lb} \qquad (14\text{-}15)$$

The brake torque per rotor is

$$T_B = \frac{(18{,}150)(16)(0.95)}{(11)(12)} = 2{,}090 \text{ lb·ft}$$

The hydraulic pressure required for the production of this brake torque is

$$p_l = \frac{(2{,}090)(12)}{(8.5)(0.60)(2)(3.14)(0.92)} = 851 \text{ psi}$$

For the secondary brake a slightly larger brake factor was assumed. The reason for this is the larger static pad-rotor friction coefficient as compared to the smaller sliding value. The secondary system uses the same wheel cylinder and brake pads for the brake force production. The actuation mechanisms are different from those of the service brake.

14-8.2 THERMAL ANALYSIS

The temperature response of the brake during a continued downhill brake operation must be determined for a vehicle speed of 17 mph, 10% slope, and travel distance of 6 mi. The thermal energy to be absorbed and dissipated by one brake rotor may be obtained by Eq. 4-3 as

$$q_o = \frac{(33{,}000)(24.9)(0.10 - 0.045)(3600)}{(778)}$$

$$= 209{,}122 \text{ BTU/h}$$

The time required for the continued braking process is 0.35 h or 1270.6 s.

The heat transfer coefficient of a ventilated rotor may be obtained by Eq. 3-26. The number of cooling vanes n_v may be determined by the approximate relationship

$$n_v = \frac{4\pi D_o}{D_o - D_i}, \text{ d'less} \qquad (14\text{-}16)$$

where

D_o = outer rotor diameter, ft
D_i = inner rotor diameter, ft

Substitution of the rotor data into Eq. 14-16 yields 27 vanes.

The hydraulic diameter d_h is determined by the ratio of four times the cross-sectional flow area of one cooling passage divided by the wetted perimeter of one cooling passage (Fig. 3-3). By the use of a rotor width of 3.5 in., a flange thickness of 0.5 in., and a fin thickness of 0.5 in., d_h is determined as

$$d_h = \frac{(4)(3.768)}{8.014} = 1.88 \text{ in.}$$

The hydraulic diameter is based on the vane dimensions existing at the average rotor diameter, i.e., 17.25 in. The cross-sectional area is determined from the product of vane width and vane circumferential dimension. For the example, the area is given by $(3.5 - 1.0) \times [17.25 \times \pi/(27) - 0.5] = 3.768$ in.^{2} The wetted perimeter is determined from the sum of twice the vane width and twice the circumferential dimension, i.e., $(3.5 - 1.0) \times 2 + [17.25 \times \pi/(27) - 0.5] \times 2 = 8.01$ in.

The Reynolds number for Eq. 3-26 can be determined from the hydraulic diameter, the density and viscosity of the cooling air, and the average velocity of the cooling air through the vanes. The average velocity may be determined by Eq. 3-28. The inlet velocity is determined by the outer and inner rotor diameter, and the revolutions per minute of the rotor as (Eq. 3-28)

$$V_{in} = (0.052)(1825)[(1.875)^2 - (1)^2]^{1/2}$$
$$= 150.5 \text{ ft/s}$$

The outlet velocity is determined by the inlet velocity and the inlet and outlet areas. By the use of a ratio of inlet area to outlet area of 0.534, the outlet velocity is

$$V_{out} = (150.5)(0.534) = 80.38 \text{ ft/s}$$

The average velocity determined by Eq. 3-28 is 115.45 ft/s.

The convective heat transfer coefficient obtained by Eq. 3-26 is 24.9 BTU/h·°F·ft.^{2} The thermal properties of the air were evaluated at an assumed expected mean temperature of 500°F. The parameters used in Eq. 3-26 are d_h = 1.88 in., l = 5.25 in., Re = 48,069, Pr = 0.683, k_a = 0.0231 BTU/h·°F·ft. The Reynolds number is computed for an air density of 0.0412 lbm/ft^3, air viscosity of 1.89×10^{-5} lbm/ft·s, hydraulic diameter of 0.191 ft, and an average velocity of 115.45 ft/s.

The rotor temperature may be obtained by Eq. 3-21. The rotor surface is 9.67 ft^2, the rotor volume is 0.385 ft^3, the rotor density is 455 lbm/ft^3, the rotor specific heat is 0.10 BTU/lbm·°F, the ambient temperature is 50°F, the duration of the brake application is 0.35 h, and the initial temperature is 50°F. The rotor temperature T is determined as

$$T = \left[50 - \left(50 + \frac{209{,}122}{9.67 \times 24.9}\right)\right] \times \exp\left(-\frac{24.9 \times 9.67 \times 0.35}{455 \times 0.10 \times 0.385}\right) + 50 + \frac{209{,}122}{9.67 \times 24.9}$$

$$= 925°\text{F}$$

Inspection of Fig. 3-4 indicates a heat transfer coefficient due to radiation of approximately 4 BTU/h·°F·ft^2 at a rotor temperature of 925°F. By the use of a total heat transfer coefficient of 28.9 BTU/h·°F·ft^2 in Eq. 3-21, a rotor temperature of 801°F is determined at the end of the downhill brake application. In this analysis, it was assumed that the entire surface area of the rotor contributed to convective and radiative cooling. In order to accomplish the cooling of the swept areas of the rotor, cooling air must be blown against the rotor in addition to the self-ventilating effect of the rotor.

The rotor temperature attained in an effectiveness stop from 45 mph at 0.6g deceleration may be obtained by Eq. 3-15 as

$$T = \frac{(0.52)(3{,}023{,}445)(3.42/3600)^{1/2}}{[(455)(0.10)(28)]^{1/2}} + 50°$$

$$= 1408°\text{F}$$

A stopping time of 3.42 s is determined by dividing vehicle speed by vehicle deceleration. The thermal conductivity of the rotor = 28 BTU/h·°F·ft.

The energy absorbed by one friction surface of one rotor for zero slip is obtained by Eq. 3-1, modified to yield

$$q_o = \frac{(66{,}000)(66)(0.6)(3600)}{(4)(778)} = 3{,}023{,}445 \text{ BTU/h}$$

If engine drag is considered in the braking analysis according to Eqs. 4-1 and 4-2, the braking energy absorbed per rotor friction surface is decreased to approximately 2,437,233 BTU/h. An engine retarding moment M_e = 546 lb·ft is computed by Eq. 4-1 by the use of an engine displacement V_e = 1000 in.^{3} and an average retarding pressure p_m = 84 psi. Eq. 4-2 yields a retarding force F_{ret} at the track of 7678 lb due to engine drag. The retarding force due to the brakes and the engine for a deceleration of 0.6g must be (0.6) × (66,000) = 39,600 lb and, consequently, the brakes are required to produce only 31,922 lb. Hence, the engine retarding effect reduces the braking energy absorbed by one rotor friction surface to approximately 2,437,233 BTU/h. Based on this reduced braking energy a brake rotor temperature of approximately 1145°F is determined by Eq. 3-15.

14-9 TEMPERATURE ANALYSIS OF A DRUM BRAKE SYSTEM

The objective is the temperature analysis of a bus operating in city traffic. The following data are available:

1. Vehicle weight 26,220 lb
2. Leading-trailing shoe front brakes
   a. 16.5 in. diameter
   b. 4 in. wide
   c. Brake chamber area 20 in.^{2}
   d. Semi-metallic linings
   e. Slack adjuster length 5 in.
3. Leading-trailing shoe rear brakes
   a. 16.5 in. diameter
   b. 8 in. wide
   c. Brake chamber area 30 in.^{2}
   d. Semi-metallic linings
   e. Slack adjuster length 6.5 in.
4. Cycle
   a. 5.5 s braking
   b. 17.6 s acceleration
   c. 4.8 s constant speed.

After 19 cycles the brakes began to fade on a 7% downhill grade after 29 s of operation on the downhill grade.

The temperature of the brake drum after the 19th stop may be obtained by Eq. 3-20. The paragraphs that follow present the details. The average braking energy of the vehicle is determined by Eq. 3-1 as

$$q_o = \frac{(1-0.05)(26{,}220)(44.1)(0.25)(3600)}{(2)(778)}$$

$$= 635{,}372 \text{ BTU/h}$$

A speed of 44.1 ft/s, tire slip of 0.05, and a deceleration of 0.25 are assumed.

The brake drum data follow: volume 0.28 ft^3, cooling area 4 ft^2, density 455 lbm/ft^3, and specific heat 0.11 BTU/lbm·°F. The temperature increase of a rear drum per cycle may be determined by Eq. 3-16 modified to represent one rear brake (multiply by ϕ and divide by 2) as

$$\Delta T = \frac{(635{,}372)(5.5/3600)(0.66)}{(455)(0.11)(0.28)(2)} = 22.9 \text{ deg F}$$

A braking time t_s = 5.5 s is used.

A brake force distribution of 0.66 was determined by Eq. 8-7 with identical brake factors assumed to exist on front and rear brakes. Eq. 8-7 must be modified for air brake systems to yield

$$\phi = \frac{(30)(6.5)}{(20)(5)+(30)(6.5)} = 0.66, \text{ d'less}$$

The brake chamber areas of 20 in.^{2} front and 30 in.^{2} rear, and the slack adjuster lengths 5 in. front and 6.5 in. rear, are used in computation of brake force distribution.

A convective heat transfer coefficient for the rear brakes may be determined by Eq. 3-31 as

$$h_R = 0.92 + (0.30)(44.1)\,e^{-(44.1/328)}$$

$$= 12.49 \text{ BTU/h·°F·ft}^2$$

The brake drum temperature after the 19th cycle may now be determined for a cycle time of 27.9 s and an ambient temperature of 60°F by Eq. 3-20 as

$$T - 60 = 22.9 \left\langle 1-\exp\left\{-(27.9/3600) \times [(19)(12.49)(4)]\,[(455)(0.11)(0.28)]^{-1}\right\}\right\rangle \times \left\langle 1-\exp\left\{-(27.9/3600)[(12.49)(4)] \times [(455)(0.11)(0.28)]^{-1}\right\}\right\rangle^{-1}$$

$$T = 403 \text{ deg F}$$

The energy to be absorbed by one rear brake during the downhill brake application is determined by Eq. 4-3 modified for one rear brake as

$$q_o = \frac{(26{,}220)(22)(0.07-0.01)(3600)(0.66)}{(778)(2)}$$

$$= 52{,}850 \text{ BTU/h}$$

A rolling resistance coefficient of 0.01 and a downhill speed of 15 mph (22 ft/s) are used in the analysis.

The rear brake drum temperature at the end of the downhill brake application may be determined by Eq. 3-21 as

$$T = \left\{403 - \left[60 + \frac{52{,}850}{(4)(12.49)}\right]\right\} \times \exp\left\{-\left(\frac{29}{3600}\right)\left[\frac{(12.49)(4)}{(455)(0.11)(0.28)}\right]\right\} + 60 + \frac{52{,}850}{(4)(12.49)}$$

$$= 423°F$$

14-10 DESIGN OF FULL POWER HYDRAULIC BRAKES FOR HEAVY TRUCK

The objective is the design of a full power hydraulic brake system for the tandem axle truck having the geometrical and loading data specified in Table 8-1. The accumulator design chart (Fig. 5-9) is to be used for component selection. An optimum brake force distribution front to rear of 0.33, 0.28, and 0.39 is to be used resulting in a tire-road friction utilization as illustrated in Fig. 8-26. A gas-charged accumulator capable of five successive stops is to be used.

14-10.1 DETERMINATION OF WHEEL CYLINDER AREAS

The wheel cylinder sizes are necessary to determine the master cylinder volume, a parameter required in the accumulator design chart.

The brake force produced by the front axle in 0.7g deceleration may be determined as

$$F_{xF} = (0.33)(46{,}000)(0.7) = 10.626 \text{ lb}$$

where 0.33 is used to compute the front axle portion of the total brake force.

For a drum diameter of 15 in., a typical brake factor BF of 2.9 for a leading-trailing shoe brake, a tire radius of 20.25 in., and a brake line pressure p_l of 1550 psi, Eq. 5-10 yields a front brake wheel cylinder area of 3.48 in.^{2} or 2-3/32 in. diameter. A wheel cylinder efficiency of 0.96 was used. A pushout pressure of 70 psi was assumed in the preceding analysis. By use of the same analysis, the wheel cylinder diameter of the tandem forward axle is 1-7/8 in. using a brake force portion = 0.28, that of the tandem rear axle is 2-3/16 in. using a brake force portion = 0.39.

14-10.2 DETERMINATION OF BOOSTER AND ACCUMULATOR SIZE

The master cylinder volume required for safe operation of the brake system may be obtained by Eq. 5-12 extended to include the third axle. A wheel cylinder piston displacement of 0.13 in. is used in the analysis. The minimum wheel cylinder piston displacement of approximately 0.11 in. may be obtained by Eq. 14-4. Substitution of d = 0.13 in. and the wheel cylinder area data into Eq. 5-12 yields a master cylinder volume of 6.6 in.^{3} A relative volume increase due to hose expansion of 30% was assumed.

The volume ratio V_{Ratio} required for a determination of the accumulator size by the use of Fig. 5-9 can be obtained by Eqs. 5-28 through 5-30. The booster input characteristic IC may be obtained by Eq. 5-28. The dimensions of hydraulic boosters are specified by the manufacturers. Typical ratios of booster piston diameter to push rod diameter range between 1.5 to 2.5 resulting in booster ratios of 2.24-6.25. Similarly, typical values for the pressure ratio are 1-4. Typical volume ratios may assume values between 0.5 and 3.0. For V_{Ratio} = 2.0, the accumulator size of approximately 60 in.^{3} required for safe braking of the vehicle may be obtained from Fig. 5-9. A ratio of gas charge pressure P_G to maximum accumulator pressure P_A of 0.30 was assumed. Since the accumulator design chart in Fig. 5-9 was developed for vehicles lighter than 46,000 lb, the lines must be extended for the solution of this problem. For example, the intercept of V_{MC} = 6.6 in.^{3} with the number of stops equal to 5 line lies below the horizontal axis. Also, the V_{ratio} line equal to 2 must be extended to the left to yield the intercept with the line drawn horizontally through the point found previously (6.6 in.^{3} and 5 stops). Finally, the pressure ratio line of 0.30 must be extended to the left to yield the intercept with a line drawn vertically through the point found last. The accumulator size is obtained at the vertical axis on the right-hand side of the chart. The master cylinder area is determined from the booster and pressure ratios. If a booster ratio of 10 to 1 is assumed, then Eq. 5-30 yields a pressure ratio p = 2.22 for a volume ratio of 2.0. Since the pushrod diameter is specified and normally equal to 0.75 in., the required master cylinder diameter is 1-19/32 in. as determined by Eqs. 5-28 and 5-29. Eq. 5-29 is used to determine the master cylinder bore. In order to meet the volume displacement of 6.6 in.^{3}, a master cylinder piston stroke of 3 in. is required. The booster diameter is 2.37 in. as determined by Eq. 5-28.

CHAPTER 15
BRAKE SYSTEMS AND THEIR COMPONENTS

In this chapter various brake systems and their components are described. The objective is to provide the reader unfamiliar with brake system details with a physical description of various braking systems.

15-1 PEDAL FORCE TRANSMISSION — HYDRAULIC BRAKES

15-1.1 BASIC PRINCIPLES OF HYDRAULIC BRAKES

Hydraulic brakes use the physical principle of equal pressure at all locations. The schematic of this principle is illustrated in Fig. 15-1(A). The piston to the left pressurizes the fluid with a given force. The forces exerted on each of the eight pistons to the right is equal to the force on the left piston since all piston cross sections are identical. However, the stroke of each of the eight pistons is only one-eighth of the stroke at the left piston. The schematic of Fig. 15-1(A) may be changed to that of an actual brake system by replacing the application force of the left piston by the pedal force, the left piston and cylinder by the master cylinder, and the eight pistons and cylinders by the wheel cylinders located in the wheel brakes as illustrated in Fig. 15-1(B). Fig. 15-1(B) represents a single circuit hydraulic brake system.

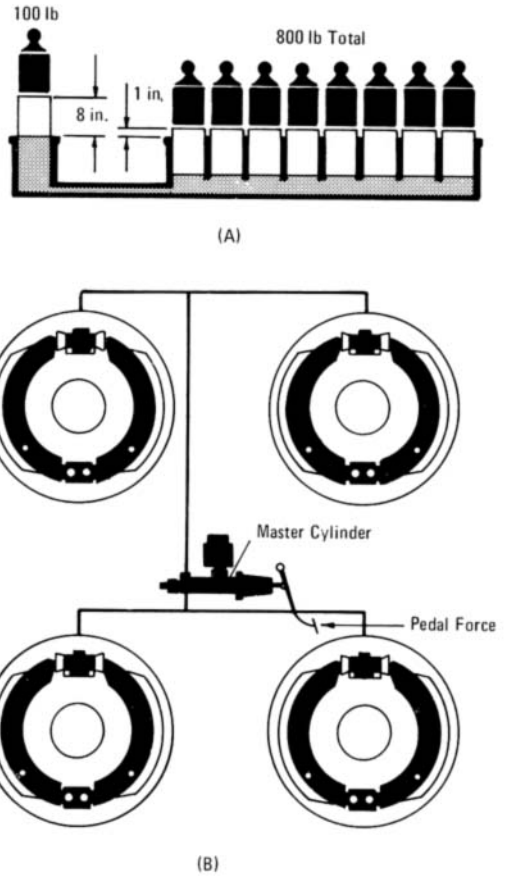

Figure 15-1. Hydraulic Brake System

15-1.2 SINGLE CIRCUIT BRAKE SYSTEM

A single circuit brake system consists of one brake line for pressure transmission between master cylinder and wheel cylinders as illustrated in Fig. 15-1(B). If a brake fluid leak develops at any point of the brake line, the entire service brake fails.

15-1.3 DUAL CIRCUIT BRAKE SYSTEM

A dual brake system consists of two brake circuits that are hydraulically separated. The individual brake systems may be designed to divide the system front to rear, diagonally, or in various other fashions. If a brake fluid leak develops in one circuit, the other circuit still provides emergency stopping capability. A dual brake system is illustrated in Fig. 15-11.

15-1.4 STANDARD MASTER CYLINDER

The master cylinder governs the braking operation. It is controlled by foot application. A master cylinder used for a single circuit brake system is illustrated in Fig. 15-2. The essential elements of any master cylinder are:

1. Reservoir
2. Piston
3. Secondary seal
4. Feed port
5. Compensation port
6. Breather hole
7. Stop-light switch (optional)
8. Primary seal
9. Seal protector
10. Residual-pressure check valve
11. Pressure chamber.

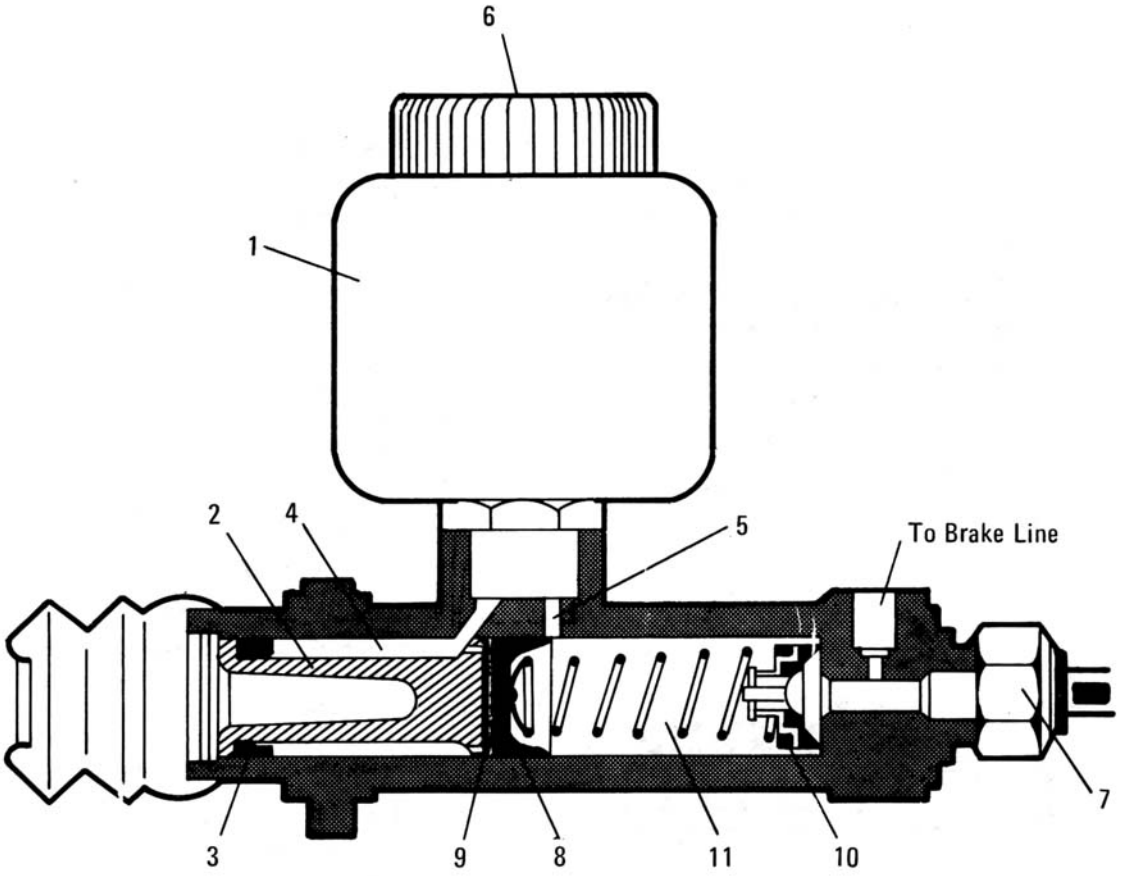

Figure 15-2. Master Cylinder

The functions of a master cylinder are as follows. The master cylinder has a self-regulating fluid supply which ensures that the brake system is always full of brake fluid and that for drum brakes a slight residual pressure remains in the brake lines. The fluid enclosed in the master cylinder, brake lines, and wheel cylinders is constantly subjected to pressure and volume variations. When the brakes are released, the brake system fluid is connected directly to the reservoir by the compensating port. The residual check valve operation is illustrated in Fig. 15-3. The check valve is used in connection with all drum brake systems and provides for a slight pressure (7-20 psi) to remain in the brake system after the brakes are released. The residual pressure keeps the pedal free-travel to a minimum, forces the wheel-cylinder-seal lips lightly against the cylinder bore to avoid entry of air, and enables bleeding of the brake systems by the use of the brake pedal. Disc brake systems must not have residual brake line pressure; otherwise brake pads constantly drag on the brake rotors. The primary seal illustrated in Fig. 15-4 serves three functions. It seals off the pressure chamber, closes off the compensation port, and allows reserve flow of fluid upon releasing the brakes. Behind the primary seal a space is provided which is always full of brake fluid and sealed off by the secondary seal. When the brake pedal is released after a brake application, the fluid in the space behind the primary seal is forced through the holes in the forward flange of the piston and the depressed primary seal into the pressure chamber (Fig. 14-4(B)). Consequently, no air can be drawn into the system due to the return flow of brake fluid past the primary seal and from the reservoir through the feed port. The reservoir is connected to the master cylinder pressure chamber by the compensation port. The reservoir may be an integral part of the master cylinder or connected by a pipe or hose.

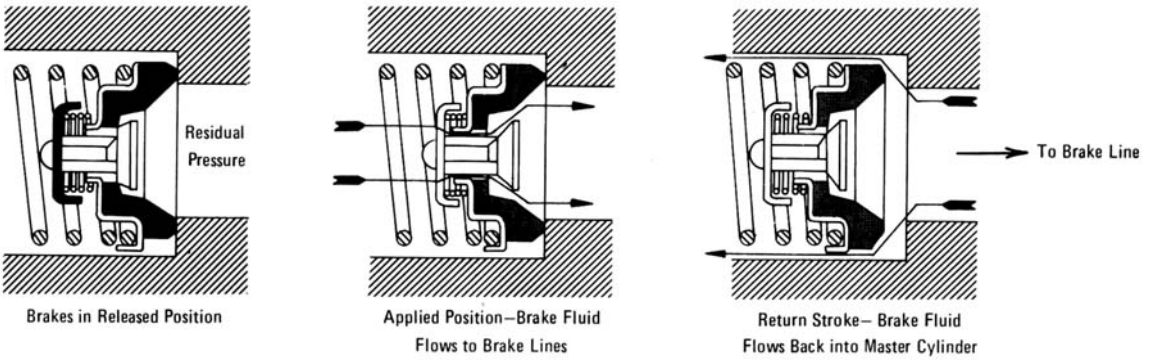

Figure 15-3. Residual-Pressure Check Valve Operation

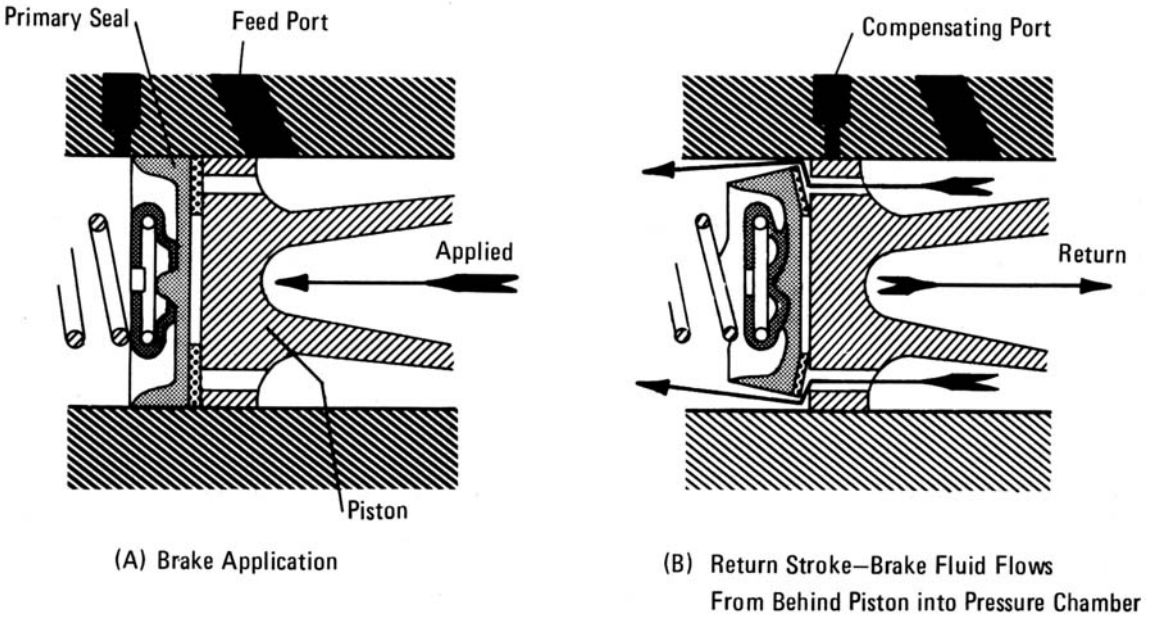

Figure 15-4. Primary Seal Operation

15-1.5 TANDEM MASTER CYLINDER

A typical tandem master cylinder is illustrated in Fig. 12-2. A tandem master cylinder basically consists of two master cylinders, behind one another in a common housing. The operation in principle is the same as a single circuit master cylinder. When the push rod piston is moved toward the floating piston, the compensation port (1 in Fig. 12-2) is closed and the resulting pressure build up in chamber (2) is transmitted by means of the floating piston to chamber (4). The floating piston moves forward and closes off compensation port (5) and the brake line pressure production begins. Details on brake circuit failure are discussed in par. 12-4.1.

15-1.6 STEPPED MASTER CYLINDER

A stepped master cylinder illustrated in Fig. 15-5 functions similar to a tandem master cylinder. The smaller diameter pressure chamber produces higher operating pressures than the larger diameter chamber. Frequently, the smaller diameter chamber is connected to the front disc brakes which require a higher brake line pressure than the rear drum brakes.

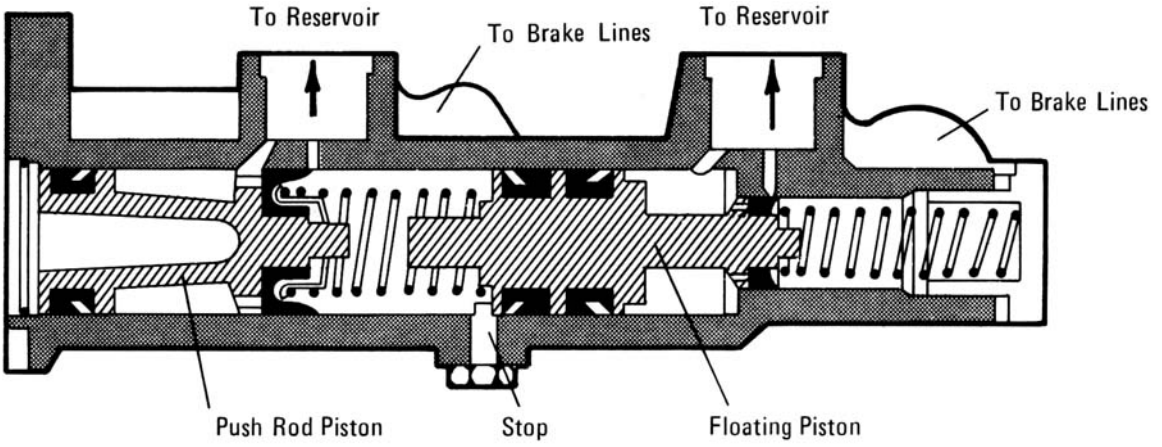

Figure 15-5. Stepped Master Cylinder

15-1.7 STEPPED BORE TANDEM MASTER CYLINDER

A schematic of a stepped bore tandem master cylinder is illustrated in Fig. 12-7. It basically functions like a normal tandem master cylinder. In the event of a brake circuit failure it provides better pedal force/deceleration characteristics than the normal tandem master cylinder. Operation details are explained in par. 12-4.1.

15-2 BRAKE TORQUE PRODUCTION

15-2.1 DRUM BRAKES

15-2.1.1 Basic Brake Shoe Configuration

Basic drum brakes are illustrated in Fig. 2-1. Shown are the leading-trailing shoe brake, two-leading shoe brake, and duo-servo brake. Sliding and pivot abutments are identified. Both eccentric and ratchet type brake shoe adjustments are marked. Although the brakes shown in Fig. 2-1 are of hydraulic brake systems, each of the shoe configurations shown can be used in connection with mechanical brake shoe actuation as in the case of mechanical brakes, and "S" cam and wedge brakes. The configurations of different drum brakes using pivots, parallel abutment, or sliding abutment are illustrated in Fig. 2-1. The shoe configuration of a duo-servo brake where the secondary shoe is supported by a parallel sliding abutment is illustrated in Fig. 2-15. The shoe configuration of a duo-servo brake where the secondary shoe is supported by a pivot is illustrated in Fig. 2-16. A more detailed view of a parallel sliding abutment is illustrated in Fig. 15-9.

15-2.1.2 Wheel Cylinder

The wheel cylinders transmit the hydraulic brake line pressure to the brake shoes. The wheel cylinders are bolted to the back plate and consist of housing, seals, piston or pistons, and tappets which link the pistons with the brake shoe. A single-acting wheel cylinder is illustrated in Fig. 15-6. A retainer spring between seal and housing is used to preload the seal by means of a spreader. A double-acting wheel cylinder is illustrated in Fig. 15-7. Wheel cylinders may be designed to have stepped bore cylinders to produce different brake shoe actuating forces for the same brake line pressure input. Long strong wheel cylinders are used for applications requiring long strokes that cannot be produced by wheel cylinders mounted inside the brake.

15-2.1.3 Wedge Brake

Wedge brakes are, illustrated in Fig. 15-8, used mostly in heavy trucks and trailers in connection with air brake systems. The brake shoe configuration can be either of the leading-trailing or two-leading shoe type. However, the two-leading shoe wedge brake is used most frequently. In a wedge brake the shoe actuation is accomplished by a wedge which is forced between the ends of the brake shoes. The wedge is actuated by an air brake chamber — in the case of an air brake system — or an externally mounted wheel cylinder — in the case of a hydraulic brake system. The entire assembly consists of the air chamber push rod, rollers, and plungers. Rollers are used to reduce friction between wedge surfaces. The air chamber may be operated strictly by air pressure or in a different design by a preloaded spring in the event the air pressure is reduced below a certain level.

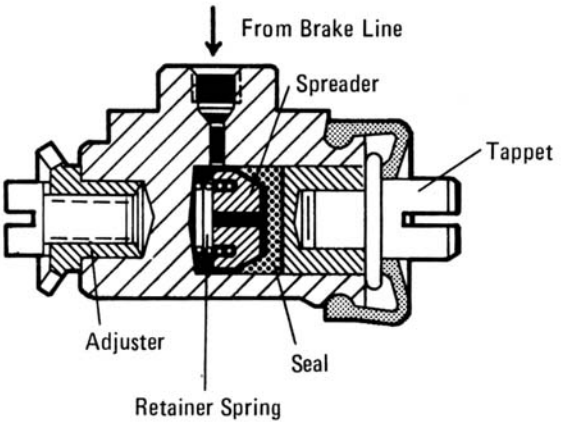

Figure 15-6. Single Acting Wheel Cylinder

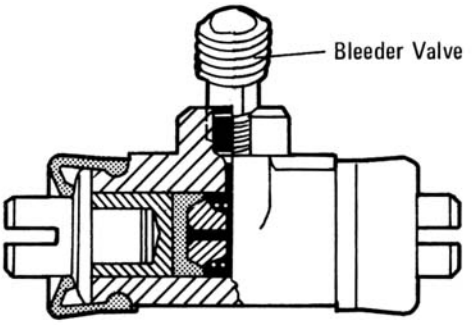

Figure 15-7. Double Acting Wheel Cylinder

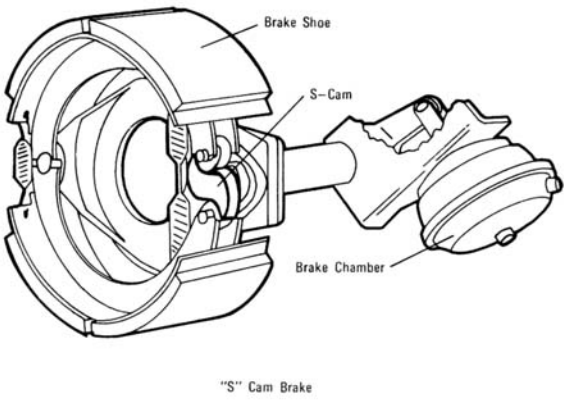

"S" Cam Brake

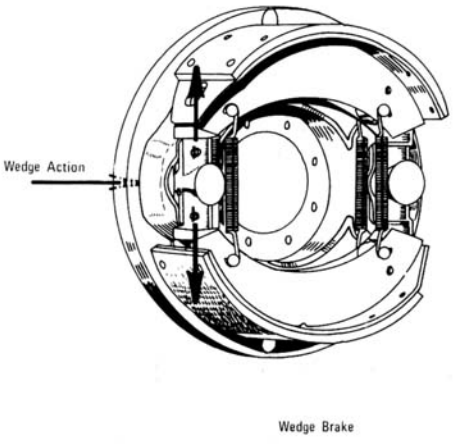

Wedge Brake

Figure 15-8. "S" Cam and Wedge Brake

15-2.1.4 "S" CAM BRAKE

"S" cam brakes are used in heavy trucks and trailers equipped with air brakes. The brake shoe configuration most frequently is of the leading-trailing shoe type as illustrated in Fig. 15-8. A cam — commonly referred to as "S" cam due to its letter "S" shape — is located between the movable ends of the brake shoes. Rollers are installed at each movable end of each brake shoe to reduce friction between cam and shoe. The rotation of the cam is accomplished by a lever arm — commonly referred to as slack adjuster — connected between cam and brake chamber. Although less frequently, different cam geometrics are used.

15-2.1.5 Brake Shoe Adjustment

Brake shoe adjustment is required to compensate for lining wear. Manual adjusters should only be adjusted when the brakes are cold and the parking brake is in the fully released position. Frequently, adjusting mechanisms consist of a screw which is turned in or out to move the position of the tappet relative to the brake shoe (Figs. 15-6 and 15-7). Manual adjusters may be located at the wheel cylinder or at the abutment as illustrated in Fig. 15-9(A). Automatic adjusters most frequently use a mechanism consisting of a threated eye bolt and a split sleeve with corresponding thread fixed to the brake shoe. After initial installation a basic play is provided. If the play increases because of lining wear to the level of basic play plus one thread, the split sleeve will snap into the next thread and thereby reestablishing the basic play (Fig. 15-9(B)). Split sleeve type adjusters may be designed to fit in a wheel cylinder.

Adjustment of "S" cam brakes can be accomplished manually by rotating the slack adjuster on the camshaft to compensate for lining wear. In some

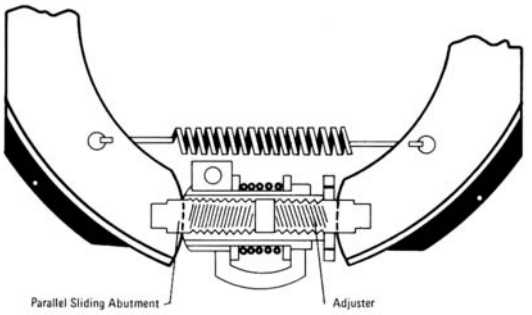

(A) Manual Adjustment

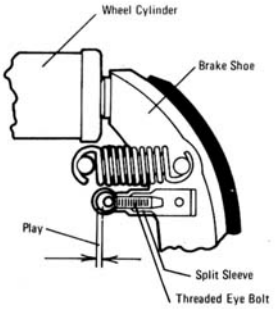

(B) Automatic Adjustment

Figure 15-9. Brake Shoe Adjustment

cases automatic slack adjusters are provided. Wedge brakes generally are equipped with automatic adjusters.

15-2.2 DISC BRAKES

15-2.2.1 Basic Configuration

Disc brakes use calipers which press the brake pads against the brake rotor (Fig. 2-2). Common disc brakes are of the fixed caliper or floating caliper design as illustrated in Fig. 2-3. The floating caliper disc brake is used when space limitations between caliper and rim do not permit the installation of a fixed caliper disc brake. Floating calipers tend to operate at lower temperatures during severe braking with reduced danger of brake fluid vaporization due to a greater exposure of the wheel cylinder to the cooling air stream. In some design applications the brake pad is extended to form a complete circular ring. In this case the pad application and pressing action between rotor and pad ring are accomplished by means of a ball and ramp mechanism as illustrated in Fig. 2-24. The ring section holding the balls is rotated by the actuation force and, consequently, the pads are forced against the rotor friction surfaces. The friction force between the stationary pads and rotating rotors causes a further wedging and hence pressing force produced by the balls. A disc brake of this type exhibits a self-energizing behavior not found in common caliper disc brakes.

The adjustment of caliper disc brakes is always automatic as illustrated in Fig. 2-5.

Disc brake rotors may be solid or self-ventilated. Solid rotors frequently are found on light weight vehicles.

15-2.2.2 Parking Brake

Parking or secondary brake systems have been designed for disc brakes. The actuation is accomplished by forcing the brake pad against the rotor by means of wedges or cams. In designing the system care must be taken that the entire parking brake assembly is as rigid as possible to avoid elastic distortions which reduce the design application force below levels generally required for acceptable parking brake performance. Since hand application force and displacement are limited by human factors, parking disc brakes generally are not found on heavy vehicles because of their low brake factor.

15-3 BRAKE FORCE DISTRIBUTION VALVE

A detailed discussion is presented in par. 9-1.5.

15-4 HYDRAULIC BRAKE LINE

Brake lines transmit the brake line pressure from the master cylinder to the wheel brakes. Brake lines are made of coated steel tubing. The pipe lines are connected by flared end sections and, "T" and other special fittings. Fittings should be mounted as accessible as possible to provide for proper brake system inspection. Pipes should be installed such that protection against grit and stones is maximized. Loops that might trap air must be avoided. Brake lines must be installed such that heat from the exhaust system will not cause fluid overheating and possibly brake fluid vaporization.

Brake hoses are used to connect a movable component of the brake system to the rigid chassis or body unit. Brake hoses must be as short as possible while still providing sufficient length to allow all movement as, e.g., wheel vertical displacement and front wheel steering rotation. Torsional and tensile stress must be excluded in the installation. When undercoatings are applied to the bottom side of the car, extreme care must be taken to protect brake hoses from exposure to sprays and paints.

15-5 VACUUM ASSIST SYSTEMS

The two basic assist units in use in motor vehicles are discussed in par. 5-3. The hydraulically controlled vacuum unit — commonly referred to as hydrovac — is illustrated in Fig. 5-2. A single circuit hydraulic brake system with hydrovac is illustrated in Fig. 15-10. The system uses two master cylinders, one operated by the foot pedal and one directly attached to the hydrovac and controlled by the hydraulic brake line pressure produced by the other master cylinder.

The mechanically controlled vacuum assist unit — commonly referred to as mastervac — is illustrated in Fig. 5-3. A dual circuit hydraulic brake system with mastervac is illustrated in Fig. 15-11. A simple function check of the vacuum assist unit may be conducted in the following manner: with the engine not running apply the brakes several times to deplete vacuum; apply a small pedal force and hold pedal in place; start the engine. If the vacuum assist is functioning properly, the brake pedal will move automatically forward toward the floor board caused by the additional brake line pressure produced by the assist device.

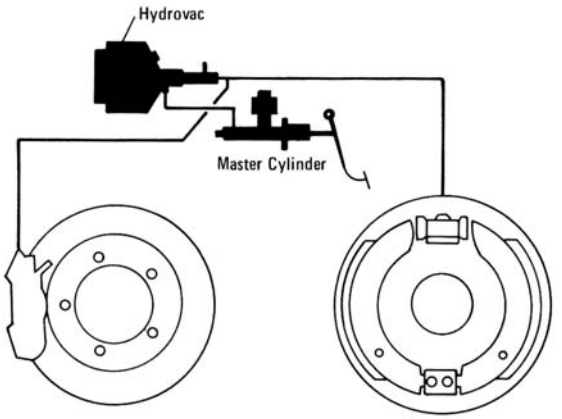

Figure 15-10. Hydrovac Brake System

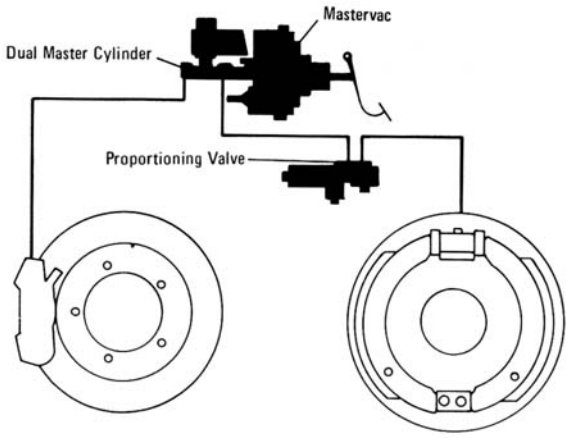

Figure 15-11. Dual Circuit Mastervac Brake System

15-6 COMPRESSED AIR-OVER-HYDRAULIC BRAKE SYSTEM

The fundamentals associated with compressed air-over-hydraulic brake systems are discussed in par. 5-6. Air-over-hydraulic brakes are designed so that in the event of an air pressure failure a manual brake application can be achieved. The schematic of a typical air-over-hydraulic booster unit is illustrated in Fig. 15-12. The released position of the brakes is shown in Fig. 15-12(A). Compressed air is separated from the booster section. Both sides of the diaphragm (1) are exhausted to ambient air and the return spring (2) forces the piston to the far left position. The maximum braking application is illustrated in Fig. 15-12(B). A brake pedal displacement causes the chambers located to the left and right side of the diaphragm (1) to be separated by the small valve (3). Further movement of the brake pedal causes the compressed air to be applied to the diaphragm by opening of the compressed air valve (4). The result is a booster application to the master cylinder. If a medium brake application is desired, the compressed air valve (4) closes and a constant air pressure is applied to the booster piston (5). In the event of a full application the compressed air valve always remains open as illustrated in Fig. 15-12 (B).

15-7 COMPRESSED AIR BRAKES

The air brake system produces compressed air, stores the air, and makes its use possible by converting its energy into mechanical work used to actuate the wheel brakes of the vehicle.

A schematic diagram of a tractor-semitrailer air brake system is illustrated in Fig. 15-13. The compressor (1) takes air from the atmosphere, compresses it, and pumps it into the reservoirs (2) where it is stored for use. The governor, mounted on or near the compressor, controls the compressor so that when maximum reservoir air pressure is obtained no further air is pumped to the reservoir. The reservoir capacity should be no less than 12 times the combined volume of all brake chambers used on the vehicle. Through the compression process, the humidity in the air liquefies and collects in the reservoir. To

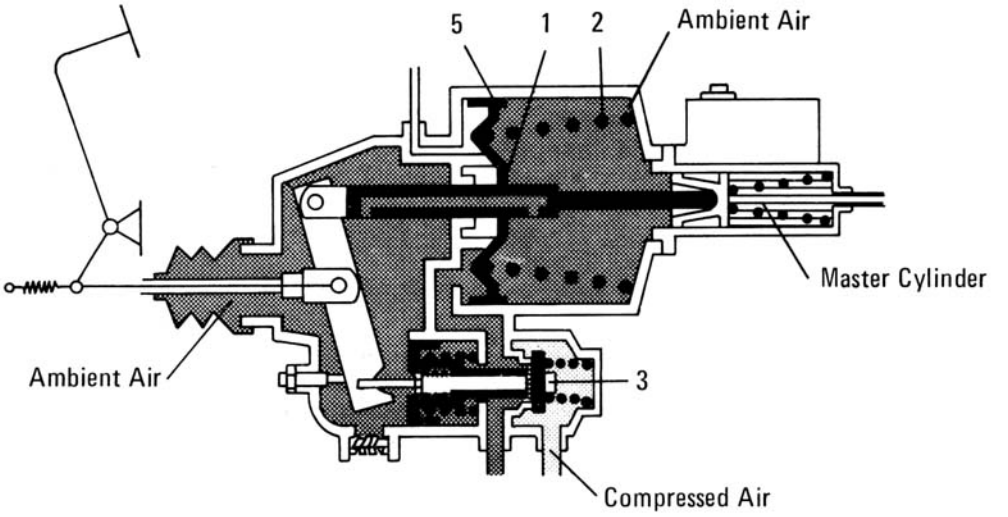

(A) Released

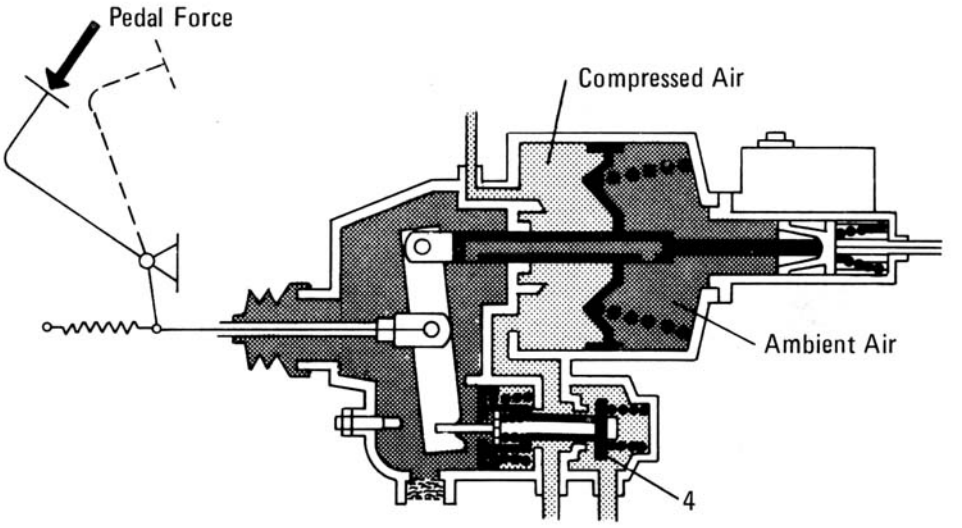

(B) Applied

Figure 15-12. Air-Over-Hydraulic Brake Operation

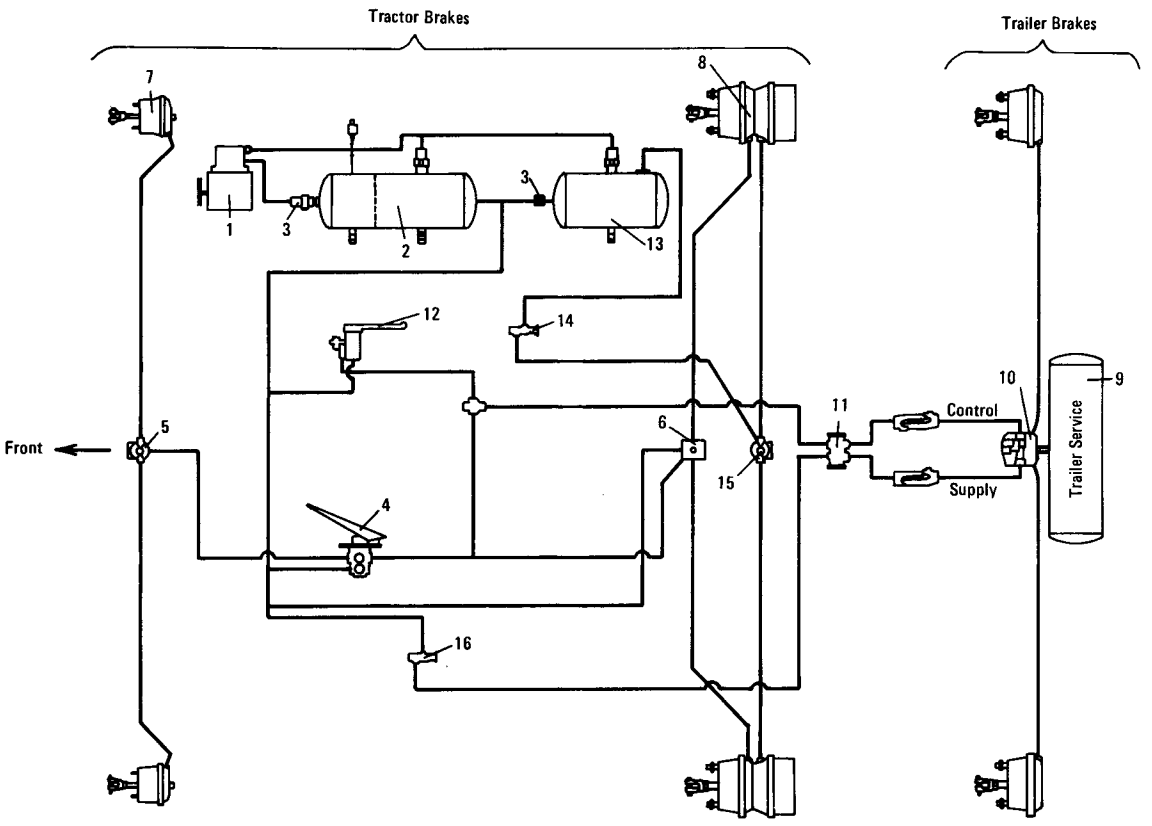

Figure 15-13. Tractor-Semitrailer Air Brake System

keep the brake system in good condition, daily draining of the reservoirs is required. To overcome the water vapor problem, standard air brakes use two reservoirs. The first one in line is called the wet (or supply) reservoir. The second one is called the service reservoir and stores the air which is used for brake actuation. In Fig. 15-13 a single reservoir with two compartments is illustrated. A reservoir mounted moisture ejector is sometimes used which automatically ejects moisture with each brake application. Finally, an air dryer may be used which removes water from the compressed air before it gets into the reservoir. To protect the air in the reservoir in case of compressor or supply failure, a one-way check valve (3) is installed in front of the reservoir which it protects.

The brake application valve (4) is used to control the flow of air to the wheel brakes and to allow modulation of the braking process. Air at reservoir pressure is constantly supplied to the brake application valve. Brake lines, running from the brake application valve to the front and rear brakes, contain air only when the brakes are applied, and then only at the pressure demanded by the driver. A schematic of a brake application valve is illustrated in Fig. 15-14. From the push rod, pedal force is transferred to the metering spring, which strokes the piston against its return spring. During this stroke the inlet-exhaust valve cartridge closes off the exhaust port. The continuing stroke unseats the inlet poppet, permitting compressed air to flow through the valve delivery ports into the brake system. Compressed air also is bypassed to the piston through an equalization orifice and pressure beneath the piston forces it to move to compress the metering spring. The piston reaches a balanced position between these opposed forces. Further movement of the push rod unbalances the forces and admits higher air pressure to increase brake force. Brake pedal release exhausts the system.

Air brake systems are equipped with one or more quick release valves to achieve a faster brake release. The valve exhausts brake line pressure at the point of installation, thus supplementing the exhaust at the

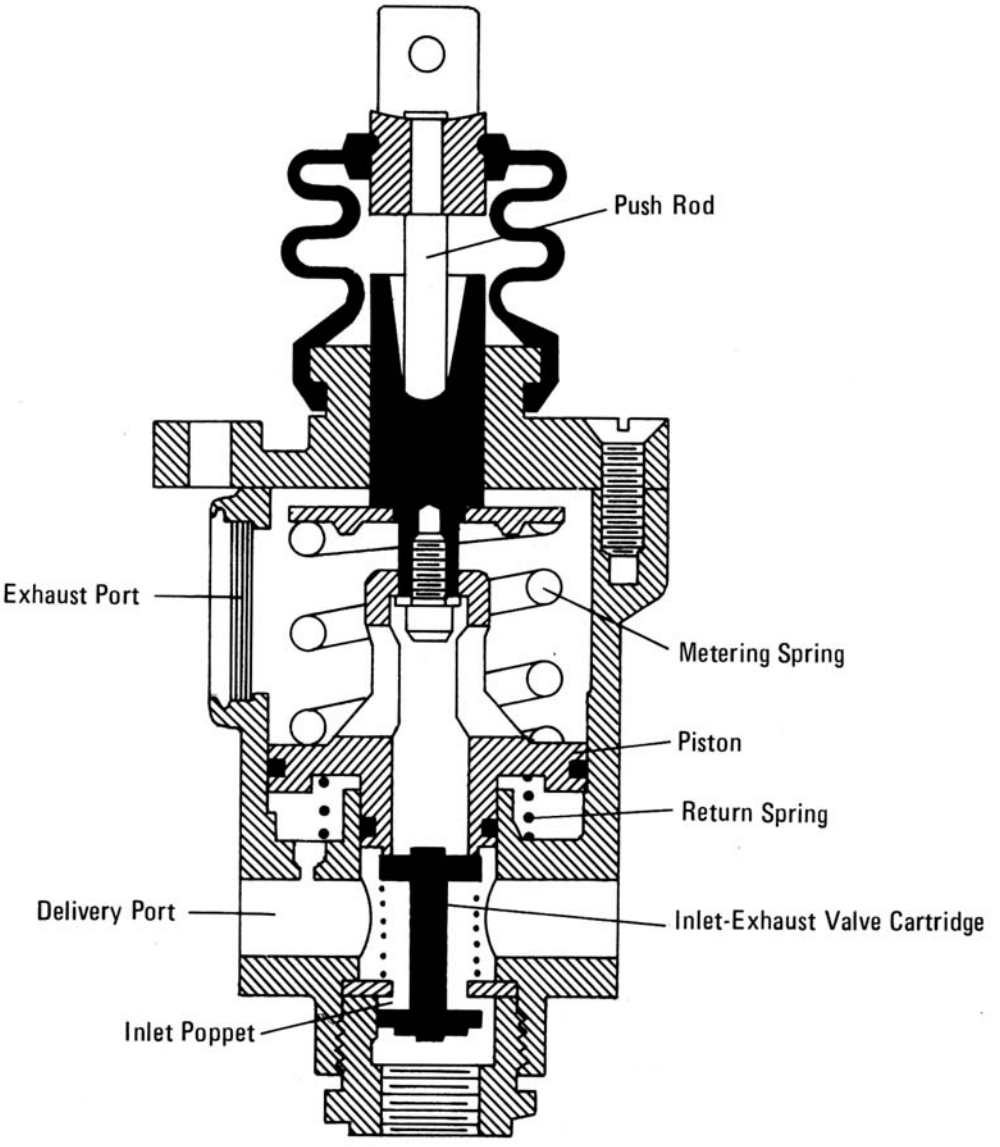

Figure 15-14. Brake Application Valve

brake application valve. A quick release valve is illustrated in Fig. 15-15. Air pressure from the brake application valve enters the quick release valve through the port above the diaphragm and forces the center of the diaphragm to seat tightly against the exhaust port. Air pressure also overcomes diaphragm cup tension to deflect the outer edges of the diaphragm and air flows through the side ports to the brakes. During release the pressure above the diaphragm is released quickly and brake line pressure coming from the wheel brakes raises the center of the diaphragm from the exhaust port and permits direct air escape to the atmosphere.

The relay quick-release valve (6) is connected into the line leading to the rear brakes as shown in Fig. 15-13. The valve helps speed brake application and re-

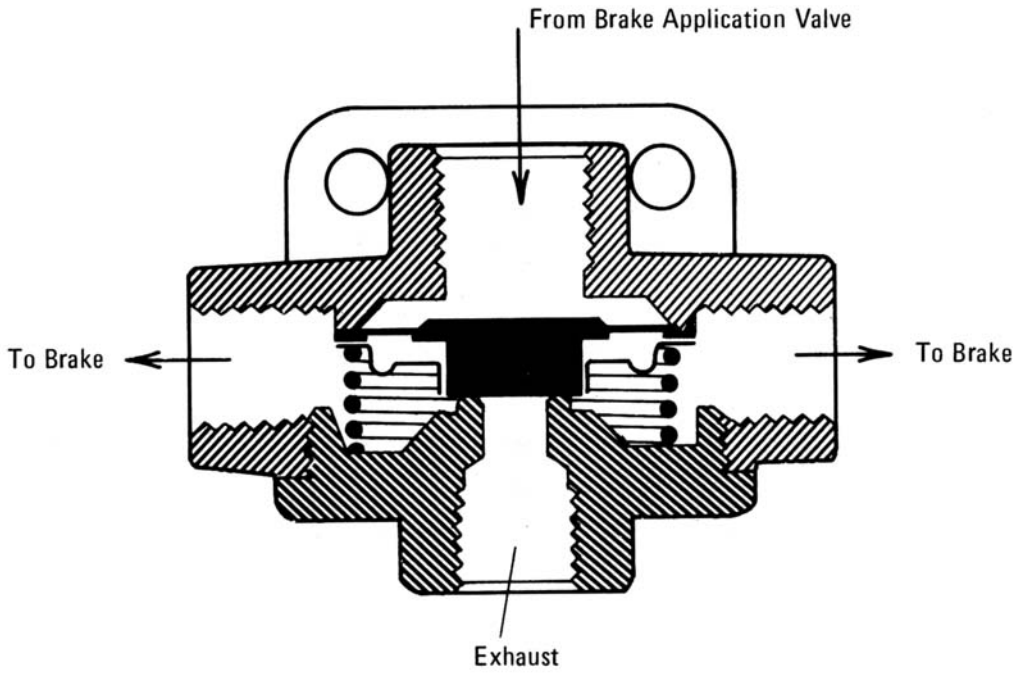

Figure 15-15. Quick-Release Valve

lease. A relay quick-release valve schematic is illustrated in Fig. 15-16. Until the brake application cycle starts, the relay-inlet valve is closed and the exhaust valve is open to the atmosphere. When brakes are applied, the metered air pressure from the brake application valve forces the relay piston down, closing the exhaust port. Further movement of the piston opens the inlet valve, allowing air pressure from the auxiliary reservoir to enter the valve, pass through the delivery ports, and on to the brake application lines. As braking pressure underneath the piston equals controlling pressure above, the piston balances and allows the inlet valve return spring to close the inlet exhaust valve. When the brakes are released, the decrease in controlling pressure unbalances the relay piston and permits the exhaust port to open, thus releasing braking pressure directly to the atmosphere.

The compressed air at the wheel brakes is converted into mechanical energy by the brake chamber (7) and slack adjuster (or wedge). Movement of the slack adjuster arm causes it to rotate a cam shaft which forces the brake shoes to contact the brake drum. An air brake chamber with slack adjuster is shown in Fig. 15-17. Details on brake chamber application force are presented in par. 5-5. A typical air brake combined with a spring brake (8) is illustrated in Fig. 15-18. During normal operation the spring is pressed together by compressed air. Only during an emergency when the system pressure falls below a certain level, or when the brake system is exhausted as in a parking application, does the spring force actuate the pushrod and the brake shoes.

When a trailer is added to the tractor, special provisions are made to apply the trailer brakes. A trailer reservoir (9) as shown in Fig. 15-13 is used to store the compressed air for the trailer brakes. A relay-emergency valve (10) installed on the trailer is used to supply the trailer reservoir with compressed air from the tractor reservoir and to control the brake line pressure and hence the brake force of the trailer — as demanded by the driver. The control line comes from the brake application valve and, when the driver depresses the foot pedal, pressure equal to the tractor brake line pressure opens a port in the relay-emergency valve and allows air at the same pressure level to leave the trailer reservoir and go through the relay-emergency valve to the trailer brake chambers. The relay-emergency valve also acts as an emergency device in case of severe air loss or trailer breakaway.

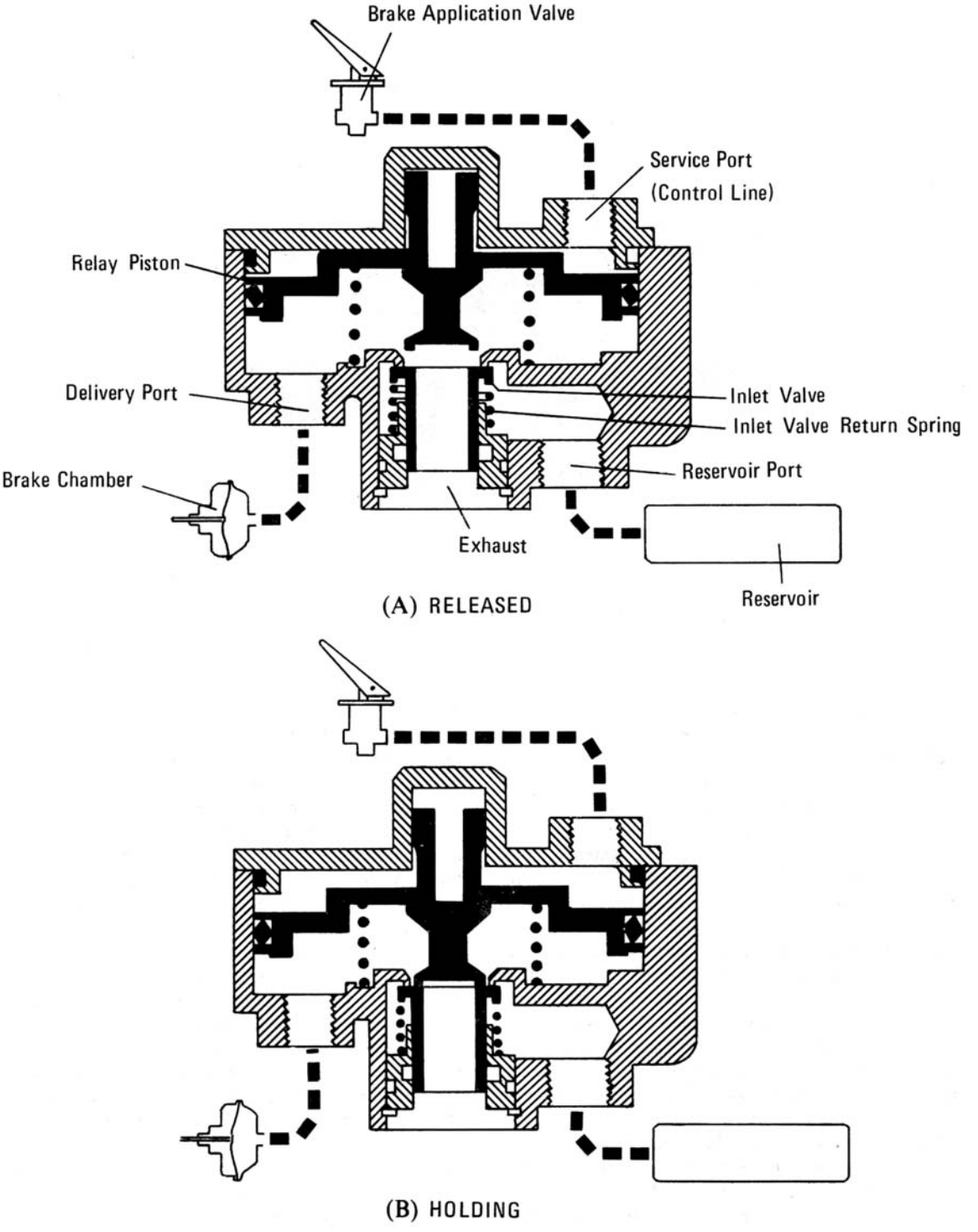

Figure 15-16. Relay Quick-Release Valve

In case of a trailer breakaway the trailer brakes will be applied automatically because the emergency section of the relay-emergency valve will use full trailer reservoir pressure to apply the trailer brakes. If a severe trailer brake leak or trailer breakaway occurs, the tractor brake system is protected by the tractor protection valve (11) as illustrated in Fig. 15-13. It is designed to control the service and supply lines to the trailer. It is both automatic and manual. In an emergency the driver can activate it by use of the manual control (12) located in the cab. If the driver does not operate the control, the tractor protection valve automatically will apply the trailer brakes — when the trailer brake line pressure has decreased to between 20 and 45 psi — by venting the supply or emergency line and thereby triggering the emergency section of the relay-emergency valve. The relay-emergency valve is combined with a quick-release valve to allow a quick release of the air from the brake chambers when the brakes are released.

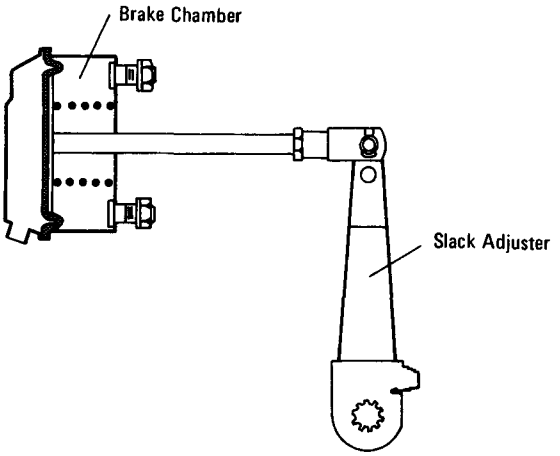

Figure 15-17. Air Brake Chamber

Since the tractor-protection valve is easy to use by the driver by means of the control lever in the cab, it is frequently used to apply the trailer brakes for parking the tractor-semitrailer. However, this should not be done. If a leak develops, no more air can be supplied to the trailer reservoir from the tractor since the tractor protection valve has vented the supply or emergency line between the tractor protection valve and relay-emergency valve.

The most widely used parking brake system on air braked vehicles is the spring brake (Fig. 15-18). It operates the vehicle service brakes (tractor rear axle brakes) by the energy stored in compressed coil springs. When the parking is not applied, the reservoir pressure is used to compress the coil springs and hold the brakes in the released position. A separate reservoir (13) as illustrated in Fig. 15-13 is used for this purpose. A tractor parking valve (14) is used to apply the parking brakes. A quick-release valve (15) is used to exhaust the air of the "parking" chamber in case of a parking brake application.

Frequently, a dash mounted tripping control valve (16) is used to apply the trailer service brake through

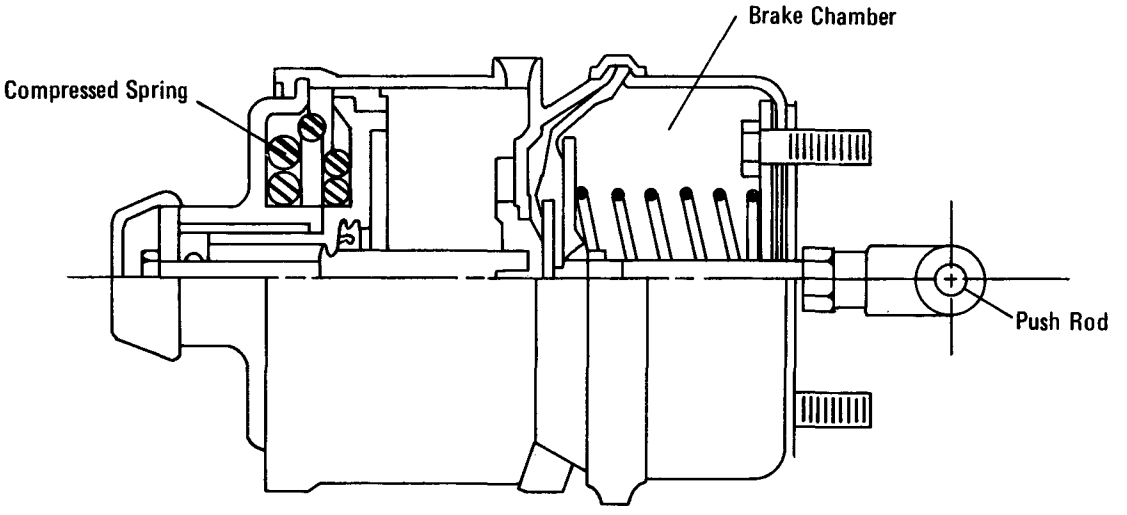

Figure 15-18. Brake Chamber With Spring Brake

the action of the relay-emergency valve when the tractor reservoir pressure drops to 55-60 psi.

15-8 SECONDARY BRAKE SYSTEMS

In the case of passenger cars secondary brake systems are provided in form of the hand or parking brake. Although the parking brake may use the friction surface of the service brake, i.e., the same brake shoes and drums, an independent application is provided. Partial failure performance of the service brake is not considered a secondary brake system.

In the case of heavy trucks and tractor-semitrailer combinations various secondary systems have been designed. If air brakes are used, the entire system can be duplicated and multi-diaphragm chambers can be used. More commonly, spring brakes are used which use a compressed spring as actuator of the wheel brakes in the event of a malfunctioning of the service brake. Recently, spring brakes have been installed on both tractor and semitrailers to provide increased parking brake performance. Light to medium weight trucks frequently use a band brake — mounted on the propeller shaft behind the transmission — as a secondary brake system.

INDEX

C

D

S

T

(DRCDE-L) DARCOM-P 706-358

FOR THE COMMANDER:

H. B. GIBSON, JR.
Major General, USA
Chief of Staff

OFFICIAL:

S/ Saw

G. J. HAROLD
LTC, GS
Adjutant General

DISTRIBUTION:
Special

☆ U.S. GOVERNMENT PRINTING OFFICE: